SPECTROCHIMICA ACTA

COMMENTARIUM SCIENTIFICUM INTERNATIONALE
TRACTANS DE RE SPECTROCHIMICA

PRIMO EDITUM A

A. GATTERER S.J. †
SPECOLA VATICANA CASTEL GANDOLFO

COLLABORANTIBUS

Á. BARDÓCZ-BUDAPEST · **C. G. CARLSSON**-STOCKHOLM **R. CASTRO**-UGINE · **N. D. COGGESHALL**-PITTSBURGH, PA. · **G. H. DIEKE**-BALTIMORE · **J. H. ENNS**-ANN ARBOR, MICH. · **Wa. GERLACH**-MUNICH · **G. HANSEN**-OBERKOCHEN · **G. R. HARRISON**-CAMBRIDGE, MASS · **J. JUNKES S.J.**-CASTEL GANDOLFO · **J. M. LÓPEZ de AZCONA**-MADRID **R. MANNKOPFF**-GÖTTINGEN · **W. MARTI**-WINTERTHUR · **A. E. MARTIN**-NEWCASTLE **O. MASI**-TURIN · **R. MECKE**-FREIBURG · **W. F. MEGGERS**-WASHINGTON, D.C. · **A. C. MENZIES**-LONDON · **FOIL A. MILLER**-PITTSBURGH, PA. · **F. MIZUSHIMA**-TOKYO · **K. PFEILSTICKER**-STUTTGART · **J. M. PHÉLINE**-UGINE · **W. ROLLWAGEN**-MUNICH · **R. A. SAWYER**-ANN ARBOR, MICH. · **R. SCHMIDT**-AMSTERDAM · **R. O. SCOTT**-ABERDEEN · **B. F. SCRIBNER**-WASHINGTON, D.C. · **D. M. SMITH**-WEMBLEY · **L. W. STROCK**-BAYSIDE, NEW YORK **F. TWYMAN**-LONDON

VOL.
8
56/57

EDITUM A

R. BRECKPOT — LOUVAIN
V. A. FASSEL — AMES, IOWA
H. KAISER — DORTMUND
E. LOEUILLE — PARIS
S. L. MANDELSTAM — MOSCOW
R. L. MITCHELL — ABERDEEN
E. H. S. van SOMEREN — LONDON
H. W. THOMPSON — OXFORD

VOLUME VIII
1956–57

PERGAMON PRESS LONDON · NEW YORK · PARIS

Spectrochim. Acta

SPECTROCHIMICA ACTA

EDITORS

BELGIUM AND THE NETHERLANDS

Prof. R. Breckpot, Institut de Chimie, 98 Rue de Namur, Louvain, Belgium

FRANCE

E. Loeuille, Laboratoire Central de l'Armament, Place St. Thomas d'Aquin, Paris, France

GERMANY AND AUSTRIA

Dr. H. Kaiser, Institut für Spektrochemie und Angewandte Spektroskopie, Dortmund-Aplerbeck, Marsbruchstr. 186, Bau I, Germany

GREAT BRITAIN AND BRITISH COMMONWEALTH OF NATIONS

Dr. R. L. Mitchell, Macaulay Institute for Soil Research, Craigiebuckler, Aberdeen, Scotland

Dr. H. W. Thompson, F.R.S., St. John's College, Oxford

E. H. S. van Someren, B.Sc., F.Inst.P., 4 Churchfields, Broxbourne, Herts, England

UNION OF SOVIET SOCIALIST REPUBLICS

Prof. S. Mandelstam, The Physical Institute of the Academy of Sciences of the U.S.S.R., Moscow, U.S.S.R.

UNITED STATES OF AMERICA

Dr. V. A. Fassel, Iowa State College, Ames, Iowa, U.S.A.

VOL.
8
1956/5

CONTENTS OF VOLUME VIII

No. 1

Page

ROBERT G. CHARLES, HENRY FREISER, ROBERT FREIDEL, LELAND E. HILLIARD, and WILLIAM D. JOHNSTON: Infra-red absorption spectra of metal chelates derived from 8-hydroxyquinoline, 2-methyl-8-hydroxyquinoline, and 4-methyl-8-hydroxyquinoline 1

E. M. TANNER: The infra-red absorption spectra of some hydroxypyrimidines . . 9

C. HAAS: Vibration spectra of crystals 19

J. R. BARCELÓ and J. BELLANATO: Contribution to the study of the structures of methyl derivatives of ammonia from spectroscopical data 27

H. STAMMREICH: Technique and results of excitation of Raman spectra in the red and near infra-red region 41

H. STAMMREICH and ROBERTO FORNERIS: Raman spectra and structure of tetratomic sulphur and selenium halides 46

Spectrochemical Notes:

H. STAMMREICH and ROBERTO VORNERIS: Raman spectrum of iodoform . . 52

PAULINE J. DUNTON: Two second-order tellurium lines listed in M.I.T. tables as first-order lines 53

DAVID C. MANNING and W. O. PHILLIPS: Photographic film washer 54

Report of Meetings 56

No. 2

Page

J. Gaunt: The analysis of heavy water by infra-red spectrometry 57

V. v. Keussler: Eine Methode zur genauen Eichung der Wellenlängen-und Wellenzahlskala von Spektralphotometern 66

R. P. Thorne: The spark spectrum of americium 71

R. M. McKenzie: The effect of current control in spectrographic analysis with a direct-current arc 88

Spectrochemical Notes:

F. W. J. Garton, W. Ramsden, R. Taylor, and R. J. Webb: The assessment of the performance of spectrographic methods 94

C. Park: A rotating filter-paper disc method for spectrographic analysis 102

Reports of Meetings:

Annual Pittsburgh Conference on Analytical Chemistry and Applied Spectroscopy . . 107

Book Review:

"Spectrochemical Abstracts." Vol. IV, 1946–1951, by E. H. S. van Someren and F. Lachman (reviewed by Velmer A. Fassel) 128

No. 3

H. W. Thompson and B. A. Green: The fundamental vibration band of nitric oxide 129

R. A. Russell and H. W. Thompson: Vibrational spectra and geometrical isomerism in amides 138

R. D. Kross, K. Nakamoto, and V. A. Fassel: Infra-red dichroism studies of some molecular complexes 142

Á. Bardócz: Untersuchungen über Lichtquellen für Spektralanalyse—VII. Universal Einstellbares Abreissbogengerät mit elektronischer Steuerung . . 152

F. T. Birks: The spectrographic analysis of alpha-active materials by the copper spark method. 167

A. M. Ure: A stabilized microphotometer-lamp power supply 180

Report of Meetings 184

OL.
8
6/57

Nos. 4/5

Page

VELMER A. FASSELL and RAYMOND W. TABELING: The spectrographic determination of oxygen in metals—I. Plain-carbon steels 201

S. F. D. ORR: An infra-red spectroscopic investigation of steric hindrance in some *trans*-stilbene derivatives. 218

J. ROMAND et V. VODAR: Contribution à l'étude de l'ultraviolet lointain . . 229

S. BRATOŽ, D. HADŽI, and N. SHEPPARD: The infra-red absorption bands associated with the COOH and COOD groups in dimeric carboxylic acid—II. The region from 3700 to 1500 cm^{-1} 249

C. CANDLER: A linear-plate characteristic and an intensity scale 262

Reports of Meetings:

Symposium on Molecular Structure and Spectroscopy 280

Letter to the Editors:

K. BUNGE: Bemerkung zu einer Notiz von Herrn BARDOCZ 316

No. 6

BARBARA J. RUSSELL, J. P. SHELTON, and A. WALSH: An atomic-absorption spectrophotometer and its application to the analysis of solutions 317

J. K. BRODY, F. S. TOMKINS, and M. FRED: Photoelectric Fabry-Perot interferometer for assay of lead and uranium isotopes 329

R. F. REKKER and W. TH. NAUTA: Steric effects in the electronic spectra of substituted benzophenones 348

GILBERT MICHEL et GEORGES DUYCKAERTS: Contribution à la spectrométrie Raman—I Construction d'un spectromètre enregistreur à grande dispersion . . . 356

V. C. FARMER: Effects of grinding during the preparation of alkali-halide disks on the infra-red spectra of hydroxylic compounds 374

Reports of Meetings:

Society for Applied Spectroscopy 390

Notices of Meetings 394

Announcement 395

Author Index to Volume VIII 396

Subject Index to Volume VIII 397

Publishing offices: 4 & 5 Fitzroy Square, London W.1 (EUSton 4455). Subscription per volume (including postage) £7 7s. (U.S.A. $20.60). Back numbers £9 ($25.20) per volume.

Distributors: U.K. only—*Hilger & Watts Ltd. (Hilger Division), 98 St. Pancras Way, London N.W.1*

U.S.A.—*Pergamon Press, Inc., 122 E. 55th Street, New York 22, N.Y.*

All other countries—*I. R. Maxwell & Co. Ltd., 4 & 5 Fitzroy Square, London W.1*

PERGAMON PRESS

4 & 5 FITZROY SQUARE, LONDON W.1

122 E. 55TH STREET, NEW YORK 22, N.Y. 24 RUE DES ÉCOLES, PARIS, Ve.

VOL. 8 1956/5

Announcement

An intensive program in Infra-red Spectroscopy will be given from 17 to 28 June during the 1957 Summer Session at the Massachusetts Institute of Technology. The program, to be offered jointly by the Institute's Spectroscopy Laboratory and Department of Chemistry, is designed for those who wish an introduction to infra-red instrumentation and laboratory methods for those interested in the use of infra-red spectra in the solution of chemical problems. It will consist of two intergrated one-week courses, one on the Technique of Infra-red Spectroscopy and the other on the Application of Infra-red Spectroscopy. Both are to be under the direction of Dr. Richard C. Lord, Director of the M.I.T. Spectroscopy Laboratory, assisted by Dr. Foil A. Miller of the Spectroscopy Laboratory at the Mellon Institute of Industrial Research, and Professor E. R. Lippincott of the Department of Chemistry, University of Maryland.

Guest experts from academic and industrial laboratories who will participate in the presentation of material related to their special fields include: Dr. R. Norman Jones, of the Division of Pure Chemistry, National Research Council of Canada, and Dr. Willis J. Potts, Spectroscopy Laboratory, Dow Chemical Company.

In the course on Technique of Infra-red Spectroscopy (17–21 June), lectures will be devoted to the elementary theory of infra-red spectra, a survey of infra-red instrumentation, and discussion of techniques for measurement of spectra. Afternoon laboratory exercises will be carried out by small groups with a variety of infra-red instruments and related equipment. This work will be supervised by experienced academic personnel from the Spectroscopy Laboratory and by technical personnel from manufacturers of infra-red equipment.

The course on Applications of Infra-red Spectroscopy (24–28 June) will cover the theory of infra-red absorption by molecules, the interpretation of infra-red absorption spectra, and the relation between spectra and molecular structure. Particular attention will be paid to hydrocarbons, high polymers, natural products, and other substances whose infra-red spectra have proved especially valuable. Afternoon hours will be devoted to supervised practice in the interpretation of infra-red spectra of complex molecules. Instruction in the use of the generally available catalogues of infra-red spectra and in punched-card methods will also be given.

All facilities of the Institute will be open to members of these courses in Infra-red Spectroscopy. Lecture, laboratory, and library facilities used in the courses are air-conditioned. Registrants may reserve rooms in the Institute's dormitories during the program.

Application forms and full information may be obtained from Dr. James M. Austin, Director of the Summer Session, Room 7–103, Massachusetts Institute of Technology, Cambridge 39, Massachusetts.

AUTHOR INDEX TO VOLUME VIII

Barceló, J. R., and Bellanato, J.: Contribution to the study of the structures of methyl derivatives of ammonia from spectroscopical data. p. 27

Bardócz, Á.: Untersuchungen über Lichtquellen für Spektralanalyse. VII. Universal einstellbares Abreißbogengerät mit elektronischer Steuerung. p. 152

Bellanato, J.: *see* Barceló, J. R.

Birks, F. T.: The spectrographic analysis of alpha-active materials by the copper spark method. p. 167

Bratož, S., Hadži, D., and Sheppard, N.: The infra-red absorption bands associated with the COOH and COOD groups in dimeric carboxylic acid. II. The region from 3700 to 1500 cm^{-1}. p. 249

Brody, J. K., Tomkins, F. S., and Fred, M.: Photoelectric Fabry-Perot interferometer for assay of lead and uranium isotopes. p. 329

Candler, C: A linear plate characteristic and an intensity scale. p. 262

Charles, R. G., Freiser, H., Friedel, R., Hilliard, L. E., and Johnston, W. D.: Infra-red absorption spectra of metal chelates derived from 8-hydroxyquinoline, 2-methyl-8-hydroxyquinoline, and 4-methyl-8-hydroxyquinoline. p. 1

Dunton, P. J.: Two second-order tellurium lines listed in M.I.T. tables as first-order lines. p. 53

Duyckaerts, G.: see Michel, G.

Farmer, V. C.: Effects of grinding during the preparation of alkali-halide disks on the infra-red spectra of hydroxylic compounds. p. 374

Fassel, V. A.: *see* Kross, R. D.

Fassel, V. A. and Tabeling, R. W.: The spectrographic determination of oxygen in metals. I. Plain carbon steels. p. 201

Forneris, R.: *see* Stammreich, H.

Fred, M.: *see* Brody, J. K.

Freiser, H.: *see* Charles, R. G.

Friedel, R.: *see* Charles, R. G.

Garton, F. W. J., Ramsden, W., Taylor, R., and Webb, R. J.: The assessment of the performance of spectrographic methods .p. 94

Gaunt, J.: The analysis of heavy water by infra-red spectrometry. p. 57

Green, B. A.: *see* Thompson, H. W.

Haas, C.: Vibration spectra of crystals. p. 19

Hadži, D.: *see* Bratož, S.

Hilliard, L. E.: *see* Charles, R. G.

Johnston, W. D.: *see* Charles, R. G.

Keussler, V. v.: Eine Methode zur genauen Eichung der Wellenlängen- und Wellenzahlskala von Spektralphotometern. p. 66

Kross, R. D., Nakamoto, K., and Fassel, V. A.: Infra-red dichroism studies of some molecular complexes. p. 142

Lachman, F.: *see* Someren, E. H. S. van

McKenzie, R. M.: The effect of current control in spectrographic analysis with a direct-current arc. p. 88

Manning, D. C., and Phillips, W. O.: Photographic film washer. p. 54

Michel, G., et Duyckaerts, G.: Contribution à la spectrométrie Raman. I. Construction d'un spectromètre enregistreur à grande dispersion. p. 356

Nakamoto, K.: *see* Kross, R. D.

Nauta, W. Th.: *see* Rekker, R. F.

Orr, S. F. D.: An infra-red spectroscopic investigation of steric hindrance in some *trans*-stilbene derivatives. p. 218

Park, C.: A rotating filter-paper disc method for spectrographic analysis. p. 102

Phillips, W. O.: *see* Manning, D. C.

Ramsden, W.: *see* Garton, F. W. J.

Rekker, R. F., and Nauta, W. Th: Steric effects in the electronic spectra of substituted benzophenones. p. 348

Romand, J., et Vodar, V.: Contribution à l'étude de l'ultraviolet lointain. p. 229

Russell, B. J., Shelton, J. P. and Walsh, A.: An atomic-absorption spectrophotometer and its application to the analysis of solutions. p. 317

Russell, R. A., and Thompson, H. W.: Vibrational spectra and geometrical isomerism in amides. p. 138

Shelton, J. P.: *see* Russell, B. J.

Sheppard, N.: *see* Bratož, S.

Someren, E. H. S. van, and Lachman, F.: Spectrochemical Abstracts, vol. IV, 1946–1951. (Rev.) p. 128

Stammreich, H.: Technique and results of excitation of Raman spectra in the red and near infra-red region. p. 41

Stammreich, H., and Forneris, R.: Raman spectra and structure of tetratomic sulphur and selenium halides. p. 46

Stammreich, H., and Forneris, R.: Raman spectrum of iodoform. p. 52

Tabeling, R. W.: *see* Fassel, V. A.

Tanner, E. M.: The infra-red absorption spectra of some hydroxypyrimidines. p. 9

Taylor, R.: *see* Garton, F. W. J.

Thompson, H. W.: *see* Russell, R. A.

Thompson, H. W. and Green, B. A.: The fundamental vibration band of nitric oxide. p. 129

Thorne, R. P.: The spark spectrum of americium. p. 71

Tomkins, F. S.: *see* Brody, J. K.

Ure, A. M.: A stabilized microphotometer-lamp power supply. p. 180

Vodar, V.: *see* Romand, J.

Walsh, A.: *see* Russell, B. J.

Webb, R. J.: *see* Garton, F. W. J.

VOL. 8 1956/5

SUBJECT INDEX TO VOLUME VIII

PAGE

Absorption:
- Atomic — spectrophotometer . . 317
- IR — bands due to COOH and COOD 249
- UV — spectroscopy . . 234, 393

Alkali-halide disc technique, Grinding effects on IR spectra . . . 374
Alpha-active materials, Analysis by copper spark method . . 167
Americium, Spark spectrum . . 71
Amides, Vibrational spectra and geometrical isomerism . . . 138
Amino and methyl groups, Mutual vibrations 30
Ammonia methyl derivatives, Structure 27
Analytical emission spectroscopy . . 107, 196, 392
Announcement:
- M.I.T. Summer Session Courses in IR Spectroscopy, 17–28 June 1957 395

Anthracene-sym-trinitrobenzene, IR dichroism 145
Assessment of performance of spectrographic methods . . . 94
Atomic absorption spectrophotometer . 317
Atomic spectroscopy 288
Band spectra, Electronic — . . 280
Benzoic acids: Grinding effects in IR spectra using pressed alkali-halide disc technique 376
Benzophenones, Substituted: Steric effect in electronic spectra . . 348
Bias in spectrographic methods . . 95
Book review:
- Spectrochemical Abstracts, 1946–1951 (van Someren) . . . 128

Calibration of spectrophotometers for wavelengths and wave numbers 66
Carboxylic acids:
- Grinding effects on IR spectra using pressed alkali-halide discs . . 380
- IR bands associated with COOH and COOD 249

Coated electrodes and filter-paper disc technique 103
Concentration range in spectrographic methods 96
Controlled d.c. current, Effect in spectrochemical analysis . . . 88
Copper and copper-base alloys, Analysis 390
Copper spark in α-active material analysis 167

PAGE

Cryostat in vacuum UV absorption spectroscopy 234
Crystals:
- Dispersion theory of cubic — . . 20
- of uniaxial — 24
- Spectroscopy of low symmetry — 298
- Vibration spectra 19

Current control in spectrochemical analysis 88
Detection sensitivity of spectrographic methods 96
Detectors:
- in Raman red and near IR spectroscopy 44
- in UV vacuum 233

Dichroism in the IR of some molecular complexes 142
Electronic band spectra: . . . 280
- of substituted benzophenones . . 348

Emission spectroscopy, Analytical 107, 196, 390, 392
Excitation sources:
- Current controlled d.c. arc . . 88
- D.c. arc discharge in rare-gas . . 208
- for Raman red and near IR spectroscopy 42
- for vacuum UV spectroscopy . . 229
- Hollow cathode tube . . . 319
- Interrupted arc, adjustable and electronically controlled . . 152
- Sliding spark 232
- Unidirectional discharge . . . 207

Fabry-Perot interferometer, Photoelectric, for assay of Pb and U isotopes 329
Film washer 54
Filter-paper disc, Rotating . . 102
Flame photometry . . . 124, 198
Fluorescence spectroscopy:
- Optical — 124
- X-ray — 112, 198

Grinding effects in IR spectra of hydroxylic compounds using alkali-halide discs 374
Heavy water, Analysis by IR spectroscopy 57
High-dispersion IR spectroscopy . . 300
Hollow-cathode tube for atomic absorption spectroscopy . . . 319

PAGE

Hydroxylic compounds:
Grinding effects on IR spectra of — using pressed alkali-halide disc technique 374
Hydroxypyrimidines, IR spectra . . 9
Structure 14
8-Hydroxyquinoline (and derivatives) chelates of metals, IR spectra . 1
Illumination of spectrographs in plate calibration 264
Infra-red spectra:
Absorption associated with COOH and COOD 249
of ammonia methyl derivatives . . 27
of hydroxypyrimidines 9
of 8-hydroxyquinoline (and derivatives) metal chelates . . 1
Infra-red spectroscopy: 117, 198, 297, 391
Analysis of heavy water . . . 57
Applied to chemical problems . . 301
Dichroism of some molecular complexes 142
Near IR Raman spectroscopy . . 41
Studies of steric hindrance in *trans*-stilbene derivatives . . . 218
Instruments (*see* also Detectors, Excitation sources, Methods):
in IR spectroscopy . . . 64, 307
in vacuum UV spectroscopy . . 238
Photoelectric Fabry-Perot interferometer 329
Spectrographs for Raman spectroscopy in red and near IR 42
Spectrophotometer for atomic absorption 317
for Raman spectroscopy . . 356
Intensities in band spectra . . 312
Intensity scale and linear plate characteristic . . . 262, 276
Iodoform, Raman spectrum . . 52
Isomerism and vibrational spectra of amides 138
Isotopes: 185
Dtn of Pb and U — by photoelectric interferometry 329
Kaiser-Seidel transformation . . 266
A-transform for linear plate characteristic 271
Letter to the editor (BUNGE, K.) . . 316
Lead isotopes, Dtn by photoelectric interferometry 329
Line widths in band spectra . . . 312
Linear plate characteristics . . 262

PAGE

Management problems in spectroscopy . 126
Mass spectroscopy 393
Metal chelates of 8-hydroxyquinoline (and derivatives), IR spectra . . 1
Methods (*see* also Excitation sources, Photographic photometry, Spectral analysis):
Cryostat technique in vacuum UV absorption spectroscopy . . 234
Current control of d.c. arc . . . 88
Performance characteristics of spectrographic — 94
Pressed alkali-halide disc technique . 374
Rotating filter-paper disc . . . 102
Separation of orders in vacuum UV spectroscopy 237
Methyl:
and amino groups, Mutual vibrations . 30
Vibrations of — radical . . 29, 32, 36
Methylamine: Structure of mono— . 28
of di— 32
of tri— 35
Methylbenzene, (Hexa—) -picryl-chloride: IR dichroism . . 143
β-Methylnaphthalene-picric-acid, IR dichroism 147
Microdensitometer, Stabilized lamp for— 180
Microwave spectroscopy . . . 310
Molecular complexes:
and IR dichroism 142
of anthracene-sym-trinitrobenzene 145
of β-methylnaphthalene-picric-acid 147
of hexamethylbenzene-picryl-chlo- . 143
ride of piperidine-picric-acid . . 149
Spectra of — 290, 299
Nitric oxide, Fundamental vibration band 129
Notices of Meetings:
American Association of Spectrographers, 8th Annual Symposium, Chicago, 29 April to 1 May, 1957 396
8th *Pittsburgh Conference on Anal. Chemistry and Applied Spectroscopy*, 4–8 March, 1957 . . 396
Society for Applied Spectroscopy, 11th Annual Meeting, New York, 1–2 November, 1956 . . . 200
Optical fluorescence spectroscopy . . 124
Order separation in vacuum UV spectroscopy 237
Oxygen, Dtn in plain carbon steel . . 201

VOL. 8 1956/5

PAGE

Phenols, Grinding effects on IR spectra using pressed alkali-halide disc technique 383
Photoelectric Fabry-Perot interferometer 329
Photographic photometry:
Film washer 54
in the vacuum UV spectroscopy . 236
Linear plate characteristics . . 262
Stabilized photometer lamp . . 180
Polyhydroxyalcohols, Changes in IR spectra using pressed alkali-halide disc technique . . . 385
Pressed-disc technique: Grinding effects on IR spectra of hydroxylic compounds 374
Piperidine-picric-acid, IR dichroism 149
Raman spectra:
of iodoform 52
of S_2 = and Se_2 = halides . . 46
Raman spectroscopy: 310
in red and near infra-red . . 41
Large dispersion spectrometer for — . 356
Reliability of spectrographic methods 96
Reports of Meetings:
American Association of Spectrographers, 7th Annual Symposium, Chicago, 4 May 1956 . 196
Pittsburgh Conference (7th) *on Analytical Chemistry and Applied Spectroscopy* 107
Analytical emission spectroscopy . 107
X-ray fluorescence spectroscopy . 112
Infra-red spectroscopy 117
Ultra-violet spectroscopy . . 121
Optical fluorescence spectroscopy . 124
Flame photometry 124
Management problems in spectroscopy 126
Society for Applied Spectroscopy, 11th Annual Meeting, 1–2 November, 1956, New York 390
Spectrochemical analysis of copper and copper-base alloys . . 390
Infra-red and related techniques . 391
Fundamental aspects of emission and X-ray spectroscopy . . 392
Applied and theoretical papers in UV absorption, mass, and pertinent nuclear spectroscopic techniques 393
Spectroscopy Symposium at Argonne National Laboratories, 15–17 Feb., 1956 184

PAGE

Reports of Meetings (*continued*):
Symposium on molecular structure and spectroscopy, Ohio, 11–15 June, 1956 280
Electronic band spectra . . 280
Atomic spectroscopy . . . 288
Spectra of molecules . . . 290
Infra-red spectroscopy . . . 297
Solid-state spectra . . . 297
High-dispersion 300
Applied to chemical problems . 301
Instrumentation . . . 307
Microwave and Raman spectroscopy 310
Intensities, line breadths, etc.. . 312
Western Spectroscopy Association, 3rd Annual Conference, 26–27 Jan., 1956 (Titles only, Program) . 56
Reproducibility of spectrographic methods 95
Rotating filter-paper disc . . . 102
Seidel-Kaiser transformation . . 267
Selenium (tetratomic) halides, Raman spectra and structure. . . 46
Sensitivity:
in atomic absorption spectroscopy . 324
in rotating filter disc method . . 105
in spectrographic methods . . 96
Separation of orders in vacuum UV spectroscopy 237
Sliding spark technique in vacuum UV spectroscopy 232
Solid state spectra 297
Solution analysis by atomic absorption spectroscopy 317
Spark:
Copper — for α-active material analysis 167
Sliding — in vacuum UV spectroscopy 232
— spectrum of Am 71
Spectra (*see* Infra-red, molecular —, ultra-violet, vibrational —)
Spectral analysis (*see* also Instruments, Methods, Reports of meetings, X-ray spectroscopy):
by atomic absorption spectra . . 317
by emission spectra . . 107, 392
by flame photometry . . 124, 198
by optical fluorescence . . . 124
by X-ray fluorescence spectroscopy 112, 198
in the infra-red . . 57, 117, 297, 391
in the vacuum UV 229
of α-active material. . . . 167
of Cu and Cu-base alloys . . . 390

PAGE

Spectral analysis (*continued*):
of heavy water in the IR . . . 57
of Pb and U isotopes 329
of solutions by atomic absorption spectra 317
Spectrochemical Abstracts (rev.) . . 128
Spectrophotometer:
Calibration for wavelengths and wave numbers 66
for atomic absorption 317
of large dispersion (for Raman spectroscopy) 356
Spectroscopy:
Analytical emission — 107, 196, 392
Atomic — 288
Infra-red — . . 117, 198, 297, 391
Management problems in — . . 126
Optical fluorescence — . . . 124
Raman — 310, 356
UV absorption — . . . 234, 393
X-ray fluorescence — . 112, 198, 392
Steel, Plain carbon — : Dtn of O_2 . 201
Stepped sector in plate calibration . 263

PAGE

Steric effects:
in electronic spectra of substituted benzophenones 348
in *trans*-stilbene derivatives . 218
Stilbene (*trans*- —) derivatives, Steric hindrance 218
Sulphur (tetratomic) halides, Raman spectra and structure . . 46
Tellurium, Dtn with second-order lines . 53
Ultra-violet spectroscopy: . . 121, 393
Detectors for vacuum — . . . 233
in the vacuum UV . . . 229
Spurious light, Elimination . . 237
Uranium isotopes, Dtn by photoelectric interferometry 329
Vibrational spectra: . . . . .
of amides 138
of crystals 19
of nitric oxide (Fundamental band) . 129
Water, Heavy: Analysis by IR spectrometry 57
Wavelengths and wave numbers, Calibration of spectrometers for — . 66
X-ray fluorescence spectroscopy: . 112, 199
Fundamental aspects of — . . 392

VOL. 8 1956/5

OL.
8
6/57

VOL.
8
1956/5

Spectrochimica Acta, 1956, Vol. 8, pp. 1 to 8. Pergamon Press Ltd., London

Infra-red absorption spectra of metal chelates derived from 8-hydroxyquinoline, 2-methyl-8-hydroxyquinoline, and 4-methyl-8-hydroxyquinoline

ROBERT G. CHARLES,* HENRY FREISER, ROBERT FRIEDEL,†
LELAND E. HILLIARD, and WILLIAM D. JOHNSTON*
Department of Chemistry, University of Pittsburgh, Pittsburgh, Pennsylvania‡

(*Received for review* 11 *March* 1955; *accepted for publication* 25 *November* 1955)

Abstract—The infra-red absorption spectra of solid 8-hydroxyquinoline, 2-methyl-8-hydroxyquinoline, 4-methyl-8-hydroxyquinoline, and of a number of metal chelates derived from these reagents, have been studied. In general, the spectra of the metal chelates derived from a given reagent were found to be quite similar. Significant differences were, however, observed in several instances, which may be useful analytically. An absorption peak at about 9 μ was found in the spectra for the chelates of all three reagents. It is suggested that this peak is associated with C-O vibrations in these molecules. When the "9 μ" peak positions for divalent-metal 8-hydroxyquinolates are plotted against the atomic weights of the corresponding metals, the points for the transition-metal chelates fall near one straight line, while the points for the remaining metal chelates fall near another. It is suggested that this may indicate either involvement of 3*d* orbitals in metal-ligand bonding for the transition-metal 8-hydroxyquinolates or, alternatively, a difference in crystal structure for the two classes of chelates.

OL.
8
6/57

As part of a general research programme dealing with metal chelate compounds which is currently in progress at the University of Pittsburgh, the infra-red absorption spectra of a number of metal chelates of 8-hydroxyquinoline have been determined. 8-Hydroxyquinoline chelates were chosen for this study, since their importance in analytical chemistry is well known [1]. Further, much data of both a theoretical and a practical nature concerning these compounds are available. In order to study the effect of simple substituents, chelates of the corresponding 2- and 4-methyl compounds have also been investigated.

There were several objectives to this study. First, it was hoped that the spectra obtained might provide information concerning the structure of the various chelates. Secondly, relationships were sought between various features of the spectra and other properties of the chelates and of the parent metal ions. Thirdly, it was thought desirable to determine whether the spectra might prove sufficiently distinctive to serve as a basis for a method of identification of the various metals involved.

Experimental

Preparation of chelates—In general, the chelates were prepared by the following procedure. 50 ml of a 0·01 M aqueous solution of the metal nitrate or perchlorate was diluted to 200 ml with distilled water, and heated to 60°C. A small excess of a 1% alcoholic solution of the chelating agent was then added, followed by sufficient ammonium hydroxide to make the solutions slightly basic. After cooling, the precipitated chelates were collected on sintered-glass

* Westinghouse Research Laboratories, East Pittsburgh, Pa.
† U.S. Bureau of Mines, Bruceton, Pa.
‡ Contribution No. 962 from the University of Pittsburgh, Pittsburgh 13, Pa.

crucibles and washed thoroughly with hot water. The 8-hydroxyquinoline chelates were dried for several hours at the temperatures recommended by WELCHER [1] to give the anhydrous compounds. The temperatures were generally in the range 105°C to 140°C. The nickel and cobalt chelates of 8-hydroxyquinoline were dried for two hours at 120°C. Chelates of 2- and 4-methyl-8-hydroxyquinoline were dried at 130°C. The aluminium, gallium, and indium chelates of 8-hydroxyquinoline were samples which had been recrystallized from absolute ethanol for another study.

The potassium salt of 8-hydroxyquinoline was prepared by the following procedure. To 14·5 g of 8-hydroxyquinoline dissolved in a minimum of hot 95% ethanol were added 5·6 g of potassium hydroxide in 20 ml of ethanol. The mixture was heated for a few minutes, and allowed to cool. On standing overnight, the potassium salt separated as yellow prisms, which were filtered off and dried at room temperature, *in vacuo*, over $CaCl_2$. The sodium salt was prepared in the same manner, except that it was necessary to use 50 ml of ethyl alcohol to dissolve an equivalent amount of sodium hydroxide. The sodium and potassium salts so obtained were not analysed and may be hydrates. The 8-hydroxyquinoline and the corresponding 2- and 4-methyl compounds, used to obtain the spectra of the reagents, were recrystallized samples, dried *in vacuo*, over $CaCl_2$.

Experimental procedure—The spectrometer employed was a single-beam Perkin Elmer instrument, model 12-C, equipped with sodium chloride optics. Since all the chelates studied were infusible solids with very low solubilities in organic solvents, they were studied as mineral-oil mulls. 50 mg of the compound were mulled for ten minutes with five drops of heavy white mineral oil in a "mullite" mortar. A drop or two of the mull was pressed between two sodium chloride plates in a demountable cell.

The spectra shown in Fig. 1 were obtained at the most rapid speed of the instrument, which speed gives adequate resolution within the wavelength-region studied. The nine-micron (1100 cm^{-1}) region was repeated at the slowest speed of the instrument. The italicized wave-number values given in the legend to Fig. 1 were obtained from spectra run at this speed.

The present study was restricted to the region 8 to 15 μ for two reasons. First, differences between spectra which might be useful in analysis were expected to be greater in this region than at shorter wavelengths. Secondly, with the single-beam instrument employed, interpretation was more difficult below 8 μ, due to the superposition on the spectra of bands arising from atmospheric water-vapour.

VOL. 8 1956/5

Results and Discussion

At the time this study was initiated, few infra-red spectra had been reported for metal chelate compounds [2]. Since that time, however, a number of papers have appeared on this subject [3–7]. The only spectra which have been reported for 8-hydroxyquinoline chelates are those recently published by STONE [7] for magnesium and bismuth 8-hydroxyquinolates. STONE's curve for the anhydrous magnesium compound is essentially identical with that given for this compound in Fig. 1 of the present paper.

The spectra for 8-hydroxyquinoline and its 2- and 4-methyl derivatives are given as spectra 2, 3, and 4 in Fig. 1. In the longer-wavelength region there are significant differences between the three spectra. Absorption peaks in this region are difficult to interpret, since the majority of such peaks are probably associated with vibrations of the molecules which are more complex than those due to simple stretching or bending motions of diatomic groupings within the molecules.

The spectra of the metal chelates derived from 8-hydroxyquinoline are all quite similar to one another, in general resembling one another more closely than they do the spectrum of the parent reagent. The greatest differences among the spectra of the 8-hydroxyquinoline metal chelates are found between 13 and 14

OL.
8
6/57

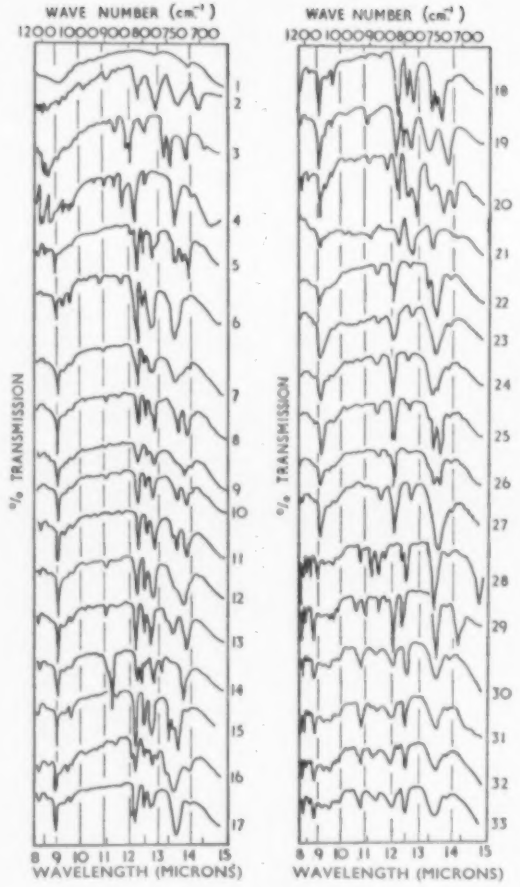

Fig. 1. Infra-red absorption spectra for 8-hydroxyquinoline, 2-methyl-8-hydroxyquinoline, 4-methyl-8-hydroxyquinoline, and their metal chelates. (Numbers given below are principal absorption peaks in cm^{-1}. The peak at about 9 μ is given in italics.)

1. Blank.

Reagents

2. 8-Hydroxyquinoline 711, 741, 781, 788, 806, 818, 865, 897, 974, 1058, 1093, 1163, 1201, 1202.
3. 2-Methyl-8-hydroxyquinoline 696, 723, 749, 759, 793, 798, 831, 836, 876, 1092, 1156, 1180, 1210.
4. 4-Methyl-8-hydroxyquinoline 690, 744, 805, 827, 861, 883, 915, 951, 1034, 1053, 1082, 1149, 1163, 1203, 1221.

8-Hydroxyquinoline chelates

5. Cu(II) 723, 734, 742, 745, 746, 786, 800, 819, 828, 834, 852, 1039, *1118·1*, 1145, 1178, 1223.
6. Ni(II) 736, 744, 784, 790, 804, 815, 854, 914, 951, 1033, 974, 1068, *1110·1*.
7. Co(II) 744, 783, 790, 804, 820, 857, 908, 1032, 1069, *1107·5*.
8. Mn(II) 730, 745, 787, 804, 820, 824, 902, *1106·4*.
9. Zn 731, 786, 802, 821, 908, 1032, *1107·3*, 1232.
10. Cd 727, 744, 792, 803, 820, 903, *1106·3*.
11. Pb(II) 727, 744, 751, 785, 800, 818, 1040, 1065, *1104·8*, 1223.
12. Mg 731, 748, 790, 804, 822, 903, *1108·3*, 1215.
13. Ca 726, 751, 758, 787, 803, 824, 867, 902, 1030, 1059, 1070, 1078, *1108·2*, 1233.
14. UO_2 732, 753, 770, 785, 798, 805, 812, 821, 893, 899, 1033, 1065, *1107·1*, 1224.
15. Fe(III) 739, 750, 754, 788, 803, 823, 869, 1034, 1062, 1082, *1106·5*, 1234.
16. Al 753, 761, 779, 788, 797, 804, 826, 836, 877, 979, 1032, 1050, 1090, *1114·7*, 1169, 1229.
17. Ga 742, 782, 790, 802, 823, 1034, 1056, *1114·6*, 1223.
18. In 737, 747, 754, 784, 801, 823, 832, 864, 868, 909, 1036, 1063, *1107·3*, 1132.
19. La(III) 725, 756, 789, 807, 821, 899, 1034, 1070, *1104·8*.
20. Na 715, 732, 752, 781, 793, 799, 817, 820, 844, 894, 928, 937, 978, 1032, 1065, *1102·3*, 1130, 1170, 1197, 1226.
21. K 714, 718, 754, 791, 796, 821, 824, 890, *1098·8*, 1139.

2-Methyl-8-hydroxyquinoline chelates

22. Cu(II) 742, 758, 793, 829, 836, 873, 1050, *1104·4*.
23. Ni(II) 744, 792, 835, 870, 1028, *1101·1*, 1138, 1168, 1204.
24. Co(II) 739, 751, 795, 835, 869, 919, 954, 972, 1029, 1062, *1101·0*, 1138.
25. Mn(II) 736, 749, 757, 793, 801, 827, 831, 870, 920, 974, 1032, *1099·8*, 1136.
26. Zn 739, 749, 756, 795, 831, 845, 869, *1104·8*, 1135.
27. Mg 740, 795, 830, 868, 915, 1026, 1057, *1100·1*, 1131.

4-Methyl-8-hydroxyquinoline chelates

28. Cu(II) 680, 749, 802, 814, 854, 872, 894, 934, 952, 1016, 1030, 1057, 1104, *1153·1*, *1158·6*, 1186, 1213.
29. Ni(II) 705, 737, 807, 824, 844, 867, 907, 937, 1017, 1035, 1054, 1103, *1159·3*, 1186, 1214.
30. Co(II) 743, 801, 813, 832, 873, 927, 1009, 1026, 1059, 1091, *1154·0*, 1186, 1208.
31. Mn(II) 740, 801, 813, 834, 872, 888, 925, 1008, 1028, 1058, 1090, *1153·2*, 1185, 1207.
32. Zn 740, 800, 812, 834, 882, 926, 1009, 1028, 1058, 1095, *1155·1*, 1188, 1209.
33. Mg(II) 743, 801, 816, 832, 873, 926, 1007, 1027, 1059, 1090, *1153·8*, 1188, 1205.

microns. In certain of the spectra (for example, spectra 7 and 17) a single strong peak appears in this region. In others (8, 10, 11) this is replaced by two strong peaks. In still others (5 and 18) three strong peaks appear in this region. These differences, while relatively small, may nevertheless prove useful in metal identification and analysis.

The general similarity between all the spectra of the 8-hydroxyquinoline chelates suggests that all the metals have similar effects on the vibrations responsible for the absorption peaks in this wavelength region. While one can divide the 8-hydroxyquinoline chelates into groups depending on the appearance of the spectra in the 13–14-micron region, there seems to be no obvious reason for the metals forming the groups which they do. It is particularly striking that there is no obvious distinction between the spectra for the divalent and trivalent metal chelates. For the two monovalent metal chelates studied there are somewhat greater differences in the 12–13-micron region.

The spectrum of the uranyl compound (spectrum 14) deserves special attention. A strong band appears at about 11·2 μ in this spectrum which does not appear in the spectra of the other chelates. A peak in this general region also appears in the spectrum of uranyl nitrate and has been assigned to the UO_2 group [8]. Since the peak at 11·2 μ is not found in the other spectra shown, it may have analytical potentialities.

The uranyl ion reacts with three molecules of 8-hydroxyquinoline to form a compound of the empirical formula $UO_2(C_9H_6NO)_2(C_9H_7NO)$. The third 8-hydroxyquinoline molecule is presumably held, as such, in the crystal lattice by purely crystal forces. It is interesting that some of the absorption peaks of 8-hydroxyquinoline (for example, the peak at 14·1 μ) are not found in the uranyl chelate spectrum. This suggests that the forces holding the 8-hydroxyquinoline molecules are sufficiently strong to modify the vibrational frequencies of all three 8-hydroxyquinoline groups.

The spectra of the 2-methyl-8-hydroxyquinoline chelates are all quite similar to one another. Like the spectra of the 8-hydroxyquinoline chelates, the greatest differences occur in the 13–14 region. The spectra of the 2-methyl-8-hydroxyquinoline chelates are significantly different from those of the 8-hydroxyquinoline chelates, particularly in the 12–13-μ region.

The spectra of the 4-methyl-8-hydroxyquinoline chelates differ both from those of the 2-methyl and of the unsubstituted 8-hydroxyquinoline. While the spectra of the Co, Zn, Mn, and Mg chelates of the first-named reagent resemble one another very closely, the spectra of the copper and nickel chelates of this reagent are significantly different. Of particular interest are the peaks at 14·7 μ in the copper chelate and 14·2 μ in the nickel chelate. Since these peaks do not appear in the spectra of the other chelates of this reagent, they offer interesting analytical potentialities. These differences suggest that, for this reagent, a difference in structure may exist between the copper and nickel chelates as opposed to the chelates of the other metals investigated. Whether this represents an actual difference in molecular structure or merely a difference in crystal type cannot be decided on the basis of present evidence.

In the spectra of all the 8-hydroxyquinoline chelates studied, a strong peak

VOL. 8 1956/5

appears at about 9 μ. It is difficult to decide which, if any, of the peaks in the 9-μ region of the reagent spectra corresponds with this peak in the chelate spectra. These peaks occur near the wavelength region commonly assigned to C-O vibrations (8–8·3 μ) [9]. This fact, plus the facts that the peak occurs in the spectra of all the 8-hydroxyquinoline chelates, suggests that the 9-μ peak is characteristic of the bond A (below) of the 8-hydroxyquinolate anion. Further evidence for this is found in the fact that similar strong peaks at about 9 μ are also found in the spectra of the 2-, and of the 4-methyl-8-hydroxyquinoline chelates (Fig. 1).

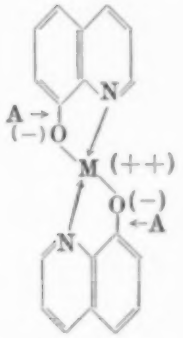

Divalent metal chelate of 8-hydroxyquinoline

The appearance of the 9-μ peak in all the metal chelate spectra is a strong indication that this peak is due to a diatomic vibration, such as that associated with the C-O group, rather than to more complex vibrations.

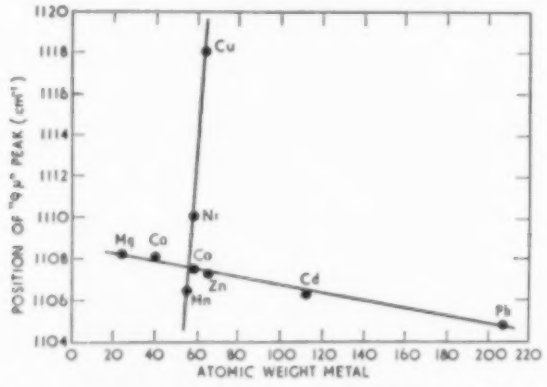

Fig. 2. Relationship between position of 9-μ absorption peak and atomic weight of metal for divalent metal chelates of 8-hydroxyquinoline.

The exact position of the 9-μ peak was found to vary, by a small but easily measurable amount, from one 8-hydroxyquinoline metal chelate to another. Attempts were made to relate the 9-μ peak position with various properties of the metal cation. HUNT, WISHERD, and BONHAM [10] have observed that the position of one of the absorption peaks of metal carbonates varies with the atomic weight of the metal present, being displaced (logarithmically) to lower frequencies

as the atomic weight of the metal is increased. In Fig. 2 the positions of the 9-μ peaks for divalent-metal 8-hydroxyquinolates are plotted against the atomic weight of the metal.* The points appear to fall into two groups. The points for the Mg, Ca, Zn, Cd, and Pb chelates obey a relationship similar to that found for the metal carbonates [10]. On the other hand, the points for the transition-metal chelates Mn, Co,† Ni, and Cu fall near another straight line of quite different slope, the absorption frequency in this case increasing sharply with increasing atomic weight of the metal. The differences just noted suggest that a fundamental difference in structure of some sort may exist between the two groups of chelates. The most obvious difference between the transition-metal cations and the other metal cations mentioned is the presence of available 3*d* orbitals in the former. One possible explanation, then, for the differences noted in Fig. 2 is the possible participation of 3*d* orbitals in metal-ligand bonding. Magnetic susceptibility measurements have frequently been used to shed some light on the question of participation of 3*d* orbitals in metal-ligand bonding for transition-metal chelates [11]. The magnetic susceptibility of nickel 8-hydroxyquinolate has been measured by MELLOR and CRAIG, who found a magnetic moment corresponding to that of the simple Ni(II) ion [12]. Unpublished results obtained at the Westinghouse Research Laboratories show that the moments of the anhydrous Co(II), Mn(II), and Fe(III) 8-hydroxyquinolate are also close to the moments found for the corresponding uncomplexed cations. These results would seem to indicate that, if 3*d* orbitals are involved in metal-ligand bonding for these chelates, they are not involved to the extent of forming $3d4s4p^2$ hybridized bonds [11]. Some question, however, has been raised regarding the interpretation of magnetic data for metal complexes and chelates [13], so that it seems necessary to leave open the question of participation of 3*d* orbitals in bonding for the 8-hydroxyquinolates, pending additional evidence.

A second possible explanation for Fig. 2 may involve a difference in crystal structure for the two groups of chelates. As pointed out by MILLER and WILKINS [14], the crystal environment of a molecule or ion should be of importance in modifying the position of absorption bands. The dihydrates of a number of divalent-metal 8-hydroxyquinolates have been shown to be isomorphous [15]. This isomorphism may or may not persist in the anhydrous compounds. It would be of considerable interest to have X-ray data for the latter.

In addition to the relationship shown in Fig. 2, a number of additional correlations were observed for the divalent transition-metal 8-hydroxyquinolates. More or less smooth curves were obtained for these chelates by plotting the 9-μ absorption peak against each of the quantities: atomic number, metal-ion electronegativity, second ionization potential of the metal, and the logarithm of the stability constant [16] for the chelate as determined in solution. All of these quantities are interrelated, and it is difficult to see which relationship may be the more fundamental. None of the simple relationships mentioned were found to fit the data for the trivalent-metal 8-hydroxyquinolates.

* The agreement of the points to two straight lines is not appreciably different if the logarithm of the 9-μ peak position is plotted against the atomic weight of the metal.

† The position of the point for the Co chelate is such that it could fall on either line. It is logical to assume, however, that it belongs with the points for the other transition metals.

VOL. 8 1956/5

An attempt was made to extend the relationships just described to the chelates of 2- and of 4-methyl-8-hydroxyquinoline. Insufficient data were obtained in both cases to establish whether the apparent division into two classes of chelates, as shown in Fig. 2, also exists for the methyl-substituted 8-hydroxyquinolates. In Fig. 3 the 9-μ peak positions for the chelates derived from these two reagents are plotted against the corresponding peak positions for the 8-hydroxyquinoline chelates. A satisfactory correlation is observed with the peak positions for the 2-methyl chelates, indicating that relationships observed for the 8-hydroxyquinoline chelates also apply to the chelates of the 2-methyl reagent.* The plot against the peak positions of the 4-methyl chelates in Fig. 3 is inconclusive. For the 4-methyl copper chelate the 9-μ peak is actually a doublet, although this is not apparent in the small spectrum shown in Fig. 1. The position of both components of this doublet have been plotted in Fig. 3. The possible difference in structure between the copper and nickel chelates as opposed to the other

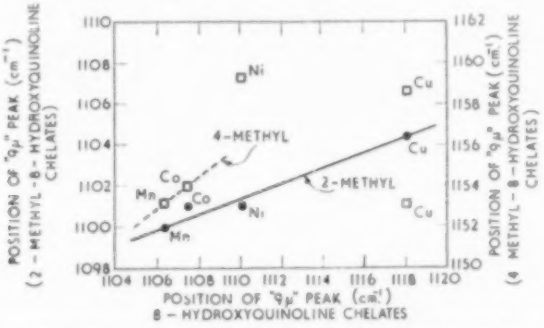

Fig. 3. Relationship between the position of the 9-μ absorption peak of transition-metal 8-hydroxyquinoline chelates and the position of the corresponding peaks for 2-methyl- and 4-methyl-8-hydroxyquinoline chelates.

4-methyl chelates studied has already been mentioned, and it may be responsible for the lack of agreement in Fig. 3. It is obvious from this figure that relationships of the type found for the 2-methyl and unsubstituted 8-hydroxyquinolates are much less satisfactory in the case of the 4-methyl compounds.

Acknowledgement—The authors are indebted to the Atomic Energy Commission for financial support of this work.

References

[1] Welcher, F. J.; *Organic Analytical Reagents*, D. Van Nostrand Co., Inc., New York, 1947.
[2] Lecomte, J.; *Disc. Faraday Soc.*, 1950, **9**, 125.
[3] Voter, R. C., Banks, C. V., Fassel, V. A., and Kehres, P. W.; *Anal. Chem.*, 1951, **23**, 1730.
[4] Bellamy, L. J., and Branch, R. F.; *J. Chem. Soc.*, 1954, 4491.
[5] Pariand, J., Fernelius, W. C., and Bryant, B. E.; *J. Org. Chem.*, 1954, **19**, 1889.
[6] Sen, D. N., Mizushima, S., Curran, C., and Quagliano, J. V.; *J. Amer. Chem. Soc.*, 1955, **77**, 211.

* The relationship between the 9-μ peak position and the stability constants for the 2-methyl-8-hydroxyquinolates [15] is, however, much less satisfactory than that for the chelates of 8-hydroxyquinoline itself. This would seem to imply that this sort of relationship is not as fundamental as the others mentioned.

[7] STONE, K. G.; *J. Amer. Chem. Soc.*, 1954, **76**, 4997.
[8] BELLAMY, L. J.; *The Infra-red Spectra of Complex Molecules*, John Wiley & Sons, Inc., New York, 1954.
[9] THOMPSON, H. W.; *J. Chem. Soc.*, 1948, 328.
[10] HUNT, J. M., WISHERD, M. P., and BONHAM, L. C.; *Anal. Chem.*, 1950, **22**, 1478.
[11] MARTELL, A. E., and CALVIN, M.; *Chemistry of the Metal Chelate Compounds*, Prentice-Hall, Inc., New York, 1952.
[12] MELLOR, D. P., and CRAIG, P.; *J. Roy. Soc. New S. Wales*, 1940, **74**, 475.
[13] SELWOOD, P. W., in *Annual Review of Physical Chemistry*, G. K. ROLLEFSON, Editor, Annual Reviews, Inc., 1953, p. 445.
[14] MILLER, F. A., and WILKINS, C. H.; *Anal. Chem.*, 1952, **24**, 1253.
[15] MERRIT, L. L.; *Anal. Chem.*, 1953, **25**, 718.
[16] JOHNSTON, W. D., and FREISER, H.; *J. Amer. Chem. Soc.*, 1952, **74**, 5239.

VOL.
8
1956/5

Spectrochimica Acta, 1956, Vol. 8, pp. 9 to 18. Pergamon Press Ltd., London

The infra-red absorption spectra of some hydroxypyrimidines

E. M. Tanner
Research Department, Parke, Davis & Co., Ltd. Hounslow, Middlesex, England

(*Received* 14 *March* 1956)

Abstract—The infra-red absorption spectra of some 2-substituted derivatives of 4:5- and 4:6-di- and 4:5:6-tri-hydroxypyrimidines and their 5-tetrahydropyranyl ethers have been examined from 3600 cm^{-1} to 650 cm^{-1}.

The spectra show evidence of the presence of both carbonyl and hydroxyl groups in the molecules. Bands between 2700 cm^{-1} and 2500 cm^{-1} are believed to be due to strongly bound hydroxyls. Except for the 5-ethers, the frequency of the carbonyl absorptions are very dependent on the nature of the substituents in the 2 position.

Tentative assignments suggest that the 4:6-dihydroxypyrimidines exist with one ketonic group and one enolic group, the 4:5-dihydroxypyrimidines possibly with a 4-ketonic and a 5-enolic group, and the 4:5:6-trihydroxypyrimidines as 4-keto-5:6-diols. These best represent the classes as a whole, but individual exceptions may occur with change of substituent at position 2.

Owing to their importance in nature, much work has been devoted to the structure of derivatives of pyrimidine, substituents round the pyrimidine ring being numbered as follows:

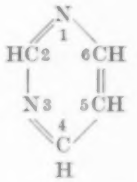

Recourse has been made to infra-red absorption spectroscopy for elucidation of the structure of important amino- and hydroxy-pyrimidines, but, unfortunately, the infra-red spectra themselves are somewhat ambiguous, and have been the subject of considerable discussion.

Brownlie [1], who examined the infra-red spectra of some di-, tri-, and tetra-substituted pyrimidines, all containing OH or NH_2 groups, indicated that his evidence supported the existence of these compounds in the imino and enolic forms, but simple pyrimidines containing nontautomeric substituents were not included in his work.

The fully enolic form was also accepted by Tipson and Cretcher [2] for dialuric acid monohydrate.

At the other extreme, Randall, Fowler, Fuson, and Dangl [3] have given the structures of alloxan monohydrate, barbituric acid, and uramil in the fully ketonic forms.

Thompson, Nicholson, and Short [4] and Short and Thompson [5] have recorded the infra-red spectra of a large number of pyrimidines, some of which were simple substitution products in which tautomerism could not occur, while

many were amino- and hydroxy-derivatives. After surveying all the data available, Short and Thompson [5] suggested that 2-hydroxy- and 4-hydroxy-pyrimidines would best be represented by a ketonic structure, and probably 2:4-dihydroxy-derivatives by a diketonic form, while in 4:6-dihydroxy-derivatives one ketonic and one enolic group might be present. They thought that, in general, amino-substituents exist in the nontautomerized form and have the character of an amido-group. Short and Thompson [5] have been careful to point out, however, that the tautomerism in amino- and hydroxy-pyrimidines may be influenced by the electronic effects of different substituent groups, and also by the quantitative degree of interaction through hydrogen bonding.

More recently, Brown and Short [6] have shown that 2- and 4-hydroxy-pyrimidines exist in the ketonic form, for, on comparing their spectra with those of 2- and 4-methoxypyrimidines for the region 1300–1800 cm^{-1}, they found each of the hydroxy-compounds had very strong absorption in the 1600–1700 cm^{-1} region, which had no counterpart in the spectra of the methoxy-compounds, and so must have been due to C=O stretching vibrations. Comparison of the spectra of 2- and 4-hydroxypyrimidines with their N-methyl derivatives has also led to a similar conclusion [7].

Brown and Short [6] also showed that, in dilute solution in carbon tetrachloride, 2- and 4-aminopyrimidines exist in the amino form, because each had two N—H stretching bands.

There are few infra-red absorption spectra of 5-hydroxy-substituted pyrimidines recorded in the literature, and that of dialuric acid [2] is, possibly, the sole exception.

The present work describes the spectra of some 2-substituted derivatives of 4:5- and 4:6-di- and 4:5:6-tri-hydroxypyrimidines. The 5-tetrahydropyranyl ethers, from which the 5-hydroxy-compounds were prepared, have also been examined. They may be formulated as:

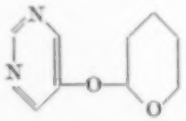

Experimental

All spectra were recorded on Nujol mulls of the solids, using a Grubb Parsons S3A infra-red spectrometer equipped with a sodium chloride prism.

The compounds examined were prepared by Davoll and Laney. Their preparation, purification, ultra-violet absorption spectra and *p*K values have been reported previously [8, 9].

Results

The wave-numbers of the band peaks of the hydroxypyrimidines examined are shown in Table 1. The peaks obscured by the Nujol bands have been omitted from the table. No description of the infra-red spectra of any of these compounds could be found in the literature, with the exception of dialuric acid (2:4:5:6-tetrahydroxypyrimidine monohydrate) [2] and 2-methyl-4:6-dihydroxypyrimidine [5], and their spectra are in substantial agreement with the literature.

VOL. 8 1956/5

The work described above has shown the complexity of the infra-red spectra of the simpler hydroxypyrimidines, and of the ambiguity encountered when structural correlations were attempted. It is not surprising, therefore, to find that the present series, containing in many cases fully substituted pyrimidine rings, have yielded even more complex spectra, with correspondingly greater difficulty in interpretation. It is very unfortunate that solution studies on these compounds were impossible owing to their insolubility in the solvents suitable for infra-red work. Examined as they were in the solid state, the spectra must be considerably modified by varying degrees of hydrogen bonding, and crystal lattice effects.

The high-frequency region

The region 3600–3000 cm^{-1}, where absorptions due to O—H and N—H stretching vibrations are found, is fairly complex in most of the compounds examined, and, in general, it is not easy to distinguish between OH and NH groups. If solution studies had been possible, differentiation would have been much simpler. Short and Thompson [5] have found a pair of bands near 3150 and 3350 cm^{-1} in monoaminopyrimidines. Similar absorptions are present in a number of the aminopyrimidines listed in Table 1, but in others they are obscured, probably by overlapping hydroxyl absorptions unresolved by a rocksalt prism.

An interesting band is found in many of the compounds in the region 2600–2700 cm^{-1}, normally regarded as a clear region of the spectrum. The band is very broad, and varies considerably in intensity from one compound to another. Brownlie [1] noticed similar bands in a few of his compounds, and attributed them to overtones. In position and appearance they resemble the bands due to the very strongly hydrogen-bonded hydroxyl groups found in carboxylic acids and β-diketones capable of enolization, and it is suggested that they may be caused by the extreme strength of the hydrogen bonds. Other physical properties such as the high melting-points and low solubilities of the compounds are also indicative of unusually strong hydrogen bonding. Recently, Willits, Decius, Dille, and Christensen [10] found similar bands near 2700 cm^{-1} in purine derivatives which they interpreted as due to hydrogen bonds of varying strengths. If the bands in question are due to strongly bonded hydroxyls, they should vanish in pyrimidines of similar type from which hydroxyl groups are definitely excluded. Such a compound, the only one of its type examined, is found in number 22 of Table 1. In this, there can be no question of the presence of an OH group, and, significantly, there is no band between 2700 and 2500 cm^{-1}. Three of the compounds, namely, 2-phenyl-4:6-dihydroxy-, 2-phenyl-4:6-dihydroxy-5-tetrahydropyranyl-2′-oxy-, and 2-methyl-4:6-dihydroxy-5-tetrahydropyranyl-2′-oxy-pyrimidine possess no bands at all in the normal OH or NH stretching region, but each has at least one band in the 2700–2500 cm^{-1} region. Reference will be made to these again in the section under Structure.

1600–1800 cm^{-1} region

The infra-red absorption bands expected in this region are those due to C=O stretching, to C=C and C=N vibrations of the pyrimidine ring, and to NH_2 deformation.

Table 1. Infra-red absorption bands of hydroxypyrimidines in cm^{-1}

Compound No.	1	2	3	4	5	6	7	8	9	10	11	12	13[a]
Substituents 2	CH_3	C_6H_5	NH_2	CH_3	CH_3	NH_2	NH_2	NH_2			CH_3	CH_3	C_6H_5
4	OH	OH	OH	OH	OH	OH	OH	OH	OH	OH	OH	OH	OH
5				OH	OR_2		OR_1	OR_2	OH	OR_1	OH	OR_1	OH
6	OH	OH	OH						OH	OH		OH	OH
	3060	—	3420 s 3110 s	G.A. 3100–3000	3550 3430 3290	3390 3110 br	3295 3060	3300 3060 br	3135 3065	3550 }br 3440 }cx	3490 }cx 3445 }	—	3600 (sharp) 3390 G.A. 3200–3000
	2605 s 2345 sh	2650 s 2355	2730 s 2530 2365	G.A. 2760–2250	—	2685 br	—	2730 w	2575 br 2050 w 1938 w	2590 1990 w	2590 br 1912 w	2570 br 1900 w	2760
	1892 1691 1636 s 1575 s	1839 w 1778 w 1615 s 1572 s 1517 s 1440	1825 w 1734 }cx 1687 } 1645 }e 1565 }	1665 s }d 1617 } 1577 w 1459 }s 1445 }d	1665 }a.d 1614 } 1575 }a.d 1561 }	1705 }e 1676 } 1658 }cx 1628 } 1579 w 1544 w 1496 w	1658 s 1619 1503 s	1653 s 1614 1518 }s 1506 }cx 1493 }	1825 w 1700 }a.d 1653 } 1550 }a.d 1521 } 1453	1645 s 1559 }d.s 1542 } 1398	1655 }s 1640 } 1622 }cx 1522 s 1421 1400	1650 sh 1628 s 1559 }a.d 1542 } 1398	1670 } 1650 } c 1622 } xs 1577 1487
	1351 1327 s 1298 1274 1213 1045 944 935 837 w 814 s 734 w 722 w 668 w	1360 1322 s 1271 w 1196 w 1154 w 964 954 sh }cx 932 866 w 797 s 777 w 725 686 s 671	1360 1321 s 1264 1226 }d 1212 } 1155 s 1100 1092 981 949 }d 932 } 844 792 777	1389 1332 1246 }s 1222 } 1201 }cx 1172 } 1032 988 918 sh 908 797 sh 788	1388 s 1360 1324 1291 w 1283 w 1262 w 1235 1205 s }cx 1185 1125 }d 1115 } 1052 }s 1042 } 1024 }cx 982 948 s 913 }s.d 907 } 885 }s.d 874 } 822 793 w 777 744	1242 }d 1226 } 1189 1105 sh 1047 br 1002 977 917 w 843 w 820 764 w 754	1322 w 1300 1287 w 1235 1204 1184 1121 1104 }d 1074 w 1050 1037 1019 959 918 885 w 871 858 w 827 w 813 789 751 725 694	1240 }d 1219 } 1172 w 1138 1080 1008 987 }cx 972 } 982 892 w 862 }d 851 } 813 w 801 w 787 774 w 750 s 732 sh 700	1386 s 1303 }d 1287 } 1233 s 1157 1043 }d 934 } 915 }d 891 } 747 731	1362 1344 sh 1306 }d 1296 } 1251 s 1204 1183 w 1163 1118 }d 1108 } 1055 1047 }cx 1035 } 1024 939 s 914 }s 907 }d 868 816 781 766 749 }w 741 }d	1302 s 1199 1107 w 1041 992 942 793 w 752	1341 } 1306 }cx 1289 w 1259 w 1202 }d 1179 } 1121 }d 1108 s } 1046 } 1037 } 1017 951 909 881 w 869 831 w 817 w 807 w 772 w 759	1309 1265 1229 1164 w 1118 w 1076 964 w 942 w 917 }d 907 } 847 w 825 w 776 759 w 747 696 686

VOL. 8 1956/57

Table 1. (*contd.*)

Compound No.	14	15	16[3]	17[1]	18	19	20[1]	21	22	23[3]	24	25
Substituents 2	C_6H_5	H8	NH_2	NH_2	NH_2	NH_2	NH_2	NH_2	NH_2	OH	OH	OH
4	OH	OH	OH	OH	OH	OH	NH_2	NH_2	NH_2	OH	NH_2	NH_2
5	OR_1	OH	OH	CH_2OH	OR_1	OR_1	OH	OR_1	OR_1	OH	OH	OR_1
6	OH	OH	OH		OH	CH_2OR_1		OH	CH_2OR_1			OH
	—	3420 br 3040 br	G.A. 3600–3020	3295 G.A. 3270–3000	3520 (sharp) 3370 3090 br	3352 (sharp) 3070	3430 (sharp) 3350 G.A. 3200–3000	3320 3135 3060	3255 }cx 3155 }	G.A. 3600–3000	3440 (sharp) 3320 3155	3580 3490 3335 3120 br
	2620	2375 w	2730 2050	2605	2610 br	2740	2680	2725	—	G.A.	2490 w 2075 w	—
	1650 }cx 1635 }s 1620 } 1591 s 1540 1521 }d.s 1510 } 1431	1679 }cx 1655 }s 1622 } 1583 s	1738 } 1702 }cx 1682 } 1654 }s 1636 } 1622 } 1540 1509	1700 } 1689 }cx 1679 } 1660 }s 1643 } 1515 }d 1508 }	1676 1653 s 1614 }cx 1594 1581 1538 }d 1523 }	1655 s 1557 1545 sh 1495	1700 }cx 1655 }s 1579 1545 s 1497	1655 }cx 1640 }s 1614 } 1560 s 1498 w 1493 w	1667 sh 1658 1561 s 1540 }d.s 1520 } 1408	1746 sh }s 1700 } 1654 }cx 1600 1420	1700 s 1650 sh }cx 1635 } 1587 }cx 1520 } 1393 s	1698 s 1682 s 1651 s } 1622 s }cx 1596 } 1576 } 1520 } 1405
	1312 1291 sh 1261 w 1212 }d 1204 }s 1182 1161 w 1132 }cx 1103 }s 1092 } 1047 sh 1037 1018 949 s 924 w 903 s 880 871 841 w 822 813 sh 779 w 766 }d 755 } 714 w 689 br	1347 1305 1242 s 1190 1148 1110 w 983 w 879 783 745 661 w	1275 br 1221 1152 1055 w 936 w 892 w	1256 }cx 1224 } 1133 1083 1055 1032 989 w 974 870 812 708 w	1310 1277 1256 w 1246 1199 1178 1144 w 1125 }w 1118 }d 1062 1034 s 972 w 940 900 879 845 w 814 w 758 699 w	1351 1315 1275 w 1245 }d 1232 } 1205 1180 1150 1132 1118 1102 1065 1058 sh 1039 }d 1023 } 1007 w 991 980 }cx 966 } 939 903 885 870 847 816 784 743 w 734 w	1253 }d 1237 } 1176 w 1145 1064 } 1047 }cx 1015 } 967 865 w 808 }cx 792 } 742 722	1315 1274 1256 w 1229 1206 1193 w 1166 w 1160 w 1144 1125 w 1113 w 1093 w 1065 1037 }d 1021 } 977 w 942 902 878 br 848 w 811 770	1322 1300 w 1281 w 1268 1199 }d 1185 } 1128 s 1083 s 1034 }cx 1022 }s 1012 } 978 w 944 s 903 869 816 720 w	1367 w 1339 w 1312 s 1254 w 1238 s 1164 w 1122 w 861 825 s 756 s 739 722 w 712 w	1336 1288 w 1214 1110 w 1076 980 }cx 936 } 813 s 802 sh 740 }d 735 }	1355 1315 w 1283 w 1245 1203 1182 w 1155 1114 1100 1073 1045 1034 }cx 1023 } 946 912 879 w 843 815 802 758 w 751

Key to Table 1:

R_1 = Tetrahydropyranyl-2′-. R_2 = Benzyl-.

1. As sulphate. $\frac{1}{2}H_2SO_4$
2. As hydrate. $\frac{1}{2}H_2O$
3. As hydrate. $1H_2O$

br. Broad band.
cx. Complex band.
d. Doublet.
G. A. General absorption.
s. Strong.
sh. Shoulder.
w. Weak.

Short and Thompson [5] have shown that simple nontautomeric derivatives of pyrimidine give a strong band in the region 1520–1580 cm^{-1}, which they have assigned to a ring vibration, but the region above 1620 cm^{-1} is clear. It seems, then, that vibrations due to the fully aromatic pyrimidine ring will not appear above 1620 cm^{-1}. However, in systems in which tautomerism can occur, the aromatic nature of the pyrimidine may be lost, the double bonds then being more localized in C=C and C=N vibrations which could give rise to absorption between 1600 and 1670 cm^{-1}. Complications arise in amino-substituted pyrimidines owing to the NH_2 deformation frequency which occurs in this region. Short and Thompson [5] have found a strong band near 1650 cm^{-1} in all their monoaminopyrimidines, which they have assigned to the NH_2 deformation.

In the compounds examined, the 1600–1750 cm^{-1} region contains a very broad and intense band with, in many cases, several submaxima. It is obviously a very complex absorption, the resultant of a number of bands which are only partially resolved. With one or two exceptions, the compounds appear to fall into two groups:

(a) Those in which the band of highest frequency lies around 1700 cm^{-1} or higher.

(b) Those in which the band of highest frequency lies between 1650 and 1680 cm^{-1}.

The compounds in group (a) must contain at least one carbonyl group, as it is very unlikely that strong bands having frequencies of 1700 cm^{-1} or higher would be produced by anything other than C=O stretching modes. The compounds in group (b) are less easy to interpret. Amide-type carbonyls would be expected to absorb in this region, but so also do NH_2 deformation vibrations. In compounds free of amino-group substituents, the bands are probably due to carbonyls, as their intensity, alone, makes them unlikely to be due to ring vibrations.

VOL. 8 1956/5

Structure of hydroxypyrimidines

A. 4:6-*Dihydroxypyrimidines*

The difficulty of interpreting the structure of the amino- and hydroxy-pyrimidines has been stressed by earlier workers [1, 4, 5]. Short and Thompson [5] found the evidence confusing, but they suggested that in 4:6-dihydroxypyrimidines one ketonic and one enolic group might be present, although the tautomerism could, possibly, be influenced by the electronic effects of different substituent groups. The three 4:6-dihydroxypyrimidines examined, compounds 1–3, show a wide variation in the frequency of the strong bands in the carbonyl region. Whereas the band of highest frequency in this region is at 1734 cm^{-1} in 2-amino-4:6-dihydroxypyrimidine, the corresponding band for the 2-methyl analogue is at 1691 cm^{-1}, whilst in the case of 2-phenyl-4:6-dihydroxypyrimidine there is no strong band in the region above 1615 cm^{-1}. This suggests that the 2-amino and 2-methyl derivatives contain at least one C=O group, while it is doubtful whether 2-phenyl-4:6-dihydroxypyrimidine possesses a carbonyl at all. It might be that, in the 2-phenyl derivative, an effect is operative similar to that in β-diketones capable of enolization, in which the carbonyl band is shifted into the range 1640–1540 cm^{-1} by chelation [11]. Some support is found for this structure in that

no bands are found in the normal OH and NH stretching region, but there is a strong band at 2650 cm^{-1} which, again, resembles that in β-diketones. 2-Amino-4:6-dihydroxypyrimidine also shows a strong band at 2730 cm^{-1} and, in addition, bands at 3420 cm^{-1} and 3110 cm^{-1}. The last two, presumably due to the amino-group, could mask other OH or NH absorptions, as the resolution of a rock-salt prism is poor in this region.

It is suggested, then, that 2-methyl- and 2-amino-4:6-dihydroxypyrimidine each contain one ketonic and one enolic group, in agreement with the work of SHORT and THOMPSON [5], and that the whole system, in each case, is involved in unusually strong hydrogen bonding. The structure of 2-phenyl-4:6-dihydroxy-pyrimidine is more doubtful, although a similar system is not excluded.

Table 2. 4.6-Dihydroxypyrimidines.

2-Substituent	Highest-frequency band in double-bond region (cm^{-1})
C_6H_5	1615
H [5]	1681
CH_3	1691
NH_2	1734
OH [5]	ca. 1750

The nature of the substituents in the 2 position evidently exerts a profound effect upon the carbonyl-stretching frequency of the 4:6-dihydroxypyrimidines, as can be seen from the series in Table 2, showing the gradual increase of frequency of the highest-frequency band in the double-bond region with different substituents in the 2 position.

It may be significant that the frequency increases with increase in electron-donating power of the 2 substituent.

B. 4:5-*Dihydroxypyrimidines*

The 4:5-dihydroxypyrimidines and their 5-ethers, compounds 4-8, are fairly similar in the double-bond region, with the exception of compound 6, 2-amino-4:5-dihydroxypyrimidine, which has absorption at a higher frequency than the rest.

2-Methyl-4:5-dihydroxypyrimidine and its 5-tetrahydropyranyl ether correspond in the double-bond region, an indication that the 5-hydroxyl is in the enolic form. The assignment of the 4-hydroxyl is more difficult, although the similarity of the spectra infers that both compounds exist in the same form. The intensity of the bands at 1665 cm^{-1} suggests that they are due to carbonyls. However, complications arise in the high-frequency region, because the 5-ether shows three bands, at 3500, 3430, and 3290 cm^{-1}, the first two of which are more likely to be due to OH than NH.

2-Amino-4:5-dihydroxypyrimidine differs from both its 5-tetrahydropyranyl ether and its 5-benzyl ether in having its absorption in the carbonyl region extended from ca. 1655 cm^{-1} in the ethers, to 1705 cm^{-1}. Although this certainly

indicates the presence of a carbonyl group, it does not necessarily infer that the 5 position is ketonic. Even in the 4:6-dihydroxy compounds, in which the 5 position is unsubstituted, in the 2-amino-derivative the carbonyl frequency is raised to a value, (1734 cm^{-1}), which is high for a C=O group adjacent to nitrogen in a 6-membered ring. Hence in 2-amino-4:5-dihydroxypyrimidine, the carbonyl may equally well be in the 4 position. The two 5-ethers, compounds 7 and 8, are very similar and show no absorption in the high-frequency region which could, apparently, be accounted as OH, although the NH_2 bands obscure a good deal of the region. There is no absorption in the 2700–2500 cm^{-1} region in the 5-tetrahydropyranyl ether, and only a weak band at 2730 cm^{-1} in the 5-benzyl ether. The possibility that the bands at 1658 cm^{-1} (compound 7) and 1653 cm^{-1} (compound 8) are carbonyls is, therefore, upheld. It is interesting to note that the compounds 17 and 19 behave in a similar manner. These compounds resemble, respectively, 2-amino-4:5-dihydroxypyrimidine and its 5-ethers, but have position 6 occupied by groups incapable of tautomerism.

Although the infra-red evidence is not without ambiguity, the balance seems to favour a 4-keto-5-enol form for the 4:5-dihydroxypyrimidines. The ultraviolet absorption data [9] tend to favour this assignment.

C. 4:5:6-*Trihydroxypyrimidines.*

The spectra of the trihydroxypyrimidines are necessarily even more complex than those of the dihydroxy derivatives.

In the carbonyl region, all of the 5-ethers of the 4:5:6-trihydroxypyrimidines are similar, and have their highest frequency band in the neighbourhood of 1650 cm^{-1} or a little higher, regardless of the nature of the substituent at position 2. In this respect they resemble the 4:5-dihydroxypyrimidine 5-ethers, and differ from the 4:6-dihydroxypyrimidines unsubstituted at position 5, whose carbonyl frequencies are very dependent on the nature of the substituent at position 2. Since most of the 4:5:6-trihydroxy-5-ethers examined had no amino-group substituents, the strong bands at ca. 1650 cm^{-1} cannot be NH_2 deformation frequencies, and are most probably carbonyl vibrations. The high-frequency region shows some evidence of OH groups. It is true that the 2-methyl and 2-phenyl derivatives show no absorption at all in the 3600–3000 cm^{-1} region, but they both absorb in the 2700–2600 cm^{-1} region. It could be, then, that the 4:5:6-trihydroxy-5-ethers possess one carbonyl and one hydroxyl group, and are in this way similar to the 4:6-dihydroxypyrimidines.

If the 5-ether groups are replaced by hydroxyl groups to give compounds such as 9, 11, 13, 15, 16, and 23 in Table 1, the values of the highest-frequency bands in the double-bond region change from their fairly constant value of 1650 cm^{-1}, and again become dependent on the substituent group at position 2. In the 4:5:6:trihydroxypyrimidines, the highest-frequency bands in the double-bond region range from 1655 to 1746 cm^{-1}, the highest frequencies being given by the 2-amino (1738 cm^{-1}) and 2-"hydroxy" (1746 cm^{-1}) derivatives. The 2-methyl- and 2-phenyl-4:5:6-trihydroxypyrimidines are only slightly different from their 5-tetrahydropyranyl ethers in the double-bond region, and the 3600–3000 cm^{-1} region now shows bands which were absent from the 5-ethers. It

VOL. 8 1956/5

appears, then, that the 5-hydroxyl in the 2-methyl and 2-phenyl derivatives exists in the enolic form.

Although the 5-ether was not examined, the hydroxyl groups of compound 15 probably form a similar structure, because the carbonyl region is so similar to those of compounds 11 and 13 in Table 1. However, the SH linking is not observed in its normal position of 2600–2550 cm^{-1}. There is no strong general absorption in this particular compound to mask the band, and it is concluded that the thioketone structure must be present.

At first glance it might appear that 4:5:6-trihydroxypyrimidine and its 2-amino-derivative exist in the 5-keto form because they differ in the carbonyl region from their 5-ethers. This is not necessarily true, because, in similar compounds unsubstituted at position 5, namely the 4:6-dihydroxypyrimidines discussed in Section A, the values of the highest-frequency bands in the carbonyl region have an even wider range (1615–1750 cm^{-1}) than the trihydroxypyrimidines. It merely means that the frequency of a C=O link next to a ring nitrogen can be considerably modified by the joint effects of the 2- and 5-position substituents.

2:4:5:6-Tetrahydroxypyrimidine (dialuric acid), compound 23, has a carbonyl-region spectrum similar to 2:4:6-trihydroxypyrimidine [5], and it is therefore unlikely that the former contains any additional C=O groups. Hence it is probable that the 5-position hydroxyl in dialuric acid is in the enolic form.

There is, therefore, a certain amount of infra-red evidence to suggest that some, if not all, of the 4:5:6-trihydroxypyrimidines exist in the 4-keto-5:6-diol form. There is also considerable chemical and ultra-violet absorption evidence supporting this view [8].

D. *Miscellaneous Aminohydroxypyrimidines*

So far, the only aminohydroxypyrimidines discussed have had the amino-group in the 2 position. A few compounds with the amino-group in the 4 position have also been examined.

In the carbonyl region, no absorption can be seen in the spectrum of 4-amino-2:5:6-trihydroxypyrimidine which is additional to that of its 5-tetrahydropyranyl ether, an indication that in the former the 5 substituent is hydroxylic. The strong bands, in both compounds, around 1700 cm^{-1} signify that either the 2- or the 6-position substituent must be ketonic. It is unlikely that both are ketonic, as the structure CO—NH—CO usually gives rise to absorption at considerably higher frequencies than 1700 cm^{-1} [12] and, in addition, the 3580-cm^{-1} band in the 5-tetrahydropyranyl ether is more likely to be due to an OH- than a NH-stretching frequency.

Of the 2:4-diaminopyrimidines, compound 22 contains no hydroxyl groups. The band of medium intensity near 1660 cm^{-1} is presumably due to an NH_2 bending mode. Compound 21 is so similar in the carbonyl region that it might appear that the hydroxyl in position 6 exists as such. Additional evidence is found in the appearance of three bands instead of two in the region 3320–3060 cm^{-1}. However, the intensity of the 1655-cm^{-1} band in compound 21 is greater that that of the 1660-cm^{-1} band in compound 22, and so the keto-form might be present. It has already been mentioned in an earlier section that the fact that the NH_2 deformation frequency can occur in the same region as the amide carbonyl causes confusion.

Conclusions

The infra-red absorption spectra of the hydroxypyrimidines show unusually strong hydrogen bonding, and bands in many of the compounds between 2700 cm^{-1} and 2500 cm^{-1} are believed to be due to strongly bonded hydroxyl groups.

The compounds fall roughly into two main classes, (a) those in which absorption occurs in the C=O stretching region at ca. 1700 cm^{-1} or higher, and (b) those in which the highest frequency in this region lies below 1680 cm^{-1}. Those in class (a) contain C=O groups, while those in class (b) may contain C=O groups, but their detection is more difficult.

The highest-frequency band in the double-bond region in the 5-tetrahydropyranyl ethers is fairly constant, and lies around 1650 cm^{-1} or a little above, and is independent of the nature of the substituent at position 2. If, however, the 5 position is unsubstituted or contains a hydroxyl group, the peak of highest frequency in the double bond region varies over a wide range, i.e. from 1615 cm^{-1} to 1746 cm^{-1} for the compounds examined, depending on the substituent at position 2. The highest frequencies for these bands are found in 2-amino and 2-"hydroxy" derivatives.

In general, there is evidence to show that the 5-hydroxyl group exists as such. While there may be individual exceptions, tentative assignments indicate that the 4:6-dihydroxypyrimidines are best represented by one ketonic and one enolic group, in agreement with the work of SHORT and THOMPSON [5], the 4:5-dihydroxypyrimidines probably as 4-keto-5-enol systems and the 4:5:6-trihydroxypyrimidines possibly as 4-keto-5:6-diols. Chemical and ultra-violet-absorption data offer additional evidence for these structures [8, 9]. However, it must again be emphasized that the infra-red evidence is frequently ambiguous owing to the fact that the compounds had to be examined in the solid state, and the structures suggested are believed to be the most suitable for the three classes of hydroxypyrimidines as a whole. Individual exceptions with different substituents may very well occur.

Acknowledgement—The author is indebted to Dr. J. DAVOLL for many helpful discussions.

References

[1] BROWNLIE, I. A.; *J. Chem. Soc.* 1950 3062.
[2] TIPSON, R. S., and CRETCHER, L. H.; *J. Org. Chem.* 1951 **16** 1091.
[3] RANDALL, H. M., FOWLER, R. G., FUSON, N., and DANGL, J. R.; *Infra-red Determination of Organic Structures*, D. Van Nostrand Co., 1949.
[4] THOMPSON, H. W., NICHOLSON, D. L. and SHORT, L., N.; *Disc. Faraday Soc.* 1950 233.
[5] SHORT, L. N., and THOMPSON, H. W.; *J. Chem. Soc.* 1952 168.
[6] BROWN, D. J., and SHORT, L. N.; *J. Chem. Soc.* 1953 331.
[7] BROWN, D. J., HOERGER, E., and MASON, S. F.; *J. Chem. Soc.* 1955 211.
[8] BOWMAN, R. E., and DAVOLL, J.; *Chem. and Ind.* 1956 138.
[9] DAVOLL, J., and LANEY, D. H.; *J. Chem. Soc.* In the press.
[10] WILLITS, C. H., DECIUS, J. C., DILLE, K. L., and CHRISTENSEN, B. E.; *J. Amer. Chem. Soc.* 1955 **77** 2569.
[11] BELLAMY, L. J.; *The Infra-red Spectra of Complex Molecules*, page 123. Methuen & Co. Ltd., London, 1954.
[12] BELLAMY. L. J.,; *Ibid.* page 190.

VOL. 8 1956/5

Spectrochimica Acta, 1956, Vol. 8, pp. 19 to 26. Pergamon Press Ltd., London

Vibration spectra of crystals*

C. Haas
Laboratory for General and Inorganic Chemistry of the University of Amsterdam, the Netherlands.

Abstract—A review of some experiments is given which shows that the assumption, that one vibration in a crystal gives rise to extrema in infra-red absorption, reflection, and emission spectra at the frequency of the corresponding Raman shift, is a too simple one. Especially for vibrations, which are very active in absorption, anomalies, such as frequency shifts and very broad reflection bands, appear. These effects are explained by the classical dispersion theory.

1. Introduction

There are several ways of obtaining information about the vibrations of crystals. The most important are the optical methods: infra-red absorption, reflection and emission spectra, and Raman spectra.

The most simple interpretation of these spectra is to assume that a vibration of frequency ω_0 gives rise to extrema in the absorption, reflection, and emission spectra, while the corresponding Raman spectrum consists of lines at a frequency $\omega \pm \omega_0$ (ω is the frequency of the exciting radiation).

Though this appears to hold at first approximation for most vibrations, experimental results have shown that for some vibrations the phenomena are much more complicated. In this article we will first discuss some of the experimental work, and then try to explain the apparent anomalies by the classical dispersion theory.

2. Review of experimental results

(a) Zincblende (ZnS), having a simple cubic lattice, cannot have more than one optically active vibration. The Raman spectrum of this crystal, however, consists of two lines at 274 and 349 cm^{-1} [1]. The infra-red reflection spectrum shows a broad band with a maximum at about 300 cm^{-1} [2].

(b) The Raman spectrum of different uniaxial crystals has been measured: if the orientation of the crystal in the mounting was varied, the frequency of some lines changed. For example, the frequency of a Raman line of quartz varied from 776 to 784 cm^{-1} [3].

(c) From crystals of sodium nitrate (which is a uniaxial crystal), plates making different angles φ with the crystal axis can be obtained. Reflection spectra of these plates were measured, using polarized light falling normally on the plate; these spectra show a reflection band in the 7-μregion. For light, polarized in the plane of the crystal axis and the normal on the plate (extraordinary ray), the position and shape of the band strongly varies with the angle φ [4], contrary to the behaviour of the ordinary ray.

* Presented at the Meeting of the European Molecular Spectroscopy Group, Oxford, July 1955. This work is part of the research programme of the "Stichting voor Fundamenteel Onderzoek der Materie" (Foundation for Fundamental Research of Matter—F.O.M.), and was made possible by financial support from the "Nederlandse Organisatie voor Zuiver-Wetenschappelijk Onderzoek" (Netherlands Organization for Pure Research—Z.W.O.).

The results are shown in Fig. 1; similar effects were found for other non-cubic crystals [5].

(d) Emission spectra of these crystal plates, heated at 270°C, were determined. The emitted light was analysed by a polarizer. The emission coefficient, defined as the emission of the crystal, divided by the emission of an ideal black body of

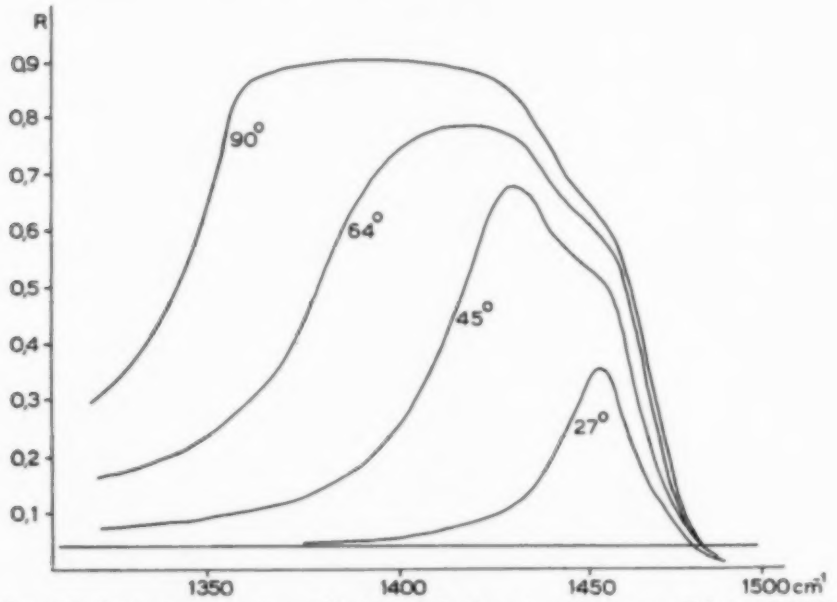

Fig. 1. Reflection spectrum (normal incidence) for the extraordinary ray of plates of $NaNO_3$, making different angles with the crystal axis.

the same temperature, has a minimum at about 1400 cm^{-1}. The curves for the extraordinary ray, which are represented in Fig. 2, show a behaviour similar to that of the reflection: the position and the shape of the band depend on the orientation of the surface of the plate with respect to the crystal axis [6].

We see that in all these cases one fundamental vibration gives rise to complex phenomena which are certainly not consistent with the simple concept given in Section 1. The anomalies only appear for those vibrations which are associated with a very strongly varying electric dipole moment, i.e., those vibrations which are strongly active in the infra-red. This suggests that the electric dipole itself causes the anomalies.

3. Dispersion theory of cubic crystals

The fact that the electric interaction of the vibrating dipoles was the origin of these phenomena was recognized by H. Poulet *et al.* immediately after the discovery of the anomalies in the Raman spectrum [7]. His theory, however, could not explain adequately the shift of the reflection band in uniaxial crystals which was found later. We shall show that the classical dispersion theory explains all anomalies and establishes the correct relation between infra-red and Raman spectra of crystals.

VOL. 8 1956/5

We assume that in the crystal, harmonic oscillators of mass m, charge e, and frequency ω_0 are present. These oscillators give rise to electromagnetic waves, which can be described by the polarization $\boldsymbol{P}$ (dipole moment per cm³): $\boldsymbol{P} = \boldsymbol{P}_0 e^{-i(\boldsymbol{K}r+\omega t)}$; $\boldsymbol{K}$ is a wave vector of length $2\pi/\lambda$ pointing in the direction of propagation of the wave of wavelength λ, ω is the circular frequency. According

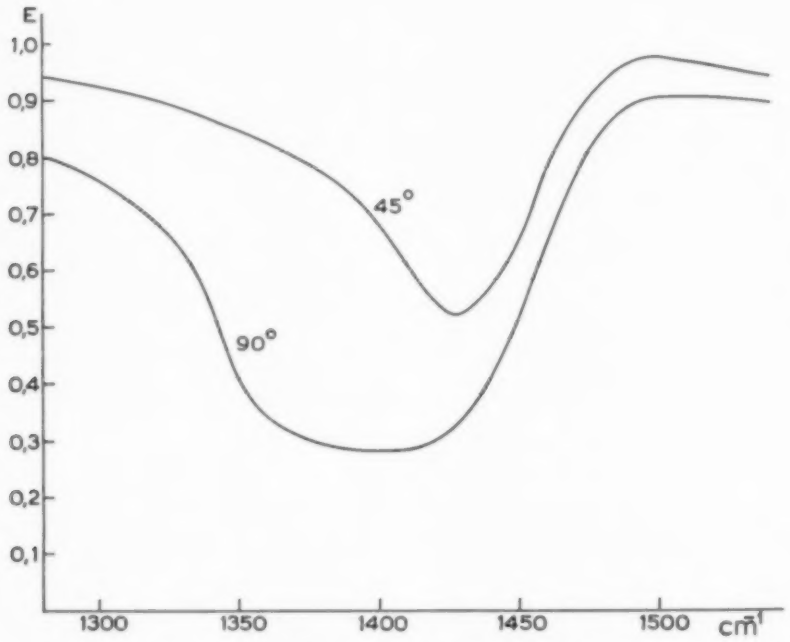

Fig. 2. Emission spectrum for the extraordinary ray of plates of $NaNO_3$ at 260°, making different angles with the crystal axis.

to the dispersion theory, developed by HUANG [9], there exist in cubic crystals two types of waves:

(a) longitudinal waves, where the vibrating dipole is parallel to the direction of propagation: $\boldsymbol{P}//\boldsymbol{K}$.

The frequency of these waves is independent of the wavelength, and is given by $\omega_l^2 = \omega_0^2 + \dfrac{4\pi A e^2}{m n_0^2}$, where A and n_0 represent respectively the number of oscillators per cm³, and the (normal) index of refraction extrapolated from higher frequencies.

(b) transverse waves: $\boldsymbol{P} \perp \boldsymbol{K}$. The frequency of these waves depends on the wavelength; the relation between λ and ω is:

$$\left(\frac{2\pi c}{\lambda\omega}\right)^2 = n_0^2 + \frac{4\pi A e^2}{m(\omega_0^2 - \omega^2)}.$$

The quantity $2\pi c/\lambda\omega$ is usually called the complex refractive index N for

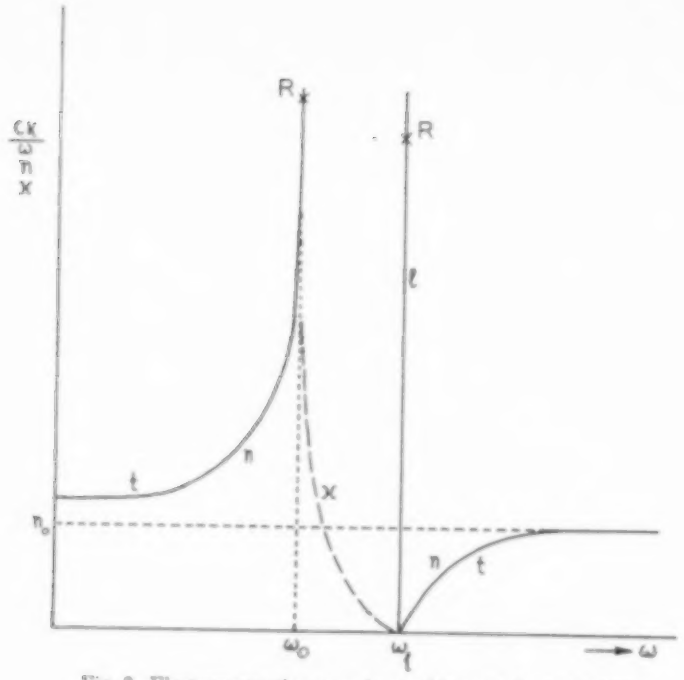

Fig. 3. Electromagnetic waves in a cubic crystal, containing undamped harmonic oscillators of frequency ω_0.

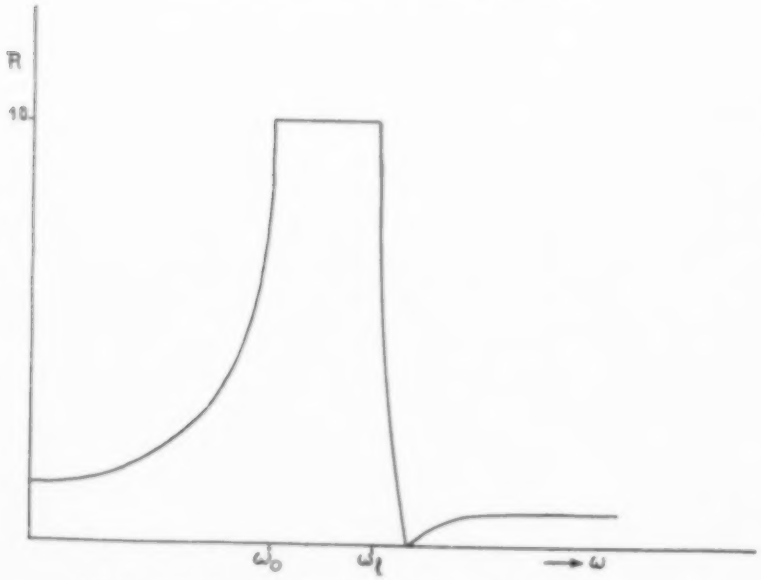

Fig. 4. Reflection coefficient for a cubic crystal, containing undamped harmonic oscillators of frequency ω_0.

VOL.
8
1956/5

transverse waves. The refractive index n and the absorption index κ are respectively the real and the imaginary part of N:

$$\frac{2\pi c}{\lambda\omega} = N = n - i\kappa.$$

In Fig. 3 the quantities ck/ω, n, and κ are given for transverse (t) and longitudinal waves (l) in a cubic crystal with simple harmonic oscillators.

The reflection coefficient R for transverse waves, falling normally on the crystal plane, can readily be calculated from $R = \dfrac{(n-1)^2 + \kappa^2}{(n+1)^2 + \kappa^2}$. The curve of R, corresponding to Fig. 3, is shown in Fig. 4.

If we measure the emission of a crystal plate, thick enough to prevent transmission, the emission coefficient will, according to KIRCHHOFF's law, be given by $E = 1 - R$, if R is the reflection coefficient at the same temperature. Thus the emission curve will show a minimum at the frequency where the reflection has a maximum.

Between ω_0 and ω_l, $\dfrac{2\pi c}{\lambda\omega}$ becomes imaginary, and waves with these frequencies will have the form $\boldsymbol{P} = \boldsymbol{P}_0 e^{-\omega\kappa r/c} e^{i\omega t}$. These waves are strongly damped, and will penetrate the crystal only over a small distance. The region between ω_0 and ω_l corresponds to a forbidden zone in the crystal; waves with these frequencies are not possible in the crystal. Therefore waves with a frequency between ω_0 and ω_l will be totally reflected, and cannot be emitted by the crystal. This causes the maximum in the reflection curve and the minimum in the emission curve.

The range of the frequency interval is directly determined by the electric dipole moment of the oscillator: the phenomena described above will be prominent for vibrations which are strongly active in the infra-red.

Raman spectra of crystals [7] are produced by a scattering of the primary radiation (wave vector $\boldsymbol{K}_1$, frequency ω_1) by a wave ($\boldsymbol{K}$, ω) in the crystal; the result is a wave ($\boldsymbol{K}_1 + \boldsymbol{K}$, $\omega_1 + \omega$) which is observed.

The Raman spectrum is usually observed under the following conditions: (a) the scattered light is observed in a direction perpendicular to that of the primary radiation: $\boldsymbol{K}_1 \perp \boldsymbol{K} + \boldsymbol{K}_1$; (b) the frequency ω_1 is much larger than ω; (c) the crystal does not absorb light of frequency ω_1, hence $cK_1/\omega_1 = n_0$.

These conditions lead to $K = \dfrac{n_0\omega_1}{c}\sqrt{2}$; only waves with this wave vector can produce the observed Raman scattering. Because $\omega_1 \gg \omega_0$, the quantity $\dfrac{2\pi c}{\lambda\omega} = \dfrac{cK}{\omega} = \dfrac{n_0\omega_1}{\omega}\sqrt{2}$ for these waves is much larger than 1. According to Fig. 3, waves with a large value of cK/ω (indicated by R in Fig. 3) will have frequencies ω_l and (approximately) ω_0. Therefore Raman scattering in the crystal will be due to transverse waves of the frequency ω_0 and longitudinal waves of frequency ω_l. The Raman spectrum of a cubic crystal, only containing one kind of harmonic oscillator, will consist of two lines with the frequencies ω_0 and ω_l. These frequencies just form the limits of the infra-red reflection and emission band.

4. Uniaxial crystals

For uniaxial crystals the phenomena become more complicated. An extension of the theory [4] given above shows that the relation of ω and λ for transverse waves depends on the polarization of the wave in the crystal. The results for a

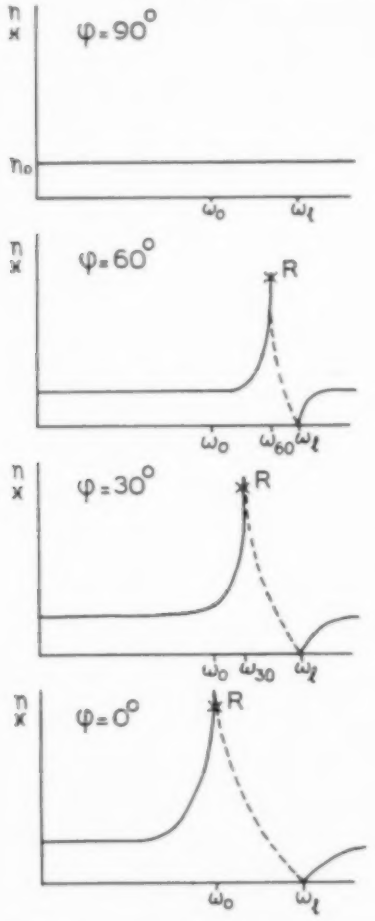

Fig. 5. Transverse waves (extraordinary ray) in a uniaxial crystal, containing harmonic oscillators with a dipole moment perpendicular to the crystal axis, for different directions of propagation $\boldsymbol{K}$ (φ = angle between $\boldsymbol{K}$ and the crystal axis).

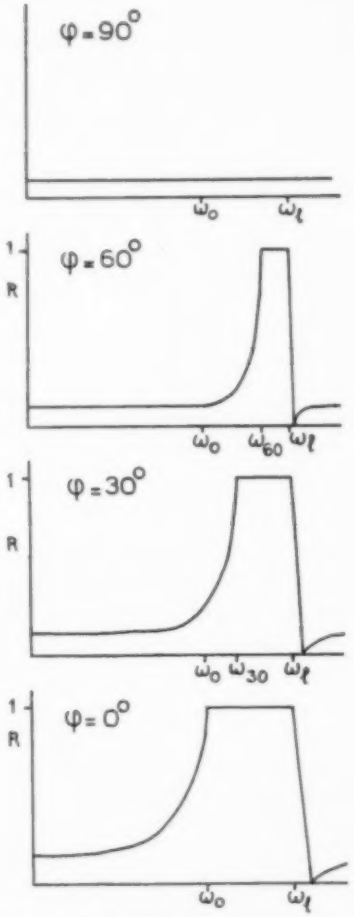

Fig. 6. Reflection curves corresponding to Fig. 5.

uniaxial crystal, containing harmonic oscillators with an electric dipole moment perpendicular to the crystal axis, are given in Fig. 5; the corresponding reflection curves are represented in Fig. 6. We notice that the width and position of the reflection band changes if the orientation of the crystal surface with respect to the crystal is varied. The emission coefficient $E = 1 - R$ for thick plates will

VOL.
8
1956/5

obviously show a similar behaviour. The Raman frequency ω_0, indicated by R in Fig. 5, varies between ω_0 and ω_l if the orientation of the crystal in the mounting is varied.

5. Damping

In the foregoing sections we used the model of undamped harmonic oscillators. Because of coupling with lattice vibrations, etc., the vibrations are damped and the introduction of a small damping constant gives results which are more consistent with the experimental data. In Fig. 7 the reflection coefficient and the

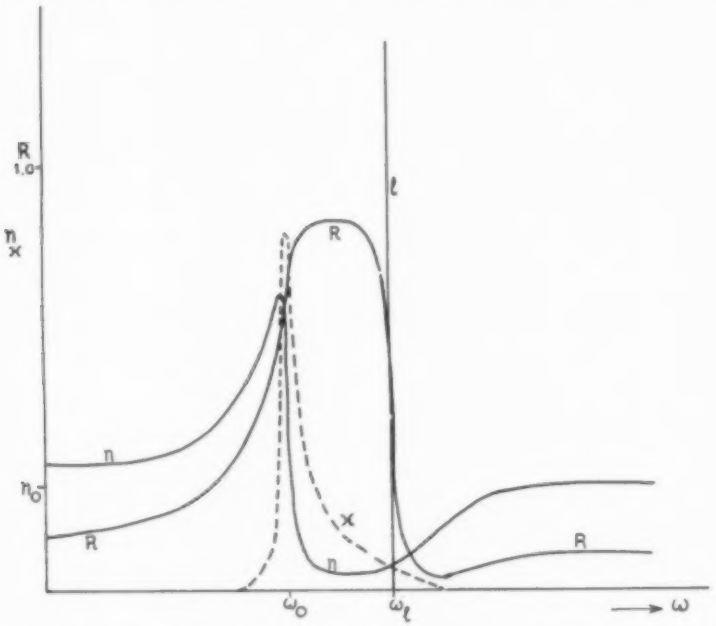

Fig. 7. Reflection coefficient and indexes of absorption and refraction for a cubic crystal, containing damped harmonic oscillators.

indexes of absorption and reflection for a cubic crystal, containing damped harmonic oscillators, are shown. We see that there does not exist a region of total reflection any more, but the spectrum still shows a broad reflection band between ω_0 and ω_l. Analogous changes appear in the reflection spectra of uniaxial crystals. The curves are slightly modified by the introduction of a small damping, but they remain essentially the same.

6. Discussion

The above theory explains all experimental data given in Section 2. From the reflection band of ZnS, Raman frequencies could be calculated which were in good agreement with the experimental values [10]. Calculation showed that the shift of the reflection band in sodium nitrate (Fig. 1) could be explained quantitatively [4]. The relation $E = 1 - R$ was confirmed for sodium nitrate and calcite [6].

Resuming, we may say that, for vibrations with a strongly varying dipole moment, complications arise which are due to the interaction of the vibrating dipoles. These vibrations give rise to broad reflection bands; the width is not determined by a coupling with lattice modes, as has sometimes been supposed in the literature [11], but it is a direct consequence of the dipole moment itself. Even an undamped oscillator will give a reflection band of the same width. The height of the reflection band is determined by the damping of the vibration.

The emission spectra are complementary to the reflection spectra measured at the same temperature.

The reflection spectrum of a uniaxial crystal strongly depends on the orientation of the reflecting surface.

For the Raman spectrum, apparent anomalies only appear for vibrations which are also active in the infra-red: in this case a vibration in a cubic crystal gives rise to two Raman lines, while the frequency of a Raman line in a uniaxial crystal depends on the orientation of the crystal.

In principle, all these effects could be found for absorption spectra as well. However, several difficulties almost prevent a determination of the pure absorption spectrum of vibrations which are very active. The preparation of crystal plates, thin enough to have a considerable transmission, is very difficult; the transmission of these plates will be influenced by reflection and by interference effects. The transmission of a powder is subjected to the same influences, together with anomalous scattering. If the particles are much smaller than the wavelength of the light (e.g., KBr-disks), one expects that the difference between longitudinal and transverse waves will disappear, which will certainly have influence on the optical properties.*

The conclusion is that the interpretation of the spectra of vibrations associated with a large dipole moment, such as the vibrations of ionic crystals, requires a careful examination of the effects discussed above.

References

[1] Couture-Mathieu, L., and Mathieu, J. P.; *Compt. Rend.*, 1953, **236**, 371.
[2] Rubens, H., and Liebisch, T.; *Sitz. Ber. Berlin*, 1919, 876.
[3] Mathieu, J. P., and Couture-Mathieu, L.; *Compt. Rend.*, 1952, **234**, 1868.
[4] Ketelaar, J. A. A., Haas, C., and Fahrenfort, J.; *Physica*, 1954, **20**, 1259.
[5] Couture-Mathieu, L., Ketelaar, J. A. A., Vedder, W., and Fahrenfort, J.; *Physica* 1952, **18**, 762.
[6] Haas, C., and Ketelaar, J. A. A.; *Physica*, to be published.
[7] Couture-Mathieu, L., Poulet, H., and Mathieu, J. P.; *Compt. Rend.*, 1952, **234**, 1761.
[8] Poulet, H.; *Compt. Rend.*, 1952, **234**, 2185.
[9] Kun Huang; *Proc. Roy. Soc.*, 1951, **A208**, 352.
[10] Haas, C., and Mathieu, J. P.; *J. Phys. Radium*, 1954, **15**, 492.
[11] Burstein, E., Oberley, J. J., and Plyler, E. K.; *Proc. Ind. Acad. Sci.*, 1948, **A28**, 388.

* This effect must not be confused with the formation of mixed crystals with the alkalihalide of the disk, which we could observe in several cases. Ketelaar, J. A. A., Haas, C., and v.d. Elsken, J.; *J. Chem. Phys.*, 1956, to be published.

Spectrochimica Acta, 1956, Vol. 8, pp. 27 to 40. Pergamon Press Ltd., London

Contribution to the study of the structures of methyl derivatives of ammonia from spectroscopical data*

J. R. Barceló and J. Bellanato
Instituto de Optica "Daza de Valdés," Madrid, Spain

Abstract—The infra-red absorption spectra of the methylamines are given between 4500 and 400 K. The spectra of di- and trimethylamine were run for the first time; that of monomethylamine was revised.

Using data on electron diffraction and assuming that in the replacement of hydrogen in ammonia by methyl groups, the ammonia molecule suffers little change, the symmetry C_s is assumed for the mono- and dimethylamine and C_{3v} for the trimethylamine. On this basis we assign the normal modes of vibration of these molecules to the experimental frequencies measured in the Raman and infra-red spectra.

We have compared the frequencies for the bond C—H, N—H, and C—N in the compounds studied. Also, the force constants for N—H and C—N have been calculated for the amines studied on the valence force hypothesis.

Little work on the infra-red spectrum of the methyl derivatives of ammonia is recorded, and we therefore thought a study of the simpler ones would be interesting, with a view to relating the results to those contained in the literature on their Raman spectra, and to facilitate the interpretation of other more complex compounds which can also be regarded as derivatives of this molecule.

Furthermore, it is interesting to compare the infra-red spectra of these derivatives of NH_3 with those of CH_4, and to seek analogies between the two, both in the characteristic vibrations of the CH_3 groups and in those related to the "skeleton" of the molecule involved.

In another publication [1] we have given a bibliography on the Raman and infra-red spectra of these compounds. The Raman spectrum has been studied by various workers and has recently been revised. Polarization studies are few: for monomethylamine, there only exist qualitative values for four lines, for dimethylamine there are no data, and for the trimethylamine only there are quantitative values for some lines. Only the infra-red spectrum of monomethylamine appears to have been recorded previously.

Experimental method and results

We have recorded the infra-red spectra of these three substances between 4500 and 500 K. The preparation of these compounds, the spectrometer used, the measured transmission curves, and the survey of the Raman spectra in the anhydrous amines have been described elsewhere [1].

Discussion

The molecules of these compounds may be considered derivatives of ammonia, inasmuch as the hydrogens have been successively replaced by one, two, or three methyl groups, with the NH_3 pyramid undergoing little distortion.

* Presented at the meeting of the European Molecular Spectroscopy Group, Oxford, July 1955.

For ammonia (Fig. 1) the values for the r(N–H) and for the angle H–N–H have been calculated from spectroscopic data. The values are r(N–H) = 1·014 Å and ∠H–N–H 108° 6′; 107°, or 106° 47′; according to different authors [2, 3, 4].

In the case of dimethylamine, the following values have been found by the electronic diffraction method, r(C–H) = 1·08 Å; r(C–N) = 1·46 Å or 1·47 Å, according to different authors; and ∠ C–N–C = 108° ± 4° or 111° ± 3°, according to different authors [5, 6].

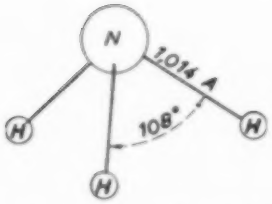

Fig. 1. Point group C_{3v}. Model of the ammonia molecule.

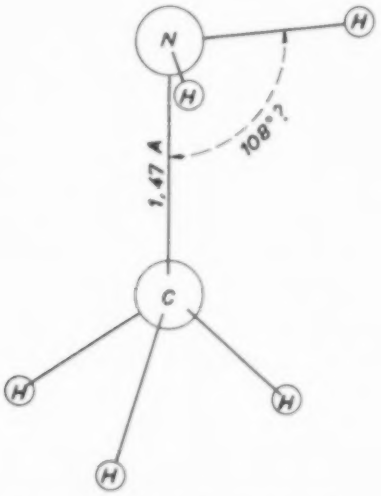

Fig. 2. Point group C_s. Model of the monomethylamine molecule.

With trimethylamine, by electronic diffraction, the distance C–N is found to be 1·47 Å; and the angle C–N–C = 108° ± 4° by electronic diffraction, and 110° by X-ray diffraction [7, 8].

From all these data it follows that the pyramidal shape of ammonia is retained in the dimethyl and trimethyl derivations, and it would seem logical that this should also occur in the monomethylamine.

Monomethylamine

Admitting that, in the replacement of a hydrogen atom of ammonia by a CH_3 radical, no great changes occur in the original pyramid, the monomethylamine molecule will have a plane of symmetry which contains the C–N bond and one of the hydrogen atoms of the CH_3 group, and which, moreover, passes through the bisector of the angle NH_2 (Fig. 2). Therefore, it belongs to the point group C_s, and, with a number of atoms equal to 7, it will show fifteen fundamental vibrations, nine of which will be polarized symmetrical vibrations of the species A', and six depolarized asymmetrical vibrations of the species A''. The fifteen fundamental vibrations must appear in the infra-red and Raman spectra, and the degeneracies of the fundamental vibrations of the CH_3 group will disappear in consequence of the disappearance of the ternary axis of this group. It is to be expected, however, that

VOL. 8 1956/5

the splitting of these CH_3-group vibrations will not be large, and perhaps it may not be detected, since the molecule approximates to a symmetrical top.

As first approximation, we may consider that of these fifteen fundamental vibrations, six belong to the CH_3 radical, three to the NH_2 radical, and six to the relative motions of the CH_3 and NH_2 radicals, taken as rigid entities.

Vibrations of the amino radical—In the neighbourhood of 3350 K, where the valency vibrations should appear, we have found an infra-red band the outline of which is irregular, probably due to the existence of two superposed bands with centres at 3360 and 3387 K. Using the Raman data, we attribute the former to the symmetrical vibration and the latter to the corresponding asymmetrical one.

We ascribe the infra-red band at 1622 K to the symmetrical deformation vibration of the NH_2 radical. Since in the Raman spectrum of several compounds containing the NH_2 group, including methylamine, the corresponding line has escaped the notice of various authors owing to the proximity of strong Hg lines, this frequency has not always been interpreted as corresponding to the deformation vibration of the NH_2 group.

In the Raman spectrum of the deuterium compound of methylamine there exists a Raman line at 1214 K, and the relation between the frequency 1622 K and this value corresponds to the ratio to be expected between the fundamental frequencies for the N–H and N–D radicals.

These infra-red values agree, within the limits allowed, with the approximate theoretical values calculated on the hypothesis of valency forces for the NH_2 radical considered as a symmetrical nonlinear molecule of the XY_2 type. In the calculation, use has been made of the constants of valency and deformation force of ammonia [4], although it is known that, more particularly in the case of the deformation constant, the value is often affected by the changes in the state of hybridization, and it is not always possible to attribute approximately fixed-force constants to the angles comprised between two given bonds.

On the basis of the infra-red data, we have calculated the values of the force constants for the N–H bond in the monomethylamine molecule (Table 1).

Vibrations of the methyl radical—four of the six vibrations are symmetrical to the plane of symmetry and polarized; and two are asymmetrical and depolarized.

In the observed spectrum, the region corresponding to the valency vibrations, in the neighbourhood of 3000 K, shows a very complex absorption, with intense bands which mask one another. It must moreover, be remembered that harmonics appear, and their intensity increases through Fermi resonance with the neighbouring vibrations. It is, therefore, difficult to assign the fundamental frequencies.

The region of 1400 K, where the angular deformation vibrations of the CH_3 radical occur, was complicated by the presence of the rotational bands of water.

The assignment of these frequencies which we have made, bearing in mind the Raman data, is given in the appropriate table.

The relation of intensities in the infra-red and Raman spectra is not always in accordance with the symmetry or asymmetry of the vibrations; never heless, it is approximately the same as in the spectra of hydrocarbons. In the latter, Sheppard and Simpson [9] draw attention to the fact that the C–H valency vibrations are

habitually intense in the infra-red and Raman spectra, and the same thing occurs in the case of the doubly degenerate asymmetrical deformation vibration; but, by contrast, the symmetrical deformation vibration is intense in the infra-red, and is usually lacking in the Raman spectrum.

Mutual vibrations of the methyl and amino groups—Three of these six vibrations are asymmetrical with respect to the plane of symmetry and are therefore depolarized; and three are symmetrical and polarized.

The valency vibration between the methyl and amino groups in which the dipole moment vibrates parallel to the plane of symmetry can be located immediately by analogy with similar compounds of the ethane type, and by an approximate calculation, using Badger's formula for calculating the force constant. It corresponds to the intense infra-red band at 1044 K corresponding to a polarized Raman line.

It is to be expected that, by analogy with methyl alcohol, the torsional vibration may have a very low frequency. In this substance it appears in the infra-red at 270 K [10]; and in ethane, in which it is inactive, it is estimated at 275 K on the basis of the specific heat [11]. Bailey *et al.* [12], on the basis of possible combination bands, infer that the torsional frequency in methylamine lies at 233 K; and, using this value, they found that the calculated specific heat C_p at 0°C agreed with the experimental value found by Felsing and Jessen [13]. Owens and Barker [14] suggested that the value of 620 K adopted by Cleaves and Plyler [15] for the torsional frequency is too high; and they refer to the observations of Randall and Lawson (unpublished), in which a region of fairly intense absorption is said to occur in methylamine at 270 K. With the KBr prism, we have not been able to study this area. However, we are inclined to think that the frequency is low and that the absorption which we find at around 500 K, using high pressures, the outline of which cannot be accurately given owing to the rotational bands of water-vapour, is due, at least in part, to the first harmonic of the torsional frequency, which would thus lie at approximately 250 K. A. Hadni [16] has observed a band in this region.

As regards the infra-red band which appears at 779 K, which has a high intensity in infra-red absorption and a small intensity in the Raman spectrum, and which appears only with the vapour, we are rather inclined to think that it corresponds to a vibration involving the asymmetrical rocking motion in which the hydrogen atoms oscillate in opposite directions, perpendicularly to the N–H bonds. The other symmetrical rocking vibration of the amino group, in which the two hydrogen atoms move in the same direction perpendicularly to the N–H bonds and approximately parallel to the plane of figure, must probably be assigned to the infra-red band which is found near 600 K; although it may also possibly lie in the neighbourhood of 1100 K superposed on another vibration.

The two remaining vibrations are those in which the C–N bond is deformed either in the plane of symmetry or normally to this plane, and these are related to the two rocking vibrations of the CH_3 group. We assign the asymmetrical vibration to the infra-red band at 1129 K; and the symmetrical one is probably associated with the weak absorption at 1244 K. No corresponding Raman line has been recorded in earlier work, but recently a very weak line has been found at

VOL.
8
1956/5

Table 1. Fundamental frequencies of gaseous CH_3—NH_2

		A'	A''
NH	stretching	ν_1 3360	ν_{10} 3387
CH	stretching	ν_2 2842 ν_3 2822	ν_{11} 2962
NH_2	bending	ν_4 1622	
CH_3	bending	ν_5 ν_6 1410	ν_{12} 1460
CH_3	rocking	ν_7 1244	ν_{13} 1129
CN	stretching	ν_8 1044	
NH_2	rocking	$\nu_9 \sim 600$?	ν_{14} 779
	twisting		ν_{15} 235?

Force constants

NH k $= 6{\cdot}2 \cdot 10^5$ dynes/cm
NH_2 $k_{\beta/\beta'}$ $= 0{\cdot}75 \cdot 10^5$ dynes/cm
CN k $= 5{\cdot}0 \cdot 10^5$ dynes/cm

Table 2. Frequency assignments for the monomethylamine bands, not given among the fundamentals.

	Calculated	Observed
$\nu_5 + \nu_{11}$, $3\nu_{12}$	4372, 4380	4385
$\nu_4 + \nu_7 + \nu_{12}$, $\nu_3 + \nu_6$	4211, 4232	4232
$2\nu_{12} + \nu_8$	3966	3945
$2\nu_4$	3244	3223
$2\nu_{12}$	2920	2917
$2\nu_{14} + \nu_8$	2604	2630
$\nu_7 + \nu_{12}$	2589	2565
$\nu_5 + \nu_8$	2456	2470
$\nu_4 + \nu_{14}$	2401	2425
$\nu_{12} + \nu_{14}$	2239	2234
$2\nu_8$	2088	2072
$\nu_8 + \nu_{14}$	1823	1826
$\nu_3 - \nu_8$	1778	1764
$2\nu_{14}$	1558	1520
$\nu_{14} - \nu_{15}$		515
$2\nu_{15}$		470

1221 K [1]. The assignment of these two vibrations may possibly be reversed and, in order to verify it, polarization data are required.

Dimethylamine

For the same reasons as outlined in the case of monomethylamine, the dimethylamine molecule belongs to the C_s point group. The plane of symmetry of this molecule would thus contain the NH radical and be perpendicular to the C–N–C plane (Fig. 3).

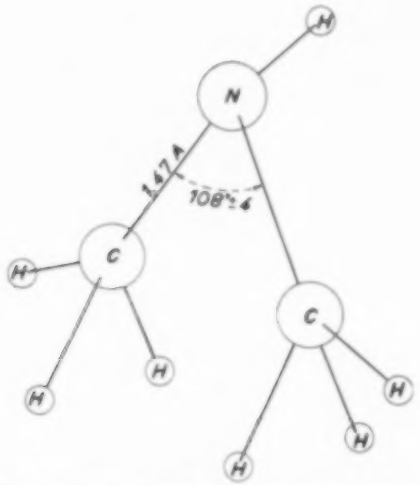

Fig. 3. Point group C_s. Model of the dimethylamine molecule.

The twenty-four fundamental vibrations are active in Raman and infra-red; it is, however, very probable that two vibrations of the same class, of similar frequencies, cannot be distinguished. It may be considered that twelve of these twenty-four fundamental vibrations are internal vibrations of the CH_3 groups, in which the degeneracy disappears when the ternary axis disappears; six are external vibrations of the CH_3 groups; three are vibrations of the NH group; and the remaining three belong to the C–N–C– chain.

No polarization data are known for the Raman lines and, in order to attribute frequencies in the majority of cases (apart from the comparison between the infra-red and Raman spectra), we shall also take as a basis the comparison with the spectra of the relative molecules, dimethylether and propane. In some cases we shall also use the Raman spectrum of the deuterated compound.

Vibrations of the methyl radical—The assignment of the valency and deformation vibrations can be seen in the relevant table. As is to be expected, the assignment of such a high number of frequencies is only tentative, and it is particularly doubtful in some cases.

As regards the rocking vibrations, it is to be expected, in principle, that they will appear in the spectrum mixed with others of similar magnitude and of the same species, and, in this case, with the bands of the skeletal and N–H bending vibrations.

VOL. 8 1956/5

We relate these vibrations to the intense infra-red band at 1155 K, which corresponds to the very weak Raman line recently found at 1154 K in the liquid substance [1], and to the 1137 and 1189 K given in the bibliography for the aqueous solution. These vibrations should probably be associated with the very weak Raman lines at 1226 and 1077 K, only the former one of which corresponds to a very weak and doubtful absorption in infra-red.

It is to be expected that, as in other similar compounds, the twisting vibrations will have a very low frequency, below 300 K. In the Raman spectrum of dimethylamine there is no line that can be attributed to them; in the infra-red we have not been able to study this region. PITZER [17] locates these vibrations in propane at 202 and 283 K, inferring the former frequency from the infra-red band at 720 K, and the latter from thermodynamic data. In dimethylether the frequencies quoted in the bibliography [4] are 160 and 300 K, which appear in the Raman spectrum with a very low intensity. As in the infra-red spectrum of dimethylamine, we have found some weak bands at 575 K, 525 K, and 482 K; we suppose these must probably be harmonics of the twisting vibrations found in the 250–300 K region.

Chain vibrations—Dimethylamine, like other similar polyatomic molecules, can be considered approximately as a system of three nuclei which behave in the same way as those of a nonlinear symmetrical molecule, where the skeletal vibrations are concerned.

Of the three corresponding vibrations, we assign that of the asymmetrical valency to the infra-red band at 1024 K, which has no counterpart in the Raman spectrum of dimethylamine, but corresponds in the hydrochloride [18] to the depolarized Raman line at 1029 K. Since this does not exist in dimethylamine, some authors have considered that this vibration should be related to the Raman line at 1077 K, since in the hydrochloride there also exists a depolarized line at 1099 K. Nevertheless, in view of the infra-red data, it would seem that our assignment is more logical. However, what is assumed in the case of propane may occur here, i.e., that the infra-red band at 1155 K may be a combination of a CH_3 rocking vibration and the asymmetrical chain vibration; and, in turn, that the 1024-frequency vibration may be a different combination of the two vibrations.

The symmetrical vibrations of the chain may be easily assigned if we bear in mind the Raman data for dimethylamine and the dimethylammonium ion, in which the polarization values help. The symmetrical valency vibration is associated with the infra-red band at 930 K, of equal frequency in the Raman spectrum, which, in the dimethylammonium ion, corresponds to the polarized line of frequency 895 K. The symmetrical deformation vibration gives rise to an intense absorption at approximately 420 K, which corresponds to a Raman line in the liquid at 397 K and to 415 K in the solution. In the Raman spectrum of the dimethylammonium ion, the line that is polarized is found at 412 K.

These assignments agree with the approximate theoretical values obtained in the hypothesis of valency forces, bearing in mind the electronic diffraction data. For this purpose, the simplest way is to calculate the valency force constant for the C–N bond by BADGER's formula, or, alternating, to use the one calculated for methylamine. With this value, and assuming the experimental value of the symmetrical deformation frequency, we can calculate the theoretical values of the two other frequencies.

On the basis of the experimental frequencies, we can, conversely, calculate the values of the force constants, which are given in Table 3.

N–H vibrations—The valency vibration must appear in the 3350-K region, as in the case of methylamine. In this region we have the infra-red band at 3355 K which is assigned to this vibration. It corresponds to the Raman line at 3350 K in the liquid substance and to 3384 K for the gas.

Table 3. Fundamental frequencies of gaseous $(CH_3)_2$—NH

		A'	A''
NH	stretching	ν_1 3355	
CH	stretching	a ν_2 2912 s ν_3 2855 ν_4 2802	ν_{14} 2967 ν_{15} ν_{16} 2802
CH_3	bending	a ν_5 1496 s ν_6 ν_7 1404	ν_{17} 1466 ν_{18} ν_{19} 1404
CH_3	rocking	ν_8 1245? ν_9 1155	ν_{20} 1155 ν_{21}
CN	stretching	ν_{10} 930	ν_{22} 1024
NH	bending	ν_{11} ?	ν_{23} 724
CNC	bending	ν_{12} 397*	
CH_3	twisting	ν_{13} 290?	ν_{24} 250?

Force constants

NH k = 6·2 . 10^5 dynes/cm
CN k = 3·9 . 10^5 dynes/cm
CN $k_{\delta\beta}$ = 0·43 . 10^5 dynes/cm

*Raman frequency

The two bending vibrations of the N–H group have not been fully studied in compounds containing this group, and different authors disagree about them. In the case of dimethylamine we assign the asymmetrical N–H bending vibration to the infra-red band at 724 K, the most intense in the whole spectrum. In the Raman spectrum of the liquid, gas, and aqueous solution, this frequency has not been recorded. Recently, a very weak Raman line has been found at 699 K, and this may be related to the infra-red band concerned.

The symmetrical N–H bending vibration must correspond to an intense Raman line and a less-intense infra-red line. We have found no frequency that could be clearly attributed to this vibration. If we bear in mind the assignments given by

VOL. 8 1956/5

AXFORD *et al.* [19] in the cases of symmetrical dimethylhydrazine and methylhydrazine, and that given by LORD and MILLER [20] for pyrrole and its derivatives, we may suppose that it must appear in the neighbourhood of 1100 K, in which case it will appear superposed on some one of the frequencies that appear in this region. Perhaps the Raman line at 1077 K should be attributed to this vibration, or alternatively that at 784 K.

Table 4. Frequency assignments for the dimethylamine bands, not given among the fundamentals.

	Calculated	Observed
$\nu_2 + \nu_{17}$, $3\nu_{17}$	4378, 4398	4370
$\nu_7 + \nu_{16}$	4206	4210
$\nu_{14} + \nu_{20}$	4122	4110
$\nu_4 + \nu_{20}$	3945	3930
$2\nu_{19} + \nu_{23}$	3532	3522
$2\nu_{22} + \nu_{20}$	3203	3182
$\nu_{10} + \nu_{20} + \nu_{22}$	3113	3113
$\nu_{10} + \nu_{22} + \nu_{23}$	2678	2685
$\nu_{17} + \nu_{20}$	2621	2607
$\nu_7 + \nu_{20}$	2559	2575
$2\nu_{23} + \nu_{22}$	2512	2510
$\nu_{17} + \nu_{22}$	2490	2492
$2\nu_{23} + \nu_{10}$	2378	2400
$\nu_{10} + \nu_{20}$	2085	2079
$2\nu_{10}$	1879	1895
$\nu_{22} + \nu_{23}$	1642	1650
$2\nu_{24}$?		575
$\nu_{13} + \nu_{24}$?		525
$2\nu_{13}$?		482

Recently, several authors suggest an NH-bending band at 1550–1650 K for the secondary amines and in the vicinity of this region for the amides. Nevertheless, the results are not in good agreement, and the origin of the band that sometimes appears in this region is not clear. We have found a weak absorption at 1650 K in the spectrum of dimethylamine, but we consider that assignment as doubtful.

Trimethylamine

The electron and X-ray diffraction data prove that in the trimethylamine molecule the ammonia pyramid is retained and the NC_3 chain belongs to the C_{3v} point group. On the other hand, it may be considered that the introduction of the methyl groups does not alter the symmetry, if a hydrogen atom of each methyl group is situated on the plane which passes through the CN axis and is the bisector of the angle formed by the other two CN axes (Fig. 4).

Assuming the C_{3v} symmetry for trimethylamine, there will be twenty-two fundamental frequencies, eleven of which are doubly degenerate. These twenty-two frequencies are classified as follows: seven are vibrations of the A_1 species, polarized

in the Raman spectrum; four are vibrations of A_2 species, forbidden in the Raman and infra-red spectra; and eleven are vibrations of E species, doubly degenerate, depolarized in the Raman spectrum. Of the A_1 species vibrations, two belong to the CN_3 chain, and five are CH vibrations, whereas those of E species include two of the chain and nine of the CH groups.

In the literature we find polarization data for the Raman lines of trimethylamine, which, in some cases, makes it easier to assign the frequencies.

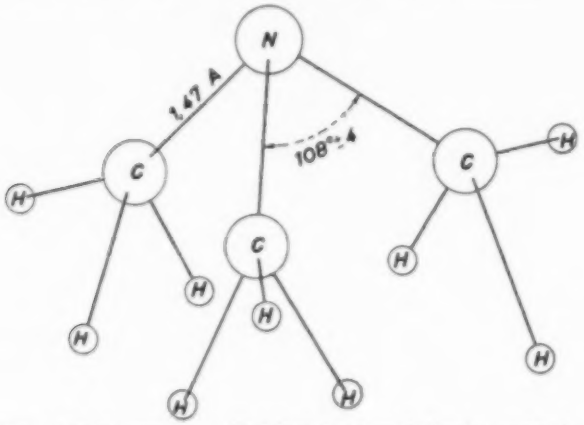

Fig. 4. Point group C_{3v}. Model of the trimethylamine molecule.

The spectrum of trimethylamine will resemble that of isobutane, the chief differences between them being that in the latter the two characteristic frequencies of the CH group appear.

Vibrations of the methyl radical—In the region of valency vibrations there appear four very intense bands which overlap one another. In the Raman spectrum [1] three weak lines appear, which are probably due to harmonics or combination frequencies. The assignment of the frequencies is given in Table 5.

The region of the deformation vibrations is confused, as in the previous cases, and, likewise, where the valency vibrations are concerned, the original vibrations of the CH_3 radical do not seem to be split.

In the region corresponding to the CH_3 rocking vibrations we find three intense infra-red bands, at 1104, 1183, and 1272 K, the first of which has no counterpart in the Raman spectrum of the liquid, although it is found with the solution. These three infra-red bands appear to correspond to the three rocking vibrations that are allowed in the infra-red spectrum, and the assignment has been made in relation to the Raman data.

Of the twisting vibrations, only one, of E species, is active; and we assign this to the depolarized Raman line at 264 K, since it is to be expected that it will be wholly depolarized and found in this region of the spectrum.

Chain vibrations—The chain vibrations have been assigned by Anantha-krishnan and Kohlrausch from a study of the Raman spectrum. Kohlrausch [21], on the basis of the experimental values, has calculated the molecular force constants and the valency angle, using a system of valency forces; and his assignment has

VOL. 8 1956/5

been confirmed by ANANTHAKRISHNAN's [22] polarization values. EDSALL [18] draws attention to the fact that the Raman line at 274 K in trimethylamine does not correspond to any line in the spectrum of the trimethylammonium ion or in isobutane, and that it may therefore correspond to one of the fundamental vibrations. The assignment of frequencies made by KOHLRAUSCH would, therefore, seem to require revision.

Tables 5. Fundamental frequencies of the gaseous $(CH_3)_3N$

		A_1	A_2	E
CH	stretching	a ν_1 2967 s ν_2 2777	ν_8	ν_{12} 2967 ν_{13} ν_{14} 2822
CH_3	bending	a ν_3 1466? s ν_4 1402	ν_9	ν_{15} 1466 ν_{16} ν_{17} 1402
CH_3	rocking	ν_5 1183	ν_{10}	ν_{18} 1272 ν_{19} 1104
CN	stretching	ν_6 826		ν_{20} 1043
CN	bending	ν_7 365*		ν_{21} 425*
CH_3	twisting		ν_{11}	ν_{22} 264*

Force constants

NC_3 k $= 3{\cdot}9 \cdot 10^5$ dynes/cm

k_{s/t^2} $= 0{\cdot}39 \cdot 10^5$ dynes/cm

* Raman frequencies.

In the infra-red spectrum we have only been able to find the bands corresponding to the valency vibrations, the frequencies of which coincide with Raman intervals. In the region covered by the KBr prism there is intense absorption at about 395 K, but at this low frequency the contour cannot be defined accurately. Furthermore, in this range covered by the KBr prism several weak bands appear; they are more or less doubtful, and have been assigned to harmonics and combination frequencies.

By means of an approximate calculation, using a system of valency forces, it is possible to show that it is highly improbable that the Raman line at 264 K should correspond to a chain vibration. Thus, if we consider that this line, together with that of 1044-K frequency, both of which are depolarized, corresponds to the degenerate vibrations of the chain, the calculation for the force constants gives the values $k = 3{\cdot}9 \times 10^5$ dynes/cm and $k_{s/t^2} = 0{\cdot}2 \times 10^5$ dynes/cm, so that the theoretical value of the symmetrical frequencies comes out at 800 K and 260 K.

On the other hand, if we consider 425 K and 1044 K as frequencies of the asymmetrical vibrations, the values of the force constants are $k = 3{\cdot}6 \times 10^5$

dynes/cm and $k_{8/1^2} = 0{\cdot}5 \times 10^5$ dynes/cm, which gives us 810 K and 410 K for the frequencies of the symmetrical vibrations in good accord with the two polarized lines 826 and 365 K. Of course, we reach the same conclusions if we calculate the values of the asymmetrical vibration frequencies on the basis of the experimental values of the symmetrical vibration frequencies.

Table 6. Frequency assignments for the trimethylamine bands, not given among the fundamentals.

	Calculated	Observed
$\nu_4 + \nu_{12}$	4369	4373
$2\nu_{15} + \nu_{17}$	4204	4207
$\nu_{12} + \nu_{20}$	4010	4010
$\nu_1 + \nu_6$	3793	3820
$\nu_1 + \nu_{21}$	3393	3398
$\nu_2 + \nu_{21}$	3201	3215
$3\nu_{20}$	3129	3127
$\nu_{14} + \nu_{22}$	3093	3102
$2\nu_{15}$, $\nu_4 + \nu_{15}$	2932, 2868	2885
$\nu_5 + \nu_{15}$	2649	2637
$2\nu_{17}$	2544	2560
$\nu_4 + \nu_{18}$	2509	2502
$\nu_2 + \nu_{20}$	2366	2400
$3\nu_5$	2226	2240
$\nu_5 + \nu_{20}$	2208	2208
$2\nu_{18}$	2098, 2086	2097
$\nu_6 + \nu_{17}$, $2\nu_{20}$	2009	2008
$\nu_6 + \nu_{20}$	1869	1872
$2\nu_6$	1652	1645
$2\nu_7$	740	742
$\nu_{21} + \nu_{22}$	700	720
$2\nu_{22}$	528	521
?		487
$\nu_6 - \nu_7$	456	450

Comparative study of the three methylamines

As is known, we can qualitatively assign the normal modes of vibration of a molecule to particular vibrations of groups of atoms in that molecule, although, actually, a normal mode of vibration comprises the movement of all the atoms. Accordingly the comparative study of the spectra of the methylamines as a series may be of interest, and also the observation of the variation of the frequencies attributed to vibrations of the NH, CH, and CN groups in the different compounds.

The four fundamental frequencies of ammonia are represented in the first column of the attached table. These frequencies, which correspond to NH movements, are approximately retained in the infra-red spectrum of monomethylamine. In this, we found frequencies 3360 K and 3387 K in the region of the stretching vibration frequencies which correspond to those of ammonia. Also, the 1622 K

VOL. 8 1956/5

and 779 K frequencies assigned to the bending and rocking movements of the NH_2 group are in accordance with the two remaining frequencies of ammonia, especially the former.

Dimethylamine shows, in the region of NH valency vibrations, a band at 3355 K. The frequency at 1622 K disappears, as was to be expected; but one of the bending vibrations appears as a very intense infra-red band at 724 K; that is in the same range as in the case of monomethylamine. The other bending vibration is not clearly located.

Table 7. Comparison of ammonia and their methylderivates as regards frequencies of the vibration modes of similar groups.

		NH_3	MMA	DMA	TMA
NH vibrations	ν_a	3414	3387		
	ν_s	3337	3360	3355	
	δ	1628	1622		
	γ	950	779 600?	724 ?	
CN vibrations	ν_s		1044	930	826
	ν_a			1024	1043
	δ			397	365 425

In the spectrum of trimethylamine, since NH groups no longer exist, there is no frequency corresponding to these vibrations.

The CN vibrations, which are naturally absent from ammonia, are found in the three amines. The symmetrical stretching vibration is found in all three cases; but its frequency falls by about 100 K on passing from monomethylamine to dimethylamine and again on passing to trimethylamine; on the other hand, the asymmetrical stretching vibration, which is only present in di- and trimethylamine, keeps its frequency practically unaltered. Something similar occurs with the bending vibration which splits into two in the case of trimethylamine.

A comparative study of the force constants of different bonds both in ammonia and in the methylamines is given in the attached table.

As regards the CH_3 valency and deformation vibrations, the differences in intensity of the common bands and the appearance of new bands can be explained easily by the increase in contents of methyl radicals. As regards the CH_3 rocking vibrations, we observe an analogy in the presence of the bands around 1150 K. However, there is a marked difference in the case of trimethylamine, in which an intense infra-red band appears at 1272 K. This has been assigned to a

rocking vibration, and, in the other derivatives, it corresponds to very weak bands, which are especially doubtful with dimethylamine.

Finally, although the existing data are doubtful, there would seem to be a concordance in the range in which the twisting vibrations of these compounds appear.

Table 8. Comparison of the force constants ($\times 10^5$ dynes/cm) in the methylamines

	NH_3	MMA	DMA	TMA
νNH	6·35	6·2	6·2	
δNH_2	0·54	0·75		
νCN		5·0	3·9	3·9
δCN			0·43	0·39

References

[1] Bellanato, J., Sardina, M. T., and Barceló, J. R.; *Anal. Soc. Esp. Fis. Quim.*, 1955, **51B**, 271
[2] Migeotte, M. V., and Barker, E. F.; *Phys. Rev.*, 1936, **50**, 418
[3] Dennison, D. M.; *Rev. Mod. Phys.*, 1940, **12**, 175
[4] Herzberg, G.; *Infra-red and Raman Spectra of Polyatomic Molecules* (D. Van Nostrand Company, Inc., New York, 1945)
[5] Bauer, S. H.; *J. Amer. Chem. Soc.*, 1938, **60**, 524
[6] Schomaker, V., according to Allen, P. W., and Sutton, L. E.; *Acta Cryst.*, 1950, **3**, 46
[7] Brockway, L. O., and Jenkins, H. O.; *J. Amer. Chem. Soc.*, 1936, **58**, 2036
[8] Richter, H.; *Phys. Z.* 1935, **36**, 85
[9] Sheppard, N., and Simpson, D. M.; *Quart. Rev.*, 1953, **7**, 19
[10] Lawson, J. R., and Randall, H. M., unpublished, according to Koehler, J. S., and Dennison, D. M.; *Phys. Rev.*, 1940, **57**, 1006
[11] Kistiakowsky, G. B., Lacher, J. R., and Stitt, F.; *J. Chem. Phys.*, 1939, **7**, 289
[12] Bailey, C. R., Carson, S. C., and Daly, E. F.; *Proc. Roy. Soc.* 1939, **173**, 339
[13] Felsing, W. A., and Jessen, F. W.; *J. Amer. Chem. Soc.*, 1933, **55**, 4418
[14] Owens, R. G., and Barker, E. F.; *J. Chem. Phys.*, 1940, **8**, 229
[15] Cleaves, A. P., and Plyler, E. K.; *J. Chem. Phys.*, 1939, **7**, 563
[16] Hadni, A., Private communication
[17] Pitzer, K. S.; *J. Chem. Phys.*, 1944, **12**, 310
[18] Edsall, J. T.; *J. Chem. Phys.*, 1937, **5**, 225
[19] Axford, D. W. E., Janz, G. J., and Russel, K. E.; *J. Chem. Phys.*, 1951, **19**, 704
[20] Lord, R. C., and Miller, F. A.; *J. Chem. Phys.*, 1942, **10**, 328
[21] Kohlrausch, K. W. F.; *Mh. Chem.*, 1936, **68**, 349
[22] Ananthakrishnan, R.; *Proc. Ind. Acad. Sci.*, 1936, **4**, 204

VOL. 8 1956/5

Spectrochimica Acta, 1956, Vol. 8, pp. 41 to 45. Pergamon Press Ltd., London

Technique and results of excitation of Raman spectra in the red and near infra-red region*

H. STAMMREICH
Department of Physics, University of São Paulo, São Paulo, Brazil

(*Received* 9 *November* 1955)

Abstract—This paper is a brief report on some recent work of the Department of Physics at São Paulo University, on the excitation of Raman spectra in the red and near infra-red region of the spectrum. Discussion of results in detail with respect to the spectra of specific molecules and their structural interpretation is omitted, but attention is drawn to the experimental technique which seems promising, particularly if executed with larger resources than were available.

PROGRESS in Raman spectroscopy has fallen behind in recent years, compared with the rapid development of infra-red spectroscopy and other spectroscopic techniques which can give more detailed information on complicated molecules, especially from the chemist's viewpoint. But for the physical and mathematical treatment of such topics as force fields, force constants, intra- and intermolecular interactions, thermodynamic properties, etc., knowledge of the vibrational constants of simple molecules is of the greatest interest, and there is a surprisingly large number of simple molecules whose vibrational spectra are not yet known. This is the case for many, particularly inorganic, compounds where high-vibrating masses and low-force constants give rise to fundamental frequencies below 300 or 200 cm^{-1}, lying in the region between 35 μ and 200 μ, which is not easily accessible to normal infra-red methods. On the other hand, these compounds are frequently strongly coloured or even opaque to visible light, or photochemically unstable or fluorescent, and therefore not suitable for the conventional excitation techniques in Raman spectroscopy.

Raman spectra of such molecules can be obtained by excitation in the long-wave region of the visible spectrum or in the near infra-red. Until a few years ago this possibility did not appear very promising, for the following reasons.

Dispersion and resolving power of prism-spectrographs, used almost exclusively in Raman spectroscopy until recently, decrease rapidly in the long-wave region, and the intensity-determining scattering factor decreases with the fourth power of wavelength. The sensitivity of radiation detectors too, especially of photographic plates, was poor above 6500 or 7000 Å, and further, it is difficult to find in this region a light source suitable for excitation of Raman spectra with characteristics comparable to those of the mercury arc.

In spite of these rather unfavourable conditions, some work on Raman spectra, employing other light sources than the mercury lamp, has been described. WOOD and others used helium discharge tubes with the strong ultra-violet radiation 3889 Å for excitation. KRISHNAMURTI employed a cadmium-lamp and excited the spectra by the two green Cd-lines, and also by the red line 6439 Å. The first

* Presented at the Meeting of the European Molecular Spectroscopy Group, Oxford, July 1955.

and apparently the only one who worked with the helium-radiation 5876 Å was H. W. THOMPSON, who reported in 1938 the Raman spectrum of thiophosgene obtained in this way. It seems, however, that these methods were more or less impracticable, except in special circumstances; and a more generally suitable technique, or, better still, a routine method, was never worked out. However, there have been some recent technical advances which provide conditions for the solution of the different problems involved, and we shall now discuss possible ways of removing the difficulties.

Spectrographs

Recent successes in ruling diffraction gratings and in obtaining replicas of high precision from blazed original gratings now permit us to concentrate up to 70% or even 80% of the light entering in the collimator in a determined spectral region of one order of the spectrum. Plane gratings from BAUSCH and LOMB are used, but we understand that equivalent gratings will shortly be manufactured in England. This great progress has been made possible by controlling the surface of the grooves and the angle between groove-surface and grating-plane. A large choice of these gratings of different dimensions, grating constants, and blazed wavelengths is now available. On account of lower reflection losses, spectrographs built with these gratings of suitable blaze have a higher luminosity than prism instruments of equal numerical aperture; compared with two- or three-prism spectrographs, frequently used in Raman work, the gain in luminosity is significant.

The linear dispersion of the grating as a function of wavelength corresponds to an increasing dispersion towards higher wavelengths in scale of frequency or of wave number, which is the quantity of interest here. Employing gratings of a ruled area of about 60 by 70 mm and with 15,000 or 30,000 grooves per inch, it is possible to build small spectrographs of high aperture, let us say 1 : 3·5, which in the red and near infra-red region are very much superior to large-prism instruments, as regards both luminosity and dispersion. Such an instrument equipped with a 30,000/in. grating in the first order has a reciprocal dispersion of about 30 Å/mm, corresponding to 45 cm^{-1}/mm in the 8000-Å region. In order to obtain the same dispersion in frequency scale in the region of the mercury-line 4358 Å, we need a reciprocal dispersion of about 9 Å/mm; a prism spectrograph with aperture of 1 : 3·5, and this dispersion would be very large and expensive.

Light sources for excitation

The most difficult problem is to find suitable light sources for the excitation of Raman spectra in the long-wave region. We need an intense monochromatic radiation in a sufficiently "free spectral range," especially on the long-wave side of the exciting wavelength. The fact that the rapid development of Raman spectroscopy in the past was due largely to the characteristics and to the simplicity and flexibility of the construction of mercury lamps, has been frequently stressed. A comparable light source in the long-wave region does not exist.

Hitherto we have worked with discharge tubes of the cold cathode type filled with noble gases, particularly with helium, whose radiations 5875·6, 6678·2,

VOL. 8 1956/5

7065·2, and to a less extent 7281·4 Å, are suitable for our purpose. But the helium-atom is, compared with the mercury-atom, extremely unfavourable for producing radiations of the desired wavelength. As it has an ionization potential of 24·47 eV and first excitation potentials of 19·77 and 20·55 eV respectively for the lowest triplet and singlet state, we have to expend at least this amount of energy in order order to produce one photon of an energy of 2 eV or less. The ionization potential of the mercury-atom is 10·44 eV, and the excitation wavelength of 4358 Å corresponds to a photon of nearly 3 eV. Thus we have much more favourable conditions for obtaining a satisfactory ratio of excitation radiation to total power input in the discharge tube than in the case of helium, where between manifold other processes the absorption of resonance radiation and the impact of metastable atoms of high energy contribute to heat the walls of the lamp.

Even when the power input of the discharge tubes is increased to the limit of the thermal resistivity of the different elements of the tube, we have to be satisfied with an intensity of the excitation light beam, incident in the Raman tube, which is in the most favourable case—that is, for 5876 Å—three or four times less than that in excitation units equipped with mercury lamps. For the helium radiations 6678·2, 7065·2, and 7281·4 Å, used by us for excitation of Raman spectra, this unfavourable factor becomes of the order of 6, 20, and 50 respectively.

The discharge tubes consist of about 1-m tubing of 5-mm diameter wound helicoidally around the Raman tube. Such lamps have an operating voltage of about 1200 to 2000 volts and can be charged with a current of about 500 mA. The power input of nearly one kilowatt calls for a very efficient cooling system, and in order to secure an efficient heat transfer, the lamps work in a circulating bath of paraffin oil, or, when the applied voltage is not too high, of water.

The helium has to be carefully purified, especially from neon, whose numerous lines in the red and near infra-red would be very troublesome. Even the commercially spectroscopical pure helium contains generally one part of neon in 1000 or 10,000 parts of helium and is not sufficiently pure for our purpose. It can be purified by adsorption of neon on charcoal at the temperature of liquid hydrogen or by diffusion through a thin-walled quartz tube at 1000°C, or more easily by an electrophoresitic method, kindly indicated to us by Prof. G. H. Dieke. As a rule, we prepare our helium in the known manner from monazite, and this product is naturally free from neon.

The helium radiations 5876 Å and 7065 Å correspond to transitions between triplet levels, and the lines 6678 Å and 7281 Å are transitions between singlet states. This means that the first pair are produced nearly exclusively by ionization of the helium atom, while the other two are partially obtained by excitation processes. By convenient choice of the gas-pressure in the discharge tube (low pressure up to 2 mm favours ionization, higher pressures of the order of 6 or 10 mm favour excitation) we are able to influence the relative intensities of these lines and consequently to build lamps specially suited for the desired radiation. The spectrum of lamps of higher pressure shows the bands of the He_2 molecule with relatively strong intensity, and these bands affect the observation of Raman shifts between the yellow and the first red helium line, but since the first one belongs to the triplet system, we use here low-pressure lamps.

For exciting radiations of longer wavelengths we used discharge tubes of similar characteristics filled with argon, krypton, and xenon. The strongest lines in the spectra of these noble gases which are suitable for excitation of Raman spectra in the near infra-red are 8115 Å and 8408 Å of argon; 8113 Å and 8298 Å of krypton; and 8232 Å, 8280 Å, and possibly 8819 Å of xenon. The arc spectra of these elements have a large number of lines in the range of interest, and it is therefore only possible to investigate by this method the Raman spectra of very simple (especially diatomic or triatomic) molecules with low fundamental vibrations. We easily obtained, for example, the Raman spectrum of liquid bromine, which is completely opaque to visible light, by excitation with argon lamps.

Finally, we shall mention some preliminary experiences with rubidium and caesium lamps, whose resonance radiations seem very suitable for the excitation of Raman spectra. Here the ratio of intensity of excitation radiation to power input is particularly favourable. The resonance doublet of rubidium has a wavelength of 7800 Å and 7948 Å, that of caesium of 8521 Å and 8943 Å. The P levels are both normal, and the components of shorter wavelength of the doublets have twice the intensity of those of higher wavelength. We hope to be able soon to report in detail some results obtained by this technique.

Radiation detectors

At present we work exclusively with photographic methods, since multiplier-photocells with sufficient sensitivity above 7000 Å are not yet available, at any rate not commercially. But it seems that this situation may change soon, and that multiplier cells sensitive to 1 μ or more will be available for general spectroscopic purposes. These photocells would create important facilities for the Raman work of this kind, particularly for excitation with caesium lamps and possibly for excitation by the very strong helium line 10,830 Å.

VOL. 8 1956/5

As regards photographic plates, continuous progress has been made in recent years in extending the useful range of spectral sensitivity towards longer wavelengths and in increasing the absolute sensitivity in the range which interests us. For example, the Eastman Kodak plates with sensitizer of the N class had eight years ago a useful range up to 8500 Å, and the absolute sensitivity here was more or less one-sixtieth of a non-sensitized plate of the same type in the blue region. Now the spectral sensitivity of the N plates extends to near 9000 Å, and the absolute sensitivity has been increased ten-fold. Even so, we have to work in this region with plates six or ten times less sensitive than those for the blue region. This ratio is much more favourable in the near red, where we use sensitizers of class E and F.

Scattering factor and resonance denominator

The intensity of the scattered radiation and therefore the intensity of the Raman spectrum depends on the fourth power of the reciprocal of the wavelength. Assuming this scattering factor to be unity for 4358 Å, we find for higher wavelengths the following values: for the yellow helium line, $3{\cdot}3^{-1}$; for 6678 Å, $5{\cdot}5^{-1}$; for 7065 Å, $6{\cdot}9^{-1}$; and for wavelengths between 8000 and 8700 Å, values between 12^{-1} and 16^{-1}.

Naturally, we can do nothing about the loss of light caused by the decreasing scattering factor, and taking into account the other unfavourable factors which we have mentioned, we should expect, in the long-wavelength region, exposure times from ten to a thousand times higher than in the conventional Raman spectroscopy. The situation is, however, to some extent improved by the fact that we work always with the shortest wavelength possible for a given compound. This means that we excite generally near an absorption band. In this case the resonance denominator $(\nu_{el}^2 - \nu_0^2)^2$ is small, and therefore the intensity of the Raman shifts is high. The calculation of the resonance denominator is in general only possible for diatomic molecules whose electronic levels are known, but the effect is always very pronounced. For instance, the Raman spectra of even weak solutions of a coloured compound in a colourless solvent show generally the Raman lines of this substance very much stronger than the shifts corresponding to the solvent.

Some results

Brief mention may be made of molecules whose Raman spectra we were able to obtain by using the above techniques; some results have already been published, and others will be published soon.

Of diatomic molecules, we measured the Raman frequency of bromine, of bromine-monochloride in equilibrium with Br_2 and Cl_2, of iodine-monochloride, and of the ions $(ClO)^-$ and $(BrO)^-$, the last being extremely unstable.

Of triatomic linear molecules, we obtained the spectra of all triatomic poly-halide-ions of the type I_3^-, Br_3^-, $(ICl_2)^-$, $(BrICl)^-$, etc. Of triatomic molecules, mention may be made of sulphur dichloride.

We obtained the complete Raman spectra of the tetra-atomic molecules sulphur monobromide, selenium monochloride, and selenium monobromide.

For penta-atomic molecules we have now determined the six fundamental vibrations of iodoform, and the total-symmetrical vibrations (breathing frequencies) of the planar ions I_5^-, Br_5^-, $(ICl_4)^-$.

In addition to work with these simple molecules, we obtained by the same methods the Raman spectra of a number of strongly-coloured substances corresponding to more complicated molecules.

Acknowledgements—I should like to express my gratitude to the National Research Council of Brazil, who supported this work, and to my collaborators ROBERTO FORNERIS, KLAUS HAIN, and OSWALDO SALA.

Spectrochimica Acta, 1956, Vol. 8, pp. 46 to 51. Pergamon Press Ltd., London

Raman spectra and structure of tetratomic sulphur and selenium halides*

H. STAMMREICH and ROBERTO FORNERIS
Department of Physics, University of São Paulo, São Paulo, Brazil

(*Received* 16 *January* 1956)

Abstract—The Raman spectra of S_2Br_2, Se_2Cl_2, Se_2Br_2 have been obtained by excitation with helium and argon radiations in the red and near-infra-red region of the spectrum. The spectra consist of six frequencies corresponding to the six fundamentals of each molecule. A satisfactory assignment of the spectra has been made on the basis of C_{2v} and C_2 symmetry. The known vibrational data of S_2Cl_2 have been reviewed.

WE report in the following paper the Raman spectra of the sulphur and the selenium monohalides of the type S_2X_2 and Se_2X_2 where X represents chlorine or bromine. The existence of fluorides and iodides of this type is doubtful. S_2F_2 has been prepared but cannot be obtained in the pure state since it decomposes readily to give sulphur and the difluoride SF_2.

The Raman spectra of three of the four stable halides have not been obtained previously. The Raman spectrum of S_2Cl_2 has been investigated by MATOSSI and ADERHOLD [1], MEYER [2], VENKATESWARAN [3], MORINO and MIZUSHIMA [4], GERDING and WESTRIK [5], GERDING [6], and MAJUMDAR [7]. The last-mentioned author has also described observations on S_2Cl_2 in the solid state.

BERNSTEIN and POWLING [8] measured the infra-red spectrum of S_2Cl_2 from 2–25 μ; three of the fundamentals of the molecule occur in this region. The structure of sulphur monochloride was investigated using electron diffraction by ACKERMANN and MAYER [9] and by PALMER [10]; MORINO and MIZUSHIMA [4] determined the dipole moment of S_2Cl_2, which was found to be $1{\cdot}0 \cdot 10^{-18}$ e.s.u.

It seems that no spectral data on the other three halides have been published, although at the Oxford Meeting, July 1955, of the European Molecular Spectroscopy Group, Prof. J. A. A. KETELAAR reported the determination of some fundamental vibration frequencies of sulphur monobromide by his method of "simultaneous transition" in mixtures with CS_2, whilst one of the present authors (H. S.) described at the same meeting the determination of the Raman spectrum of the molecule. In the meantime Prof. KETELAAR was kind enough to send us the manuscript of a paper on the simultaneous transition spectrum of S_2Br_2 and CS_2 to be published soon in collaboration with HOOGE and BLASSE [11]. The data obtained by this investigation are in excellent agreement with our Raman values, and we wish to express our gratefulness to Prof. KETELAAR for making his data available to us before publication.

The work of the above-mentioned authors leads to the following conclusions with regard to the structure of sulphur monochloride. The electric moment of the molecule and the number of Raman-active fundamentals exclude the configurations possessing a centre of symmetry, namely the linear and the planar *trans*

* This work was supported by the "Conselho Nacional de Pesquizas" Rio de Janeiro; the authors are grateful for the facilities created by the aid of the C.N.Pq.

VOL. 8 1956/5

form. The remaining possibilities are two planar forms of symmetry C_{2v}, the axial-symmetric top S=S=Cl_2 or the *cis* structure, and one nonplanar form of symmetry C_2 with one Cl atom attached to each S atom and the two Cl–S–S planes forming an angle different from 0 degrees or 180 degrees.

VENKATESWARAN [3] and others observed that the values of Raman shifts corresponding to vibrations involving a stretching motion of the sulphur atoms are incompatible with a double bond S=S; this is confirmed by the results of PALMER [10], who found the S–S distance to be 2·05 Å, corresponding to a single bond. The radial distribution curve of the electron diffraction investigation of the last author indicates clearly a configuration with one Cl atom attached to each S atom, and excludes the *cis* form, but permits no decision between the static right-angled structure and a more or less hindered rotation of the Cl atoms around the S–S axis. However, the work of MAJUMDAR [7] provides a strong evidence for the fact that the structure of S_2Cl_2 in the solid state (at about −170°C) corresponds, at least partially, to S=S=Cl_2.

The final determination of the true structure should be possible by an investigation of the state of polarization of the Raman lines, or possibly by the absorption spectrum of S_2Cl_2 in the far infra-red. The six fundamental vibrations of a molecule with C_{2v} symmetry are all active, both in Raman and in the infra-red, the three symmetric vibrations corresponding to polarized Raman shifts (of type A_1), the three others to depolarized lines (two of type B_1 and the remaining "out of plane" vibration of type A_2). Following the notation used by KOHLRAUSCH [12] and also by GERDING and WESTRIK [5], we designate the symmetric vibrations as ω_1, ω_2, and ω_3, the vibrations of type B_1 as ω_4 and ω_5, and the torsional (out of plane) oscillation as ω_6.

The absence of a plane of symmetry in the molecule belonging to C_2 point group affects the last-mentioned torsional vibration ω_6 so that it will be expected in this case to become inactive in the infra-red and to give a polarized line in the Raman spectrum. The absorption spectrum of S_2Cl_2 in the 100-μ region ($\omega_6 = 102\ cm^{-1}$) should therefore permit the choice between the possible configurations in an unambiguous manner, but the difficulties of this investigation are well known.

The observed Raman spectrum of liquid S_2Cl_2 consists of five lines. MORINO and MIZUSHIMA [4] assumed these five frequencies to be ω_1 to ω_5, and supposed ω_6 to be unobserved. Employing a quadratic potential function with 5 force constants these authors calculated the secular equations for the vibrations of the "right-angled" molecule of symmetry C_2. The numerical values of the force constants calculated by MORINO and MIZUSHIMA are not satisfactory. In particular the force constant $K'_{S\text{-}Cl}$ for the cross term is found to have a value of the same order as the two valence force constants due to an erroneous assignment, since these authors considered the torsional vibration ω_6 as the symmetric vibration ω_1. Using a correct assignment, BERNSTEIN and POWLING [8] obtained a good agreement between observed and calculated frequencies using the same equations.

It is almost certain that the appearance of five instead of six fundamental frequencies in the spectrum of S_2Cl_2 is due to an accidental degeneracy of ω_1 and ω_3, and since the interaction between the two vibrations is weak, no splitting

due to Fermi resonance is observed. This was assumed by GERDING and WESTRIK [5] and by BERNSTEIN and POWLING [8]; the last-mentioned authors succeeded in resolving the infra-red absorption band 443 cm^{-1} into two bands of nearly equal intensity at 438 cm^{-1} and 448 cm^{-1}. We have photographed the corresponding Raman line excited by He 5875·6 Å with large dispersion (19 Å mm^{-1} in the 6000 Å region); the microphotometric trace of the line (Fig. 1) suggests that we have here two overlapping lines.

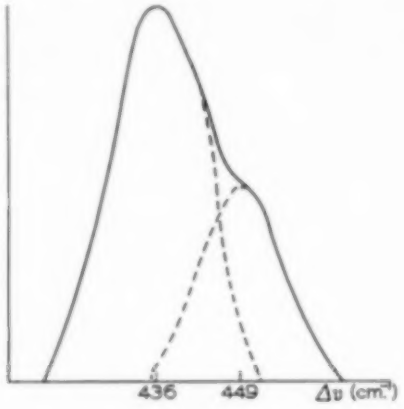

Fig. 1.

The state of polarization of the Raman lines of S_2Cl_2 was investigated by GERDING and WESTRIK [5] who found the line at 106 cm^{-1}, corresponding to the torsional vibration ω_6, to be depolarized. This result indicates the *cis* structure of symmetry C_{2v} or at any rate a configuration not deviating considerably from the *cis* form [13]. On the other hand the results obtained from the electron diffraction by PALMER [10] are inconsistent with this structure and suggest the right angled model of symmetry C_2. BERNSTEIN and POWLING [8], analysing the result of GERDING and WESTRIK, believe that the overlapping of the line 106 cm^{-1} with the background of the exciting line makes it difficult to distinguish between a weakly polarized line and a depolarized line, and conclude in favour of symmetry C_2.

Our Raman spectra of S_2Cl_2 taken with large dispersion show the shift in question at 102 cm^{-1} and completely free from overlapping with the exciting line He 5875·6 Å and, in agreement with GERDING and WESTRIK, we found the line to be depolarized. As our polarization measurements are only qualitative we cannot however exclude the possibility that we have here a weakly polarized line.

In spite of the fact that our investigations of the Raman spectrum of S_2Cl_2 do not contribute significantly to the decision between the configurations C_{2v} or C_2, we have reviewed the known data referring to the structure of the molecule since our measurements of the Raman spectra of sulphur monobromide, selenium monochloride, and selenium monobromide suggest that the four molecules possess an identical structure. This is shown clearly by the rate of decrease of the corresponding frequencies going from S_2Cl_2 to Se_2Br_2 and particularly by comparing

VOL. 8 1956/5

the spectra of S_2Br_2 and Se_2Cl_2. The frequencies of vibrations corresponding essentially to motions of the halogen atoms are to be expected higher in Se_2Cl_2 than in S_2Br_2; and the converse will occur for the other frequencies. This is confirmed by our results which are shown in the following Table 1 together with the complete assignment of the observed Raman shifts. The Raman spectra of the three last-mentioned halides show six lines each, corresponding to the six fundamentals; we have observed no overtones even in strongly over exposed spectra. Nearly all shifts (with exception of ω_4) were observed as Stokes and anti-Stokes lines. For S_2Cl_2 and S_2Br_2 we have included in the table the results of some of the above-mentioned authors in order to compare values obtained by different methods.

All the Raman spectra were excited by helium or argon radiations in the red or near-infra-red region of the spectrum. The experimental details of the technique employed are described by one of us elsewhere in this journal [14]. Qualitative polarization measurements were made in the spectra of the two sulphur halides; unfortunately it was not possible to make these measurements at wavelengths above 7500 Å. Since the selenium halides are nearly opaque for visible light it was necessary in this case to use dilute solutions, and therefore the state of polarization was obtained only for the three strongest lines of Se_2Cl_2.

Since the preparation of the four halides involves no particular difficulties and is described thoroughly in the chemical literature, the methods used will be only briefly described.

S_2Cl_2 was prepared by direct combination of the elements. The crude product was first distilled at normal pressure at about 138°; the first fraction which contained the sulphur dichloride was excluded. The product was then submitted to a vacuum distillation at about 1 mm, and the fraction boiling at 60° employed for the investigation of the Raman spectrum. The light-yellow final product was completely transparent at 5875·6 Å; the yellow helium line was therefore used for excitation.

The Raman scattering of S_2Cl_2 is intense; with the most rapid spectrograph (reciprocal dispersion 100 Å mm^{-1}) a complete spectrum was obtained in 30 sec. The spectra taken with large dispersion, and for which the polarization measurements were made required exposure times up to 150 min. Ordinary plates of high sensitivity, such as Kodak Super Panchro-Press or P 1500 and Ilford HP3 plates were employed.

S_2Br_2 was prepared by heating stoichiometric quantities of sulphur and bromine in a closed tube for some hours at 120°. The product was then purified by fractional distillation at a pressure of about 1 mm. The first fraction containing bromine was excluded, and the middle fraction distilling at 68° was used.

Sulphur monobromide is a garnet red liquid with a transmittance of about 84% at 7065 Å with a 1 cm layer; above 7500 Å it becomes completely transparent. The spectra were excited by helium radiations 7065·2 Å and 7281·4 Å and recorded on Kodak IN plates. Exposure times ranged from 30 min to 4 hours; qualitative polarization measurements were possible for all the Raman lines and required an exposure time of 12 hours.

Se_2Cl_2 was prepared by four different methods:

(1) By action of an excess of chlorine on granulated metallic selenium, $SeCl_4$ was formed and purified by sublimation; $SeCl_4$ and the calculated quantity of powdered metallic selenium were then heated in a sealed tube for some hours at 120°.

(2) Stoichiometric quantities of granulated metallic selenium and liquid chlorine were brought together in a thick-walled glass tube at −70°; the tube was sealed off and warmed up slowly to room temperature and then to 120°.

(3) Red amorphous selenium was added to a solution of selenium dioxide in concentrated hydrochloric acid and then treated with sulphuric acid [15].

Table 1

Vibration	Vibration type of molecule with symmetry		S_2Cl_2			S_2Br_2		Se_2Cl_2	Se_2Br_2
	C_{2v}	C_2	Raman (GERDING and WESTRIK) [5]	*I.R.* (BERNSTEIN and POWLING) [8]	Raman (this work)	*I.R.* and "Simultaneous transition" (KETELAAR, HOOGE, and BLASSE) [11]	Raman (this work)	Raman (this work)	Raman (this work)
ω_6	A_2	A	106(dp)(~6/7)		102(5b)(dp?)		66(7b)(dp?)	87(8)(dp?)	50(10)
ω_2	A_1	A	206(p)(0·7)		206(4)(p)	176(*S.T.*)	172(5)(p)	130(7)(p)	94(3)
ω_5	B_1	B	245(dp)(6/7)		240(2)(dp)	196(*S.T.*)	200(3)(dp)	146(3)	106(7)
ω_1	A_1	A	443(p)(0·4)	438	436(3b)(p)		302(1)(p)	288(2)	204(2)
ω_3	A_1	A		448	449(10b)(p)	354(*S.T.*)	356(10b)(p)	367(10b)(p)	265(10)
ω_4	B_1	B	537(dp)(~6/7)	538	540(1)(dp)	531(*I.R.*)	529(1)(dp)	418(1)	292(1)

VOL. 8 1956/5

(4) A slow stream of chlorine was passed through a suspension of red amorphous selenium in CS_2 until the selenium dissolved completely and precipitation of the insoluble white selenium tetrachloride began.

Attempts were made to purify the crude product by distillation in a high vacuum, but since an appreciable decomposition occurred the compound was simply filtered from the solution in CS_2 through a dense-fritted glass filter in vacuum. Identical spectra were obtained from all samples and it is therefore probable that no impurities were present in disturbing amounts.

Se_2Cl_2 is a brown-red oily liquid the transmittance of which, even in the near infra-red, is not sufficient for the observation of Raman scattering. We used therefore 0·3 and 0·6 molar solutions in CS_2 and C_6H_6 respectively for our purposes. 1 cm layer of the 1 molar solution shows at 6500 Å a transmittance of 47%, and at 7500 Å one of 85%. The spectra were excited by He 6678·2 Å using Kodak 103a F plates and exposures ranged from 30 min to 6 hours; polarization measurements were possible for the three strongest lines with an exposure time of 8 hours.

Se_2Br_2 is the sole selenium bromide stable in the liquid state and therefore easier to prepare than selenium monochloride. The preparation was made by direct combination of the elements in the pure state or in a solvent analogous to the above-mentioned methods (2 and 4) for Se_2Cl_2. It decomposes by distillation in vacuum since the vapour dissociates into $SeBr_2$ and selenium.

Selenium monobromide is a very deep red liquid, nearly opaque to visible light. A 0·25 molar solution in CS_2 or CCl_4 has, at 6650 Å, a transmittance of 21%, at 7050 Å of 48%, and at 8000 Å one of 95%. 0·06 and 0·12 molar solutions in C_6H_6, CS_2 and CCl_4 were used and excited by He 6678·2 and 7065·2 Å and with the argon radiation 8115·3 Å; the spectra were recorded on hypersensitized Kodak IN plates: Due to the low concentration exposure times up to 15 hours were required, and observations on the state of polarization of the Raman lines could not therefore be made.

Our thanks are due to Dr. Kôzô Sone,* of the Aichi College of Liberal Arts, Nagoya, Japan, for his valuable aid in preparing the above-mentioned compounds.

At present, attempts are being made to prepare some "mixed molecules," such as S_2ClBr and $SSeCl_2$, from which better information may be obtained on the state of polarization of the Raman shift corresponding to the torsional vibration of the molecule. These results, together with some theoretical considerations, will be published in a later paper.

References:

[1] Matossi, F. and Aderhold, H.; *Z. Phys.*, 1931, **68,** 683.
[2] Meyer, J.; *Z. anorg. allg. Chem.*, 1931, **203,** 146.
[3] Venkateswaran, S.; *Ind. J. Phys.*, 1931, **6,** 275.
[4] Morino, Y. and Mizushima, S.; *Sci. Pap. Inst. Phys. Chem. Res., Tokio* 1937, **32,** 220.
[5] Gerding, H. and Westrik, R.; *Rev. Trav. Chim. Pays-Bas*, 1941, **60,** 701.
[6] Gerding, H.; *J. Chim. Phys.*, 1948, **45,** 55.
[7] Majumdar, N. C.; *J. Sci. Ind. Res. (India)*, 1949, **8B,** 25.
[8] Bernstein, H. J. and Powling, J.; *J. Chem. Phys.*, 1950, **18,** 1018.
[9] Ackermann, P. G. and Mayer, J. E.; *J. Chem. Phys.*, 1936, **4,** 377.
[10] Palmer, K. J.; *J. Amer. Chem. Soc.*, 1938, **60,** 2360.
[11] Ketelaar, J. A. A., Hooge, F. N., and Blasse, G.; private communication, *Rev. Trav. Chim. Pays-Bas* (in press).
[12] Kohlrausch, K. W. F.; *Der Smekal-Raman-Effekt, Ergänzungsband*, 1931–1937, Berlin 1938, p. 69.
[13] Gerding, H.; *Colloques Internationaux*, 1948, **VII,** Bordeaux, p. 118.
[14] Stammreich, H.; *Spectrochim. Acta*, 1956, **8,** 41.
[15] Lenher, V. and Kao, C. H.; *J. Amer. Chem. Soc.*, 1925, **47,** 772.

* Fellow of the University of São Paulo.

Spectrochimica Acta, 1956, Vol. 8, pp. 52 to 55. Pergamon Press Ltd., London

SPECTROCHEMICAL NOTES

Raman spectrum of iodoform*

H. STAMMREICH and ROBERTO FORNERIS
Department of Physics, University of São Paulo, São Paulo, Brazil

(*Received* 18 *December* 1955)

THE complete vibrational spectrum of iodoform is not known. Incomplete data on the infra-red spectrum were reported by G. EMSCHWILLER and J. LECOMTE [1], P. BARCHEWITZ and M. PARODI [2], and by E. K. PLYLER and W. S. BENEDICT [3], the last-mentioned authors indicating also some Raman frequencies.

At the Oxford Meeting 1955 of the European Molecular Spectroscopy Group, R. M. HEXTER from Cornell University, Ithaca, New York, reported the polarized infra-red spectrum of a single iodoform crystal, and from his observations he made an assignment of the fundamental frequencies of CHI_3. Dr. HEXTER was so kind as to compare his values with the Raman frequencies obtained by the present authors, that were reported by one of us (H. S.) at the same meeting. The infra-red values of HEXTER and our Raman values are in good agreement, and we wish to express our gratitude to Dr. HEXTER for his communication.

Iodoform is an axial-symmetrical tetrahedral molecule belonging to point group C_{3v}. One has to expect, therefore, six fundamentals: three totally symmetric ones (class A_1) and three degenerate ones (class E), all of them being active both in infra-red and in Raman. Following the notation used by PLYLER and BENEDICT [3], we designate the two symmetric C-I vibrations with ω_3 and ω_4, the two degenerate ones with $\omega_{2,5}$ and $\omega_{7,9}$, the symmetric C-H vibration with ω_1, and the degenerate (deformation-) vibration C-H with $\omega_{6,8}$. ω_1, ω_3, and ω_4 correspond to polarized Raman shifts, the degenerate vibrations to depolarized ones.

We succeeded in obtaining the complete Raman spectrum of CHI_3, using an experimental technique described by one of us in this journal [4]. The Raman spectrum was excited by the helium radiations 5875·6 and 6678·2 Å. The optical arrangement has been described already in a previous paper [5]. Iodoform is a good example of the applicability of this technique, since its solutions are strongly coloured and photochemically unstable, and the decomposition products in some solvents are strongly fluorescent.

The chemical and photochemical instability of CHI_3 seems particularly strong in non-polar solvents such as CCl_4 and C_6H_6; on the other hand, solutions in pyridine are very stable, and show, even after prolonged intense illumination, no appreciable darkening. But, since interaction with this later solvent might possibly influence the Raman shifts of CHI_3, we used diethylether, bromoform, and methylenebromide as solvents also. The following samples were investigated:

CHI_3 0·35 molar solution in $(C_2H_5)_2O$ at room temperature
CHI_3 1·3 molar solution in $CHBr_3$ at 50°
CHI_3 1·3 molar solution in CH_2Br_2 at 40°
CHI_3 1·3 molar solution in C_5H_5N at room temperature

* This work has been supported partly by the "Conselho Nacional de Pesquisas," Rio de Janeiro; the authors are much indebted for the facilities created with the aid of the C.N.Pq.

VOL. 8 1956/5

The observed Raman shifts of CHI_3 in the different solvents agree perfectly within the limits of our experimental error, which is, for sharp lines, of the order of ± 1 cm^{-1}.

The Raman shifts corresponding to C-H vibrations, ω_1 and $\omega_{6,8}$, are extremely weak compared with the other ones; we obtained the four lower frequencies with exposure times ranging from 30 min to 2 h, and needed up to 20 h to bring out the Raman lines corresponding to the C-H vibrations. We were therefore unable to make observations on the state of polarization of the last ones, but qualitative polarization measurements were made on the more intense Raman shifts. The following table gives our results, and also the infra-red values of HEXTER, obtained from a single CHI_3 crystal.

Table 1

Vibration	Class	Raman (cm^{-1}) (this work)	Infra-red—HEXTER (priv. com.)
$\omega_{2,3}$	E	105 (10) dp	108
ω_4	A_1	153 (10) p	148–150
ω_5	A_1	437 (4) p	426
$\omega_{7,9}$	E	578 (6) dp	577
$\omega_{6,8}$	E	1067 (0, b) —	1064
ω_1	A_1	3038 (0, b) —	2972

We believe that the values given above constitute the complete fundamental vibrational spectrum and assignment of the iodoform molecule. We are now calculating, from the observed frequencies, the force constants, including several interaction terms, of the molecule, using the method indicated by J. C. DECIUS [6], and we hope to report our results soon in a following paper.

References

[1] EMSCHWILLER, G., and LECOMTE, J.; *J. Phys. Radium*, 1937, **8**, 130.
[2] BARCHEWITZ, P., and PARODI, M.; *J. Phys. Radium*, 1939, **10**, 143.
[3] PLYLER, E. K., and BENEDICT, W. S.; *J. Research N.B.S.*, 1951, **47**, 202.
[4] STAMMREICH, H.; *Spectrochim. Acta*, 1956, **8**, 41.
[5] STAMMREICH, H., FORNERIS, R., and SONE, K.; *J. Chem. Phys.*, 1955, **23**, 972.
[6] DECIUS, J. C.; *J. Chem. Phys.*, 1948, **16**, 214.

Two second-order tellurium lines listed in M.I.T tables as first-order lines

PAULINE J. DUNTON
U.S. Geological Survey, Denver, Colo.

(*Received* 3 *December* 1955; *accepted for publication* 11 *January* 1956)

WHILE searching the spectrum for tellurium lines showing greater sensitivity than those usually used in the ultra-violet region at 2385·76 Å and 2383·25 Å, two tellurium lines were found in the visible region at 4771·56 and 4766·03 Å. These latter lines are listed as first-order lines in the M.I.T. wavelength tables [1]. Line 4771·56 Å proved to be a particularly useful and sensitive line under conditions of analysis in the U.S. Geological Survey. The

method of analysis used is a d.c. arc, semiquantitative method, using carbon powder as a buffer and Eastman III-O plates to record the spectrum [2].

When these two wavelengths were divided by a factor of 2, the resulting wavelengths gave a close correspondence to the ultra-violet first-order lines listed above. Therefore it was evident that the lines found in the visible region are second-order ultra-violet tellurium lines. To check this further, a tellurium spectrum was prepared with a prism spectrograph. The so-called first-order tellurium lines listed at 4766·03 and 4771·56 Å in the M.I.T. wavelength tables were not present.

The use of tellurium lines listed in the M.I.T. tables at 4766·03 and 4771·56 Å allowed detection of as little as 0·08 per cent of the element. Thus, these ultra-violet lines, are more sensitive in the second order than in the first under our experimental conditions.

References

[1] M.I.T. *Wavelength Tables*, John Wiley and Sons, 1939.
[2] Myers, A. T., and Barnett, P. R.; *Amer. J. Sci.*, 1953, **251**, 823.

Photographic film washer*

David C. Manning and W. O. Phillips
Technical Division, Goodyear Atomic Corporation, Portsmouth, Ohio

(*Received* 17 *January* 1956; *accepted for publication* 23 *February* 1956)

Abstract—A specifically designed 35-mm film washer of simple glass construction is described. It provides thorough removal of undesired chemicals from the photographic emulsion.

VOL. 8 1956/5

Introduction

Photographic processing requires that the plate or film be washed after fixation to remove the processing chemicals and soluble silver salts from the gelatin. The washing of plates is provided for in most commercial developing machines. Films are washed by the use of adapters or special holders. Little has been reported on the design of photographic washers specifically for film. In this note an efficient film washer (Fig. 1) of simple glass construction is described. The adaptation of the washer design as the basis for a completely automatic film-processing unit is being investigated.

Construction

The body of the washer, the length of which may be varied, is made from 38-mm I.D. (for 35-mm film) Pyrex tubing flanged at the top for support. The tubing is reduced in diameter at the bottom for a hose connection to the drain. Four slots (Fig. 1) are cut in symmetrical positions around the cylinder 4 cm below the top. An annular chamber with two water inlets is centred on the cut slots. All of the glasswork can be fabricated in approximately two man-hours.

The two inlets are joined by plastic tubing to a glass "Y" which connects to the water supply. One end of the film is attached to the freely suspended clip of a metal cap. A small clip is attached to the other end of the film to keep the film in place during the washing operation.

The washer unit fits into a bench top through a 5·6-cm hole and is held in suspension by a split metal collar.

* This work was performed under Contract AT-(33-2)-1, United States Atomic Energy Commission.

Operation

The wash water enters the pressure-equalizing annular chamber, which feeds the slots, spraying water into the tubing body. Water-flow rates from 2 litres per minute to 10 litres per minute provide efficient operation. At the minimum water rates, a continuous film of water flows quietly down the emulsion. At the higher flow rates, great turbulence can be formed by bleeding air into the tube through the normally sealed cap. This effect, however, was not found to improve the washing action.

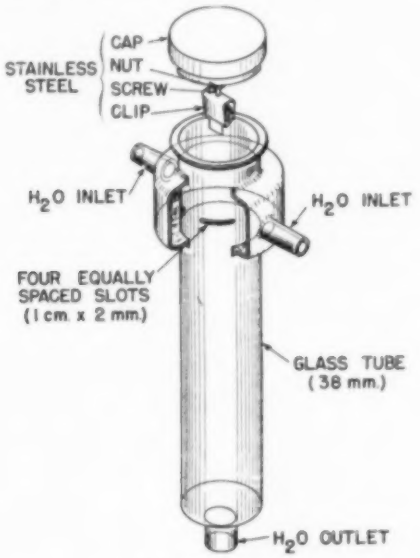

Fig. 1. Film washer.

For minimum water use, it is possible to add a siphon arrangement of the Soxhlet extractor type to the outlet. An air inlet hole in the cap is also required. In this modification the washer alternately fills and empties, providing successive dilution of the wash water. Water-flow rates from one litre per minute down to one-quarter litre per minute may be used.

Acknowledgement—The original design of this washer was proposed by LOUIS E. OWEN of this laboratory.

REPORT OF MEETINGS

Western Spectroscopy Association Third Annual Conference

26 AND 27 JANUARY 1956

PROGRAMME

WILLIAM T. SIMPSON, University of Washington: "Electronic Emission Studies of Cyanine and Triphenylmethane Dyes."

ROBERT A. SATTEN, University of California at Los Angeles: "Problems in the Interpretation of the Spectra of Rare-earth ions in Crystals."

E. BRIGHT WILSON, JR., Harvard University: "Frontiers of Research in Microwave Spectroscopy."

S. I. WEISSMAN, Washington University, St. Louis: "Paramagnetic Resonance Spectra of Free Radicals."

MARTIN PACKARD, Varian Associates: "Instrumental Problems in Paramagnetic Resonance Spectroscopy."

A. MCKELLAR, Dominion Astrophysical Observatory: "Molecules in the Solar System."

JOHN G. PHILLIPS, University of California: "Anomalous Abundances of Elements in the Cool Stars."

VOL.
8
1956/5

Spectrochimica Acta, 1956, Vol. 8, pp. 57 to 65. Pergamon Press Ltd., London

The analysis of heavy water by infra-red spectrometry

J. GAUNT
United Kingdom Atomic Energy Authority,
Atomic Energy Research Establishment, Harwell, Didcot, Berks

(*Received* 15 *March* 1956)

Abstract—Methods are described for the analysis of the deuterium content of heavy water in the concentration ranges 50% D_2O, 3% D_2O, 0·2% D_2O, and the natural range. The accuracy of determination rises from $\pm 2\%$ in the natural range to $\pm 0{\cdot}05\%$ in the 50% range.

The measurements are made directly on the samples without any previous dilution or enrichment, and in consequence the methods developed are suitable for application to continuously flowing plant streams.

Instrumentation for the laboratory and the plant is discussed.

Introduction

IT has already been shown in an earlier paper [1] that the deuterium content of heavy water in the concentration range 99·6–100% W/W D_2O can be estimated with speed and accuracy by means of an infra-red spectrometric technique, and in addition it was also shown that the low concentration range from 0–1% W/W D_2O could be covered by a similar technique. In the production of heavy water it is necessary to monitor over intermediate concentration ranges, and hence suitable techniques have to be developed. Such ranges are likely to be as follows:

(a) ca. 50% D_2O
(b) ca. 3% D_2O
(c) ca. 0·2% D_2O } with increased accuracy over that
(d) Natural range } previously obtained.

In each case an accuracy of measurement of $\pm 1\%$ of the analytical figure is desirable.

The work described in the following sections represents an attempt to fulfil such analytical requirements.

Discussion of methods

In the production of heavy water it would be desirable to have a series of instruments which could not only monitor the product from the various stages of the process but which could also be used as controllers. Such instruments must be rapid in response to be effective, and it is this factor beyond all others which makes the infra-red technique highly desirable. In addition to the requirement for flow analysis, however, instruments are required in the control laboratory. Although such instruments do not require the robust construction and long-term stability as plant instruments, the preliminary investigations which are reported here have been

made with the object of providing laboratory analytical techniques, at the same time bearing in mind the possible extension of these techniques to plant-control. For this reason every effort has been made to use samples of heavy water in the form in which they will be available from the plant. Better methods could probably have been devised by diluting or enriching the samples, as required, to bring them all to a specific concentration range; such techniques, however, would be extremely difficult to carry out in a continuous-flow stream, and were ignored. It was also anticipated at the outset of this work that some difficulty would be experienced in continuously flowing representative samples from a bypass through very thin cells. Consequently, every effort has been made to use cells as thick as possible.

One point of importance which has been observed is the effect of temperature on the absorption coefficient of H_2O/D_2O mixtures. This was first reported by TRENNER and WALKER [2], and although in the present author's previous work this factor was ignored, this was because all the samples used and the spectrometer employed were housed in a thermostatically controlled laboratory. In the present work, however, this has not been the case, and the day-to-day temperature of the laboratory has varied. As a consequence, the effect noticed by TRENNER and WALKER has been confirmed. It has, however, also been noticed that the effect of temperature decreases as the deuterium content of the heavy water increases, and samples of heavy water in the high concentration range are not noticeably affected by quite large temperature variations. Because of the fluctuating temperature, it would have been desirable to use thermostatted cells for this work; but as these were not available, the technique employed has in every case been one in which a complete calibration curve has been drawn up each time a sample was estimated. Although this may seem tedious, it shows very clearly the rapidity of the infra-red method, since it takes only 30 min to draw up a complete calibration curve using five or six standard samples and carry out the estimation of an unknown sample. During this relatively short period, the temperature changes were negligible.

VOL. 8 1956/5

Although in some types of analysis the infra-red method can be made absolute, in the analysis of heavy water this is not the case, and a calibration curve must be drawn up from known standards. The technique involves observing changes in the absorption of a band characteristic of the material to be analysed. The choice of a suitable band is, however, very important and is complicated to some extent in heavy water by the equilibrium which is rapidly established when pure D_2O and pure H_2O are mixed.

$$H_2O + D_2O \rightleftharpoons 2HOD$$

If x g D_2O are mixed with $(100 - x)$ g H_2O, the resultant mixture is defined as containing $x\%$ W/W D_2O. Although this "nominal" figure is often used to define heavy-water samples, the real conditions prevailing in the mixture are rather different from this, and in order to appreciate the problem more fully, calculation of the relative concentrations of the three species is desirable.

The equilibrium constant for the reaction is given by

$$K = \frac{[HOD]^2}{[H_2O]\,[D_2O]} = 3{\cdot}80 \text{ at } 25°C$$

From the experimental data ($W/W\%$), the mole per cent D may be obtained when

$$\frac{[HOD] + 2[D_2O]}{2[HOD] + [H_2O] + [D_2O]} = \frac{\text{mole per cent D}}{100}$$

and

$$[HOD] + [H_2O] + [D_2O] = 100$$

The solution of these equations gives the mole per cent of each component. Typical examples of this are given in Table 1 for the region around 50% W/W.

Table 1. Relationship of H_2O, D_2O, and HOD in heavy water. 50% W/W Range

% D_2O W/W (nominal)	Mole % D	HOD		D_2O		H_2O	
		Mole %	W/W %	Mole %	W/W %	Mole %	W/W %
56·00	53·39	49·13	48·95	28·82	30·23	22·05	20·82
54·00	51·37	49·32	49·25	26·71	28·07	23·97	22·68
52·63	50·00	49·36	49·36	25·32	26·65	25·32	23·99
52·00	49·37	49·35	49·38	24·76	26·02	25·95	24·60
50·00	47·37	49·22	49·35	22·76	24·03	28·02	26·62
48·00	45·38	48·94	49·18	20·91	22·12	30·15	28·70

Similar calculations show that a solution which is nominally 3·0% W/W D_2O comprises 94·377% H_2O, 0·085% D_2O, and 5·538% HOD, by weight. When the deuterium concentration is less than this, the solution contains essentially only the two species H_2O and HOD, and similarly when greater than 97% D_2O, only D_2O and HOD. It is thus obvious that just as measurements based on an HOD absorption band at 2·95 μ gave the greatest sensitivity in the 99–100% W/W D_2O range [1], so the maximum sensitivity will be achieved by making measurements on an HOD absorption band for the 3%, 0·2%, and natural concentration regions.

From Table 1, it is clear that attempts to make measurements on HOD absorption bands will lead to little success in the 48–56% W/W D_2O range, since over this concentration range the HOD concentration is practically constant. On the other hand, both the H_2O and D_2O concentrations vary quite markedly over this range, and measurements on either of these species should give the desired results.

Details of the methods are described below.

50% W/W D_2O *Range*

In this range, the concentration of all three components of the mixture is high, and it consequently becomes necessary to use a weak absorption band in order to obtain measurable intensities. As a fairly high precision is required over a small range of concentration, a differential comparison technique is indicated. The most suitable band for this concentration range was found to be the H_2O absorption centred at 1·445 μ, which is a weak combination band ($\nu_1 + \nu_3$) and is not obscured

by overlapping HOD and D_2O bands. An initial survey on a Hilger H800 double-beam spectrometer showed that a 5-mm glass cell filled with 50% *W/W* D_2O transmitted about 2% at 1·445 μ. This transmission is adequate at this wavelength for carrying out accurate measurements, and the following technique was worked out.

Two 5-mm glass cells were filled with 51·93% *W/W* D_2O and placed at the foci of the two beams in the spectrometer, the slits were opened to 1 mm, and the reference beam trimmed to give about 10% absorption at the peak wavelength. The absorption band was then scanned from 1·39 to 1·47 μ, and the maximum absorption recorded. This was repeated, using different samples of D_2O in the sample cell but maintaining the reference sample at the focus of the reference beam throughout the investigation. In this way a calibration curve was obtained, the relevant figures being given in Table 2.

Table 2. Calibration of spectrometer for 50% *W/W* D_2O region

% *W/W* D_2O	Recorder reading mV at 1·445 μ					Mean value
51·93	8·74	8·80	8·70	8·90	8·65	8·76
51·55	8·37	8·45	8·47	8·50	8·43	8·44
50·71	7·93	7·80	7·80	7·83	7·69	7·81
49·74	6·90	7·05	7·11	7·00	6·84	6·98
48·76	6·25	6·25	6·27	6·17	6·12	6·21
47·81	5·53	5·54	5·54	5·55	5·42	5·52

VOL. 8 1956/5

The samples of heavy water used for this calibration were made up by direct weighing of D_2O and H_2O, and were kept and analysed in a thermostatically controlled room.

In order to test the repeatability of the method, a fresh sample of heavy water was made up by weighing, and analysed as though it was an unknown. The figures are given in Table 3.

Table 3. Analysis of "unknown" sample
(Real value = 51·74% *W/W* D_2O)

Recorder mV	% *W/W* D_2O	
8·68	51·82	Mean = 51·73 ± 0·06
8·68	51·82	
8·66	51·80	
8·62	51·74	
8·58	51·70	
8·58	51·70	
8·62	51·74	
8·52	51·62	
8·52	51·62	
8·63	51·76	

As an alternative to the double-beam differential method, just described, this analysis can also be carried out on a single-beam spectrometer. A Harwell Grating spectrometer [4] was used, employing a lead sulphide cell as detector and a 2400 line-per-inch grating in the second order (blazed for maximum intensity at 3 μ in the first order). The filter for eliminating overlapping orders was an additively coloured alkali halide crystal of the type described by BURNS and GAUNT [5], the transmission starting at 1·2 μ. The results obtained were comparable to those outlined above.

Although the changes in the absorption coefficient due to changes in temperature are small in this region, it is nevertheless still desirable to use thermostatted cells to achieve maximum repeatability. No special precautions were found to be necessary in handling samples of this concentration, and they were treated throughout in a straightforward manner.

3% *W/W* D_2O *Range*

It has already been shown [1] that the range 0–1% *W/W* D_2O can be covered by measurements on the O-D fundamental vibration band of HOD at 3·98 μ, using a 0·25-mm cell. TRENNER and WALKER [2] have also shown that measurements can be made on samples of concentrations up to 5% *W/W* D_2O, using thinner cells. Because of the high concentration of H_2O in samples in this concentration range, it was not possible to make measurements with any accuracy on the HOD band at 1·6 μ, whilst the HOD band at 2·95 μ was totally obscured by the H_2O fundamental occurring at the same wavelength. Attempts were, therefore, made to improve the accuracy of measurements on the 3·98-μ band of HOD. One of the difficulties encountered when working at this wavelength arises from the absorption of H_2O at approximately 3·6 μ. This band is normally weak, but the high concentration of H_2O in the samples develops it into a strong absorption whose wings badly overlap the 3·98-μ HOD absorption band. As a consequence, the sensitivity of measurements on HOD at 3·98 μ is reduced because of the limitation of cell thickness imposed by this high-background absorption.

Two alternative methods of attack were tried, both being single-beam methods. For this work, the Harwell Analytical Grating spectrometer was used, employing a 2400-line/inch grating with an "F-centre" filter which started to transmit at 2·2 μ. A Hilger-Schwarz 8W thermocouple was used as detector with a 300 : 1 matching transformer and Grubb-Parsons 10-c/s amplifier, the output being fed into a 10-mV Brown recorder. The slits were set at 1·0 mm and the grating set to give 3·98 μ in the first order. The amplifier was set to give the maximum workable gain (i.e. maximum tolerable noise). Under these conditions, a 0·25-mm cell containing 3% *W/W* D_2O gave zero transmission and no stray light was detectable. Two alternative techniques were examined.

(1) A standard technique in which various cells were tried, to find the conditions under which a 3% *W/W* D_2O mixture would give rise to a full-scale deflection on the recorder, followed up by sensitivity tests over the range 3·0–3·4% *W/W* D_2O in that cell.

(2) A technique in which a thinner cell than in (1) was used such that when filled with 3·0% *W/W* D_2O it would give rise to an output from the amplifier

equal to $(x + 10)$ mV, and to apply a backing-off potential of x mV so that a full-scale deflection of the recorder was obtained, followed up by sensitivity tests over the range 3·0–3·4% W/W D_2O in the same cell, maintaining a constant back-potential.

Because of the background absorption due to H_2O, there is an optimum cell thickness for this range, and this was found to be 0·07 mm for the second technique, which was found to give much greater sensitivity than the more conventional method [1]; the cell windows were synthetic sapphires.

It was found that measurements in this range were much more influenced by temperature fluctuations than in the 50% range, and it was not found possible to repeat absolute measurements from day to day. In the absence of thermostatted cells, this difficulty was overcome by making observations on a number of standard samples at the same time as the unknown sample and drawing up a fresh calibration curve for each set of readings. Although the absolute readings could not be repeated under these conditions, the total number of points can be placed on a single calibration curve by means of normalizing to standard values. This is shown for five sets in Table 4.

Table 4. Calibration points for 3% W/W D_2O range
(Normalized readings (mV))

% W/W D_2O	*A*	*B*	*C*	*D*	*E*	Mean
3·000	8·98	9·14	9·02	9·19	9·05	9·08
3·146	6·76	6·78	6·78	6·86	6·85	6·81
3·274	4·98	4·95	4·96	4·99	4·90	4·96
3·404	3·41	3·35	3·32	3·31	3·40	3·36
"Unknown"	5·57	5·44	5·53	5·40	5·50	—
			Backing-off potential = 10 mV			

A calibration curve was drawn through these mean points from which the "unknown" values were obtained.

Series	Normalized reading	% D_2O	Mean
A	5·57	$3·23_0$	
B	5·44	$3·24_0$	
C	5·53	$3·23_3$	$3·23_6 \pm 0·00_4$
D	5·40	$3·24_2$	
E	5·50	$3·23_4$	

The real value of the "unknown" sample was $3·23_7$% W/W D_2O.

VOL. 8 1956/5

0·2% *W/W* D_2O *Range and Natural Range*

Because of the low deuterium content of samples in the 0·2% range and the natural range, thicker cells than were needed for the 3% range must be used, and in consequence those factors which influence measurements in the higher range become even more pronounced. By experiment it was found that the identical spectrometric conditions for the 3% range were required for the 0·2% and the natural ranges, with the exception of the cells.

For the 0·2% range a 0·19-mm sapphire cell was required, and for the natural range a 0·25-mm sapphire cell was used, the techniques being identical in both cases with the technique used in the 3% range.

Here again the influence of temperature on the absorption coefficient of the samples was large, and the day-to-day variations were such that the absolute measurements could not be repeated. It was again found convenient to draw up a separate calibration curve for each unknown sample analysed, but all the points recorded can be placed on one curve, as was done for the 3% range.

The results of these investigations are shown in Tables 5 and 6.

Table 5. Calibration points for 0·2% *W/W* D_2O range (normalized readings (mV))

% *W/W* D_2O	*A*	*B*	*C*	*D*	*E*	*F*	*G*	*H*	Mean
0·186	8·62	8·61	8·28	—	8·65	9·20	8·05	7·99	8·48
0·221	5·11	5·24	5·31	5·09	5·20	4·87	5·21	5·22	5·16
0·251	2·51	2·55	2·71	2·52	2·43	2·26	2·88	2·92	2·60
"Unknown"	—	—	—	5·82	5·55	5·31	5·77	5·72	—

Backing-off potential = 25·5 mV

From the calibration curve based on these points, the unknown was estimated.

Series	Normalized reading	% D_2O	
D	5·82	0·214	Mean = 0·216 ± 0·002
E	5·55	0·217	
F	5·31	0·219	
G	5·77	0·214	
H	5·72	0·215	

The real value of this "unknown" was 0·217% *W/W* D_2O

Finally, an attempt has been made to improve the sensitivity of measurement in the very low concentration range, from the natural concentration (0·0167% *W/W* D_2O) to 0·07% *W/W* D_2O. The technique has already been described, and the results are tabulated below.

Table 6. Calibration points for natural range (Normalized readings mV))

% W/W D_2O	*A*	*B*	*C*	*D*	*E*	*F*	*G*	Mean
0·0167	9·4	9·5	10·1	—	—	9·8	—	9·7
0·0234	9·1	9·2	9·3	9·4	9·1	9·4	9·3	9·2
0·0301	8·7	8·7	8·7	8·6	8·6	8·5	8·7	8·6
0·0434	7·1	7·0	6·9	6·9	7·1	6·6	6·9	6·9
0·0667	4·6	4·4	3·9	—	—	—	—	4·3
0·0762	—	—	—	—	—	2·4	2·5	2·4
"Unknown"	8·0	7·9	7·9	7·9	7·9	7·6	7·8	—

Backing-off potential = 30·0 mV

From the calibration curve based on these points, the unknown was estimated.

Series	Normalized reading	% D_2O	
A	8·0	0·0355	
B	7·9	0·0365	
C	7·9	0·0365	
D	7·9	0·0365	Mean = 0·0368 ± 0·0008
E	7·9	0·0365	
F	7·6	0·0390	
G	7·8	0·0375	

The real value of the "unknown" was 0·0367% W/W D_2O

Discussion of instruments

It is obvious from the results of the investigations described in the previous sections that analytical control of the product from the various stages of a heavy-water production plant can be achieved in the laboratory with a fairly high degree of accuracy by means of an infra-red technique. The methods devised are rapid, and require only a small quantity of material (ca. 3 ml) for each estimation.

There is little doubt that the repeatability and accuracy of measurements can be improved by temperature control of the samples and absorption cells.

Although analyses of the type described in this paper, and in the previous one relating to the high concentration range, can be carried out by means of a conventional infra-red spectrometer, to do so would mean the introduction of a number of unnecessary complications to the techniques and would immobilize an otherwise versatile and elaborate instrument. The simplest form of analytical device based on infra-red spectrometry is one which consists of a source, narrow band filter, and detector. Filters of this type are not readily available for most purposes, although it is possible under some circumstances to devise means for

VOL. 8 1956/5

doing this. In the case of the analytical problems in question, suitable filters have not been found, and in consequence some alternative must be sought. This requirement is fulfilled to some extent by the analytical spectrometer described previously [4]. Although this instrument is capable of a degree of resolution somewhat better than conventional prism spectrometers, it was originally designed as a simple monochromator to serve the function of a narrow-band filter, and, in the author's opinion, is best used in that capacity. Instruments of this type have been in operation at Harwell and elsewhere for some considerable time and have proved to be both accurate and reliable. In order to obtain precision results, it is probably better to design a special instrument for each purpose than to use one instrument to cover a wide variety of problems. Therefore, to cover the five ranges of heavy water, as described, on a routine basis, a minimum of three laboratory instruments would be required.

(a) 99% *Range*

An instrument set at 2·946 μ equipped with PbS cell and 800-c/s amplifier, with 0·25-mm silica cells.

(b) 50% *Range*

An instrument set at 1·445 μ (second order), equipped with PbS cell and 800-c/s amplifier, with 5-mm glass cells.

(c) 3%, 0·2%, *and Natural Ranges*

An instrument set at 3·98 μ, equipped with thermocouple and 10-c/s amplifier, using 0·07-mm, 0·19-mm, and 0·25-mm cells with windows of calcium fluoride or synthetic sapphire.

Although instruments of the type envisaged are essentially single-beam devices, the cell-in/cell-out technique employed, in which a "grey" standard is compared against the sample, gives results which are highly reproducible, because the short-period instability of the equipment is very small. If long-term stability is required, it is much better to use self-compensating double-beam devices.

It is only within very recent years that attempts have been made to meet the very rigid requirements of stable plant-control equipment for liquid flow analysis, and this work has been almost exclusively the prerogative of the U.S.A. At present, two general types of equipment are available. In one case a dispersive system is used [6], and the other is of a nondispersive type [7]. This latter type has already been sensitized for use in the analysis of heavy water in the 99–100% range, and preliminary reports are very encouraging. Modified forms of this nondispersive type of instrument could probably be used for the other ranges of heavy-water concentration, as described in this present paper.

References

[1] Gaunt J. *The Analyst* 1954 **79** 580.
[2] Trenner N. R. and Walker R. W. *Perkin-Elmer News* 1952, Vol. 4, No. 1.
[3] Kirschenbaum I. *Physical Properties and Analysis of Heavy Water*. McGraw Hill, New York, 1951.
[4] Gaunt J. *J. Sci. Inst.* 1954 **3** 315.
[5] Gaunt J. and Burns W. G. Institute of Petroleum—Conference on Molecular spectroscopy, 1954, p. 66.
[6] Woodhull E. H., Siegler E. H., and Sobcov H. *Ind. Eng. Chem.* 1954 **46** 1396.
[7] Savitzky A. and Bresky D. R. *Ind. Eng. Chem.* 1954 **46** 1382.

Spectrochimica Acta, 1956, Vol. 8, pp. 66 to 70. Pergamon Press Ltd., London

Eine Methode zur genauen Eichung der Wellenlängen- und Wellenzahlskala von Spektralphotometern

V. v. Keussler
Institut für Physikalische Chemie der Universität Freiburg i.Br

(*Received* 22 *October* 1955)

Abstract—An exact method for photoelectric spectrophotometer wavelength and wave-number scale calibration is described. It consists of photographing the light passed through the exit slit by means of a spectrograph together with an iron comparison spectrum. The exit slit image is rotated by a mirror system to be perpendicular to the spectrograph slit. In this way, for every scale division the corresponding wavelength can be determined and the calibration easily performed with great accuracy.

Die beim Arbeiten mit Spektralphotometern entstehenden Abweichungen der eingestellten Wellenlänge vom richtigen Wert sind durch systematische Fehler der Skalenteilung und des Antriebsmechanismus bedingt. Bei Apparaten mit rein optischer Ablesung fällt die zweite Fehlerquelle naturgemäss fort. Fehler bei der Wellenlängeneinstellung können ferner durch toten Gang der Einstellvorrichtung (bei rein optischer Ablesung nicht vorhanden) und durch physiologische Effekte entstehen. Schliesslich ist die Frage nach der effektiven Bandbreite in den verschiedenen Wellenlängengebieten von grosser Wichtigkeit.

Bisher wurden zur Eichung der Wellenlängen- bzw. Wellenzahlskala vorzugsweise die Linien der Quecksilberlampe verwendet. Ausserdem sind die Emissionslinien des Wasserstoffs sowie die Bogenlinien von Helium und Neon herangezogen worden [1]. Zur Einstellung einer beweglichen Skala in die richtige Lage ist im langwelligen Gebiet das Absorptionsspektrum von Didymglas sehr geeignet, das aus einer Reihe hinreichend scharfer genau vermessener Banden besteht. Im *UV* hat sich die Einstellung auf die scharfe Phenolgasabsorptionsbande 2750 Å bzw. 2693 Å sehr gut bewährt [2]. Da nur eine sehr beschränkte Anzahl geeigneter Spektrallinien bzw. Absorptionsbanden zur Verfügung steht, ist eine Kontrolle für beliebige Wellenlängen nicht möglich. Es ist daher ausgeschlossen, mit Hilfe dieser wenig zahlreichen, teilweise ungünstig gruppierten Linien bzw. Banden eine kontinuierliche Eichkurve zu erhalten, die zur lückenlosen Ermittlung der Korrekturwerte für die einzelnen Skalenteile erforderlich ist. Daher wurde eine Methode entwickelt, welche gestattet, die jeder Ablesung der Skala entsprechende wahre Wellenlänge genau zu bestimmen. Sie macht es auch grundsätzlich möglich, die eingangs gestellte Frage nach der Einstellgenauigkeit sowie die nach der effektiven Bandbreite zu beantworten. Die Methode ist in einer unlängst erschienenen Veröffentlichung des Verfassers [2] kurz erwähnt und inzwischen weiter ausgebaut und verbessert worden.

Eine genaue Bestimmung der einem Skaltenteil entsprechenden Wellenlänge bzw. Wellenzahl ist möglich, wenn man das durch den Austrittsspalt austretende Licht auf den Spalt eines Spektrographen fallen lässt und zusammen mit einem Eisenvergleichsspektrum photographiert. Man kann auf diese Weise bei nicht

VOL.
8
1956/5

allzulangen Belichtungszeiten bequem und verhältnismässig schnell eine Spektralphotometerskala eichen und jeden Skalenteil an das Eisenspektrum anschliessen.

Das aus einem Monochromator austretende Licht stellt ein Gemisch verschiedener Frequenzen dar, d.h. die Wellenzahl nimmt nach der einen Spaltbacke zu, nach der anderen ab oder umgekehrt. Aus diesem Grunde muss der Spalt des Spektrographen zu demjenigen des Monochromators senkrecht orientiert sein. Es ist zu überlegen, ob es in Hinblick auf die für nur eine Wellenlänge kompensierte Krümmung des Spaltbildes zulässig ist, einen sehr schmalen Teil, etwa in der Mitte des Spaltbildes herauszugreifen, während doch beim lichtelektrischen Messen ein grosser Teil des Spaltes mit Licht gefüllt ist. Eine Überschlagsrechnung zeigt aber, dass hierdurch kein merklicher Fehler verursacht werden kann.*

Eine zum Spektrographenspalt senkrechte Orientierung des Bildes des Austrittsspaltes liess sich durch ein "Aufdieseitelegen" des Spektralphotometers nicht erreichen. Es zeigte sich alsbald, dass nach dessen Wiederaufrichten eine geringe Verschiebung der Wellenlänge im ganzen Spektrum eintrat. Aus diesem Grunde wurde das Spaltbild auf *optischem* Wege um 90° gedreht. Es wurde der Quarzspektrograph Qu 24 von Carl Zeiss verwendet.

Die Wirkungsweise der optischen Drehanordnung ist aus Abb. 1 ersichtlich.

OL.
8
6/57

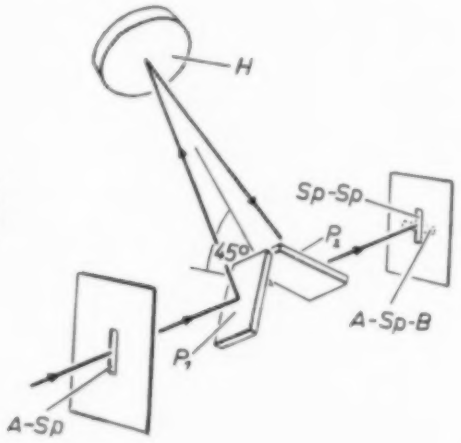

Abb. 1. Spiegelanordung zur Bilddrehung. Die optische Achse des Hohlspiegels *H* ist um 45° gegen die Horizontalebene geneigt.

* Die Krümmung im kontinuierlichen Spektrum hat zur Folge, dass unabhängig von der Breite des Spaltes eine Verschiebung des Schwerpunktes der aus dem Monochromator austretenden Strahlung stattfindet, und zwar im Betrage von $\frac{1}{4}$ der Durchbiegung des gekrümmten Spaltbildes. Unter "Durchbiegung" wird hier die Entfernung des Scheitelpunktes von der die den beiden Endpunkten des Spaltes entsprechenden Bildpunkte verbindenden Sehne verstanden. Gewöhnlich werden die Spalte entsprechend einem Mittleren Brechungsexponenten des Prismenmaterials gekrümmt. Wird dieser Brechungsexponent mit n_0, die dazugehörige Durchbiegung des Spaltes mit Δ_0 bezeichnet, so gilt bei einer einem anderen Brechungsexponenten n entsprechenden Durchbiegung Δ des Spaltbildes

$$\frac{\Delta - \Delta_0}{\Delta_0} = \frac{\frac{1}{n_0^2} - \frac{1}{n^2}}{1 - \frac{1}{n_0^2}}.$$

Daraus folgt, dass der Wert von $\Delta - \Delta_0/\Delta_0$ etwa $\pm 0{,}05$ nicht überschreiten kann. Es ist leicht zu ersehen, dass diese geringe Abweichung bei allen Apparaten zu vernachlässigen ist, und bei der Eichung nach dem angegebenen Verfahren der Spektrographenspalt das Bild des Austrittsspaltes in der Mitte, aber auch an anderen Stellen schneiden kann.

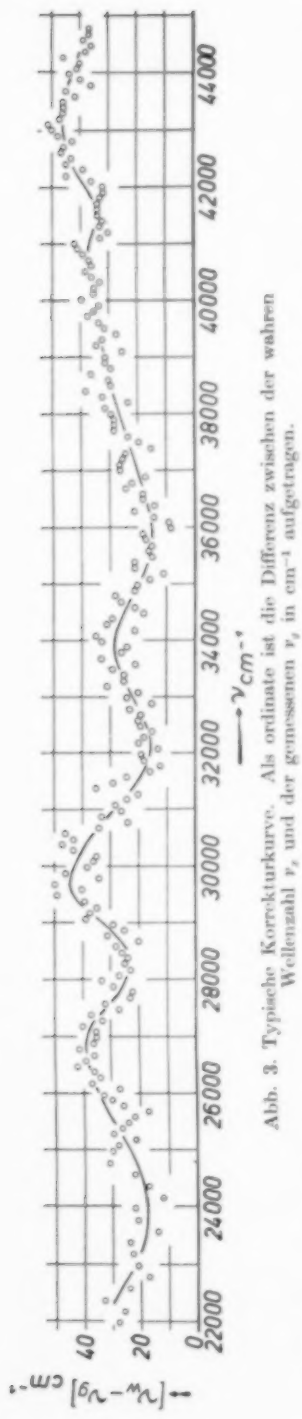

Abb. 3. Typische Korrekturkurve. Als ordinate ist die Differenz zwischen der wahren Wellenzahl ν_g und der gemessenen ν_w in cm^{-1} aufgetragen.

Das den senkrechten Austrittsspalt *A-Sp* verlassende Licht wird von dem Planspiegel P_1 zum sphärischen Hohlspiegel *H* abgelenkt. Die Achse des Hohlspiegels ist um 45° gegen die Horizontalebene geneigt. Nachdem das Licht vom Hohlspiegel zurückgeworfen und vom Planspiegel P_2 nochmals abgelenkt worden ist, entsteht in der mit der Ebene des ebenfalls senkrechten Spektrographenspaltes *Sp-Sp* zusammenfallenden Bildebene des optischen Systems das *horizontale* Bild *A-Sp-B* des Austrittsspaltes. Damit auch im *UV* eine hinreichend starke Reflexion stattfindet, sind alle drei Spiegel mit Aluminium durch Aufdampfen im Vakuum verspiegelt. Die beiden Planspiegel haben eine Grösse von 35 mm × 50 mm, der Durchmesser der freien Fläche des Hohlspiegels beträgt 35 mm. Die Halterungen der Spiegel sind auf einem um 45° geneigten Holzbrett montiert, das an einem auf einer Schiene verschiebbaren Reiter befestigt ist. Jede Halterung ist mit einem Paar Zug- und einem Paar Druckschrauben versehen, die eine sehr genaue und bequeme Ausrichtung der Spiegel gestatten. Der Winkel zwischen dem auf den Hohlspiegel auffallendem Strahl und dem von ihm reflektierten beträgt etwa 8°. Durch diesen Winkel wird ein leichter Astigmatismus hervorgerufen, der aber eher erwünscht ist, damit der auf der photographischen Platte entstehende Lichtfleck eine gewisse Ausdehnung in Richtung des Spektrographenspaltes bekommt. Die Verwendung eines abbildenden Hohlspiegels bringt den Vorteil mit sich, dass die sehr lästige Nachfokussierung entsprechend der jeweiligen Wellenlänge fortfällt.

Eine schnelle und einfache *Justierung* der ganzen Anordnung lässt sich auf folgende Weise erreichen. Zunächst wird nach Entfernen der Kassette des Spektrographen eine mattierte Glühlampe in die Gegend des sichtbaren Spektralbereiches gebracht und der weitgeöffnete Spektrographenspalt auf diese Weise beleuchtet. Sodann wird der Planspiegel P_1 so eingestellt, dass die Mitte des aus dem Spektrographenspalt austretenden Lichtbündels auf die Mitte des Hohlspiegels *H* fällt. Das aus dem Spektralphotometer austretende Lichtbündel wird gleichfalls in der selben Weise durch Neigen des Planspiegels P_2 auf die Mitte des Hohlspiegels geworfen. Sodann wird durch entsprechende Ausrichtung des Hohlspiegels eine Abbildung jedes Teiles des Austrittsspaltes auf den Spektrographenspalt leicht erreicht. Bei dieser Art der Justierung ist eine vollständige Lichtausfüllung der Öffnungswinkel in jedem Falle gewährleistet. Die Abbildung erfolgt im Verhälntis von etwa 1 : 1. Zur Fokussierung wird das ganze Spiegelsystem auf der Schiene bewegt.

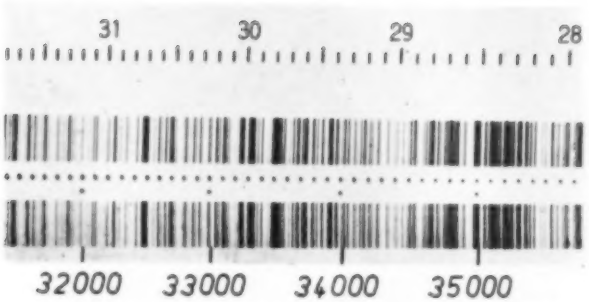

ABB. 2. Ausschnitt auf einer Eichaufnahme. Lichtfleckreihe im unter-erochenen Eisenver gleichs Spektrum. Unten wellenzahlen in cm^{-1}. Skala des quarzspektrographen (0·102 Å).

OL.
8
6/57

VOL.
8
1956/5

Mit Hilfe der beschriebenen Anordnung ist die Wellenlängenskala eines Spektralphotometers mit mechanischer Skaleneinstellung und die Wellenzahlskala eines solchen mit rein optischer Skaleneinstellung geeicht worden. Die Eichung wurde zunächst auf das Gebiet 4555 Å bis 2237 Å beschränkt. Sie lässt sich auch ausserhalb dieses Gebietes unter Zuhilfenahme geeigneter Aufnahmen des Eisenspektrums durchführen. Es wurden "Spektralplatten 450 blau" von Perutz verwendet. Die Belichtungszeiten betrugen bei der Eichung beider Spektralphotometer im Gebiet 4600 Å bis 2800 Å von einigen Sekunden bis zu 1^m, von 2800 Å bis 2350 Å bis zu 2^m und stiegen unterhalb der letztgenannten Wellenlänge bis zu 8^m an. Dabei waren die Spaltbreiten sowohl des Spektralphotometers, als auch des Spektrographen auf 0,03 bis 0,05 mm eingestellt. Es wurde zu jedem Teilstrich der Skala eine Aufnahme des entsprechenden Lichtfleckes auf der Platte gemacht. Um die Koordinierung der Lichtflecke mit den Skalenteilstrichen zu erleichtern, wurden die jeweils einem zehnten Teilstrich entsprechenden Aufnahmen nach Verschiebung des Lichtfleckes durch eine in den Strahlengang eingeführte geneigte planparallele Quarzplatte wiederholt. Ein Ausschnitt aus einer bei der Eichung einer Wellenzahlskala gemachten Aufnahme ist in Abb. 2 wiedergegeben.

Die Bestimmung der zu den Lichtfleckbildern gehörigen Wellenlängen gestaltet sich besonders einfach bei Verwendung eines mit einer Wellenlängenskala versehenen Eisenatlasses (es wurde der von F. Gössler [3] benutzt) und eines Spektrenprojektors, dessen Vergrösserung so eingestellt werden kann, dass sie derjenigen des Atlasses genau entspricht. Die Wellenlängen wurden durch Interpolation zwischen zwei benachbarten den Lichtfleck einschliessenden Teilstrichen der Skala bestimmt. Die zugehörigen Wellenzahlen wurden der Tabelle von H. Kayser [4] entnommen.*

Die für die beiden oben genannten Spektralphotometer erhaltenen Korrekturkurven unterscheiden sich die wenig voneinander. In beiden Fällen liess sich der Verlauf durch Wiederholung der Eichung nach der gleichen Methode reproduzieren. Auch die Einstellgenauigkeiten sind angenähert gleichgross. Eine solche Korrekturkurve ist in Abb. 3 wiedergeben. Eine Periodizität in der Folge der Maxima ist nicht vorhanden. Die Streuung der Messpunkte entspricht der Einstellgenauigkeit einzelner Wellenzahlwerte am Spektralphotometer. Um diese Einstellgenauigkeit festzustellen, wurde eine grössere Anzahl Einstellungen auf den selben Teilstrich vorgenommen und die entsprechenden Aufnahmen auf der gleichen Platte in einem Zwischenraum zwischen zwei Eisenlinien gemacht, wobei der Lichtfleck in der bereits erwähnten Weise durch Neigen einer Quarzplatte verschoben wurde. Für 27800 cm^{-1} (4400 Å) ergab sich für den mittleren Fehler der Einzelmessung (Standartabweichung) der Wert $\pm 5{,}3\ cm^{-1}$, was mit der Streuung der Messpunkte gegen die ausgezogene Kurve ungefähr übereinstimmt. Ein Unterschied der Abweichung von dem Mittelwert in Abhängigkeit davon, ob von links nach rechts oder umgekehrt eingestellt wurde,† konnte nicht festgestellt werden.

* Bei der festgestellten Genauigkeit der Ablesung muss der Einfluss der Luft auf die Wellenlänge berücksichtigt werden. Es ist daher nicht zulässig, einfach Reziproktafeln zu benutzen.

† Einen Hinweis auf diesen möglicherweise auftretenden Effekt verdanke ich Herrn Dr. H. J. Höfert. Er tritt bei der benutzten Dispersion offenbar nicht auf und mag vorzugsweise subjektiver Art sein.

Zum Schluss möchte ich dem Institutsvorstand Herrn Prof. Dr. R. MECKE für sein Interesse, der Gesellschaft zur Förderung der Spektrochemie und angewandten Spektroskopie für die Ermöglichung der Arbeit meinen besten Dank aussprechen.

Zusammenfassung

Der Austrittsspalt des Spektralphotometers wird durch ein drehendes Spiegelsystem auf den Spalt eines Spektrographen so abgebildet, dass sein Bild horizontal und zum Spektrographenspalt senkrecht liegt. Die den einzelnen Teilstrichen der Spektralphotometerskala entsprechenden Wellenlängen bzw. Wellenzahlen werden nacheinander eingestellt und die auf der photographischen Platte entstehenden monochromatischen Spaltbilder zusammen mit einem Eisenvergleichsspektrum aufgenommen. Auf diese Weise ist es leicht möglich, die Skala mit grosser Genauigkeit an das Eisenspektrum anzuschliessen.

Literatur

[1] GIBSON K. S. und BALCOM M. M. *Res. Bu. St.* 1947 **38** 601.
[2] KEUSSLER V. v. *Z. Elektrochem. u. angew. phys. Chem.* 1954 **58** 136.
[3] GÖSSLER F. *Bogen- und Funkenspektrum des Eisens*. Jena 1942.
[4] KAYSER H. *Tabelle der Schwingungszahlen*. Leipzig 1925.

VOL.
8
1956/5

Spectrochimica Acta, 1956, Vol. 8, pp. 71 to 87. Pergamon Press Ltd., London

The spark spectrum of americium

R. P. THORNE
Atomic Energy Research Establishment, Harwell, Didcot, Berks*

(*Received* 17 *March* 1956)

Abstract—The wavelengths of some thirteen hundred lines of the spark spectrum of americium have been measured in the spectral range 2500–8000 Å. Below 5000 Å they were recorded in the third order of a Baird three-meter grating spectrograph, with an estimated accuracy of ±0·03 Å. Wavelengths above 5000 Å were determined in the first order with an accuracy of ±0·1 Å. The spectrum consisted of a number of strong and a multitude of weaker lines. Some of the lines recorded at the higher dispersion were resolved into flag patterns.

Introduction

WHEN this investigation opened in 1953, the only published wave length data of the americium spectrum was that of TOMKINS and FRED [1], whose main object was to obtain a list of lines for use in spectrochemical analysis. Examination of the spectrum of americium submitted for spectrochemical analysis at the Atomic Energy Research Establishment, Harwell, revealed that certain of these lines were absent and others less intense than reported

About one milligram of purified americium became available, which enabled a systematic study to be made of its spectrum. About two hundred and thirty americium lines were measured by the author [2].

This preliminary work showed that many of the strongest lines reported by TOMKINS and FRED [1] were either impurity lines or lines from overlapping orders. No lines were found in the infra-red, due to the low concentration of americium on the electrodes. The information obtained yielded an important wave-number difference of 2598,† which is believed to determine the ground state of Am-II. This difference has been independently reported by FRED and TOMKINS [3].

It was decided that when more americium became available an extensive investigation would be made of its spectrum with the object of compiling sufficient information for the term analyses of Am-I and Am-II. The first part of this programme, which is summarized here, was to repeat the previous spark work at higher dispersion with a greater concentration of americium on the electrodes.

Experimental

The "copper spark" technique of FRED, NACHTRIEB, and TOMKINS [4] was used to obtain the spectra. For each spectrum, 600 μg of americium were excited by an A.R.L. multi-source unit, the Feussner-type high-wattage source used for the preliminary work [2] being no longer available. For the spectral range 2500–5000 Å, third-order spectra were taken on the Baird three-meter grating spectrograph. Wavelengths in excess of 5000 Å were recorded in the first

* Now at U.K.A.E.A. Industrial Group, Capenhurst.
† R. P. THORNE, unpublished work, 1953.

order. After each exposure the plate mask was closed to about 2 mm and an iron arc superimposed. Details of the spectral ranges and the photographic plates and optical filters used to eliminate overlapping orders, are listed in Table 1.

Table 1. Optical filters

Range	Order	Photographic plate	Filter
2470–2930	Third	Ilford ordinary	1 cm Backstrom filter solution
2760–3210	Third	Ilford ordinary	1 cm Backstrom filter solution
3140–3590	Third	Ilford ordinary	0·5 cm $CuSO_4 \cdot 5H_2O$. 12·5 gm/litre solution 0·5 cm Backstrom firm solution
3520–3960	Third	Ilford ordinary	1 cm 6% $Co(No_3)_2 \cdot 6H_2O$. Solution
3890–4320	Third	Ilford ordinary	Corning 738 filter
4260–4690	Third	Ilford ordinary	Corning 738 filter
4620–5040	Third	Astra III	Corning 3389 filter
4810–6210	First	Astra III	Corning 738 filter
5980–7360	First	Ilford L.R.S.	Corning 3389 filter
7130–8510	First	Kodak II N	Corning 2418 filter

To eliminate possible errors due to extraneous orders, the filter efficiency was checked by making weaker exposures with the optical filters removed. Filtered and unfiltered spectra were compared, and in no instance did strong lines from other orders coincide with weak lines in the filtered plates.

Each spectrum consisted of an americium spectrum 1 cm wide with a 2-mm wide centrally superposed iron spectrum. A trace of each of the three resulting sections was recorded on a Hilger recording microphotometer. Both upper and lower portions of the spectrum were recorded, to eliminate errors due to plate imperfections. The central portion enabled the wavelengths to be measured by linear interpolation relative to the iron spectrum.

VOL. 8 1956/5

Results

Some 1300 lines of the americium spark spectrum are listed in Table 2. Each line has been checked for impurity interference by reference to the Massachusetts Institute of Technology's Wavelength Tables [5] and to the Spectra of the Heavy Elements [1]. Spectra were taken of the main impurities, Fe, Cr, and Mg, under identical experimental conditions. By visual comparison of intensities, lines due to these foreign elements were eliminated.

Any movement of the iron reference spectrum relative to the americium spectrum on the same plate has been determined by the measurement of impurity and electrode material lines. When any bias was found, the greatest being 0·03 Å, the wavelengths have been corrected. By repeated measurements of selected lines it was concluded that those wavelengths measured in the third order are accurate to $\pm 0{\cdot}03$ Å. Above 5000 Å the accuracy figure should be better than 0·1 Å; the error may increase slightly at the highest wavelengths due to the low population of reference lines.

No attempt was made to make absolute measurements of line intensities, the figures quoted in Table 2 are by visual inspection and corrections have been applied for overlapping plates.

Table 2. The spark spectrum of americium

Wavelength	Intensity	Wavelength	Intensity
2548·05	10	2722·38	100
2572·71	40	2723·66	100
2585·38	20	2725·12	10
2586·28	20	2725·27	200
2590·96	10	2726·41	40
2614·10	20	2726·83	20
2620·12	20	2728·32	40
2643·36	10	2728·67	500
2650·55	10	2731·78	30
2650·62	40	2731·93	200
2655·00	80	2732·13	50
2656·97	10	2734·91	20
2661·48	20	2735·20	10
2662·85	10	2735·46	200
2665·44	10	2737·11	80
2668·66	20	2737·83	80
2682·34	50	2738·32	50
2686·41	20	2740·03	40
2686·77	50	2740·24	40
2687·37	30	2740·54	10
2687·43	10	2740·93	10
2690·14	100	2741·35	50
2696·33	250	2742·30	100
2696·99	50	2743·49	20
2697·36	10	2749·75	100
2697·54	100	2750·31	80
2697·71	10	2750·59	20
2698·57	10	2751·05	80
2698·67	10	2751·41	10
2700·40	100	2752·47	10
2704·15	10	2753·46	10
2705·24	100	2755·14	1000
2706·30	250	2756·52	1000
2706·97	40	2757·08	20
2707·17	40	2758·21	10
2712·61	10	2758·88	70
2712·73	10	2759·21	10
2713·89	200	2760·00	10
2714·14	10	2760·19	10
2714·72	20	2760·87	20
2714·90	10	2761·34	40
2715·13	10	2762·03	10
2715·94	10	2762·17	40
2716·02	10	2762·54	100
2716·43	200	2763·12	80
2716·89	20	2764·76	20
2717·37	30	2765·03	20
2720·38	20	2765·35	10
2721·29	40	2765·58	10

Table 2 (*continued*)

Wavelength	Intensity	Wavelength	Intensity
2765·96	20	2796·06	10
2767·08	20	2796·49	10
2767·38	20	2796·81	250
2769·55	50	2798·53	10
2770·20	50	2798·73	10
2770·58	80	2798·85	10
2771·08	80	2799·12	100
2771·74	10	2799·96	10
2771·90	20	2800·57	10
2772·44	100	2803·12	10
2774·16	10	2803·23	10
2775·97	200	2804·36	20
2776·36	250	2805·63	20
2776·71	20	2805·81	20
2776·99	20	2806·07	20
2778·86	20	2806·44	10
2779·03	10	2806·66	10
2779·56	10	2807·81	100
2779·67	10	2808·40	10
2781·04	10	2808·52	20
2781·18	20	2810·32	100
2781·42	10	2810·68	100
2781·69	10	2810·83	10
2782·03	10	2811·04	10
2782·39	10	2811·40	10
2782·57	10	2811·53	10
2783·91	50	2812·08	250
2784·30	100	2812·74	10
2784·48	80	2812·93	1000
2784·88	20	2813·84	10
2785·18	10	2813·96	20
2785·41	10	2814·25	10
2786·08	100	2814·72	20
2786·30	20	2815·28 HFS	500
2786·70	20	2815·98	500
2786·80	20	2816·45	400
2787·36	10	2816·81	40
2787·85	10	2816·96	10
2788·19	20	2817·71	20
2789·04	10	2817·81	10
2789·63	10	2818·12	10
2791·59	50	2818·32	10
2791·82	30	2818·51	10
2792·54	50	2818·88	40
2793·44	10	2819·13	10
2793·60	10	2819·27	10
2793·83	20	2819·45	10
2794·08	20	2819·58	10
2794·80	50	2820·03	40

VOL. 8 1956/5

Table 2 (*continued*)

Wavelength	Intensity	Wavelength	Intensity
2820·49	20	2844·11	10
2820·97	10	2844·40	50
2821·11	40	2844·79	40
2821·36	10	2845·20	10
2821·52	10	2846·34	10
2822·45	10	2846·50	10
2822·84	20	2846·84	10
2823·77	10	2847·16	10
2824·69	20	2847·65	10
2825·13	50	2847·87	80
2825·36	40	2848·83	10
2826·24	10	2849·02	10
2826·42	20	2849·27	10
2826·84	200	2849·64	100
2827·20	20	2849·75	20
2827·66	40	2850·02	10
2828·09	40	2850·07	10
2828·41	40	2850·46	80
2828·67	40	2850·76	20
2829·40	10	2850·96	10
2829·76	50	2851·63	10
2830·02	10	2852·46	20
2830·38	10	2852·53	10
2830·60	10	2852·97	20
2830·98	50	2853·40	20
2831·23	400	2853·72	20
2831·54	20	2854·03	20
2832·26	10,000	2854·33	50
2832·93	10	2854·66	10
2833·22	10	2854·95	20
2833·94	100	2855·86	10
2834·33	50	2856·07	20
2834·60	50	2856·46	10
2835·37	50	2856·63	10
2836·47	50	2857·01	20
2836·86	50	2857·13	10
2838·35	80	2857·36	20
2839·19	10	2857·77	50
2839·61	10	2858·08	50
2840·23	50	2859·17	10
2840·49	10	2859·32	100
2840·86	40	2860·73	10
2841·10	10	2861·29	10
2842·04	40	2861·53	100
2842·29	10	2861·90	200
2842·48	100	2862·68	10
2842·58	10	2863·02	10
2843·03	10	2863·14	10
2843·77	10	2863·98	10

Table 2 (*continued*)

Wavelength	Intensity	Wavelength	Intensity
2864·27	10	2888·87	100
2864·88	50	2889·60	100
2865·51	100	2889·95	10
2865·99	10	2891·64	20
2866·17	200	2891·96	10
2866·89	10	2892·47	80
2867·33	50	2893·08	10
2867·86	30	2893·27	500
2868·24	30	2893·70	100
2868·55	20	2894·27	50
2869·36	10	2894·39	50
2869·81	10	2894·61	100
2870·04	10	2895·42	10
2870·26	80	2895·57	20
2870·75	50	2896·02	20
2871·16	20	2896·13	80
2871·41	10	2896·50	10
2871·70	10	2896·86	20
2872·31	10	2897·37	100
2872·67	20	2897·65	20
2872·85	80	2897·84	20
2873·26	800	2898·25	10
2873·65	20	2898·68	50
2874·64	20	2899·07	50
2874·97	10	2899·56	500
2875·23	10	2900·47	10
2875·74	40	2900·78	10
2876·39	10	2901·21	10
2876·70	80	2901·50	50
2876·81	10	2902·18	10
2877·48	40	2902·51	20
2878·76	10	2902·70	20
2878·90	50	2903·10	10
2879·20	20	2903·29	10
2879·64	40	2903·63	10
2880·15	20	2903·78	10
2882·01	10	2904·04	100
2882·46	80	2904·39	50
2883·38	40	2905·33	10
2884·69	10	2905·55	10
2884·93	10	2905·86	20
2885·31	10	2906·17	100
2885·47	10	2906·72	20
2886·58	50	2907·56	20
2886·87	50	2907·86	10
2887·20	80	2908·21	10
2888·02	100	2908·54	10
2888·25	20	2908·87	10
2888·49	2000	2909·47	10

VOL. 8 1956/5

Table 2 (*continued*)

Wavelength	Intensity	Wavelength	Intensity
2909·84	100	2935·17	20
2910·45	100	2935·47	10
2911·13	2000	2935·84	10
2912·10	10	2936·13	10
2912·86	80	2936·98	1000
2913·44	20	2937·21	20
2913·74	10	2938·19	20
2914·04	10	2939·04	300
2914·69	10	2939·34	20
2914·97	10	2940·55	20
2915·08	10	2941·02	20
2915·24	10	2941·77	20
2915·43	10	2942·30	20
2915·76	50	2942·43	20
2916·32	10	2942·82	10
2916·53	10	2943·36	20
2916·81	80	2943·82	20
2917·21	10	2945·19	80
2917·57	100	2946·10	20
2918·34	80	2946·41	20
2918·90	100	2948·99	10
2919·32	500	2950·40	100
2919·65	20	2951·53	10
2920·09	20	2952·10	40
2920·60	5000	2952·69	20
2921·09	10	2953·27	10
2921·60	10	2953·39	10
2922·58	20	2954·32	20
2922·91	10	2955·67	50
2923·19	10	2955·93	20
2923·95	10	2957·04	2000
2924·37	10	2957·52	10
2925·65	10	2957·67	10
2926·42	10	2958·46	250
2926·56	10	2958·79	10
2926·79	10	2959·02	100
2927·51	1000	2959·62	10
2927·91	10	2961·97	10
2928·05	40	2962·25	20
2929·21	10	2962·60	10
2929·47	50	2962·96	50
2930·24	10	2963·08	50
2930·43	10	2963·51	50
2931·96	10	2963·84	80
2932·92	20	2965·65	80
2933·03	20	2966·08	50
2933·89	20	2966·73	4000
2933·98	20	2967·07	10
2934·21	10	2968·11	10

Table 2 (*continued*)

Wavelength	Intensity	Wavelength	Intensity
2969·31	5000	3005·49	10
2969·79	10	3005·96	10
2970·68	100	3007·37	50
2971·23	100	3007·63	20
2971·91	100	3009·30	10
2972·56	4000	3010·33	10
2974·14	10	3012·59	250
2974·63	10	3013·52	10
2975·31	20	3013·74	10
2975·79	20	3014·12	10
2976·01	10	3014·64	10
2976·98	150	3016·33	10
2977·16	10	3017·17	10
2977·47	40	3018·12	20
2977·74	10	3023·75	40
2978·41	50	3025·67	20
2979·15	20	3025·73	10
2979·79	50	3026·92	10
2980·12	10	3027·22	20
2981·09	100	3028·00	3000
2981·80	20	3028·87	250
2982·18	20	3030·37	100
2982·50	10	3030·94	10
2985·10	20	3031·19	10
2985·54	10	3032·03	10
2985·64	10	3032·47	20
2986·20	20	3034·10	10
2986·31	20	3035·63	10
2987·25	2000	3036·70	10
2988·05	10	3038·38 HFS	2000
2988·52	20	3040·52	20
2989·07	20	3042·54	10
2989·30	20	3043·03	80
2989·93	10	3043·48	10
2990·13	10	3043·66	80
2990·50	10	3044·10	10
2990·95	10	3045·80	20
2991·21	10	3048·92	20
2992·01	20	3050·25	80
2993·51 HFS	800	3051·48	10
2994·07	10	3053·72 HFS	1000
2996·49	10	3054·41	10
2996·79	10	3056·59	10
2997·02	20	3059·01	40
2999·13	100	3059·61	10
3001·01	10	3060·18	10
3001·63	10	3062·35	10
3004·25	3000	3062·54	10
3004·74	50	3064·02	10

VOL. 8 1956/5

Table 2 (*continued*)

Wavelength	Intensity	Wavelength	Intensity
3065·35	10	3133·02	20
3066·38	10	3133·46	20
3066·66	10	3134·60	10
3066·79	10	3135·17	20
3068·00	50	3135·59	20
3071·30	1000	3136·83	10
3072·09	250	3140·71	10
3074·67	250	3144·20	10
3076·19	50	3145·38	10
3079·83	10	3145·56	10
3080·61	20	3148·40	40
3083·28	50	3148·78	20
3085·06	30	3149·59	10
3085·86	40	3150·23	20
3086·93	50	3151·02	10
3087·31	50	3152·33	10
3090·06	10	3153·39	20
3091·61	10	3154·34	20
3092·29	10	3159·01	20
3095·20	80	3160·49	200
3095·71	10	3161·85	3000
3096·01	10	3164·73	10
3096·27	10	3164·87	20
3096·81	80	3167·44	50
3097·26	20	3167·87	1500
3097·87	50	3170·17	10
3101·14	20	3171·09	10
3102·39	50	3172·01	10
3102·75	20	3172·51	10
3103·26	20	3173·56	10
3104·01	50	3174·03	10
3105·20	20	3177·47	20
3105·73	200	3177·65	20
3106·88	10	3180·58	10
3111·33	10	3182·48	10
3112·05	20	3186·39	10
3113·79	100	3190·13	50
3114·89	10	3190·27	50
3116·00	80	3199·30	80
3116·65	80	3200·38	80
3117·75	20	3200·59	80
3120·51	5000	3202·76	40
3121·80	50	3203·26	800
3127·19	10	3204·55	20
3127·54	10	3206·00	20
3127·84	10	3208·98	10
3129·72	10	3209·18	100
3130·28	50	3213·13	20
3130·63	10	3216·67	50

Table 2 (*continued*)

Wavelength	Intensity	Wavelength	Intensity
3216·93	50	3410·72	100
3217·80	100	3415·97	250
3218·55	80	3418·94	50
3221·51	100	3419·42	50
3221·77	80	3419·68 HFS	1000
3226·39	80	3420·64	200
3229·60	40	3428·03	400
3233·21	80	3431·57	200
3234·31	80	3432·03	100
3254·50	80	3435·58	50
3258·73 HFS	200	3439·81	5000
3260·07	100	3441·81	100
3264·39	100	3446·20	500
3264·82	80	3448·21	500
3266·46	80	3451·29	1000
3281·26	100	3452·08 HFS	2000
3282·34	500	3453·66	50
3286·68 HFS	1000	3456·23	50
3297·03	50	3476·95	50
3304·44	50	3483·35 HFS	1000
3305·01	50	3484·80	100
3310·73	50	3486·54	100
3313·89	500	3509·57	250
3324·64	500	3510·16	500
3325·51	500	3530·96	100
3335·71	200	3533·27	50
3342·79	100	3534·96	80
3347·95	80	3538·25	50
3348·92	100	3542·77	250
3362·57 HFS	1500	3543·68	50
3372·59	80	3544·42	20
3373·03	200	3548·07	500
3374·00	50	3549·57	40
3378·67	100	3551·89	10
3384·08	80	3552·81	20
3385·93	50	3559·62 HFS	500
3387·48	250	3561·89	500
3388·09	200	3562·70	5000
3391·82	100	3566·16	250
3392·18	1000	3568·00	20
3394·00	100	3569·18	1500
3394·94	1000	3572·96	20
3398·50	250	3573·70	3000
3398·95	100	3575·22	100
3399·07	20	3579·92	10
3403·27	500	3580·25	20
3403·97	200	3582·59	200
3405·11	300	3584·09	20
3409·40	100	3584·36	2000

VOL. 8 1956/5

Table 2 (*continued*)

Wavelength	Intensity	Wavelength	Intensity
3586·15	10	3631·72	40
3587·34	10	3632·09	40
3588·49	200	3633·58	10
3589·08	10	3633·79	50
3589·72	40	3634·19	10
3589·93	50	3634·48	10
3590·36	20	3635·75	10
3591·73 HFS	100	3636·94	50
3592·49	10	3637·53	100
3592·91	10	3637·89	10
3593·04	10	3638·09	10
3593·30	10	3638·67	10
3593·74	20	3639·85	20
3594·13	20	3641·00	100
3594·37	10	3643·04	100
3594·96	500	3643·70	10
3596·03 HFS	500	3644·06	10
3600·84	50	3644·19	10
3602·75	10	3644·70	10
3603·02	10	3646·43	10
3603·44	500	3646·84	10
3604·88	50	3646·95	10
3607·59	80	3647·20	200
3608·17	80	3648·29	20
3609·87	20	3648·84	20
3610·73	80	3650·32	100
3611·36	50	3652·42	100
3612·62	100	3653·49	250
3614·99	20	3654·03	200
3616·27	10	3655·07	200
3616·55	10	3657·90	10
3616·96	10	3658·11	10
3617·19	50	3658·27	20
3617·59	500	3659·03	750
3618·38	50	3660·47 HFS	100
3621·80	200	3662·71	50
3622·56	20	3662·97	10
3622·87	80	3663·20	20
3623·28	100	3664·19	100
3626·24	10	3665·25	10
3626·50	10	3666·45	10
3627·92	10	3667·00	10
3628·74	10	3667·18	20
3629·03	10	3668·69	50
3629·20	10	3669·04	20
3629·92 HFS	200	3669·19	50
3630·36	20	3669·86	10
3630·60	50	3672·41	10
3630·87	50	3673·11	2000

Table 2 (*continued*)

Wavelength	Intensity	Wavelength	Intensity
		3759·22	200
3674·40	10	3761·69	1500
3675·40	10	3762·84	10
3675·54	10	3764·04	20
3676·35	200	3764·63	50
3677·92	50	3766·36	20
3683·48	2000	3769·12	80
3683·63	10	3776·93	80
3684·56	250	3777·50 HFS	5000
3687·98	100	3782·39	20
3691·46 HFS	100	3782·61	10
3693·05	50	3782·71	20
3695·52 HFS	200	3783·02	50
3696·42 HFS	5000	3783·55	10
3701·06	10	3783·84	10
3701·27	20	3787·77	100
3702·58	200	3789·03	50
3704·93	50	3793·23	100
3705·77	2000	3793·35	10
3706·18	1000	3793·58	100
3706·28	1000	3796·01	100
3706·34	500	3796·75	50
3707·86	2000	3798·33	100
3709·02	20	3799·62	50
3709·84	20	3801·38	50
3711·24	10	3801·74 HFS	1000
3712·44	250	3802·83	10
3713·21	40	3803·03	80
3713·49	40	3806·22	20
3714·47	20	3806·46	10
3720·56	200	3807·94	10
3721·20	150	3808·14	10
3726·05	40	3809·17	20
3726·23	20	3814·86	10
3726·43	250	3816·14	40
3726·95	40	3817·13	10
3732·82	200	3817·66	10
3737·77	80	3818·64	10
3739·75	20	3819·25	10
3740·42	250	3820·96	80
3742·20	80	3825·23	10
3751·03	100	3828·86	10
3751·13	20	3831·82	10
3752·05	10	3833·66	10
3752·68	250	3837·53	20
3753·25 HFS	1000	3844·72	20
3753·66	10	3845·47	10
3755·87	50	3861·07	750
3756·12	50	3862·78	250
3757·78 HFS	1000	3867·40	20

VOL. 8 1956/5

Table 2 (*continued*)

Wavelength	Intensity	Wavelength	Intensity
3870·18	80	4009·17 HFS	250
3872·76	50	4013·70 HFS	200
3892·98	100	4017·91	80
3901·57	100	4019·67	250
3904·27	80	4020·24	20
3907·90	50	4021·24	50
3914·93	20	4026·12	10
3921·80	10	4027·44	250
3922·46	50	4027·86 HFS	250
3923·25	50	4032·85	100
3926·25 HFS	5000	4033·56	100
3929·62	10	4036·36	3000
3936·33	10	4039·06	10
3936·57	10	4039·25	10
3943·81	200	4039·63	10
3944·45 HFS	200	4041·25	10
3946·03	80	4041·74	10
3948·02	10	4042·15	10
3949·57	50	4042·90	200
3952·57 HFS	500	4044·93	20
3953·83	10	4045·18	50
3956·75	100	4045·72	50
3958·42	10	4057·90	20
3958·80	10	4062·82	250
3960·55	10	4064·58	10
3962·05	10	4065·53	10
3963·24	50	4066·31	10
3965·15	10	4069·79	250
3966·25	50	4071·27	10
3966·58	50	4078·09	10
3966·80	50	4079·38	10
3972·56	10	4083·40	10
3972·72	10	4085·33	10
3973·07 HFS	500	4085·62	10
3975·23	100	4089·24 HFS	5000
3982·37	10	4089·77	10
3983·12	10	4095·02	10
3984·68	10	4098·98	10
3987·55	10	4099·49	10
3991·03	10	4102·19	100
3991·94	200	4106·97	100
3994·11	10	4108·75	50
3995·81	400	4109·88	100
3996·66	10	4121·25	20
3998·35	10	4124·43	100
3998·44	10	4128·93	20
3998·71	10	4130·70	10
4000·57	100	4136·67	10
4006·27	20	4144·02	80

Table 2 (*continued*)

Wavelength	Intensity	Wavelength	Intensity
4146·88	10	4509·21	1000
4147·95	10	4509·49	3000
4152·53	10	4511·21	200
4154·70	80	4512·02	100
4162·47	10	4519·84	200
4164·54	10	4520·32	80
4178·34	100	4550·40	200
4179·09	100	4563·53	250
4188·13 HFS	4000	4573·70	20
4193·68	10	4575·57 HFS	5000
4197·46	20	4576·79	50
4197·91	20	4593·28	500
4200·03	50	4600·42	50
4233·61	10	4605·57	50
4234·04	20	4608·88	20
4261·80	10	4615·45	20
4261·89	10	4639·53	250
4262·37	100	4645·03	100
4265·54	2000	4660·64	200
4273·25	50	4662·80	2000
4282·40	10	4680·15	50
4289·29	1500	4681·67	1000
4300·97	20	4699·65 HFS	5000
4302·48	20	4706·80	500
4302·85	80	4712·17	100
4309·66	1000	4721·84	10
4324·56	5000	4723·30	20
4335·65	50	4725·65	20
4337·18	50	4727·32	100
4341·84	50	4728·27	50
4348·27	200	4735·26	10
4352·50	50	4737·75	80
4353·18	50	4739·68	10
4358·31	50	4742·47	20
4364·85	50	4744·64	10
4372·40	250	4754·75	10
4372·64	20	4755·74	50
4373·53	20	4762·10	40
4384·86	50	4770·78	10
4386·78	20	4771·97	20
4400·74	50	4772·86	200
4403·03	50	4773·45	200
4441·37	5000	4778·41	50
4451·20	100	4782·40	50
4475·85	50	4787·00	2000
4476·87	100	4792·90	1000
4489·67	250	4814·52	1000
4498·45	100	4817·80	20
4500·23	100	4825·24	10

VOL. 8 1956/5

Table 2 (*continued*)

Wavelength	Intensity	Wavelength	Intensity
4825·98	20	5141·9	10
4830·61	20	5160·1	50
4840·40	20	5164·05	10
4848·16	20	5166·8	10
4849·66	20	5173·4	500
4853·28	500	5180·2	20
4853·62	1000	5183·75	200
4854·03	250	5185·2	50
4860·98	20	5198·2	10
4868·15	50	5208·65	20
4872·14	5000	5225·0	50
4877·83	10	5231·6	20
4878·35	80	5232·3	50
4880·20	10	5234·2	20
4881·06	10	5242·3	20
4884·77	10	5246·9	50
4887·47	10	5254·6	10
4893·64	50	5262·5	10
4902·72	200	5264·9	100
4905·85	200	5288·9	250
4929·20	50	5300·75	10
4945·53	50	5306·6	50
4962·42	80	5318·7	10
4965·87	80	5319·55	200
4978·92	20	5333·7	80
4982·66	50	5338·7	80
4990·36	10	5345·8	80
4990·82	500	5350·75	80
5000·5	50	5378·45	20
5009·9	20	5380·8	20
5021·0	1000	5383·3	20
5024·45	10	5384·8	10
5028·8	10	5386·4	20
5035·85	10	5398·1	20
5040·75	10	5402·65	2000
5046·4	100	5406·7	20
5055·1	10	5410·7	500
5061·9	500	5422·9	50
5071·15	50	5424·7	1000
5082·75	10	5444·0	20
5096·15	10	5447·3	10
5103·45	20	5454·65	20
5115·2	2000	5460·8	20
5117·45	20	5465·85	20
5118·3	50	5492·9	10
5123·1	10	5498·4	10
5133·95	10	5501·45	20
5135·4	50	5503·45	10
5140·95	10	5509·6	500

Table 2 (*continued*)

Wavelength	Intensity	Wavelength	Intensity
5513·55	80	6054·5	4000
5537·1	500	6405·1	2000
5553·5	10	7224·4	50
5560·7	20	7256·9	500
5572·8	10	7267·6	200
5575·8	100	7368·6	50
5584·15	3000	7374·7	50
5591·8	50	7530·5	200
5598·1	1000	7546·2	250
5601·1	20	7547·2	250
5611·75	500	7599·7	100
5652·4	10	7615·4	100
5654·0	10	7641·3	100
5662·0	50	7687·4	100
5690·2	20	7717·8	50
5694·0	250	7745·4	80
5706·1	20	7796·3	100
5761·9	20	7836·2	200
5833·25	200	7955·7	50
5835·65	200	8086·1	100
5841·1	50	8122·6	100
5892·0	200	8333·2	1000
5929·0	80	8370·6	50
6014·2	50	8376·3	5000
6016·4	50		

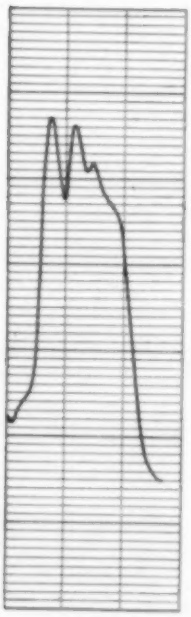

Fig. 2. Photometer trace of Am-3926·25.

By inspection of Table 2 it can be seen that the spark spectrum of americium consists of some very intense lines and a multitude of weaker ones. In this respect it is similar to Eu-II, and this may be taken as some evidence that Am-II has a normal configuration of $5f^7 7s^1$ analogous to $4f^7 6s^1$ of Eu-II. Russell, Albertson, and David [6] have shown that the strongest Eu-II lines arise from transitions based on the f^7 core of Eu-III to which s or p electrons are added. Here the simple analogy appears to end. The ground state of Eu-II is determined by four wave-number differences of 1669·21 cm^{-1}, whereas the difference 2598 appears more times amongst the strongest lines of the Am-II spectrum.

In the region of the spectrum photographed in the third order, a number of lines, those labelled HFS in Table 2, appeared as flag patterns. At some wavelengths, four members of a probable six-component flag pattern were easily resolved. Fig. 1 is a reproduction of the line at 3926·25 Å, and Fig. 2 is a microphotometer trace of the same line. Tomkins and Fred [7] have published a photograph of the

VOL. 8 1956/5

FIG. 1. Americium 3926·25 Å.

VOL.
8
1956/5

6054-Am line, taken in the fourth order of a 30-ft Paschen-Runge grating spectrograph, showing it resolved into six components. A six-component flag pattern leads to a nuclear spin of 5/2 for americium. An interferometric study of the hyperfine structure of americium, carried out as the third phase (the second being the hollow cathode spectrum) of this investigation, has confirmed the six component patterns.

Full details will be subsequently published.

Acknowledgement—The author is indebted to Dr. J. MILSTED of the Chemistry Division, A.E.R.E., Harwell, for the supply and purification of americium for this project.

References

[1] TOMKINS F. S. and FRED M. *J. Opt. Soc. Amer.* 1949 **39** 5.
[2] THORNE R. P. A.E.R.E. C/R. 1309 1953.
[3] FRED M. and TOMKINS F. S. *J. Opt. Soc. Amer.* 1954 **44** 10 824.
[4] FRED M., NACHTRIEB N. H., and TOMKINS F. S. *J. Opt. Soc. Amer.* 1947 **37** 279.
[5] HARRISON G. R. *Massachusetts Institute of Technology, Wavelength Tables*, J. Wiley & Sons, New York.
[6] RUSSELL H. N., ALBERTSON W., and DAVIS D. N. *Phys. Rev.* 1941 **60** 641.
[7] TOMKINS F. S. and FRED M. *Spectrochimica Acta* 1954 **6** 139.

OL.
3
6/57

Spectrochimica Acta, 1956, Vol. 8, pp. 88 to 93. Pergamon Press Ltd., London

The effect of current control in spectrographic analysis with a direct-current arc

R. M. McKenzie

Division of Soils, Commonwealth Scientific and Industrial Research Organisation, Adelaide, Australia

(*Received* 13 *March* 1956)

Abstract—A sulphated plant ash was arced repeatedly, both with the current controlled at 15 amperes throughout the arcing period, and with the current set to 15 amperes at the beginning of the arcing period and then allowed to proceed without further adjustment.

It was found that current control resulted in a marked reduction in the analytical error for a very involatile element, while it had little or no effect for elements of low to medium volatility. It was concluded that the greater part of the increase in precision was due to more reproducible volatilization of the elements during the latter part of the arcing period.

1. Introduction

The methods used for the establishment and control of the arc current in the spectrographic analysis of mineral powders vary considerably in different laboratories. In methods suggested by Jaycox [1] and Dunn and Mitteldorf [2], the arc is struck, and the current adjusted to the required value, after which no further adjustment of current is made. Harvey [3] recommends setting the current to the required value while the electrodes are momentarily short-circuited, on the grounds that if the current is measured after the arc is struck, the spacing of the electrodes, the type of sample, and the period of the arcing cycle will give variable measurement of the current. Mitchell [4] and Farmer [5], working with the cathode layer method, struck the arc by bringing the electrodes together with sufficient resistance in series to give a current of 2–3 amperes. The arc gap was then opened to the required distance, at the same time increasing the current to 9 amperes, after which this current was maintained throughout the arcing period by means of a variable resistance. The method used in these laboratories is similar to the above, the arc being started at a current of 5 amperes, and increased to 15 amperes as the electrodes are separated to the required distance. The current is then maintained at this level by a variable resistance.

A number of workers have shown that their devices for control of current do really control the current, but no one appears to have demonstrated conclusively that the use of such devices with samples of mineral powders increases spectrographic precision. Manual control of the arc current involves a considerable amount of manipulation on the part of the operator. If it could be shown that current control was unnecessary, then the operator could give the whole of his attention to keeping the arc length and position constant. This would not only simplify the method, but would give more accurate control of the arc itself. It was therefore decided to test whether any loss in precision would result if the current

VOL. 8 1956/5

was set to the required value as soon as the correct arc gap had been established, and then allowed to proceed without further adjustment.

The difference in steadiness of current between no control after initial setting and continuous manual control is certainly greater than that between manual control and automatic control. If the former difference has little effect on precision, the latter is unlikely to have a measurable effect, whereas if manual control results in an improvement in precision, at least the same improvement could be expected from automatic control relative to no control.

2. Experimental

Sulphated plant ash was chosen as the mineral powder, because of its homogeneity and arcing qualities. Lead (100 p.p.m), silver (10 p.p.m.), and beryllium (40 p.p.m) were added to 20 g of finely ground plant material, and the sample was sulphated and ashed as usual. The ash was well ground and mixed, and from it 120 electrodes were filled. Sixty of these electrodes were arced with controlled current, and the remainder without current control.

The current was controlled through a tapped resistance with a variable resistance in parallel. The arc was struck by bringing the electrodes together, with the tapped resistance fully in, allowing a current of 5 amperes to pass. The electrodes were then separated to a distance of 4 mm at the same time increasing the current to approximately 15 amperes by reducing the tapped resistance. At this point a second operator adjusted the current to 15 amperes with the variable resistance, and, for the "controlled current" samples, maintained this current for the duration of the arcing period. For the "no control" samples, the second operator set the current at 15 amperes as soon as the full current had been turned on, and then made no further adjustment. The sample was made the anode, and the exposure continued until all of the sample had left the electrode.

Ten plates were used to record the spectra, with twelve samples per plate. The sixty "no control" samples were distributed over the ten plates in random order, with the "controlled current" samples filling the rest of the spaces. The plates were exposed in order, each sample being arced with or without current control, as decided by the random selection.

Density measurements were made on Pb-2833A, Ag-3281A, Cu-3274A, Mo-3170A, Be-3321A (arc line), Be-3130A (spark line), Mn-2798A (arc line), and Mn-2606A (spark line). This selection was made in order to cover a wide range of volatilities, from the very volatile lead to the involatile beryllium, as well as lines arising from both atoms and ions. Plate calibration curves were prepared and used to convert the measured densities of the lines to log intensities. Separate estimations of the standard deviations for each element for each method of arcing were made and compared, using standard statistical techniques.

Separate moving-plate studies were made by racking the plate forward at five-second intervals during the arcing period, to provide information on the relative volatilities of these elements.

3. Discussion of results

During the arcing of the "no control" samples, the current remained at 15 amperes for approximately 20 seconds, and then dropped gradually to 13 amperes at the end of the arcing period. In both cases the voltage across the arc gap slowly increased from 25 to 50 volts.

The standard deviations for each element are set out in Table 1, together with those for the ratios of arc and spark lines for beryllium and manganese, and for the ratio of the copper and silver lines. The level of significance is also given. A level of significance of $p = 0{\cdot}001$ means that a difference as large as the one obtained would occur by chance only once in a thousand times.

Table 1 shows that current control has resulted in a marked reduction in the S.D. for both beryllium lines, and a small, though not quite significant, reduction for Cu-3274A and Mn-2606A, while there was no significant effect on the other lines measured. It has been shown [6] that the intensity of a line depends on the level of the arc current, and it might therefore be expected that there would be some

Table 1. Standard deviations of a single measurement for lines and line ratios under different arcing conditions

Line	Log S.D.* no control	Log S.D. controlled current	Variance ratio	Significance level p
Be-3321A	0·090	0·048	3·49	0·001
Be-3130A	0·085	0·045	3·46	0·001
Ag-3281A	0·062	0·059	1·10	N.S.†
Cu-3274A	0·071	0·057	1·60	N.S.
Mo-3170A	0·060	0·074	1·52	N.S.‡
Pb-2833A	0·060	0·065	1·16	N.S.‡
Mn-2798A	0·049	0·046	1·14	N.S.
Mn-2606A	0·084	0·065	1·68	N.S.
Be-3130A / Be-3321A	0·038	0·039	1·07	N.S.‡
Mn-2798A / Mn-2606A	0·052	0·051	1·04	N.S.
Ag-3281A / Cu-3274A	0·063	0·046	1·87	0·02

*To obtain an approximate Coefficient of Variation, multiply the log S.D. by 230.
†N.S. = not significantly different.
‡In these three cases the no-control samples actually had a numerically smaller error.

reduction in intensity with no current control, since the current dropped to 13 amperes. However, there was no effect on the mean integrated intensity, the drop in current apparently being too small.

The mean arcing time for the "no control" samples was $59{\cdot}8 \pm 4{\cdot}8$ seconds, and that for the "controlled current" samples was $55{\cdot}5 \pm 2{\cdot}9$ seconds. Both the times and the standard deviations are different, at the level of significance $p = 0{\cdot}002$. Thus the time required to volatilize the sample with no current control was more variable, and, on the average, longer than when the current was controlled.

These results may be explained on the basis of the volatilization curves shown in Figs. 1 and 2, and on the assumption that the volatilization of the elements into the arc, and the conditions in the arc stream itself were more variable during the latter part of the arcing period when the current was not controlled. That this is a reasonable assumption is shown by the fact that the current did remain constant for the first 20 seconds, and that the total arcing time was more variable when the current was not controlled. The curves in Figs. 1 and 2 were drawn from an average of four moving-plate exposures. To facilitate comparisons, the ordinates were

VOL. 8 1956/5

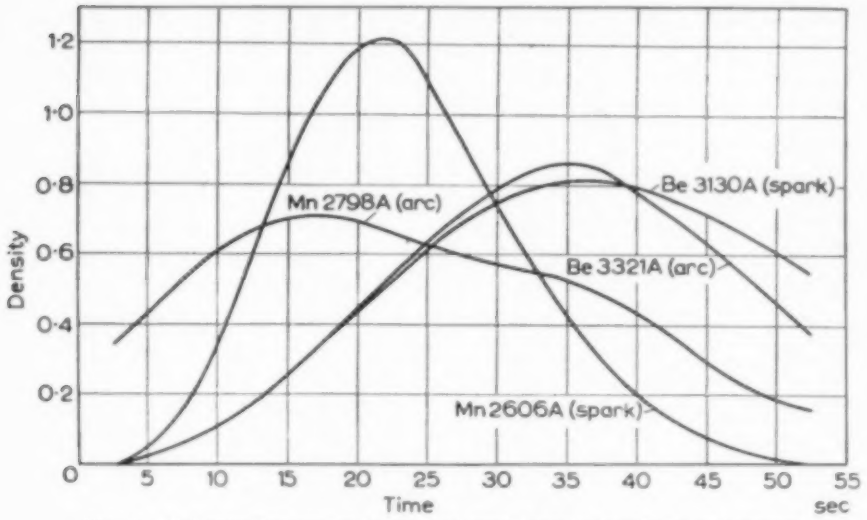

Fig. 1. Volatilization curves for arc and spark lines of beryllium and manganese.

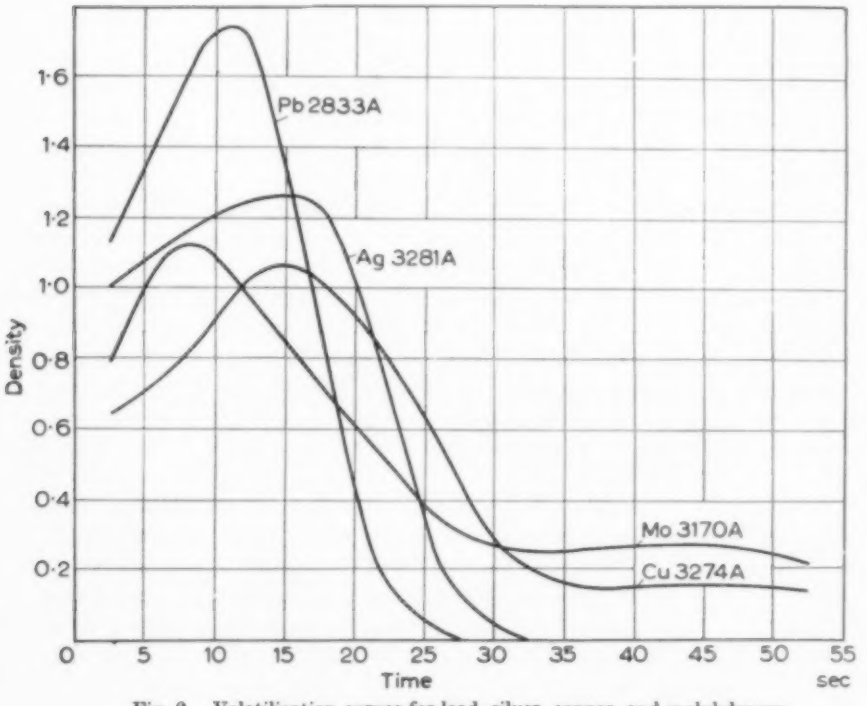

Fig. 2. Volatilization curves for lead, silver, copper, and molybdenum.

adjusted to give equal areas under each curve. Although these curves are commonly known as volatilization curves, they are in actual fact "emission" curves. Fig. 1 shows that the curves for an arc and a spark line from the same element are not necessarily the same, and it is probable than neither curve gives an exact picture of the volatilization of the element into the arc stream. It would appear from Fig. 1 that the peak emission of the spark lines occurs at a slightly later stage than that of the arc lines. Reference to these curves shows that the fraction of the total emission which occurred during the first 20 seconds was approximately 95% for lead, 80% for silver, 60% for copper and molybdenum, 40% for manganese, and 10 per cent for beryllium. It is then obvious that current control has had its greatest effect on the involatile element, with no effect on the volatiles, and only small effect on the intermediate elements. The fact that the spark line Mn-2606A had a slightly smaller S.D. when the current was controlled, while the arc line Mn-2798A did not, may be due to the fact that the emission curve for the spark line (Fig. 1) has a sharp peak, whereas the emission of Mn-2798A is distributed more evenly over the arcing period. Large fluctuations in the conditions in the arc stream would therefore be expected to have more effect on the spark line. This is supported by the fact that in both cases the S.D. for the spark line is greater than that for the arc line. For beryllium, the curves are extremely similar, and thus both lines have similar standard deviations.

Table 1 shows that current control has had no effect on the precision of the ratios of the arc line to the spark line for beryllium and manganese. An arc line and a spark line need not necessarily respond in the same way to fluctuations in the arc stream as, for example, an increase in temperature would be expected to increase the emission of the spark line more than that of the arc line. On the other hand, both lines arise from the same element, and there can be only one real volatilization curve. This indicates that a large part of the difference in the standard deviations between the "controlled current" and "no control" samples is due to fluctuations in the volatilization, rather than fluctuations in current. The correlation between the arc and spark lines was improved when the current was not controlled. The correlation coefficients were for beryllium, 0·65 with controlled current, and 0·91 with no control, and for manganese 0·63 with controlled current, and 0·83 with no control. This indicates that the arc and spark lines follow each other more closely under the influence of large fluctuations without current control than they do under the influence of smaller fluctuations when the current is controlled. If these larger fluctuations occur in the volatilization of the elements into the arc stream, then the arc and spark lines would be forced into closer correlation.

It is of interest to note that the use of silver as an internal standard has done nothing to overcome the increased S.D. of copper without current control. In fact the effect of current control on the ratio Ag-3281A/Cu-3274A is greater than it is on either element alone. Ag-3281A would appear to be the perfect internal standard line for Cu-3274A. The slight difference in boiling points is reflected in the volatilization curves (Fig. 2), showing that although the peaks occur at the same time, the emission of silver during the early part of the arcing period is greater than that of copper, while the reverse is the case during the latter part of the arcing period. The

VOL. 8 1956/5

result of this difference in the volatilization curves is the rather poor correlation between the two lines, the correlation coefficients being 0·68 with current control and 0·57 with no current control.

4. Conclusions

It can be concluded that, while current control has little or no effect on the volatile and intermediate elements, it results in a marked increase in precision in the case of a very involatile element. This increase in precision is probably due to better reproducibility of the volatilization of the involatile elements during the latter part of the arcing period. The use of an internal standard, however good it may appear, does not necessarily correct for this loss of precision.

The relatively small change in current occurring when no current control is used has no effect on the mean intensity of a line, and therefore has no effect on sensitivity.

References

[1] Jaycox E. K. *Methods for Emission Spectrochemical Analysis.* pp. 135, 172 and 273, Amer. Soc. Test. Mater., Philadelphia, 1953.

[2] Dunn E. J. and Mitteldorf A. J. *Methods for Emission Spectrochemical Analysis.* p. 94, Amer. Soc. Test. Mater., Philadelphia, 1953.

[3] Harvey C. E. *Spectrochemical Procedures,* p. 335, Applied Research Laboratories. Glendale, Calif., 1950.

[4] Mitchell R. L. *The Spectrographic Analysis of Soils, Plants and Related Materials.* Commonwealth Bureau of Soil Science, Harpenden, England, 1948.

[5] Farmer V. C. *Spectrochim. Acta* 1950 **4** 224.

[6] Oertel A. C. and McKenzie R. M. *Aust. J. Appl. Sci.* 1954 **5** 330.

Spectrochimica Acta, 1956, Vol. 8, pp. 94 to 101. Pergamon Press Ltd., London

SPECTROCHEMICAL NOTES

The assessment of the performance of spectrographic methods*

F. W. J. Garton,† W. Ramsden,‡ R. Taylor,§ and R. J. Webb†

(*Received* 19 *October* 1955)

1. Introduction

In the development of spectrographic methods of analysis where the experimental results are subject to a number of random variations, the logical approach is through statistical methods and parameters. These, besides being convenient in that they give a factual measure of the reproducibility and sensitivity, are entirely independent of any bias on the part of the observer when it comes to comparisons. That this is generally recognized by spectrographers is indicated by the fact that most reports of methods quote one of the measurements of dispersion (standard deviation, coefficient of variation, or mean deviation, etc.) to express reproducibility.

However, the wide range of statistics used and misused for this purpose and the diversity of terminology used for each is most disconcerting, particularly for the reader who is not familiar with statistical expressions and the inter-relationship between the different terms. The aim of this report, therefore, is to provide a basis for a more uniform approach to the problem of analysing and presenting spectrographic results by enumerating what is considered to be the most suitable means of assessing and expressing the performance characteristics of a method.

The paper is utilitarian rather than original, the procedures recommended being based mainly on the authors' experience in the development and assessment of spectrographic methods and on discussions with other spectrographers on the presentation of analytical results.

VOL. 8 1956/5

2. The performance characteristics of a method

It is recommended that the performance of a method should be assessed by:

(a) *Accuracy*, which represents the degree of confidence which can be placed on a particular analysis. This may be subdivided into
  (i) *Reproducibility*, i.e. the random errors inherent in the method.
  (ii) *Bias*, i.e. any systematic inaccuracy not eliminated in the design of the method.

(b) *Concentration range*, i.e. the concentration range which may be determined by the method with a stated degree of accuracy.

(c) *Sensitivity of Detection*, i.e. the lowest concentration which can be determined with a given degree of confidence.

(d) *Reliability of the method*, i.e. a long-term indication of the performance of the method in routine use. This includes drifts in the reproducibility and in the analytical results.

Each of the above performance characteristics is considered with respect to its assessment and interpretation. The term "assessment" is self-explanatory. The validity of any interpretation which may be made, however, will be dependent upon a knowledge of the frequency distribution of the errors. Lack of information on this point does not invalidate the use of such statistics as the mean and the standard deviation to represent the location and scatter of a set of data, but to draw inferences as to the correlation of results, assessment of confidence limits, etc., a reasonably precise knowledge of the distribution must be available.

In some methods there is evidence that the distribution of results (i.e. concentration) is normal; however, in certain cases, particularly in the less precise methods, it has been found

* Prepared for the Interservices/D.S.I.R. Panel on Emission Spectroscopy by a Study Group consisting of the authors.

† United Kingdom Atomic Energy Authority, Royal Arsenal, Woolwich.
‡ British Non-Ferrous Metals Research Association.
§ Post Office Research Station.

that the distribution of log (concentration) is normal, and where this is known to be the case the alternative and often more convenient method of using log R (assumed to be a near linear function of log (concentration) should be used in the statistical analysis.

Definitions of the terms used are given in Appendix I.

2.1 *Reproducibility*

Because of the difference between research and routine conditions and personnel, the variation between individual results occurring during the development of a method may differ from that obtained in its application. Thus it should be made clear under which conditions the figures reported were obtained.

The working reproducibility, which is the parameter of prime interest, includes variations arising from:

(a) the source of excitation,
(b) the response and measurement of the photographic plate,
(c) the plate calibration factor, i.e. the factor correlating the results on one plate with those on another plate.

Representing the variance of each of these as V_S, V_R, V_C, respectively

$$V_T = V_S + V_R + V_C \tag{1}$$

Thus any set of data used as a basis for estimating the reproducibility should include observations from as many different plates as possible.

The coefficient of variation (i.e. the standard deviation expressed as a percentage of the mean) is the statistic generally accepted as being the best to express reproducibility. The mean percentage deviation is sometimes used, but has the disadvantage that it cannot be used directly in any significance tests.

To define the reproducibility precisely, two facts should be given:

(i) the dispersion of the observations about the mean, expressed as the coefficient of variation,
(ii) the number of observations on which the estimate is based, from which the reader can compute the degree of confidence in the figure quoted (see Appendix I).

In addition the concentration or the range of concentration to which the coefficient of variation applies should be stated.

If the coefficient of variation of a single observation is $C\%$, then, in the absence of bias, 95% of the observations will be within $2C\%$ of the true value. Alternatively, it is reasonably certain that the true value will be within $2C\%$ of the observed value. Furthermore, if the mean of n observations is taken as the observed value, then it is reasonably certain that the true value will be within $\pm 2C\%/\sqrt{n}$ of the observed mean. It should be observed here that when all the replicates are on one plate, the practice of dividing by $\sqrt{n}$ to give the standard error of the mean is not strictly accurate. (See Appendix II for further discussion of this point.)

2.2 *Bias*

Bias is a measure of the systematic errors in a method (e.g. those arising from errors in standardization). It is assessed by considering the difference between the observed concentration and the "true" concentration in relation to the reproducibility of the method. In a good method, bias should not be detectable by the usual statistical tests. If a significant bias is detected, its cause should be traced and the method redesigned or an appropriate correction factor applied. The purpose of this test is to examine the practical significance of any apparent bias.

The above considerations assume that the true concentration is known or can be determined, and in certain classes of work, for example in solution analysis, tests can be carried out on synthetic solutions whose composition is known accurately. In the majority of cases, however, the true concentration can never be known, it can only be assessed by an alternative method of analysis (e.g. chemical analysis) which also has performance characteristics possibly comparable with the method under test; this is particularly so in trace analysis. In this case the test for the significance of the bias must include the performance characteristic of the alternative method. The primary requirement is a number of samples of which the true composition is known or an independent analysis has been carried out. The chemical and spectrographic methods of analysis should be identical with those used in the primary standardization, and bias can only

be assessed relative to the particular methods. Standard "referee" chemical methods can be relied upon to provide results not significantly different from the true figure, and in these cases a good estimate of the true bias can be obtained.

A possible cause of a significant bias could be the presence of extraneous elements either not present in the standards or occurring in variable concentrations in both samples and standards. When this is suspected, tests must be made on standards containing similar amounts of the interfering element and the significance of any bias assessed. Bias may also occur between the results obtained in different laboratories using a similar method.

2.3 *Concentration Range*

The concentration range of a method is an entirely arbitrary limitation on the concentrations which may be determined to a required degree of accuracy. In general, the upper range is most accurate, being limited at the upper end by such things as line reversal, reading errors, etc. At the lower end of the range, where the coefficient of variation tends to increase rapidly, it is advisable to decide upon some limit for lowest concentration which can be determined using a particular line pair. This limit may be defined as that concentration at which the coefficient of variation reaches a value dependent on the particular problem. SCHEUER [1] and VAN SOMEREN [2] have shown the type of variation of accuracy with concentration which may be obtained in practice.

2.4 *Sensitivity of Detection*

This is of particular importance in "trace" methods when it is essential to know with reasonable certainty the smallest concentration detectable. The impurity line is recorded on top of a background which arises from plate fog and from the light source, and hence inherits the variations in the background in addition to its own variations. Thus, as the concentration is decreased, a point is reached when the density difference between the blank and the blank plus a trace of impurity, or, in the case where a background correction is applied, the difference in density at the wavelength of the analysis line and the wavelength at which the background is measured, is no longer significant because of these errors. It is proposed to call this point the *limit of detection*.

In many cases the standard deviation S expressed as concentration reaches a constant low value at low concentrations, and twice this standard deviation is recommended as the limit of detection. In terms of the treatment given by KAISER [3], this limit corresponds to $2\sqrt{2} \times$ the standard deviation of the background.

For a normal distribution, this means that:

(i) if no impurity is detected, there is a 95% degree of confidence that not more than $2S$ of the impurity is actually present,

or

(ii) there is but a 5% chance that up to $2S$ of impurity will pass undetected.

For other probable distributions, a 95% degree of confidence can be obtained by using $3S$ as the limit (corresponding to a 99·8% degree of confidence for a normal distribution). It should be stated whether $2S$ or $3S$ has been used.

2.5 *Reliability of the Method*

As stated before, this is essentially an indication of the long-term performance of a method. To obtain this, the use of a control sample and two control charts is recommended.

The control sample should be typical of the routine samples being analysed, and it should be included on each plate and treated exactly the same as the other samples. Preferably an independent analysis figure should be known, but this is not essential. Two quality control charts [4, 5] should be constructed:

I Should show the mean concentration for the control sample plotted against plate number, with the control limits $2S/\sqrt{n}$ and $3S/\sqrt{n}$ (where n is the number of exposures per determination and S the standard deviation determined as in Section 3) plotted on the chart.

II Should show the range (maximum–minimum) of concentrations, expressed as a percentage of the mean concentration, obtained for the control sample, and, if desired, for the analysis samples. (It is assumed here that replicate exposures are carried out on each sample.

VOL. 8 1956/5

If analysis figures are based on single exposures, this naturally does not apply.) The upper control limits for the range on this chart are given by D_1C and D_2C (where C is the coefficient of variation determined as in Section 3), where D_1 and D_2 depend on the number of replicates as follows:

n	$D_1(0{\cdot}975)$	$D_2(0{\cdot}999)$
2	3·17	4·65
3	3·68	5·06
4	3·98	5·31
5	4·20	5·48
6	4·36	5·73

The two charts give an almost complete indication of the reliability of the method.

Chart I ensures that the accuracy of the method is maintained. If this is so, practically all the points should be scattered randomly between the inner control limits. A point outside the outer limits indicates a lack of control somewhere in the process, probably in the plate factor, and the whole plate should be repeated; any drift of the index point will be indicated by a general drift in the plotted points. If such a drift is suspected, its significance may be assessed by a test for nonrandomness [6,] such as the theory of runs or the mean-square successive difference test. A depreciation in the reproducibility will be indicated by an increased scatter of the points, with a larger proportion lying outside the inner limits.

Chart II is a more sensitive indication of any change in reproducibility. This is indicated by the proportion of points falling outside the control limits. Further, it enables one to pick out individual samples for which the mean analysis figure is unreliable because the range of replicate determinations is greater than would normally be expected. Such a case would probably be due to one erratic observation which will unduly bias the mean for the sample.

While it is appreciated that there is a certain loss of time, and that a little extra computation is involved in keeping control charts on these lines, their institution is strongly recommended, both as a means of maintaining the performance of a method and an indication of the source of the trouble when the method does not function properly.

3. Experimental determination of the performance characteristics

It is assumed that a method has been devised of which the characteristics need to be determined. The determination of the range, and the experimental procedures necessary to assess the reliability of a method, have been discussed in detail in Sections 2.3 and 2.5 respectively, and will not be considered further.

In any spectrographic method operating under specified conditions there is a definite relationship between the measured quantity (i.e. log R (corrected)), log intensity ratio, etc., and the concentration. When a series of spectra of standard samples is taken on one plate and read, an estimate of this relationship may be made from the observations. Another similar standard plate will give, possibly, a slightly different, but equally good, estimate of the same relationship. If a number of such plates are taken, then a very good estimate of the correlation between the reading and the concentration (i.e. of the standard curve) may be obtained. Now, if the coefficient of variation of all the results for each standard about the grand mean for that standard is calculated, a true indication of the reproducibility of the method is obtained. If, on the other hand, the reproducibility is calculated on the results of individual plates separately, then the figure obtained represents the variation of individual results about particular estimates of the standard curve which may themselves be in error.

Two methods of standardization and of determining the reproducibility are considered. In method A, reference is made to a standard working curve; in method B, standard samples are exposed on every plate and individual calibration curves are drawn.

3.1 *Establishment of Working Curve and Determination of Reproducibility for Method A*

The following experiment is recommended to establish a standard working curve and to determine the overall reproducibility. Five or six standard samples, covering the required concentration range, are each exposed five times on each of ten plates, giving fifty exposures of

each sample. The exposures on each plate should be arranged in five groups, each consisting of a single exposure of each sample, leaving a margin of not less than $\frac{1}{2}$ in. at the top and bottom of each plate.

The values of log R (corrected for plate factor), or preferably the log intensity ratios, for each line pair in each exposure are determined. The mean value for a line pair for each sample is computed (averaged over all the plates) and plotted against log concentration as abscissa. The best straight line or smooth curve is drawn through the points, and constitutes the working curve.

The practical work involved in the above procedure will normally take some time to complete, and it is in fact desirable to spread it over a period of several weeks. In order to put the method into service during the period, if required, the final standard curve may be built up gradually by successive corrections to a provisional curve based on the first few plates.

The reproducibility is determined from the information obtained in establishing the working curve, by computing the standard deviation of the log ratios (for a particular line pair in a sample) from the grand mean for each sample, according to the formula given in Appendix I. These standard deviations are converted to log concentration units by dividing by the slope of the working curve at the appropriate concentration. If the log concentration values obtained are not significantly different, their r.m.s. value S is computed and converted to the coefficient of variation C by the formula

$$C = 100 \,(\text{antilog}\, S - 1)$$

This coefficient gives the reproducibility over the range of concentrations covered by the samples.

If there are significant differences between the standard deviations on a log concentration basis, i.e. if the ratio of any two standard deviations is higher than 1·4 (for fifty exposures), the individual coefficients of variation should be quoted.

VOL.
8
1956/5

3.2 *Determination of Reproducibility for Method B*

The following experiment is recommended to determine the overall reproducibility when the method requires duplicate exposures of standards and samples: for three or more exposures, the experiment would be correspondingly modified. Five standard samples, covering the required concentration range, and fifteen samples of unknown composition within the range, are each exposed in duplicate on each of ten plates. For each exposure the electrodes are freshly prepared and the spectra for each sample are distributed over the plate, leaving a margin of not less than $\frac{1}{2}$ in. at the top and bottom.

In accordance with the method, the mean log deflection ratios for the standard samples are plotted against concentration or log concentration. The best straight line or smooth curve is drawn through the points to constitute the calibration curve for each plate.

From the calibration curve the concentration corresponding to the mean log R for each sample is determined. This is done for all the plates, and gives ten values for each sample. The mean value and an estimate of the coefficient of variation from that mean is computed for each sample. Provided that no coefficient is more than twice another, i.e. the differences are not significant, the r.m.s. value is calculated and represents the reproducibility of the method over the range of concentrations covered by the samples. If there are significant differences, the composition of the sample or samples which are not compatible will be a guide in deciding whether the range is to be limited or whether sample heterogeneity may have caused the discrepancy.

Alternatively, the reproducibility may be estimated from the range of the ten values of concentration for each sample; each range is expressed as a percentage of corresponding concentration, and the coefficient of variation is obtained by dividing the mean value by the factor 3·08.

3.3 *Bias*

The experimental work involved in the detection of bias has been outlined in 2.2. Spectrographic analyses should be carried out on a number of standards, say twenty or more, covering the whole concentration range, in parallel with chemical checks. The percentage deviations of

the spectrographic results from the chemical are plotted against concentration for each element. The inner control limits can also be marked on the chart.

These are: $$\pm 2\sqrt{\left(\frac{C_1^2}{n} + C_2^2\right)}$$

where C_1 is the coefficient of variation of the spectrographic results per exposure, n is the number of exposures per determination, and C_2 is the standard error of the chemical results expressed as a percentage of the mean.

A study of the pattern of the resultant plot will show the presence and magnitude of any bias. If the chart shows a bias to be present, necessary corrections can be worked out and applied. Points falling outside the control limits should be checked and, if necessary, investigated more fully.

3.4 *Sensitivity*

The determination of the absolute sensitivity of a method, as defined in Section 2.4, is mainly of importance in trace analysis. To determine this limit, it is necessary to carry out replicate exposures, say thirty or more, of several samples having low impurity contents. It is not usually necessary to spread the exposures over a large number of plates.

4. Conclusion

It is the hope of the authors that the recommendations made in this report will be of value to spectrographers who wish to put their routine methods of analysis on a firm statistical basis, and, in consequence, may lead to some uniformity in the statistical terms used in published statements about the performance of spectrographic methods.

The advice and criticisms given during the preparation of the paper by Messrs. J. Cross, J. R. Churchill, M. Milbourn, D. A. Sinclair, E. H. S. van Someren, and the members of the Inter-Services/D.S.I.R. Panel on Emission Spectrocopy, are gratefully acknowledged.

References

[1] E. Scheuer, F. H. Smith, *Metallurgia* 1949, **41** 44–46.
[2] E. H. S. van Someren, *Metallurgia* 1950, **42** 52.
[3] H. Kaiser, *Spectrochimica Acta* 1947 **3** (1) 40.
[4] British Standard 600R: 1942, *Quality Control Charts*.
[5] K. A. Brownlee "*Industrial Experimentation*" H.M.S.O. Publication.
[6] Carl A. Bennett *Ind. & Eng. Chem.* 1951 **43** 9 p. 2063.

Appendix I

Definitions

Log R is the density difference between the impurity line and the internal standard line.
Mean $\bar{x}$ (or *average*) is the sum of the observations divided by their number.

$$\bar{x} = \frac{x_1 + x_2 + x_3 + \ldots + x_n}{n}$$

where $x_1, x_2, x_3 \ldots x_n$ are the individual observations.

Deviation is the difference between an individual observation in a group and the mean for that group.

e.g. Deviation of $x_1 = (x_1 - \bar{x})$

Mean deviation is the average of the deviations when all are given a positive sign

$$\text{M.D.} = \frac{|x_1 - \bar{x}| + |x_2 - \bar{x}| + \ldots + |x_n - \bar{x}|}{n}$$

In a normal distribution the mean deviation is approximately four-fifths the standard deviation.

Variance (S^2) is the sum of the squares of the deviations divided by one less than the number of observations

$$S^2 = \frac{(x_1 - \bar{x})^2 + (x_2 - \bar{x})^2 + \ldots + (x_n - \bar{x})^2}{n - 1}$$

$$= \frac{\sum_1^n x^2 - n\bar{x}^2}{n - 1}$$

This is a most useful measure of the dispersion of results, since most statistical tests of significance are based upon it. Further, it has the valuable property of being additive, that is, if a procedure is subject to a number of sources of variation having variances S_1^2, S_2^2, etc., the total variance is equal to their sum.

Standard deviation S is the square root of the variance.

Coefficient of variation C is the standard deviation expressed as a percentage of the mean.

$$C = 100S/\bar{x} \text{ per cent.}$$

Standard error of the mean is the standard deviation of the means of groups of observations, i.e. it defines the confidence limits of the mean.

$$\text{S.E. of the mean} = S/\sqrt{n}$$

Standard error of the standard deviation cannot be expressed as simply as can the standard error of the mean for small numbers of observations, and in any case the resulting figure has not the same preciseness of meaning. It is only useful as an indication of the reliability of the estimate of standard deviation, and is of no value in significance tests.

The following table gives the confidence limits on the standard deviation for small numbers of observations; for larger numbers of observations the standard deviation S_s of the standard deviation S is given by

$$S_s = \frac{S}{\sqrt{2n}}$$

i.e. the 5% confidence limits, expressed as a percentage of the observed value, are given by

$$\pm \frac{2S}{\sqrt{2n}} \cdot \frac{100}{S} = \pm 100\sqrt{\frac{2}{n}}.$$

Table 1.

Number of observations	5% confidence limits expressed as a multiple of the observed value
2	7·1 to 0·45
3	6·3 to 0·52
5	2·9 to 0·60
10	1·83 to 0·69
15	1·56 to 0·73
20	1·46 to 0·76
25	1·39 to 0·78
30	1·34 to 0·80

VOL. 8 1956/5

Appendix II

The Effect of Replication on the Standard Error of the Mean

It is normally correct practice to take the standard error of the mean of n observations as $S/\sqrt{n}$, where S is the standard deviation of single observations. In spectrographic work, however, where the replications are not in fact true replications because all the variable factors involved are not replicated, this is not strictly accurate. This is considered in detail by J. Sherman in *Physical Methods in Chemical Analysis*. Vol. II, page 578. (Edited by Walter G. Berl, Academic Press Inc., New York, 1951.)

One of the most common examples of this arises when all replicates are taken on one plate. In these circumstances, factors affecting source and recording errors are replicated, but not those affecting plate calibration. Thus, if C_p is the coefficient of variation of results within individual plates (i.e. source and recording errors only), and C_c is the coefficient of variation arising from the method of plate calibration, then the total coefficient of variation C_T of individual observations is given by

$$C_T = \sqrt{(C_p^2 + C_c^2)}.$$

The standard error of the mean of n observations on one plate is given by

$$\sqrt{(C_P^2/n + C_c^2)}.$$

Clearly the efficiency of using $C_T/\sqrt{n}$ as an estimate for the standard error depends on the relative importance of C_p and C_c. In many methods, C_c is of a lower order than C_p, and $C_T/\sqrt{n}$ gives an adequate estimate. On the other hand, in methods involving the use of standards on each plate, C_c can be comparable with C_p, since each exposure of the standard will be subject to the same errors as the exposures for the samples, so that under the test conditions

$C_c = C_p/\sqrt{m}$ where m is the total number of exposures of standards

Thus the standard error of the mean of n observations is given by

$$\sqrt{\left(\frac{C_P^2}{n} + \frac{C_P^2}{m}\right)} = C_P\sqrt{\left(\frac{1}{n} + \frac{1}{m}\right)}$$

Spectrochimica Acta, 1956, Vol. 8, pp. 102 to 106. Pergamon Press Ltd., London

Spectrochemical Note

A rotating filter-paper disc method for spectrographic analysis

C. PARK
Department of the Government Chemist, Clements Inn Passage, London

(*Received* 9 *February* 1956)

Abstract—A method is described for the spectrochemical analysis of samples in solution form, using a rotating filter disc for carrying the solution into the analytical gap. Results are given of a statistical comparison with the coated-electrode method.

Introduction

FOR some years the standard method in this laboratory of spectrographic analysis of samples in solution form has been the coated-graphite-electrode method described by MCCLELLAND [1]. Although the precision and sensitivity of this method is satisfactory, the preparation and coating of large numbers of electrodes is a lengthy process, and the danger of contamination is considerable. More direct methods of transferring the solutions to the analytical gap have been tried, including the rotating lower electrode dipping into the solution, originally described by PIERRUCCI and BARBANTE-SILVA [2], the porous cup-electrode of FELDMAN [3], and various methods devised here for sparking directly to the surface of the solution. None of these methods attained the degree of sensitivity normally obtained from the coated-electrode technique, probably owing to the fact that difficulties were encountered which in every case precluded the use of a high-amperage source of the intermittent a.c. arc type.

The use of filter-paper spills as carriers for a solution has been described by RAMAGE [4], who fed the papers by hand into a flame source; ROACH [5] described a method in which filter-paper spills were fed into a flame by means of a motor-driven feeding device.

BERTON [6] impregnated a strip of paper with solution, and fed it into a spark discharge by means of a revolving drum; paper strips were also used by RUSANOV [7] to carry ore powder into the arc. HEGEMANN and ZOELLNER [8] used shellac to stick a powder to the edge of a paper disc and rotated the disc into the arc.

Apparatus

An electric motor geared to 1 r.p.m. is mounted on the base of the arc stand with its output spindle vertical and positioned 3·3 cm from the analytical gap (Fig. 1). Filter discs 7 cm in diameter are mounted between two discs of an asbestos-based heat-resistant material (4·5 cm diam., 3 mm thick), attached to a spindle which engages with and forms an extension of the motor spindle, and the whole assembly is fixed rigidly in order to prevent any change in the alignment of electrodes and filter disc, since such changes may cause variations in the ratio of element to internal standard line intensities. The direction of rotation is so arranged that the rim of filter paper left exposed is moving towards the slit of the spectrograph as it feeds into the analytical gap. Using a peripheral speed of 22 cm per minute, the intermittent a.c. arc discharge is very steady, and the paper burns

VOL. 8 1956/5

OL.
8
6/57

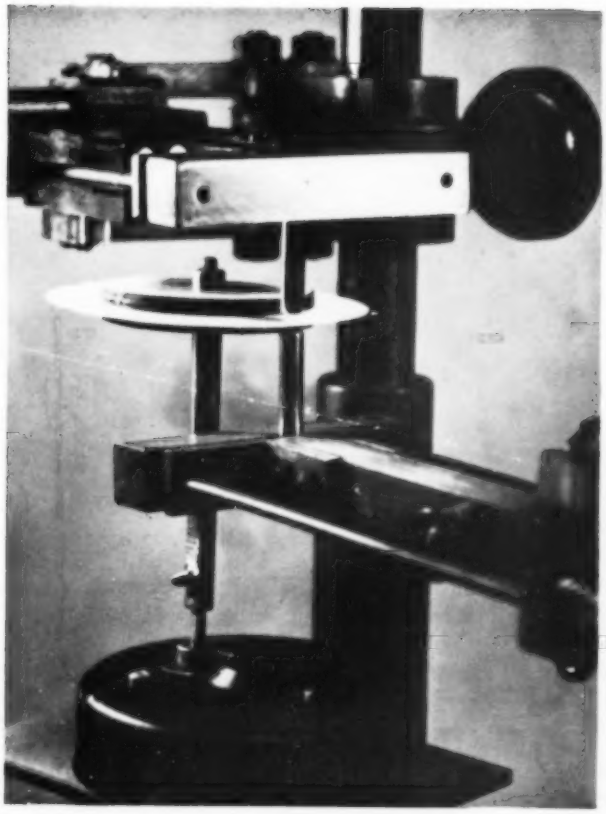

FIG. 1. Filter disc assembly mounted on the arc stand.

VOL.
8
1956/5

smoothly as it passes between the electrodes. Increasing the peripheral speed whilst keeping the time of exposure constant results in a decrease in intensity, and the discharge tends to become unsteady; a decrease in speed increases the intensity but enhances the OH bands. Whilst satisfactory conditions were attained for the author's particular problem, it has not been possible, as yet, to investigate every possible combination of peripheral speed and exposure time.

The electrodes are Matthey pure copper rods, 5 mm in diameter and 2·5 cm long, with the ends machined flat. An electrode separation of 2 mm is used, as increasing the analytical gap to more than 2·5 mm causes the arc to flare around the edge of the paper, but at the recommended setting, this undesirable characteristic is completely absent.

Experimental procedure

The method of preparing the solutions for analysis is as described by McClelland [1]; the particular solution used in the comparative tests described later contained 30 μg of Pb and 200 μg of Bi in 2 ml of 10 per cent $NaNO_3$ solution. Eight drops of the solution (0·3 ml) are evenly distributed by means of a pipette around the margin of the filter paper, which is already mounted between the insulating discs. Two spindle assemblies are used, so that the filter paper for one exposure is impregnated whilst the previous sample is being exposed; the time between impregnation and exposure is thus approximately two minutes, by which time there should be no surplus moisture on the surface of the paper. Particular attention is drawn to this, as experiments have shown that excess moisture on the paper results in some instability of the discharge, whereas a dry paper ignites and burns away before reaching the gap. On being impregnated, the rim of filter paper crinkles, but as long as a paper with a good wet strength is used, the leading edges of the electrodes act as guides and smooth out the corrugations. Whatman No. 54 filter discs are very suitable for the purpose.

The copper electrodes are changed after each exposure and subsequently cleaned by washing in dilute nitric acid; not until each electrode has been used six times is it necessary to reskim the ends on the lathe. This results in a great economy of electrode material. Furthermore, the rotating-disc method effects a saving in time of over 30%, and although the precision is, so far, not as high as than of the coated-electrode technique, the difference is not of practical importance in many applications. Finally, it is likely that the method here described will prove more versatile than the old method, where a high concentration of salts in the sample, or the presence of small amounts of insoluble matter, results in an unsatisfactory electrode coating.

Comparison of results obtained with the rotating filter disc and coated-electrode methods

The comparison of results show that the precision of the filter-disc method is of a similar order to that of the method using coated electrodes. Three plates were exposed each containing ten spectra of both methods recorded alternately down the plate. Separate variances were calculated for each method from the results on each plate. These variances proved to be consistent from plate to plate and were, therefore, combined to give a variance representing results of thirty exposures per method, from which the coefficients of variation given below were calculated.

Rotating filter disc	Coated electrode
13·4%	6·7%

Operating conditions

	Rotating filter disc	Coated electrodes
Spectrograph	Hilger medium	Hilger medium
Source to slit (with condensing lens)	38 cm	38 cm
Slit-width	0·025 mm	0·025 mm
Electrodes	J. M. 30. Copper 5 mm diam. Ends machined flat	J. M. 4B. Graphite 6·5-mm diam. Ends cupped
Electrode separation	2 mm	4 mm
Source	Intermittent a.c. arc	Intermittent a.c. arc
Strike frequency	100/sec	100/sec
Pulse-length	1/20 of the interval between pulses	1/20 of the interval between pulses
Hot-wire mean current	5·0 amp	5·0 amp
Hot-wire short-circuit current	5·2 amp	5·2 amp
Plate	Kodak B. 10.	Kodak B. 10.
Exposure	50 sec	40 sec
Periphery speed	22 cm/min	—
Filter disc	Whatman No. 54. 7-cm diam.	—
Line pairs	Pb-2833·1A–Bi-2898·0A.	Pb-2833·1A–Bi-2898·0A.

VOL. 8 1956/5

It is of interest to note that over a period of several months the coefficient of variation of the coated electrode method at this concentration was 8·5%.

The results of typical routine analyses by both methods are tabulated below:

	Rotating filter disc	Coated electrode
Sample No.	Pb (p.p.m.)	Pb (p.p.m.)
P. M. 45	5	5
P. M. 21	8	6
P. M. 38	20	17
P. M. 43	66	60
P. M. 1343	400	390

Fig. 2 shows a typical working curve obtained with the new method.

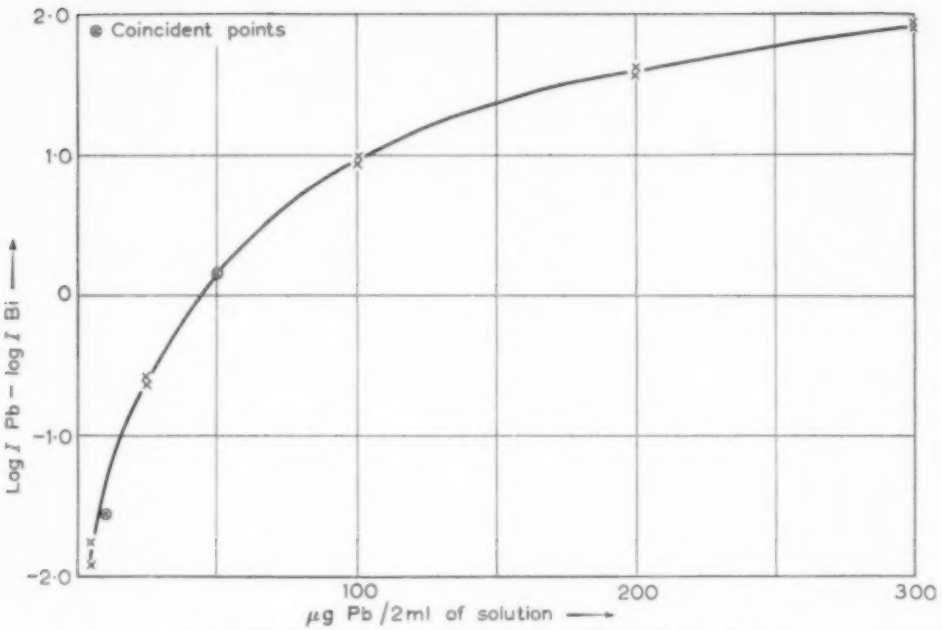

FIG. 2. Working curve using the lines Pb-2833·1 and Bi-2898·0

Interelement interferences

No special study of interelement interferences has been made, as the method has been particularly applied to the analysis of airborne dusts containing little other than the element to be determined; usually Pb, Cr, or Be. A further application of the method has been the analysis for trace elements of metals and alloys received in the form of drillings, or which were otherwise unsuitable for the making of self-electrodes. Samples of manganese bronze were examined for traces of Pb, an appropriate range of standards being prepared by adding varying amounts of Pb to solutions containing a known weight of Pb-free manganese bronze. The working curve obtained by using these standards was found to be identical with the curve obtained from a similar range of Pb solutions which contained no manganese bronze. All these solutions, of course, contained the $NaNO_3$ buffer. However, until more is known about interferences, it would seem to be safer to make the composition of sample and standard as nearly identical as possible.

Sensitivity to trace elements

The following sensitivities are expressed as the minimum weight of element which must be fed into the analytical gap to produce a detectable line on the plate. In the case of the sensitivities shown as <1 μg, the ultimate detection limit has not yet been determined.

Be	<1 μg	Mn	<1 μg
Co	1 μg	Mo	<1 μg
Cr	<1 μg	Ni	1 μg
Fe	<1 μg	Sn	5 μg
Pb	1 μg	V	1 μg

Acknowledgement—I wish to thank the Government Chemist for permission to publish this work.

References

[1] McClelland J. A. C. *Analyst* 1946 **71** 129-139.
[2] Pierrucci M. and Barbante-Silva L. *Nuovo Cimento* 1940 **17** 275.
[3] Feldman C. *Anal. Chem.* 1949 **21** 1041.
[4] Ramage H. *Nature* 1929 **123** 601.
[5] Roach W. A. *J. Soc. Chem. Ind.* 1946 **65** 33.
[6] Berton A. *Compt. Rend.* 1947 **225** 289–290.
[7] Rusanov A. K. *Bull. Acad. Sci. URSS, Ser. phys.* 1940 **4** 145-148.
[8] Hegemann F. and Zoellner H. *Glas. Email-Keramo Technik.* 1952 **3** 316.

VOL.
8
1956/5

REPORTS OF MEETINGS

Annual Pittsburgh Conference on Analytical Chemistry and Applied Spectroscopy

The 7th Annual Pittsburgh Conference on Analytical Chemistry and Applied Spectroscopy was held at Pittsburgh, Pennsylvania, from 27 February to 2 March 1956. Abstracts of papers in spectroscopy presented at the meeting are as follows:

Analytical Emission Spectroscopy

Observations on the spectrographic determination of the gaseous elements in metals: V. A. Fassel, Iowa State College, Ames, Iowa.

The presence of the gaseous elements in metals may greatly influence the physical properties of the metal. Although considerable progress has been made in applying chemical methods to the determination of these elements in metals, the actual analyses remain singularly difficult tasks. The possibilities of determining these elements by spectroscopic approaches has virtually gone unexplored. The problems encountered in extending conventional spectrographic techniques to these determinations will be surveyed and techniques for surmounting some of these problems will be presented. A d.c. carbon arc excitation method for the determination of oxygen in steel in the concentration range 20 to 2000 p.p.m. will be discussed and preliminary results on the extension of this and other excitation techniques to various metals will be summarized.

High-sensitivity spectrographic method for the analysis of titanium tetrachloride: Martha M. Darr and Bourdon F. Scribner, National Bureau of Standards, Washington, D.C.

An investigation was made to develop a method for determining trace impurities in high-purity titanium tetrachloride (99·9 + %). Dissolution of the titanium tetrachloride in conc. HCl results in stable solutions that are favourable for trace-element determinations. A measured amount of the solution is dried on a graphite electrode and the spectrum of the sample is obtained by d.c. arc excitation. Separate observation of the spectra of the early and later stages in the arc results in enhanced sensitivity for the more and the less volatile elements, repectively. With a moderate dispersion of 5 Å per mm, sensitivities in p.p.m. have been observed as follows: Be, 0·02; Ca, Mg, 0·05; Cu, Fe, Mn, 0·1; Ag, B, 0·2; Ni, 0·5; and Al, Cr, Si, 1·0. Details will be given of the procedure including spectral line pairs, sensitivities, and precision for the determination of an extended group of elements.

Spectrographic analysis of soils and soil clays: Jane Connor and Neil F. Shimp, Rutgers University, New Brunswick, N.J.

A method for the quantitative analysis of soils and soil clays for their major and minor chemical constituents is presented. The sample is brought into solution by treatment with H_2SO_4—HF. An aliquot of the solution is mixed with $NaNO_3$ in ratio of at least 20 : 1 $NaNO_3$ to sample ash. HNO_3 and H_2O are then added to give a solution of 20% $NaNO_3$ and 5% HNO_3. A drop of the solution is dried on a flat carbon electrode and the resultant cap analysed spectrographically in the a.c. arc, using Mo as an internal standard. The elements determined are Al, Cu, Fe, Mg, Mn, and Ti. Knowing the Al and Fe content of the digested sample, a suitable aliquot of the digested sample solution is calculated for use in the second part of the analysis. Fe and/or Al is added to the aliquot to give a ratio of 5 : 1 of Al_2O_3 to Fe_2O_3. Fe, Al, and trace elements are then separated from the alkali metals, alkaline earths, phosphates and sulphates by precipitation with quinolinol tannic acid and thionalide. The precipitate is ashed and mixed with graphite containing Ge and Pd internal standards. This is analysed spectrographically with the d.c. arc. The elements determined are Cd, Co, Cr, Ga, Mo, Ni, Pb, Sn, V, and Zn. Standards are prepared by making appropriate solutions of the elements to be determined and treating these in a like manner to the samples. Although soils and soil clays exhibit a wide range in chemical composition, quantitative analysis by these methods is possible for any sample since sample composition is altered to a constant matrix in both methods. The precision of the analyses is between 5% and 15% for each element.

A spectrochemical method for determining silicon in silicone resin solutions: J. Rudolph, Westinghouse Electric Corp., East Pittsburgh, Pa.

A rapid and precise spectrochemical method for the determination of silicon in silicone resin solutions is described. The method is applied to a routine check of tanks containing these solutions to determine the concentration of the silicone resin.

A spectrochemical technique not only produces the required accuracy, but fulfils the necessary speed requirements and low cost of routine analysis of large numbers of samples.

After dilution of the resin solution with toluene, cobalt naphthenate is added as an internal standard. An aliquot of the prepared sample is then introduced into the sample electrode which is placed under an infra-red lamp to distill the solvent. The remaining sample is charred in a furnace at 350°C.

A coefficient of variation of $\pm 5\%$ was obtained using direct current excitation. Comparison with chemical values on routine samples showed an average error of 8%.

Emission spectrographic analysis of high alloy magnetic materials: Arthur C. Bowen, The Indiana Steel Products Company, Valparaiso, Ind.

A detailed description is given of a spectrographic procedure for the analysis of Alnico alloy, a complex ferrous material. To permit the accurate determination of the high percentage concentrations of aluminium, cobalt, nickel, and copper, a "concentration ratio" method is used which allows for variations in the matrix material, iron. The precision of the spectrographic method is shown to compare favourably with that obtainable by routine chemical methods.

The paper concludes with a résumé of the variety of applications of spectrochemical analysis as used by the Indiana Steel Products Company.

Curves, tables, and miscellaneous photographs will be illustrated by slides.

The spectrochemical analysis of cathode nickel alloys by a graphite to metal arcing technique: Edwin K. Jaycox and Betty E. Prescott, Bell Telephone Laboratories, Inc., Murray Hill, N.J.

A technique is described for the analysis of thermionic cathode nickel alloys for the determination of aluminium, cobalt, chromium, copper, iron, magnesium, manganese, silicon, and titanium in the general concentration range of 0·003 to 0·2% for each element.

In this procedure, 10 milligrams of acid-cleaned nickel metal is placed in the crater of a $\frac{3}{16}$ in. diameter graphite cup and burned to extinction in the d.c. arc. This technique has two advantages over the procedure ASTM E-2 SM 5-1, now in general use, wherein all samples are converted to nickel oxide and mixed with graphite powder. These are:

1. An appreciable increase in the speed of analysis, achieved primarily in the area of sample preparation.
2. The elimination of several sources of contamination of the samples, namely: the reagents, glass or platinum ware, and the mortar and pestle used for grinding and mixing.

A present disadvantage of the method is the general lack of certified standard samples adequately covering all the desired elements and concentration ranges. However, samples can be standardized in the laboratory by other analytical procedures, and committees in ASTM are now working on the standardization of several nickel alloys.

Data will be presented to indicate the precision and accuracy of the procedure.

Spectrochemical determination of silver in stainless-type steels: J. F. Woodruff, T. Harris, jr., and Lillian J. Canody, Research Laboratories, Armco Steel Corporation, Middletown, Ohio.

A spectrochemical method is described for the determination of silver in stainless-type steels. This method uses briquetted drillings, millings, or nibblings. Details of the method, such as sample holders, the line pair used, excitation conditions, and precision and accuracy data are discussed.

The spectrographic determination of lead in leaded steel: J. E. Paterson, Graham Laboratory, for J. & L. Research, Jones & Laughlin Steel Corporation, Pittsburgh, Pa.

A spectrographic procedure for the determination of lead in leaded steels will be described. The procedure is based on interrupted direct current excitation of a nitric acid solution of the sample using the Rotrode. The concentration range covered by the method is 0·10%–0·50% lead in leaded steels with a 95% confidence interval of $\pm 8\%$.

An emission spectrographic technique of analysis for Sr in silicate materials: Karl K. Turekian and Paul W. Gast, Columbia University, Palisades, New York.

A general spectrographic method of analysis for strontium in all silicate materials has been developed which claims accuracy as well as precision. The accuracy of the technique was established by comparison with stable-isotope dilution determinations.

VOL. 8 1956/5

The effect of the calcium content on the intensity ratio I_{Sr4607}/I_{Ca4578} has been determined and shown to be greatest for low values of calcium. The presence of buffers such as graphite does not alleviate this matrix effect. It was observed that the effect becomes negligible at high concentrations of calcium. Hence each silicate sample was mixed 1 : 1 with strontium free calcium carbonate. This latter reagent was prepared by a careful ion-exchange separation of the Ca from the Sr and Ba.

Approximately 5 mg of the mixture was arced at 16·5 amperes (d.c. arc) in a $\frac{1}{16}$ in. deep necked high purity electrode to prevent spattering when the carbon dioxide was released. The spectrograph used was a Jaco Ebert mount and recording was on SA No. 1 photographic plates.

The standard curve was set up adding known amounts of $SrCO_3$ to Sr-free albite. A preliminary check for accuracy was made by adding known amounts of Sr to the rock standards G-1 and W-1 and by diluting these with albite thus giving three points each. If one value is obtained from the working curve then the remaining two of the addition-dilution series can be calculated. The agreement between calculated and experimental values was excellent. Finally a number of samples were analysed by both the above technique and isotope dilution. The results presented below indicate the level of accuracy attained.

	Emission Spectrograph	Isotope Dilution
Granite G-1	267	262
Diabase W-1	158	178
Granite 29A5	218	230
	(p.p.m. strontium)	

One thousand rock and mineral samples have been analysed to date and the method is being actively extended to include the accurate analysis of barium as well.

Direct reading analysis of alloy cast iron: Roger Bartel and Alan Goldblatt, Chicago Spectro Service Laboratory.

The routine use of a point to plane technique will be described for the analysis of manganese 0·2 to 1·0%, silicon 0·1 to 3·0%, nickel 0·1 to 3·5%, chromium 0·1 to 3·5%, and molybdenum 0·2 to 5·0%.

A Multisource discharge is used which eliminates the metallurgical effect of carbon and permits the use of alloy steel standards for setting up the alloy iron curves.

Direct reading spectrochemical analysis of nonmetallics used in the aluminium industry: R. H. Black and P. E. Lemieux, Aluminium Laboratories Limited, Arvida, Quebec.

Direct-reading instrumentation has been applied to the analysis of alumina, carbon, bauxite, and other nonmetallics of interest to the aluminium industry, with a view to reducing analytical costs. D.c. arc excitation is employed, alumina samples being mixed with two parts of pure graphite and carbon materials with equal parts of pure alumina and graphite. For the determination of major constituents (Si, Ti, Fe, and Al) in bauxite, CuO is added as an internal standard.

Total analytical time is 15–20 man-minutes per sample, including quadruplicate arcings. Precision is about 5% (coefficient of variation) for individual arcings, and accuracy (for analyses in quadruplicate) is also in the order of 5% of the amount present.

Photographic techniques approach this precision and accuracy with some sacrifice in speed.

Direct reading spectrochemical analysis of stainless steel: L. O. Eikrem and J. S. Fippĥen, Engineering Department, Baird Associates, Inc., Cambridge, Mass.

The use of the apparent concentration system has not proved satisfactory for the analysis of stainless steel in this laboratory. Stainless alloys of the same alloy type do not conform to a single apparent concentration curve to a degree sufficient for accurate analysis, even though results of high precision are obtainable. Stainless alloys of different types do not fit a single apparent concentration curve. Accurate results have been obtained using curves of actual concentration. Stainless alloys of different type may be analysed on a curve selected from a family of parallel curves. The proper curve to be used is defined by the sum of the concentration of iron and of the concentration of the element being analysed. Only approximate values of the iron content need be determined. If the type of alloy is already known, then the proper curve may be selected with no calculation. Other significant factors in the technique are the use of a long pre-spark (60 seconds) and a counter electrode of tungsten.

Accuracy data will be shown, comparing wet chemical results obtained by an independent laboratory with direct reader results on the same samples obtained without previous knowledge of wet chemical values.

Narrow wavelength interval direct reading spectrometer: Louis E. Owen, Goodyear Atomic Corporation, Portsmouth, Ohio.

Progress in the assembly of a narrow wavelength interval direct reading spectrometer based upon the principles proposed by Brehm and Fassel* is described. The attempt is being made to contruct such an instrument with the maximum utilization of commercially available electronic components. Initial work has been with an oscillating slit on the Leeds and Northrup monochromator.† The electronic components are assembled in a manner to provide a unit useful with other spectrographs in which oscillatory movement of spectra can be produced.

Innovations and performance of the Fisher Spectro Analyser: A. M. Laing and D. D. Harmon, Fisher Scientific Company, Pittsburgh, Pa.

In order to achieve optimum performance from a direct reading spectrograph, consideration of all factors which effect the final result must be made. Calibration drift has been found to be caused mainly by small movements of the receiver slits with respect to the spectrum lines. After the sample itself, the major cause of nonreproducibility has been found to be the fluctuations of the spark column about the optical centre line. These problems and their solutions will be discussed.

A new direct concentration readout system, either recording or nonrecording, will be described, as will the performance of the Fisher Spectro Analyser on specific analytical problems.

Improving the sensitivity of high dispersion spectrographs: Robert J. Meltzer and John Keller, Bausch & Lomb Optical Co., Rochester 2, N.Y.

A series of experiments were conducted to improve the speed and sensitivity of the echelle spectrograph. The experiment first used a quartz-fluorite achromat to focus the cathode layer onto the horizontal slit of a Littrow echelle spectrograph. The finite depth of source makes it impossible to get good focus of the cathode layer from the entire source. Since a nonachromat will produce in focus images from different depths of the source, down to 2400 Å, no gain is obtained using the achromat. However, a smaller diameter source is helpful. Because of these considerations the position of the condenser and the source are critical. With the techniques developed lead may be determined down to 1 microgram on the electrode. Boron in steel may be measured at 0·0006% with a one-minute exposure.

Semiquantitative spectrographic analysis in a truck-mounted laboratory for geochemical exploration—a preliminary report: A. T. Myers, F. C. Canney, and P. J. Dunton, U.S. Geological Survey, Denver Federal Centre, Denver, Colo.

Application of a semiquantitative spectrographic method of rock and soil analysis has been made with a truck-mounted spectrographic laboratory, assembled and tested by the U.S. Geological Survey. An air-conditioned van-type truck body carries complete equipment for making semiquantitative analyses of geological materials. The spectrograph is a fixed-position 1·5-metre grating instrument in a Wadsworth stigmatic mounting which records the region from 2063 Å to 4837 Å in the second order on a 20-in. strip of film. Companion units include a projection type comparator-densitometer, film processor, and other accessory equipment. Trailer-mounted motor generators supply 230 volts d.c. for the arc source unit and 115 volts a.c. for lights and accessories. Crushing and grinding equipment is mounted on a separate truck to prepare the sample for analysis. Some control of contamination is effected by the use of ceramic grinding plates.

The truck was driven more than 500 miles from Denver to Eureka (Tintic district), Utah, and then 39 drill-core samples were analysed for 15 elements. Comparison of the results for copper, lead, and zinc from the field spectrograph with chemical and spectrographic laboratory determinations show acceptable agreement.

Spectrographic determination of trace metals in petroleum fractions: W. D. Perkins, Martinez Research Laboratory, Shell Oil Company, Martinez, Calif.

When trace metal concentrations in refinery streams lie in the parts per billion range, it is necessary to concentrate the sample before sparking. This is usually done by ashing. A method for analyzing the acid solutions of such petroleum ashes is described, in which maximum detectability has been obtained by a suitable choice of electrode systems, power source settings, and pre-spark and exposure times. Further line enhancement has been obtained by the addition of a suitable concentration of lithium as lithium carbonate. Using this method, metal concentrations as low as 0·4 to 0·6 micrograms per millilitre of acid solution can be determined with a precision of 5 to 10% for vanadium and chromium and 20 to 25% for nickel and magnesium. The procedure can be easily extended to include other elements.

---

* Brehm R. K. and Fassel V. A. *Spectrochim. Acta* **6** 1954 373.

† Fastie W. G. *J. Opt. Soc. Am.* **42** 1952 641.

VOL. 8 1956/5

A rapid method for the spectrochemical analysis of lead in blood: Kathleen Kumler and Thomas P. Schreiber, General Motors Research Laboratories, Detroit, Mich.

Compared to the wet-ash dithizone technique routinely used in this laboratory, the spectrochemical method described is capable of producing twice the number of analyses per man-hour.

The unique features of the method are as follows:

1. A partially digested (ten to fifteen minutes) blood specimen is used for analysis.

2. A drop of sample is placed on a warm graphite electrode 20–30 seconds after a 10-second prearc at 10 amperes, direct current. Eliminating unnecessary handling and exposure reduces the possibility of contamination to a minimum.

3. After the sample has dried on the electrode it is arced 10 seconds at 10 amperes (250 volt d.c. arc —sample electrode positive) in a special electrode holder. This holder is so designed that a stream of nitrogen gas is directed along the axis of, and surrounds the electrode. Thus arc wandering is reduced and the line to background ratio of the 3833 Å lead line so improved that background correction is not required.

Bismuth is used as the internal standard 2898 Å line) and sodium chloride as the spectrographic buffer. These materials (1·0 g NaCl and 0·2 mg Bi per 10–25 g blood) are added to the blood before partial digestion.

The analytical curve was obtained from synthetic standards and bloods analysed chemically. Over 300 comparative analyses were made. The emulsion calibration and other steps in the analysis follow normal spectrographic procedures.

The chemical separation of rare earths from thorium prior to spectrographic analysis: Cyrus Feldman and Janus Y. Ellenburg, Oak Ridge National Laboratory, Oak Ridge, Tenn.

Kember* has suggested the use of a column of slightly nitrated ("activated") cellulose for separating rare earths and certain other impurities from thorium. This method has been used as the basis of a considerably faster batch separation technique. This procedure makes it possible to isolate microgram quantities of rare earths from solutions containing 20 grams or more of thorium in three hours or less.

Activated cellulose adsorbs rare earths directly from a mixture of 95–85 vol. per cent diethyl or di-n-propyl ether and 5–15 vol. per cent of concd. HNO_3, provided that all water other than that contained in the nitric acid is excluded. The rare earths are recovered by treating the cellulose with nitric acid at pH 2. Contaminants such as zirconium, iron and residual thorium are removed by extraction into a 0·5 M solution of thenoyltrifluoroacetone (TTA) in xylene.

This procedure is being used principally as a preliminary group separation of rare earths from thorium prior to spectrographic determination of individual rare earths. As the size of the thorium sample may be increased more or less indefinitely, the concentrational limit of detection of rare earth in thorium may be lowered to meet any desired specifications.

An aid for visual comparison in spectrographic analysis: William K. Baer and Edwin S. Hodge, Mellon Institute. Pittsburgh 13, Pa.

Several well-known methods of qualitative and semi-quantitative analysis involve the visual estimation of line intensity. The subjective nature of such observations and the repetitious handling of plates or films has led to the development of a visual intensity scale.

A selected single line at several different intensities was enlarged to make a transparent intensity scale. This was placed behind the viewing screen of an ARL projection-comparator. A table of intensities measured by the scale was prepared for about 40 elements ranging from 0·0001 to 100% concentration. Over 90% of the individual analyses of 15 standard samples were in agreement with the certified values.

The advantages of this aid include faster analysis, freedom from handling standard spectrograms on plates or films, elimination of eye strain in using a plate magnifier, and the elimination of comparison and memory of line intensities.

Use of commercial sheet film in spectrochemical analysis†: Morris Slavin, Department of Chemistry, Brookhaven National Laboratory, Upton, Long Island, N.Y.

Based on several years' experience, the substitution of commercial sheet film for glass plates is advocated for spectrochemical purposes. Advantages of sheet film are freedom from breakage, ease of cutting and filing, and ability to photograph wide spectral regions in one piece. Commercial emulsions

---

* Kember, N. F., "The Extraction of Thorium Nitrate with Ether Containing Nitric Acid in the Presence of Activated Cellulose, and the Application of this Process to the Analysis of Monazite Sands and Urano-Thorianite," CRL-AE-23 (Sept., 1948). U.S. Office of Technical Services, Washington 25, D.C.

† Research carried out under the auspices of the U.S. Atomic Energy Commission.

are more uniformly coated and are much more free from blemishes. Holders for glass plates can be used for film with no structural changes. A list of available emulsions which can be used in place of spectroscopic plates is presented.

Recent improvements in uniformity of spectroscopic electrodes: R. B. Dull and Norman Simpson, The National Carbon Company, Fostoria, Ohio.

The high level of uniformity of AGKS and AGKSP spectroscopic electrodes has been further improved both within the electrode and from electrode to electrode. The results of a statistical study of variations in density and electrical resistivity will be presented.

Sample transport and temperature studies in porous cup discharges: Cyrus Feldman and Margaret K. Wittels, Oak Ridge National Laboratory, Oak Ridge, Tenn.

The temperature of porous cup (and other) discharges can be obtained by measuring the distribution of rotational energies in the ultra-violet spectrum of OH. Temperature measurements can be made with a spectrograph having 2·5 A/mm dispersion. The labour of calculation is greatly reduced by the use of a special graph paper. Measurements in porous cup discharges indicate that (1) such discharges are at thermal equilibrium; (2) the region near the porous cup surface essentially obeys the Saha-Semeonova relationship between temperature and ionization potential; (3) the temperature of the region near the counter electrode is essentially independent of solute identity or concentration, and (4) the temperature distribution curve is essentially independent of polarity in a pulsed d.c. discharge. Explanations of the sample transport mechanism derived from temperature observations correlate well with those obtained from high-speed colour motion pictures of the discharge.

Statistical evaluation of spectrographic methods: Benjamin N. Nelson, Westinghouse Electric Corp., Bettis Plant, Pittsburgh 30, Pa.

The tools of statistical analysis can be of tremendous help to the spectroscopist in developing and evaluating his methods. A realistic evaluation of the precision and bias of a method is needed to attach some reliability estimate to results. An aim towards a control programme should be made by evaluation of the variables that could seriously affect precision and bias. Rejection of extreme results, homogeneity studies, differences between spectrographic plates, various excitation conditions, operators, levels of concentrations and effect of different matrices are some of the things of interest to the spectroscopist.

The purpose of this paper then will be, first of all, to review some of the valuable tools, as related to actual applications in spectrographic work. Examples will be given where conclusions are not obvious on inspection—and where statistics acts as a regulator against making hasty conclusions. Other examples will be given of some of the benefits and shortcuts achieved by the use of statistical tools.

X-ray Fluorescence Spectroscopy

X-ray optics of fluorescence analysis instruments: W. Parrish, K. Lowitzsch, and N. Spielberg, Philips Laboratories, Irvington-on-Hudson, N.Y.

The effects of the X-ray optics on the resolution, line profile, peak and integrated line intensity, scattered background, and peak-to-background ratio have been studied with various experimental arrangements. Some of the factors considered in the flat crystal arrangement include: (1) the angular aperture of the Soller (parallel) slit assembly; (2) the use of two sets of Soller slits instead of a single set, with one set between the specimen and crystal analyser and another set between analyser and detector; (3) the divergence of the beam in the plane normal to the Soller slits; (4) the area of the apertures; (5) the macroperfection and dispersion of the crystal analyser. A comparison is made of flat and focusing crystal arrangements and the advantages and limitations of both methods are discussed. Some experimental data on crystal analysers are included.

Nondispersive analysis with proportional and scintillation counters: H. Friedman, U.S. Naval Research Laboratory, Washington, D.C.

Proportional counters are suitable for isolating the characteristic radiations of light elements separated by two atomic numbers or more. Scintillation counters are well adapted to the detection of elements of higher atomic number with cruder resolution. The reduction of air path with nondispersive arrangements makes it possible to detect radiations as soft as Al$K\alpha$ in air. Examples will be given of resolution and sensitivity in the different portions of the spectrum.

Nondispersive X-ray analysis with proportional counters: C. F. Hendee, S. Fine, and W. B. Brown, Philips Laboratories, Irvington-on-Hudson, N.Y.

A compact, rugged xenon-filled X-ray proportional counter has been developed for the linear high speed detection of Cu$K\alpha$ radiation. This tube has good quantum-counting efficiency in the region 0·5 to 3·0 ångstroms. The unique construction of this counter results in a linear relationship between X-ray

VOL. 8 1956/5

photon energy and output pulse amplitude. Therefore, the counter is a spectrometric device and has been used in a nondispersive X-ray fluorescence system.

The energy resolution for a counter of this geometry is chiefly limited by the natural statistical fluctuation of ion-pair production. The half-width of the peak in the pulse height distribution for monochromatic radiation varies as the square root of the energy. According to Moseley's law, a similar square root relationship exists between atomic number and energy of the characteristic X-radiations. This results in a set of pulse height distributions for the detection of K-radiation of adjacent elements with a constant overlap of the peaks for all the elements. This indicates that the severity of the problem of analysing mixes of neighbouring elements is similar over the whole periodic table.

Despite the overlap of the pulse height distributions, working curves of binary mixtures of adjacent elements have been obtained by means of a two-channel electronic pulse height analyser and Philips EIT decade scaler tubes. Working curves have been obtained also for interesting simpler cases, where the binary mixtures contain nonadjacent elements. For rapid analysis of some systems, it is possible to identify elements by observing the amplified pulses on an oscilloscope.

In the analysis of rare earth elements with a xenon-filled proportional counter, considerable increase in sensitivity and resolution is obtained by utilizing the escape peak in the pulse height distribution. In this region the peaks corresponding to adjacent rare earths are almost completely resolved.

A gas-flow proportional counter for third period element X-rays: W. B. Brown, C. F. Hendee, S. Fine, and T. Stahre, Philips Laboratories, Irvington-on-Hudson, N.Y.

One of the major problems of analysis in the soft X-ray region is the limitation due to low transmission of the window materials of sealed-off X-ray detectors. This paper describes the properties and use of a gas-flow proportional counter system for the X-ray analysis of elements in the third period of the periodic table, with special reference to aluminium and silicon. The use of gases flowing continuously through the counter at atmospheric pressure in conjunction with helium also at atmospheric pressure in the optical path permits the use of ultra-thin non-vacuum tight windows with high transmission in this region.

It is possible to establish a low minimum flow rate for which the deleterious effects on counter operation of outgassing and diffusion through the window are no longer noticeable. Stability and reproducibility are comparable to that found in the harder X-ray region where sealed-off detectors are used. This system retains the characteristics of proportional counters in regard to counting and energy linearity, and the ability to discriminate against background and unwanted radiations.

Comparative data, obtained on a Norelco fluorescence spectrometer, show a tenfold increase in counting efficiency for Al$K\alpha$ over detectors previously available for this application. The facility with which K-lines of elements in the third period are recorded at high counting rates above a low background will be illustrated by slides showing spectra of materials containing these elements in varying proportions.

Work has begun on the extension of the above techniques to windowless flow counters, where the gas in the optical path and the counter are identical, and the gas pressure is adjusted for optimum operation. Such a system offers the possibility of detecting X-rays of elements in the second period of the periodic table.

Performance characteristics of a new three-specimen rotating-head X-ray spectrograph: Howard F. Carl and William J. Campbell, U.S. Bureau of Mines, College Park, Md.

A three-specimen rotating-head spectrograph is described that allows rapid changing and precise positioning of samples in the X-ray beam while providing maximum radiation protection to the operator. When used with the helium attachment the loss and contamination of gas during sample changing is negligible. Holders are provided that are suitable for liquids, solids, and powders.

Rotation of the sample during exposure provides integrated intensities from the entire sample radiated. This is particularly valuable for the analysis of films and precipitates that may not be homogeneous or of uniform thickness.

Results obtained from this instrument and from the laboratory's original spectrograph are compared. Its advantages for the analysis of liquids and for elements of atomic numbers below 22 are discussed.

Increased sensitivity for elements of atomic numbers 45–60 is gained by the higher available voltage of the FA60 tungsten target X-ray tube. The relatively high purity of the spectra from this tube allows more precise analyses of traces of copper, nickel, and iron.

Continuous analytical and gauging control of X-ray emission: P. S. Goodwin, J. L. Jones, and M. F. Hasler, Applied Research Laboratories, Glendale, Calif.

X-radiations emitted by an irradiated, continuously moving sample can be utilized for continuous analytical and gauging control. These emitted radiations consist of the scattered tube-target spectrum, and the characteristic spectra of the elements in the gauged material.

The utility of these various radiations, as well as other essential requirements of such controls, are developed, utilizing the most recent findings in the field of X-ray emission analysis.

Examples in the field of metal coating thickness gauging, and continuous ore analysis for a single element, will be given. Typical instrumentation suitable for these types of control analysis will be described and performance discussed.

A monochromatic diffraction-absorption technique for direct quantitative X-ray analysis· D. H. LENNOX, Department of National Health and Welfare, Ottawa, Canada.

Investigation in this laboratory of limitations in the classical internal standard technique led to studies of a diffraction-absorption method to eliminate the need for an internal standard. In an earlier paper a method employing a polychromatic beam for the absorption measurement was described. An alternative method employing a monochromatic beam for the absorption measurement is reported in this paper. An experimental equation relating diffraction and absorption measurements to quartz concentration in crystallite mixtures is developed. Differences between the experimental equation and that theoretically predicted are studied and are ascribed mainly to non-linearity of Geiger counter response. The results obtained in the analysis of a series of known mixtures by the three methods are compared and it is concluded that under the experimental conditions described the monochromatic diffraction-absorption technique gives superior results. Types of problems for which the diffraction-absorption methods should be especially suitable are discussed.

Refinements in X-ray emission techniques: J. W. KEMP and GEORGE ANDERMANN, Applied Research Laboratories, Glendale, Calif.

In the field of analysis of nonmetallic materials, a new technique has been investigated for application to a wide variety of ores, slags, tailings, petroleum products, etc. It has been found in many cases that selected portions of the scattered tube-target spectrum can perform the same function as the internal standard used in the usual internal standard technique. Although not universally applicable, the new technique provides correction for particle size, sample density, sample-tube distance, sample surface, and interelement effects over limited ranges. An advantage of the technique is that it does not require mixing of the sample with a standard or other treatment such as fusion. Several examples will be given.

In the field of analysis of metallic materials, a detailed study of various iron base alloys has been made to determine the best data handling technique for complex alloys. Interelement correction factors, type working curves, and type standards have been considered. Results obtained with iron alloys containing 0 to 10% molybdenum, 0 to 20% cobalt, 0 to 30% tungsten, 0 to 30% chromium, and 0 to 50% nickel will be reported on.

Selective analysis for elements using modified X-ray absorption techniques: W. M. FLOOK, JR. and D. D. FRIEL, E. I. du Pont de Nemours & Co., Inc., Wilmington, Del.

A practical method of elemental analysis of liquid samples has been developed using the X-ray absorption edge technique. This method involves the use of filters in conjunction with proper selection of excitation potential to isolate two bands of wavelengths, one on either side of the critical absorption edge of the desired element. Analysers based on this technique have been made for copper, with a sensitivity of about 100 parts per million, and for chlorine, with a sensitivity of about 300 parts per million. A method of reducing interference from other elements in the sample through the use of three separate pass bands has been developed, and the performance of a copper analyser using this technique is described.

Dynamic diffusion studies by X-ray spectroscopy: L. S. BIRKS and E. J. BROOKS, U.S. Naval Research Laboratory, Washington, D.C.

The focusing X-ray spectrometer has been adapted for diffusion studies in both liquid and solid phases. Solution of $CuSO_4$ in water is used as a simple example to illustrate two types of results: (1) Determination of concentration gradients in a static system, and (2) Rate of change of concentration in a dynamic system.

Analysis of multicomponent systems by X-ray fluorescence: J. HOWER, L. C. JONES, and H. D. BURNHAM, Shell Oil Company, Wood River, Ill.

A general scheme of analysis based on the equations of SHERMAN* has been attempted. Novel alterations and extensions of the original equations were required before a suitable analytical procedure

* SHERMAN, J., ASTM Special Technical Publication 1953 No. 157, 27.

VOL. 8 1956/5

was developed. For a three-component system the working equations take the form of three simultaneous equations, linear with respect to the concentrations and reciprocal intensities and third order with respect to a geometric factor. The value of the method is greatly enhanced by the use of time-saving graphical solutions for these equations. In addition, the X-ray fluorescence method developed can now handle quantitatively samples of nonidentical geometry, i.e., specimens in the form of plate, wire, chips, turnings, and filings can be treated with equal ease. Calculation of the interaction coefficients required in setting up the method from a series of standards has been facilitated by the use of IBM equipment. Application of the method to the analysis of steels for chromium, iron, and nickel will be described.

Rapid and improved mineral analyses with fluorescent X-ray spectrography: Merlyn L. Salmon and James P. Blackledge, Denver Research Institute, University of Denver, Denver, Colo.

Progress in the field of fluorescent X-ray spectrography is very rapid at the present, yet the future is practically unlimited in the need for improved equipment and the need for the development of techniques for the optimum use of the existing equipment.

Minerals are presently analysed routinely by fluorescent X-ray spectrography with no question that the speed of analysis is unsurpassed by any other method. The greatest limitation in the application of the method is the interference effect that may be encountered in the quantitative analysis for a single element.

Several techniques and equipment developments are reported in the literature to yield suitable accuracy with reasonable speed of quantitative analysis; however, there is still the need for improved accuracy-speed ratios.

Research programmes at the Denver Research Institute have yielded techniques with accuracy/speed ratios that are very favourable compared to other procedures of mineral analyses. These ratios vary from $\pm 10\%$ of the actual concentration of an element at the rate of ten determinations per hour to $\pm$ a fraction of a percentage of the actual concentration with one determination per hour.

Radioisotope X-ray sources and applications: S. Fine and C. F. Hendee, Philips Laboratories, Irvington-on-Hudson, N.Y.

The initial cost, bulk, and power requirement of X-ray tube installations have been the motivation for a search for compact portable sources of X-rays in many fields of application. Such sources are available among the many artificially produced radioisotopes which emit characteristic X-rays immediately subsequent to electron-capture or isomeric transitions toward the stable state.

Emission energies range from 5 to 80 keV. Calculations were made showing that the emission intensity per cm^2 of surface of a number of these isotopes averages about 10^5 to 10^7 photons/sec/cm^2, which compares favourably to the 10^3 to 10^6 c/s available at the detecting end of a typical X-ray fluorescence arrangement. These characteristics, plus the natural stability calculable from the half-life, make the sources useful for testing X-ray sensitive detectors, checking the counting and energy linearity of X-ray detection systems, and determining the overall stability of X-ray equipments. Other practical applications exist in the fields of thickness gauging, diffractometry, absorptionometry, nondispersive fluorescence analysis, and radiography.

Work has been done in depositing layers of Fe55, which emits MnK-radiation, on source holders suitable for portable use around the laboratory or insertable in the exit slit position of the Norelco X-ray diffractometer goniometer arm. Similar work has been done with Zn65, which emits CuK-radiation. It has been possible to firmly bind the radioactive layers to the backing material so that there is no danger of contaminating the laboratory and equipment even though no X-ray absorbing covers are used. Specific metal foils, which are highly absorptive of the $K\beta$ component of the characteristic radiation emitted, can be employed as covers for these sources to further monochromatize the radiation.

Facilities exist at the National Laboratories for the production of X-ray emitting radioisotopes by piles of cyclotrons. The yield of the radioisotope production process will depend on such factors as the natural abundance and purity of the target material, the available flux of the bombarding particle and the cross section of the target material for this particle, the half-life of the produced radioisotope and its degree of purification. The radioisotope X-ray yield will depend on factors such as the specific activity, the fraction of competing decay processes, the fluorescence yield, the self-absorption of the radioisotope for its own characteristic radiation.

Some work has also been done with naturally radioactive polonium whose alpha particles, when stopped in Al or Ni foils of proper thickness, produce characteristic X-radiations of the bombarded element. It is interesting to note that radioisotope β-emitters, such as Sr90-Y90, P32, Ca45 can be utilized in target bombardment arrangements (analogous to the X-ray tube) or in intimate mixture with the target material for the production of characteristic X-lines superimposed on a bremsstrahlung continuum.

Trace analysis with Norelco X-ray spectrometer: Frederick Behr, North American Philips Co., Inc., Mt. Vernon, N.Y.

Examples will be given of trace analyses made with the various Norelco spectrometric instruments such as the Autrometer and the 50 kV and 100 kV spectrometers. Detection limits reached for low-percentages of various elements in liquids, metals, and ores will be presented.

The reduction of background and scatter by means of electronic energy discrimination will be described.

Orientation and diffraction effects in metals and powders and the effects of specimen rotation will be presented. The practical aspects of resolution limits achieved by various geometries and their relation to quantitative analytical results will be discussed.

Fluorescent X-ray spectrographic analyses of traces of germanium: William J. Campbell and Howard F. Carl, Eastern Experiment Station, U.S. Bureau of Mines, College Park, Md.

Germanium usually occurs as a trace or a minor element, in concentrations of less than 0·1%, in certain minerals and in coals. Chemical analyses for this element are often difficult and may be unreliable for various reasons. A sensitive fluorescent X-ray spectrographic method has been developed which involves a preliminary chemical concentration of germanium.

Germanium is separated from the sample by distillation as the volatile tetrachloride. This distillate is precipitated as an organic complex, e.g., cinchonine germanomolybdate, and collected on filter paper. Standards are prepared by precipitating aliquots of a standard germanium solution under identical conditions as the unknowns.

The intensities of the Ge$K\alpha_1$ lines of the unknowns are compared to a calibration curve prepared by use of the standard filter papers. Either a quartz or topaz analysing crystal is used to provide sufficient resolution of the Ge$K\alpha_1$ line from the second order Mo$K\beta$ lines.

By this technique germanium analyses are made on a one-gram sample to within ±10% of the amount present, in the concentration range of 5–100 p.p.m. (0·0005 to 0·01%). These limits can be extended by the use of a greater or lesser amount of initial sample. The analysis of a group of eight samples and two standards requires an average of 2 hours per sample.

VOL. 8 1956/5

Fluorescent X-ray spectrographic determination of uranium in waters and brines: W. L. Kehl and R. G. Russell, Gulf Research & Development Company, Pittsburgh 30, Pa.

In a search for a method sensitive to small concentrations of uranium in water and brine, a modification of a fluorimetric method was adopted. The uranium is precipitated from the water or brine by the method of Smith and Grimaldi,* and the ashed precipitate is analysed by fluorescent X-ray spectrography. The sample holder of the Norelco X-ray spectrograph was modified to place the small precipitate samples in the most intense part of the beam from the molybdenum target X-ray tube. The sensitivity of the method is such that as little as 0·01 mg of uranium, equivalent to 0·01 p.p.m. in a one-litre water sample, can readily be measured. The time for analysis is about 10 minutes per sample, exclusive of the precipitation process.

Determination of chromium nickel and copper in jute and paper by X-ray fluorescence methods: J. P. Wright and K. H. Storks, Bell Telephone Laboratories, Murray Hill, N.J.

A rapid direct X-ray fluorescence method for the determination of metals in fungus proofed cellulosic materials will be described. Various instrumental arrangements, suited for the analysis of single strands or extensive flat samples will be discussed. The method is applicable to continuous analysis during treatment, or spot to spot scanning to determine uniformity of treatment.

With commercially available apparatus, the lower detectability limits for chromium, copper, and nickel using the single strand method are 0·015, 0·002, and 0·001. With the extensive sample method these values are considerably improved.

Application of X-ray emission spectroscopy to air-borne dusts in industrial hygiene studies: R. C. Hirt, W. R. Doughman, and J. B. Gisclard, American Cyanamid Company, Stamford, Conn.

The ability of X-ray emission spectroscopy to determine quantitatively the heavy metal elements in the range of 1 to 100 micrograms in the absence of interferences has been applied to industrial hygiene studies. Airborne dusts containing heavy metals may constitute a health hazard in the manufacture, processing, and packaging of catalysts, ores, and pigments. The atmosphere is sampled by drawing the air at a known rate through a glass fibre filter disc which catches the air-borne dust. The dust is imprisoned on the disc by application of an acrylic resin spray to protect the sample during shipment to

* Smith, A. P., and Grimaldi, F. S., Fluorimetric Determination of Uranium in Nonsaline and Saline Waters. *Geol. Survey Bull.* 1954 No. 1006, 125–131.

the laboratory. The filter disc is examined directly in a "Norelco" X-ray emission spectrograph. Calibration curves, extending down to one to five micrograms, have been prepared for cobalt, chromium, iron, lead, mercury, nickel, platinum, vanadium, and zinc. Examples are presented for air-borne dusts from catalysts (platinum, vanadium), ores (cobalt), and pigments (chromium). Extension to many other elements is quite feasible.

Application of the X-ray spectrograph to the analysis of chlorine in resins: Earl R. Walter, Research and Development Department, Carbide and Carbon Chemicals Company, South Charleston, W. Va.

A rapid method has been developed for the determination of chlorine in resins using the X-ray spectrograph. The method is equally applicable to dry powder or moulded plaques. Precision and accuracy are comparable to the best wet chemical methods and the time required for an analysis is less than that required by the usual routine chemical methods.

One calibration curve was found to fit all copolymers of vinyl chloride in which the other component contained carbon and hydrogen either alone or in combination with nitrogen, oxygen, or chlorine. The method has also been applied to materials containing chlorine in the presence of fluorine. Although these materials required different calibration curves, the precision was equal to that obtained when fluorine was not present.

Determination of platinum in reforming catalyst by X-ray fluorescence: E. L. Gunn, Humble Oil & Refining Company, Baytown, Texas.

An X-ray fluorescence method has been developed and applied to the routine inspection of reforming catalyst for platinum content. The specimen is prepared for analysis by briquetting the sample with 5% Sterotex binder. At the 0·6% level the precision of measurement is expressed as a standard deviation of 0·0066% platinum. Excellent agreement with other methods is shown. High precision is obtained irrespective of the time of measurement or of specimen preparation. Optimum tube conditions are selected for maximum peak-to-background ratio. The influence of carbon, iron, and water contamination in a catalyst is minor or negligible. Heat treatment does not affect the value obtained on a catalyst. Helium offers no marked advantage over air as an atmosphere in the optical path of the instrument.

Infra-red Spectroscopy

Effects of resolution in infra-red analysis: John U. White, White Development Corporation, Stamford, Conn.

Some of the factors affecting repeatability in the measurement of absorbance are discussed from the instrumentation point of view. The widths of liquid absorption lines and the correction of errors will be considered.

Infra-red microspectroscopy and the effect of convergence: S. S. Mitra and D. L. Wood, University of Michigan, Ann Arbor, Mich.

The large angle of convergence necessarily encountered in infra-red microspectroscopy can introduce serious difficulties in the interpretation of spectra. With fibres where there is molecular orientation along one direction the effect of convergence is small. With single-crystal sections, however, the effects can become large, introducing both shifts in frequency and incorrect intensities. For such specimens the various factors involved will be discussed, and evaluated. The results will be presented in terms of forbidden absorption intensity and frequency shift versus angle of convergence.

Improving the performance of the Perkin-Elmer Model 21 spectrophotometer: H. G. Conner, W. M. Trippeer, and D. J. Troy, Engineering Research Laboratory—Engineering Dept., E. I. du Pont de Nemours & Company, Inc., Wilmington, Del.

The performance of the Perkin-Elmer Model 21 infra-red spectrophotometer has been improved several fold by reduction or elimination of stray pickup, thereby reducing the total noise level. The modifications necessary to achieve this and experimental results that illustrate the improvement obtained are described.

Design and performance of a fore prism-grating infra-red spectrometer: E. H. Siegler, jr. and J. W. Huley, The Perkin-Elmer Corporation, Norwalk, Conn.

A high resolution fore prism-grating spectrometer was constructed using a newly designed fore prism monochromator and a Perkin-Elmer 12-C spectrometer converted to grating use. Fore prism design considerations will be discussed. The performance of the system will also be described. Improved resolution (approximately 1 cm^{-1} in the rock salt region) and low scattered light are observed.

Design and performance of the Beckman Model IR-4 infra-red spectrophotometer: William M. Ward, Beckman Instruments, Inc., Fullerton, Calif.

A new infra-red spectrophotometer has been designed for greater facility in analytical and research problems. Among the described features will be the following: double beam operation for high speed qualitative work; single beam operation for high accuracy in quantitative analysis; double monochromator for high resolution and low stray light. Other unique design features will be discussed, and curves will be shown depicting the performance.

The electronics of the Beckman Model IR-4 infra-red spectrophotometer: Noel B. Braymer and N. G. Kabuss, Beckman Instruments, Inc., Fullerton, Calif.

The electronics of the Beckman IR-4 infra-red spectrophotometer consists of four major parts: A high gain eleven cycle signal amplifier which incorporates a unique feedback path for decreasing the response time of the system; a slit width programmer which provides a slit width that is a function of wavelength; a wavelength scan speed control that is a function of slit width; and the servo amplifiers for driving the slits, wavelength scan, pen, and comb.

Near-infra-red spectroscopy. The association of alcohols: Wilbur I. Kaye, Research Laboratories, Tennessee Eastman Company, Division of Eastman Kodak Company, Kingsport, Tenn.

The association of alcohol molecules into dimers and polymers can be readily observed from the "free" and hydrogen-bonded OH absorption bands at 1·4 and 2·8 μ. Careful measurements of the band intensities permit the calculation of association equilibrium constants, free energy, heats of association, and entropy change. These values are found to be properties not only of the alcohol but also of the solvent used. Rather drastic differences are observed when n-amyl alcohol associates in carbon tetrachloride, Fluorolube, carbon disulphide, and chlorobenzene.

The infra-red spectra of aromatic compounds II. Evidence concerning the interaction of π-electrons and σ-bond orbitals in C—H out-of-plane vibrations: R. D. Kross, V. A. Fassel, and M. Margoshes, Institute for Atomic Research and Department of Chemistry, Iowa State College, Ames, Iowa.

In certain monosubstituted and para-disubstituted benzenes the frequency of one of the C—H out-of-plane bending vibrations falls above the characteristic frequency range assigned to that vibration. A property common to all of the substituents which cause this positive shift in frequency is that they are electrophilic in nature, i.e., they tend to deplete the aromatic nucleus of π-electronic charge. These experimental observations are consistent with the theory of orbital following during molecular vibrations. The depletion of π-electron density of the aromatic nucleus by electrophilic substituents leads to a decreased ability of the carbon bonding orbital to follow the out-of-plane movement of the hydrogen atom. This results in higher bending vibration frequencies because the vibrations occur with greater difficulty as orbital overlap decreases. Application of this theory to other spectral anomalies will also be discussed.

The infra-red and ultra-violet characterization of some selenides, selenoxides, and selenones: Sister Miriam Michael Stimson, O.P., Siena Heights College, Adrian, Mich.

The infra-red spectra of p-tolyl selenide, p,p′-dimethoxy selenide and of p,p′-ethoxy selenide have been determined in carbon tetrachloride, and the infra-red spectra of these compounds as well as of p,p′-dimethoxy-selenoxide and p,p′-dimethoxyselenone and the corresponding p,p′-diethoxy-compounds have been determined in KBr disks. Certain spectral changes, especially splitting of bands occurring between 6–9 microns in the KBr sample as compared to the CCl_4 sample have been observed. On the other hand the absorption in the 12 micron region is much sharper in the solid specimen.

In the study of the ultra-violet spectrum, solutions were run in ethanol as well as the KBr disks. Ethanol solutions of the selenoxides were sufficiently different from those in KBr disks to suggest interaction with the solvent. The change of selenium to the selenoxide and to the selenone is reflected in the infra-red region in the ether link in such a way that there is a greater similarity in the symmetrical compounds, which is reflected in the stability of these compounds to changes in pH as shown in the ultra-violet region.

Ultra-violet and infra-red absorption spectra of some metal anthranilates: Sister Ann Gertrude Hill, O.S.U. and Brother Columba Curran, University of Notre Dame, Notre Dame, Ind.

The usual effect of chelation is to shift the ultra-violet absorption maxima of the ligand to longer wavelengths. It is to be expected that the direction of this shift might be reversed when one of the donor centres is a nitrogen atom of an aryl amine. This reversal has been observed for the complexes of the anthranilate ion with cadmium, zinc, and magnesium cations. The above complexes have long

VOL. 8 1956/5

wavelength absorption maxima in potassium bromide disks at 298, 296, and 294 mμ respectively, compared to the corresponding maxima for barium, strontium, and calcium anthranilates at around 322 mμ. Ultra-violet spectra reveal that the cadmium complex is partially dissociated and the magnesium complex completely dissociated in absolute ethanol. All three complexes are completely hydrolysed in 95% ethanol.

Infra-red spectra reveal that the configuration of these complexes is the same as that of bis-(anthranilato)copper(II). The absorption patterns in the 6-micron region indicate electrostatic COO^-—M bonds. The spectra in the caesium bromide region suggest a partial covalent character for the N—M bonds in the anthranilates of the alkali and alkaline earth metals.

A microfilm catalogue of infra-red spectra and X-ray powder patterns of biochemicals; inclusive biochemical analysis:* Carl Clark, Biophysics Division, Naval Aviation Medical Acceleration Laboratory, Johnsville, Pa.

Further contributors to the standard data catalogue are desired. A goal is to assemble in one file, available to others at reproduction cost, with suitable indices, the published and unpublished data of all biochemicals and the common tissue fractionation products which can be uniquely identified by these techniques. The form of the catalogue will be presented. A biochemical index (name index) of the principal molecules whose data are sought will be available. Preliminary fractionation procedures of biological fluids or tissues, involving the study of all fractions, and IBM computational procedures for automatic mixture analysis, utilizing all the information of the spectrum, as absorptivities per unit spectral slit width across the spectrum, with the minimization of the sum of the squared differences of the observed and computed spectra, will be reviewed. A subsequent goal is a machine for automatic inclusive small molecule (to molecular weight 300–600) biochemical analysis.

Infra-red determination of hydrocarbon structural groups: S. A. Francis, Beacon Laboratories, The Texas Company, Beacon, N.Y.

The use of structural group intensities for the quantitative determination of structural group concentrations will be reviewed. Methods for the determination of saturated, olefinic, and aromatic hydrocarbon groups will be discussed and applications of these methods will be presented. Present limitations and possible future developments will be indicated.

Group type analyses for oxygenated materials by infra-red absorption: Eleanor L. Saier and Richard H. Hughes, Gulf Research & Development Company, Pittsburgh, Pa.

This paper will discuss group type analyses for oxygenated materials by infra-red absorption. Quantitative analyses for the following groups will be considered: alcohols, acids, ketones, aldehydes, esters, and ethers.

When only one type is present, its concentration can readily be determined. The intensity of the OH absorption at 2·76 μ is a measure of the alcohol concentration. Acids can be determined from the acid OH absorption at 2·82 μ in dilute solution if a calibration curve is used. Either acids, aldehydes, ketones, or esters can be determined from the carbonyl absorption at 5·8 μ. The absorption at 8·5 μ is a measure of the ester concentration and that near 9·0 μ a measure of the ether content. Integration methods should be employed whenever absorptions for individual members vary in wavelength or are split into components. Integrated intensities are not influenced by small shifts in line position and are more independent of changes in chemical structures than are maximum absorptivities.

The problems of analyses for one or more of these groups types in the presence of others will be discussed. For example, a base line method can be employed to determine acid in the 2·82 μ region in the presence of background absorption from other group types.

The design and performance of a simplified die for the preparation of potassium bromide windows: H. T. Grendon and H. L. Lovell, The College of Mineral Industries, The Pennsylvania State University, University Park, Pa.

The construction of this evacuable die was based upon the requirements of minimum cost combined with maximum performance and convenience as well as ease of construction. The salient features include ease of operation, maintenance and adjustment, versatility in regard to window shape and thickness according to the spectrometer requirements or the amount of sample available, and the use of window holders as part of the forming die to facilitate handling of the windows. Excellent window quality is consistently obtained. The nature of the windows and the resulting spectra will be discussed.

---

* This work is supported in part by a grant from the American Cancer Society on the recommendation of the Committee on Growth of the National Research Council.

Spurious infra-red bands due to grinding small amounts of KBr in mortars of various composition: W. B. Mason and J. Salvatore, Atomic Energy Project and Department of Biochemistry, School of Medicine and Dentistry, The University of Rochester, Rochester, N.Y.

KBr disks prepared from powder obtained by grinding the sample with a small amount of coarse KBr in a motor driven mortar give spurious absorption bands, predominantly in the 7–10 μ region. With KBr alone, the magnitude of these absorptions vary with the grinding time, amount of KBr ground, size of KBr particles taken for the disk, and the composition and cleaning of the grinding unit. Of these, composition appears to be the primary variable. Data are presented for porcelain, mullite, tool-steel and Kennametal (tungsten carbide) mortars. With a moderately polished Kennametal unit, good spectra substantially free of spurious bands are obtained with powder prepared by grinding 2–3 mg of sample with 500 mg of KBr for 15 minutes in a Fisher Mortar Grinder.

This paper is based on work performed under contract with the United States Atomic Energy Commission at the University of Rochester Atomic Energy Project, Rochester, New York.

Adaptation of potassium bromide disc technique for infra-red micro analysis: H. P. Schwarz, R. Childs, L. Dreisbach, and S. V. Mastrangelo, Philadelphia General Hospital, Philadelphia, Pa.

The KBr-disc technique has been adapted for quantitative micro analysis in the microgram range. The improvements include: (1) Specimen preparation by improved freeze drying techniques; (2) Disc preparation with lubrication of dies with graphite; and (3) Avoidance of contamination of any kind during the whole sample processing operation. Water soluble specimens are frozen dried with a Cryochem apparatus. Water insoluble specimens are processed by a two-step freeze drying procedure. An apparatus for freeze drying of both types of specimens on a relatively large scale is demonstrated. Lubrication of the dies with graphite permitted use of evacuable single and double plunger dies. Calibration curves for a number of compounds are shown. The feasibility of the technique for infra-red micro analysis is demonstrated.

Micro method for the infra-red identification of carbohydrates in the solid state: Joseph Fugger, The Buckeye Cellulose Corporation, Memphis 8, Tenn.

Spectral absorption curves, covering the 2 to 15 micron region, are presented for twenty carbohydrate substances.

The existence of a highly distinctive pattern of absorption bands in the 10–15 micron region is demonstrated for all the compounds tested. Methods are given which permit use of this "sugar fingerprint region" for the identification of carbohydrates.

An inexpensive and easily manipulated die has been constructed for the preparation of KBr—sample discs under vacuum. Anderson's equipment has been simplified without sacrificing its utility. Samples weighing about 0·15 mg are dispersed in 20 mg of KBr and pelletized to form a one-quarter inch diameter plate firmly mounted inside a metal ring. Less than one ton of force, applied briefly, is required for pressing. A method is given for obtaining good spectra of these micro samples using the Perkin-Elmer Model 21 double-beam spectrophotometer. The necessary, easily constructed, accessories are described.

Study of the interaction between surface OH groups and adsorbed nonpolar molecules by infra-red spectrometry: R. S. McDonald, G. E. Research Laboratory, Box 1088, Schenectady, N.Y.

The sharp 3749 cm^{-1} OH absorption of a thoroughly outgassed burned silica, such as Cabosil, is due to isolated surface OH groups. When molecules are adsorbed adjacent to OH groups, the 4739 cm^{-1} band decreases in intensity and a new band appears at lower frequency. The residual intensity of the 3749 cm^{-1} band is a measure of the amount of free surface OH groups remaining. The magnitude of the band shift is a measure of the strength of interaction between surface OH groups and adsorbed molecules. The sharpness of the 3749 cm^{-1} band allows measurement of very small shifts caused by adsorbed nonpolar molecules such as N_2, O_2, CF_4, CH_4, C_6H_{12}, C_6H_6, and the rare gas atoms A, Kr, and Xe.

The infra-red and mass spectra of eight high purity nitroparaffins: Richard A. Jewell and Theron J. Allen, Commercial Solvents Corporation, Terre Haute, Ind.

This paper presents infra-red and mass spectral data on eight high-purity nitroparaffins from nitromethane through the four isomeric nitrobutanes.

Within the rock-salt region of the infra-red spectrum, symmetrical and unsymmetrical stretching vibrations of the nitro-group produce absorption peaks at 7·24 to 7·42 microns and 6·47 $\pm$ 0·05 microns respectively.

The mass spectral data includes fragmentation patterns relative to the standard breakdown pattern of n-butane.

VOL. 8 1956/5

Ultra-violet Spectroscopy

Organic group analysis with ultra-violet spectroscopy: J. M. VANDENBELT, The Research Laboratories, Parke, Davis & Co., Detroit 32, Mich.

Group identification by ultra-violet absorption is not usually accomplished by means of a direct correspondence of structure and band like that obtaining in parts of the infra-red spectrum. This results from the number of relatively wide bands which must be accommodated in a relatively short region, the tendency of many structural types to absorb at similar wavelengths, the pronounced effect of contiguous structure and arrangement on the absorptive wavelength, and the effects produced by combination of chromophores, in which the individual characteristics of each are obscured in the pattern of the larger unit.

Assignments are effected rather on a permissive basis. Groups are first qualified tentatively in the light of wavelength, absorptivity, and contour of bands; probabilities are selected against a background of sample origin and chemical properties. These are complemented by additional effects and behaviour, such as dissociation with change in pH, and more subtle influences such as change in solvent. Within a given frame, choice of possibilities may be quite discerning, especially when supplemented by model compounds, derivatives, and calculations.

Modification of a Beckman Model DU Quartz spectrophotometer for measurements to 192 millimicrons: L. W. TAYLOR and L. C. JONES, JR., Wood River Research Laboratory, Shell Oil Company, Wood River, Ill.

A Beckman Model DU Quartz spectrophotometer has been modified so that reliable absorbance measurements at wavelengths as short as 192 millimicrons can be obtained with solutions. The modification involved rotation of the collimating mirror, construction of a new wavelength scale, substitution of a photomultiplier with fused silica window (EMI 6255) for the usual detector, replacement of the Beckman u.v. source with an Allen-Nester hydrogen discharge tube, use of thin-spacer absorption cells, installation of a Vycor filter for measurement of the residual stray energy; provision was also made for flushing the monochromator with nitrogen. Spectra obtained with the modified instrument are in excellent agreement with those measured with a recording vacuum spectrometer* over the entire spectral range. The modified instrument is an adequate substitute for a vacuum spectrometer in a number of applications of practical importance where the conventional ultra-violet spectrometer is not suitable.

The precision, accuracy, and sensitivity of quantitative measurements with the Beckman DK-1 spectrophotometer: FREDERICK C. STRONG III and EDWARD S. O'CONNOR, Stevens Institute of Technology, Hoboken, N.J.

Repeated measurements of the absorption of solutions were made with a Beckman DU spectrophotometer over a wide range of absorbances. The results were studied statistically for precision, absolute accuracy and sensitivity. The classical error curve for transmittance measurements was tested experimentally to determine whether mechanical and electrical considerations require it to be modified.

Definition and variation of the performance of an ultra-violet-near infra-red spectrophotometer: B. D. HENDERSON, Beckman Division, Beckman Instruments, Inc., Fullerton, Calif.

Extensive tests have been developed to define and evaluate the performance of Beckman DK Spectrophotometers when they are made, which may be applied to any spectrophotometer operating in the same wavelength range. The tests have been applied to several hundred instruments, and the results analysed to determine the variation in performance parameters between different instruments of the same design. These variations are significant, and must be considered when attempting to generalize from the performance of any single instrument.

Ultra-violet water vapour measurement: T. A. CHUBB and H. FRIEDMAN, U.S. Naval Research Laboratory, Washington, D.C.

Water vapour absorbs strongly in the extreme ultra-violet. At the wavelength of the Lyman α line of hydrogen (1216 Å) molecular oxygen and nitrogen are both relatively transparent. By means of photon counters, sensitive to a narrow band of wavelengths centred about 1216 Å, it is possible to measure the absorption of water vapour in open air over a path length of several centimetres, without the use of a dispersive monochromator. Similar techniques are applicable to absorption measurements of traces of molecular oxygen in the rare gases, nitrogen, and hydrogen.

---

* JONES L. C., JR. and TAYLOR L. W. *Analytical Chemistry* 1955 **27** 228–37.

Spectroscopic studies in dyes. II. The structure of N,N′-dimethylindigo: Julius Weinstein and George M. Wyman, Quartermaster Research and Development Centre, U.S. Army, Natick, Mass.

In contrast with other indigo dyes, N,N′-dimethylindigo is a low-melting green compound which is very soluble in organic solvents and has little affinity for fibres. The wavelength of the visible absorption band of this dye is strongly dependent on the nature of the solvent; hydroxylic solvents, in particular, cause a strong bathochromic shift. The absorption band shifts to still longer wavelengths in the solid phase. Rapid trans to cis isomerization occurs when a solution of this dye is irradiated with yellow or red light; reversal of the reaction in the dark is almost instantaneous. The compound also forms hydrogen-bonded complexes with phenol. These observations suggest that, probably due to the steric effect of the methyl groups, the central double bond of this compound has considerably more single-bond character than in other indigo or thioindigo dyes.

The determination of 2,6-di-tertiary-butyl-para-cresol in edible fats by ultra-violet spectrophotometry: M. A. Phillips and R. D. Hinkel, Koppers Company, Inc., Verona, Pa.

2,6-Di-tertiary-butyl-para-cresol (I) is a very effective agent for inhibiting oxidation in a wide variety of organic substances. Recently, by approval of the Meat Inspection Division of the U.S. Department of Agriculture, its use has been extended to edible fats, notably lards, where prior studies have shown that the development of rancidity can be effectively delayed through the use of quantities as low as 100 to 200 p.p.m. (0·01 to 0·02%).

To maintain effective control over food processing operations and ensure adherence to governmental regulations, a quantitative method was developed for determining 20 to 200 p.p.m. (0·002 to 0·02%) of (I) in lards in the presence of other allowable preservatives, including butylated hydroxy anisole, nordihydroguaiaretic acid, propyl gallate, citric acid, citric acid esters and phosphoric acid.

In this method the lard sample is dissolved in cyclohexane and percolated through a chromatographic column packed with 100-mesh silicic acid. By washing the column with successive portions of cyclohexane, (I) is selectively removed from the adsorbent and recovered in the column filtrates. The filtrates are subsequently analysed by ultra-violet spectrophotometry, and the amount of (I) is calculated from optical density measurements made at a wavelength of 284 millimicrons.

This procedure has been tested with synthetic formulations of commercial-brand lards with (I) and other additives in concentrations and combinations as permitted by law. A large number of analyses indicates that recoveries consistently better than 93% can be obtained, with the majority of recoveries being over 97% of the amount added.

The absorption of 2-(o-hydroxyphenyl)benzothiazoline and some of its metal chelates: Otho E. Harris and Henry Freiser, Department of Chemistry, University of Pittsburgh, Pittsburgh, Pa.

The compound 2-(o-hydroxyphenyl)benzothiazoline has been found to form chelates with a considerable number of metallic ions. Spectral analyses have been made of these complexes in the ultra-violet, visible, and infra-red regions of the spectrum; however, most of the attention will be focused on the visible region.

In the examples to be discussed, only small shifts in λ_{max} of the ligand absorption are brought about by complex formation. Since the absorption of light by complexes can arise through transitions of nonbonding electrons of the ligand, nonbinding electrons of the cation, or bonding electrons between the cation and the ligand, an attempt has been made to interpret these spectra in terms of the possible structures of the respective complexes.

Ultra-violet determination of phenolic antioxidants in rubber: C. W. Wadelin, Research Division, Goodyear Tire & Rubber Co., Akron 16, Ohio.

The determination of phenolic antioxidants in rubber extracts by direct ultra-violet measurement is subject to interference from other extractable materials. Reliable average correction factors cannot be established because the magnitude of the interference varies from sample to sample.

It was found that in extracts of both hot and cold GR-S the only substances which undergo an ultra-violet spectrum shift as a function of basicity are phenolic antioxidants. A wavelength is chosen where the antioxidant has a low absorptivity in neutral solution and a higher absorptivity in 0·1 N potassium hydroxide solution. Since the other materials present are insensitive to the change in basicity, the measurement in neutral solution serves as a background correction factor for that particular sample and permits accurate determination of the antioxidant.

The method has been applied to Wing-Stay S (styrenated phenol), 2,6-di-t-butyl-4-methyl phenol, and methylene bis-2,2′-(6-t-butyl-4-methylphenol).

VOL. 8 1956/5

A new optical test for minerals with narrow absorption bands in the visible region: HARRY BASTRON and K. J. MURATA, U.S. Geological Survey, Washington 25, D.C.

The property of discontinuous absorption of visible light shown by certain minerals, notably those containing cerium earth elements, has long been used to identify these minerals. The characteristic absorption bands have been observed by illuminating the mineral with white light and looking at either the reflected or transmitted light through a visual spectroscope.

In the new method, white light is replaced with a special source that emits only two wavelengths of visible radiation, and observations are made with the naked eye. The wavelength of one radiation is selected to lie in the middle of a strong absorption band and that of the other to lie nearby on either side of the absorption band in a spectral region of low absorption. The mineral assumes the colour of the unabsorbed radiation. The principle is illustrated through the use of the green and yellow radiations of a mercury vapour lamp for identifying cerium earth minerals.

Spectrophotometric titration of olefins with electrically generated bromine: JOHN W. MILLER and DONALD D. DEFORD, Department of Chemistry, Northwestern University, Evanston, Ill.

This investigation was undertaken to develop a spectrophotometric titration procedure in which a plot of absorbance versus time of generation of bromine was recorded and to apply the technique for the precise and accurate determination of small quantities of olefins. The Cary spectrophotometer was used to obtain the recorded titration curves, and a new cell holder was constructed to allow the use of a 100 ml electrolysis beaker as the titration cell. A new cover for the sample compartment was made to allow the entrance of the two electrodes and of the shaft of a stirrer. A wavelength of 360 mμ was used to determine the end point. The generator electrolyte consisted of 95 ml of a 3 : 1 mixture of glacial acetic acid and methanol to which had been added a small amount of potassium bromide and concentrated hydrochloric acid. 8 ml of 15% methanolic mercuric chloride was added to serve as a catalyst. Bromine numbers of 14 olefines of all structure types were determined with a precision of better than 2% on samples ranging from 5 to 20 mg.

The results of the coulometric bromination procedure were compared with the values obtained from bromination by the method of LUCAS and PRESSMAN* and by the A.S.T.M. procedure [D1158-52T] as well as with hydrogenation values. The new procedure compares favourably with the hydrogenation method, but the method of LUCAS and PRESSMAN gives high results.

The use of impure compounds as calibration standards for quantitative infra-red spectrophotometry: R. S. MUNGER and E. L. GAVIN, Continental Oil Company, Ponca City, Okla.

A technique is described which, under favourable circumstances, permits impure compounds to be used for spectrophotometric calibration purposes. Purity of the standards is estimated from the calibration data.

This technique can be used if two conditions are met:

1. Each component of the system has strong absorption at some wavelength at which each of the other components has only smooth background absorption.
2. None of the calibration standards contain any material other than those for which calibration is being conducted.

The technique is especially useful for "one shot" determinations which do not warrant the preparation of high purity standards.

Calibration data for the determination of the three mono chloro toluene isomers are used to demonstrate the method.

The analysis of liquid chlorine by infra-red absorption spectroscopy: D. ANDRYCHUK, Diamond Alkali Company, Cleveland 14, Ohio.

A refrigerated infra-red liquid cell is described. The application of the cell to the analysis of liquid chlorine for the concentration of impurities carbon tetrachloride, hexachloroethane, phosgene and chloroform is given.

Near infra-red determination of H_2O in D_2O. Application to the determination of water of crystallization and readily exchangeable hydrogens in organic and inorganic compounds: JOHN H. JONES and MARIE ALICE HALL, Food and Drug Administration, Department of Health, Education, and Welfare, Washington 25, D.C.

From 1 to 10% H_2O in D_2O can be easily and accurately determined from the absorbance of the mixture at 1·4 μ. The H_2O of crystallization and/or readily replaceable hydrogens in various samples are

* LUCAS and PRESSMAN *Ind. Eng. Chem., Anal. Ed.* 1938 **10** 140–2.

determined by equilibrating the sample with D_2O, separating the H_2O—D_2O equilibrium mixture and determining the H_2O content of the mixture.

Application of this procedure to various compounds and to analytical problems are described.

Optical Fluorescence Spectroscopy

Modification of the Beckman DK-1 spectrophotometer for use as a recording spectrofluorometer: Chalmers L. Gemmill, Department of Pharmacology, School of Medicine, University of Virginia, Charlottesville, Va.

The Beckman DK-1 spectrophotometer was modified in the following manner in order to record fluorescence spectra. The lamp from the back plate was removed and a hole bored into this back plate. When ultra-violet light passed through this hole, it excited fluorescence in the sample which occupied the former position of the lamp. The fluorescent light of the sample was picked up by the mirror mounted in its usual position on the back plate and passed into the spectrophotometer. A 150-watt Hanovia xenon arc lamp (10-C-1) was used as the source of light. In the first modification a Corning filter No. 9863 was placed over the hole in the back plate in order to cut off wavelengths above 410 μ. Later the light from the xenon arc was passed through a Bausch and Lomb Monochromator in order to vary the wavelengths of the exciting light. In operation the solution is placed in a quartz cell, the cell placed in position and the arc ignited. The DK-1 spectrophotometer is placed on "Energy." The sensitivity and 100% adjustment are set in order to get maximal energy deflection for the solution under study. The slit is kept open at 2·0 mm. Examples will be shown of the use of this instrument for the study of the energy exchange of mixed phosphors excited by ultra-violet light.

Applications of spectrophotofluorometry to the analysis of organic compounds in solution: Daniel E. Duggan, Robert L. Bowman, Bernard B. Brodie, and Sidney Udenfriend, Laboratory of Chemical Pharmacology, and Laboratory of Technical Development, National Heart Institute, National Institutes of Health, Bethesda, Md.

A spectrophotofluorometer capable of continuous activation and measurement of fluorescence throughout the ultra-violet and visible regions has been developed in this laboratory.* Activation and fluorescent spectra which are rapidly displayed on a cathode-ray oscillograph or X-Y recorder offer several unique advantages over conventional fluorometers. In addition to the specificity inherent in spectral characterization, they provide a ready means for detecting the presence of fluorescent contaminants, for the survey of new compounds and for the determination of environmental effects upon the intensity and position of fluorescent bands. A brief survey of organic compounds of biological interest has revealed useful fluorescence in many compounds not previously known to fluoresce in solution and analytical methods for several have been evolved. Some important compounds now being routinely assayed in biological extracts with this instrument include serotonin, tryptophan and LSD. Details of the spectrofluorometric estimation of tryptophan in proteins and in blood will be presented.

Fluorometric determination of vitamins B_1 and B_2 in mixtures: Wm. E. Ohnesorge and L. B. Rogers, Department of Chemistry and Laboratory for Nuclear Science, Massachusetts Institute of Technology, Cambridge 39, Mass.

A procedure has been developed for the fluorometric determination of vitamins B_1 and B_2 in mixtures. Standard deviations of the order of 5% for each substance have been attained for concentrations from 0·5 to 4·0 p.p.m. The effects of a number of variables have been evaluated.

Flame Photometry

Some anion effects in flame photometry. Barbara Milan and Edwin S. Hodge, Mellon Institute, Pittsburgh 13, Pa.

The intensity changes caused by different anions as present in salts of sodium, potassium and calcium have been studied at cation concentrations of 1, 10, 100, and 1000 p.p.m. with the Beckman DU flame photometer. About 80 compounds have been investigated, and the intensity of the cation emission in each case has been compared to similar concentrations of sodium hydroxide, potassium hydroxide, or calcium chloride as the case might be.

Most of the anions caused little or no deviation in the intensity as produced by the hydroxide or chloride solutions used for standards. Generally, the complex radicals, such as phosphates and borates, showed the greatest changes.

* Bowman R. L. *et al. Science* 1955 **122** 32.

VOL. B 1956/5

Flame spectrophotometric determination of copper in ferrous alloys: John A. Dean and J. Harold Lady,* Department of Chemistry, University of Tennessee, Knoxville, Tenn.

This investigation describes the application of organic solvent extraction to the isolation of copper from ferrous alloys, followed by the flame spectrophotometric determination of copper in the organic phase. An aqueous solution of the alloy is shaken with a 1% solution of salicylaldoxime in chloroform or amyl acetate. Copper salicylaldoxime is formed at the interface and passes directly into the organic phase without intervening precipitation. A portion of the organic phase was aspirated directly into an oxyacetylene flame. The luminescence of the copper emission line at 324·7 μ, corrected for the flame background at 325·0 μ, was measured and compared with standard solutions of copper salicylaldoxime in the same organic solvent. In a citrate solution at pH 2·5 to 3·0 the iron was firmly masked against extraction. No interferences were found when the method was applied to all types of ferrous alloys.

Flame photometric determination of chlorides: Grace E. Marsh, Standard Oil Company (Indiana), Whiting, Ind.

The copper chloride emission-band head at 436 mμ has been employed for the quantitative determination of both organic and inorganic chlorides. The sample size is chosen within the working range of 0·1 to 1% Cl for organic chlorides (DDT, 2,4-D, etc.) and 0·01 to 0·1% Cl for inorganic chlorides. A carefully measured amount of a copper salt is added to each sample. When a very cool flame is used in the Beckman Model DU flame photometer, and the photomultiplier tube is set for highest amplification, the reproducibility of the method is 3% of the amount of chlorine present. Although certain ions interfere with the inorganic chloride determination, their influence can be minimized by proper buffering of the working solution.

The flame photometric determination of lead and copper in plating bath solutions: Ed. G. Wasilko, *Engineering Department, Cleveland Graphite Bronze Co., Cleveland 10, Ohio.*

The Beckman Model DU Flame spectrophotometer has been utilized in the determination of copper and lead in lead-tin-copper and lead-tin plating bath solutions. This method has proven to be extremely rapid and more accurate than the volumetric and electroplating methods used previously. However, standard operating procedures for the Beckman DU are not followed in this analysis because high sensitivities under optimum conditions are needed to obtain the desired accuracy. Therefore, the sensitivity is fixed at its highest level leaving only the dark current and slit dials to make the proper adjustments. The instability of the Fluoborate additives necessitated using plain Cu and Pb standards. Therefore, a unique situation is developed whereby standards on one slope are used to control a working curve with an entirely different slope. Interference from other elements is cut to a minimum by diluting an aliquot from the bath solutions one hundred times with deionized water. Outside of this, no other preparations are made to the plating bath solutions.

A new calcium filter for flame photometry: Stanley J. Sage, Engineering Department, Baird Associates, Inc., Cambridge, Mass.

The major component of the flame emission of calcium occurs as a molecular band, several hundred ångstroms wide. It is, therefore, important, if maximum sensitivity is to be obtained, to use a wide band wavelength selector.

It is also important that the edge of the band be steep to reject efficiently the emission of sodium, potassium and other ions present in the sample. Until recently, this combination was impossible in filter photometers. However, new advances in the manufacture of interference filters have made possible the development of a new calcium filter which has a band width previously obtainable only with glass filters, and the excellent rejection characteristics inherent in interference filters. This paper compares glass filters, narrow band interference filters, and the new wide band interference filters.

A multi-channel flame spectrometer: Frederick Brech, Jarrell Ash Company, 26 Farwell St., Newtonville 60, Mass.

A Direct Reading Flame spectrometer employing four channels will be described. The instrument is based on a folded Wadsworth mounting, employing a 30,000 LPI grating of 70 cm focal length, to achieve a reciprocal dispersion of 12·5 Å/mm. An automatic method to minimize the effect of background radiations is incorporated in the instrument, and alternative methods to achieve this will be detailed. The measuring system is based upon photomultiplier transducers. Performance data will be given.

---

* Present address: Westinghouse Research Laboratories, Pittsburgh 35, Pa.

Management Problems in Spectroscopy

The optimum utilization of spectroscopy in industrial research—from the viewpoint of a practising spectroscopist: H. E. LUMPKIN, Research and Development Div., Humble Oil & Refining Company, Baytown, Texas.

The title subject is discussed from the viewpoint of a practising spectroscopist. The role of the spectroscopist in industrial research must necessarily be determined, to some extent, by the size of the organization or installation in which he works. In small organizations devoted primarily to routine analyses, his research efforts are limited; however, in large research groups the spectroscopist should be free to carry out application and fundamental research. His responsibilities to management, service laboratories, research chemists and chemical engineers in his organization, and to the scientific profession in general are discussed. He should anticipate the analytical requirements of the exploratory groups, act as advisor on spectroscopic problems, acquaint process and research personnel with the available analytical procedures, and publish promptly the results of his fundamental research studies.

The optimum utilization of spectroscopy in industrial research—from the viewpoint of a department head: N. WRIGHT, The Dow Chemical Company, Midland, Mich.

A spectroscopy laboratory will be described which comprises X-ray methods, infra-red absorption, mass spectrometry, emission, ultra-violet, Raman and microwave spectroscopies, colour measurement, radiochemistry (including neutron activation analysis) and physical separation methods (including vapour phase chromatography). Situated in close proximity to production plants and other research laboratories its function is to apply this growing array of instrumental methods as a service to both production and research. It has a further vital function of basic research on the methods themselves and of developing new methods and techniques. The increasing amount of service analysis carried out by the various methods will be discussed as will the co-ordination between these methods and the analysis by chemical methods carried out in other laboratories. Communications between customer and spectroscopist and the system of selection of proper methods within the laboratory will be outlined. The organization of the laboratory, the scientific training and interests of its personnel, and the philosophy behind the manner of carrying out its functions will be discussed.

The optimum utilization of spectroscopy in industrial research—from the viewpoint of a research director: H. W. FIELD, The Atlantic Refining Co., Philadelphia, Pa.

The primary concern of the Research Director in the use of molecular spectroscopy lies in both the development of new and versatile spectroscopic methods and in providing all divisions in the research and development department with the best possible methods of analyses. In working out a policy to promote the optimum utilization of these techniques, management must give careful consideration to a number of problems.

The organization of the spectroscopic group must of course conform to the requirements of the entire department, but usually it is desirable to split the development and fundamental work from the routine work. Efforts should be directed towards the acquisition of trained personnel, up-to-date instrumentation, and the encouragement of fundamental analytical research studies to ensure the steady growth of spectroscopy technology. It is also important that the other divisions in the department be kept informed as to the capabilities and new developments in the field of spectroscopy and conversely the spectroscopists should be made aware of the analytical problems existing in the department. The various aspects of these and other similar problems will be discussed and some of the approaches to their solution will be suggested.

It is our experience that close communication between the spectroscopists and other departmental personnel has proven to be invaluable in the successful application of molecular spectroscopy to research problems.

The optimum utilization of spectroscopy in industrial research from the viewpoint of the instrument manufacturer: H. F. COLVIN, Consolidated Electrodynamics Corporation, Pasadena, Calif.

The functions of the instrument manufacturer are to make available useful, reliable instruments, to furnish instructions on the proper operation of these instruments, and to supply replacement parts and service as needed.

Because most instruments are used by industries undergoing rapid technological change, instrument obsolescence and use flexibility are important factors both to the manufacturer and the purchaser. The technical problems and the economic problems must be considered together, for modern instruments require the manufacturer to make substantial investments in development, design, tooling, manuals, and personnel training, as well as in the tools of production. One special problem created by these costs

VOL 8 1956/

is how to provide quickly and at a low cost small numbers of an instrument designed for a limited application, and to handle the specialized service these instruments may require.

Instrument companies need co-operation in forecasting, at the start of a development programme, not only the market potential of a given instrument, but also the specific needs this instrument must fulfil by the time it is ready to be marketed. Furthermore, the initial testing and evaluation of designs requires close co-operation between the manufacturer and the potential user.

Various approaches to these and other related problems are being followed by the different manufacturers, and their relative success will have considerable bearing on the future plans and organization of industrial research laboratories.

VOL.
8
56/57

Book review

ERNEST H. S. VAN SOMEREN and F. LACHMAN: **Spectrochemical Abstracts,** Vol. IV, 1946–1951. Hilger and Watts, Ltd., London, 1955. 179 pp., 30s.

THE present and future workers in the field of analytical emission spectroscopy are very fortunate in that two bibliographic surveys of the published literature are available. The classification of the abstracts and subject-indexing of these bibliographies are such that the two series complement each other to a high degree.

This book is the fourth volume in one of these bibliographic series. The 826 abstracts which constitute this volume cover the fields of analytical emission spectroscopy and flame photometry. About two-thirds of the papers published during the time period 1946–1951 are abstracted. The papers selected for abstracting are those which the authors felt recorded more than the mere results of emission spectrometric analyses or which contributed in some way to the development of the subject. About half of the abstracts are original; the remainder are quoted from other abstracting journals or authors' summaries.

The abstracts are classified according to type of substance analysed (biological materials, minerals, solutions, metals, etc.), methods, apparatus, reviews, tables, and books. A serial number is assigned to each abstract. Unfortunately, multiple listing of communications in which several subjects are discussed is not provided. For these papers, the authors have used their judgment in selecting the main subject of a communication, and this subject is denoted by a keyword for subject classification. Thus, a paper which describes a direct-reading spectrometer and which includes performance data on the analysis of steel may be listed under "Methods, Direct" only, with no listing under the keyword "Steel." This lack of a detailed subject cross-referencing is compensated by a valuable index of elements observed as minor constituents in various matrices. A minor annoyance is that the abstracts contain the names of the authors but not the literature references. To obtain the literature citation, it is necessary to refer to the author index, where the reference is listed opposite the identification number. This bibliography would be easier to use if the literature references were included in the abstract and the author index provided serial number cross-references.

Although this bibliography can be criticized on the points mentioned above, there can be no doubt that this compilation is of great value to analytical emission spectroscopists, especially those concerned with the development of methods. The value is great enough for this reviewer to prefer more frequent publication of these volumes.

VELMER A. FASSEL

VOL.
8
1956/

Spectrochimica Acta, 1956, Vol. 8, pp. 129 to 137. Pergamon Press Ltd., London

The fundamental vibration band of nitric oxide

H. W. THOMPSON and B. A. GREEN
The Physical Chemistry Laboratory, Oxford

(*Received* 23 *May* 1956)

Abstract—The rotational structure of the fundamental vibration band of nitric oxide has been remeasured with high resolving power. The component of the lines in the P_2 and R branches of the bands corresponding to the $^2\Pi_{1/2}$ and $^2\Pi_{3/2}$ states have been resolved better than previously and lines in one of the Q branches have also been measured. The rotational constants B and D for the different states have been determined and compared with previous estimates by other workers. It is concluded that $B_e = 1{\cdot}7050 \pm 0{\cdot}001$, $\alpha = 0{\cdot}0179$, $D_0 \sim 5{\cdot}1 \times 10^{-6}$ cm^{-1}, $I_e = 16{\cdot}418 \times 10^{-40}$ g cm^2, and $r_e = 1{\cdot}1506$ Å.

THE ultra-violet spectrum of nitric oxide has been studied by a number of workers [1]. Certain inconsistencies in the derived molecular constants led GILLETTE and EYSTER [2] to measure the fundamental vibrational absorption band in order to obtain independent values for the rotational constants B_0 and B_1. In view of the recent technical improvements leading to higher resolving power, it seemed profitable to remeasure this band. During the course of our work results were described by NICHOLS, HAUSE, and NOBLE [3] for the overtone bands $v = 0 \rightarrow v = 2$ and $v = 0 \rightarrow v = 3$, and shortly after its completion SHAW [4] described new measurements on the fundamental band. In view of the fact that we have obtained rather better resolution of the lines in the P and R branches and have also made a partial analysis of the Q branch, it seems desirable to report our data. While they agree fairly closely with the results of SHAW, we differ somewhat in the values of the derived molecular constants.

Experimental method

Nitric oxide was prepared by reducing a solution of sodium nitrate with acidified ferrous sulphate in the absence of air. It was passed over caustic soda followed by phosphorus pentoxide, and refractionated from a liquid-air trap.

The grating spectrometer has been described elsewhere [5]. The grating had 7200 lines per inch, with blaze near 3 μ, and sharp lines about 0·1 cm^{-1} apart could just be resolved. A path-length of 10 cm, with pressures 15–550 mm, were used.

Wavelength calibration was carried out with lines of deuterium chloride [6] and of deuterium bromide [7], the values for the latter being corrected as indicated previously [8]. Further checks were made, using lines of the water-vapour bands [9] at 2·8 μ and 1·7 μ in the second and third order respectively, although these are less satisfactory. The position of most lines could be established to about 0·02 cm^{-1}. Although over thirty lines were measured in the R branches, fewer were recorded in the P branches, since the grating was being used far from its blaze and the falloff in intensity beyond 5·5 μ was rapid for this reason and also owing to the decreasing sensitivity of the lead-telluride detector. The instrument was swept with dry air, but some overlapping with intense lines of water vapour could not be avoided.

Results and discussion

The ground state of nitric oxide is $^2\Pi$ with substates $^2\Pi_{1/2}$ and $^2\Pi_{3/2}$, separated by about 120 cm^{-1}. The transition $v = 0 \rightarrow v = 1$ for each substate gives rise to a

band with P, Q, and R branches, and the origins of the two bands lie very close to each other. The lines in these P, Q, and R branches are in reality Λ-type doublets, but the splitting is too small [10] to be detected in our work.

In Table 1 the positions are given for the observed lines and Fig. 1 shows the appearance of the bands. The energy levels in the two substates are given with sufficient accuracy by the following expressions.

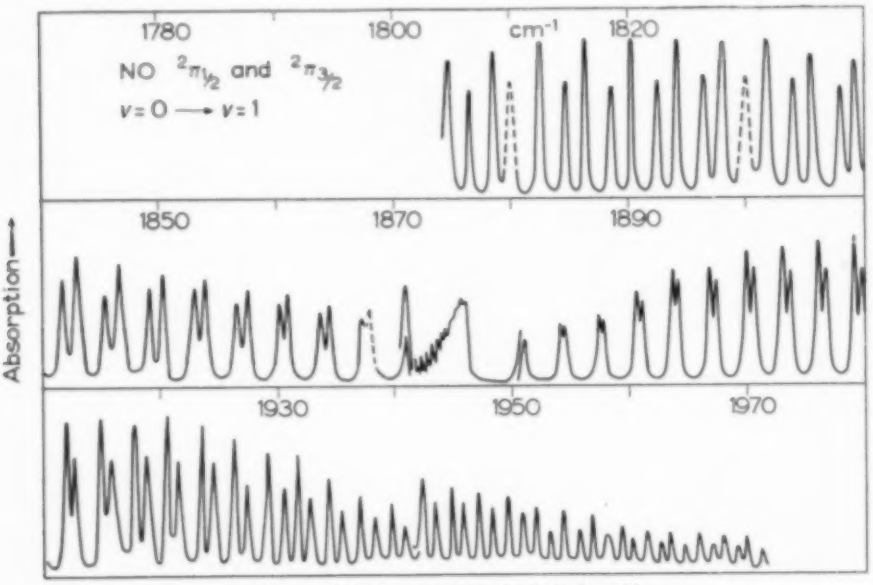

Fig. 1. Fundamental band of nitric oxide.

For the $^2\Pi_{1/2}$ state,

$$F_1 = T_v - \frac{A}{2} + G_1(v) + \frac{B_{v1}}{4} = B_{v1}J(J+1) + D_{v1}J^2(J+1)^2$$

and for the $^2\Pi_{3/2}$ state,

$$F_2 = T_v - \frac{A}{2} + G_2(v) - \frac{7B_{v2}}{4} + B_{v2}J(J+1) + D_{v2}J^2(J+1)^2$$

in which the mean rotational constants B_v and D_v are given by

$$2B_v = (B_{v1} + B_{v2}) \qquad \text{and} \qquad 2D_v = (D_{v1} + D_{v2}).$$

The following combination relations can then be applied. For both $^2\Pi_{1/2}$ and $^2\Pi_{3/2}$ states, using the combination differences

$$[R(J-1) - P(J+1)] \quad \text{and} \quad [R(J) - P(J)]$$

we have

$$\frac{\Delta_2 F_i(J, v)}{(J + \frac{1}{2})} = (4B_{vi} + 6D_{vi}) + 8D_{vi}(J + \tfrac{1}{2})^2$$

Table 1. Nitric oxide fundamental band
Positions of lines given in cm^{-1} (vac).

$^2\Pi_{1/2}$ *State*

$J+\frac{1}{2}$	R	P	Q	$J+\frac{1}{2}$	R	P
1	1881·04			18	1931·71	1812·66
2	84·34	1870·95		19	34·39	08·75
3	87·56		(1875·92)	20	37·00	1804·74
4	90·73	1864·22	(75·76)	21	39·61	
5	93·84	60·78	(75·57)	22	42·21	
6	1896·97	57·27	(75·34)	23	44·67	
7	1900·04	53·73	(75·14)	24	47·15	
8	03·10	50·17	74·66	25	49·60	
9	06·13	46·57	74·34	26	52·01	
10	09·10	42·96	73·98	27	54·39	
11	12·06	39·28	73·61	28	56·73	
12	1914·97	35·60	73·20	29	59·01	
13		31·84	72·73	30	61·24	
14	1920·69	28·06	72·26	31	63·48	
15	23·45	24·27	1871·72	32	65·68	
16	26·27	20·45		33	67·82	
17	1929·01	1816·58		34	1969·91	

$^2\Pi_{3/2}$ *State*

Table 1 (*continued*)

$J+\frac{1}{2}$	R	P	$J+\frac{1}{2}$	R	P
2	1884·34		19	1935·49	1806·70
3	87·66	1867·24	20	38·16	
4	90·87	63·69	21	40·77	
5	94·13	60·12	22	43·35	
6	1897·34	56·51	23	45·89	
7	1900·49	52·88	24	48·39	
8	03·62	49·22	25	50·86	
9	06·71	45·51	26	53·27	
10	09·79	41·80	27	55·66	
11	12·77	38·02	28	58·01	
12	15·75	1834·22	29	60·31	
13	18·67		30	62·59	
14	21·59	1826·50	31	64·79	
15	24·44	22·62	32	67·06	
16	27·26	18·67	33	69·12	
17	30·05	1814·70	34	1971.21	
18	1932·71				

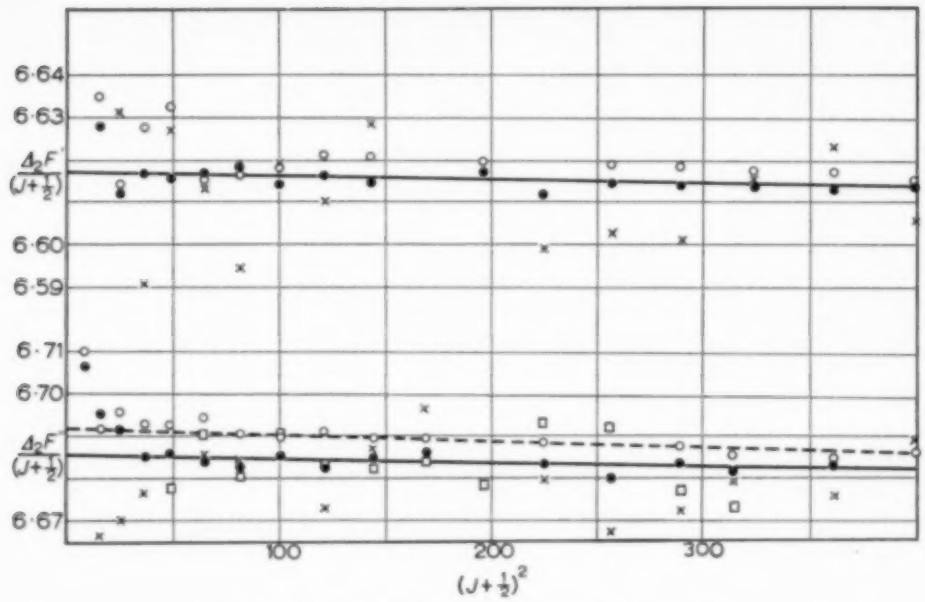

Fig. 2. Plots of $\frac{\Delta_2 F}{(J+\frac{1}{2})}$ against $(J+\frac{1}{2})^2$ for $^2\Pi_{1/2}$ state.

● Thompson and Green × Gillette and Eyster
○ Shaw □ Nichols, Hause, and Noble.

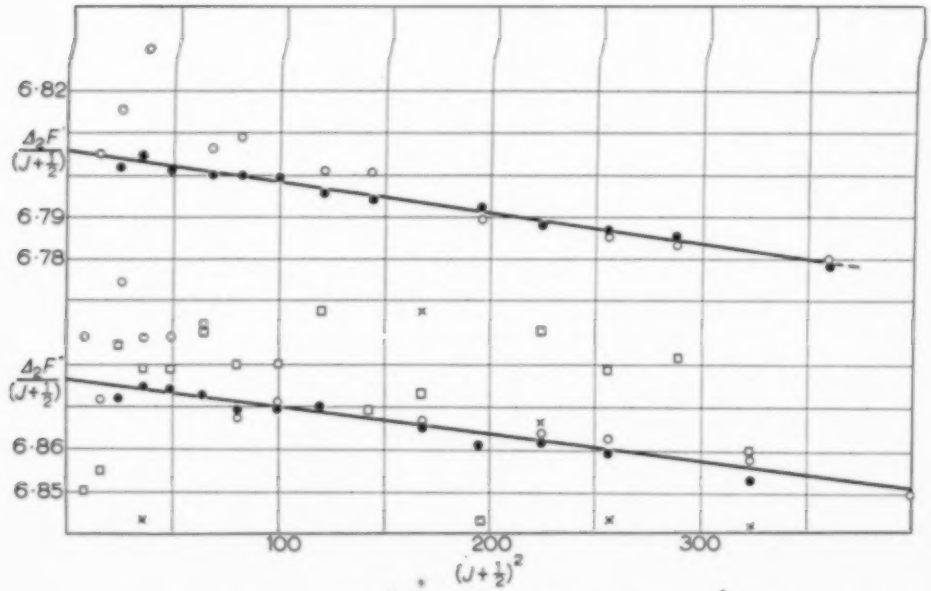

Fig. 3. Plots of $\frac{\Delta_2 F}{(J+\frac{1}{2})}$ against $(J+\frac{1}{2})^2$ for $^2\Pi_{3/2}$ state.

● Thompson and Green × Gillette and Eyster
○ Shaw □ Nichols, Hause, and Noble.

VOL.
8
1956/5

For the $^2\Pi_{1/2}$ state, neglecting the term involving the difference $(D_{01} - D_{11})$,

$$R(J-1) + P(J) = 3\,\Delta G_1(0) + 2(B_{11} - B_{01})(J^2 + \tfrac{1}{4})$$

and

$$\nu^{Q(J)} = \Delta G_1(0) + (B_{11} - B_{01})(J + \tfrac{1}{2})^2.$$

Similarly, for the $^2\Pi_{3/2}$ state,

$$R(J-1) + P(J) = 2\Delta G_2(0) + 2(B_{12} - B_{02})(J^2 - \tfrac{7}{4}).$$

The results were analysed by means of these combination relationships. Figs. 2 and 3 show plots of $\Delta_2 F''$ and $\Delta_2 F'$ for each of the substates.

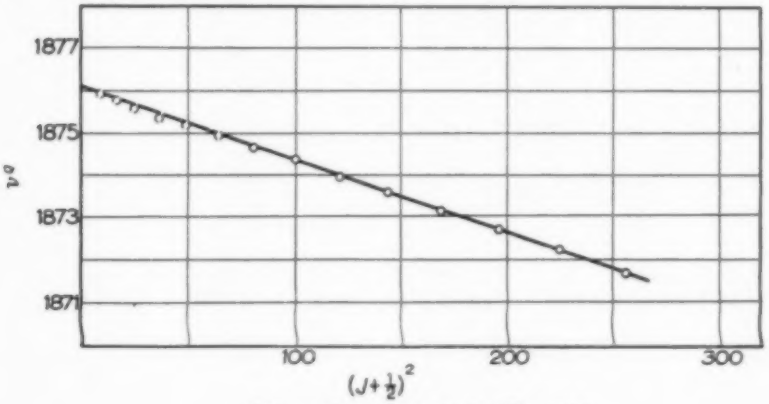

Fig. 4. Plot of Q lines for $^2\Pi_{1/2}$ state.

The data of other workers are also shown in the $\Delta_2 F''$ plots of Figs. 2 and 3, but appear to show greater scatter than our own. The dotted line in Fig. 2 corresponds to that used by SHAW. Our results lead to the following values for the molecular constants:

State $^2\Pi_{1/2}$

$B_{01} = 1{\cdot}6713$	$\alpha = +0{\cdot}172$
$B_{11} = 1{\cdot}6542$	$D_{01} = -1{\cdot}3 \times 10^{-6}$
$\Delta G_1(0) = 1876{\cdot}09$	$D_{11} = -1{\cdot}3 \times 10^{-6}$

State $^2\Pi_{3/2}$

$B_{02} = 1{\cdot}7191$	$\alpha = +0{\cdot}0179$
$B_{12} = 1{\cdot}7014$	$D_{02} = -8{\cdot}9 \times 10^{-6}$
$\Delta G(0) = 1875{\cdot}86$	$D_{12} = -8{\cdot}8 \times 10^{-6}$.

The assignment of lines in the resolved Q branch to J values was determined by plotting ν^Q against $(J + \frac{1}{2})^2$ so that a straight line was obtained passing through the origin determined from the P and R branches. This plot is shown in Fig. 4, and gave $\alpha = +0{\cdot}0172$ cm^{-1}. Also, the good accordance of the relation

$$R(J) - Q(J) = Q(J+1) - P(J+1)$$

confirmed the assignment adopted for the Q lines.

Table 2

	Infra-red				Ultra-violet		Microwave	
	Present work	Shaw [4]	Gillette and Eyster [2]	Nichols, Hause, and Noble [3]	Gero and Schmid [11]	Schmid, König, and Farkas [12]	Burrus and Gordy [13]	Gallagher, Bedard, and Johnson [14]
B_{01}	1·6713	1·6733	1·6696	1·6706	1·6703	1·6706	1·67198	1·67196
B_{11}	1·6542	1·6561	1·6525					
D_{01}	$-1·3\times10^{-6}$	$-2·8\times10^{-6}$				$-0·53\times10^{-6}$		
D_{11}	$-1·3\times10^{-6}$	$-2·8\times10^{-6}$						
$\Delta G_1(0)$	1876·09	1876·11	1876·10					
B_{02}	1·7191	1·7200	1·7200	1·7224	1·7182	1·7239		
B_{12}	1·7014	1·7023	1·7015					
D_{02}	$-8·9\times10^{-6}$	$-9·1\times10^{-6}$			$-6·6\times10^{-6}$	$-10·1\times10^{-6}$		
D_{12}	$-8·8\times10^{-6}$	$-9·1\times10^{-6}$						
$\Delta G_2(0)$	1875·86	1875·85	1875·64					
B_0	1·6952	1·6966	1·6948	1·6965	1·6943	1·6973	1·6956*	1·6956*
B_1	1·6778	1·6792	1·6770					
$D_0 \sim D_1$	$-5·1\times10^{-6}$	-6×10^{-6}	-5×10^{-6}					

* Using our value for B_{02} with the microwave value for B_{01}.

VOL. 8 1956/57

The lines in the P and R branches should therefore be represented by the expressions:

$$^2\Pi_{1/2}: \nu = 1876{\cdot}09 + 3{\cdot}3255m - 0{\cdot}0172m^2 - 5{\cdot}2 \times 10^{-6}m^3$$

$$^2\Pi_{3/2}: \nu = 1875{\cdot}86 + 3{\cdot}4205m - 0{\cdot}0179m^2 - 35{\cdot}6 \times 10^{-6}m^3$$

in which $m = -J$ for the P branch and $(J + 1)$ for the R branch. The coefficients in these expressions agree fairly well with those found by SHAW, but there are small significant differences. According to our data, $B_0 = 1{\cdot}6952$, $B_1 = 1{\cdot}6778$, and $\alpha = +0{\cdot}0176$ cm^{-1}, with $D_0 \sim D_1 \sim 5{\cdot}1 \times 10^{-6}$ cm^{-1}.

The values obtained by different workers for these molecular constants are collected in Table 2. It should be noted that our value for B_{01} agrees more closely with the microwave value than any other infra-red or ultra-violet spectral estimate. Also, our value for B_0 is lower than that given by NICHOLS, HAUSE, and NOBLE, or by SHAW, but it is perhaps in better accord with the remaining data. B_e can be calculated in two ways, either by using the infra-red data alone,

$$B_e = B_0 + \frac{\alpha}{2} = 1{\cdot}7040 \text{ cm}^{-1}$$

or by taking a mean from a plot of all the data on B_i values now available. The latter are given in Table 3 and in Fig. 5. B_i is plotted against $(v + \frac{1}{2})$. We thus

Table 3

i	B_i					
	Present work	Other work (reference)				
0	1·6952	1·6966 [4]	1·6948 [2]	1.6965 [3]	1·6943 [11]	1·6973 [12]
1	1·6778	1·6792 [4]	1·6770 [2]			
2		1·6631 [3]	1·6599 [15]	1·6606 [12]		
3		1·6508 [3]	1·6414 [15]	1·6422 [12]		
6		1·5856 [16]				
7		1·5752 [16]				
8		1·5546 [16]				
11		1·5006 [16]				
12		1·4778 [16]				
13		1·4645 [16]				

obtain $B_e = 1{\cdot}7050 \pm 0{\cdot}001$ and $\alpha = 0{\cdot}0179$ cm^{-1}, which we believe to represent the data more satisfactorily than the more precise estimate $B_e = 1{\cdot}7060$ quoted by SHAW. If $[B_i + 0{\cdot}0179(v_i + \frac{1}{2})]$ is plotted against $(v_i + \frac{1}{2})$, the points are scattered randomly about a value 1·7050. The values then calculated for I_e and r_e are $16{\cdot}418 \times 10^{-40}$ g cm^2 and 1·1506 Å.

The value found for D_0 is in good agreement with that calculated from the relation

$$D_0 = -\frac{4B_0^3}{\omega_0^2} = -5{\cdot}5 \times 10^{-6}$$

and the values of A calculated for the two levels $v = 0$ and $v = 1$, using the relation

$$B_{vi} = B_v\left\{1 + (-1)^i \cdot \frac{B_v}{A} + \ldots\right\}$$

are each close to 120.

Acknowledgement—We wish to thank the Hydrocarbon Research Group of the Institute of Petroleum for financial support.

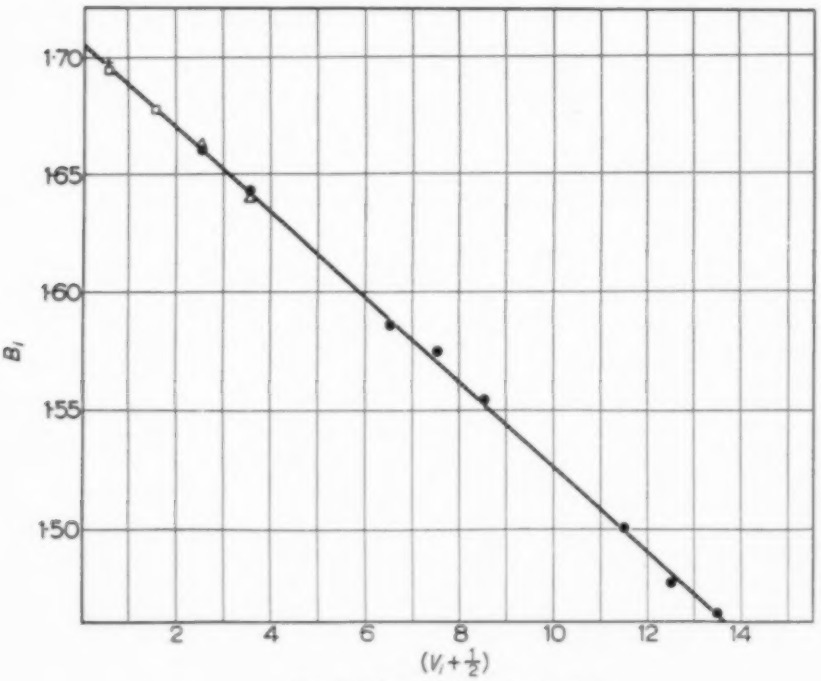

Fig. 5. Plot of B_i against $(v_i + \frac{1}{2})$.

References

[1] HERZBERG G.; *Spectra of Diatomic Molecules*, van Nostrand, New York (1950)
[2] GILLETTE R. H. and EYSTER E. H.; *Phys. Rev.* 1939 **56** 113
[3] NICHOLS N. L., HAUSE C. D., and NOBLE R. H.; *J. Chem. Phys.* 1955 **23** 57.
[4] SHAW J. H.; *J. Chem. Phys.* 1956 **24** 399.
[5] MILLER C. H. and THOMPSON H. W.; *Proc. Roy. Soc.* 1949 **A200** 1.
BOYD D. R. J. and THOMPSON H. W.; *Spectrochim. Acta.* 1952 **5** 308.
MILLS I. M., THOMPSON H. W., and WILLIAMS R. L.; *Proc. Roy. Soc.* 1953 **A218** 29.
[6] PICKWORTH J. and THOMPSON H. W.; *Proc. Roy. Soc.* 1953 **A218** 37.

VOL. 8 1956/5

[7] KELLER F. C. and NIELSEN A. H.; *J. Chem. Phys.* 1954 **22** 294.
[8] OVEREND J. and THOMPSON H. W.; *Proc. Roy. Soc.* 1956 **A234** 314.
[9] BENEDICT W. S. and PLYLER E. K.; *J. Res. Nat. Bur. Stand.* 1951 **46** 246.
NELSON R. C.; *J. Opt. Soc. Amer.* 1949 **39** 68.
[10] MULLIKEN R. S. and CRISTY.; *Phys. Rev.* 1931 **38** 87.
VAN VLECK J. H.; *Phys. Rev.* 1929 **33** 467.
BERINGER R. A., RAWSON E. B., and HENRY A. F.; *Phys. Rev.* 1954 **94** 343.
[11] GERO L. and SCHMID R.; *Proc. Phys. Soc.* 1948 **60** 533.
[12] SCHMID R., KÖNIG T., and FARKAS D. V.; *Z. Physik.* 1930 **64** 84.
[13] BURRUS C. A. and GORDY W.; *Phys. Rev.* 1953 **92** 1437.
[14] GALLAGHER J. J., BEDARD F. D., and JOHNSON C. M. ; *Phys. Rev.* 1954 **93** 729.
[15] GERO L., SCHMID R., and VON SZILY F. K.; *Physica.* 1944 **11** 144.
[16] JENKINS F. A., BARTON H. A., and MULLIKEN R. S.; *Phys. Rev.* 1927 **30** 150.

DL.
3
6/57

Spectrochimica Acta, 1956, Vol. 8, pp. 138 to 141. Pergamon Press Ltd., London

Vibrational spectra and geometrical isomerism in amides

R. A. Russell and H. W. Thompson
The Physical Chemistry Laboratory, Oxford.

(*Received* 23 *May* 1956)

Abstract—The occurrence of a close pair of absorption bands near 3 μ with *N*-monosubstituted amides is interpreted as indicating the presence of *cis* and *trans* forms of the amide skeleton, which give rise to stretching vibrations of the N—H group of slightly different frequency. In those cases where steric or other factors only permit the occurrence of one structural configuration, only one band is found. With most compounds the *trans* structure appears to be the more favoured.

As a result of resonance hybridization, the C—N bond in amides possesses considerable double-bond character [1]. Also, we may expect to find restricted rotation about this bond and a planar configuration for the amide group. This planar structure has been confirmed by measurements with X-rays and polarized radiation for substances such as acetamide [2],urea [3], acetanilide [4], and acetyl glycine [5] in the solid state. In these circumstances there is a possibility of *cis-trans* isomerism in amides of the type shown in Fig. 1. The X-ray data have so far suggested that

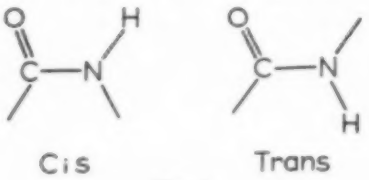

Fig. 1.

the *trans* configuration is the more stable, and it has been shown that protein chains involve this structure [6]. Further evidence for restricted rotation has recently been found [7] from the nuclear magnetic resonance spectrum of *N*-dimethyl formamide.

In the course of some infra-red measurements with compounds containing the N—H group, we noticed that most N-monosubstituted amides give rise to two close bands in the region of the N—H stretching vibration near 3 μ. It appears likely that the results can be interpreted satisfactorily in terms of the occurrence of geometrical isomers.

The substances were examined as dilute solutions in carbon tetrachloride, using a Perkin Elmer 12-C spectrometer with lithium-fluoride prism. The effective slit-widths were about 5 cm^{-1}. The results are summarized in Table 1.

Nearly all the monosubstituted amides examined gave the pair of bands, and this might at once suggest the occurrence of association through hydrogen bonds. At the high dilutions used, this is most unlikely, but in any case if such intermolecular bonding were involved, a much higher displacement of the frequency would be expected, and one of the bands would be expected to be broader than is found.

VOL. 8 1956/5

Table 1. Amides in carbon tetrachloride solution.

Compound	Frequency components of cm^{-1} N—H group		Estimates of isomers (%)	
	Stronger band	Weaker band	*trans*	*cis*
N-methyl formamide	3466	3429	95	5
N-phenyl formamide	3434	3408	65	35
N-methyl acetamide	3472	3440	95	5
N-phenyl acetamide	3445	3400	90	10
N-*p* chlorphenyl acetamide	3445	3425	95	5
N-*p* bromophenyl acetamide	3445	3400	90	10
N-*p* tolyl acetamide	3445	3425	95	5
N-*p* anisyl acetamide	3447	3420	95	5
N-*n* propyl phenylacetamide	3430			
N-tert. butyl phenylacetamide	3426	3442	30	70
N-tert. amyl phenylacetamide	3425	3445	30	70
N-cyanomethyl phenylacetamide	3435	3460	30	70
N-cyclohexyl phenylacetamide	3430			
N-phenyl phenylacetamide	3415	3441	15	85
N-*p* tolyl phenylacetamide	3416	3442	10	90
N-*o* tolyl phenylacetamide	3410			
N-methyl urethane	3473	3440	90	10
N-ethyl urethane	3461	3430	95	5
N-phenyl urethane	3446	3465	5	95
N-*o* tolyl urethane	3457	3440	80	20
N-*N* dimethyl urea	3462	3446	(70)	(30)
N-*N* dipenyl urea	3430	3445	(30)	(70)
N-*N* diphenyl thiourea	3411	3378	(50)	(50)
Thioacetanilide	3398	3368	60	40
N-phenyl benzamide	3444		100	0
N-α napthyl benzamide	3444, 3463		100	0
N-butyrolactam[8]	3420		0	100
δ-valerolactam[9]	3425		0	100
3-keto-1,2,3,4, tetrahydro-isoquinoline	3423		0	100
Succinimide	3422		0	100
Phthalimide	3441		0	100
Isatin	3442		0	100

A second possibility is that one of the bands near 3 μ is due to the overtone of the fundamental carbonyl-group vibration, which lies near 6 μ. This is also very improbable, since it would imply a substantial anharmonicity for the vibration, and of opposite sign to that usually found. The frequency of the carbonyl-group fundamental is about 1675 cm^{-1} for *N*-alkyl acetamides and about 1700 cm^{-1} for *N*-aryl acetamides. In either case the anharmonicity factor x_e would would have to be negative. If Fermi resonance were occurring between $2\nu_{CO}$ and ν_{NH}, this anharmonicity might have to be even more negative. Another argument against this interpretation as an overtone band is found in the fact that there is a similar

type of splitting of the N—H band at 3 μ with substances such as thioacetanilide and thiocarbanilide. In the latter cases, the overtone of the C=S group fundamental vibration must lie at a much lower frequency than 3400 cm^{-1}, and cannot be responsible for either of the bands found in this region.

The most plausible interpretation of the data is, therefore, in terms of a pair of isomeric structures, the *cis* and *trans* forms. Now, in certain of the compounds which have been measured, the configuration is unambiguously defined. For example, if the —CO—NH— group forms part of a closed five- or six-membered ring, the C=O and N—H groups must lie in a *cis* configuration. Thus γ-butyrolactam [8], δ-valerolactam [9], and 3-keto-1,2,3,4-tetrahydro-isoquinoline show only one band near 3425 cm^{-1}, corresponding to the *cis* modification. With *N*-methyl acetamide, and *N*-ethyl acetamide in the liquid state, dipole moment

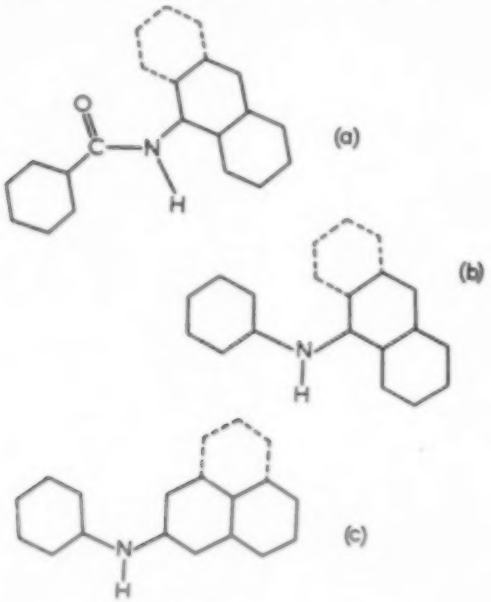

Fig. 2.

measurements [10] [11] and other theoretical considerations [11] suggest that the predominant form is the *trans* isomer. From Table 1 it is seen that with *N*-methyl acetamide the more intense band has the higher frequency, near 3472 cm^{-1}. This suggests that the band at higher frequency may in general be associated with the *trans* form, and that at lower frequency with the *cis* form. The exact location of the two bands will depend upon other groups adjacent to the —CONH— skeleton, but it seems that in carbon tetrachloride the *trans* isomer usually gives a band in the range 3440–3460 cm^{-1}, while that for the *cis* isomer lies in the region 3420–3440 cm^{-1}.

On this basis, the results imply that the majority of the *N*-monosubstituted amides exist predominantly in the *trans* form. If as a first approximation it is assumed that the intrinsic intensities are the same for both forms, the rough percentage proportions have been estimated and are given in Table 1. With

VOL.
8
1956/5

benzanilide, steric hindrance prevents the two phenyl nuclei from taking up a *cis* planar arrangement, and if there is to be the maximum resonance stabilization, the *trans* configuration will arise. In fact, only one band at 3444 cm^{-1} is found with the compound. In the case of α-naphthyl-benzamide there are two bands at 3444 and 3463 cm^{-1}, but here there is the further possibility of rotational isomerism about the N—C (naphthyl) bond as shown in Fig. 2(a). This interpretation is supported by the fact that a pair of bands at 3417–3434 cm^{-1} due to the N—H group stretching mode is found with *N*-phenyl-α napthylamine [12] and also with *N*-β naphthyl-α naphthylamine. By contrast, with *N*-phenyl-β-naphthylamine the difference in structure between the corresponding pair of rotational isomers will have less effect on the N—H group frequency, and in fact a single broad N—H band is found.

Some of the results given in Table 1 appear anomalous. For example, with *N*-phenyl formamide there appears to be a substantial proportion of the *cis* isomer, whereas *N*-methyl formamide shows almost exclusively the *trans* configuration. Also, whereas the acetamides and acetanilides seem to have predominantly the *trans* structure, the amides of phenyl acetic acid have the stronger band at lower frequency, which would suggest excess of the *cis* form. These apparent deviations may arise from the effect of steric influences of the different groups attached to the —CO—NH— skeleton.

With the derivatives of urea, the isomeric forms are probably *trans-trans* and *trans-cis*, since a *cis-cis* arrangement is unlikely on steric grounds. With these compounds, the double-bond character of the C—N bonds is less than that in other amides, and there may be a greater ease of conversion between the isomers. A similar argument may apply to the results with thioacetanilide.

Acknowledgements—We are grateful to the Hydrocarbon Research Group of the Institute of Petroleum for financial support, and one of us (R. A. R.) thanks the Department of Scientific and Industrial Research for a maintenance grant.

References

[1] Vaughan P. and Donohue J.; *Acta. Cryst.* 1952 **5** 530.
[2] Senti F. and Harker D.; *J. Amer. Chem. Soc.* 1940 **62** 2008.
[3] Waldron R. D. and Badger R. M.; *J. Chem. Phys.* 1950 **18** 516.
Goldschmidt G. H. and Llewellyn F. J.; *Acta Cryst.* 1950 **3** 294.
[4] Brown C. J. and Corbridge D. E. C.; *Acta Cryst.* 1954 **7** 711.
[5] Carpenter G. B. and Donohue J.; *J. Amer. Chem. Soc.* 1950 **72** 2315.
[6] Pauling L., Corey R. M., and Branson H. R.; *Proc. Nat. Acad. Sci.* 1951 **37** 205.
[7] Phillips W. D.; *J. Chem. Phys.* 1955 **23** 1363.
[8] Darmon G. K. and Sutherland G. B. B. M.; *Nature* 1949 **164** 440.
[9] Mizushima S. I.; *J. Amer. Chem. Soc.* 1950 **72** 3490.
[10] Kumler W. D. and Porter C. W.; *J. Amer. Chem. Soc.* 1934 **56** 2549.
[11] Mizushima S. I.; *J. Amer. Chem. Soc.* 1951 **73** 1330.
[12] Russell R. A. and Thompson H. W.; *Proc. Roy. Soc.* 1956 **A234** 318.

Spectrochimica Acta, 1956, Vol. 8, pp. 142 to 151. Pergamon Press Ltd., London

Infra-red dichoism studies of some molecular complexes*

R. D. Kross, K. Nakamoto,† and V. A. Fassel
Institute for Atomic Research and Department of Chemistry,
Iowa State College, Ames, Iowa

(*Submitted for publication* 6 *January* 1956; *Accepted for publication* 10 *May* 1956)

Abstract—The results of a study on the polarized infra-red spectra of the hexamethylbenzene-picryl chloride, anthracene-sym-trinitrobenzene, and *p,p'*-dinitrodiphenyl-p-hydroxydiphenyl molecular compounds show agreement with published X-ray crystal structures. On the basis of the observed dichroism, molecular orientations are suggested for the complexes of picric acid with β-methylnaphthalene and piperidine.

Introduction

When polarized infra-red radiation passes through an anisotropic material, maximum absorption will occur if the electric vector of the incident polarized radiation is parallel to the direction of the transition moment vector of a molecular vibration. Similarly, when the vector directions are perpendicular, minimum absorption will occur. If the two vectors are at some intermediate angle, the amount of absorption depends on the magnitude of the parallel projection of the transition moment on the *E* vector. Polarization data obtained from oriented single crystals are therefore very useful in determining the orientation of various bonds with respect to the crystal axes [1–7]. These data may be used to confirm X-ray structural predictions and, in some cases, provide structural information which is difficult to obtain by X-ray or neutron diffraction methods. Thus, Francel [1], by studying an aggregate of oriented crystals with infra-red polarized radiation, was able to determine the orientations of nitro groups substituted ortho to various groups on the benzene ring. Similarly, Waldron and Badger [4] showed that the urea molecule is completely planar, a fact only recently ascertained through neutron diffraction studies [8].

Single crystals of the well-known molecular complexes of the type formed between nitrosubstituted benzenes and aromatic hydrocarbons should be particularly amenable to infra-red polarization studies. Pertinent information on (1) the relative spatial configurations of the two molecules composing the complex, (2) the arrangement of the individual complex molecules with relation to the crystal axes, and (3) the changes of orientation of individual groups due to the complex formation, can be directly obtainable from the polarized spectra. In this paper the polarized spectra of five complexes of this type are presented. The crystal structure of three of these compounds were known; their polarized spectra served as a guide in interpreting the spectra of the other two molecular compounds whose structures have not been determined.

VOL.
8
1956/5

* Contribution No. 451 of the Institute for Atomic Research and Department of Chemistry.
† Corn Industries Research Foundation Post-Doctoral Fellow, on leave from Department of Chemistry, Osaka University, Osaka, Japan.

Experimental

A Perkin-Elmer Model No. 112 single-beam universal monochromator equipped with a reflecting-type microscope attachment, and a Perkin-Elmer Model No. 13 double-beam infra-red spectrophotometer, both equipped with an AgCl polarizer, were used in obtaining the polarized spectra of single crystals. The optical paths within the instruments were flushed with dry nitrogen.

The hexamethylbenzene-picryl-chloride complex was prepared from a 1 : 1 mole ratio solution of both components in hot chloroform. Cooling and evaporation of the solution yielded the yellow crystalline adduct (m.p. 148°). The same procedure was followed for the anthracene-sym-trinitrobenzene complex, with the substitution of methanol for chloroform (orange, m.p. 164°). The β-methylnaphthalene and piperidine-picric-acid complexes were prepared by addition of β-methylnaphthalene and piperidine to hot saturated solutions of picric acid in ethanol, followed by cooling (both yellow, m.p. 116° and 147°, respectively). The *p,p'*-dinitrodiphenyl-*p*-hydroxydiphenyl complex was prepared by cooling a warm solution of acetone containing equal amounts of both components (yellow, m.p. 228°). The first four substances form needle-like crystals and the latter were rectangular plates. The crystals were of such size as to completely fill the maximum microscope field of 650 × 220 μ. Polarization studies were made along and perpendicular to the long axis.

Results and discussion

In general, the infra-red spectra of these molecular complexes appear to be summations of the spectra of the two components. However, small frequency shifts and band splittings of a rather complex nature do occur on complex formation.

Hexamethylbenzene-picryl-chloride Molecular Complex

According to X-ray crystal-structure data [9], the structure of this complex consists of alternate layers of hexamethylbenzene and picryl chloride molecules, with the planes of the molecules being perpendicular to the needle axis. Both the picryl-chloride and hexamethylbenzene molecules are planar except for the ortho-nitro groups of picryl chloride, which are turned out of the plane of the ring because of the steric effect of the chlorine atom [9]. The angle of rotation can be estimated through comparison with the 64° rotational angle of the nitro group ortho to a chlorine atom in 3,5-dichloro-4-nitroaniline [10].

The polarization spectra of this complex shown in Fig. 1 and the polarization properties summarized in Table 1 are in agreement with this structure. The absorption of polarized radiation by the asymmetric and symmetric nitro stretching vibrations (bands 3 and 5) is of interest. An asymmetric nitro stretching vibration has its transition moment parallel to a line between the two nitro oxygens. If a nitro group is rotated out of the plane of the ring, the transition-moment vector will have a component perpendicular to the ring, and the magnitude of the component vector is directly proportional to the cosine of the degree of rotation of that group. Since the *p*-nitro group in picryl chloride is probably coplanar with the benzene ring within a few degrees, its asymmetric stretching vibration should show almost pure perpendicular polarization. The *o*-nitro groups, however, are rotated out of the plane and should contribute to both polarization spectra. Experimentally, the sum of these absorptions appears approximately equal (band 3), confirming the appreciable rotation of the *o*-nitro groups out of the plane of the ring. A symmetric nitro vibration, on the other hand, has its transition

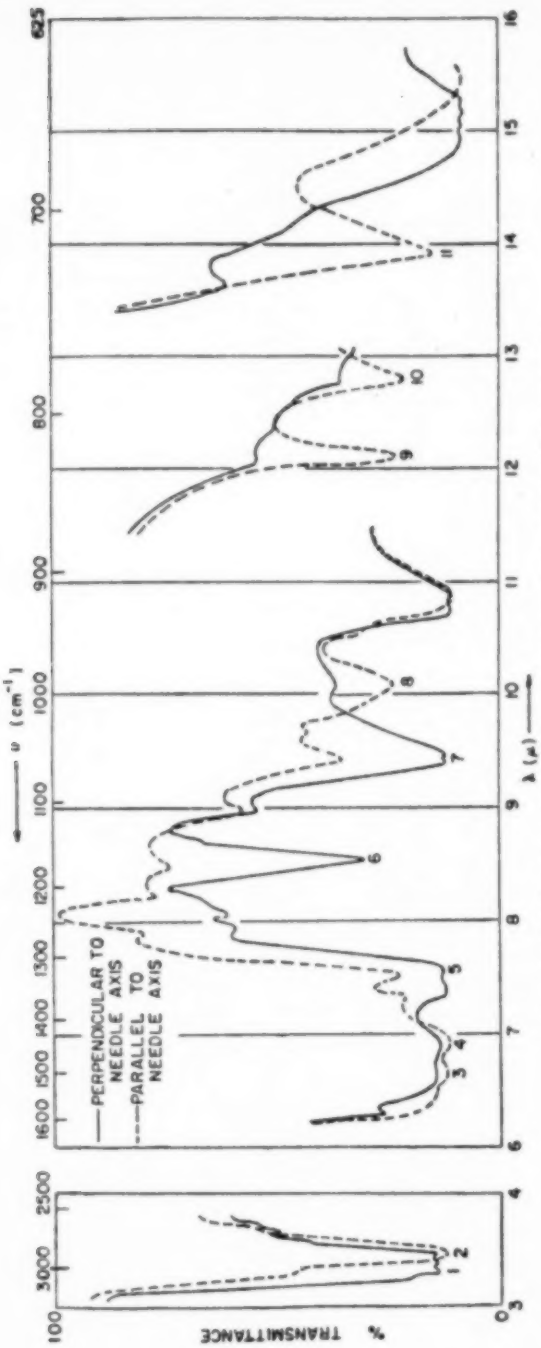

Fig. 1. Polarized spectra of hexamethylbenzene-picryl-chloride complex.

VOL. 8 1956/5

Table 1. Hexamethylbenzene (HB)-picryl chloride (PC)

No. of band	Frequency (cm^{-1})	Assignment	Predominant polarization[a]	Vibration type
1	3030	Arom. C-H stretch (PC)	$\perp$	planar
2	2886	Aliph. C-H stretch (HB)	$\approx$[b]	
	2857			
3	1522	Asymm. NO_2 stretch	$\approx$	
4	1450	CH_3 deform.	$\approx$	
5	1338	Symm. NO_2 stretch	$\perp$	planar
6	1174	C-N stretch (?)	$\perp$	planar
7	1060	C_6 ring plan. degen. vib. of both rings[c]	$\perp$	planar
	1054			
8	994	C_6 out-of-plane (HB)[c]	$\parallel$	nonplanar
9	824	C_6 out-of-plane (PC)	$\parallel$	nonplanar
10	784	C-H out-of-plane bend (PC)	$\parallel$	nonplanar
11	717	C_6 out-of-plane mode of both rings	$\parallel$	nonplanar

[a] Denotes orientation of the electric vector, with respect to the needle axis, which shows greater absorption intensity.
[b] Approximately equal intensity.
[c] Based on the assignments of MANN and THOMPSON [2].

moment along a line bisecting the O–N–O angle and in the plane of the ring, regardless of the angle of rotation of the group. Thus, band 5, the symmetric nitro stretching vibration, appears predominantly in the component of light perpendicular to the needle axis. The slight degree of absorption in the parallel component probably arises from imperfect orientations of the molecules.

Anthracene-sym-trinitrobenzene Molecular Complex

In this complex, the two kinds of molecules are stacked alternately in columns parallel to the needle axis and tilted about 6° from the position where the ring planes would be perpendicular to the needle axis [11]. The polarization spectra of the complex shown in Fig. 2 and the polarization assignments summarized in Table 2 are in agreement with the published structure. The polarized spectra of the nitro stretching vibrations are again worthy of special comment, because both the symmetric and asymmetric frequencies exhibit absorption in both planes of polarization.

The nitro symmetric stretching vibration should appear solely as a planar vibration if the following conditions are fulfilled: (a) the molecules are parallel to each other; (b) the molecules are perpendicular to the needle axis; and (c) the crystal is perfect, as well as perfectly oriented with respect to the incident polarized radiation. The significant absorption of radiation which has its E vector parallel to the needle axis (band 5) suggests that one or more of these conditions are not fulfilled. The 6° molecular tilt of the molecules with respect to the needle axis should lead to a small absorption of parallel radiation, but not to the extent

indicated in the spectrum. It is therefore probable that the greatest part of the absorption arises from orientational and/or crystalline imperfections or from

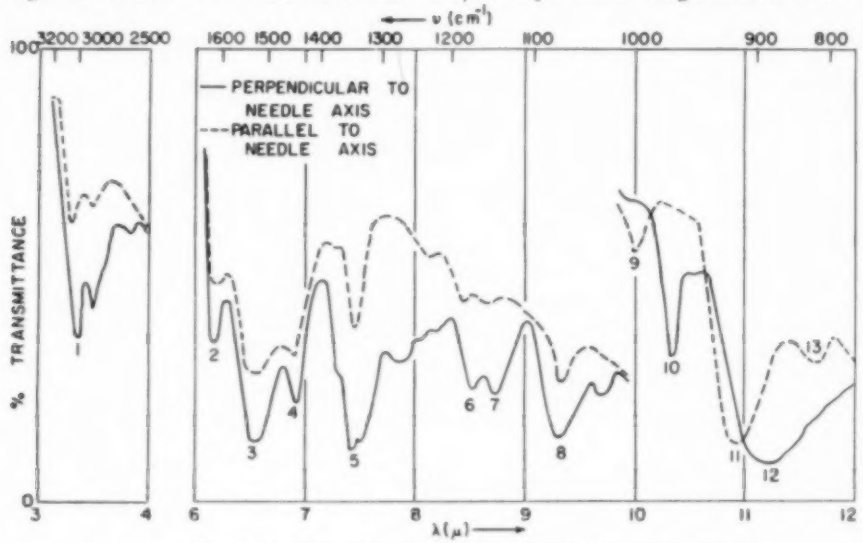

Fig. 2. Polarized spectra of anthracene-sym-trinitrobenzene complex.

the effects of radiation convergence.* It is generally observed that unhindered nitro groups are rotated about 6 to 10° with respect to the ring [2, 12], but this rotation would not contribute to absorption of radiation which has the E vector

Table 2. Anthracene (A)-sym-trinitrobenzene (TB)

No. of band	Frequency (cm^{-1})	Assignment	Predominant polarization	Vibration type
1	3030	Arom. C-H stretch of both mols.	⊥	planar
2	1620	C-C stretch of both rings	⊥	planar
3	1526	Asymm. NO_2 stretch	⊥	planar
4	1439	C-H in plane bend of both mols.	⊥	planar
5	1341	Symm. NO_2 stretch	⊥	planar
6	1167	C-N stretch (?)	⊥	planar
7	1147	Ring stretch (A)	⊥	planar
8	1068	Degen ring stretch (TB)	⊥	planar
9	998	Out-of-plane ring vib. of both mols.	∥	nonplanar
10	966	Ring stretch (A)	⊥	planar
11	917	C-H out-of-plane bend (TB)	∥	nonplanar
12	882	Ring stretch (A)	⊥	planar
13	825	C_6 out-of-plane (TB)	∥	nonplanar

* The authors are indebted to Dr. FOIL MILLER for pointing out that the large angle of convergence encountered in microspectroscopy can contribute to anomalous absorption intensities because the radiation passing through the sample is not strictly parallel.

parallel to the needle axis because of the reasons previously stated. However, the rotation of the nitro groups as well as the molecular tilt and the crystalline and orientational imperfections would contribute to the absorption of this radiation by the asymmetric nitro stretching vibrations. If the rotation of the nitro groups is within the usual limits of 6 to 10°, the absorption of the parallel radiation by this vibration should not be significantly greater than the corresponding absorption by the symmetric vibration. The approximate equal intensity of the symmetric and asymmetric nitro stretching modes (bands 5 and 3, respectively) suggests that the nitro groups retain their basic coplanarity in the complex.

p,p'-Dinitrodiphenyl-p-hydroxydiphenyl Molecular Complex

In this structure the dinitrodiphenyl molecules are in a 3 : 1 ratio with respect to the hydroxydiphenyl molecules [13], and there are no apparent strong intermolecular interactions. The dinitrodiphenyl molecules lie in the *ab* plane of the crystal and the hydroxydiphenyl molecules are arranged with their lengths nearly normal to that plane (i.e. along the *c*-axis). A large single crystal of the complex was placed over the slit of the Model No. 13 instrument and the polarizer was mounted between the sample and the source. The polarizer was rotated until maximum dichroism was obtained for settings 90° apart. The resulting strongly polarized spectra, as shown in Fig. 3 and summarized in Table 3, completely agree with the published structure.

Table 3. *p,p'*-Dinitrodiphenyl (DD)-*p*-hydroxydiphenyl (HD)

No. of band	Frequency (cm^{-1})	Assignment	Predominant polarization	Vibration type
1	3315	O-H stretch	∥	planar
2	3150	C-H stretch (HD)	∥	planar
3	3088	C-H stretch (DD)	⊥	planar
4	1505	Asymm. NO_2 stretch	⊥	planar
5	1340	Sym. NO_2 stretch	⊥	planar
6	1178	C-N stretch (?)	⊥	planar
7	770	C-H out-of-plane bend (HD)		nonplanar
8	740 733	C_6 out-of-plane deform. (DD)	∥	nonplanar

β-Methylnaphthalene-picric-acid Molecular Complex

The overall strong dichroism shown by the polarized spectra of this complex in Fig. 4 indicates that the molecular components are stacked closely perpendicular to the needle axis of the crystal. The polarization properties of the individual bands as listed in Table 4 give more information pertinent to the structure of the complex. The O–H group of picric acid is surrounded by two ortho-nitro groups, one of which forms a hydrogen bond with the O–H group, while the other is rotated out of the plane of the ring by the steric influence of the O–H group.

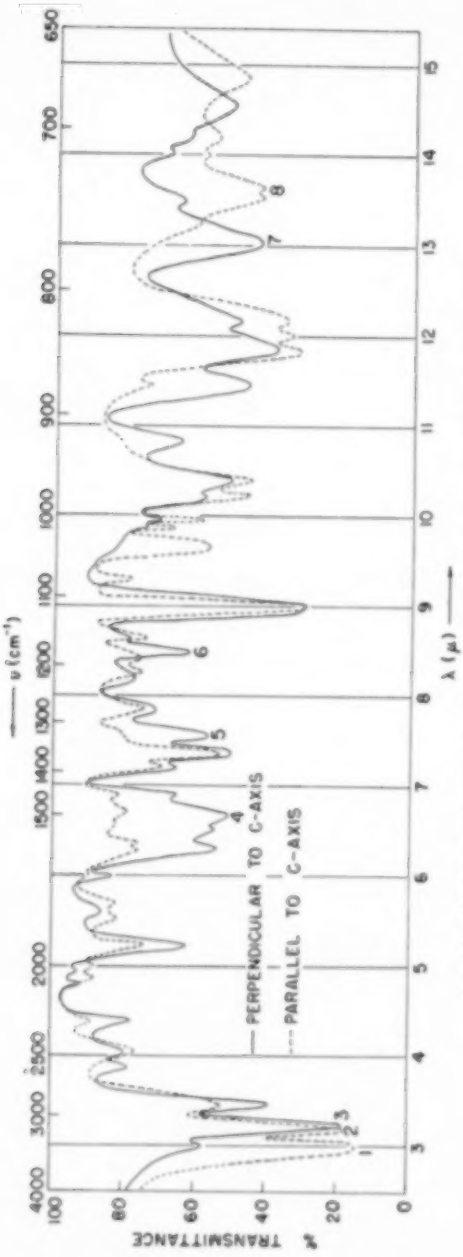

Fig. 3. Polarized spectra of *p,p'*-dinitrodiphenyl-p-hydroxydiphenyl complex.

The para-nitro group of picric acid is expected to be basically coplanar with the ring. Some idea as to the magnitude of rotation of the one ortho-nitro group can be obtained from the fact that the dihedral angle for the two ortho-nitro groups in

potassium picrate is about 27° [12]. This rotation results in absorption, by the asymmetric stretching vibration of one ortho-nitro group, of radiation which has an *E* vector parallel to the needle axis (band 4, Fig. 4, and Table 4). The symmetric

Table 4. β-Methylnaphthalene (MN)-picric acid (PA)

No. of band	Frequency (cm^{-1})	Assignment	Predominant polarization	Vibration type
1	3030	Arom. C-H stretch of both mols.	$\perp$	planar
2	2884	Aliph. C-H stretch	$\approx$	
3	1630 1608	C-C stretch of both rings	$\perp$	planar
4	1533 1505	Asymm. NO_2 stretch	$\perp$	planar
5	1422	Arom. C-H in-plane bend of both mols.	$\perp$	planar
6	1339	Symm. NO_2 stretch	$\perp$	planar
7	1259	O-H in-plane bend	$\perp$	planar
8	1148	C-N stretch (?)	$\perp$	planar
9	1082	Degen. ring stretch (PA)	$\perp$	planar
10	1038	Degen. ring stretch (MN)	$\perp$	planar
11	960 944	Ring stretch (MN)	$\perp$	planar
12	913	Ring stretch (PA)	$\perp$	planar
13	895	C_{ar}-CH_3 stretch	$\perp$	planar
14	865	Ring stretch (MN)	$\perp$	planar
15	823	C-H out-of-plane bend (MN) and C_6 out-of-plane bend (PA)	$\parallel$	nonplanar
16	778	C-H out-of-plane bend (PA)	$\parallel$	nonplanar

Table 5. Piperidine (P)-picric acid (PA)

No. of band	Frequency (cm^{-1})	Assignment	Predominant polarization	Vibration type
1	3267	N-H stretch (P)	$\perp$	planar
2	2967 2915	Overlap of C-H and CH_2 stretch of both mols. with bonded O-H stretch	$\perp$	planar
3	[a]1544 [b]1527 [c]1515	Asymm. NO_2 stretch	$\perp$	planar

nitro stretching vibrations (band 6) show little absorption of the parallel radiation because the nitro-group rotation does not alter the orientation of the vector moment.

Piperidine-picric-acid Molecular Complex

Because of the probable nonplanarity of the piperidine molecule, the dichroism

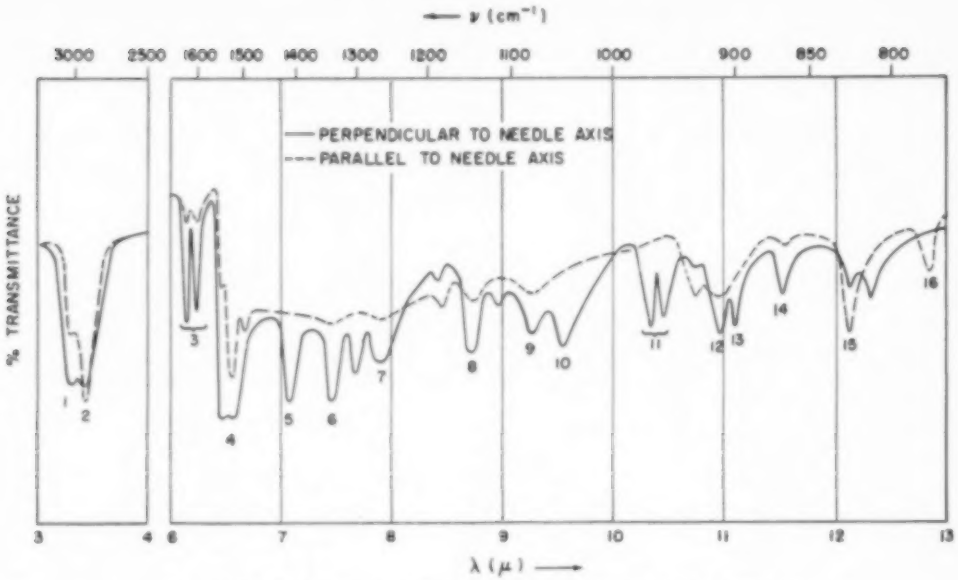

Fig. 4. Polarized spectra of β-methylnaphthalene-picric-acid complex.

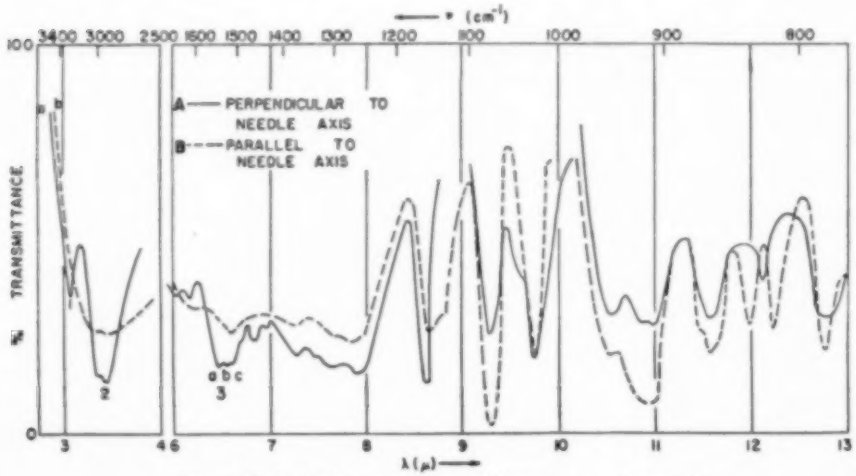

Fig. 5. Polarized spectra of piperidine-picric-acid complex.

of this complex, as shown in Fig. 5 and summarized in Table 5, is not very strong. Information on the orientation of specific portions of the piperidine molecule with respect to the predominantly planar picric-acid molecule is useful in predicting an approximate structure. Since the dichroism of band 3, the nitro asymmetric stretching vibrations, indicates that the nitro groups are essentially in a plane perpendicular to the needle axis, and since two of the three nitro groups are coplanar with the aromatic ring (cf. previous section), the picric-acid ring must be in a plane perpendicular to the needle axis. The predominant appearance of band 1,

VOL. 8 1956/5

the N-H stretching vibration of piperidine, in the *A*-spectrum, indicates that the N-H bond is parallel to the picric-acid ring. Since the N-H frequency in the complex (3267 cm^{-1}) is shifted to a lower position as compared with its value in dilute solution (3344 cm^{-1}), a hydrogen bond involving the N-H and a nitro group is suggested. If this is so, the appearance of the N-H vibration only in the *A*-direction requires that the N-H bond not only be parallel to, but actually coplanar with, the picric-acid ring.*

References

[1] Francel R. J. *J. Amer. Chem. Soc.* 1952 **74,** 1265.
[2] Mann J. and Thompson H. W. *Proc. Roy. Soc.* 1952 **A211,** 168.
[3] Kuratani K. *Rept. Inst. Sci. and Technol. Univ. Tokyo* 1952 **6,** 137; *Bull. Chem. Soc. Japan* 1952 **25,** 258.
[4] Waldron R. D. and Badger R. M. *J. Chem. Phys.* 1950 **18,** 566.
[5] Newman R. and Halford R. S. *ibid.* 1950 **18,** 1276.
[6] Crookes D. A. *Nature* 1947 **160,** 17.
[7] Jones A. V. and Sutherland G. B. B. M. *ibid.* 1947 **160,** 567.
[8] Worsham J. E. jr., Levy H. A., and Peterson S. W. paper presented at meeting of American Chemical Society, 12–17 September 1954.
[9] Powell H. M. and Huse G.; *Nature* 1939 **144,** 77, *J. Chem. Soc.* 1943 435.
[10] Zhdanov G. S. and Gol'der G. A. *Zhur. fiz. Khim.* 1955 **29,** 1248.
[11] Wallwork S. C. *Acta Cryst.* 1954 **7,** 648.
[12] Hughes E. W. private communication.
[13] Saunder D. H. *Proc. Roy. Soc.* 1946 **A188,** 31.

* X-ray crystallographic data were obtained by one of the authors (K. N.) for the piperidine-picric-acid complex. The crystal was found to be triclinic, of space group P_1 or $P_{\bar{1}}$, and of approximate density 1·60. The dimensions of the unit cell are as follows; $a = 8{\cdot}8$A, $b = 12{\cdot}1$A, $c = 6{\cdot}92$A (needle axis), $\alpha = 92°, \beta = 93°, \gamma = 108°$, and the number of complex molecules per unit cell is two.

Spectrochimica Acta, 1956, Vol. 8, pp. 152 to 166. Pergamon Press Ltd., London

Untersuchungen über Lichtquellen für Spektralanalyse—VII

Universal Einstellbares Abreissbogengerät mit elektronischer Steuerung

Á. Bardócz
Physikalisches Zentralforschungs-Institut der Ungarischen Akademie der Wissenschaften Abteilung Spektroskopie Budapest, Ungarn

(*Received* 12 *April* 1956)

Abstract—An universally adjustable interrupted arc source with electronic control is described. The interrupted arc source consists of a conventional arc circuit, an electronic high-frequency ignitor circuit and a pulse-generator circuit. The ignitor circuit is operated by a control system consisting of a thyratron tube and a double spark gap. The thyratron is controlled by the pulse generator, which sends voltage pulses to the grid of the thyratron in the desired rhythm. The design of the pulse generator facilitates the production of arcs with either direct or alternating polarity. By adjusting the controls, the repetition period and duration of the intermittent arcs can be selected.

Einleitung

In früheren Mitteilungen wurden die Vorzüge der besonderen Einstellmöglichkeiten von Abreissbogengeräten mit elektronischer Steuerung gegenüber den mechanisch gesteuerten besprochen. So wurden Abreissbogengeräte gezeigt, mit denen sich Folgen von einzelnen Bögen gleicher Polarität [1, 2] bzw. Bogenpaare wechselnder Polarität [3, 4] herstellen lassen, zwischen denen beliebig lange Pausen eingeschaltet werden können. Die einzelnen Bögen brennen dabei jeweils innerhalb einer Halbwelle der speisenden Wechselspannung.

Der bisherigen Praxis war diese Art der Abreissbogenerzeugung unbekannt, da die verwendeten mechanischen Systeme so feine Einstellungen nicht ermöglichen. Wir verstehen unter feiner Einstellung die Möglichkeit, nach Belieben Einzelbogen oder Bogenpaare in regelmässigen Zeitabständen zu erzeugen. Demzufolge wurden bei den mechanisch gesteuerten Abreissbogengeräten die gewünschten Pausen zwischen die aus Einzelbogen zusammengesetzten Bogengruppen eingeschaltet. Einen zeitgemässen Apparat dieser Art beschrieb Bückert [5].

Das hier beschriebene Abreissbogengerät mit elektronischer Steuerung ermöglicht ausser der oben erwähnten Einstellung von Einzelbogen gleicher Polarität und von Bogenpaaren positiver und negativer Polarität die Einstellung von beliebigen Bogengruppen und beliebigen Pausen dazwischen. Die Anwendung von Bogengruppen kann in vielen Fällen zu einer höheren Empfindlichkeit führen. Da ausserdem sich die Analysenvorschriften auf Anregung mit Bogengruppen beziehen, war es wichtig, die früher vom Autor beschriebenen elektronisch gesteuerten Abreissbogengeräte so zu gestalten, dass mit diesen eine ähnliche Anregung ausführbar ist.

Aufbau des Abreissbogengerätes

Das elektronisch gesteuerte Abreissbogengerät ist aus drei Teilen aufgebaut: aus dem Bogenstromkreis, dem Zündstromkreis und dem Stromkreis des

VOL. 8 1956/5

Impulsgenerators. Abb. 1 stellt die Bogen- und Zündstromkreise dar, Abb. 2 den Stromkreis des Impulsgenerators. Der im oberen Teil der Abb. 1. dick ausgezogene Bogenstromkreis ist dem in [3] beschriebenen ähnlich, der Zündstromkreis im unteren Teil der Abbildung dem in den Arbeiten [4, 6, 7, 8, 9] beschriebenen; deshalb kann auf die Beschreibung der Abb. 1. hier verzichtet werden.

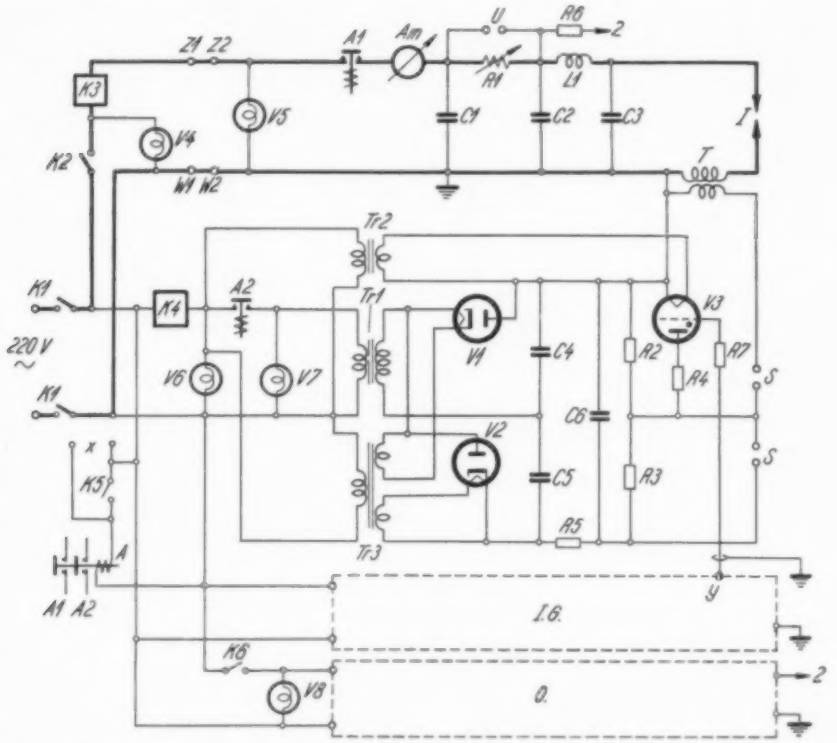

Abb. 1. Bogen-und Zündkreis des elektronisch gesteuerten Abreissbogengerätes. *A* = Magnetschalter, *A1* und *A2* dessen Schaltkontakte; *Am* = Strommesser, 15 A; *C1–3* = 0,1 μF, 1000/3000 V; *C4,5* = 0,1 μF, 6000 V; *C6* = 0,003 μF, 12000 V; *I* = Bogenstrecke *I.G.* = Impulsgenerator; *K1,2* = Schalter, 15 A; *K3,4* = Automat, 10 A; *K5,6* = Schalter; *L1* = Drosselspule, 0,35 mH, 10 A; *O.* = Oszilloskop; *R1* = max. 102 Ω, 10 A; *R2,3* = 5 × 3,3 MΩ, 3 W; *R4* = 8 × 1,2 kΩ, 3 W; *R5* = 25 × 30 kΩ, 3 W; *R6* = 2 × 0,2 MΩ, 0,5 W; *R7* = 50 kΩ, 1 W; *S* = Doppelsteuerfunkenstrecke; *T* = Tesla-Transformator, Primärspule ϕ 110 mm, 10 Wdg. Drahtdurchmesser 2 mm, Sekundärspule ϕ 80 mm 290 Wdg., Drahtdurchmesser 1 mm, *Tr1* = Transformator, 220/4000 V, 200 VA; *Tr2* = Heiztransformator, 220/2,5 V, 5 A; *Tr3* = Heiztransformator, 220/2 × 6, 3 V, 2 A; *U* = Überbrückung; *V1,2* = Hochspannungs-Gleichrichterdiode, V22/7000; *V3* = Thyratronröhre GRG 250/3000, 6000 V, 0,25 A; *V4–8* = Signallampen; *W1,2–Z1,2* = Gleichstromanschluss; *x* = Anschluss des Fernsteuerschalters; *y* = Ausgangsignal des Impulsgenerators.

Durch die Bogenstrecke *I* des Bogenstromkreises in der Abb. 1 kann innerhalb einer Halbwelle der speisenden Wechselspannung nur dann ein Strom fliessen, wenn zuvor die Bogenstrecke durch einen hochfrequenten Spannungsstoss gezündet worden ist, der über den Tesla-Transformator *T* in den Kreis eingespeist wird. Dieser Zünds spannungsstoss wird durch die Entladung des Konden

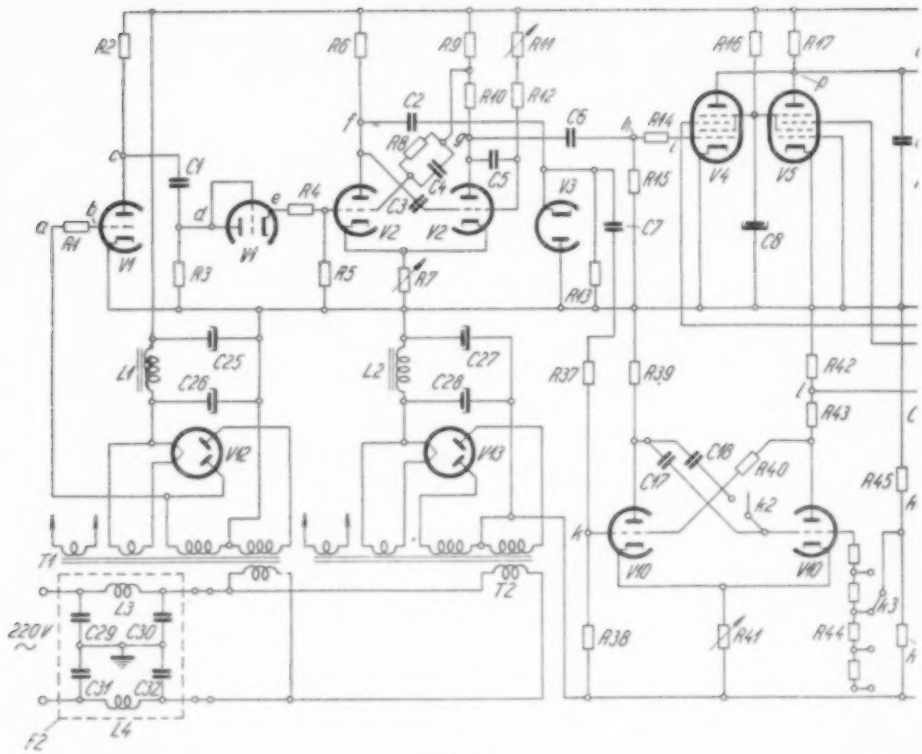

Abb. 2a.

Abb. 2. Elektrisches Schaltschema des Impulsgenerators. *a*, *b*, ... *x* = Stellenbezeichnungen; *C1,2* = 680 *pF*; *C3* = 0,05 *μF*; *C4* = 330 *pF*; *C5* = 100 *pF*; *C6,7* = 680 *pF*; *C8* = 8 *μF* (elektrolytisch) 350/385 V; *C9* = 2200 *pF*; *C10* = 680 *pF*; *C11* = 0,05 *μF*; *C12,13* = 1000 *pF*; *C14* = 1000 *pF*; *C15* = 5000 *pF*; *C16* = 0,1 *μF*; *C17* = 0,05 *μF*; *C18* = 0,2 *μF*; *C19* = 500 *pF*; *C20* = 2500 *pF*; *C21* = 0,05 *μF*; *C25–28* = 16 *μF* (elektrolytisch) 500/550 V; *F1,2* = Filterglied; *C23–24, 29–32* = 250 *pF*; *L3,4,5* = 6,4 mH; *k1–k4* = Umschalter; *L1,2* = 6 H; *R1* = 1MΩ, 0,3 W; *R2* = 60 *k*Ω, 2 W; *R3* = 0,2 MΩ, 0,5 W; *R4* = 0,2 MΩ, 0,5 W; *R5* = 0,5 MΩ, 0,5 W; *R6* = 60 kΩ, 2 W; *R7* = 15 kΩ, 1 W; *R8* = 1,5 MΩ, 0,5 W; *R9,10* = 30 kΩ, 1 W; *R11* = 0,5 MΩ, 1,5 W; *R12* = 55 kΩ, 0,5 W; *R13* = 2 MΩ, 0,5 W; *R14,15* = 0,2 MΩ, 0,5 W; *R16* = 20 kΩ, 3 W; *R17* = 0,3 MΩ, 2 W; *R18* = 0,5 MΩ, 0,5 W; *R19* = 0,5 MΩ, 0,5 W; *R20* = 0,2 MΩ, 0,5 W; *R21* = 60 kΩ, 3 W; *R22* = 1,5 MΩ, 3 W; *R23* = 15 kΩ, 1 W; *R24* = 60 kΩ, 3 W;

sators *C6* bewirkt, dessen Entladungsstrom als hochfrequente Schwingung durch den Tesla-Transformator und die beiden Funkenstrecken *S* abfliesst. Diese Entladung wird mit Hilfe der Thyratronröhre *V3* gezündet u. zw. durch ein Signal, das vom Impulsgenerator *I.G.* (Abb. 2.) kommt und auf das Gitter der Thyratronröhre *V3* wirkt. Es ist die Aufgabe des Impulsgenerators, diese Signale im gewünschten Rythmus zu liefern.

Abb. 2 stellt das Schaltungsschema des Impulsgenerators, Abb. 3 dessen Blockschema dar. Die Form der an den einzelnen Punkten der Schaltung erscheinenden Spannungssignale ist aus Abb. 4 ersichtlich. Die mit gleichen Buchstaben bezeichneten Punkte in den Abb. 2 und 3 sind identisch.

Auf Grund des Blockschemas der Abb. 3 arbeitet der Impulsgenerator in folgender Weise:

VOL. 8 1956/5

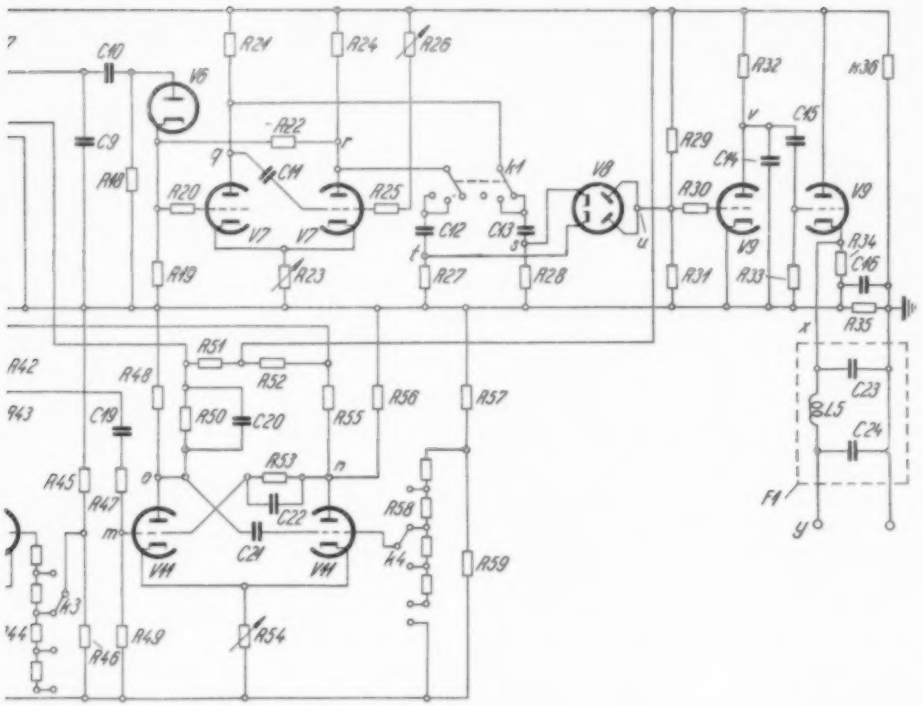

Abb. 2b.

R25 = 0,4 MΩ, 0,5 W; *R26* = 0,5 MΩ, 1,5 W; *R27,28* = 0,1 MΩ, 0,5 W; *R29* = 0,2 MΩ, 0,5 W; *R30* = 0,3 MΩ, 0,5 W; *R31* = 0,2 MΩ, 0,5 W; *R32* = 60 kΩ, 2 W; *R33* = 0,5 MΩ, 0,5 W; *R34* = 10 kΩ, 1 W; *R35* = 25 kΩ, 2 W; *R36* = 40 kΩ, 2 W; *R37* = 0,2 MΩ, 0,5 W; *R38* = 0,5 MΩ, 0,5 W; *R39* = 60 kΩ, 2 W; *R40* = 1,5 MΩ, 0,5 W; *R41* = 15 kΩ, 1 W; *R42,43* = 30 kΩ, 1 W; *R44* = nach Tabelle 1., 0,25 W; *R45* = 45 kΩ, 2 W; *R46* = 7,5 kΩ, 0,5 W; *R47* = 1,5 MΩ, 0,5 W; *R48* = 60 kΩ, 2 W; *R49* = 0,5 MΩ, 0,5 W; *R50* = 0,5 MΩ, 0,5 W; *R51,52* = 2 MΩ, 0,5 W; *R53* = 1,5 MΩ, 0,5 W; *R54* = 15 kΩ, 1 W; *R55* = 0,5 MΩ, 0,5 W; *R56* = 60 kΩ, 3 W; *R57* = 45 kΩ, 2 W; *R58* = nach Tabelle I., 0,5 W; *R59* = 7,5 kΩ, 0,5 W; Die veränderlichen Widerstände *R7*, *R23*, *R41* und *R54* sind nur bei Röhrenwechsel einzustellen. *V1,2* = Doppeltriode, ECC40; *V3* = Diode, 6AL5; *V4,5* = Pentode, 6BE6; *V6* = Diode, 6AL5; *V7* = Doppeltriode, ECC40; *V8* = Doppeldiode, 6AL5; *V9–11* = Doppeltriode, ECC40; *V12–13* = Vollweggleichrichter, AZ21; *y* = Ausgang des Impulsgenerators.

Aus der Speisespannung von etwa 350 Volt, 50 Hz, werden mit Hilfe eines gitterseitigen Begrenzers, Verzerrungverstärkers *V1* und Differenzierkreises Spannungssignale gebildet. Mittels dieser Signale wird nach Gleichrichtung *V1* ein Univibrator *V2* gesteuert, der zur Einstellung der Phasen lage dient. Von den aus dem Univibrator kommenden zwei Signalen wird eines durch einen Differenzier-und Begrenzerkreis in die Stufe *V4* geleitet. Das andere Signal geht nach Durchlaufen eines Differenzier- und Gleichrichterkreises, des Univibrators *V10* und eines zweiten Differenzierkreises in einen weiteren Univibrator *V11*. Mit Hilfe der durch letzteren gesteuerten Mischstufe *V4–V5* wird der übrige Teil der Schaltung ein oder ausgeschaltet. Mit Hilfe der Univibratoren *V10* und *V11* können verschiedene Zeitdauern eingestellt werden, während denen die Signale durchgelassen werden. Das Prinzip der Anordnung besteht

darin, dass nur dann Signale an das Gitter des Thyratrons *V3* der Abb. 1. weitergegeben werden, wenn der Weg durch die Mischstufe *V4–V5* offen ist. Auf diese Weise können verschiedene Verhältnisse von Brennzeit und Pause und verschiedene Periodenlängen des gesamten Vorgangs eingestellt werden. Mit dem Univibrator *V10* wird die Gesamtlänge von Brennzeit und Pause, mit dem Univibrator *V11* die Länge der Brennzeit allein eingestellt. Brennzeit + Pause können zwischen 0,04 und 5 sec verändert werden, die Brennzeit allein zwischen 0,02 und 1,2 sec. Die Periodenlänge (Brennzeit + Pause) bezeichnen wir in der Folge mit T, die Brennzeit mit t. Die Zeitdauer der Pausen wird dann T-t sein.

Da der Impulsgenerator mit dem Netz synchron arbeitet, folgen die am Punkt *i* der Mischstufe ankommenden Signale im Abstand von 1/50 sec. Dasselbe gilt auch für die Signale, welche durch die Mischstufe während der Brennzeit durchgelassen werden. Um auch Bogen mit wechselnder Polarität zu erzeugen, ist hinter die Mischstufe noch ein Univibrator *V7* geschaltet, welcher die Signale verdoppelt, sodass die einzelnen Signale im Zeitabstand von 1/100 sec aufeinander folgen. Mit Hilfe eines Umschalters *k1* kann man wählen, ob man nur das eine oder das andere, oder beide Signale, die vom Univibrator *V7* kommen, weiterlaufen lassen will. Nach dem Umschalter *k1* werden die Signale differenziert und gelichgerichtet. Ist die Stellung des Schalters *k1* wie in Abb. 3, so erfolgen nach der Gleichrichterrohre *V8* die Signale bennin die Brennzeit *t* in Zeitspannen von 0,01 sec. Diese Signale gelangen nach durchlaufen eines Phasenumkehr-Verstarkers *V9* und Kathoden-Verstarkers *V9* zum Gitter der Thyratronröhre *V3* der Abb. 1.

VOL.
8
1956/5

Die ausführliche Wirkungsweise des Impulsgenerators ist folgende (Abb. 2):

Die erste Stufe (erste Hälfte von *V1*) ist ein Verzerrungsverstärker, welcher aus der seinem Gitter zugeführten Sinusspannung von 350 Volt eine Rechteckspannung macht, welche durch *C1*, *R3* differenziert wird. Die zweite Hälfte der Röhre *V1* richtet die differenzierten Signale gleich und lässt die positiven Signale durch. Abb. 4 zeigt schematisch die in den Punkten *a*, *b*, *c*, *d* und *e* der Abb. 2 bzw. 3 erscheinenden Spannungssignale. Das durch die Röhre *V1* durchgegangene positive Spannungssignal betätigt den aus den Röhren *V2* bestehenden Univibrator, welcher auf Einwirkung eines jeden positiven Spannungssignals ein Rechtecksignal bildet, dessen Anfang mit dem Anlass-Signal synchron ist, während das Ende durch die veränderliche Zeitkonstante von *C3*, *R11*, *R12* gegeben ist. Die am Anfang der Periode an der Anode der ersten Röhre erscheinende Rechteckwelle entspricht einem negativen, das verzögerte und regulierbare Ende einem positiven Potential-sprung. An der Anode der zweiten Röhre tritt das Umgekehrte ein. Durch letztere Rechteckwelle, die durch die Glieder *C6*, *R15* differenziert und durch *R14* und das erste Gitter der Röhre *V4* (als Diode) begrenzt wird, erhält man im Verhältnis zur Netzspannung beliebig einstellbare phasenverzögerte negative Signale. Der Univibrator *V2* ersetzt eigent lich eine Phasenschieberbrücke, mit deren Hilfe die Phasenlage der im Punkt *i* der Abb. 2 ankommenden Signale gegenüber der Netzspannung um 90-270 elektrische Grade verschiebbar ist. Wie später noch gezeigt wird, ist diese Phaseneinstellung nötig, um die Zündung des Bogens mittels Hochfrequenz in der gewünschten Phasenlage zu gestatten. Die so

erzeugten negativen Signale gelangen in die aus *V4* und *V5* bestehende Mischstufe.

Die in dem Punkt *i* der Mischstufe eintreffenden Spannungssignale steuern das erste Gitter der Röhre *V4*. Das erste Gitter der Röhre *V5* liegt an Masse. *V4* verstärkt die Spannungssignale und kehrt sie in der Phase um, wenn sie arbeitet (*V5* ist dann gesperrt). Wenn *V4* gesperrt ist, *V5* jedoch arbeitet, erscheint am gemeinsamen Anodenwiderstand *R17* der Röhren kein Signal. Es können also die zur Röhre *V4* im Punkt *i* eintreffenden Signale weiter-geleitet oder ausgeschaltet werden. Diesen Schaltvorgang kann man durch Steuerung der Röhren mit dem Univibrator *V11* erreichen. Die Steuerungsart der Mischröhren *V4* und *V5* ist bei der Beschreibung der Stufe *V11* besprochen.

Die Abb. 4*p* stellt die den Punkt *p* der Abb. 2 verlassenden Spannungssignale für den Fall dar, wenn die Zahl der Glieder der durch die Mischstufe weiter beförderten Signalreihen drei ist und die dazwischen liegenden Pausen dem Ausbleiben von zwei Signalen entsprechen. Der Zeitabstand bei der Wiederholung der Signalreihen wurde in der Abb. 4 mit *T* bezeichnet und früher Periodenlänge genannt. Die Länge der Signalreihen, die Brenndauer, ist in Abb. 4 mit *t* bezeichnet.

Die aus dem Punkt *p* der Mischstufe kommenden Signale werden nach Durchlaufen der Diode *V6* dem aus den Röhren *V7* bestehenden Univibrator zugeführt, dessen Rückkippzeit auf 1/100 sec eingestellt ist. Die an den Punkten *q* und *r* der Anoden der Röhren des Univibrators erzeugten Spannungssignale zeigen die Abb. 4*q* und 4*r* Die durch die Glieder *C12*, *R27*, bzw. *C13*, *R28* differenzierte Form dieser Signale geben die Abb. 4*s* und 4*t* wieder. Die so differenzierten Signale werden durch die Röhre *V8* gleichgerichtet, in welchem Fall an dem Arbeitswiderstand *R31* der Röhre die Summe der beiden negativen Signale erscheint, d.h. eine Signalreihe, in welcher die einzelnen Signale in einem Zeitabstand von 1/100 sec aufeinander folgen. Mit der Betätigung des Schalters *k1* kann man erreichen, dass während der Zeitdauer der Signalreihe (Brennzeit) ein Bogen in jeder der beiden Halbperioden, oder in jeder positiven oder negativen Halbperiode des Netzstromes von 50 Hz entsteht. Abb. 4*u*. zeigt die Signale entsprechend der Mittelstellung des Schalters.

Die die Röhre *V8* verlassenden Signale werden einem Phasenumkehr-Verstärker (erste Hälfte des *V9*) zugeführt. Das Gitter dieser Röhrenstufe begrenzt die eintreffenden Signale in der Weise, dass am Teiler *R29–R31* die Spannung des Punktes *u* positiv wird. Es fliesst also durch den Widerstand *R30* ein Gitterstrom wenn die Röhre keine negative Signalsteuerung bekommt. Hiedurch werden die in den Signalpausen entstehenden Fehlsignale abgeschnitten. Infolge der Übersteuerung der Röhre *V9* werden die erzeugten Signale, als nur vom Widerstand *R32* abhängend, gleich gross. Die Form der an der Anode im Punkte *v* erscheinenden Signale ist aus der Abb. 4*v* ersichtlich.

Die andere Hälfte der Röhre *V9* ist ein Kathoden-Verstärker. Die von der Kathode der Röhre ausgehenden Signale dienen zum Steuern des Gitters der Thyratronröhre *V3* der Abb. 1. Die Abb. 4*x* zeigt die Spannungssignale an der Kathode der Röhre auf das Erdpotential bezogen. Sämtliche andere Signale beziehen sich auf das Kathodenpotential. Das vom Punkt *x* ausgehende Signal schliesst sich, nach Durchgang durch das Filterglied *F1*, mit dem Punkt *y* an den

ebenso bezeichneten Punkt der Abb. 1 an. Die Thyratronröhe *V3* der Abb. 1 bekommt ihre negative Gittervorspannung vom Impulsgenerator durch den Spannungsteiler *R35*, *R36*.

Schliesslich sei die Steuerung der aus den Röhren *V4* und *V5* (Abb. 2) bestehenden entgegengesetzten Mischstufe besprochen.

Die vom Punkt *f* der ersten Hälfte der Röhre *V2*entnommenen Signale werden zum Anlassen des aus Röhre *V10* gebildeten Univibrators benützt. Zu diesem Zweck werden durch die Elemente *C2*, *R13* die an der Anode der ersten Hälfte der Röhre *V2* erscheinenden und in der Abb. *4f* abgebildeten Signale differenziert und ihre negativen Teile mittels der Diode *V3* abgeschnitten. Hiedurch wird die Gestalt der Signale im Punkt *k* vor dem Gitter der ersten Hälfte der Röhre *V10* der Abb. 4*k* entsprechen. Die Rückkippzeit des Univibrators *V10* ist mit den Schaltelementen *C17*, *C18*, *R44* einstellbar. Die Einstellung zwischen 0,04 und

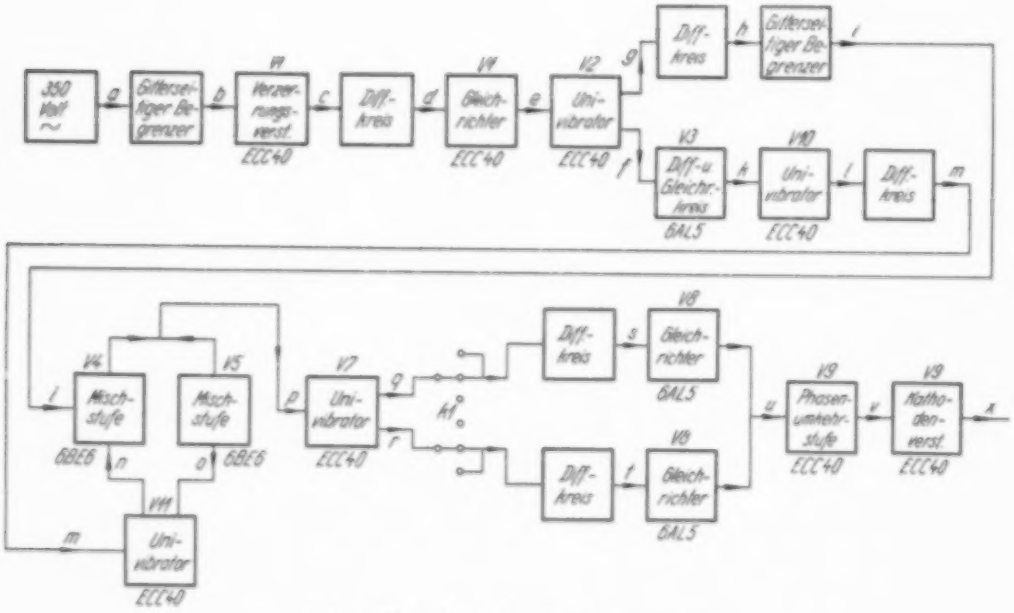

Abb. 3. Blockschema des Impulsgenerators

etwa 5 sec erfolgt in mehreren Abstufungen durch die Schalter *k2* und *k3*. Die zu verschiedenen Schwingungszahlen des Univibrators *V10* gehörenden Werte von *R44* sind in der Tabelle 1 angegeben. Wenn die Stufe rückgekippt ist, wird sie durch das nächste positive Signal (Synchronisierungssignal) neuerdings betätigt und es beginnt eine neue Periode. Aus dem Aufbau des Impulsgenerators geht hervor, dass von der Röhre *V2* zum Punkt *k* zwar fortlaufend Betätigungssignale eintreffen, diese aber solange unwirksam sind, als das Rückkippen des Univibrators *V10* erfolgt. An der zweiten Anode im Punkt *l* erscheint synchron mit dem Anlasssignal ein positiver, beim Rückkippen ein negativer Spannungssprung.

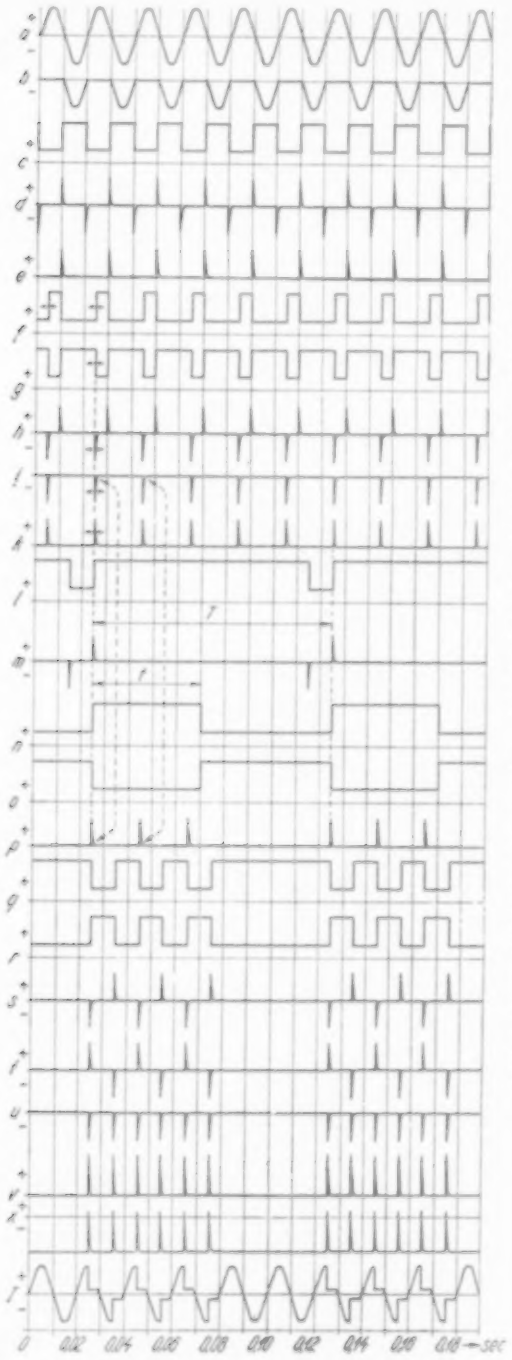

Abb. 4. Form der Spannungssignale an den gleichbezeichneten Punkten der Abb. 2 und 3. Kurve *l* zeigt den Verlauf der Spannung in der Bogenstrecke *l* der Abb. 1.

Die Spannungsverhältnisse im Punkt *l* der Abb. 2 zeigt die Abb. 4*l*. Mittels dieser durch die Elemente *C19*, *R47*, *R49* differenzierten Spannungssignale kann man den Univibrator *V11* steuern, welcher durch die Wirkung des positiven Anlasssignals umkippt und nach der durch *C21*, *R58* einstellbaren Zeit zurückkippt. Die im Punkt *m* eintreffenden differenzierten Signale zeigt die Abb. 4*m*, das im Punkt *n* des Univibrators *V11* erscheinende Signal zeigt die Abb. 4*n*, und das im Punkt *o* erscheinende Abb. 4*o*. Die Änderung des Widerstandes *R58* geschieht mit Hilfe des Schalters *k4*. Die Rückkippzeit des Univibrators *V11* kann man zwischen 0,02 und 1,2 sec. ändern. Im Ruhezustand sperrt die Stufe durch *R52*, *R55* die erste Röhre (*V4*) der Mischstufe und öffnet über *C20*, *R50*, *R51* die Gegentakt-Röhre *V5*. Wie schon früher erwähnt wurde, lässt in diesem Zustand die Mischstufe überhaupt keine Signale durch. Demgegenüberwie ebenfalls schon erwähnt wurde-verstärkt und leitet die Mischstufe im umgekippten Zustande des Univibrators *V11* das Signal weiter. Es wird somit die Zeitdauer des Umkippens die Länge *t* der Brennzeit bestimmen (*t* in der Abb. 4).

In Anbetracht der langen Betätigungsdauer schliesst sich die Stufe *V11* durch Gleichstromkoppelung an *V4* und *V5*. Deshalb ist die Kaskadenausgestaltung der Anodenstromspeisequellen durch die Elemente *T1*, *V12*, *L1*, *C25*, *C26* und *T2*, *V13*, *L2*, *C27*, *C28* notwendig. Die Widerstände *R50*, *R51*, *R52*, *R55* und die Kapazität *C20* dienen zum genauen Beschneiden der zum Steuern der Mischstufe *V4–V5* nötigen Rechteckform. Dieses Beschneiden erfolgt in der Weise, dass die dritten Gitter der Röhren *V4* und *V5* über die Widerstände *R51*,

VOL. 8 1956/5

Tabelle 1. Einstellbare Schwingungszahlen der Univibratoren *V10* und *V11* (Abb. 2 und 3) und die dazu gehörigen Widerstandswerte.

Univibrator *V10*			Univibrator *V11*		
Periodenlänge *T* gemessen in Netzperioden als Einheit		*R44*	Brennzeit *t* gemessen in Netzperioden als Einheit		*R58*
Schalter *k2*			Schalter *k2*		
Ausgeschaltet	Eingeschaltet		Ausgeschaltet	Eingeschaltet	
2	7	200 kΩ	1	1	80 kΩ
3	11	380 kΩ	2	2	213 kΩ
4	19	695 kΩ	3	3	346 kΩ
5	23	895 kΩ	4	4	496 kΩ
6	27	1,1 MΩ	6	6	796 kΩ
8	37	1,5 MΩ	8	8	1,1 MΩ
12	58	2,4 MΩ	12	12	1,9 MΩ
16	78	3,3 MΩ	16	16	2,9 MΩ
20	98	4,2 MΩ	20	19	4,9 MΩ
25	127	5,4 MΩ	36	34	10,9 MΩ
36	183	7,7 MΩ		60	25,9 MΩ
50	247	10,7 MΩ	∞ (100)	∞ (100)	Gitter geerdet

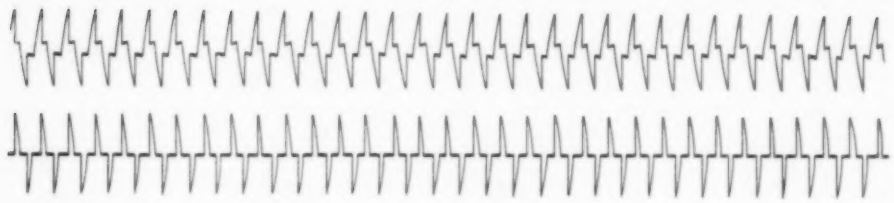

(a)

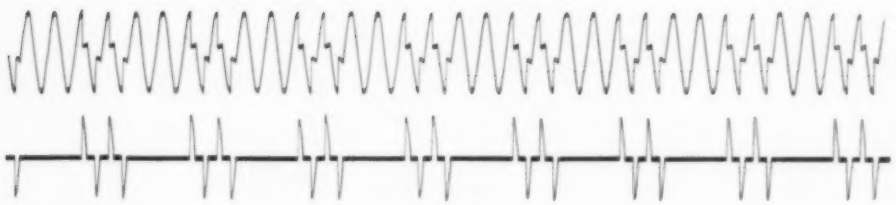

(d)

OL.
8
6/57

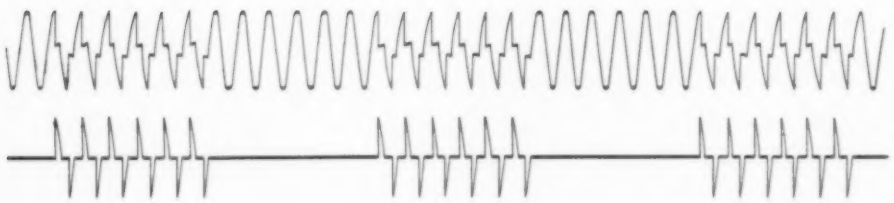

(c)

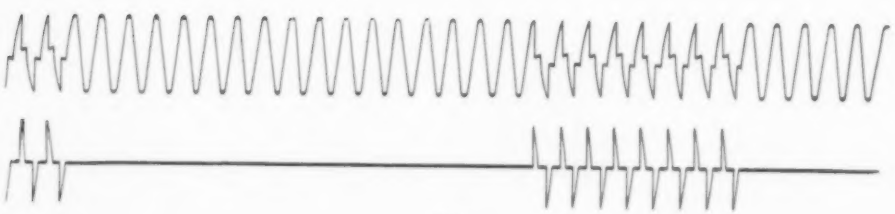

(b)

Abb. 5. Wirkungsweise des Abreissbogengerätes. Verlauf der Spannung und des Stromes in der Bogenstrecke *I* der Abb. 1. Bogen wechselnder Polarität.

R52 positive Spannung erhalten und dadurch die exponentiellen Teile der Anodensignale der Stufe *V11* abschneiden.

Der bei der Stufe *V4–V5* immer entstehende Wechselfehler (Verspätung der Einschaltung der einen Seite) würde ein am Anodenwiderstand *R17* erscheinendes kurzes Störsignal hervorrufen, welches durch den Kondensator *C9* ausfiltriert wird.

Wirkungsweise des Apparates

Die Wirkungsweise des Apparates ist am besten aus den Abb. 4*I*, 5, 6 und 7, ersichtlich. Abb. 4*I* zeigt schematisch die Spannungsverhältnisse in der Bogenstrecke *I* der Abb. 1 im Falle, dass $T = 5$ Netzperioden und $t = 3$ Netzperioden betragen. Die Sinusgrundkurve ist die Netzspannungskurve. Im Zeitpunkt der Zündung fällt diese Spannung auf die Bogenspannung. Die Kurven in Abb. 5, 6 und 7. wurden mit einem Siemensschen Dreischleifenkurvenschreiber aufgenommen. Hier zeigen die oberen Kurven den Verlauf der Spannung in der Bogenstrecke *I* der Abb. 1, die unteren den Verlauf des Stromes im Bogenstromkreis. Bei der Aufnahme sämtlicher Kurven betrug die Höchstspannung 300 V, der maximale Strom 5 *A*.

Die Einstellung der den Abb. 4*I*, 5, 6 und 7. entsprechenden Betriebsverhältnisse des Abreissbogengerätes erfolgt auf Grund der Tabelle der Abb. 8 durch die Schalter *k1*, *k2*, *k3* und *k4* der Abb. 2.

Die Wirkungsweise des Impulsgenerators ist prinzipiell nur in dem Falle richtig, wenn die Periodenlänge T grösser ist als die Brennzeit t, das heisst, die Umkippzeit des Univibrators *V10* soll länger sein als die von *V11*. Eine Ausnahme bildet der Fall, wenn der Schalter *k4* auf unendliche Zeit eingestellt wird, wodurch das Gitter des zweiten Röhrenteils des Univibrators *V11* an den negativen Zweig gebunden wird und die Mischstufe *V4–V5* ohne Unterbrechung weiterleitet. In diesem Fall ist das Einstellen der Periodenlänge T gleichgültig. Abb. 5*a* zeigt bei dieser Einstellung des Impulsgenerators die Spannungs- und Stromverhältnisse in der Bogenstrecke *I* der Abb. 1.

Die Aufnahme der Abb. 5*b* erfolgte bei Periodenlänge $T = 4$, Brennzeit $t = 2$, in Abb. 5*c* ist $T = 12$, $t = 6$, in Abb. 5*d* ist $T = 25$, $t = 8$. Einheit von T und t ist die Periode des Netzstromes.

Früher wurde schon erwähnt, dass der Univibrator *V2* (Abb. 2) zur Einstellung der Phasenlage dient. Abb. 6 veranschaulicht den Vorgang. Abb. 6. wurde bei $T = 12$ und Brennzeit $t = 6$ aufgenommen also bei gleichen Verhältnissen wie Abb. 5*c*. Der Unterschied zwischen den beiden Abbildungen ist der, dass bei der Aufnahme der Abb. 5*c* die Bogenzündung im Scheitelpunkt der Netzspannung, bei der Abb. 6*b* vor dem Scheitelpunkt und bei der Aufnahme der Abb. 6*a* nach dem Scheitelpunkt der Netzspannung einsetzt. In dieser Weise kann das Brennen des Bogens bei einer bestimmten Einstellung innerhalb einer Halbperiode der Netzspannung auf kürzere oder längere Zeit eingestellt werden.

Bei der Aufnahme der Abb. 5 und 6 stand der Schalter *k1* (Abb. 2.) in Mittelstellung, deshalb folgten die Zündfunken innerhalb der Brennzeit in Zeitspannen von 1/100 sec aufeinander. Diese Einstellung ermöglicht also die Erzeugung eines Bogens in jeder Halbperiode der Netzspannung. Die Abb. 7*a–e* zeigen

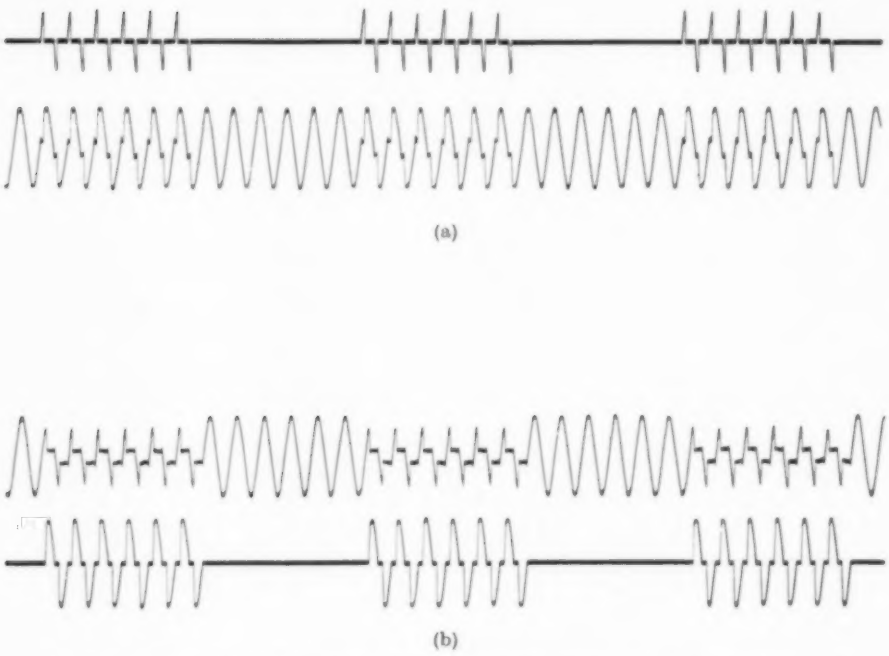

Abb. 6. Verlauf der Spannung und des Stromes in der Bogenstrecke *I* der Abb. 1, wenn die Zündung in verschiedenen Phasenlagen erfolgt. Bogen wechselnder Polarität.

Aufnahmen bei denen der Schalter *k1* der Abb. 2 in der eingezeichneten Stellung stand und von den vom Univibrator *V7* kommenden Signalen nur das eine weiterlief. Bei dieser Einstellung folgen die Zündungen mit einer Verzögerung von 1/50 sec aufeinander und es entsteht je Periode der Netzspannung nur ein Bogen. Die Abb. 7*a–e* zeigt die Betriebsverhältnisse des Gerätes in obiger Einstellung und zwar in 7*a* bei $t = \infty$, in 7*b* bei $T = 25$ und $t = 2$, in 7*c* bei $T = 25$ und $t = 4$, in 7*d* bei $T = 25$ und $t = 8$, in 7*e* = bei $T = 25$ und $t = 12$. Die auf Abb. 7 bezüglichen Betriebsangaben sind mit denen der Abb. 5 identisch.

Allgemeine Bemerkungen

Um die Erwärmung der Elektroden möglichst zu vermindern, ist bei der Anregung mittels des Abreissbogens ein Zwischenschalten von längeren oder kürzeren Pausen üblich, wobei sich die Elektroden abkühlen können. Auf Grund der Abb. 8 kann man feststellen, dass diese Forderung mit dem beschriebenen elektronisch gesteuerten Abreissbogengerät befriedigend erfüllt werden kann. Die Einstellungsmöglichkeiten können durch weitere Änderung der Schalt-

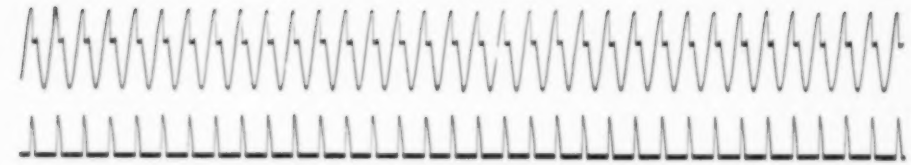

(a)

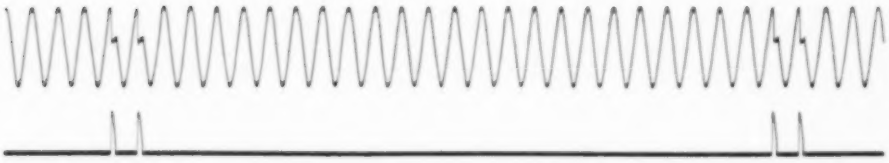

(b)

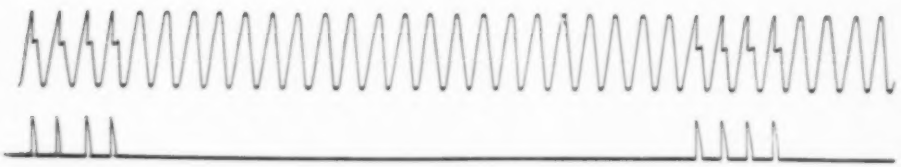

(c)

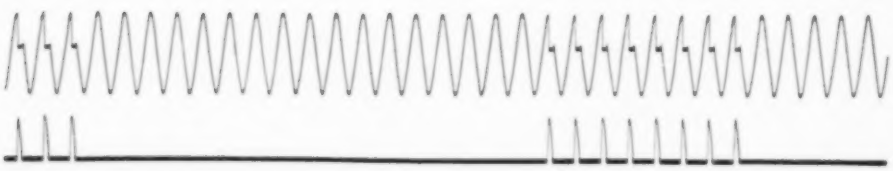

(d)

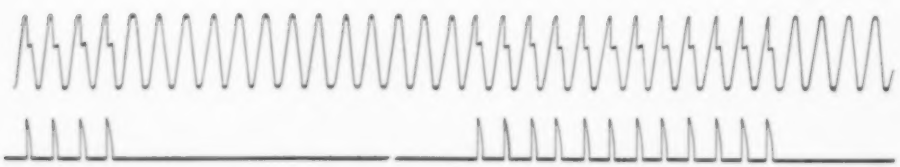

(e)

Abb. 7. Wirkungsweise des Abreissbogengerätes. Verlauf der Spannung und des Stromes in der Bogenstrecke *I* der Abb. 1. Bogen gleicher Polarität.

VOL.
8
1956/5

elemente *C17*, *C18*, *C21*, *R44* und *R58* (Abb. 2) unbegrenzt vermehrt werden, wenn dies erwünscht ist. Mit Hilfe dieses Gerätes sind selbstredend sämtliche Anregungsverhältnisse einstellbar, welche die früher beschriebenen ermöglichen [1, 2, 3, 4]. Zum ungefähren Vergleich sind in der Abb. 8 die mit dem von BÜCKERT [5] beschriebenen Gerät möglichen Einstellungen mit schwarzen Punkten bezeichnet.

In Bezug auf die Genauigkeit der Schaltvorgänge und der Reproduzierbarkeit des elektronisch gesteuerten Abreissbogengerätes kann festgestellt werden, dass

Brenndauer "t"	Periodenlänge "T" Schalter k2 ausgeschaltet											
	2	3	4	5	6	8	12	16	20	25	36	50
1	○	○	○	○	○	○	○	○	○	○	○	○
2		○	○	○	○	○	○	○	○	○	○	○
3			○	○	○	○	○	○	○	○	○	○
4				○	○	○	○	○	○	○	○	○
6						○	○	○	○	○	○	○
8							○	○	○	○	○	○
12								○	○	○	○	○
16									○	○	○	○
20										○	○	○
36												○
50												
∞ (100)	×	×	×	×	×	×	×	×	×	×	×	×

Brenndauer "t"	Periodenlänge "T" Schalter k2 eingeschaltet											
	7	11	19	23	27	37	58	78	98	127	183	247	300
1	○	○	○	○	○	○	○	○	○	○	○	○	
2	○	○	○	○	◉	○	◉	○	◉	◉	○	○	
3	○	○	○	○	○	○	○	○	○	○	○	○	
4	○	○	○	◉	○	○	◉	○	◉	○	◉	○	
6	○	○	○	○	○	○	○	○	○	○	○	○	
8		○	○	○	○	○	◉	○	◉	○	○	○	
12			○	○	○	○	○	○	○	○	○	○	
16			○	○	○	○	○	○	○	○	○	○	
19				○	○	○	◉	◉	○	◉	○	○	•
34						○	○	○	○	○	○	○	
60								◉	◉	◉	◉	○	•
∞ (100)	×	×	×	×	×	×	×	×	×	×	×	×	

Abb. 8. Tabelle zum Einstellen der Betriebsverhältnisse des Impulsgenerators. Die Einheit der in der Abb. angegebenen Zahlen ist die Dauer einer Periode der Netzspannung. Bei den mit Kreuzen bezeichneten Einstellungen liefert der Impulsgenerator 50 bzw. 100 Signale pro sec. Die Kreise geben die Einstellungen der anderen möglichen Betriebsverhältnisse an. Die schwarzen Punkte stellen annähernd die Einstellungsmöglichkeiten des BÜCKERT-schen [5] Gerätes dar.

das System innerhalb verhältnismässig kleiner Zeitabstände ohne Fehler arbeitet. Dies ist so zu verstehen, dass die Zahl der Bögen innerhalb der eingestellten Periodenlänge bzw. Brennzeit stets genau dieselbe bleibt. Mit dem beschriebenen Gerät ist diese Genauigkeit in der Zeitspanne von einer Sekunde (entsprechend 50 Netzperioden) gültig. Diese Genauigkeit kann mit keinem mechanisch gesteuerten Gerät erreicht werden. Ist die Periodenlänge T bzw. die Brennzeit t grösser, so ist die Reproduzierbarkeit im Falle der hier vorkommenden $T = 5$ sec innerhalb einer Netzperiode genau.

Wir danken Herrn A. KLATSMÁNYI für den Entwurf des Impulsgenerators, seine Teilnahme in der Ausgestaltung der Einrichtung und an den Versuchen. Dank gebührt Herrn K. BERTA für die Mitwirkung beim Ausmessen der Einrichtung und Anfertigung der Oszillogramme, sowie Herrn F. MANCZ für die Ausführung des elektronischen Teils der Einrichtung.

Zusammenfassung

Es wird ein spektroskopischen Zwecken dienendes universal einstellbares, elektronisch gesteuertes Abreissbogengerät beschrieben. Das Gerät besteht aus einem Bogenstromkreis von gebräuchlichem Aufbau, einem elektronischen Hochfrequenz-Zündstromkreis und einem Impulsgenerator. Die Steuerung des Zündstromkreises erfolgt durch eine mit Doppelfunkenstrecke gekoppelten Thyratronschaltung. Die den Zündstromkreis betätigende Thyratronröhre wird durch einen Impulsgenerator gesteuert, der das Gitter der genannten Thyratronröhre im erwünschten Rythmus mit Spannungssignalen beschickt. Der Impulsgenerator ermöglicht die Erzeugung von Bogen gleicher und wechselnder Polarität. Durch entsprechende Einstellung der Steuerung können Bogenreihen mit beliebiger Zeitdauer in beliebiger periodischer Wiederholung hergestellt werden.

Literaturverzeichnis

[1] Bardócz Á. *Acta Physica Hungarica* 1953 **2,** 265.
[2] Bardócz Á. *J. Opt. Soc. Amer.* 1952 **42,** 257.
[3] Bardócz Á. *Spectrochim. Acta* 1953 **5,** 397.
[4] Bardócz Á. *Acta Physica Hungarica* 1954 **4,** 91.
[5] Bückert H. *Spectrochim. Acta* 1952 **4,** 525.
[6] Bardócz Á. *Spectrochim. Acta* 1955 **7,** 307.
[7] Bardócz Á. *Nature* 1953 **171,** 1156.
[8] Bardócz Á. *Spectrochim. Acta* 1955 **7,** 238.
[9] Bardócz Á. *Acta Technica Hungarica* 1955 **13,** 407.

VOL.
8
1956/

Spectrochimica Acta, 1956, Vol. 8, pp. 167 to 179. Pergamon Press Ltd., London

The spectrographic analysis of alpha-active materials by the copper spark method

F. T. Birks
Atomic Energy Research Establishment, Harwell, Didcot, Berks

(*Received* 12 *May* 1956)

Abstract—The active samples are sparked in a disposable plastic cassette which is enclosed in a secondary chamber. The excitation source is a 30,000-volt high-wattage generator of the Feussner type, with Tl^{204} sources in place of the usual mercury lamp to ionize the synchronous interrupter gap. The spark source and the spectrograph are housed in separate laboratories: the light passing through a quartz window and reflecting from a mirror into the spectrograph. Four micrograms of molybdenum are added as the internal standard. The line ratios and working curves are given for fourteen elements and the detection sensitivities are given for thirty-eight impurity elements.

The coefficient of variation of the estimations is from 5 to 10% at the five-microgram level.

1. Introduction

Of the standard methods of spectrographic analysis, the direct current arc gives, in general, high absolute sensitivity of detection, but, because of the instability of the arc, the reproducibility of the results is likely to be poor unless careful attention is given to such factors as electrode design and to finding suitable buffering agents and internal standards. The spark method gives better reproducibility, but the sensitivity is less, partly due to lower temperature of the electrodes and smaller consumption of the sample. The copper-spark method of Fred *et al.* [1] was devised to retain the reproducibility of the spark and at the same time give high sensitivity by confining the sample to the electrode surface as a thin film of the volatile chlorides, so that in a short period of time the whole of the sample is consumed in the spark with little consumption of the electrode material. By this method adequate analyses may be carried out using only very small amounts of sample. This is of great advantage for the analysis of highly alpha-active materials, where it is desirable to restrict the amount of material that has to be vaporized, and where frequently the total quantity available is very small.

The method was first investigated at AERE by Todd and was applied to active materials by Wise, who used the high-wattage spark generator described in this report. Bettison and Coe developed the method for use with the 15-kV Hilger spark generator, and their results were applied to active materials by Hartley and Timms.*

Sparking of the sample to completion involves the dispersal of all the alpha activity as an aerosol, and precautions must be taken to ensure that all of this activity is trapped on a suitable filter system. Wise and Outteridge [2] discussed the safety aspects in the case of active analyses, which were at the time

* The work acknowledged here is in reports not yet published.

carried out in a laboratory which was not designed specifically for dealing with active materials. This report contains a brief description of the laboratory designed for this purpose.

2. Description of apparatus

A plan of the optical arrangement is shown in Fig. 1. The spark is enclosed in a cassette, a secondary container, and a dry box; and the light from it is transmitted through two quartz windows and a lens and is reflected from a front-surface mirror into a Hilger large quartz spectrograph.

The laboratory is divided into two sections by double panels of 3-mm sheet aluminium which have two Perspex windows inserted at convenient heights for the spectrographs. One section is used for all operations which involve the handling of alpha activity while the other larger section houses the two spectrographs and is kept free from activity. The two sections are connected via an outside corridor. Plate-reading instruments are kept in the spectrograph section and the dark room and office lead off from it.

The spark output leads are brought through the laboratory walls in polythene sleeves from the generator, which is stored conveniently in the access corridor. The generator is a 30-kV high-wattage source (Fig. 2) developed by Gillieson and Todd.[2] It is a scaled-up Feussner circuit [3] designed to give very energetic excitation, the primary circuit consuming about 2 kW. In place of the more usual ultra-violet irradiation of the secondary interrupter gap, a 500-microcurie source of thallium-204 is placed near each of the fixed electrodes to ionize the gap. This has the advantage that no attention is necessary for a long period, since the thallium has a half-life of 3·5 years. The operating switches for the motor and transformer relays, and the variac control for the primary of the transformer, are detached from the generator and are mounted on a control panel beneath the glove box.

The sparking is done in an enclosed container (Fig. 4) which is separately vented in order to confine most of the activity. For his early work Wise used a stainless-steel cassette of the type described by Feldman *et al.* [4] but found that the handling time was too long for routine use. Subsequently Gillieson and Wise developed a plastic cassette which was cheap when manufactured in quantity and could therefore be disposed of in the event of its becoming heavily contaminated. This cassette, which is shown in Fig. 3, has been used for all subsequent work. It consists of a cruciform body with two screwed caps which retain the quartz end windows. It is used in the horizontal plane with the central 10-deg taper hole uppermost to provide an attachment point to the extract filter system. The copper electrodes are fitted through the 6·4 mm holes in the side arms and are locked at the correct spark-gap setting with self-tapping screws. Electrical contact with the electrodes is made by coarse-threaded wing screws in brass plates which are screwed to the ends of the cassette holder. These screws lock the cassette in position on the optical axis after the spark gap has been set. The plastic carrier which supports the cassette is shown in Fig. 4. One of the 5-mm-thick brass end plates can be seen.

A secondary chamber is used to enclose the cassette so that any traces of activity which may leak out will not contaminate the dry box. This chamber, Fig. 4, is a small Perspex box bolted to a standard Hilger optical bar fitting, via a brass stiffening platform. The light from the spark is transmitted through a 25-mm-diameter hole that may be covered with a Perspex cap when the box is not in use. The main dry-box extract is drawn through this hole and out to the filter system. A positive air leak through a filter from the atmosphere is provided by fitting a 12-mm bore tap on the roof of the dry box. By this means a good scavenging air flow through the Perspex sparking box is ensured, with the added advantage that all air passing into the dry box is filtered from atmospheric dust. The cassette is maintained at a lower air pressure than the dry box by a flow through an independent filter system. An 8-mm o.d. polythene tube has at one end a small tufnol cone which fits into the 10° tapered hole of the cassette, and the other end passes through a coupling in the wall of the spark box to a double D41 Porton resin-wool filter clamped inside the dry box and then through a second double filter on the roof of the dry box. The high activity vaporized by the spark accumulates on the first filter unit, which may be

VOL. 8 1956/5

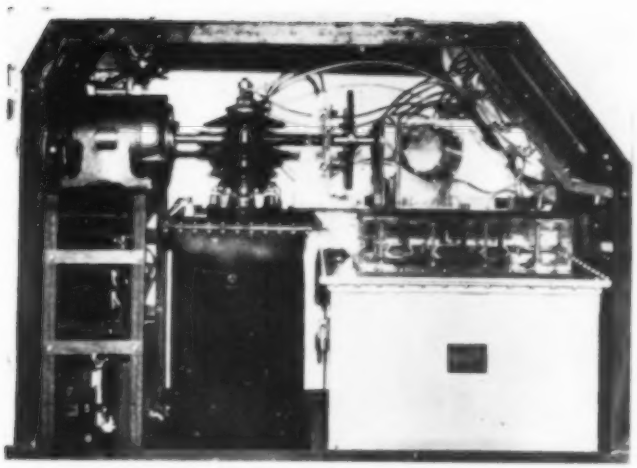

Fig. 2. High-wattage spark generator.

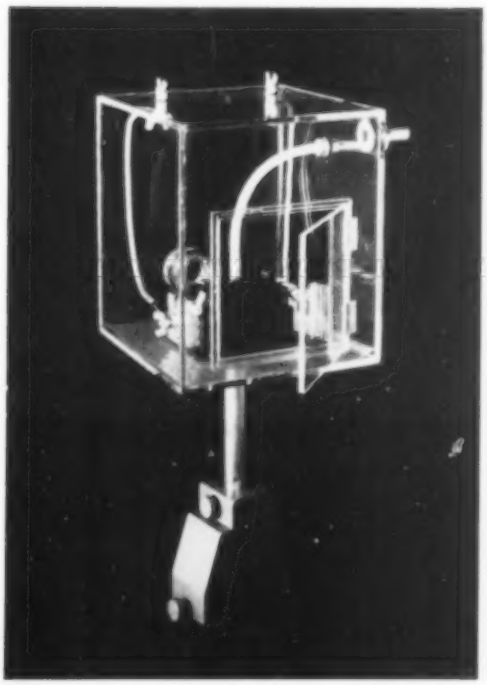

Fig. 4. Spark-chamber assembly.

VOL.
8
1956/5

replaced when necessary from inside the box and brought out completely sealed. A small filter-paper trap can be inserted in the extract line in order to recover any valuable samples after sparking.

The electrodes are aligned by an auxiliary optical system. A shielded 6-V 18-W lamp rotates on a pivot on the wall of the box into the optical axis, the shield thereby covering the exit window. An image of the illuminated electrodes is focused by a glass lens on to a small PVC screen cemented to the perspex front of the dry box, and a standard cassette with accurately positioned 2-mm gap is kept as a check on the optics. A length of optical bar bolted to the floor of the box supports the various components on the optical axis.

The dry box is constructed in two sections (Fig. 1) joined in L-shape by a port which can be closed. The smaller section has a transfer box attached and is used for the loading of electrodes with solution and the decontamination of quartz windows removed from used cassettes. Access to the larger compartment can be made only through the dividing port or through a PVC seal-bag. The latter compartment is used for making the spectrographic exposures and also for any operations involving large amounts of dry alpha-active material.

The optical arrangement outside the dry box consists of a quartz condensing lens (focal length 15 cm) fixed 24 cm from the spark in the perspex panel which is built into the dividing wall between the laboratory sections. 47 cm from the lens and 11 cm from the slit there is a front-surface aluminized mirror inclined at 45° to reflect the light beam along the axis of the optical bar of the quartz spectrograph. To produce lines uniform in density over their length for quantitative measurement, a Hilger quartz 1025 lens is placed 2 cm from the slit. If the spectrograph is required for nonactive samples, it is only necessary to remove the mirror from the bar. To facilitate accurate replacement, fixed stops are provided for each component used on the optical bars. Plate racking is controlled from the active section by a flexible cable with a 2 to 1 gear reduction at the plate.

VOL. 8 56/57

3. Preparation of standards

For all but a few elements, stock solutions and working dilutions are made up in N hydrochloric-acid solution. Fred *et al.* [1] used 1% HCl and stated that larger concentrations are not harmful on copper electrodes but that nitric acid should not exceed 0·02%. They also recommend the use of 4 μg of molybdenum in each exposure as internal standard. This was adopted by Hartley and Timms, and is used in the present method.

The compounds used to prepare the stock solutions should be of high purity, but of still greater importance is the purity of the N HCl which is used to prepare the dilutions of the standards, since any trace impurities that are present will limit the sensitivity of detection of the added standards. This factor is controlled as much as possible by redistilling the hydrochloric acid and distilled water from fused silica apparatus, rejecting the first portion of the distillates.

Most of the elements listed in Table 1 have compounds which are soluble in hydrochloric acid, but the following require special treatment:

Gold, palladium, and tellurium are dissolved in mixed HCl/HNO_3, evaporated with HCl to remove excess of HNO_3, and then dissolved in N HCl.

Thorium is dissolved in HNO_3 to which a trace of sodium fluoride has been added, evaporated with HCl to remove HNO_3, and then dissolved in N HCl.

SiO_2 and WO_3 are fused with sodium carbonate in platinum until a clear melt is obtained, and after cooling they are dissolved in water only.

Silver nitrate is dissolved in water only.

The stock solutions are made up to a concentration of 1 mg per ml in N HCl

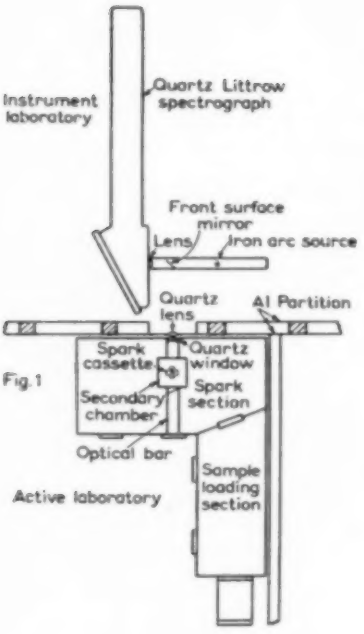

Fig. 1

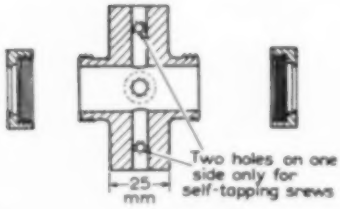

Fig. 3

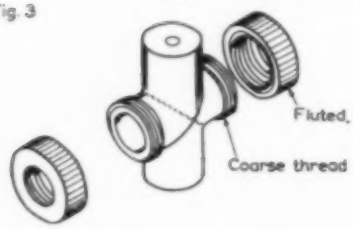

Fig. 1. Plan showing optical arrangement.

Fig. 3. Disposable plastic cassette.

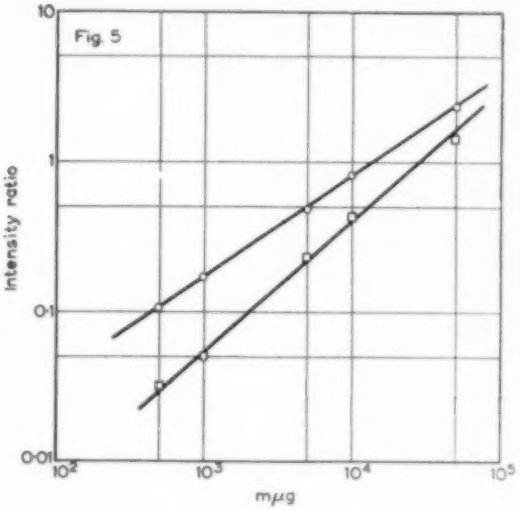

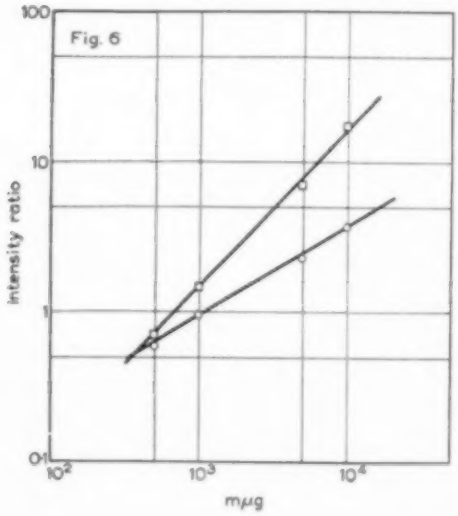

Fig. 5. ○ $\frac{\text{Th-4019·1}}{\text{Mo-3903·0}}$ □ $\frac{\text{Th-4116·7}}{\text{Mo-3903·0}}$
Plotted against mμg on electrodes.

Fig. 6. ○ $\frac{\text{B-3451·4}}{\text{Mo-3170·3}}$ □ $\frac{\text{Mg-2852·1}}{\text{Mo-2848·2}}$
Plotted against mμg on electrodes.

VOL. 8 1956/5

at which strength they store well. In order to reduce subsequent contamination, all solutions are stored in polythene bottles.

To reduce the work involved thirty-eight elements are blended in thirteen solutions and the working concentrations are made by diluting these in N HCl as described in Section 4. Molybdenum standard is added to give a concentration of 40μg of Mo per ml in each dilution.

Boron as boric acid is somewhat volatile in steam, and the standards prepared by drying out acid solutions may in consequence be too low. This loss is minimized by making the standard boron dilutions in N HCl to which has been added 1% v/v of pure glycerol, which complexes with the boric acid and thereby reduces the volatility.

4. Working dilutions

Standard dilutions of W and Ag are made with water; Si dilutions are made with N HCl immediately before taking aliquots, and the colloidal solutions are not stored. All other dilutions are made with N HCl. Redistilled water and HCl are used throughout.

Three dilution series are used as follows, the concentrations being in milli-micrograms ($g \times 10^{-9}$) in 0·10 ml.

Dilution A	10,000	5,000	2,500	1,000	500
	250	100	50	25	blank
Dilution B	1,000	500	250	100	50
	25	10	5	2.5	blank
Dilution C	50,000	25,000	10,000	5,000	2,500
	1,000	500	250	100	blank

In Table 1 the spectrograph ranges are 2260–3000, 2810–5000, and 3180–8000 Å, and the photographic plates are Ilford ordinary or long-range spectrum.

Table 1.

Solution	Elements	Dilution	Littrow spectrograph range			Ilford plate
1	Fe Cr Ni Cd Ca Al Mg	A	3000		5000	0
2	Ti Ga Be V Mn Sc	A B	3000		5000	0
3	Na Li	A		8000		LRS
4	Si	A		3000		0
5	B	A		3000		0
6	Zn Pb Bi Sn In Tl As Sb	A	3000		5000	0
7	Th	C	3000		5000	0
8	U	C	3000		5000	0
9	Te Au Pd Co	A	3000		5000	0
10	P	C	3000		5000	0
11	Ag	B		5000		0
12	W	A		5000		0
13	Ba Sr Cs Rb	A C		8000		LRS

5. Experimental

To check the effect of nitric acid, four cassettes each containing 1000 mμg of solutions 1 and 2 (Table 1) were sparked with the wavelength set at 2260–3000 Å. Two of these had 0·05 ml of 20% v/v HNO_3 dried on to the surface of the copper electrodes subsequent to the standard addition, and the results of this treatment are given in Table 2.

Table 2. Amounts in grams $\times 10^{-9}$ (mμg) read from standard plates

	Cd	Ni	Fe	Al	Cr	Mg	Be	Mn	V	Ga
Untreated	1000	1000	1000	1000	1000	1000	50	100	1000	1000
HNO_3 added	<100	<100	<250	<590	100	50	<20	10	100	300

A thick deposit of copper nitrate was obtained, and this probably prevented the spark from adequately sampling the added impurities.

Fred *et al.* [1] ascribed the high sensitivity of the method to the fact that the deposit normally remains as a thin film on the surface of the electrode and little consumption of the electrode material itself takes place in the spark. Any factors which increase the film thickness therefore tend to reduce the sensitivity. In general, there is no advantage in increasing the sample weight beyond 200 μg.

To avoid the complication of adding the internal standard to each active sample solution, the procedure used by Fowler was adopted. He first dried his internal standard (cobalt) on the electrodes, and then added his sample. The validity of this procedure for the molybdenum internal standard was checked by sparking twelve standard electrodes prepared as described and comparing the spectra with those from another twelve prepared with the molybdenum in homogeneous solution. No significant difference was found.

The effect of adding 100 μg of Pu and 100 μg of U to the standards was investigated. Some suppression was found of the lines arising from the impurities, but the molybdenum internal standard lines were also suppressed and the results obtained from the line ratios were sufficiently accurate for most requirements. If greater accuracy is necessary, then standards must be prepared using the same matrix elements as in the sample and in similar concentration.

6. Method of operation

Since the detection sensitivity of the more common elements is limited by the blanks and the quantities sought are of the order 10^{-7} g, extreme cleanliness of working is essential. Blanks are derived from (1) reagents, (2) air-borne dust contamination, and (3) impurities in the electrode copper. The purity of reagents has been dealt with under standards preparation. Dust suppression is assisted by working in a dry box and by avoiding the use of talcum powder on the gloves. It is advisable to scrub the gloves thoroughly with soap and water before fitting them to the box to remove the talcum that is always present when they are new. Plastic components are used in the box wherever possible, and any remaining metal parts are painted to stop corrosion.

The electrodes are commercial high-purity 6·35-mm-diameter copper, cut into 50-mm lengths. Before use they are degreased in trichlorethylene, pickled in 25% v/v nitric acid to remove surface contamination, washed, and dried. In a clean lathe the ends are machined flat and a tapered cut taken from the sides down to about 6 mm from the end. They are then kept in a dust-free container until required for loading with sample. Acid pickling, after they are machined, is said by Fred *et al.* [1] to increase rather than reduce the blanks.

The electrodes are sparked for 30 sec before they are loaded, since this procedure reduces blanks of Al, Mg, Si, Ca, and Fe. The residual blank is then more consistent, and a more accurate blank correction may therefore be applied. They are not stored for more than a few hours in

VOL. 8 1956/5

the presparked condition, since they are liable to become contaminated again on standing, even though covered by a Perspex box.

When required for use, one drop of a 0·1% w/v Apiezon 'M' grease solution in A.R. petroleum ether is placed onto each electrode, in order to produce a thin grease-film on the surface, then 0·02 ml of a solution containing 2 μg of Mo is evaporated under infra-red driers on to each electrode to give 4 μg per exposure. The hydrochloric-acid solution of the sample is then added in equal aliquots to each electrode, and dried. Active material is dried under an inverted glass cylinder 45 mm diameter × 55 mm long, which has a 8 mm side arm at the top to which suction is applied via the dry-box filter. The prepared electrodes are loaded into clean cassettes and locked with the self-tapping screws before transporting to the spark chamber.

Details of the exposures are as follows:

Slit-width, Hilger Littrow large quartz spectrograph 15 microns (fixed)

Instrument setting	2260–3000, 2810–5000, or 3180–8000 Å (Table 1)
Analysis gap	2 mm
Added inductance	nil
Added capacity	0·02 μF
Transformer primary current	Controlled at 16 amp during exposure
Sparking time	30 sec
Plate	Ilford ordinary or long-range spectrum (Table 1)
Developer	5 min at 20°C in Kodak D19b diluted 1 : 2.

Standards may be exposed on the same plate with the samples in order to correct for any shift in the calibration curves. An iron calibration pattern is exposed on each plate by means of the 2 : 1 seven-step sector.

The used cassettes are rejected if they are active, but those from the standards or blanks may be used again after they have been cleaned with a test-tube brush to remove the thin film of copper oxide. The quartz windows are recovered and are cleaned by immersion in 1 : 3 HCl, then distilled water, and finally methylated spirits. The reagents are stored in the dry box in wide-mouth glass stoppered bottles, and the HCl is provided with a glass cover to reduce corrosive fume in the box. The windows are held for cleaning in slots cut in a length of polythene tube.

7. Results

The limit of detection for each added impurity element was determined from the standard plates, and these are listed with the corresponding wavelengths in Table 3. The maximum sensitivities and the equivalent percentages of impurity elements on 100-μg samples are grouped together in Table 4. The limits would be lower if the Mo internal standard were not added, but the increased precision obtained justifies some loss of sensitivity. When one or two hundred micrograms of a sample are also present, it is doubtful whether the relatively slight suppression by 4 μg of Mo has much effect on the total suppression, but the suppression of the Mo lines themselves then enables a correction to be applied by the measurement of the intensity ratio of impurity/Mo.

Blanks limit the sensitivity of some common elements, in particular Ca, Si, and Mg. These elements are difficult to remove at the 10^{-8}-g level unless all air-borne dust is eliminated.

Semiquantitative results are obtained by visual comparison with the corresponding standard plates at 20× magnification in a projection comparator. More accurate results are obtained by measuring the line densities on a microphotometer. The line densities from the standard plates are converted to relative intensities by means of the plate characteristic curve which is obtained from a sectored iron-arc exposure on each plate. Suitable molybdenum lines are read off

Table 3. Limits of detection
In the presence of 4 μg of molybdenum

Element	Wavelength	Detection limit mμg (gram $\times 10^{-9}$)	Interferences
Al	2660·4	500	
	3944·0	100	blank, Pa-3944·0
	3961·5	100	Mo-3961·5 and blank
Sb	2528·5	1,000	Si-2528·1
	2598·1	1,000	
	3232·5	4,000	Pu-3232·6 >25 μg
	3267·5	5,000	
As	2349·9	2,500	U-2349·9
	2780·2	2,000	Th >10 μg
B	2496·8	100	(1% glycerol added)
	3451·4	500	U-3451·2
Be	2348·6	10	
	2650·6	15	Th >10 μg
	3130·4	0·25	
Bi	2898·0	1,000	U-2898·0 >5 μg, Pu-2898·0 >10 μg
	3067·7	75	Mo-3067·6, Pa-3067·7
Ca	3179·3	100	blank
	3933·7	100	blank
Cd	2288·0	100	
Cr	2835·6	10	Pa-2835·5, Pu-2835·5 >5 μg
	2843·3	10	Pa-2843·3
	4254·3	500	background
Co	2378·6	250	
	2388·9	200	
	3453·5	50	U-3453·6
	3474·0	250	
Ga	2943·6	250	
	4033·0	50	Th-4032·5 >5 μg
	4172·1	40	Th-4171·3 >10 μg
Au	2428·0	250	Th-2428·0 >2 μg
	2675·9	100	
	3122·8	500	
In	2932·6	10,000	Th-2932·6 >2 μg
	3039·4	200	
	3256·1	50	Th-3256·3 >1 μg
Fe	2382·0	250	blank
	2631·1	250	blank
	3581·2	250	
	4383·5	500	background
Pb	2614·2	1,000	
	2833·1	250	Pu-2833·2 >10 μg
	3683·5	100	Am-3683·4
	4057·8	100	U-4058·2
Mg	2781·4	100	
	2852·1	50	blank
Mn	2576·1	5	
	2949·2	5	Th-2949·1 >5 μg
Ni	2316·0	80	
	2416·1	80	
	3414·8	25	Th-3414·5 >50 μg
	3493·0	50	
P	2535·7	2,000	
	2554·9	5,000	
	4080·0	500	
	4422·2	5,000	

VOL. 8 1956/

Table 3 (*continued*)

Element	Wavelength	Detection limit mμg (gram × 10^{-9})	Interferences
Pd	2635·9	1,000	
	2658·7	1,000	
	3421·2	50	Cr-3421·2, Th-3421·2 >2 μg
	3441·4	50	
Se	3572·5	2·5	Pb-3572·7 >3 μg
	4246·8	5	P-4246·9, Pb-4245·0 >20 μg
Si	2516·1	100	blank
	2881·6	100	blank
Ag	3280·7	10	Random blank from copper
	3382·9	10	
Te	2383·2	250	
Tl	2767·9	1,000	
	2918·3	5,000	
	3519·2	250	
	3775·7	250	Pu-3775·7 >25 μg
Th	2898·9	500	
	2978·6	500	
	3221·3	250	Pa-3221·9, Pu-3221·4 >20 μg
	3722·2	100	
Sn	2840·0	200	Fe >2 μg
	2863·3	1,000	
	3009·1	500	Pu-3008·9 >10 μg
	3262·3	250	
Ti	3361·2	50	
	3761·3	1,000	
U	2858·9	5,000	
	4090·1	2,500	Am-4089·2
	4116·1	2,500	Pu-4115·8
	4472·3	1,000	Pu-4472·8, Th-4472·2 >5 μg
V	2700·9	100	
	2908·8	50	Pa-2909·0
	3093·1	10	U-3093·0. Resolved from Mo-3092·9
	3102·3	10	U-3102·4
W	4008·8	100	U-4009·2 Am-4009·3
	4294·6	500	
Zn	2502·0	1,000	
	2558·0	500	
	3345·0	500	
Ba	3891·8	100	
	4554·0	10	
	6141·7	100	
Cs	3597·4	10,000	
	4006·2	20,000	
	4593·2	8,000	
Li	6103·6	500	
	6707·8	25	
Rb	3940·6	10,000	Background
	4244·4	8,000	U-4244·4
	4571·8	20,000	Background
Na	5890·0	100	
	5895·9	100	
Sr	4077·7	10	Am-4077·8
	4215·5	10	Weak Rb-4215·6

OL.
8
6/57

Table 4. Maximum detection sensitivities

Maximum sensitivity gram $\times 10^{-9}$	Equivalent % on 100 μg	Elements
0.25	0·00025	Be
2·5	0.0025	Sc
5	0·005	Mn
10	0·01	Cr Ag V Ba Sr
25	0·025	Ni Li
50	0·05	Co Ga In Mg Pd Ti
100	0·1	Al B Bi Ca Cd Au Pb Si Th W Na
250	0·25	Fe Te Tl Sn
500	0·5	P Zn
1000	1	Sb U
2000	2	As
8000	8	Rb Cs

Any suppression that is exerted by the major component will reduce these sensitivities.

and, after subtracting background intensities, the intensity ratios of impurity line to Mo line are plotted against the quantity of impurity on the electrodes. The background intensities are read as close to the parent line as possible and usually on the high-wavelength side of it. From these standard curves the impurities are read off, correcting for any drift of the calibration by the standards included on the plate with the samples.

The calibration curves in some cases tail off from linearity at low concentrations owing to the blank contribution. When the blank has a consistent value, say from the copper electrodes, a correction may be applied by trial substitution until a straight line is obtained which passes through the value derived for the blank. When the blank varies, it is more likely to arise from air-borne contamination or from the reagents used for the preparation of the sample, and the correction must be assessed for each analysis.

Lines of the common impurity elements used for microphotometry are given in Table 5 together with molybdenum internal standard lines and the iron lines used for plate calibration. Below about 3100 Å a single-plate characteristic calibration suffices for all the impurity wavelengths on the plate, since the plate gamma is reasonably constant over this region [5]. Above 3100 Å it is necessary to calibrate at both the impurity and molybdenum wavelengths unless these are close together.

Standard calibration curves for Th, B, Mg, Be, V, Si, Pb, Cr, Fe, Ag, Ba, Sr, Sc, and Mn are shown in Figs. 5–12.

The reproducibility and accuracy of the method were assessed by sparking twelve pairs of electrodes, to each of which had been added 5000 mμg of a number of elements, together with 4 μg of the molybdenum internal standard. The line-intensity ratios were evaluated for each spectrum and the corresponding quantity of impurity element read off from the standard calibration curves. The results are given in Table 6.

VOL. 8 1956/5

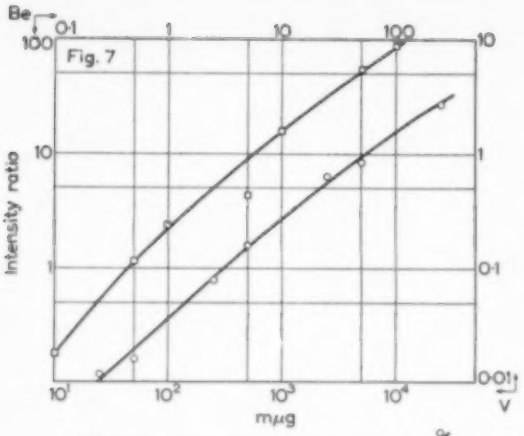

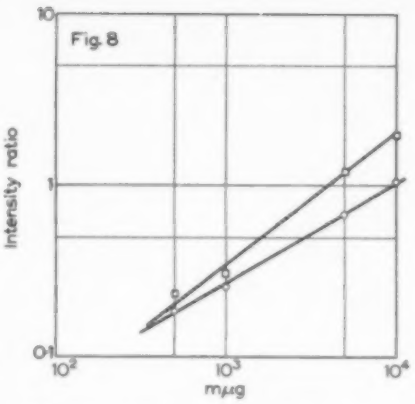

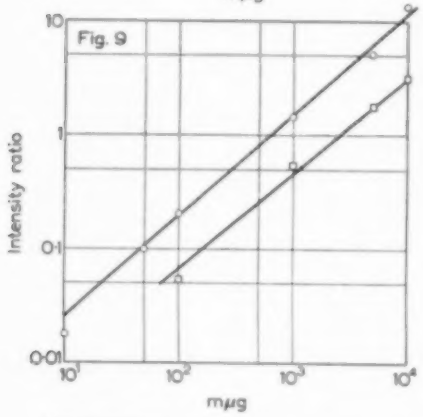

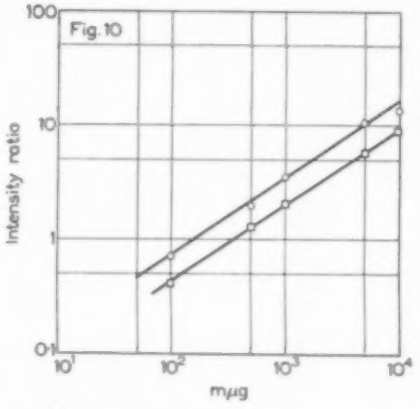

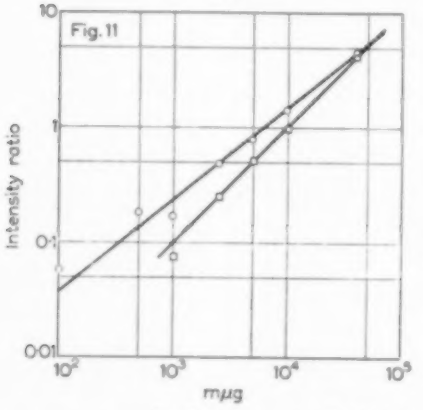

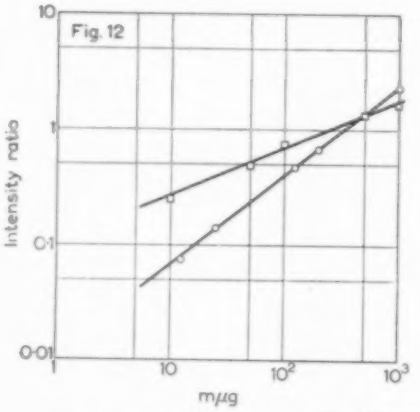

Fig. 7. ○ $\frac{\text{Be-3130·4}}{\text{Mo-3170·3}}$ □ $\frac{\text{V-3102·3}}{\text{Mo-3170·3}}$
Plotted against mμg on electrodes.

Fig. 8. ○ $\frac{\text{Si-2881·6}}{\text{Mo-2848·2}}$ □ $\frac{\text{Pb-4057·8}}{\text{Mo-3903·0}}$
Plotted against mμg on electrodes.

Fig. 9. ○ $\frac{\text{Cr-2677·2}}{\text{Mo-2684·1}}$ □ $\frac{\text{Fe-2382·0}}{\text{Mo-2684·1}}$
Plotted against mμg on electrodes.

Fig. 10. ○ $\frac{\text{Ag-3382·9}}{\text{Mo-3170·3}}$ □ $\frac{\text{Ag-3382·9}}{\text{Mo-3292·3}}$
Plotted against mμg on electrodes.

Fig. 11. ○ $\frac{\text{Ba-3891·8}}{\text{Mo-3903·0}}$ □ $\frac{\text{Sr-4161·8}}{\text{Mo-3903·0}}$
Plotted against mμg on electrodes.

Fig. 12. ○ $\frac{\text{Sc-3572·3}}{\text{Mo-3903·0}}$ □ $\frac{\text{Mn-2593·7}}{\text{Mo-2903·0}}$
Plotted against mμg on electrodes.

Table 5. Line pairs for quantitative measurements

Element	Element line (Å)	Mo control line (Å)	Fe calibration line (Å)
Ni	2416·1	2684·1	2739·5
Cd	2288·0	2684·1	2739·5
Al	2660·4	2684·1	2739·5
	3082·2	3170·3	3116·6
Fe	2382·0	2684·1	2739·5
Cr	2677·2	2684·1	2739·5
Mg	2790·8	2848·2	2739·5
	2852·1	2848·2	2739·5
Si	2881·6	2848·2	2739·5
Pb	4057·8	3903·0	4109·8
Th	4019·1	3903·0	4109·8
	4116·7	3903·0	4109·8
Be	3130·4	3170·3	3175·5
Sc	3572·3	3903·0	3873·8
B	3451·4	3170·3	3175·5
Ga	4033·0	3903·0	3873·8
Na	5890·0	3903·0	6136·6 3935·8
Ag	3382·9	3170·3	3248·2
	3382·9	3292·3	3248·2
Ba	3891·8	3903·0	4315·1
Sr	4161·8	3903·0	4315·1
Mn	2593·7	2903·1	2679·1
V	2700·9	2903·1	2679·1
	3102·3	3170·3	3175·5

Table 6. Reproducibility of results

Element	Amount taken ($g \times 10^{-9}$)	Wavelength (Å)	Mo standard (Å)	Coefficient of variation (per cent)
Cr	5000	II-2677·2	2684·1	6·8
Fe	5000	II-2382·0	2684·1	7·1
Mg	5000	II-2790·8	II-2848·2	5·1
Ni	5000	II-2416·1	2684·1	7·8
Al	5000	I-2660·4	2684·1	10·8
Be	250	II-3130·4	3170·3	8·6
V	5000	II-3102·3	3170·3	6·1
Ga	5000	I-4033·0	3903·0	8·7
Sc	1000	II-3572·5	3903·0	7·6

VOL. 8 1956/5

I denotes a line from the normal atom and II a line from the ionized atom. When a spark source such as the high-wattage generator is used for the excitation, it is best to select for measurement those lines that are derived from the ionized atom. This has been done for most of the elements listed in Table 6, but no suitable spark line could be found for Al in the region 2260–3000 Å.

Acknowledgement—The author thanks Mrs. D. WILLIAMS for assistance, and the Director, Atomic Energy Research Establishment, Harwell, for permission to publish this paper.

References

[1] FRED M., NACHTRIEB N. H., and TOMKINS F. S. *J. Opt. Soc. Amer.* 1947 **37**, 279
[2] WISE H. S. and OUTTERIDGE K. D. AERE CM, 90, November, 1950.
[3] FEUSSNER O. *Archiv. für das Eisenhüttenwesen* 1932–3 **6**, 551.
[4] FELDMAN C., HAWKINS M. B., MURRAY M., and WOOD D. R. *Analyt. Chem.* 1950 **22**, 1400
[5] AMSTEIN E. H. *J.S.C.I.* 1944 **63**, 172.

OL.
8
6/57

Spectrochimica Acta, 1956, Vol. 8, pp. 180 to 183. Pergamon Press Ltd., London

SPECTROCHEMICAL NOTE

A stabilized microphotometer-lamp power supply

A. M. URE
Department of Spectrochemistry,
The Macaulay Institute for Soil Research, Aberdeen, Scotland

(*Received* 15 *May* 1956)

Abstract—A mains-operated power unit, to provide a stabilized supply for the photometer lamp of the Hilger H451 microphotometer is described. The circuit makes use of a saturated diode to control a multivibrator oscillator, transformer coupled to the load. A 10% change in mains voltage within the range 220 V to 250 V produces a galvanometer deflection change of 0·2%. Readily available valves and components are used throughout. Reliable daily operation with the microphotometer for over 18 months has been obtained with greater convenience and less maintenance than with an accumulator supply.

VOL.
8
1956/5

THIS power pack has been designed to supply the 6-V 18-W photometer lamp of the Hilger H451 non-recording microphotometer. With our mains a simple constant-voltage transformer has proved quite inadequate. It is based on a stabilizer circuit by ATTREE [1] in which the output-amplitude-sensing device is a miniature receiving valve operated as a saturated diode [2] and the power source a multivibrator oscillator, transformer coupled to the load. The a.c. power output is 20 W, about twice that of ATTREE's circuit, and an additional amplifier stage is employed to attain a similar short-term stability at this higher output, for mains voltage variation from 220 V to 250 V. It has high stability and speed of response, and requires no special components such as saturable reactors, which are not readily available commercially and whose design and construction present some difficulty to the small laboratory. A low-voltage a.c. stabilizer, employing a saturated diode and a saturable reactor, is described by RICHARDS [3].

Description

The power source consists of a two-valve, V8, V9, multivibrator oscillator working at a frequency of about 2 kc/s, whose output is fed to the terminals *A B* through *T*3. This transformer, *T*3, is a mains type whose normal primary winding is not used. The secondary winding, nominally 235–0–235 V, is used as the input and fed from the 6·3-V winding. While the use of a mains transformer for this function is not the ideal solution, it has proved quite successful in operation. The transformer chosen for *T*3 was a war-surplus metal-clad type. Some types of transformer with the same nominal voltage windings gave different degrees of matching. With one type which also matched the load to the oscillator, a high audiofrequency oscillation severely limited the range of output voltage and the range of mains voltage over

which the stabilizer would operate. This could, however, be overcome by inserting 0·01 μF capacitors from A to earth and B to earth.

The filament of a 1T4 miniature pentode, $V5$, is connected, in series with $F2$ and $R13$, across the output, AB. The 1T4 is operated as a saturated diode with a reduced filament current and the control, screen, and suppressor grids strapped to

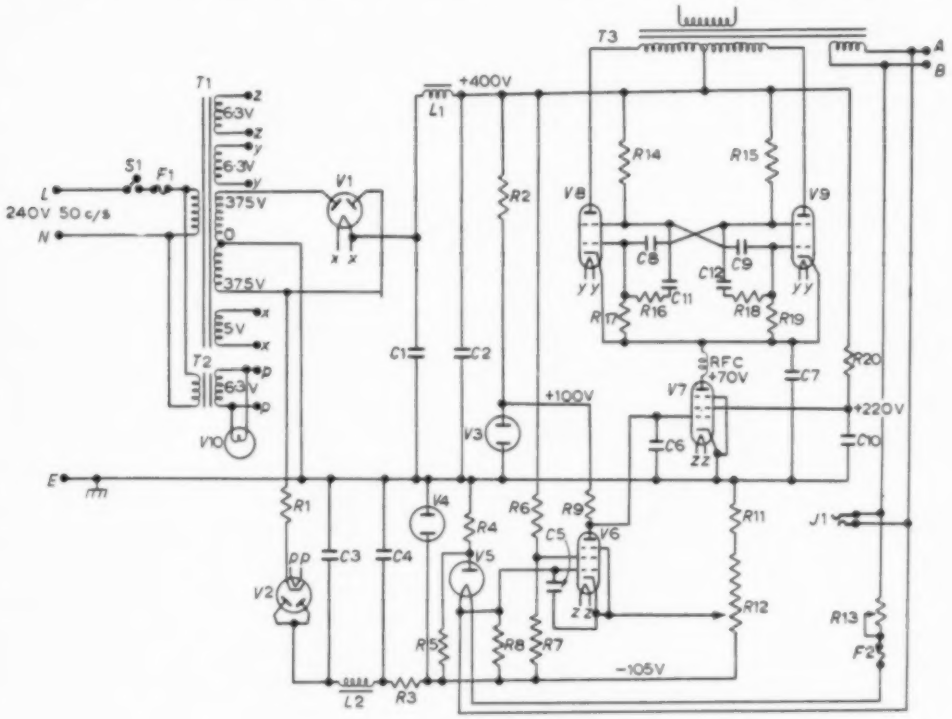

Fig. 1. Circuit diagram.

Component List

$C1$, $C2$, 4 μF, 1 kV; $C3$, $C4$, 4 μF, 600 V; $C5$, 0·05 μF, 600 V; $C6$, 0·002 μF, 600 V; $C7$, 1 μF, 1 kV; $C8$, $C9$, 0·001 μF, 500 V mica; $C10$, 0·1 μF, 1 kV; $C11$, $C12$, 0·002 μF, 500 V mica; $F1$, 2 A; $F2$, 60 mA; $L1$, 15 H, 275 mA; $L2$, 20 H, 50 mA; $R.F.C.$, 18 turns 22 S.W.G., single layer, on $\frac{1}{4}$ in. dia. former; $R1$, 5 K, 10 W, w/w.; $R2$, 60 K, 3 W, w/w.; $R3$, 3 K, 3 W, w/w.; $R4$, 500 K, H.S. carbon; $R5$, 1 M, H.S. carbon; $R6$, 220 K; $R7$, 100 K; $R8$, 4·7 M, H.S. carbon; $R9$, 100 K, H.S. carbon; $R11$, $R14$, $R15$, 5 K, 5 W, w/w.; $R12$, 5 K, 3 W, w/w. variable; $R13$, 500, 3 W, w/w. variable; $R16$, $R18$, 3·3 M; $R17$, $R19$, 470 K, (all resistors are $\frac{1}{2}$ W carbon, except where stated); $T1$, pri., 0–240 V, sec., (a) 375–0–375 V, 250 mA, (b) 6·3 V, 5 A, (c) 6·3 V, 2·5 A, (d) 5 V, 2·5 A; $T2$, pri., 0–240 V, sec., 6·3 V, 2·5 A; $T3$, pri., 0–240 V, sec., (a) 235–0–235 V, 70 mA, (b) 6·3 V, 3 A; $V1$, 5U4G; $V2$, 6X5G; $V3$, 7475; $V4$, VR 105; $V5$, 1T4; $V6$, 6J7G; $V7$, EL38; $V8$, $V9$, 6L6G; $V10$, 6·3 V, 0·3 A indicator lamp.

the anode, as described by Attree [1, 2]. A variation in the r.m.s. value of the output voltage changes the filament current and hence the anode current of the 1T4. The consequent voltage change at the grid of $V6$ is amplified and fed to a series modulator $V7$, which changes the output of the oscillator in the direction necessary to counteract the initiating change at the output terminals. The required output voltage, monitored at $J1$, can be adjusted by $R13$.

The capacitors, $C5$ and $C6$, remove unwanted oscillator-frequency voltages

without appreciably impairing the speed of response. In the prototype, there was some high-frequency oscillation in the modulator which has been suppressed by the radiofrequency choke inserted directly at the anode of *V*7. Improved performance may be obtained by the connection of a capacitor (0·0005 to 0·001 μF between the 240 V 50 c/s "live" head and output terminal A, and a grid stopper in series with the control grid of V7.

Adjustment

In setting up the stabilizer, an Avometer Model 7, range 10 V a.c. monitors the output voltage. An Avometer is adequate for this purpose, but the absolute readings may be in error by up to 10%, in terms of true r.m.s. values, since the output waveform is nonsinusoidal.

To adjust, connect the microphotometer lamp to *AB* and Avometer to *J*1. With the photocell slit closed, set *R*13 to maximum resistance and *R*12 to its most negative position. After allowing time for the valve filaments to heat, turn *R*12 in a positive direction. The lamp will light and the meter show a voltage reading. Adjust *R*12 until this reading is at its maximum (about 7·5 V). Slowly reduce resistance *R*13 until the diode takes control and the output voltage decreases. As *R*13 is reduced, a point will be reached where extinction of the lamp, immediately preceded by a slow oscillation of the output amplitude, occurs. *R*13 should be set to just short of this point, or to 6 V on the Avometer, whichever is the greater.

The stabilizer should now be in reasonable adjustment, but for optimum performance very small adjustments, principally of *R*13, may still be required. These are best made, after disconnecting the Avometer, by setting the microphotometer clear-plate reading to about full scale by means of the microphotometer sensitivity control, and observing the short-term stability of this setting. In good adjustment the short-term range of variation should be not greater than 0·2 in a deflection of 50. Small adjustments may be required during the first few days of operation to "centre" the range of stabilizing action on the range of mains variation but otherwise no attention should be required over long periods.

Although it is desirable to switch off the stabilizer immediately should the lamp burn out, no damage is in fact caused to the stabilizer by failure to do so. With a replacement lamp the stabilizer should require no more than a small readjustment of *R*13.

Performance

At optimum adjustment a 10% fall of mains voltage produces a change in galvanometer deflection of 0·1 in 50, i.e., a change of 0·2%. For a Hilger microphotometer, with its lamp near the operating point, it was found experimentally [4] that a small percentage change in lamp voltage produces a corresponding percentage change in galvanometer deflection about 3·5 times as great. Thus a 10% fall in mains voltage produces a fall of 0·2% in galvanometer deflection and a fall of about 0·06% in lamp voltage.

From a drum-camera recording of the galvanometer deflection of a Hilger microphotometer whose lamp was supplied by the stabilizer, the drift, after an initial warm-up period of 30 min, was found to be less than $\pm$0·2% over a 15-min period. The stability of the microphotometer when supplied by the

VOL. 8 1956/

stabilizer was as good as that obtained with an accumulator which had been in service for some months.

The speed of response of the combined stabilizer and microphotometer is such that a 10% fall in mains voltage, produced by switching a resistor in series with the mains, is corrected with a rapid transient deflection of only 0·3 in a deflection of 50.

Four units have been built largely from war surplus material. One unit has been in daily operation with a Hilger H451 microphotometer for up to seven hours a day for over eighteen months and another for over twelve months without major defects or maintenance problems having arisen, and with much greater convenience than when accumulators were employed.

References.

[1] Attree V. H. *Electron. Eng.* 1953 **25** 71.
[2] Attree V. H. *Electron. Eng.* 1953 **25** 27.
[3] Richards J. C. S. *J. sci. Instrum.* 1951 **28** 333.
[4] Ure A. M. Thesis: *The Application of Electronics to Spectrochemistry* University of Aberdeen, 1954.

OL.
8
6/57

Spectrochimica Acta, 1956, Vol. 8, pp. 184 to 200. Pergamon Press Ltd., London

REPORT OF MEETINGS

U. S. A.

A spectroscopy symposium was held at Argonne National Laboratories, Lemont, Illinois on 15, 16, and 17 February 1956. The following papers were presented.

The high-resolution spectroscopy laboratory at the Los Alamos Scientific Laboratory DAVID W. STEINHAUS, Los Alamos Scientific Laboratory

This small new spectroscopy laboratory contains two large Wadsworth spectrographs that can be used with or without a Fabry-Perot interferometer for either photography or photoelectric scanning of spectra. Adequate facilities have been provided for the safe handling of radioactive elements, including the preparation of sharp-line sources, such as electrodeless metal halide lamps or hollow cathodes, and their excitation. Some of the troubles will be described that had to be overcome to make this a functioning new laboratory for the basic study of the isotopic spectra of the heavy elements.

The porous-cup electrode as a spectrochemical source* MORRIS SLAVIN, Department of Chemistry, Brookhaven National Laboratory

It was possible to increase intensity, avoid corrosion and contamination, and make the preparation and handling of electrodes convenient by using a gold-plated, water-cooled electrode holder and by waterproofing the electrodes with lacquer. A study of the poor reproducibility of the porous cup source showed that it was not due to selective absorption of the solute by the graphite, as some workers suspect, but rather to poor and inhomogeneous porosity, which diminishes flow and causes local drying under the spark. The incidence of this trouble can be reduced by (1) allowing the solution to soak in the electrode for at least an hour before exposure; (2) giving a pre-exposure for at least 60 sec; (3) making the drilled hole in the electrode as large as possible.

VOL. 8 1956/5

Observations on the spectrographic determination of oxygen in metals RAYMOND W. TABELING and VELMER A. FASSEL, Institute for Atomic Research and Department of Chemistry, Iowa State College

The physical properties of many metals and alloys are greatly influenced by the presence of combined oxygen in the metal. The chemical determination of oxygen in metals has been the subject of much investigation, but the analyses remain singularly difficult tasks. The possibilities of performing this analysis by spectroscopic approaches has virtually gone unexplored. The problems encountered in extending conventional spectrographic techniques to this determination are surveyed and techniques for surmounting these problems will be presented. D.c. carbon-arc excitation methods for the determination of oxygen in steels and the rare earths will be discussed in some detail.

Narrow-wavelength-interval direct-reading spectrometer LOUIS E. OWEN, Goodyear Atomic Corporation (to be presented by DAVID C. MANNING)

This paper is to inform members of Commission laboratories of the attempt being made in the spectrochemical laboratory of the Goodyear Atomic Corporation to assemble a narrow-wavelength-interval direct-reading spectrometer. The principle of converting detected photoelectric currents into pulse counts as proposed by BREHM and FASSEL is being used. Initial work employs an L and N monochromator, but it is intended to build a versatile unit applicable to other optical systems. Emphasis is being placed upon the utilization of commercial circuit components.

* Research performed under the auspices of the U.S. Atomic Energy Commission.

The spectroscopy of small samples* FRANK S. TOMKINS and MARK FRED, Chemistry Division, Argonne National Laboratory

Some of the techniques and devices which have been developed to measure wavelengths and hyperfine structure in the spectra of small radioactive samples will be described. For arc and spark exposures 1/16-in.-diameter electrodes are commonly used, loaded in increments of 0·0005 ml in a jig using a Gilmont ultramicroburet. To obtain weak lines with 1-mg samples the electrodes have a porous cap. Discharge-tube sources will also be described. The 30-ft Paschen-Runge spectrograph is used almost exclusively because of its high intensity in low orders and high resolution in high orders. Wavelengths are measured from one standard line on each plate, using the grating law and the AVIDAC for the calculations.

Isotope shifts and nuclear structure LAWRENCE WILETS, Los Alamos Scientific Laboratory

Isotope shifts in heavy elements arise from details in the nuclear structure beyond the electric charge number or the nuclear moments. The dominant effect in isotope shifts is the finite extension of the nuclear-charge distribution. Relative to a theory which assumes uniform charge density throughout the nucleus and the nuclear radius to vary as $A^{1/3}$, one finds that the observed shifts (1) are on the average too small, (2) show regular variation with neutron number, (3) exhibit even-odd staggering.

The discrepancy in the magnitude of the isotope shifts has been partially removed recently by the smaller nuclear (charge) radius measurements (about $1{\cdot}2 \times 10^{-13} A^{1/3}$ cm). The remainder of the discrepancy appears to be accounted for on the basis of nuclear compressibility.

The variation with neutron number is apparently related to nuclear deformation. An ellipsoidally deformed nucleus leads to a potential (averaged over angles) which is equivalent to the potential of a spherical nucleus of larger radius. The observed shifts are in semiquantitative agreement with deformations obtained from other experiments. More detailed experiments would be valuable.

Even-odd staggering presents an interesting and fundamental problem in nuclear physics. Polarization of the nucleus by the atomic electrons, suggested by BREIT, ARFKEN, and CLENDENIN, appears to be too small to account for the phenomenon. One possible explanation lies in nuclear deformation. There are some theoretical reasons to suggest that odd nuclei are less deformed than their even-even neighbours, but there is no other experimental evidence except isotope shift-staggering to support this hypothesis.

Isotope shift in the neighbourhood of $Z = 50$ W. M. CLOUD,† J. E. MACK, and J. A. VREELAND,‡ University of Wisconsin§

Comparison of the experimental isotope shift data for $_{46}$Pd, $_{48}$Cd, $_{50}$Sn, and $_{52}$Te shows that the field-effect shift arising from the addition of two neutrons, times a function of Z only is, within the limits of experimental error, the same function of neutron number for Cd and Sn, but not for Pd and Te. Possible inferences from the difference are discussed.

Nuclear moments of Am^{241} and Am^{243}* THURSTON E. MANNING,¶ MARK FRED and FRANK S. TOMKINS, Chemistry Division, Argonne National Laboratory

Hyperfine structure in the americium spectrum has been measured in high orders of the Argonne 30-ft. spectrograph. Although the Am-I and Am-II term analyses are quite incomplete, some terms giving rise to wide hyperfine patterns have been identified, and it has been possible to calculate the nuclear dipole moment(μ) from the ground-state S terms of Am-II, and the nuclear electric quadrupole moment (Q) from excited P states of Am-I. The values obtained for the

---

* Based on work performed under the auspices of the U.S. Atomic Energy Commission.
† Now at Kansas State Teachers College, Emporia, Kansas.
‡ Now at Westinghouse Electric Corporation, Pittsburgh, Penn.
§ Supported in part by ONR and OOR, and by the research committee of the Graduate School from funds provided by the Wisconsin Alumni Research Foundation.
¶ On leave from Oberlin College, Oberlin, Ohio.

isotope of mass 241 are: $\mu = +1{\cdot}4$ nm, $Q = +4{\cdot}9 \times 10^{-24}$ cm^2. Comparison of the hyperfine patterns of the isotopes of masses 241 and 243 indicated that both isotopes have the same dipole and quadrupole moments within 1%.

On photoelectric Fabry-Perot spectroscopy* J. G. Hirschberg, University of Wisconsin

The employment of the photomultiplier with the Fabry-Perot interferometer has been developed for examining the fine structure of the spectra of light atoms, especially He-II. Liquid helium is used as the coolant. A complicating factor is the relative faintness of the ionized helium lines. To obtain the maximum efficiency necessary with such an expensive coolant, several refinements were found necessary.

Suitable curvature of the slits makes usable the full slit-length of 2 cm provided with the 21-ft, double-pass, stigmatic concave grating mounting. With the usual straight slit, only a much shorter segment of the slit is actually available, using a Fabry-Perot interferometer of the usual aperture. Since the amount of light falling on the photocathode is, other things being equal, proportional to the slit-length, this is an important modification.

Linearity of the pressure sweep for the interferometer is achieved by means of a vibrating bob suspended above a mercury manometer. The bob actuates a solenoid valve, which has a constant pressure across it, made available by a simple modification of an ordinary regulator.

Results are shown in the spectrum of ionized helium.

Isotopic analysis of polonium-208–209 mixtures D. J. Hunt and G. Pish, Mound Laboratory, Monsanto Chemical Company

Isotopic ratios of polonium, produced by proton bombardment of Bi^{209}, were determined from electrodeless discharge tubes by spectrographic methods, The ratios of polonium-209 to polonium-208 were calculated from intensity ratios of the bandheads due to the two molecules, $(Po^{208})_2$ and $(Po^{208}Po^{209})$. It was found that a result with a probable error of $\pm 6\%$ could be obtained from a single spectrogram. Comparison of spectrographic analysis with proton energy-yield data indicated agreement of the order of $\pm 20\%$.

Photoelectric spectroscopic isotope determinations with the Fabry-Perot interferometer J. Brody, Argonne National Laboratory†

The Fabry-Perot interferometer was used with photoelectric detection for precise intensity measurements of the complex pattern of Pb-4057·82. Radial scanning of the central fringe was accomplished by a change of pressure in the interferometer housing. Optical and electronic arrangements for employing the internal standard principle with the interferometer will be described. The Pb^{208}/Pb^{207} and Pb^{208}/Pb^{207} ratios determined by the method are essentially in agreement with mass spectroscopic ratios. A comparison of the effectiveness of aluminium and dielectric coatings for use in the Fabry-Perot interferometer was made. The practical value of the dielectric coatings for the determination of isotope ratios in Pb was demonstrated for the Pb-4057·82 line.

Small isotope shifts in the uranium spectrum were examined because of similarities with other heavy-element spectra, particularly plutonium, for which it was hoped a method might be developed. Partially resolved U^{235} hyperfine structure necessitated a search for U^{235} lines with negligible structure. Low intensity of available light sources severely limited the usefulness of the interferometer method for uranium.

Comparison of method of measurement of nuclear spins for use on radioactive nuclides V. W. Cohen, Brookhaven National Laboratory

Of the many techniques available for measurement of nuclear spin and magnetic moments, each method is definitely limited by such factors as ground-state electron configuration, vapour

* Supported in part by ONR, and by the research committee of the Graduate School from funds supplied by the Wisconsin Alumni Research Foundation.

† Based on work performed under the auspices of the U.S. Atomic Energy Commission.

[1] Hirschberg J. G. *Phys. Rev.* 1955 **99** 1898

[2] Jacquinot P. manuscript in press.

VOL. 8 1956/5

pressure of the element or its compounds, molecular species attainable, and isotopic purity. It appears that optical spectroscopy is free from many of these limitations and is badly needed to supplement nuclear-moment data which are not otherwise attainable. Present techniques in optical hyperfine structure make possible studies of microscopic samples encountered while working with radioactive nuclides. In particular, stable elements of groups 0, II, III(a), IV(a), V(a) and Pt metals have not been studied by other methods. Radioactive members of these groups might well be available for study by optical methods.

Theoretical and experimental criteria for measurement of diffraction-grating performance GEORGE W. STROKE, Massachusetts Institute of Technology, FRANCIS H. SUILIVAN and DAVID K. RICE, Jarrell-Ash Co.

Diffracted wavefront interferograms are easily obtainable, as previously described [1]. The direct physical and analytical Fourier transform relationship between wavefronts and the diffraction images they produce is well known. Optical images of simple or multiple spectral lines, hyperfine structures or Zeeman patterns are determined by the familiar convolution process involving the basic diffraction pattern and the goemetrical slit image. Furthermore, "local" accidents found in diffracted wavefronts enter by superposition independently of the main wavefront. The latter one may have the aberrations from flatness or sphericity. In particular, it is clear that good line separation can be obtained with wavefronts having rather bad "local" accidents and appreciable deviations from flatness. The first factor contributes mainly to the formation of satellites and ghosts, the second one leading to a decrease of depth of focus and increase of diffraction wings. Typical examples of very good resolution of the Hg-2537 Å line with a rejected grating will be shown.

The usual resolving-power pictures are arbitrary and have poor physical significance. Experience has borne out the fact that it is rather the wavefront interferograms which contain the simply obtainable and complete information relevant to the formation of clean, narrow, and well-separable spectral lines, without background and satellites, needed in modern, wide spectral-range, spectroscopy.

Getting rid of the Doppler effect* FRANCIS BITTER, Department of Physics and Research Laboratory of Electronics, Massachusetts Institute of Technology

A general survey will be made of the significance of the Doppler effect in obscuring the interpretation of hyperfine structure data. A few of the more promising areas for further work on HFS will be reviewed.

Various experimental approaches to the problem will be described and compared, and preliminary work with jet lamps will be discussed.

Magnetic scanning of the mercury $^3S_1$ state* H. H. PLOTKIN,† Massachusetts Institute of Technology

By means of an extension of the method of magnetic scanning [2, 3], the $^3S_1$ state of mercury was studied in samples of natural mercury, mercury enriched in the isotope Hg^{201}, and radioactive mercury produced by the bombardment of gold by deuterons. The atoms were excited into the metastable $^3P_0$ level through the absorption of 2537 Å radiation and subsequent collision with N_2 molecules. A variable wavelength source of 4047 Å radiation from a pure Hg^{198} lamp in a magnetic field was then used to excite selectively the hyperfine structure components of the 4047 Å line. The intensity of the re-emitted 5461 Å radiation was observed with a photomultiplier. The lines due to the even isotopes were not resolved. while all of the magnetic

* This work was supported in part by the Signal Corps; the Office of Scientific Research, Air Research and Development Command; and the Office of Naval Research.

† Now at Signal Corps Engineering Laboratories, Fort Monmouth, New Jersey.

[1] STROKE GEORGE W. *J. Opt. Soc. Amer.* 1955 **45** 30
[2] BITTER F. *et al. Phys. Rev.* 1953 **91** 421.
[3] BITTER F. *et al. Phys. Rev.* 1954 **96** 1531.

hyperfine structure components due to Hg^{199} and Hg^{201} were separated and measured. The frequencies were found to be in good agreement with reported values. A tentative assignment of the new components which appeared in the radioactive sample results in a nuclear magnetic moment for Hg^{197} of $\mu_{197} = 1{\cdot}055\ \mu_{199}$ and an isotope shift toward abnormally small effective nuclear radius. Other lines, presumably due to an isomeric state of Hg^{197}, have not been identified.

Radio frequency experiments in mercury $^3P_1$ PAUL L. SAGALYN*†

An apparatus has been constructed for studying radio frequency transitions in the $^3P_1$ state of the various mercury isotopes. The "double resonance" [1] technique is used. Mercury atoms are excited by polarized light from a mercury arc, containing pure Hg^{198}, and placed in a magnetic field called the "scanning field." The mercury absorption cell is placed in a steady magnetic field, called the "splitting field," and subjected to an oscillating magnetic field at right angles to the splitting field. The re-emitted light is passed through a suitable polarizer to a photomultiplier and the photomultiplier current is amplified and displayed on a long persistence screen oscilloscope as a function of the splitting field. The splitting field is swept slowly by a low-frequency sinusoidal voltage applied to an auxiliary coil. The deflection of the oscilloscope trace at resonance is the "resonance amplitude." The splitting and scanning-field magnitudes are measured with a nuclear resonance magnetometer.

With this apparatus one can study: (1) the g factors of the excited state; (2) if one plots the resonance amplitude as a function of the scanning field, the positions of the maxima provide a new method of measuring isotope shift, which eliminates the effects of overlapping lines whose g-factors differ; (3) at microwave frequencies, the splitting fields required for the odd isotope resonances provide a measurement of the magnetic hyperfine structure interaction.

Results for the even isotopes taken at 3100 mc/sec will be presented.

Proposed coincidence method for the elimination of the Doppler effect PAUL L. SAGALYN*†

BRANNEN *et al.* [2] have recently shown that the coincidence rate between pairs of photons, emitted successively by the same atom, can be measured. We have devised a method, using coincidence techniques, which in principle enables one to measure the wave-lengths of emission spectra with considerably greater resolution than would be allowed by the Doppler effect. Light from a very weakly excited source is passed through a spectrograph whose resolution is assumed high compared with Doppler width, thereby giving in the focal plane two lines with widths corresponding to the Doppler width. Two slits are used, a fixed reference slit in front of, say, line 1, and a movable scanning slit in front of line 2. Two photomultipliers are used, one behind each slit, and are connected to a coincidence counter through individual channel counters. The true coincidence rate is measured as a function of the position of the movable slit. The momentum of a photon is negligible with respect to that of an atom, and therefore, if the source is operated so that the atom is not perturbed during the lifetime of the intermediate level, the velocity of the atom will not change between the two transitions and the Doppler shifts of the two photons will be the same. The coincidence rate will then show a maximum when the two slits have the same relative positions on the two lines. The width of the response curve will depend on the slit-width and on the resolving power and aperture of the spectrograph, but not on the Doppler width. Estimated counting times for 0·1 Doppler width resolution are of the order of minutes.

---

* Work performed while Research Associate, Department of Physics and Research Laboratory of Electronics, Massachusetts Institute of Technology. Present address: Ordnance Materials Research Laboratory, Watertown Arsenal, Watertown, Massachusetts.

† This work was supported in part by the Signal Corps; the Office of Scientific Research, Air Research and Development Command; and the Office of Naval Research.

[1] BROSSEL J. and KASTLER A. *Comp. rend.* 1949 **229** 1213.
BROSSEL J. and BITTER F. *Phys. Rev.* 1952 **86** 308.
[2] BRANNEN E., HUNT F. R., ADLINGTON R. H., and NICHOLLS R. W. *Nature* 1955 **175** 810(L).

VOL. 8 1956/5

A high-resolution absorption spectroscope for the study of resonance lines of radio-isotopes* JOHN E. R. YOUNG, Department of Physics and Research Laboratory of Electronics, Massachusetts Institute of Technology

A unique but simple high-resolution absorption spectroscope has been built for the study of the hyperfine structure of the 2537 Å mercury lines. The Zeeman effect on a cooled Hg^{198} arc gives a variable wavelength source. The two circularly polarized components are divided into separate beams, traversing the same optical system, but detected separately; thus the source line scans the absorption spectrum in two directions simultaneously as the Zeeman field is varied. The light intensity from the source is monitored both before entering, and after leaving, the quartz absorption cell, by 1P28 photomultipliers. The resultant photo-currents are accurately compared on a d.c. bridge which gives a value directly proportional to the transmission through the cell.

The six abundant stable isotopes are readily investigated, and owing to the sensitivity of the apparatus, which will detect approximately 10^{12} atoms of mercury vapour, it is possible to investigate radioisotopes of mercury.

Techniques are under development to prepare very pure samples of radiomercury in vapour form in order to investigate their hyperfine structure with this instrument.

A semiautomatic method for spectroscopic wavelength and intensity measurements G. H. DIEKE, the Johns Hopkins University

Efficient and accurate wavelength measurements are a prerequisite for progress in many branches of spectroscopy.

An arrangement is described by which spectroscopic wavelength measurements are greatly simplified with an oscilloscope screen. The comparator readings are made automatically with electronic devices, and the results either recorded with an automatic typewriter or punched into cards, or both. Photographic densities are measured and recorded at the same time. The data are then further processed by electronic calculating machines.

The equipment is built largely from commercially available components. Its operation is simple and foolproof. The various stages are independent of each other and can be introduced singly or in combination as desired. Possibilities for further developments are discussed.

The emission and absorption furnace spectra of plutonium L. F. H. BOVEY, Atomic Energy Research Establishment, Harwell

The construction and operation of a King-type furnace for exciting spectra of radioactive or toxic materials will be described. Absorption spectra of scandium, yttrium, lanthanum, uranium, and plutonium have been observed within the range 2400–7000 Å in the second order of a 3-metre-grating spectrograph. The emission spectra of plutonium and uranium have also been photographed, and it is hoped to discuss preliminary results on plutonium.

The first spectra of antimony and bismuth in the region between 1·0 and 2·2 microns CURTIS J. HUMPHREYS and EDWARD PAUL, JR. U.S. Naval Ordnance Laboratory, Corona, California

The atomic emission spectra of bismuth and antimony have been observed by means of a high-resolution automatically recording grating spectrometer, in the infra-red region accessible to a lead sulphide detector. Wavelength measurements have been made by comparison with simultaneously recorded noble-gas spectra. Most of the infra-red energy emitted in these spectra is represented by lines already observed, photographically in the instance of antimony by MEGGERS and HUMPHREYS [1], and radiometrically for bismuth by RANDALL [2]. More than twenty new lines have been observed for Sb_I. New measurements of the wavelengths greater than 1 micron of all observable lines of Bi_I have been made. Current status of the term analysis will

---

* This work was supported in part by the Signal Corps; the Office of Scientific Research, Air Research and Development Command; and the Office of Naval Research.

[1] MEGGERS WM. F. and HUMPHREYS CURTIS J. The First Spectrum of Antimony. *J. Research NBS* 1942 **28** 463 RP 1464.

[2] RANDALL H. M. Some Infra-r odSpectra. *Astrophys. J.* 1911 **34** 1.

be discussed. Hyperfine structures of the bismuth lines 9657 Å and 11711 Å have been partially resolved under optimum conditions attainable, which include a resolving power of better than 100,000. These structures support existing assignments.

Preliminary analysis of Pr-I with echelle spectrograms* SUMNER P. DAVIS, Massachusetts Institute of Technology

An analysis of the spectrum of neutral praseodymium is being undertaken in order to determine the term analysis and the atomic energy levels. At present, only the ground state is known, from atomic beam work [1].

Until now analysis has not been possible because of the complexity of the spectrum, and the lack of g and J values obtainable from Zeeman patterns. When an ordinary arc containing rare earths is placed in a strong magnetic field, the atoms are ionized and the neutral spectrum does not appear. With the development of an electrodeless microwave discharge source, it was found that the neutral atom spectrum is present even in very large fields. A special type of arc source has been developed [2], which gives the neutral spectrum, although with somewhat less intensity than the discharge.

To date, over 100 lines of Pr-I in fields of about 70 kilogauss have been identified. They are now being analysed; the J-values of most of them lie between 7/2 and 15/2. No attempt has yet been made to correlate the intensities with those listed by A. S. KING, or in the M.I.T. Wavelength tables.

Echellegrams already taken indicate many more lines of Pr-I too weak to measure, but which can be brought up with a brighter source or with increased exposure times.

An analysis of the spectrum of erbium* JOHN W. LINDNER and SUMNER P. DAVIS, Massachusetts Institute of Technology

The spectrum of erbium is now being analysed in order to measure atomic-energy levels. Very little is known about this spectrum at present due to its great complexity and the difficulty in obtaining pure samples or erbium salts.

After experimenting with various types of arc and spark sources, it was found that only an electrodeless discharge tube would give sufficient intensity to obtain Zeeman spectra in a reasonable time. Resolved Zeeman patterns have been obtained for about seventy erbium lines at fields of about 70,000 gauss. These patterns are now being measured to obtain J and g values. Approximately fifty unresolved patterns have also been observed, Spectrograms were made on the M.I.T. echelle spectrograph, which is excellent for Zeeman work.

An attempt has also been made to obtain the underwater spark spectrum of erbium. Thus far we have been unsuccessful in obtaining such spectra for any of the rare earths. This is thought to be due to the rapid oxidation of the rare earths by the oxygen in the water [3]. Attempts are now being made to obtain these spectra, using oxygen-free liquids, but no suitable liquid has yet been found.

Progress report on the description and analysis of the first spectrum of thorium C. C. KIESS and R. ZALUBAS, National Bureau of Standards

Although numerous investigations have been made in recent years, of the spectra emitted by singly, doubly, and trebly ionized thorium atoms, yet very little is known of the character and structure of the spectrum, Th-I, of the neutral atom. Such information is needed for a variety of reasons, among which the manner in which the $5f$-electron enters the configuration of valence electrons and affects the spectrum is of prime importance. Before the solution to this problem can be found, however, it is necessary to have an accurate description of the spectrum, and such additional information, as Zeeman effects, before a start can be made on the analysis of the term

* This work was supported in part by U.S. Atomic Energy Commission funds under Contract No. AT(30-1)-1283.

[1] LEW H. *Phys. Rev.* 1953 **89** 530.
[2] ARCHER J. E. Course VIII Sc.D. Thesis, M.I.T. 1950 (unpublished).
[3] MEGGERS W. F. Private Communication.

VOL. 8 1956/5

structure of the spectrum. To date we have obtained concave-grating spectrograms of arcs and sparks, in air, between metallic thorium electrodes, and of the electrodeless discharge in a thorium-iodide lamp. These observations, although not yet completed, give a good picture of the complexity of the spectra emitted by these modes of excitation. In the region from 3400 to 10,400 Å nearly 12,000 lines have been measured with an average density of nearly two lines per ångström. In the spectral regions outside these limits, observed but not yet measured, there are an estimated additional 4000 lines. Obviously not all of them are characteristic of Th-I, and this is verified by the Zeeman-effect observations that we have made in the region 67–9000 Å. Many well-resolved patterns have been recorded, which, by inspection, can be ascribed to Th-I and Th-II lines. Those already measured confirm this. But the work proceeds slowly and, at the present rate of progress, will require at least three years for its completion.

Application of new techniques to Zeeman spectroscopy P. M. Griffin and K. L. Vander Sluis, Stable Isotope Research and Production Division, Oak Ridge National Laboratory*

A number of new techniques have been utilized in obtaining high precision Landé g factors from Zeeman patterns of spectrum lines. The combination of electrodeless discharge sources capable of high resolution, very uniform magnetic fields of about 33,000 oersteds, and an Echelle-Littrow spectrograph has produced very well resolved Zeeman patterns with a limit of resolution of 0·05 Lorentz units. To make maximum use of all data from a pattern, to be able to compute meaningful probable errors, and to remove difficulties from incipient Paschen-Back effect, a least-squares method of computation based on the separation of symmetric components (which leads to "best values" of the g factors) has been developed and applied. The methods of obtaining the "best values" of the g factors with their probable errors simply from comparator readings and the order number of the components as appearing in an echellogram through use of a high-speed electronic computer (the ORACLE) will be described.

The results of observations on the Zeeman spectrum of Te-II, using the aforementioned techniques, will be discussed. In the case of Te-II, g factors have been determined with an average probable error of 0·0015 Lorentz units when measurements were based on a single pattern. The g factors of levels of Te-II where at least four transitions involving the level were observed have been determined with an average probable error of 0·0006 Lorentz units.

Infra-red spectroscopy of polyatomic molecules† Harold H. Nielsen and K. N. Rao, Dept. of Physics and Astronomy, The Ohio State University

The influence of resonance on centrifugal-distortion constant. Investigations concerning the effect of Fermi resonance and l-type resonance on the centrifugal-stretching constants in linear polyatomic molecules commenced some time ago with a study [1–3] of the bands of CO_2, have been continued. The bands ν_1 and $2\nu_2^0$ of the N_2O molecule have been measured and the constants evaluated. Observations were made at low temperatures to reduce the influence of the "hot" transitions.

In order to examine the effect of l-type resonance alone on the molecular constants, the combination band $\nu_4 + \nu_5$ in C_2H_2 has been remeasured. It was found that the centrifugal stretching constant in the upper state of this band changes by about 40% as compared to the ground-state value obtained from a study of ν_5 at 14 μ to large J values. A similar transition in C_2D_2 was also measured and the results compared with the work of Talley and Nielsen [4] and Overend and Thompson [5].

---

* This paper is based on work performed for the U.S. Atomic Energy Commission by Union Carbide Nuclear Company, a Division of Union Carbide and Carbon Corporation, at the Oak Ridge National Laboratory.

† This work was supported in part by Contract No. DA-33-019-ORD-1893, with the Office of Ordnance Research.

[1] Rossmann Kurt, France W. L., Rao Narahari K., and Nielsen H. H. *J. Chem. Phys.* (in press).
[2] Amat G., Goldsmith M., and Nielsen H. H. *J. Chem. Phys.* (in press).
[3] Amat G., Goldsmith M., and Nielsen H. H. (in preparation).
[4] Talley R. M. and Nielsen A. H. *J. Chem. Phys.* 1954 **22** 2030.
[5] Overend J. and Thompson H. W. *Proc. Roy. Soc.* 1955 **232** 291.

The present status of the theory of the anomalous centrifugal stretching constants in linear polyatomic molecules will be summarized.

Instrumentation. A brief description will be given of the optical arrangement recently constructed here for obtaining wavelength calibrations simultaneously with the recording of the absorption spectrum.

A cooled hollow cathode tube filled with neon and operated at 400–500 MA and 300 volts d.c. enabled us to observe overlapping orders of neon lines over a wide spectral range in the infra-red (1–15 μ). The spectral lines from this source were found to be considerably more intense than those obtainable from the CROSSWHITE, DIEKE, and LEGAGNEUR [1] hollow cathode discharge tube.

Other Studies. The pure rotational absorption spectrum of NO in the region 100–450 μ was observed for the first time. The line positions have been determined by calibrating the far-infrared spectrograph with the pure rotational absorption lines of CO. The molecular constants of NO evaluated from these data will be discussed.

A study of some of the vibration rotation bands of allene-d_4 has been undertaken. The bands studied so far will be described.

The interferometric absorption spectrum of TlCl R. R. KADESCH,* J. C. MOLDENHAUER† and J. G. WINANS, University of Wisconsin

The absorption spectrum of TlCl was photographed with an absorbing path of eight metres, using a Fabry-Perot interferometer. A double-pass Wadsworth mounting employing a 21-ft concave grating was used as the cross dispersion. The resultant patterns obtained as a result of the superposition of the white-light Fabry-Perot fringes and the rotational fine structure will be termed "moire spectra." Wave numbers for rotational lines were determined to an accuracy of $\pm 0{\cdot}01$ cm^{-1}, and for band heads to an accuracy of $\pm 0{\cdot}1$ cm^{-1}.

A rotational analysis of the 0,0, 1,1, and 1,0 bands gave $B_e'' = 927{\cdot}3 \times 10^{-4}$ cm^{-1}, $B_e = 937{\cdot}8 \times 10^{-4}$ cm^{-1}, $D'' = 13{\cdot}61 \times 10^{-8}$ cm^{-1}, $D' = 18{\cdot}12 \times 10^{-8}$ cm^{-1}, $\alpha_e'' = 2{\cdot}48 \times 10^{-4}$ cm^{-1}, $\alpha_e' = 14{\cdot}47 \times 10^{-4}$ cm^{-1}, $r_e'' = 2{\cdot}466 \times 10^{-8}$ cm, and $r_e' = 2{\cdot}452 \times 10^{-8}$ cm. Band origins calculated from the observed wave numbers of the band heads by use of the rotational constants are given by

$$\nu_0 = 31{,}053{\cdot}78 + 209{\cdot}78(v' + \tfrac{1}{2}) - 3{\cdot}41(v' + \tfrac{1}{2})^2 - 0{\cdot}36(v' + \tfrac{1}{2})^3$$
$$-248{\cdot}850(v'' + \tfrac{1}{2}) - 0{\cdot}847(v'' + \tfrac{1}{2})^2.$$

The isotope shift for the four isotopic combinations, $Tl^{205}Cl^{35}$, $Tl^{205}Cl^{37}$, $Tl^{203}Cl^{35}$, and $Tl^{203}Cl^{37}$, was calculated using the rotational and vibrational constants. The mean deviation from the observed shifts was 0·2 cm^{-1} for 111 (heads) observations.

The value of B_e'' obtained here differed from the value $874{\cdot}0 \pm 0{\cdot}8 \times 10^{-4}$ cm^{-1} determined from a molecular beam electric resonance method. The difference is sixty times the probable error, which is approximately the same for both experiments. The plots of $\dfrac{\Delta_2 F(J)}{J + \frac{1}{2}}$ vs. $(J + \frac{1}{2})^2$ deviated from a straight line at low J, as found previously for InCl and GaCl. No explanation for the deviation has been found.

The dissociation energy has been fixed as $3{\cdot}902 \pm 0{\cdot}005$ eV. This is consistent with the presently accepted value $3{\cdot}78 \pm 0{\cdot}1$ eV determined by atomic fluorescence and thermochemical data.

Vibrational analysis of the spectrum of Po_2 G. W. CHARLES, Stable Isotope Research and Production Division, Oak Ridge National Laboratory‡

Measurement of spectrograms of an electrodeless discharge in purified polonium has yielded frequencies of more than 450 red-degraded band heads of Po^{210} and over 500 heads of mixtures of

* Now at University of Utah, Salt Lake City, Utah.

† Now at Inyokern, China Lake California.

‡ This paper is based on work performed for the U.S. Atomic Energy Commission at Mound Laboratory, operated by the Monsanto Chemical Company, and at Oak Ridge National Laboratory, operated by Union Carbide Nuclear Company, a Division of Union Carbide and Carbon Corporation.

[1] CROSSWHITE H. M., DIEKE G. H., and LEGAGNEUR C. S. *J. Opt. Soc. Amer.* 1955 **45** 270.

VOL. 8 1956/5

Po^{208} and Po^{209} in the wavelength range 3500–5100 Å. Approximately 200 bands have been classified as transitions between two sets of energy levels, the average deviation between observed and calculated frequencies being less than 0·3 K in both spectra. The levels are quite well represented by a quadratic equation with the following constants (for Po_2^{210}):

$$T_e'' = 0 \; \omega_e'' = 156{\cdot}14 \text{ K} \; \omega_e'' x_e'' = 0{\cdot}360 \text{ K}$$

$$T_e' = 25149{\cdot}5 \text{ K} \; \omega_e' = 108{\cdot}56 \text{ K} \; \omega_e' x_e' = 0{\cdot}443 \text{ K}$$

A similar equation with constants calculated from these in accordance with the theory of vibrational isotope effect, represents the levels of Po_2^{208} equally well.

A linear extrapolation of the observed levels to convergence leads to an estimate of 2·1 *V* for the dissociation energy of the lower state, assuming the dissociation products to be Po^{210} atoms in the normal state. Other regularities are presently being sought among the unassigned bands.

The present status of knowledge of the spectra of the Group VI diatomic molecules will be briefly discussed.

Symmetries of electric fields about ions in solutions. Absorption and fluorescence spectra of europic chloride in alcohol and water* SIMON FREED, EDWARD V. SAYRE, and DONALD G. MILLER

The theoretical and experimental correlations between the symmetries of the microfields about ions, the degree of splitting of energy levels and the selection rules for radiation have been so successful for ions in crystals that the extension of this approach to discover the precise point symmetries about ions in solutions appears limited only by instances where the spectra of the solutions are sufficiently discrete. In the present approach, crystals containing a rare-earth ion (Eu^{+++}) in known local symmetry had furnished the quantum states involved in the transitions and the unknown symmetry of the fields about the ions in solution was then derived from the number of lines in these transitions.

Solutions of salts of europium appear to be especially favourable for such investigations, since their absorption spectra are sufficiently sharp at room temperature, while the fluorescence spectra become adequately discrete at the temperature of dry ice (193°K). The analysis of aqueous solution was carried out by obtaining absorption spectra of the salt in pure water at room temperature and in mixtures of water and alcohol at both room temperature, and that of dry ice together with the fluorescence spectrum at the latter temperature.

It was found that the symmetry of the microfields about europium ion in methanol was C_{2v}, while there was good evidence that the point symmetry of the ion in water was D_{2h}. Some discussion will be entered upon concerning these low symmetries.

Analysis of the spectra of some solids containing rare earths in terms of the microcrystalline fields about ions* EDWARD V. SAYRE and SIMON FREED

A review of several studies, recently undertaken at Brookhaven National Laboratory, is presented which illustrates the degree and diversity of information obtainable from a detailed analysis of rare-earth spectra.

The polarization absorption and fluorescence spectra of single crystals of some praseodymium and europium salts have been observed and analysed. The analysis of these spectra has revealed the quantum nature of the observed states of the rare-earth ions, the symmetry character of sublevels into which the states were split by the microcrystalline field, and the multipole character of the transitions.

Using these same techniques, some unusual phenomena have been observed. An additional splitting of lines indicates interactions between neodymium ions in anhydrous neodymium chloride. The appearance of extra lines in the spectrum of praseodymium fluoride at liquid-helium temperatures indicates a low-temperature lattice deformation that is not a first-order phase change. The spectrum of a dilute solution of praseodymium chloride in solid strontium

* Research carried out under the auspices of the U.S. Atomic Energy Commission.

chloride indicates that the sites occupied by europic ions are well defined but different from strontium-ion sites.

The absorption and emission spectra of $AmCl_3$ JOHN G. CONWAY, University of California Radiation Laboratory, DIETER M. GRUEN, Argonne National Laboratory, RALPH D. MCLAUGHLIN and B. B. CUNNINGHAM, University of California Radiation Laboratory.

Single crystals of $LaCl_3$ containing 0·04 and 0·2 mole per cent $AmCl_3$ were grown by the Stockbarger method.

Absorption spectra were obtained at 300°K and 70°K. Polarization of some of the Am absorption lines was observed. The spectral range covered in absorption was 3000–12,000 Å.

The crystals exhibited a blue self-luminescence which was intensified by illumination with a 1000-W A-H6 mercury lamp. The emission spectrum was photographed at 300°K and 70°K in the spectral range 4100–6700 Å. At room temperature twelve fluorescence lines were observed. Two of these correspond exactly with two of the absorption lines. At 70°K, about thirty fluorescence lines were observed. There is a temperature dependence of some of the fluorescence lines.

The electronic configuration of Am^{+3} will be discussed in the light of the spectral data.

Spectra of UF_6, NpF_6, and PuF_6 JAMES K. BRODY, HOWARD H. CLAASSEN, and BERNARD WEINSTOCK, Argonne National Laboratory*

The Raman spectrum of gaseous UF_6 and the infra-red spectra of NpF_6 and PuF_6 have been observed. The vibrational spectra furnish strong evidence that the three molecules belong to the O_h symmetry group. All six fundamental frequencies have been determined from the spectra for each molecule.

The absorption spectra of NpF_6 and PuF_6 from 5000 Å to 25,000 Å have also been studied, the photographic portion at high dispersion using the Argonne 30-ft circle. For PuF_6 there are six groups of bands in this range, one of which shows considerable fine structure. For NpF_6 two groups of bands are found. Possible interpretations of some of the vibrational structure will be discussed.

VOL.
8
1956/5

The experimental validity of selection rules for rare-earth ion spectra in crystals ROBERT A. SATTEN, University of California, Los Angeles

The selection rules for atomic electric and magnetic dipole and electric quadrupole transitions in an electric field having the symmetry of each of the thirty-two crystallographic point groups has been looked into again both from a group-theoretical and perturbation-theory approach. New useful ways of summarizing the results are obtained.

When the spectra of neodymium bromate and ethyl sulphate are each examined after empirical energy levels have been drawn indicating the Stark splitting, it is evident that the selection rules are violated for a large number of transitions. This conclusion can be made independent of J assignments or knowledge of the local crystalline symmetry. Assumptions of more than one kind of local symmetry or of ions with equilibrium positions shifted from centres or planes of symmetry cannot apply here, since there are many lines present strongly in only one polarization. The transitions concerned are assumed to be electric dipole from the appearance of the σ spectrum when light is sent along the optic axis.

The explanation for the breakdown in selection rules is sought partially in the interaction of electronic and vibrational motion, the theory of which will be discussed.

High precision wavelength measurements with atomic beam lamps† K. W. MEISSNER and E. C. FINCKH, Purdue University.

The great sharpness of spectral lines obtained with atomic beam light sources permits wavelength measurements of an accuracy which surpasses the definition of the present standard

---

* Based on work performed under the auspices of the U.S. Atomic Energy Commission.
† This investigation has been supported by a grant from the National Science Foundation.

of wavelength. This state of affairs suggests investigating the possibility of constructing an atomic beam lamp which may serve as source for the production of the future primary wavelength standard. Results obtained at Purdue University with a calcium beam lamp show the feasibility of this idea.

Quantitative evaluation of the dispersion of helium W. F. MILLER* and R. L. PLATZMAN, Department of Physics, Purdue University

A complete and consistent set of oscillator strengths for dipole transitions from the ground level of the helium atom has been derived by a critical analysis of both theoretical and experimental information.

The results of the calculations of HUANG (1948), using the momentum matrix element, were adopted as the best obtainable values for oscillator strengths to the continuum. The oscillator strengths to discrete levels were chosen so as to give agreement between the theoretical and experimental value of the static dielectric constant and to be consistent internally, with the sum rule, and with the criterion of continuity at the series limit. The oscillator strengths for the 2^1P, 3^1P, 4^1P, and 5^1P levels were found to be 0·277, 0·0755, 0·0311, and 0·0158 respectively.

The derived oscillator strengths were employed to calculate the following properties of helium gas: various inelastic scattering cross-sections for fast electrons, magnetic susceptibility, refractive index, Verdet constant (Faraday effect), and the mean excitation potential for the stopping power for fast charged particles. The results are in excellent agreement with the experimental information available.

There still remain some uncertainties in the distribution of oscillator strengths among high levels of the continuum for single ionization and the doubly excited levels.

Unusual Doppler effects in calutron ion sources J. R. MCNALLY, JR. and M. R. SKIDMORE, Stable Isotope Research and Production Division, Oak Ridge National Laboratory†

Spectroscopic studies have been made of the low-voltage, low-pressure, magnetically constrained arc which is used in the Oak Ridge National Laboratory calutrons (isotope separators) as an ion source. Spectrum lines of ionized helium and carbon and recombination lines of hydrogen show unusually marked broadening and a "slant line effect," or Doppler shift, across the arc column. The slant effects are attributed to an ordered ionic drift about the arc column, the ion velocities at times exceeding 10^6 cm/sec.

Isotope analysis by nuclear magnetic resonance B. E. HOLDER and M. P. KLEIN, University of California Radiation Laboratory

Nuclear magnetic resonance absorption has been used to determine H^1/H^2 and Li^6/Li^7 isotope ratios on a routine basis. The absorption signal amplitudes of a given nuclide are compared with standard concentrations under the conditions of identical chemical-environment and instrument-operating conditions. The original standard solutions are analysed by a "spiking" technique.

The relative abundance of two isotopes also may be measured without recourse to standard comparison by operating at saturation values of the r.f. field and by using square-wave modulation to obtain the adsorption signal from a lock-in detector. The measurement of the natural Li^6/Li^7 ratio will be presented.

Determination of nuclear moments by nuclear magnetic resonance M. P. KLEIN and B. E. HOLDER, University of California Radiation Laboratory.

One of the most fruitful applications of nuclear magnetic resonance has been the precise determination of nuclear magnetogyric ratios. This quantity ($\gamma = \mu/I^h$) is given directly by a simultaneous measurement of the frequency of the oscillating magnetic field inducing the transitions and the static magnetic field intensity. For those cases where the nuclear spins are

* Now at Argonne National Laboratory, Lemont, Illinois.

† This paper is based on work performed for the Atomic Energy Commission by Union Carbide Nuclear Company, a Division of Union Carbide and Carbon Corporation, at the Oak Ridge National Laboratory.

known from optical data, a measurement of γ yields the magnetic moment. In a nuclear induction experiment, the sign of the magnetic moment is also determined.

For a large number of nuclides, a direct observation of the nuclear magnetic resonance may be precluded because of (1) residual atomic paramagnetism, (2) nuclear quadrupole interactions, and (3) inadequate signal/noise resulting from low abundances or very small magnetogyric ratios.

A double-resonance technique will be described which can alleviate some of the problems stated above. In this method, the nuclide under investigation is bonded to one or more "probe" atoms whose nuclear properties are favourable for nuclear magnetic resonance observation. Under suitable conditions, an indirect spin-spin interaction splits the resonance of the probe nuclei into a multiplet determined by the spin of the unknown nuclide. Injection of a second oscillating field at the resonance frequency for the unknown nuclide removes the multiplicity. This technique yields the nuclear spin directly and the magnetogyric ratio to high precision.

Atomic beam measurements of radioactive isotopes* L. S. Goodman, Argonne National Laboratory, Lemont, Illinois

Techniques used to adapt the Rabi-Zacharias atomic beam method to the study of radioactive isotopes will be considered.

Problems of source preparation, magnetic-field calibration, and detection will be discussed.

VOL.
8
1956/5

The American Association of Spectrographers 7th Annual Symposium was held at Chicago on May 4. The following papers were presented.

Spectrochemical analysis of high-alloy steels L. O. Eikrem, Baird Associates Inc., Cambridge 38, Mass

The authors recently presented a paper on the direct reading analysis of stainless steel, using what they termed the "M/X" concept. That paper, however, did not give the details of the simple theory which explains this method of working. This paper, therefore, will demonstrate that the usual apparent concentration analysis can be expected to be successful in only one special instance. This instance is the one in which $d \log c/d \log I$ is identical for both the element being analysed and for the reference element. In other cases, the apparent concentration system becomes awkward or unworkable. The "M/X" approach to the problem permits the use of curves applicable to a binary system for analysis of a ternary system consisting of M, X, and R. M is the matrix element, X is the element being analysed, and R represents the concentration total of everything else present. When atomic concentrations are used, an exact calculation for the binary curve shift for use with this ternary system is possible. Stainless-steel accuracy data will be shown to demonstrate how this is done. The paper will also demonstrate that different ferrous alloys other than stainless can be analysed from the same basic curve.

Emission spectrographic analysis of high-alloy magnetic material Arthur C. Bowen, Indiana Steel Products Company, Valparaiso, Indiana

A detailed description is given of spectrographic procedure for the analysis of Alnico alloy, a complex ferrous material. To permit the accurate determination of the high percentage concentrations of aluminium, cobalt, and nickel, a "concentration ratio" method is used which

* Work performed under the auspices of the U.S. Atomic Energy Commission.

allows for the variations in the matrix material, iron. The precision of the spectrographic method is shown to compare favourably with that obtainable by routine chemical methods.

The sampling and direct spectrochemical analysis of pig iron HENRY TODD, American Steel and Wire

A solution technique for the analysis of zinc in aluminium DWAINE H. BREWSTER, Kaiser Aluminum and Chemical Corporation, Spokane 69, Wash.

A rapid method for the determination of zinc in aluminium alloys in the range of 2 to 7% has been developed. The technique features the rotating electrode and is designed primarily to overcome variables associated with cast sample structure as well as providing a rapid referee method for the routine control of this element in aluminium. The procedure is particularly suited to the analysis of samples where the metallurgical history cannot be controlled. Extension to the analysis of other elements in aluminium alloys is possible.

A detailed description of the procedure will be given, including a discussion of the effects of various excitation conditions on the zinc working curve.

The quantitative spectrographic determination of zirconium and niobium in uranium metal J. A. GOLEB, Argonne National Lab., Lemont, Illinois

The spectrographic method developed enables fast routine analysis of a large number of uranium metal samples containing about 5·5% zirconium, 1·5% niobium. Excitation is by a high-voltage condensed spark. The average deviation from the mean for zirconium was ±2·89% and for niobium ±2·16%. Comparison of spectrographic and chemical results showed an average deviation of ±3·01% for zirconium and ±3·96% for niobium.

OL.
8
6/57

The role of ion exchange as a concentration tool in spectrographic analysis HENRY J. HETTEL and VELMER A. FASSEL, Iowa State College, Ames, Iowa

Although spectrographic methods are ideally suited to the determination of low concentrations of impurities, every element has a basic sensitivity of detection below which it is impossible to determine it directly. When the determination of lower concentrations is required, concentration procedures must be used to bring the element concentration within the normal spectrographic range. Concentration procedures involving ion exchange provide the advantages of speed, versatility, and freedom from effects which may produce serious, but undetectable, losses of the impurity. The basic criterion for the use of an ion exchanger as a concentration tool is that a complexing agent be chosen which will convert the matrix and the impurity to differently charged complexes. On passage through a cation exchanger, the cations and cationic complexes will be retained, while the neutral and anionic complexes pass through unaffected. Conversely, an anion exchanger will retain the anions and anionic complexes. In both cases, the neutral complexes will pass through the resin bed. The application of ion exchange to the determination of part-per-million amounts of individual rare earths in thorium, uranium, zirconium, and titanium will be discussed.

Recent developments in ratio-recording spectrophotometer ROBERT E. GOETTMAN, Beckman Instruments Inc., Chicago, Ill.

The discussion will cover the new Model DK-1 and 2 ratio-recording, double beam spectrophotometer. The instrument covers a complete range of ultra-violet, visible, and near-infra-red. Although its main function is absorption measurement, attachments are available for emission work such as flame and fluorescence spectra.

Infra-red grating spectrometers and fore-prism building block design JOHN H. RHODES, The Perkin Elmer Corp., Chicago. Ill.

The design and performance considerations of a fore-prism grating spectrometer will be discussed.

The wavelength range from 2·2 to 17 microns can be covered with a single fore-prism and a

single grating. This range can be extended from the ultra-violet to the far-infra-red by substituting suitable prisms, gratings, sources, and detectors. Band separations of better than 0·8 cm^{-1} have been observed. Scattered light is less than 0·1%.

Infra-red analysis of emulsion polishes Mr. Warren C. Schwemer, S. C. Johnson & Sons Inc., Racine, Wisc.

Protective coating formulations based on water emulsions of waxes, resins, and polymers have wide consumer, industrial, and agricultural use. It is often desirable to have a qualitative analysis of these products as to the type of wax, resin, polymer, and emulsifier used. Although these products contain between 80% and 90% water, it is possible to determine the infra-red spectra of the nonvolatile portion of these products by depositing the emulsion on AgCl disks and evaporating the water.

A collection of the spectra of waxes, resins, and ionic emulsifiers common to these polishes will be presented. Examples of the identification of the components of several emulsion polishes will be described. These examples will illustrate the amount of information which may be obtained from the single spectrum of a complete formulation.

The separation and identification of amine emulsifiers from emulsion polishes will be described. Spectra of hydrochloride derivatives of amine emulsifiers will be shown. The separation of shellac from waxes and synthetic resins will be illustrated.

A description of the quantitative determinations possible on these emulsion films will be given.

A high-resolution grating flame spectrometer Raymond W. Tabeling and Richard K. Brehm, Jarrell-Ash Company, Newtonville, Massachusetts

A high-resolution grating flame spectrometer will be described. The increase in sensitivity, precision, and scope of analysis obtainable with this apparatus will be discussed and substantiating data will be presented.

VOL.
8
1956/5

Substituent effects on the near-ultra-violet spectrum of benzene J. A. Petruska, University of Chicago

The influence of inductive substituents on the π-electron spectrum of benzene is discussed theoretically in terms of perturbation theory. It is found that all the interactions among the low-lying singlet states of benzene can be expressed in terms of two parameters which are proportional to the change of coulomb integral at the carbon atom to which the substituent is attached and to the change of resonance integral in the adjacent bonds respectively. Experimental data on the two lowest bands of substituted benzenes are interpreted in the light of these results and formulas are given for predicting the intensity increments and frequency shifts in polysubstituted benzenes in terms of parameters evaluated from data on the monosubstituted derivatives.

Isotope assay by the optical spectrographic method James K. Brody, Argonne National Laboratory, Lemont, Ill.

Isotope assay procedures have been developed for the determination of relative concentration of H^1, H^2, H^3; He^3, He^4; Li^6, Li^7; U^{235}, U^{238}; and Pb^{204}, Pb^{206}, Pb^{207}, Pb^{208}. Photoelectric intensity measurements were accomplished by scanning isotope shifts in the grating spectra of these elements. An alternative procedure using the Fabry-Perot interferometer as the high-resolution instrument was also used. Some problems related to the extension of the method to other elements will be discussed.

Six-year review of X-ray spectrography C. J. Woods, North American Philips Co. Inc., Instruments Division, Mount Vernon, New York

In the field of analytical instrumentation the X-ray spectrograph has in all probability received less attention, but has advanced instrumentation-wise extremely rapidly, over the past six years. This paper will deal primarily with the geometry of the X-ray emission spectrograph with particular emphasis placed on analysing crystals and detectors.

X-ray spectrographic determination of columbium and tantalum in high-nickel alloys C. Manning Davis, International Nickel Co., Research Laboratory, Bayonne, New Jersey

In recent years columbium and tantalum have been found to enhance the properties of high-nickel alloy weld metal compositions. In previous years the total of the two elements have been reported because of the tediousness and lack of precision in the chemical separation of tantalum from columbium.

A procedure has been developed for the X-ray spectrographic determination of both columbium and tantalum following a chemical separation. This technique allows the determination of tantalum down to 0·1% or lower, depending on the initial sample weight. Other techniques for high-temperature alloys will also be discussed.

Determination of strontium by X-ray fluorescence spectrometry Claude A. Lucchesi, Shell Development Co., Houston, Texas

A precise, rapid, and reliable X-ray fluorescence spectrometric method has been developed for the determination of strontium. This method, involving the use of yttrium as an internal standard, is applicable to the analysis of a wide variety of earth substances. Calcium does not interfere. Only 100 mg of sample is required, and a single determination can be made in 30 min. In the analysis of impure anhydrite, the standard deviation of the method is 0·005% strontium over the concentration range, 0·005 to 0·4%.

X-ray absorption analysis Robert E. Ogilvie, Massachusetts Institute of Technology

The two independent techniques of quantitative analysis by X-ray absorption— the X-ray absorption edge method and the linear absorption of a monochromatic X-ray beam—were discussed.

OL.
8
6/57

Analysis of low atomic number elements by X-ray emission spectrography R. G. Edholm, General Electric Company, Milwaukee, Wisc.

The complementary nature of X-ray fluorescence methods and optical emission methods in spectrochemical analysis Dr. M. F. Hasler and Mr. J. W. Kemp, Applied Research Laboratories, Glendale, California

Some recent activities in mass spectrometry at Argonne National Laboratory Charles Stevens, Argonne National Laboratory

The general topic will deal mainly with isotopic analysis in the heavy-element region, using the mass spectrometer, and will include a brief discussion of instruments, methods, and techniques, and applications of analytical procedures to determination of fundamental nuclear constants such as half-lives, cross-sections, etc.

A study of the influence of electrode form on selective volatilization occurring in d.c. arcs I D. O. Landon, Sperry Gyroscope Company

The author feels that a better understanding of electrode behaviour in d.c. arcs can point the way toward means of improving analyses using this type of light source. Three forms of graphite electrodes have been studied in d.c. arc of from 2 to 14 amperes. A much analysed sample of N.B.S. standard nickel oxide, with tungsten added, was used in the experiments, as the behaviour of this material is of considerable interest to many spectrographers. The data presented concerns stability of light output and selective volatilization effect. Burning curves are shown for the various elements for each set of conditions.

The application of spectroscopes in factory and field alloy identification J. E. Scott and D. R. Stoss, General Electric.

The long manufacturing cycle required to build large steam-turbine generators aggravates the task of maintaining the identification of critical high-temperature alloys. To ensure that

critical turbine parts are made from the specified alloys, a system has been set up to perform qualitative elemental determinations on finished turbine parts in the factory. Two types of spectroscopes are used in this system of testing. The Hilger steeloscope is used in testing small parts. Parts of any size can be tested with the Canadian Arsenals direct vision spectroscope modified as a portable, manually supported unit. All of the testing is performed in the factory by factory personnel.

The capabilities and limitations of the spectroscopes are discussed. A programme of training nontechnical factory personnel as spectroscope operators will be presented. The use of a microscope camera as an expedient in this training programme and as a means of providing permanent spectrochemical records in factory and field analyses will be discussed.

Notices of Meetings

Society for Applied Spectroscopy

The Eleventh Annual Meeting will be held on Thursday and Friday November 1 and 2 at the Hotel New Yorker, New York, N.Y. There will also be an exhibition of modern laboratory equipment; and an annual dinner. The main subjects to be discussed will be the spectrochemical analysis of copper and copper-base alloys, infra-red and related techniques, X-ray spectroscopy and the fundamentals of emission sources; and other spectroscopic techniques. For further particulars apply to the Secretary, Society for Applied Spectroscopy, c/o Lucius Pitkin Inc., 47 Fulton St., New York 38, N.Y.

VOL. 8 1956/5

Spectrochimica Acta, 1956, Vol. 8, pp. 201 to 217. Pergamon Press Ltd., London

The spectrographic determination of oxygen in metals—I Plain carbon steels*

VELMER A. FASSEL and RAYMOND W. TABELING†
Institute for Atomic Research and Department of Chemistry
Iowa State College, Ames, Iowa

(*Received* 4 *June* 1956; *accepted for publication* 13 *July* 1956)

Abstract—The presence of oxygen in metals may greatly influence the physical properties of the metal. Although progress has been made in applying chemical methods to the determination of oxygen in metals, the performance of the analysis is a singularly difficult task. The problems encountered in extending conventional spectrographic techniques to this determination are surveyed and techniques for surmounting some of the problems are presented. A d.c. carbon-arc excitation method for the determination of oxygen in plain-carbon steels in the concentration range 20 to 2000 parts per million is discussed in detail. The method is based on the liberation of the oxygen as carbon monoxide into an argon atmosphere which supports a conventional arc discharge between a counter electrode and the sample supported in a carbon electrode. The intensity ratio of the line pair $\frac{\text{O-7771·93}}{\text{A-7891·07}}$ is related to the oxygen concentration in the usual manner. The precision is comparable to results obtained by most vacuum fusion methods, whereas considerably less time is required per determination.

1. Introduction

IN our modern metal industries, emission spectrometric methods of analysis have largely replaced chemical procedures for the quantitative determination of both residual metal impurities and major alloying constituents. In contrast, methods for the determination of the nonmetallic impurity content of metals by emission spectrometric techniques are virtually nonexistent. Although the atomic emission spectra of the nonmetallic constituents are usually excited along with those of the metallic components, the spectra obtained are in general not sufficiently sensitive for analytical purposes, especially when conventional methods of excitation and observation are employed.

In recent years, it has become apparent that small concentrations of oxygen in metals can exert a profound effect on the physical properties of metals. Oxygen occurs in metals primarily as dissolved combined oxides, and in this form it holds the notorious distinction of being very difficult to determine by chemical methods. Among the various methods which have been suggested and used the vacuum fusion technique [1–7] or modifications thereof [8] and the bromination-carbon reduction method [9] have been found most satisfactory. However, the performance of the analysis by any of these techniques remains a singularly difficult

* Abstracted in part from a thesis presented by RAYMOND W. TABELING to the Graduate College of Iowa State College in partial fulfilment of the requirements for the degree of Doctor of Philosophy, December 1955. Contribution No. 462 of the Institute for Atomic Research. This investigation was supported by the Atomic Energy Commission.
Presented in part at the 14 December 1955 meeting of the Milwaukee Society for Applied Spectroscopy and on 1 March 1956 at the Pittsburgh Conference on Analytical Chemistry and Applied Spectroscopy.
† Present address: Jarrell-Ash Company, Newtonville, Mass.

task, and procedural subtleties must be strictly followed in order to obtain accurate results. If the total time required for changing crucibles, for outgassing, and for reducing the operating blank is taken into consideration, an hour or two is usually required per determination.

In principle, the atomic emission spectrum of oxygen is excited together with the spectra of other constituents when samples are subjected to conventional spectrographic excitation techniques. It is therefore appropriate to inquire whether conditions can be established which will make it possible to determine oxygen in metals by emission spectrometric techniques with adequate precision and accuracy.

2. Basic problems involved in the spectrographic determination of oxygen

Several basic problems must be overcome before oxygen can be included among the elements determinable in metals by emission spectrometric techniques. First

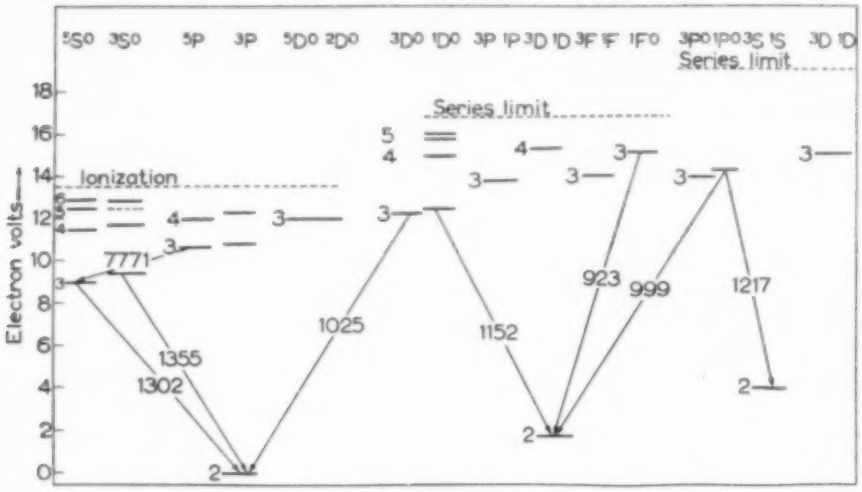

Fig. 1. Energy level diagram of oxygen [10].

and foremost is the exclusion of atmospheric oxygen from the excitation process. This imposes the requirement that the excitation be carried out either *in vacuo* or in oxygen-free atmospheres.

Another basic problem encountered in the spectrographic determination of oxygen is that the resonance and other sensitive lines of oxygen occur in the vacuum ultra-violet (Fig. 1). Although rapid progress is being made in observing spectra in the vacuum ultra-violet, the limitations imposed by optical materials in the 900–1350-Å region compound the difficulties encountered in making quantitative intensity measurements [11]. For conventional spectrographic techniques, the most sensitive atomic lines of oxygen in the photographic region are found in the triplet at 7771 Å. However, these lines are weak in intensity and require relatively high energies (10·7 eV) for excitation. The spectra of various discharges in air (Fig. 2) show that d.c. arc discharges are unable to excite the oxygen triplet

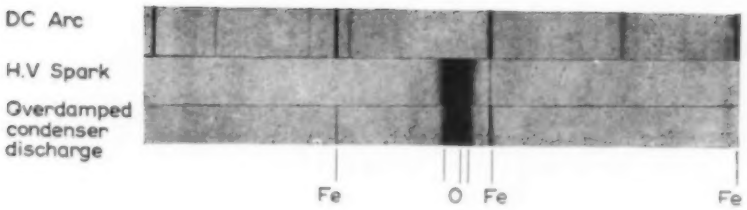

Fig. 2. Spectra of various electrical discharges in air.

OL.
8
6/57

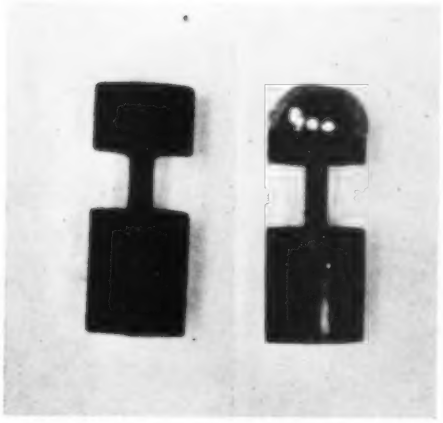

Fig. 6. Photograph of supporting electrodes before and after excitation.

VOL.
8
1956/5

with adequate sensitivity to allow the detection of 25% by weight of oxygen in air. The spectra also show clearly that the higher excitation energies available in high-voltage spark or overdamped-condenser discharges produce strong emission of the 7771-Å lines.

The apparent necessity of employing high-voltage discharges for excitation leads to a third basic problem in determining oxygen in metals. The conventional excitation sources which best provide the higher energies required to excite the oxygen lines at 7771 are able to vaporize only a fraction of a milligram of sample per minute from the surface of metal self-electrodes. Consequently, surface oxide films may contribute to unrealistically high analytical results. Moreover, the combination of small amount of sample vaporized and low-oxygen line intensity leads to poor detection sensitivity.

Because of these obstacles to exciting and observing the optical spectrum of oxygen, the possibilities of determining this element in metals by emission spectrometric methods has virtually gone unexplored. Significant progress has been made only during the time the present investigation was in progress.

STERNER [12] attempted to determine oxygen in steel by exciting self-electrodes *in vacuo* with 100,000-volt a.c. spark discharges, but was not successful. YUDOWITCH [13] explored the possibility of determining oxygen in titanium by arcing self-electrodes in pure argon atmospheres and observing the TiO band spectra, but could not detect oxygen concentrations below 2 to 3%. Oxygen has been successfully determined in steel by ROSEN [14], who used a hollow cathode discharge tube for excitation. ROSEN's technique was basically a modification of the vacuum-fusion method. The sample was placed in a graphite crucible, which served as the cathode of the hollow cathode discharge. The supporting gas for the discharge was argon at a few millimetres pressure. The discharge heated the crucible to a sufficiently high temperature to liberate the oxygen from the sample as carbon monoxide. The intensity ratio of one of the Ångström carbon monoxide band-heads with respect to an argon line was correlated with oxygen concentration. ROSEN's procedure retained many of the disadvantages of the vacuum fusion method, and the time required per analysis was about 1 hour. Since low-pressure fusion was employed, the disadvantages of excessive metal volatilization were retained. Independent analytical curves were necessary for the analysis of each group of samples.

The work of FAL'KOVA [15] in Russia came to the authors' attention after the present investigation was completed. FAL'KOVA reported the successful determination of oxygen in steel by directing single, highly energetic condenser discharges to the metal specimens. The high energy attained in these discharges can be estimated from the fact that the analysis line employed, O II 4641·8, required 39·1 eV for excitation. The intensity ratio of this line with respect to the background was related to the oxygen concentration. FAL'KOVA reported that the precision of the technique was within $\pm 25\%$ of the actual oxygen content. Since FAL'KOVA's technique predominantly sampled the surface of the specimen, oxide films or surface inhomogeneities could contribute serious errors to the determination.

No attempt apparently has been made to utilize the emission spectrum of

neutral oxygen nor has any effort been made to excite the oxygen emission spectrum by conventional arc or spark discharges operating in rare gas or other oxygen-free atmospheres. It seemed appropriate therefore, to conduct a systematic exploration of these approaches.

3. Experimental equipment

Gas purification system

A gas purification train (Fig. 3) is necessary for the removal of oxygen and oxygen-containing compounds from the gases before they are admitted into the excitation chamber. The gas from the cylinder (No. 1) enters the system through

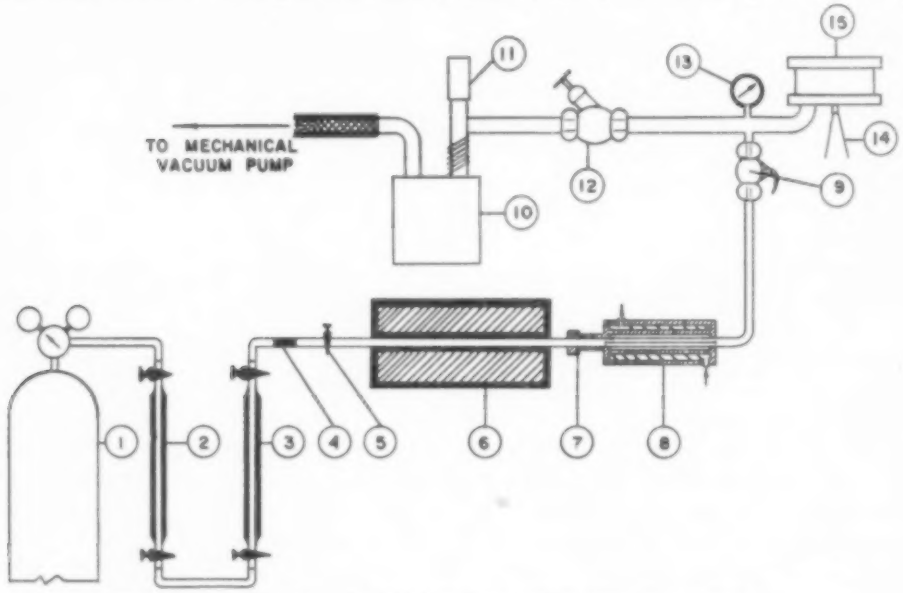

Fig. 3. Schematic diagram of high-vacuum and gas-purification system.

absorption tubes (Nos. 2 and 3), containing, respectively, sodium hydroxide on asbestos (Ascarite) for the removal of carbon dioxide and magnesium perchlorate (Anhydrone) for the removal of water vapour. A 0·2-mm capillary (No. 4) is used to limit the flow rate of the gas through the purification system. A silica combustion tube (No. 6) packed with uranium turnings and heated to 600°C by a 46 × 2·86 cm split-tube furnace (Hevi-Duty Electric Co., Type 70-S) is used to remove any molecular oxygen present [8, 16]. A high-vacuum stopcock (No. 5) permits vacuum outgassing of the uranium tube after recharging. A water-jacketed cooling chamber (No. 8) is joined to the system by a metal-to-glass coupler (No. 7) (Central Scientific Co., Cat. No. 94230). This cooling chamber permits rapid cooling of the gas prior to entry into the excitation chamber and thereby facilitates accurate pressure measurements. The cooling chamber consists of seven copper tubes (1·6-mm diameter and 15 cm long) for conducting the gas through a circulating water-bath. The gas enters the excitation chamber through a 3·18-mm toggle

VOL.
8
1956/5

vacuum valve (No. 9) (Hoke, Inc., No. 450). The flow rate of the gas through the purification system is adjusted to about 2 litres/minute by the pressure regulator on the gas cylinder.

High-vacuum system

A conventional high-vacuum system is employed for outgassing of the excitation chamber prior to the admission of the supporting atmospheres for the excitation. This system consists of an oil-diffusion pump (No. 10) (Consolidated Vacuum

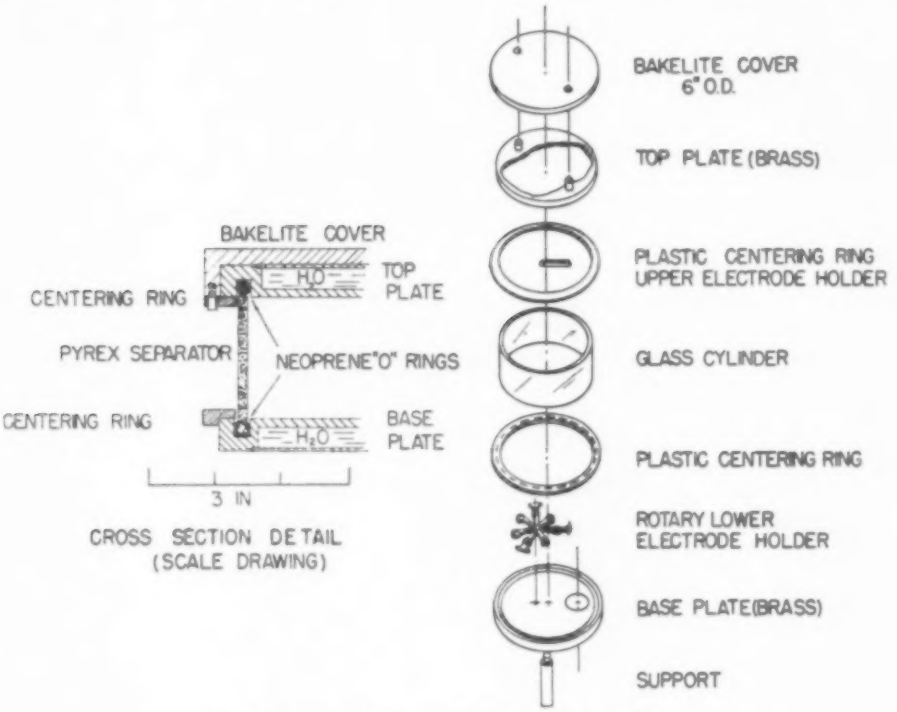

Fig. 4. Schematic diagram of excitation chamber.

Corp., VMV 20–01), a liquid nitrogen trap (No. 11) constructed of stainless steel and attached directly to the diffusion pump stack, and a 1-in. vacuum valve (No. 12) (Distillation Products, Inc., No. Kv–1). A mechanical vacuum pump (Welch No. 1305H) is used as the forepump in series with the oil-diffusion pump. The connecting tubing in the vacuum system is fabricated from 2·54-cm seamless stainless-steel pipe. A Phillips gauge (Distillation Products, Inc., Model PHGOI), mounted between the excitation chamber and vacuum valve (No. 12) is used to monitor the outgassing of the system.

Excitation chamber

An exploded view of the vacuum-tight excitation chamber (No. 15) is shown in Fig. 4. The chamber consists essentially of two brass plates, 15·24 cm outer

diameter and 1·27 cm thick, which are separated by a glass cylinder. A groove of suitable dimensions to accept a 12·1 × 0·635-cm synthetic rubber (Neoprene) "O" ring is machined into one side of each of the plates. Watertight compartments are machined into the outer side of each plate to provide cooling. The lower plate of the chamber is secured to the optical bench and the vacuum connection is made to this plate. A 2-in. borosilicate glass (Pyrex) cylinder, 12·7-cm inner diameter, placed between the plates, serves as electrical insulator and optical window. Vacuum grease is not used in the "O" ring seals because of the high temperatures generated by the electrical discharges. For excitations conducted in supporting atmospheres, the tightness of the chamber is assured by applying pressure to the synthetic-resin (Bakelite) insulating cover of the top plate and the bottom plates with three 5-in. "C" clamps placed symmetrically around the chamber. A Bourdon-dial vacuum gauge calibrated for 30 in. of mercury (No. 13, Fig. 3) is used to measure the pressure of gases introduced into the chamber. A spring-clip electrode holder is fastened to the upper plate to support a stationary-counter electrode. A stainless steel electrode holder accommodating seven electrodes is attached to the bottom plate with a pin. This holder can be rotated from outside the chamber by means of a small permanent magnet. This makes it possible to bring successive sample electrodes into the optic axis without opening the chamber.

All of the excitations reported in this paper have been conducted in static gas systems, i.e. a measured amount of gas admitted into the chamber constitutes the atmosphere for a single excitation.

VOL. 8 1956/5

Spectrographic facilities

The spectrograph employed in this study is described in Table 4. The spectrograph illuminating system is similar to the arrangement shown by FELDMAN and ELLENBURG [17], except that the central 60% of the arc image passes through the aperture of the diaphragm.

Table 1. Oxygen in steel standards

Standard	Oxygen content (%)
No. 1	0·018
No. 4	0·002
No. 6	0·007
No. 7	0·106

Standard samples

Steel samples of known oxygen content were obtained from the National Bureau of Standards. These standards were prepared by the Bureau and were analysed by several different methods in thirty-five different laboratories [5]. The "best" values reported for these standards are presented in Table 1.

4. Preliminary investigations

High-voltage a.c. spark excitation

The oxygen content of the 0·106% standard could not be detected when the steel standards were excited by conventional high-voltage a.c. spark discharges. It is well known that these discharges volatilize only a small amount of sample in air atmospheres, but in the rare gases and hydrogen the volatilization is still less by a factor of 3, as shown in Table 2. These data were obtained using the

Table 2. Sample vaporization by high frequency spark discharge

Atmosphere	Sample vaporized/minute (mg)
H_2	0·3
He	0·3
A	0·4
O_2	1·9
N_2	1·8
Air	1·8

following parameters on the National Spectrographic Laboratories Model 22 "Spec power" source: Secondary peak voltage = 30,000 volts, $C = 0{\cdot}015\ \mu F$, $L = 0$ (residual) μH, R = 0 (residual) ohms, breaks per half-cycle = 4

Unidirectional discharge excitation in oxygen-free atmospheres

It has been shown [18] that the volatilization of metal from the surface of electrodes in a high-voltage a.c. spark discharges occur primarily when the electrode is the cathode, presumably through an ion bombardment or "sputtering" mechanism. This suggests that high-power, unidirectional discharges directed towards metal samples as cathodes should provide increased metal volatilization. The data summarized in Table 3 show that this is indeed so. These data were obtained for 960-volt overdamped-condenser discharges obtained from the Applied Research Laboratories Multisource, Model No. 22 [19] with the following parameters: C = 60 μF, $L = 400\ \mu H$, $R = 5$ ohms, time = 2 min.

Table 3. Amount of sample volatilized from anode and cathode by unidirectional overdamped-condenser discharge

Atmosphere	Weight change mg/min	
	Anode	Cathode
A	0·0	−12·7
H_2	0·0	−14·2
N_2	•	− 0·6
Air	+2·9	− 4·0

• Not measured

It is seen that in argon, for example, the amount of sample volatilized has increased by a factor of about 30. The high volatilization efficiency in hydrogen atmosphere is suggestive of a chemical reaction, but this has not been proven experimentally. The spectra of the steel standards excited in both argon and hydrogen atmospheres showed detectable oxygen down to approximately 0·05%, but the same oxygen concentration in zirconium or titanium metal could not be detected. These excitation conditions do not appear to be generally useful, although they may find application when relatively high concentrations (>0·1%) are to be determined.

D.c. arc excitation in rare-gas atmospheres

The experimental observation that the oxygen triplet at 7771 could not be detected in spectrograms of d.c. carbon-arc discharges in air (which contains 25% by weight of oxygen) at first glance would tend to discourage further exploration of d.c. arc excitation methods. However, it should be recognized that a d.c. carbon arc in rare-gas atmospheres presents drastically different excitation conditions than a d.c. carbon arc in air. A d.c. carbon-arc discharge in air contains relatively high concentrations of molecular species such as N_2, O_2, CN, NO, CO, etc. The electronic excited states and dissociation energies of most of these species lie well below the energy required to excite the emission of the 7771 group of oxygen lines. When these species are absent, as for example in a d.c. carbon arc in helium the mean energy and energy distribution of the electrons would be expected to shift to a considerably higher value. These higher energies have in fact been observed by others [20–22] either directly or indirectly, and experimental data obtained by us confirm these observations. In spectrograms of d.c. carbon arcs in helium containing only a few parts per million of oxygen, the 7771 triplet is readily detectable, whereas 25% could not be detected in air atmospheres. When steel electrodes are used for d.c. arc discharges in helium, neither the residual oxygen content of the helium nor the oxygen contributed by the electrodes is detectable. Apparently the flooding of the analytical gap with iron atoms, which have ionization potentials of 7·9 eV and multitudinous excited states below this value, causes a marked shift of electron energies to lower values, analogous to the situation of a d.c. carbon arc in air. It is thus apparent that if oxygen is to be determined by d.c. arc excitation it is necessary to volatilize the more refractory oxide components of a metal sample without causing appreciable volatilization of the metal itself. To accomplish this, the basic technique used by the vacuum fusion method may be turned to good advantage. When a steel specimen is placed in the cavity of a carbon electrode serving as the anode of the d.c. arc discharge, the sample attains a temperature sufficiently high to cause melting of the specimen. The high solubility of carbon in steels at the prevailing electrode temperatures brings the carbon into intimate contact with the metal oxides and effects the chemical reduction of these oxides to gaseous carbon monoxide. The latter is readily dissociated in the arc column and the atomic emission spectrum of oxygen is then excited. Simultaneously, a saturated solution of carbon in steel is formed which reduces the volatility of the iron. In essence, the oxygen is extracted from the metal while at the same time the volatility of the metallic constituents is reduced.

VOL. 8 1956/5

A factorial study on the optimum experimental conditions for carrying out this reduction led to the electrode design shown in Fig. 5. The constricted neck of the electrode provides thermal isolation of the receptacle portion so that higher cavity temperatures are more readily obtained. The wall-thickness of the cavity is adjusted so that it is completely dissolved when 1-gram specimens of steel are

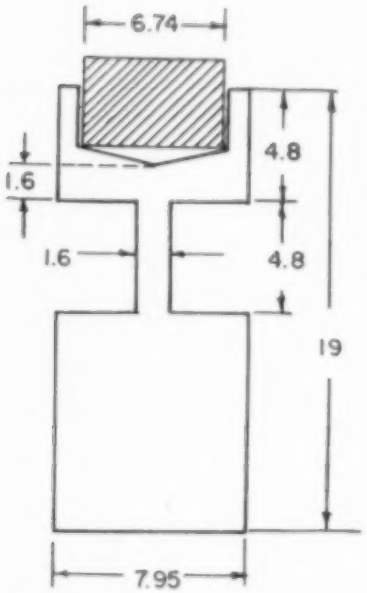

Fig. 5. Supporting electrode (anode)—dimensions are in millimetres.

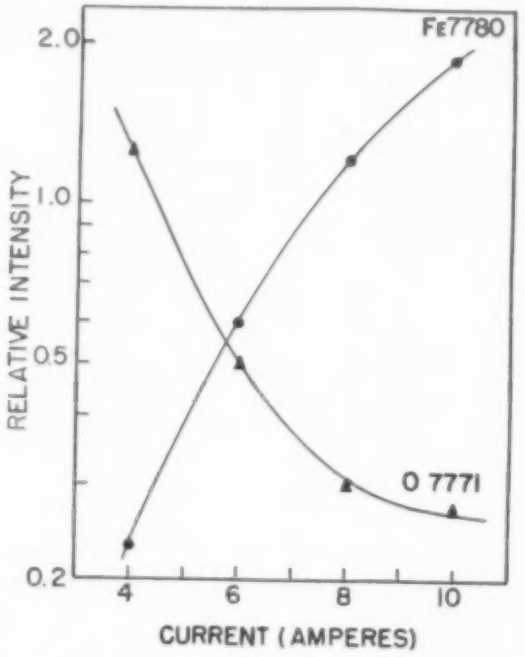

Fig. 7. Inverse relationship between oxygen and iron spectral-line intensities.

arced at currents greater than 8 amperes. The arc then strikes directly to the molten globule which sits in almost idealized fashion on the flat platform. Photographs of an empty electrode and an electrode after excitation are shown in Fig. 6. Standard samples, excited at currents large enough to cause melting (>8 amperes), showed vigorous evolution* of gases during the first 30 sec of arcing, with a rapid decrease in rate of evolution for the next 30 sec. This observation, plus others to be discussed later, suggested that complete reduction takes place in about 1 min.

Although exceptionally high sensitivity of detection could be obtained, neither oxygen-line intensities nor oxygen/iron-line intensity ratios showed any quantitativeness. Visual examination of the spectrograms consistently showed an inverse relationship between oxygen- and iron-line intensities. This dependency is quantitatively illustrated in Fig. 7. Although the iron lines showed the expected increase in intensity as arcing current increased, the oxygen intensities showed a continuous decrease. This anomalous behaviour of oxygen-line intensities again suggested

* Assuming a temperature of 1800°, atmospheric pressure, and that ideal gas laws apply, 0·1% oxygen evolved as CO occupies a volume of approximately 10 ml.

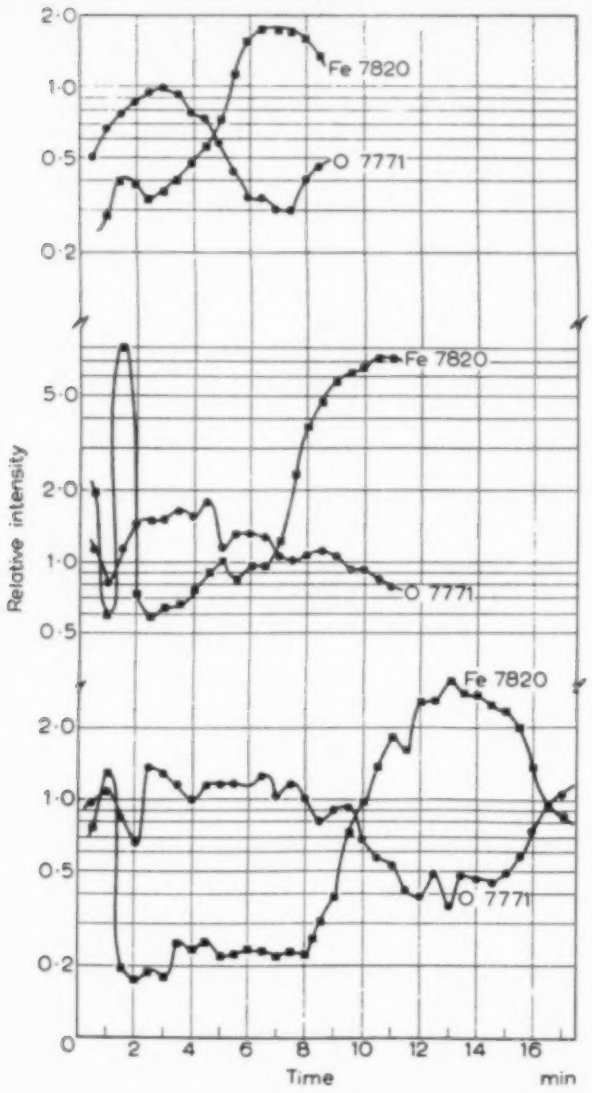

Fig. 8. Variation of relative intensities of spectral lines during excitation.

that the greater concentrations of iron atoms in the arc column at higher currents caused marked shifts in the electron energy distribution to lower values. It was also conceivable that the iron was recombining or "gettering" part of the evolved CO, thus permanently removing an increasing amount from the atmosphere as the current was increased. The role played by each of these processes could be deduced by observing the behaviour of oxygen- and iron-line intensities as a function of time. The results from three of these moving plate studies are plotted

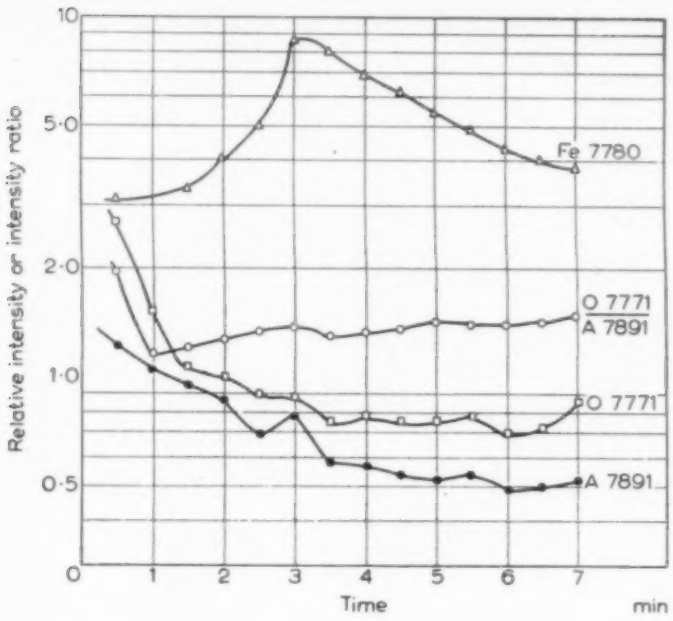

(a)

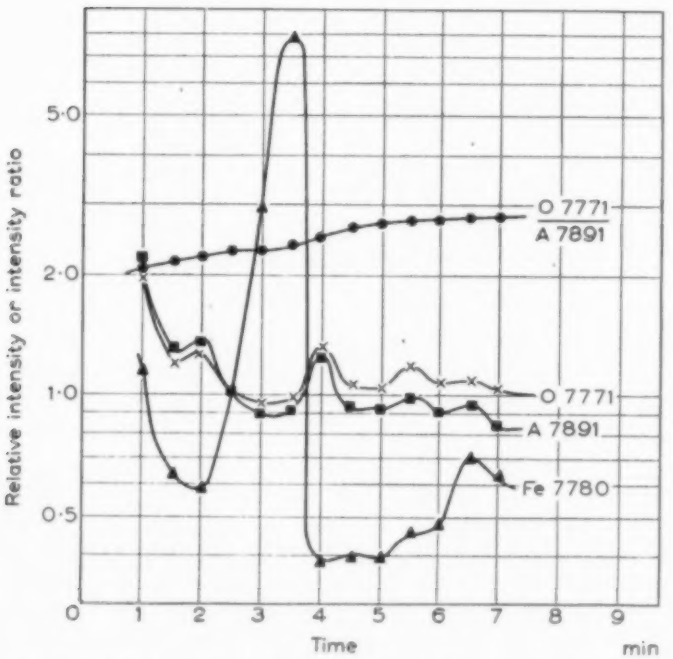

(b)

Fig. 9a and 9b. Variation of oxygen, argon, and iron spectral-line intensities during excitation (typical behaviour).

in Fig. 8. All three of the plots suggest that the oxygen suppression occurs in the excitation process rather than from gettering. The third run, covering a time period of 17 min, shows conclusively that gettering is playing a negligible role. If gettering had occurred, the oxygen-line intensity should have experienced a gradual decrease, but even after 17 min of arcing the oxygen-line intensity returned to its original general level, indicating that there was no depletion of the carbon-monoxide concentration in the atmosphere. The general reduction in oxygen-line intensities during periods of greater iron volatilization provided confirming evidence that the oxygen intensity suppression arose from lowering of the effective excitation temperature of the arc by the iron atoms.

This suppression effect is analogous to one of the manifestations of the extraneous element influence commonly observed when samples of diverse composition are excited under conventional excitation procedures. One approach for overcoming this effect is to control the iron volatilization during the course of the excitation, but this is unattractive from an experimental standpoint. In principle, the judicious application of the internal-standard principle should make it possible to provide internal compensation for this effect. In order to employ this principle to best advantage, the atmosphere of the chamber should contain a gas which possesses the following characteristics: (a) it should have excited states approximately 11 eV above the ground state, and (b) the spectral lines originating from these states should fall in the 7700-Å region. If these conditions are fulfilled, the intensities of the oxygen and selected internal standard lines should change in consort as the concentration of iron atoms in the arc column changes during the excitation. The intensity ratio of the oxygen/internal standard line pair should then be independent of the iron volatilization.

Helium does not qualify as an internal standard, because its lowest excited state is 20 eV above the ground state. Argon, however, satisfies both requirements. Rather than add a specified amount of argon to a helium atmosphere, it is more convenient to employ a pure argon atmosphere. The temperature attained by the anode in a d.c. arc in argon is considerably lower [23] than in an arc operated at the same current in a helium atmosphere. To attain a temperature of approximately 1500–1600°C for the molten globule, an arcing current of 20 amperes is required.

Fig. 9 (*a* and *b*) shows some typical moving-plate observations of intensities and intensity ratios when steel samples are arced in argon. It is seen that argon achieves an exceptionally high degree of internal standardization. The parallel behaviour of the selected oxygen/argon lines, after the initial minute of arcing, produces intensity ratios which are virtually constant with time—a condition seldom achieved in analytical emission spectroscopy. However, attention should be called to the slight but consistent increase of the oxygen/argon intensity ratio with time. If this observation is combined with other experimental data, important conclusions can be drawn regarding the evolution of carbon monoxide from the sample. Visual observation of the molten globule during arcing indicates that gas evolution is negligible after the initial 30 sec. Quantitative verification of these visual observations was obtained by arcing the standards for 1 min at 20 amperes, evacuating the gas evolved, refilling with pure argon, and then re-arcing the sample

VOL. 8 1956/5

for 3 min. Within experimental error, spectrograms of the second excitation showed oxygen contents no greater than those obtained for sample-free graphite electrodes arced under the same conditions. The slight increase of oxygen/argon intensity ratios therefore does not appear to be caused by the more complete extraction of oxygen from the sample. Rather, the liberation of oxygen or oxygen-containing compounds from the walls of the excitation chamber by the prolonged heating of the arc discharge appears to be a more logical explanation. The fact that the intensity ratio shows no decrease with time is further verification that gettering of carbon monoxide by the volatilized iron is negligible.

5. Quantitative calibrations

Source of oxygen contamination-"blank"

The actual determination of oxygen by this technique is subject to serious sources of oxygen contamination unless proper precautions are taken. The oxygen content of the graphite-supporting electrodes is reduced by outgassing them in quantity at 1000°C for 4 hours under a vacuum of 1×10^{-6} mm Hg. The blank contributed by surface oxidation of the metal specimens is difficult to evaluate, but appears to be negligible, according to data obtained by others employing vacuum-fusion techniques [6, 7]. The largest source of oxygen contamination is the liberation of oxygen or oxygen-containing compounds from the walls of the excitation chamber by the heating produced by the arc discharge. This contamination is hereafter called the chamber blank. Standard outgassing techniques, i.e. subjecting the excitation chamber to high temperatures while evacuating, could not be employed directly with the chamber employed in this investigation. However, satisfactory outgassing was achieved by arcing an auxiliary pair of graphite electrodes at 35 amperes for about 3 min at reduced pressure (approximately 100 mm Hg) without watercooling the chamber. After termination of the arcing cycle, the chamber was evacuated as quickly as possible. The chamber was then refilled with argon and the operation repeated two more times. These outgassing arcings reduced the chamber blank to a value equivalent to about thirty parts per million of oxygen in 1-gram steel samples. The chamber blank could be consistently reduced to this level if certain other precautions were observed. When not in use, the chamber was either filled with argon or evacuated. Since smaller amounts of gases are absorbed on hot surfaces, a 35-ampere arc discharge was operated, without watercooling, to heat the chamber walls before opening the chamber to the atmosphere.

The normal operating procedure for exciting samples was to load the rotary electrode holder with six sample electrodes plus an auxiliary graphite electrode for the outgassing excitations. The auxiliary electrode was then arced three times in succession as described above, after which the samples were excited in succession with intervening evacuation of the chamber and refilling with pure argon. The chamber was not opened between the series of outgassing arcings or the six successive sample excitations. Watercooling of the chamber was provided during the sample excitations to retain the chamber blank at the low value. To monitor the magnitude of the blank, spectrograms of 2-min, 20-ampere d.c. arc discharges between the

outgassing electrodes were photographed just prior to and immediately following the sample excitations.

A single counter electrode (cathode) served for the series of outgassing, blank, and sample exposures, since negligible consumption of this electrode occurs in arcs in argon. The light transmission of the glass separator gradually decreased during a series of exposures because of deposition of metal and carbon vapour. The slight decrease of overall spectral intensity during a series of exposures was accommodated by exposing four-step sectored spectrograms.

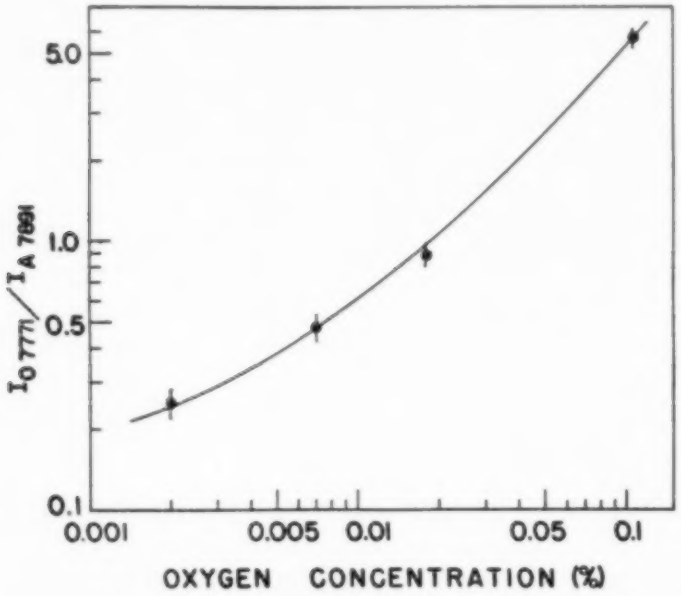

Fig. 10. Analytical curve for the determination of oxygen in steel.

In order to reproduce the number of moles of argon admitted into the chamber prior to each sample excitation, the pressure, volume, and temperature factors were reproduced from exposure to exposure. The temperature of the argon gas admitted to the chamber was kept within narrow limits by watercooling both the gas after it left the purification system and the chamber itself. Temperature fluctuations of $\pm 3°$ were permissible, since this introduced an error of only 1% in the quantity of argon admitted into the chamber. Pressure measurements were made to within $\pm 1\%$ with a Bourdon-type gauge. The nominal pressure of argon admitted to the chamber was 640 mm; the temperature-increase during excitation brought the total pressure up to near atmospheric pressure.

The National Bureau of Standard samples were prepared for excitation by sawing strips approximately $0{\cdot}4 \times 0{\cdot}4 \times 5$ cm from each of the standards. Approximately 1-gram specimens were then cut from these strips, and cleaned with a small file until smooth and bright. Any grease was removed with carbon tetrachloride. The samples were accurately weighed and stored in a vacuum.

VOL. 8 1956/5

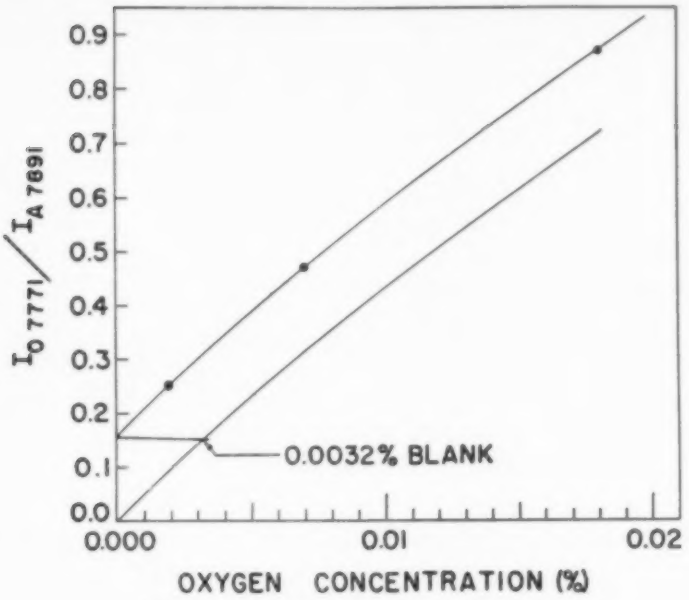

Fig. 11. Graphical determination of blank correction.

Table 4. Experimental conditions for the determination of oxygen in steel

Spectrograph	Jarrell-Ash Co., 3·4-metre plane-grating spectrograph, Ebert mounting, using a 6-in, 15,000 grooves per inch grating blazed for approximately 12,000 Å first order [24].
Line pair	$\frac{\text{O-7771·928 Å}}{\text{A-7891·075 Å}}$
Weight of sample	Approximately 1 g. (The measured oxygen concentration may be corrected to a 1·000-g sample by dividing the measured intensity ratio by the actual sample weight.)
Type of electrodes	United Carbon Co. Grade U-2.
Anode	Undercut 7·95-mm-diameter graphite, as shown in Fig. 5.
Cathode	3·18-mm diameter, graphite 2·5 cm long with a 120° point.
Argon pressure	640 mm reproduced to ±1%.
Excitation source	250 volts d.c., 20 amperes, from National Spectrographic Laboratories "Spec Power" source, Model 22.
Length of exposure	1-min prearc plus 2-min exposure.
Analytical gap	6 mm.
Emulsion	Eastman 1-N.
Wavelength photographed	7100–8400-Å, first order
Filter	Corning 2–63
Slit	0·05 mm.
Development	4 min at 21°C in Eastman Kodak D-19 with continuous agitation in an Applied Research Laboratories developing machine [25].
Emulsion calibration	Two-step sector, preliminary curve method.
Microphotometer	Jarrell-Ash Co., Console Microphotometer, Model JA-2100.

Sextuplicate runs of the standard samples were exposed under the conditions summarized in Table 1. Since the preliminary experiments discussed above showed that all of the oxygen was liberated in about 1 min, a prearc of this time-period was selected. Vigorous bubbling frequently occurred during the initial arcing cycle which caused the incandescent molten mass to expand into the optical viewing field of the spectrograph. Since the shutter was closed during this period, continuous background from this source was eliminated. Photography, microphotometry, and intensity-ratio computation followed standard practices [25]. Background corrections were made.

The analytical curve obtained from the National Bureau of Standard samples is shown in Fig. 10. The vertical lines show the spread of values obtained from sextuplicate runs. The asymptotic curvature at the lower concentration is a manifestation of the total blank. This blank can be evaluated by plotting the data on co-ordinate paper [27] and noting the lateral displacement of the experimental curve from a parallel curve drawn through the origin (Fig. 11). The measured value of the blank is about 32 p.p.m.

6. Discussion

The precision of measuring oxygen in metals with this technique is comparable to the values obtained by most vacuum-fusion methods. At higher oxygen concentrations (0·01 to 0·1%) the standard deviation is about ± 5 to 6% whereas at lower concentrations (0·002 to 0·05%) this value increases to about ± 10 to 12%. The loss in precision at the lower concentration may be attributed primarily to fluctuation in the inherited blank, which becomes increasingly significant as the oxygen content in the sample decreases.

The time required for analysis by the spectrographic method is much less than for vacuum fusion techniques. About 35 min are required to obtain single exposures of six samples, and approximately another half-hour is required for plate measurements. It should thus be possible to perform about thirty-five determinations per day. If excitation chambers are specifically designed for large-scale operations and if spectral intensities are measured photoelectrically, the number of samples which can be analysed per day could be increased to about eighty.

The standard samples used in this investigation were all plain carbon steels. Whether the technique can be applied directly to high-alloy steels has not been conclusively demonstrated. The ease with which oxides of alloying constituents are reduced varies considerably [6], hence longer arcing times and higher electrode temperatures may be required.

The experimental evidence so far obtained indicates that all of the occluded and dissolved elemental oxygen is liberated and the combined oxygen evolved as gaseous carbon monoxide in about 1 min. This leads to the conclusion that the amount of carbon monoxide in the molten metal globule in equilibrium with the carbon monoxide in the excitation chamber is negligible. In vacuum-fusion techniques, evolution of gases appears to continue for periods from ten to fifteen times longer, even though the gases are evolved into a vacuum and extracted by diffusion pumps. The greater rate of reaction and gas evolution in the spectrographic method may be caused by the high temperatures in the vicinity of the anode

VOL. 8 1956/5

spot, and the resulting convection stirring arising from the large temperature gradients. Although the temperature of the globule varies from 1700°C near the anode spot to about 1500°C at the graphite platform, the temperature of the anode spot itself has been reported to be equal to the boiling-point of the anode material [28]. Thus, the anode-spot temperature is greater than 3000°C—the boiling-point of pure iron.

7. Extension to other metals and organic compounds

The possibility of determining oxygen in such metals as titanium, zirconium, and rare earths has been under study, and preliminary data indicate that it should be possible to extend this basic method to most metals, especially if metal "bath" techniques are used. Preliminary experiments on the determination of oxygen content of solid organic compounds also show promise. Detailed results of these investigations will be reported at a later data.

Acknowledgements—The authors are grateful to R. KNISELEY, H. HETTEL, and W. GORDON for helpful discussions during the course of this investigation.

References

[1] JORDAN L. and ECKMAN J. R.; *Sci. Papers Nat. Bur. Standards* 1925 **20** 445; *Ind. Eng. Chem.* 1926 **18** 279.
[2] HESSENBRUCH W. and OBERHOFFER P.; *Arch. Eisenhuttenw.* 1927 **1** 583; *Stahl U. Eisen.* 1928 **48** 486.
[3] VON SETH R.; *Jernkont. Ann.* 1928 **83** 113.
[4] HESSENBRUCH W.; *Zeits. f. Metallkunde* 1929 **21** 46.
[5] THOMPSON J. G., VACHER H. C., and BRIGHT H. A.; *J. Res. Nat. Bur. Standards* 1937 **18** 259.
[6] SLOMAN H. A.; *J. Inst. Metals* 1945 **71** 391.
[7] SLOMAN H. A.; and HARVEY C. A. *J. Inst. Metals* 1952 **80** 1360.
[8] SMILEY W. G.; *Analyt. Chem.* 1955 **27** 1098.
[9] CODELL M. and NORWITZ G.; *Analyt. Chem.* 1955 **27** 1083.
[10] MOORE C. E.; *Atomic Energy Levels* Vol. I., National Bureau of Standards Circular 465. 1949; *An Ultraviolet Multiplet Table* National Bureau of Standards Circular 488, Section 1. 1950;
[11] INN E. C. Y.; *Spectrochim. Acta* 1955 **7** 65.
[12] STERNER J.; *First Progress Report on Spectrographic Gas Analysis* Watertown Arsenal, WAL-122/21 (August 1939).
[13] YUDOWTIHC K. K.; Armour Research Foundation Report No. NP-4486 (July 1952).
[14] ROSEN B.; *Rev. Univ. Mines* 1953 **9** 445.
[15] FAL'KOVA O. B.; *Izvt. Akad. Nauk. SSSR. Ser. Fiz.* 1955 **19** 14.
[16] GIBBS D. S., SVEC H. J., and HARRINGTON R. E.; *Ind. Eng. Chem.* 1956 **48** 289.
[17] FELDMAN C. and ELLENBURG J. Y.; *Spectrochim. Acta* 1956 **7** 349.
[18] KAISER H. and WALLRAFF A.; *Ann. Physik.* 1939 **34** 297.
[19] HASLER M. F. and DIETERT H. W.; *J. Opt. Soc. Amer.* 1943 **33** 218.
[20] VALLEE B. L. and ADELSTEIN S. J.; *J. Opt. Soc. Amer.* 1952 **42** 295.
[21] BAKER M. R., ADELSTEIN S. J., and VALLEE B. L.; *J. Opt. Soc. Amer.* 1956 **46** 138.
[22] VON ENGEL A.; *Ionized Gases* Ch. 8 and 9. Oxford University Press, London, 1955.
[23] VALLEE B. L. and BAKER M. R.; *J. Opt. Soc. Amer.* 1956 **46** 77.
[24] JARRELL R. F.; *J. Opt. Soc. Amer.* 1955 **45** 259.
[25] SCHUCH J.; *J. Opt. Soc. Amer.* 1942 **32** 116.
[26] CHURCHILL J. R.; *Ind. Eng. Chem., Analyt. Ed.* 1944 **16** 653.
[27] HURWITZ J. H.; *Analyt. Chem.* 1953 **25** 1028.
[28] LOEB L. B.; *Fundamental Processes of Electrical Discharge in Gases* page 616, John Wiley and Sons, Inc., New York, 1939.

Spectrochimica Acta, 1956, Vol. 8, pp. 218 to 228. Pergamon Press Ltd., London

An infra-red spectroscopic investigation of steric hindrance in some *trans*-stilbene derivatives

S. F. D. Orr
The Chester Beatty Research Institute, The Institute of Cancer Research: Royal Cancer Hospital, Fulham Road, London S.W.3.

(*Received* 12 *July* 1956)

Abstract—Seventeen *trans*-stilbenes, of which some are expected to be planar and others to be buckled because of the size of their *ortho*-substituents, have been examined. All absorb strongly at about 960 cm^{-1} due to the out-of-plane in-phase vibration of the olefinic hydrogen atoms. It has been found that, as the expected steric hindrance increases, the width of this band greatly increases, up to threefold, although there is no significant change in intensity and only a slight increase in frequency. The increase in band width has been explained as being due to a transfer of energy from the vibration of the olefinic hydrogen atoms to a motion involving the group in the *ortho*-position, probably a partial rotation of the aromatic ring containing the hindering *ortho*-group about the bond to the olefinic bridge. The original vibration has been characterized by its lifetime, which can be derived from the increase in band width.

Introduction

The examination of a series of derivatives of 4-aminostilbene has shown a relationship between their growth-inhibitory effects and chemical constitution [1]. One of the features required for activity appears to be an unbroken conjugation of the amino group with both benzene nuclei, and this is only possible when a coplanar arrangement of the two nuclei obtains. A consideration of atomic models and plane diagrams suggests that steric hindrance to a planar configuration may occur in certain cases. In *trans*-stilbene derivatives, rotation of the benzene rings to give the planar arrangement brings the atoms or groups on the *ortho*-positions of the rings closest to those on the olefinic bridge. When these are all hydrogen atoms, the separation between any pair exceeds the sum of the van der Waals radii and weak attractive forces operate, but with sufficiently large substituents this is no longer the case, and strong repulsive forces are brought into play. These forces increase very rapidly with the degree of interpenetration [2], so that the molecule has its stable configuration of minimum energy when nonplanar, for the consequent reduction in interpenetration energy exceeds the increase in bonding energy due to reduced conjugation.

These expectations have been confirmed by examination of the ultra-violet absorption spectra, which show the effects to be expected for enforced nonplanarity in compounds of this type, *viz.* a shift of absorption to higher frequencies [1] and a lowered absorption intensity [3]. It has been found that any substitution on the olefinic bridge produces considerable steric hindrance, and that the effect of substitution at the *ortho*-positions is very dependent on the size and number of substituents.

A preliminary survey of the infra-red spectra of a number of substituted stilbenes has already been carried out [4], in an attempt to obtain further

information on the degree of steric hindrance in the *ortho*-substituted compounds. The stilbenes examined, being unsubstituted on the olefinic bridge, absorb strongly at about 960 cm^{-1} like all *trans*-disubstituted ethylenes, and there is some indication that the frequency of the absorption band is raised slightly in compounds which are expected to be sterically hindered. This band has been shown [5] to be due to a mode in which the vibrations are almost completely localized in the motion of the two olefinic hydrogen atoms in phase and out of the plane containing them and the CC double bond. As it is the interaction between one or both of these atoms and large *ortho*-substituents which leads to nonplanarity, a band arising from their vibration might be expected to be affected. This investigation describes measurements on the frequency, intensity and width of this band, carried out in dilute solutions.

Theoretical considerations

1. *Frequency.* The actual frequency of the band at 960 cm^{-1} in *trans*-disubstituted ethylenes has been shown [5, 6] to be determined almost entirely by the out-of-plane bending force constant of the CH link, and dependent on the rest of the molecule only as its electronic structure affects this constant. An increase in electronegativity in the substituents leads to a decrease in the force constant and hence to a decrease in frequency. Conjugation with the unsaturated phenyl groups in *trans*-stilbene might also be expected to affect the frequency, so that any decrease in conjugation resulting from steric hindrance to a planar configuration should be apparent as a decrease of such an effect. Now *trans*-stilbene itself absorbs at 959 cm^{-1} in carbon disulphide; Δ^{22} steroids, for which figures are available [7] in the same solvent, absorb at 970–974 cm^{-1}. Conjugation of the olefinic bond with the two phenyl groups thus leads to a reduction in frequency of 10–15 cm^{-1}, so that the maximum effect of steric hindrance can only be the reversal of this small effect.

2. *Intensity.* The intensity of absorption due to any vibrational mode is proportional to the square of the rate of change of dipole moment associated with that vibration. For a deformational mode, calculations of the latter quantity can readily be made [8, 9]. In the present case, assuming the vibration to be completely localized in the hydrogen atoms, it can be shown that the intensity of absorption will be proportional to the square of the CH bond moment and the frequency of absorption, and inversely proportional to the square of the CH bond length. In the same manner in which it has been shown that reduction of conjugation caused by steric hindrance can result in only a small frequency shift, it can be concluded that the CH bond moment and length will be but little affected, so that the intensity of absorption of this band at 960 cm^{-1} should show only a small variation.

3. *Band Width.* It has been explained above that the steric hindrance to a planar structure arising from the presence of a large *ortho*-substituent is due to the strong repulsion which would exist in the planar configuration between that substituent and the olefinic hydrogen atom to which it approaches so closely in space. In the resulting nonplanar structure, there is little or no force of repulsion between the interfering groups because of their increased separation. This separation, however, will vary during the out-of-plane vibration of the hindered

olefinic hydrogen atoms. The resultant increase of repulsion as the separation decreases will far exceed the opposite effect in the other direction [cf. 2], so that there will be a net increase of repulsion. If the *ortho*-group were completely rigid, the effect would simply be to make the amplitude of vibration of the hydrogen atom asymmetric with respect to the equilibrium position, as in any stretching vibration, with possibly a small frequency shift. However, a motion of the *ortho*-group is possible, and the repulsive force can cause either a bending of the group itself out of the plane of the aromatic ring or a partial rotation of the whole ring. The energy of this motion can only be obtained from the energy of vibration of the hydrogen atom, but there are two ways of envisaging this process of energy transfer. In one case, a part of the vibrational energy of the hydrogen atom is presumed to be transferred at each vibration, so that the energy and amplitude are progressively reduced, that is, the vibration is damped by the presence of the blocking group. In the other case, it is supposed that there is a definite probability of transition from the state in which the hydrogen atoms are vibrationally excited to that in which the *ortho*-group(s) is (are) involved, so that steric hindrance reduces the mean lifetime of the original vibrationally excited state. Both processes can be shown to result in a widening of the absorption band, but, before considering this, it is necessary to discuss the factors governing band width in general.

All absorption bands have finite width and, in order to allow for this, it is usually considered that the best quantity to take as a measure of a band intensity is the integrated absorption intensity, that is, the area under the absorbance/wave-number plot [8, 10]. The factors influencing band widths have been considered by Ramsay [10], who has concluded that the widths of infra-red absorption bands for materials in the liquid state are due almost entirely to pressure broadening and Stark broadening. The shape of an absorption band modified by these factors [cf. 11] can be represented by the Lorentz equation

$$\log_e \left(\frac{I_0}{I}\right)_\nu = \frac{a}{(\nu - \nu_0)^2 + b^2}, \qquad (1)$$

where I_0 and I are respectively the true intensities of the incident and transmitted radiation of frequency ν, ν_0 is the frequency of the band maximum, and a and b are constants. Ramsay has shown that this equation describes the observed band shapes to a reasonable degree of accuracy, when allowance is made for the effect of finite-resolving power in the measuring spectrometer. The peak absorbance of a band described by equation (1) is a/b^2, and the band width, that is the interval between the frequencies at which the absorbance is equal to half its peak value, $2b$.

The effect of the transfer of vibrational energy, postulated as occurring in the sterically hindered stilbene derivatives, can now be considered. First, let us examine the process as being one of vibration damping. The exact form of the damping will depend on the variation of the force of repulsion between the hindering groups with the degree of their interpenetration. The interaction energy of two nonbonded atoms is at a minimum at an interatomic distance equal to the sum of their van der Waals radii; it increases slowly as the separation widens and increasingly rapidly as it narrows, corresponding to the weak attractive and strong repulsive forces in these directions. The net repulsive force arising

in hindered *trans*-stilbenes must therefore be related to the amplitude of vibration by an exponential or power series. It follows that each cycle of the vibration will be progressively less damped, and it seems reasonable to assume that the damping decreases exponentially with time.

The energy and amplitude of the vibration after time t can then be written

$$E_t = E_0 e^{-2\pi\gamma t} \tag{2}$$

$$A_t = A_0 e^{-\pi\gamma t} \tag{3}$$

where γ is a constant defining the rate of damping. The vibration is more conveniently characterized by the time taken for the energy to be reduced to $1/e$ of its original value, referred to as the lifetime (T_0), and equal to $1/2\pi\gamma$. Equation (2) can be expressed as the sum of a series of sine waves with an intensity distribution given by equation (1), where a and b are equal to $\gamma/4\pi^2$ and $\gamma/2$ respectively. The absorption of electromagnetic radiation corresponding to the damped vibration will be described by this distribution, that is a band of Lorentz shape and width γ. It has been shown [12] that the band width resulting from a damping and a pressure-broadening effect is the sum of the separate widths. The damping of the vibration corresponding to the band at 960 cm^{-1} in the hindered stilbenes should therefore lead to a broadening of the band, with the difference in band width between the hindered and unhindered compounds equal to γ, expressed in sec^{-1}. Hence, if Δw represents this increase in cm^{-1}, the lifetime of the vibration will be given by

$$T_0 = 5{\cdot}30 \times 10^{-12}/\Delta w \text{ secs}$$

$$= 153/\Delta w \text{ vibrations at } 960 \text{ cm}^{-1}. \tag{4}$$

Let us now consider the transfer of vibrational energy as occurring by a transition to another vibrationally excited state. As the probability increases, the mean lifetime (τ) of the original state decreases. From the Heisenberg uncertainty principle, it follows that the energy distribution in this state will be wider so that the absorption band corresponding to excitation to this level will be broader. This is the same result as obtained on the damping hypothesis. Furthermore, it can be shown from quantum mechanics [11] that the band broadened by a transition mechanism will also be described by the Lorentz equation and have a width equal to $1/2\pi\tau$ due to this cause. The lifetimes obtained from the increase in band width on steric hindrance are therefore the same on both theories, although they do have a slightly different physical significance in the two cases.

Experimental details

1. *Purification of materials.* In any measurement involving intensities, the purity of the materials is particularly important. In this work, the samples prepared for the biological work [1] were taken and purified by recrystallization and/or fractional vacuum sublimation. The *cis*-isomer, expected as the main impurity, can be removed by these methods for it differs from the *trans*-isomer in having a higher solubility and vapour pressure. Purification was continued until a constant sharp melting point was obtained. In three cases, as indicated in Table 2, this stage was not reached, for further purification was prevented by lack of material; these samples may therefore contain a certain amount of impurity.

2. *Spectral measurements.* These were made on a Perkin-Elmer model 12C spectrometer, using an NaCl prism and adapted as a double-pass monochromator. The slit-width was 0·40 mm,

equivalent to 3·5 cm^{-1} at 960 cm^{-1}. The frequency calibration was carried out using the frequencies of bands due to ammonia and water vapour, by plotting their deviation from calculated values[13]. From the smooth curve drawn through these points, corrections were obtained which enabled the final calibration table to be drawn up. In the 800–1100 cm^{-1} region, the standard deviation of points from the correction curve was 0·25 cm^{-1}, and their reproducibility was about 0·1 cm^{-1}. The calibration was checked before each run from the position of the 1685 cm^{-1} band of water vapour.

Measurements were made in carbon disulphide in a cell whose thickness of 3·03 mm was deduced from the thickness of spacers used and checked from the difference in thickness of the whole cells and of its plates. Three solvent and three solution runs were made for each compound; the three concentrations were chosen to give successive maximal absorbances of approximately 0·36, 0·54, and 0·72 for which they were in the range 0·1 – 0·5% (w.v.). I_0 values were taken from the average of the three solvent runs; any changes in amplification and source intensity between these and the solution runs were allowed for by measuring the energy before and after each run at a fixed frequency. In this manner absorbance/wavenumber plots were obtained at the three concentrations for each compound.

3. *Calculation of results.* In order to derive the quantities characterizing the band under investigation, it was first necessary to allow for the overlap of neighbouring bands. This was

Table 1. Absorption bands in the stilbenes close to that due to the olefinic CH deformation vibration, giving frequencies (ν) in cm^{-1}, extinction coefficients (E) in litres/mole/cm (common logs.) and band widths ($\Delta\nu$) in cm^{-1}

Compound	ν $E\sim5$	ν $E\sim5$	ν E $\Delta\nu$	ν E $\Delta\nu$	ν E $\Delta\nu$	ν $E\sim10$	$\nu(E)$
trans-Stilbene				979·8 41 6·4			
4-Methyl-				978·6 27 6·6			
2 : 2′-Dimethyl-		939			972·8 34 7·0		989 (8)
2 : 4 : 6-Trimethyl-				979·8 44 6·5			
2 : 4 : 6 : 2′ : 4′ : 6′-Hexamethyl-							1013 (28) 1031 (52)
4-Dimethylamino-	928		948·9 117 8·8	977·1 28 7·0		1005	
-4′-methyl-	928		948·6 125 9·5			1005	938 (5)
-2′-methyl-	926	938	948·6 111 8·6		970·8 20 7·2	1006	988 (5)
-2′ : 4′-dimethyl-	928		948·4 118 8·9			1005	
-2′ : 5′-dimethyl-	928		948·5 128 9·4			1006	990 (25)
-2′-ethyl-	925	940	948·6 112 9·0		971·3 20 7·0	1006	
-2′ : 5′-diethyl-	926		948·6 115 8·7			1006	989 (3)
-2′-*iso*propyl-	928	940	948·7 113 9·8		971·7 14 7·0	1006	
-2′ : 5′-di*iso*propyl-	925		948·3 120 8·9			1006	944 (22)
-2 : 2′-dimethyl-		938			*968·7 63 10·1		990 (5) 1012 (60)
-2′ : 6′-dimethyl-	928		949·0 108 8·8			1006	961 (5) 990 (10)
-2′ : 4′ : 6′-trimethyl	926		948·9 105 9·0			1006	
Assignment			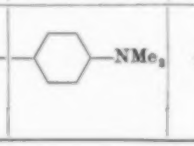	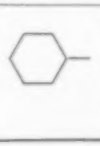	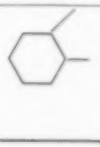		*Unassigned*

* Probably overlapped by absorption from another structure.

done by graphical separations fulfilling the following requirements: that the total of the separated absorbances should equal that observed, that the bands should be as symmetrical as possible, and that their shapes should approximate to the Lorentz equation as closely as possible. Most of the subsidiary bands can be assigned to specific structures as in Table 1, and it will be seen that in each series the absorption coefficient and band width, as well as the frequency, have characteristic values. In general, these bands do not overlap the main band very seriously and the separation may easily be carried out. The band at 949 cm^{-1}, due to the *p*-dimethylaminophenyl structure, does, however, overlap the main band considerably, except in three cases where the main band is at a higher frequency (see Table 2) and an accurate separation is possible. The constancy of the frequency, intensity and width of the minor band obtained in all

Table 2. Values of frequency (ν) in cm^{-1}, integrated absorption intensity (A) in litres/mole/cm^2 (nat. logs.), extinction coefficient (E) in litres/mole/cm (common logs.) and band width ($\Delta\nu$) in cm^{-1} for the olefinic CH deformation band of the stilbene derivative

Compound	ν	$A \times 10^{-3}$	E	$\Delta\nu$	
				obs.	calc.
trans-Stilbene	958·8	6·50	340	5·3	5·28
4-Methyl-	960·0	6·60	335	5·5	5·43
2 : 2′-Dimethyl-	960·8	5·41	255	5·8	5·80
2 : 4 : 6-Trimethyl-	968·0	5·50	152	9·8	9·94
2 : 4 : 6 : 2′ : 4′ : 6′-Hexamethyl-*	976·8	5·70	110	14·7	14·32
4-Dimethylamino-	957·0	6·70	347	5·4	5·32
-4′-methyl-	958·4	6·70	352	5·5	5·26
2′-methyl-	958·3	6·68	326	5·6	5·64
-2′ : 4′-dimethyl-	959·2	6·72	336	5·5	5·53
-2′ : 5′-dimethyl-	959·2	6·58	300	6·0	6·06
-2′-ethyl-	958·1	6·75	291	6·5	6·40
-2′ : 5′-diethyl-	958·6	6·81	267	7·1	7·05
-2′-*iso*propyl-	958·6	6·50	231	7·9	7·77
-2′ : 5′-di*iso*propyl-*	965·0	5·42	127	12·2	12·33
-2′ : 2′-dimethyl-*	957·9	6·17	284	6·0	6·00
-2′ : 6′-dimethyl-	968·9	6·37	166	11·3	10·57
-2′ : 4′ : 6′-trimethyl-	968·5	6·41	172	10·8	10·26

* Known to contain some impurity (see text).

cases suggests the separation procedure to be reliable even when the overlap is considerable. As a test, in one of the latter cases band separations were carried out in which the intensity of the subsidiary band was respectively over- and under-weighted as much as possible. Its intensity showed an overall variation of 10% and this produced in the main band a variation of 5% in its area and 2% in its peak absorbance. These were extreme values and the actual error involved should always be less than these amounts.

Following the band separations, the frequency, integrated absorption intensity (band area), peak extinction coefficient and band width were obtained. The three latter quantities varied somewhat with concentration; this was because the effect of the finite resolving power of the spectrometer on the absorption curves, which varies with absorption intensity, had not been considered. The true values of these quantities must therefore be derived from the apparent ones. It has been shown [14] that the true integrated absorption intensity can be obtained by extrapolating the observed values to zero concentration; for extinction coefficients, however, the true value cannot be obtained by a similar extrapolation [15]. Ramsay [10] has considered the

problem fully and has published tables from which single observed values of integrated absorption intensity, extinction coefficient and band width can all be corrected to true values when the spectral slit width is known.

Although strictly applicable only to isolated bands, the methods and tables compiled by Ramsay were applied directly to the separated bands. Only in the case of the band at 949 cm^{-1} already mentioned is a subsidiary band sufficiently intense and near to the main band in position to have any appreciable effect on the correction. The effect of the subsidiary band is to increase the effective band width and reduce the difference between the observed and the true absorption curve. Corrections were therefore applied to the separated bands on the basis of a band width derived from the total absorption. For isolated bands, the corrections are probably accurate to within 10–15%, and should not exceed 20% for the greatest amount of overlap here considered. The actual corrections applied were 1–5% on integrated absorption intensity and 10–25% on extinction coefficient and band width, so that the errors introduced in deriving the true from the observed values for these quantities should not exceed 1% and 5% respectively.

This method of correcting the observed band parameters to true values is only valid when the true band shape is described by the Lorentz equation. Ramsay verified this experimentally and it appears to be true in the present case. It does therefore follow that the integrated absorption intensity (A), extinction coefficient (E) and band width ($\Delta\nu$) are related by the equation:

$$A = \frac{\pi}{2} \log_e 10 \cdot E \cdot \Delta\nu \qquad (5)$$

Values for all three parameters were obtained experimentally, but in addition, values of the band width were calculated from the observed values of A and E by means of equation (5). The two sets of figures may be compared in Table 2; it will be seen that they agree closely, the r.m.s. difference being 2·5%.

4. *Accuracy of results.* In order to assess the significance of the results, it is necessary to consider their accuracy. The band frequency in individual solutions was never more than 0·1 cm^{-1} from the mean value, and from the accuracy of the calibration the latter should be accurate to within $\pm 0{\cdot}2$ cm^{-1}. For the intensity measurements, each value of the absorbance is subject to a random instrumental error; from the signal-to-noise ratio, it is estimated that this introduces an error of about $\pm 1\%$ in the mean of A and E. In addition, the band separation introduces an error which affects mainly band area, while the uncertainty in the slit correction affects mainly peak height. These errors have already been discussed; as a result, the mean values of the integrated absorption intensity and the extinction coefficient cannot be expected to be more accurate than to within about $\pm 5\%$.

The errors in the band width are more difficult to assess. Experimentally, it is the least accurate quantity to measure; although estimated to 1/40 cm^{-1}, its value cannot be accurate to better than 1/10 cm^{-1}. On the other hand, errors in band separation and slit correction should produce a smaller effect in this case, for band width depends on the ratio of A to E, and these would be affected in the same direction by such errors. Because of the greater experimental uncertainty in measuring band width, values calculated from A and E by equation (5) are probably more accurate than those derived from the observed absorption, and should be about as accurate as the values of A and E, that is within $\pm 5\%$. It should also be noted that the band width is much less dependent than A or E on the purity of the materials and is indeed completely unaffected by the presence of an impurity which does not absorb near the main band. This condition should be fulfilled in the present case, for the *cis*-isomers, the main impurity, have no strong band in this region.

Discussions of results

The data for the 17 *trans*-stilbenes measured are given in Table 2.

It can be seen that the frequency of absorption shows little variation with structure. Compared with the value in *trans*-stilbene, most of the frequencies are consistent with a decrease of about 2 cm^{-1} due to the *p*-dimethylamino group and an increase of about 1 cm^{-1} due to a methyl group in positions *ortho* or *para* to

VOL. 8 1956/5

the olefinic bridge. These small shifts are in the directions expected on the basis of the electronegativities of the substituents. For five compounds, in all of which considerable steric hindrance is expected, the frequency is appreciably higher than normal, a result which has been predicted above and explained in terms of reduced conjugation. In the hexamethyl compound, in which all four *ortho*-hydrogen atoms are substituted, the increase in frequency is about 12 cm^{-1}, suggesting an almost complete lack of conjugation between the aromatic rings and the olefinic bridge, and therefore considerable nonplanarity. In the three compounds with both *ortho*-positions in one ring substituted the increase is about 6—10 cm^{-1}, and a similar shift is found in 4-dimethylamino-2′ : 5′-di*iso*propylstilbene. The corresponding 2′-mono*iso*propyl compound does not show this shift, and the effect of the second *iso*propyl group in a nonhindering position will be discussed further below. Except in these extreme cases, however, the shift is small and not of sufficient magnitude to provide a sensitive criterion of steric hindrance, for the effect of other structural factors cannot be predicted with sufficient accuracy.

Comparison of the values of the integrated absorption intensity shows them to be remarkably constant. The three samples of questionable purity give low values, as do two other compounds. The other 12 stilbenes have a mean value of $6{\cdot}62 \times 10^3$ litres/mole/cm^2 with a standard deviation of $0{\cdot}13 \times 10^3$. The latter leads to a limit of 4% for significant variation, reflecting the expected accuracy of not better than 5%. No explanation of the low values for 2 : 2′-dimethyl- and 2 : 4 : 6:-trimethyl-stilbene can be given; the purity of the samples was most carefully checked and the reductions are much greater than could be caused by experimental error. Apart from these cases, it must be concluded that the integrated absorption intensity remains constant within experimental error.

In contrast with the frequencies and intensities, the extinction coefficients show large variations, with correspondingly large differences in band widths. On general theoretical considerations it has been shown above that an increase of band width is to be expected as a result of steric hindrance. If the variations in band width be due to differing extents of steric hindrance, the changes in structure which increase the band width must be those by which the hindrance can be increased. That this is so is apparent from Table 3 where the compounds have been classified according to the size and number of their *ortho*-substituents, and are listed in the order of expected steric hindrance. Examination of the table shows that, except for one type of structure, the order of band widths follows exactly the order of steric hindrance expected from the nature of the *ortho*-substituents. It will be seen below that this exception can readily be explained and there seems little doubt, therefore, that the increase in band width is caused by an increase in steric hindrance.

An explanation of the origin of the effect has been given above. This supposes the energy of vibration of the olefinic hydrogen atoms to be transferred to the rest of the molecule when steric hindrance is present, and relates the resultant increase in band width to a characteristic lifetime of the vibration. Those compounds unsubstituted in their *ortho*-positions are unhindered and their band widths can be taken as standard. The increases in the other compounds, together with the derived lifetimes, are given in Table 3.

Table 3. Band widths (calculated from A and E) of the stilbenes classified according to structure; Δw is the increase in band width, compared to the non-*ortho*-substituted compounds, and T_0 is the derived life-time, expressed in numbers of vibrations

Substituents in *ortho* positions	Band width		Δw	T_0
	Individual	Average		
None	5·28 5·43 5·32 5·26	5·32	—	—
One methyl	5·64 5·53	5·59	0·3	500
One methyl (with an *m*-methyl)	6·06	6·06	0·7	220
Two methyl, one in each ring	5·80 6·00	5·90	0·6	250
One ethyl	6·40	6·40	1·1	140
One ethyl (with an *m*-methyl)	7·05	7·05	1·7	90
One *iso*propyl	7·77	7·77	2·4	64
One *iso*propyl (with an *m*-*iso*propyl)	12·33	12·33	7·0	24
Two methyl, both in same ring	9·94 10·57 10·26	10·26	4·9	31
Four methyl	14·32	14·32	9·0	17

The derivation of an exact relationship between the lifetime of the vibration and the degree of steric hindrance would require a knowledge of the force field within the molecule. Although this final step is not possible at the moment, the effect, expressed directly as an increase in band width or interpreted in terms of lifetimes, does provide an accurate measure of the relative degree of steric hindrance in the various derivatives. It should be noted that these results, like those derived from dipole moment data [16], refer to the electronic ground state and are not dependent on the configuration in the excited state as are conclusions derived from ultra-violet intensities [3], although the results obtained by each method are very similar.

The degree of steric hindrance in the several structures must now be discussed. From a consideration of probable errors, the increase in band width of 0·3 cm^{-1} obtained for the *ortho*-monomethyl compounds would be expected to be at about the limit of significance. The fact that the value taken for the unhindered molecules

is an average of four individual values does, however, increase the probability that the increase for the monomethyl compounds is a real one. The physical picture of this difference, that the vibration would have a lifetime of 500 vibrations in the absence of other factors reducing its lifetime, indicates that there is but slight interaction, and suggests the sensitivity of the method to be high.

The values for the other compounds, except where *meta*-substituents occur, are as might be expected. An increase in size of the single *ortho*-substituent leads to steadily greater hindrance, as shown by the 2′-ethyl and 2′-*iso*propyl compounds. A second methyl substituent in the same ring has a very large effect, but if it is in the other ring, it has only about the same additional effect as the first such group. This difference is in line with the observation on models that a single *ortho*-group can interfere with one of the olefinic hydrogen atoms much more than the other; two groups in different rings can therefore be accommodated so that each interferes no more than a single group, but this is not possible when both are in the same ring [3]. A very large effect is observed when all four *ortho*-positions are filled with methyl groups. The band is almost trebled in width and the life-time of the vibration is now only 17 vibrations.

As substituents in the *meta*- and *para*-positions cannot interfere sterically with the olefinic hydrogen atoms, their size might be expected to be without effect on the band widths. Although this appears to be true in the case of *para*-substitution, an increase in size of the *meta*-substituent appears to increase the band width further in already hindered compounds. Thus, the band width in 4-dimethylamino-2′ : 5′-dimethylstilbene is just significantly greater than in the 2′-monomethyl compound; the difference between the corresponding ethyl compounds is somewhat greater, and in the case of the *iso*propyl compounds is very great indeed. Although substituents in the *meta*-positions cannot affect the degree of steric hindrance directly, their effect on band width can still be explained on the hypothesis that any increase in the width of this band is caused by steric hindrance, and indeed throws further light on the mechanism involved.

The increase in band width has been explained as being due to a transfer of energy from the vibration of the olefinic hydrogen atoms, which gives rise to the band, to a motion involving the group in the *ortho*-position, whose presence is causing the steric hindrance. This forced motion could be either a bending of the group in the *ortho*-position out of the plane of the aromatic ring, or a partial rotation of the whole ring about the bond to the olefinic bridge. In the latter case, the size of a *meta*-substituent might be expected to be important, due to its affecting the moment of inertia of the ring about the axis of rotation. As this increases, more energy is required to produce that displacement of the group in the *ortho*-position away from the olefinic hydrogen atom, which is necessary to relieve steric strain. A greater proportion of the original vibrational energy is, therefore, transferred in each vibration, so that a more rapid transfer of energy results, leading directly to an increase in band width. The observed effect of substituents in the *meta*-position is thereby explained, and suggests a rotation of the aromatic ring to be the motion induced by the transfer of vibrational energy. This increase in energy of rotation may cause a slight increase in the deformation force constant and thus explain the higher frequency for the 2′ : 5′-di*iso*propyl compound. It should be

noted that substituents in the *para*-position should have a much smaller effect; the bulky *p*-dimethylamino group might be expected to have an effect no greater than that for an *m*-methyl group. In the two cases where comparison is possible, the 2 : 2′-dimethyl and 2 : 4 : 6-trimethyl pairs of derivatives, the compound with the *p*-dimethylamino group does have a slightly larger band width in each case, but these differences are not significant.

It has thus been shown that steric hindrance in the substituted stilbenes can readily be demonstrated by its effect on their infra-red spectra. The band at 960 cm^{-1} due to the out-of-plane in-phase vibration of the olefinic hydrogen atoms, whilst almost constant in frequency and intensity, shows a nearly threefold variation in band width. The lowest values are for the unsubstituted compounds; the increase in other cases has been correlated with the presence of steric hindrance and a possible explanation of the connection has been given.

Acknowledgements—The author wishes to thank Dr. E. M. F. Roe for her interest in this work, and for helpful suggestions. He is indebted to Mr. J. L. Everett, who specially prepared samples of some of the compounds. The investigation has been supported by grants to this Institute from the British Empire Cancer Campaign, the Jane Coffin Childs Memorial Fund for Medical Research, the Anna Fuller Fund, and the National Cancer Institute of the National Institutes of Health, US Public Health Srevice.

References

[1] Haddow A., Harris R. J. C., Kon G. A. R., and Roe E. M. F.; *Phil. Trans. Roy. Soc. London* 1948 **A241** 147.
[2] Dostrovsky I., Hughes E. D., and Ingold C. K.; *J. Chem. Soc.* (*London*) 1946 173.
[3] Beale R. N. and Roe E. M. F.; *J. Amer. Chem. Soc.* 1952 **74** 2302.
[4] Thompson H. W., Vago Eva E., Corfield M. C., and Orr S. F. D.; *J. Chem. Soc.* (*London*) 1950 214.
[5] Sheppard N. and Sutherland G. B. B. M.; *Proc. Roy. Soc. London* 1949 **A196** 195.
[6] Brown J. K. and Sheppard N.; *Trans. Faraday Soc.* 1955 **51** 1611.
[7] Jones R. N.; *J. Amer. Chem. Soc.* 1950 **72** 5322.
[8] Bell R. P., Thompson H. W., and Vago E. E.; *Proc. Roy. Soc. London* 1948 **A192** 498.
[9] Cole A. R. H. and Thompson H. W.; *Trans. Faraday Soc.* 1950 **46** 103.
[10] Ramsay D. A.; *J. Amer. Chem. Soc.* 1952 **74** 72.
[11] White H. E.; *Introduction to Atomic Spectra* McGraw-Hill Book Co. 1934 p. 418.
[12] Margenau H. and Watson W. W.; *Rev. Mod. Phys.* 1936 **8** 22.
[13] McKinney D. S. and Friedel R. A.; *J. Opt. Soc. Amer.* 1948 **38** 222.
[14] Wilson E. B. and Wells A. J.; *J. Chem. Phys.* 1946 **14** 578.
[15] Philpotts A. R., Thain W., and Smith P. G.; *Analyt. Chem.* 1951 **23** 268.
[16] Everard K. B. and Sutton L. E.; *J. Chem. Soc.* (*London*) 1951 2816.

VOL. 8 1956/5

Spectrochimica Acta, 1956, Vol. 8, pp. 229 to 248. Pergamon Press Ltd., London

Contribution à l'étude de l'ultraviolet lointain

J. Romand et V. Vodar
Laboratoire des Hautes Pressions (CNRS-DEFA) Bellevue
(Seine et Oise) France

Résumé—Dans le but de compléter les articles d'ensemble déjà publiés sur l'ultraviolet lointain, les auteurs passent en revue un certain nombre de questions relatives à cette région spectrale. Quelques techniques particulières de spectroscopie d'absorption sont décrites. Les possibilités de l'analyse spectrochimique d'émission sont aussi données. Enfin quelques aspects théoriques de la spectroscopie d'absorption dans cette région sont indiqués.

1. Introduction

La région spectrale de l'ultraviolet lointain est comprise entre 2.000 Å et les rayons X; la limite assez artificielle de 2.000 Å correspond au début de l'absorption atmosphérique (celle de l'oxygène) de sorte que cette partie du spectre ultraviolet peut s'appeler également "ultraviolet à vide" car pour l'étudier on doit placer tout l'appareillage dans un vide élevé.

Bien qu'ayant été explorée et étudiée depuis plus de cinquante ans, elle était jusqu'à ces dernières années peu familière aux spectroscopistes en partie par suite des difficultés expérimentales. Les progrès de la technique ont permis de résoudre certaines de ces difficultés et depuis une dizaine d'années nous assistons à un développement rapide des recherches dans cette région spectrale.

Les techniques particulières, les méthodes, les problèmes théoriques et les principaux résultats obtenus au cours de travaux effectués dans ce domaine ont fait l'objet d'ouvrages et d'articles d'ensemble parmi lesquels nous pouvons citer par ordre chronologique: Lyman [1], Bomke [2], Boyce [3], Platt et Klevens [4], Price [5], Vodar et Romand [6], et enfin Inn [7].

L'intéressant article de Inn qui est le dernier en date, donne une revue rapide des méthodes et techniques en insistant sur les perfectionnements les plus récents notamment dans le domaine de la spectrophotométrie photoélectrique. Cet auteur donne également une discussion très pertinente des possibilités de l'ultraviolet lointain principalement au point de vue des problèmes concernant la structure moléculaire, l'état solide et la haute atmosphère.

Le but du présent article est de compléter ces données par une brève revue des travaux effectués postérieurement à la rédaction de l'article de Inn ou concernant les quelques questions que cet auteur a moins développées. Nous insisterons plus particulièrement sur les méthodes et les techniques expérimentales et surtout sur celles employées dans notre laboratoire et qui ont fait l'objet des travaux de Mme S. Robin, Mme A. Johannin-Gilles, Mlle N. Astoin, et Mr. V. Schwetzoff.

2. Sources

Pour effectuer des études d'absorption la source idéale devrait fournir un spectre continu et être raisonnablement stable. Ces conditions sont difficiles à réaliser dans l'ultraviolet lointain.

Si l'on excepte les radiations émises par les électrons accélérés de grande énergie [8, 9] la source de Lyman est la seule source donnant un spectre continu dans *l'ensemble* de l'ultraviolet lointain. Cette source est couramment utilisée [10, 11, 12], mais le capillaire s'use et la reproductibilité est médiocre, aussi nous avons préconisé [13] l'utilisation d'un matériau réfractaire tel que l'alumine qui s'use moins vite que le pyrex ou le quartz habituellement utilisés.

Nous avons proposé récemment [14] une version très simplifiée de la décharge de Lyman classique, en utilisant une décharge "glissante" sur isolant ou semi-conducteur dans le vide (voir plus loin).

Le dispositif que nous utilisons (figure 1) consiste en un tube capillaire en verre ou en alumine dans lequel sont enfilées les deux électrodes métalliques, l'observation

Fig. 1. Disposition des électrodes et du capillaire pour la production d'un spectre continu dans l'ultraviolet lointain.

étant faite perpendiculairement à l'axe par un trou latéral. L'ensemble est disposé dans une chambre à étincelles ordinaire dans laquelle on maintient le vide en permanence au moyen d'une pompe à diffusion. A l'origine de la décharge il n'y a donc pas de gaz dans le capillaire et le rôle fondamental joué par la vapeur de ce dernier est ainsi mis en évidence. Outre son intérêt théorique au point de vue de l'explication du mécanisme de l'émission, les avantages pratiques de cette source sont: utilisation d'une chambre normale, absence de gaz de remplissage, remplacement facile du capillaire. Des essais préliminaires ont donné des spectres continus limités vers 1000 Å. Cette limitation est peut être due à la faible profondeur optique de la source.

Quand un spectre continu n'est pas absolument indispensable dans l'ensemble de l'ultraviolet lointain, on préfère, au lieu de la décharge en impulsions de Lyman, employer une décharge entretenue usuelle comme celle de la lampe à hydrogène. A titre d'exemple la figure 2 représente une lampe sans fenêtre de forte puissance et de forme compacte, mise au point par Mme Robin [15, 16].

La décharge en haute fréquence dans les gaz rares (récemment décrite par les auteurs américains) permet également d'obtenir un spectre continu dans différentes régions de l'ultraviolet lointain. Ce spectre s'étend de 1500 à 2250 Å avec le xénon, de 1250 à 1850 Å avec le krypton, de 1070 à 1650 Å avec l'argon [17, 18, 19]. L'excitation est obtenue à partir d'un générateur haute fréquence à 2450 Mc. Il semble que cette source offre des possibilités intéressantes pour les études d'absorption.

Les sources de raies n'en restent pas moins fort utiles particulièrement dans le domaine des très courtes longueurs d'onde; le spectre continu de Lyman descend en effet difficilement au dessous de 600 Å. La source classique est l'étincelle dans le vide (étincelle de Millikan) où l'excitation est très forte et qui permet de descendre à quelques dizaines d'Ångströms. Mais elle nécessite des champs disruptifs très intenses, donc pour les potentiels usuels, un espacement très faible des électrodes, d'où des collages fréquents de ces dernières et la nécessité de

VOL.
8
1956/5

régler continuellement leur espacement du fait de l'usure; la reproductibilité est très médiocre.

L'étincelle ordinaire dans un gaz transparent peut être utilisée dans la région spectrale de transparence du gaz et de la fenêtre nécessaires [20, 21, 22]. Néanmoins la pollution de la fenêtre et la limitation en longueur d'onde à 1100 Å restent des inconvénients majeurs de ce type de source. Récemment SHENSTONE [23] a supprimé la fenêtre entre la chambre à étincelles et le spectrographe; il utilise une étincelle ordinaire dans l'hélium très pur, ce gaz étant à la pression de 30 à 60 cm Hg dans la chambre à étincelles et de 4 à 10 mm Hg dans le spectrographe où

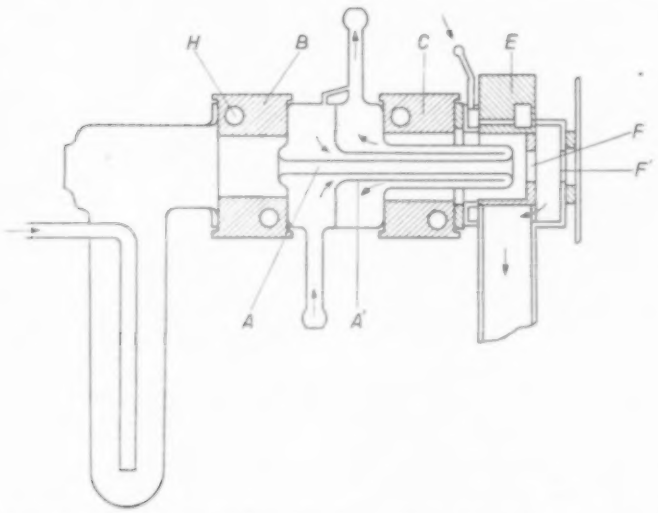

Fig. 2. Lampe à décharge sans fenêtre—On distingue en *A* le capillaire en quartz fondu, en *B* et *C* les électrodes en aluminium refroidies par circulation d'eau (*H*); en *E* la pièce permettant le repompage du gaz entre les fentes *F* et *F'* situées devant la fente de l'appareil dispersif.

il ne pénètre que par la fente et où il est pompé en permanence par une pompe primaire. Le spectre a pu être observé dans ces conditions jusqu'à 600 Å.

Citons encore l'étincelle condensée dans le vide, utilisée par WAHR, MCCORMICK et SAWYER [24], dans laquelle les inconvénients de l'étincelle de MILLIKAN sont évités, car l'initiation de l'étincelle est déclenchée par l'admission dans la chambre d'une "bouffée" de quelques cm³ d'hélium à la pression atmosphérique.

Enfin on peut utiliser des décharges faiblement condensées dans un capillaire contenant un gaz à basse pression. Ce type de source est utilisé en particulier par WEISSLER et ses collaborateurs pour des travaux sur l'absorption et la photoionisation [25, 26, 27]. Récemment PO LEE [28] a pu effectuer des mesures jusqu'a 200 Å en associant une source de ce type à un spectrographe muni d'un réseau en incidence tangentielle. DITCHBURN [29] utilise une source analogue sur un montage particulièrement étudié pour donner le minimum de lumière diffusée.

La source au perfectionnement de laquelle nous nous sommes attachés, et qui nous paraît convenir le mieux surtout dans la région des courtes longueurs d'onde est

un type différent d'étincelle dans le vide, proposé par Vodar et Astoin [30, 31, 32]. On fait jaillir l'étincelle entre deux électrodes en contact avec un support semi-conducteur ou isolant. Ce type d'étincelle est connu depuis longtemps dans l'air sous le nom d''étincelle glissante''. Dans le vide le caractère de la décharge est différent de celui des étincelles glissantes classiques, mais une propriété fondamentale subsiste, celle de se produire sur des intervalles longs pour des potentiels modérés; le potentiel disruptif est abaissé et l'émission lumineuse est stable. Nous avons essayé plusieurs dispositions d'électrodes [33] et retenu les dispositions 1–2–3 représentées figure 3; l'étincelle glisse à la surface intérieure de l'isolant qui a la

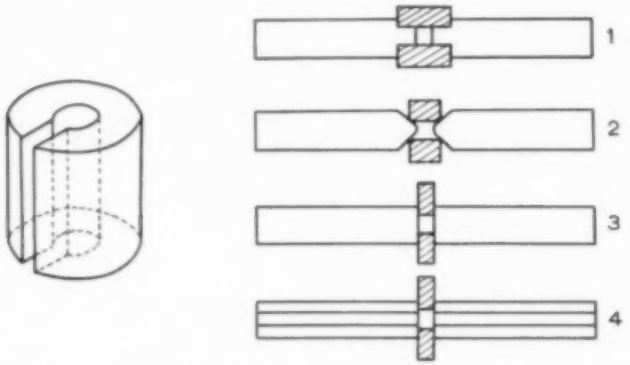

Fig. 3. Diverses dispositions des électrodes et du support pour la réalisation d'étincelles glissantes dans le vide.

forme d'une rondelle comportant une fente latérale. La disposition 3 est celle décrite par Bockasten [34].

Le spectre comportant outre les raies des électrodes des raies provenant du matériau du support, et ce type d'étincelle pouvant être utilisé pour l'analyse spectrale comme nous le verrons plus loin, nous avons choisi l'alumine qui est un matériau dur, réfractaire, et donnant peu de raies (le spectre de l'aluminium est relativement pauvre). L'alimentation électrique est la même que celle qui est utilisée couramment pour la décharge condensée dans le vide. La richesse des spectres obtenus est telle qu'ils conviennent très bien comme fond pour l'étude des spectres d'absorption. La reproductibilité de cette source est assez bonne (5%). Remarquons d'autre part que Bockasten a attiré l'attention sur le fait que les raies émises par l'étincelle glissante dans le vide sont plus fines que celles des étincelles condensées dans le vide habituelles (étincelles de Millikan) car l'élargissement par effet Stark est moindre.

3. Utilisation des étincelles glissantes pour l'analyse spectrale dans l'ultraviolet lointain

Parmi les éléments qu'il est difficile de détecter avec les techniques habituelles de l'analyse spectrale nous remarquerons les halogènes, les gaz rares et les métalloïdes dont les raies intenses sont dans l'ultraviolet lointain. Il nous a semblé intéressant d'examiner au point de vue de l'analyse spectrale les possibilités des étincelles

VOL. 8 1956/5

glissantes dont le fonctionnement est plus stable que celui des étincelles dans le vide habituelles. Nous avons pu ainsi doser quantitativement le soufre, le phosphore et le carbone dans les aciers [35, 36] en utilisant des raies d'atomes fortement ionisés: P_{IV} (950,7 et 1118,6 Å), S_{VI} (933,4 et 944,5 Å), C_{III} (977 et 1176 Å). Les concentrations limites détectables ont été évaluées à 0,005% pour ces trois éléments dans les aciers. Leur détection dans d'autres métaux est également possible et des résultats obtenus récemment donnent une sensibilité pour le soufre et le phosphore meilleure dans l'aluminium que dans les aciers (limite inférieure à 5 p.p.m. dans l'aluminium).

On peut aussi obtenir le spectre d'émission d'une substance non conductrice réduite en poudre, en tassant celle ci dans un canal axial ménagé dans des électrodes d'aluminium (dont le spectre propre est pauvre en raies); on utilise alors la disposition 4, figure 3. Nous avons pu ainsi détecter le carbone, le soufre, le phosphore, l'azote, le selenium, le chlore dans des poudres d'alumine et de zircone contenant différentes impuretés.

D'une façon générale les raies que nous utilisons sont celles d'ions ayant une configuration de la couche externe analogue à celles des atomes alcalins ou alcalino-terreux. L'examen du tableau des raies les plus sensibles nous a conduits à une extension de la notion de raie ultime [37, 38]: les raies les plus sensibles sont émises par l'ion ne possédant plus qu'un électron sur sa couche externe lorsque cet électron passe de l'état s à l'état p. Ces raies sont analogues aux doublets des atomes alcalins.

L'utilisation des étincelles glissantes ouvre de grandes possibilités à l'analyse spectrochimique d'émission dans l'ultraviolet lointain.

4. Récepteurs de radiations

Nous ne parlerons pas des surfaces photographiques, mais nous signalerons dans le domaine des récepteurs photoélectriques les récepteurs à fenêtre de quartz soufflé construits par Mr Schwetzoff et qui ont permis de descendre jusqu'à 1450 Å [39, 40, 41]. Les surfaces sensibles sont des couches complexes Cs sur argent oxydé et des couches aux antimoniures alcalins; ces couches, connues pour leur rendement photoélectrique élevé dans le visible se sont également montrées excellentes dans la région de Schumann. Les couches de Cu-Be peuvent également être utilisées et en principe autoriseraient même l'exposition à l'air [42]. Mais une étude complète des perfectionnements à apporter aux récepteurs sans fenêtre est nécessaire en ce qui concerne la stabilité; aussi n'avons nous réalisé et étudié que des multiplicateurs à fenêtre de quartz mince [41, 43] (figure 4), qui, à notre connaissance ont été les premiers photomultiplicateurs répondant directement au rayonnement ultraviolet dans la région de Schumann.

Les photocompteurs, dont nous parlerons plus loin, sont également utilisables dans l'ultraviolet lointain.

5. Cuves et cryostats

Lorsqu'on se limite aux mesures dans la région de Schumann ou dans une partie seulement de cette région, l'utilisation de matériaux transparents tels que la fluorine, le fluorure de lithium et le quartz permet d'étudier les matières dans des

conditions aussi variées que dans l'ultraviolet moyen ou le visible. On peut ainsi réaliser les montages en lumière convergente classiques; voir par exemple les références [44, 45]. Il est également possible de chauffer ou de refroidir l'absorbant; c'est ainsi qu'en placant une cuve en silice "homosil" dans un enroulement chauffant on a pu étudier le spectre de la vapeur d'eau en fonction de la température jusqu'à 900°C dans la région de Schumann [45, 46, 47]. Signalons aussi nos mesures quantitatives de la transparence de la fluorine, du quartz et du corindon dans l'ultraviolet de Schumann [48, 49, 50]. Pour le corindon ces mesures sont à notre connaissance les seules qui aient été publiées jusqu'ici (figure 5).

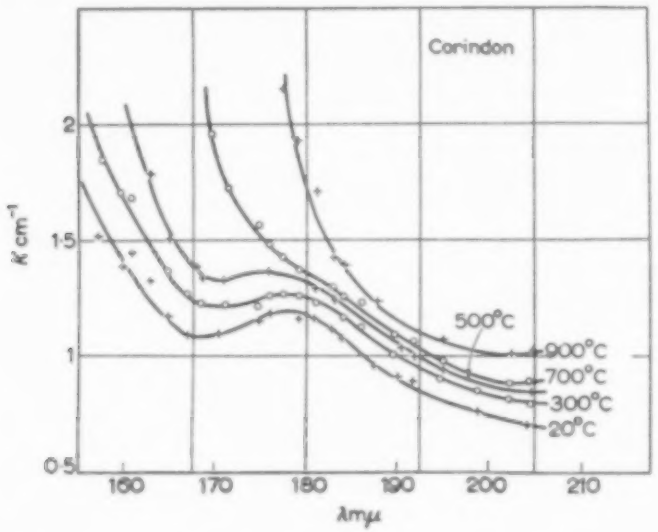

Fig. 5. Courbes d'absorption d'un échantillon de corindon pour diverses températures.

D'autre part pour étudier les spectres d'absorption des couches minces solides obtenues par congélation d'un jet gazeux nous avons utilisé le montage cryostatique, voisin de celui de Thomas [51] représenté sur la figure 6. Ce cryostat [52] comporte une double enceinte refroidie et d'autre part peut tourner d'un bloc autour d'un axe vertical. On évapore la couche dans une position donnée, puis on tourne l'ensemble pour observer cette couche, et enfin on mesure l'absorption dans une troisième position. Ce cryostat nous a permis d'étudier les spectres d'absorption du benzène solide [53], de l'oxyde azoteux solide [54, 55]; de l'oxyde azotique solide [56] et de l'oxygène solide [57]. A titre d'exemple la figure 7 représente la courbe d'absorption de l'oxygène solide comparée à celle de l'oxygène gazeux dans la même région spectrale.

Il est également possible d'effectuer l'étude des spectres d'absorption des fluides sous pression. En utilisant des fenêtres de fluorine ou de quartz sélectionné de 7 à 10 mm d'épaisseur ainsi que de l'argon suffisamment pur comme fluide nous avons pu faire des mesures jusqu'a 1430 Å environ sous des pressions atteignant 650 kg/cm² et étudier en particulier la perturbation de la raie 1469 Å du xénon par

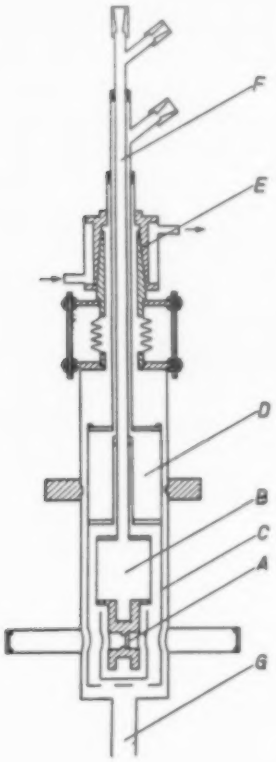

Fig. 6. Cryostat pour l'étude des spectres d'absorption des couches solides obtenues par congélation d'un jet gazeux. En *A* on aperçoit la fenêtre refroidie par l'hydrogène liquide situé dans le récipient *B*. En *C* se trouve une enceinte refroidie par l'azote liquide contenu en *D*. En *E* rodage permettant de faire tourner l'ensemble de l'appareil. En *F* se trouvent les tubes de remplissage.

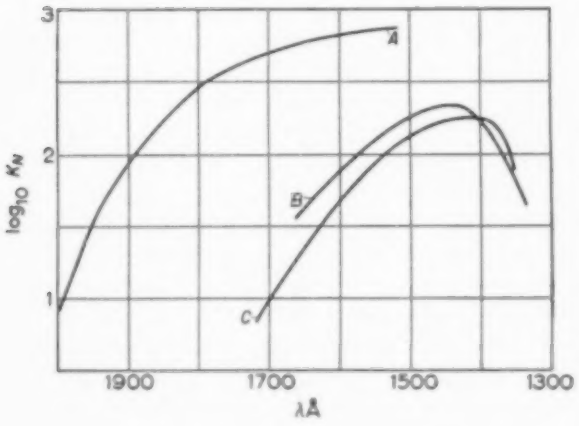

Fig. 7. Courbes d'absorption de l'oxygène. En *A* courbe de l'oxygène solide à basse température. En *B* et *C*, courbes de l'oxygène gazeux obtenues respectivement par LADENBURG et VAN VOORHIS et par WATANABE.

l'argon sous pression [58]. L'utilisation des gaz comprimés comme solvants apporterait à l'ultraviolet lointain les solvants qui lui manquent. A titre d'exemple nous avons pu ainsi obtenir la courbe d'absorption du phénanthrène dans la région de Schumann en utilisant comme solvant l'argon sous pression [59].

Au dessous de la limite de transparence du fluorure de lithium (1.100 Å) on ne connaît aucun solide transparent sous des épaisseurs macroscopiques. Cependant on peut réaliser des films très minces (quelques centaines d'Ångström) transparents jusqu'à 100 Å et qui soient étanches et résistent à des pressions de quelques mm Hg [60, 61]. On peut donc en faire des fenêtres de lampe, de cuve, et des

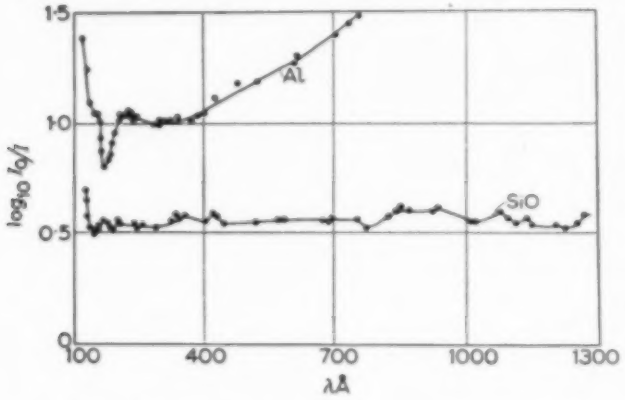

Fig. 8. Courbes d'absorption de pellicules minces d'aluminium et de monoxyde de silicium.

supports pour étudier des pellicules évaporées. Nous avons principalement employé le collodion ainsi que le monoxyde de silicium évaporé sous vide. Ces pellicules sont supportées par des grilles fines de microscopie électronique. La figure 8 représente la courbe d'absorption d'une telle pellicule de SiO et la courbe d'absorption d'une pellicule d'aluminium (ce dernier absorbe trop pour être utilisé pratiquement). Dans cette région spectrale de l'ultraviolet extrême il n'est plus possible d'utiliser des lentilles. Aussi la source est elle placée relativement près de la fente et l'absorbant est disposé entre la fente et le réseau [60, 32]. Néanmoins nous verrons dans un paragraphe ultérieur qu'il est possible d'utiliser des miroirs toriques sous des incidences autorisant un pouvoir réflecteur suffisant pour que l'on puisse par conséquent focaliser la lumière même dans la région de l'ultraviolet extrême.

6. Spectrophotométrie photographique

Le principal problème est celui de la gradation des clichés. Avec des sources fonctionnant en impulsions on ne peut guère songer aux secteurs tournants; la gradation avec une source auxiliaire [62] ne peut d'autre part être utilisée qu'avec les émulsions sensibilisées par une couche fluorescente.

Par contre les grilles photométriques conviennent bien. Avec un spectrographe à réseau en incidence normale les grilles habituelles peuvent être utilisées à condition de les placer dans une région assez large du faisceau [44, 45], au besoin au

vosinage du réseau [63]. Dans le cas où la partie utilisable du faisceau est toujours de faible section on peut utiliser des grilles très fines de microscopie électronique, les dimensions des mailles pouvant être 1/20 × 1/20 mm. De telles grilles peuvent être utilisées par exemple avec un spectrographe à réseau en incidence rasante [32]. Entre la chambre à étincelles (source) et le réseau se trouve une tige coulissante portant les différents échantillons dont on veut étudier l'absorption ainsi que les grilles pour la gradation photométrique de la surface sensible.

7. Réduction de la lumière parasite par des procédés photoélectriques

La lumière parasite (diffusée, réfléchie, réémise par fluorescence) est une gêne sérieuse dans l'étude de l'ultraviolet lointain. Signalons deux procédés que l'on peut utiliser dans le cas de récepteurs photoélectriques en vue d'éliminer cette cause d'erreur.

(a) on peut moduler la lumière directe utile en ne modulant pas la lumière parasite et effectuer ensuite une amplification sélective du signal obtenu. On peut profiter du fait que la lumière parasite est en général assez uniformément répartie de chaque côté du spectre et on obtiendra simplement la modulation en effectuant un mouvement relatif périodique du spectre par rapport à la fente. Ceci peut être réalisé en utilisant la vibration d'un miroir [64]. Nous pensons [6] qu'il serait également possible de faire osciller la fente parallèlement à elle même dans le cas d'un spectre à peu près stigmatique. Au lieu d'une oscillation mécanique, toujours délicate à réaliser, on pourrait utiliser un secteur tourant muni de trous complémentaires. Dans le cas d'un spectre très astigmatique (réseau tangent) une oscillation de la fente parallèlement au spectre semble seule possible, mais le procédé ne s'appliquerait qu'à un spectre de raies relativement isolées. Evidemment ces procédés de modulation ne sont applicables que lorsque l'émission de la source est continue dans le temps.

(b) la lumière parasite étant de longueur d'onde relativement grande, en général, on pourrait l'éliminer ainsi que l'a proposé Schwetzoff [41] soit en choisissant des récepteurs photoélectriques dont le seuil soit assez loin dans l'ultraviolet (cependant on ne connaît guère de matériau dont le seuil soit en dessous de 2000 Å) soit en reculant artificiellement le seuil du récepteur par application d'un potential retardateur, réalisant ainsi un filtre passe-haut (en fréquence). Les essais faits dans ce sens aux Etats-Unis ont montré la validité de ce procédé [65] qui est applicable à tous les types de sources.

(c) Un récepteur sensible exclusivement dans une certaine bande spectrale peut être réalisé en utilisant des photocompteurs. En combinant convenablement le gaz de remplissage et le filtre optique associé au photocompteur, il est possible de réaliser des détecteurs à bande relativement étroite pour l'ultraviolet lointain, ainsi que le montrent les travaux récents de Chubb et Friedman [66, 67, 68].

8. Séparation des ordres

Dans la région des courtes longueurs d'onde, avec les réseaux habituellement utilisés en incidence rasante, on observe la superposition des spectres de plusieurs ordres (jusqu'au quatrième dans notre cas). Cette circonstance est très gênante en spectrographie d'absorption et rend le dépouillement des spectres particulièrement

laborieux; en particulier l'utilisation d'un spectre continu est pratiquement impossible surtout pour des mesures spectrophotométriques. Une limitation des spectres du côté des courtes longueurs d'onde permettrait de résoudre cette difficulté. Un tel filtre passe-bas (en fréquence) peut être réalisé en utilisant les variations du pouvoir réflecteur en fonction de la longueur d'onde, les radiations de longueurs d'onde plus courtes que celle correspondant à la région d'apparition de la reflexion totale étant fortement affaiblies [69]. On dispose donc un miroir sur le trajet de la lumière entre la source et la fente. La figure 9 représente, à titre d'exemple, juxtaposées, deux mêmes portions du spectre d'une étincelle glissante du fer, pris avec un miroir auxiliaire en aluminium sous une incidence de 45° (spectre du haut) et sans miroir (spectre du bas). Avec un tel miroir la région au dessous de 250 Å n'est plus observable, celle comprise entre 250 et 400 Å est affaiblie; mais on observe la suppression totale des raies du 4 ème ordre et l'affaiblissement de celles du 2 ème ordre. Remarquons que l'on sait que la longueur d'onde limite dépend de l'incidence mais doit aussi théoriquement dépendre de la nature de la couche réfléchissante. Un réglage de ce filtre passe-bas, par exemple par modification de l'angle d'incidence sur le miroir permettrait en combinaison avec la méthode des potentiels retardateurs appliqués aux récepteurs photoélectriques, l'isolement d'une bande spectrale.

D'autre part il est possible même jusqu'à 250 Å, d'utiliser des miroirs à condition d'opérer sous une incidence suffisante. Comme l'avait déjà proposé Terrien [70] il y a longtemps et comme nous l'ont montré quelques essais, des miroirs toriques, qui donnent des images acceptables pour des incidences relativement élevées, permettraient la réalisation de montages en lumière convergente pour l'ultraviolet extrême.

VOL. 8 1956/5

9. Monochromateurs

Alors que seuls les spectrographes étaient utilisés au début des recherches dans l'ultraviolet lointain, depuis quelques années on observe un nombre croissant de monochromateurs. Ceci est dû principalement aux travaux effectués sur les récepteurs photoélectriques et en particulier à la facilité avec laquelle on peut utiliser des récepteurs commerciaux en les associant avec une substance fluorescente [71, 72, 73]. D'autre part une source monochromatique est indispensable pour certaines études telles que la photoionisation et la photodissociation.

Comme les spectrographes, les monochromateurs pour l'ultraviolet lointain sont le plus souvent des appareils à réseau. Divers systèmes mécaniques ont été proposés pour assurer une focalisation convenable sur la fente de sortie. Les mouvements mécaniquement simples n'assurent pas en général une focalisation parfaite pour toutes les longueurs d'onde, ou encore présentent l'inconvénient de produire un déplacement du rayon lumineux à la sortie du monochromateur; c'est le cas par exemple pour la simple rotation du réseau autour du centre du cercle de Rowland. Le procédé qui nous paraît le plus avantageux [74, 16] est dérivé du procédé de Rowland (figure 10) (bras rigide $C'D$ de longueur R glissant sur Px et Py), mais il semble préférable d'adopter deux bras articulés en E, PE et EC', de longueur $R/2$ dont l'un $C'E$ est lié au réseau dont il commande la rotation, le mouvement de E étant assuré par exemple par une glissière GG' se déplaçant parallèlement à elle

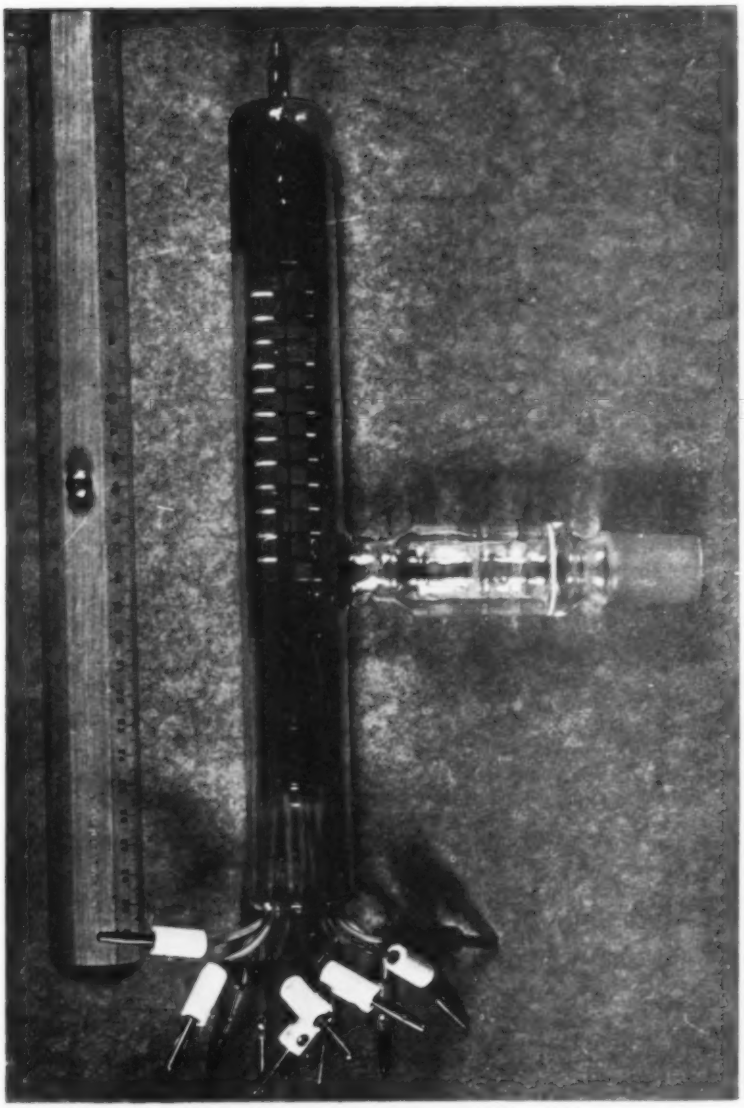

Fig. 4. Multiplicateur d'électrons à fenêtre de quartz mince soufflée. En bas les connexions des étages multiplicateurs, en haut la sortie d'anode. Le raccordement au monochromateur se fait sous vide grâce au rodage qu'on aperçoit à droite.

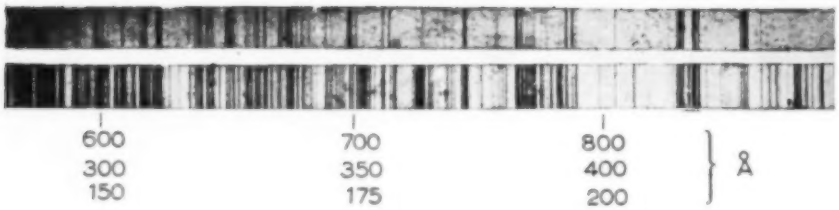

Fig. 9. Spectres d'une étincelle glissante entre électrodes de fer, dans la région 600–800 Å. Le spectre du bas a été pris directement, et celui du haut a été obtenu après une réflexion à 45° sur un miroir d'aluminium. Remarquer dans ce deuxième spectre la suppression des raies du quatrième et du deuxième ordre.

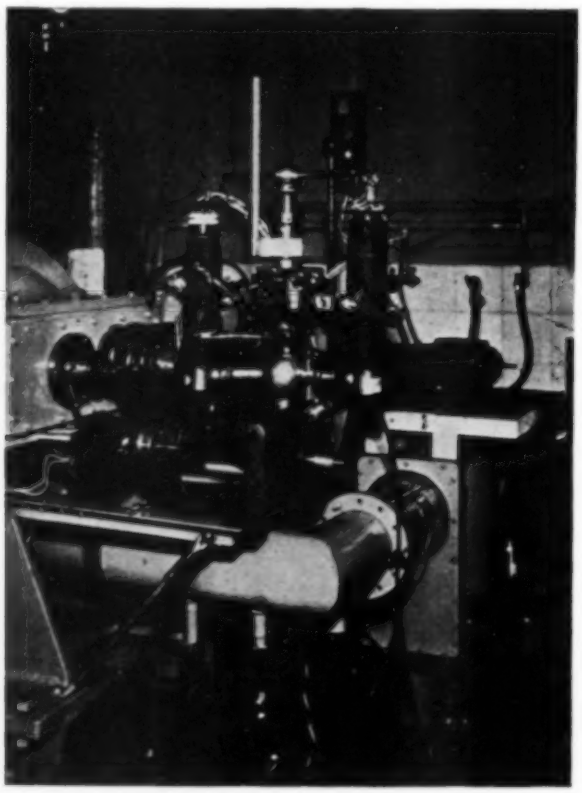

Fig. 11. Vue de la "tête" du monochromateur et du dispositif pour l'étude des pouvoirs réflecteurs.

VOL.
8
1956/5

même suivant Px. Signalons aussi la disposition décrite récemment par NAMIOKA [75] dans laquelle les fentes sont fixes et le réseau ne subit qu'une rotation autour d'un axe vertical passant par son centre. La disposition des trois éléments, fentes et réseau est déterminée par le calcul. La solution est unique et impose une valeur fixée pour $\alpha - \beta$ et r (α: angle d'incidence, β: angle de diffraction, r: distance fentes réseau) avec un réseau de rayon de courbure donné. On a ainsi $\alpha - \beta = 70° 15'$ et $r = 44$ cm pour un réseau de 54 cm de rayon. Ce procédé simple, qui assure aux auteurs une bonne focalisation jusqu'à 6.200 Å, semble le plus intéressant dans tous les cas où la condition relative aux angles ne constitue pas un inconvénient (astigmatisme).

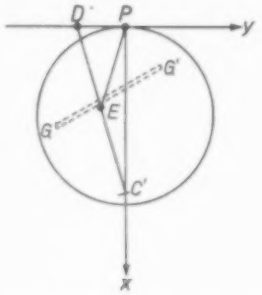

Fig. 10. Dispositif de focalisation pour monochromateur

10. Pouvoirs réflecteurs

Comme nous l'avons vu plus haut les miroirs sont appelés à jouer un rôle de plus en plus important dans l'ultraviolet lointain; aussi, outre son intérêt théorique, l'étude et la mesure des pouvoirs réflecteurs dans l'ultraviolet présente-t-elle un intérêt pratique indéniable. De telles mesures ont été faites avec l'appareil représenté figure 11 et 12 associé à un monochromateur [76]. Les récepteurs photoélectriques sont disposés en I pour la réflexion à 18°, en II pour la transmission directe, et en III pour la réflexion à 45°. La tige coulissante B peut porter plusieurs échantillons dont certains pourraient être préparés sur place grâce à des ampoules à évaporation. Les résultats obtenus, qu'il serait trop long d'exposer ici [16] confirment l'intérêt du platine par rapport à l'aluminium pour les longeurs d'onde inférieures à 1000 Å.

Cet intérêt, qui avait déjà été signalé par LYMAN [1] a été indiqué à nouveau par l'un d'entre nous il y a quelques années [44, p. 535]. Par ailleurs des mesures récentes [77, 78, 79] montrent que des couches évaporées de certains matériaux réfractaires comme le tungstène et le tantale ont dans l'ultraviolet lointain un pouvoir réflecteur acceptable (20% à 1200 Å) et sont assez reproductibles (figure 13). Les pouvoirs réflecteurs relativement élevés (30% à 1400 Å) de certaines couches de silicium évaporé dans des conditions particulières laissent à penser qu'une étude systématique des pouvoirs réflecteurs des alliages dans l'ultraviolet lointain ne serait pas sans intérêt. De même les couches évaporées de matériaux semiconducteurs tels que le germanium, le sélénium, et le tellure ont d'assez bons pouvoirs réflecteurs dans l'ultraviolet lointain (20 à 30% entre 1000 et 2000 Å).

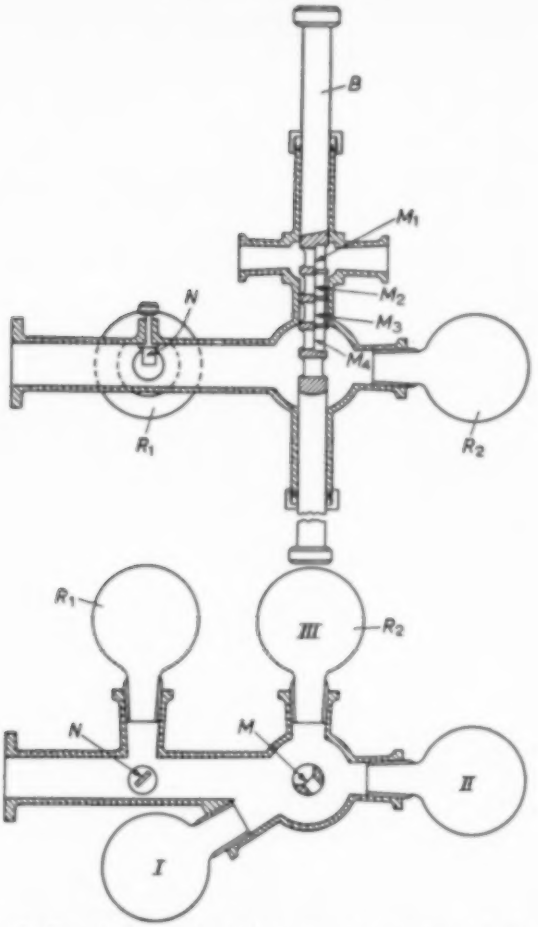

Fig. 12. Schéma du dispositif pour l'étude des pouvoirs réflecteurs. Les récepteurs photoélectriques sont disposés en I pour la réflexion à 18°, en II pour la transmission directe, en III pour la réflexion à 45°. *B* tige coulissante portant les échantillons *M* à étudier, *N*: miroir pour le faisceau du contrôle.

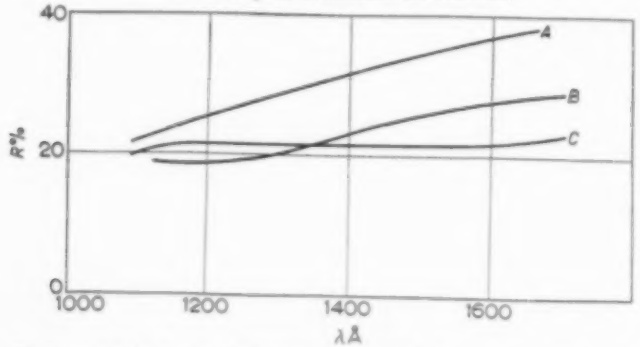

Fig. 13. Courbes du pouvoir reflecteur de couches évaporées de Tungstène, Tantale et Silicium.

VOL.
8
1956/5

11. Spectres d'absorption

Un exposé complet des résultats expérimentaux et des conclusions théoriques qui en découlent dépasserait de beaucoup le cadre de ce bref exposé. Nous nous bornerons donc à quelques points particuliers concernant principalement l'interprétation des bandes d'absorption continues ainsi que des spectres des solides; nous laisserons donc de côté des questions trop particulières comme la détermination des constantes optiques dans l'ultraviolet lointain par la mesure des pouvoirs réflecteurs sous diverses incidences [80, 81]. Nous ne parlerons pas non plus de la détermination des potentiels d'ionisation à partir des séries de RYDBERG correspondant à des électrons se mouvant sur des orbites quasi atomiques, cette question étant discutée en détail dans l'article de INN.

(A) L'étude des interactions entre les molécules d'un corps à l'état condensé peut être faite par l'observation de diverses propriétés de ce corps. En particulier les spectres d'absorption peuvent apporter des données sur ces interactions si l'on connaît d'une part le spectre de la molécule isolée (absorption du corps à l'état vapeur) et d'autre part le spectre de la molécule soumise à l'action des molécules voisines (absorption du corps à l'état solide ou liquide). Les résultats seront d'autant plus faciles à interpréter que les molécules à étudier sont plus simples. On étudiera donc de préférence des molécules di ou tri atomiques simples. L'examen et la comparaison des courbes d'énergie potentielle fournira alors des renseignements sur les interactions. Or ces corps de constitution simple ont le plus souvent leur région d'absorption dans l'ultraviolet et aussi l'ultraviolet lointain. Même pour les corps dont l'absorption est plus proche du visible, l'ultraviolet lointain est encore intéressant pour les renseignements qu'il peut donner sur la nature des transitions se produisant dans la molecule (cas de IH par exemple).

Nous nous sommes particulièrement intéressés aux bandes continues, c'est à dire produites par une transition ayant lieu à partir d'un niveau de l'état fondamental à un niveau quelconque de l'état excité se trouvant au dessus de l'énergie de dissociation. La détermination de la partie répulsive de la courbe d'énergie potentielle de l'état excité à partir de la courbe de l'état de base et de la courbe d'absorption peut se faire par différents procédés. Signalons la méthode de la réflexion dans laquelle on ne tient pas compte des fonctions d'onde de l'état excité, et la méthode d'integration compléte en fonction de l'écartement des noyaux en supposant le terme électronique constant. Cette dernière méthode [82, 83, 44] conduit à des calculs laborieux, et on emploie généralement la méthode de la réflexion, plus simple, et d'approximation suffisante dans la plupart des cas. GOODEVE et TAYLOR ont utilisé une méthode différente. Celle-ci, dans l'application qu'ils en firent à BrH et IH [84, 85] était très simplifiée et critiquable sur beaucoup de points. FINK et GOODEVE [86] la perfectionnèrent notablement et l'appliquèrent à $BrCH_3$. Enfin PORRET et GOODEVE [87] l'utilisèrent dans le cas de ICH_3.

Nous avons étudié il y a quelques années les gaz ClH [88] BrH et IH [89, 44] et nous avons analysé les résultats par les méthodes de la réflexion. Le cas de IH est particulièrement intéressant, car on ne peut représenter correctement la courbe expérimentale par une formule théorique en utilisant une seule transition: par contre nous avons pu faire cette représentation en utilisant deux transitions.

La figure 14 représente ainsi la décomposition de la courbe expérimentale et la figure 15 les deux courbes d'énergie potentielle de l'état excité correspondantes.

Ces méthodes s'appliquent bien dans le cas des molécules diatomiques, ou que l'on peut considérer comme telles, par exemple lorsque la bande d'absorption étudiée correspond à une liaison entre deux groupes individuellement assez stables pour pouvoir être considérés comme des ensembles (cas de $Br\text{-}CH_3$ et $I\text{-}CH_3$). Mais l'application devient difficile dans le cas de molécules triatomiques. Ainsi dans le cas de l'oxyde azoteux gazeux [90, 91] on observe sur la bande de 1830 Å un effet de température [92]; le maximum de la bande se déplace vers les grandes fréquences

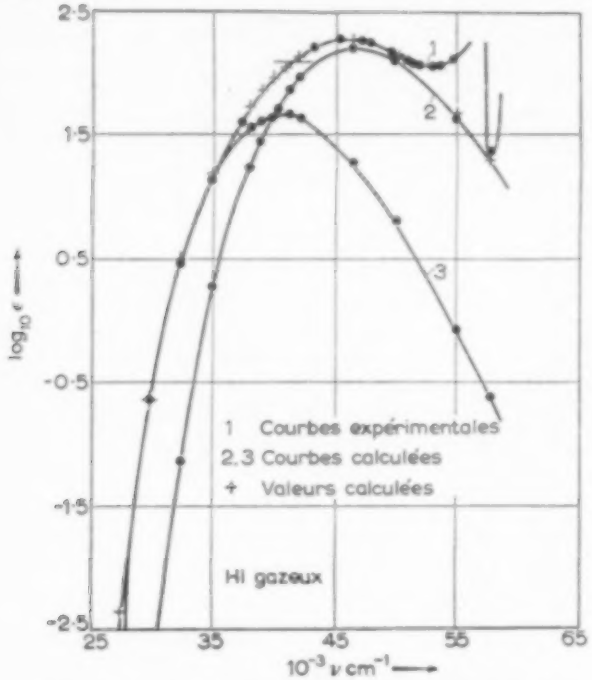

Fig. 14. Courbes d'absorption de l'acide iodhydrique gazeux.

avec diminution de l'absorption lorsque la température décroît. Cet effet peut être attribué à la variation de la population sur les différents niveaux de l'état de base; cependant dans le cas de N_2O, molécule triatomique et linéaire, la dissociation se faisant (processus primaire) selon toute probabilité en N_2 et O, la fréquence $\overleftarrow{N\ N\ O}\rightarrow$ correspondante (1.285 cm^{-1}) est trop élevée pour rendre compte d'un tel effet de température et l'on doit faire intervenir la fréquence de déformation (589 cm^{-1}). Un calcul approché que nous avons entrepris ne donnant pas de bon résultat, il sera nécessaire de faire un calcul complet au moyen des surfaces d'énergie potentielle [93].

(B) Les résultats actuels sur les spectres d'absorption des couches solides obtenues par congélation d'un jet gazeux, selon la technique signalée plus haut,

sont encore peu nombreux, mais néanmoins intéressants parce qu'ils montrent la diversité des cas possibles.

Ainsi dans le cas de l'oxyde azoteux solide à 20°K [54, 55] on observe une bande analogue en forme et en position à la bande *B* du gaz, mais déplacée vers les courtes longueurs d'onde et légèrement élargie. Les modifications de l'état de base étant minimes (selon les résultats donnés par le spectre Raman), ce déplacement est presque totalement dû à une modification de l'état excité seul; nous sommes donc ici dans le cas le plus simple.

Dans le cas du benzène [53] des modifications plus profondes apparaissent.

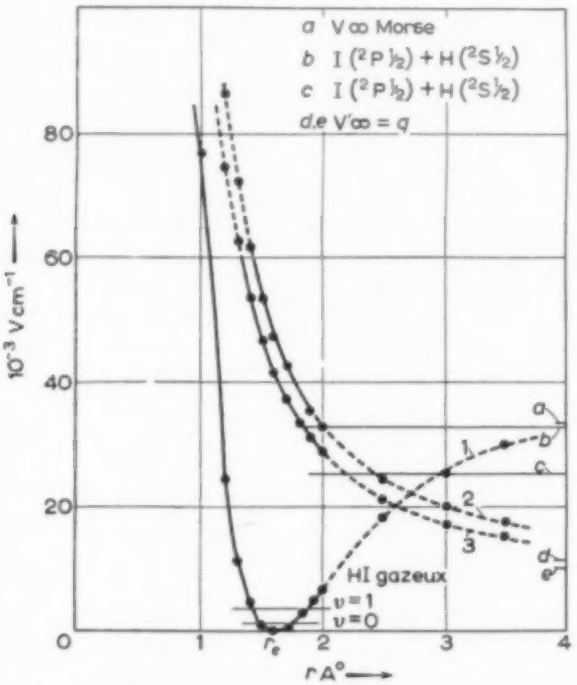

Fig. 15. Courbes d'énergie potentielle de la molécule d'acide iodhydrique.

On observe dans le spectre de la vapeur un système de bandes diffuses qui se groupent sur une courbe dont le maximum est 1990 Å. Ce système se déplace de 1970 cm^{-1} vers les basses fréquences. Le maximum n'existe plus pour le solide, probablement par suite d'une bande voisine, très aplatie, et dont le maximum est vers 1920 Å. Si l'on admet qu'elle correspond à la bande de 1780 Å de la vapeur, cette dernière subirait un déplacement de 4100 cm^{-1} vers les basses fréquences. Le comportement nettement différent de ces deux bandes lors de la condensation montre que deux transitions différentes interviennent. La bande de 1780 Å se déplace et se déforme beaucoup; les bandes diffuses de 1990 Å se déplacent sans beaucoup se déformer. L'effet des perturbations est maximum pour l'état le plus excité ainsi qu'on pourrait l'escompter. Enfin les bandes étroites qui se trouvaient

dans la région de 1790 Å pour la vapeur ont disparu. Ceci constitue un argument en faveur de leur indépendance par rapport à la bande continue de 1780 Å.

Un troisième cas se présente lorsque la molécule étudiée s'associe à l'état condensé. Ainsi le spectre de l'oxyde azotique solide à 20°K [56] est absolument différent de celui de la vapeur. Il se compose d'une unique bande continue, dont le maximum se trouve à 2100 Å environ. On n'observe aucune trace des divers systèmes de bandes électroniques du gaz. Différentes considérations conduisent à attribuer cette bande continue à la molécule associée. De même dans le cas de l'oxygène solide à 20°K [57] (figure 7) il est difficile d'expliquer les différences relativement importantes entre les spectres des deux états sans tenir compte de l'association de l'oxygène en molécules O_4.

Enfin dans le cas de l'oxyde azoteux solide nous avons observé un phénomène particulier [55]. Les mesures sont médiocres et peu reproductibles dans la région 2000–2400 Å. On observe un changement de pente brusque de la courbe d'absorption et une variation anormale de l'absorption avec l'épaisseur de la couche. Par irradiation l'absorption augmente dans cette région avec parfois un maximum vers 2120 Å. L'ensemble de ces phénomènes nous a suggéré que cette absorption pouvait être due à un produit de dissociation de l'oxyde azoteux, dont la formation et la teneur dépendraient essentiellement des conditions d'évolution de la couche. D'après la position de cette bande on peut supposer que ce produit peut être l'oxyde azotique (maximum à 2100 Å comme nous l'avons vu, plus haut). Nous aurions donc à côté du processus de décomposition photochimique de N_2O généralement admis:

$$N_2O \rightarrow N_2 + O - 89{,}5 \text{ kc}$$

$$O + O \rightarrow O_2 + 58{,}2 \text{ kc}$$

le processus secondaire:

$$O + N_2O \rightarrow 2NO + 35{,}2 \text{ kc}$$

(C) Les mesures d'absorption des gaz et vapeurs dans la région de courte longueur de l'ultraviolet lointain (de 1100 Å aux rayons X) sont encore peu nombreuses à cause des difficultés expérimentales. Néanmoins elles présentent un grand intérêt par suite de l'observation des phénomènes de photoionisation, et par les données qu'elles peuvent apporter à la connaissance des processus physicochimiques intéressant la haute atmosphère.

L'emploi d'une source de spectre continu est difficile dans l'ultraviolet extrême, mais on peut espérer obtenir une approximation satisfaisante de la courbe d'absorption (tout au moins du continu) en utilisant une source émettant des raies nombreuses et rapprochées. Ainsi Weissler et ses collaborateurs ont étudié jusqu'à 400 Å les spectres d'absorption des gaz suivants: oxygène, hydrogène, azote, argon, oxyde de carbone, anhydride carbonique, ammoniac, méthane etc . . . [94, 95, 96].

En utilisant un spectrographe à réseau en incidence rasante, les spectres d'absorption de l'oxyde azoteux, de l'oxyde azotique et la vapeur d'eau ont pu être étudiés par N. Astoin jusqu'à 170 Å [97, 98, 99]. Un certain nombre de potentiels d'ionisation ont pu être mis en évidence spectroscopiquement par

VOL. 8 1956/5

l'observation d'une discontinuité dans le spectre d'absorption continu qui accompagne le spectre de bandes. Les potentiels ainsi observés sont en accord avec les prévisions théoriques ou les autres observations (impacts d'électrons).

A titre d'exemple la figure 16 représente la courbe d'absorption de la vapeur d'eau dans l'ultraviolet extrême [99]. On remarquera les discontinuités d'absorption vers 270.000 cm^{-1} — (33,4 eV), 200.000 cm^{-1} (24,2 eV), 135.000 cm^{-1} (16,7 eV), en accord avec les quatrième, troisième et second potentiels d'ionisation.

L'étude de la photoionisation peut être effectuée directement par la mesure des courants de photoionisation. Signalons les mesures de WEISSLER [100] qui, à

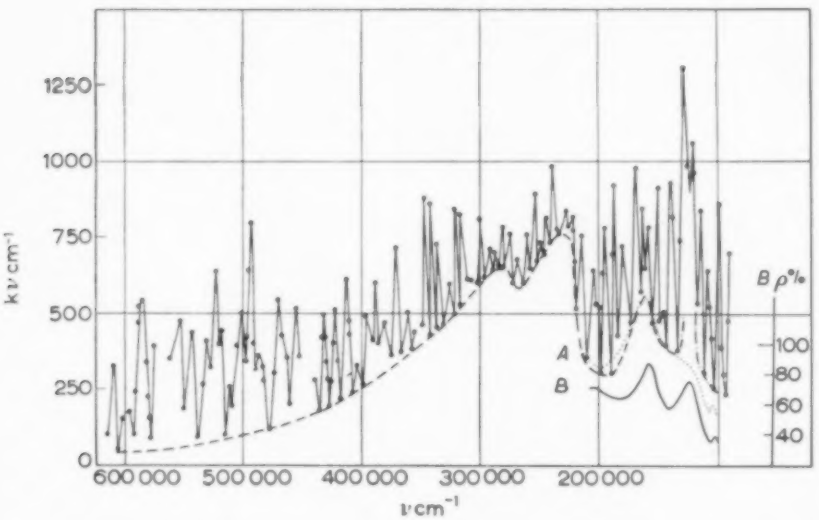

Fig. 16. Courbe d'absorption de la vapeur d'eau dans l'ultraviolet extrême. Les courbes A et B sont déduites des résultats publiés par WAINFAN, WALKER et WEISSLER pour les sections droites (A) et les rendements de photoionisation (B).

l'aide de deux chambres d'ionisation séparées, a pu étudier les rendements de photoionisation d'un certain nombre de gaz en dessous de 1100 Å.

(D) La spectrochimie d'absorption dans l'ultraviolet lointain est susceptible d'importantes applications analytiques. En effet dans cette région spectrale toutes les substances absorbent, en général de façon intense et sélective. Signalons les bandes intenses observées dans les spectres des corps présentant des doubles liaisons [101, 104]. Le benzène par exemple, peut être détecté par son absorption intense dans la bande de 1790 Å ($K_N = 3800$ pour ce maximum) [53]; Un détecteur de fuite dans les appareils à vide qui utilise cette absorption a été proposé [105]. Les raies de résonance des gaz rares présentent également des absorptions considérables [96, 105, 106]. De même les séries de RYDBERG observées dans l'ultraviolet lointain, par exemple sur la vapeur d'eau [107] pourraient également être utilisées à des fins analytiques. Ces raies sont voisines de celles de l'oxygène atomique, on pourrait ainsi doser les atomes d'oxygène engagés dans des

molécules, et même peut être par le déplacement des raies observées caractériser le type de liaison auquel participent ces atomes.

Il ne semble pas que, actuellement, toutes ces possibilités soient exploitées, mais l'avenir verra certainement leur développement s'étendre de plus en plus.

12. Conclusion

Dans le cadre de ce bref exposé, destiné à compléter les articles d'ensemble déjà publiés sur l'ultraviolet lointain, nous nous sommes particulièrement attachés à décrire les grandes lignes des méthodes expérimentales; nous avons également donné quelques considérations d'intérêt plutôt théorique sur les spectres d'absorption. Ceci ne doit pas faire oublier l'intérêt pratique de cette région spectrale au point de vue analytique. Il suffit de rappeler que toutes les substances y absorbent et généralement d'une manière fort sélective. Enfin l'analyse spectrochimique d'émission semble devoir y trouver de nouvelles possibilités, comme nous l'avons vu plus haut.

Bibliographie

[1] Lyman T. *The Spectroscopy of the Extreme Ultraviolet*, Longmans, Green and Co, London, 1928.
[2] Bomke H. *Vakuumspektroskopie*, J. A. Barth, Leipzig, 1937.
[3] Boyce J. C. *Rev. Mod. Phys.* 1941 **13** 1.
[4] Platt J. R. et Klevens H. B. *Rev. Mod. Phys.* 1944 **16** 182.
[5] Price W. C. *Reports on Progress in Phys.* 1951 **14** 1.
[6] Vodar B. et Romand J. *Mikrochimica Acta* 1955 no. 2–3 429.
[7] Inn E. C. Y. *Spectrochim. Acta* 1955 **7** 65.
[8] Hartman P. L. et Tomboulian D. H. *Phys. Rev.* 1953 **91** 1577.
[9] Johnston R. W. et Tomboulian D. H. *Phys. Rev.* 1954 **94** 1585.
[10] Collins G. et Price W. C. *Rev. Sci. Instrum.* 1934 **5** 423.
[11] Worley R. E. *Rev. Sci. Instrum.* 1942 **13** 67.
[12] Garton W. R. S. *J. Sci. Instrum.* 1953 **30** 119.
[13] Romand J. et Vodar B. *C.R. Acad. Sci. Paris* 1947 **225** 574.
[14] Romand J., Balloffet Mlle G., et Vodar B. *C.R. Acad. Sci. Paris* 1955 **240** 412.
[15] Robin Mme S., Robin S, et Vodar B. *J. Phys. Radium* 1952 **13** 671.
[16] Robin Mme S. *Rev. Optique* 1954 **33** 193.
[17] Tanaka Y. et Zelikoff M. *J. Opt. Soc. Amer.* 1954 **44** 254.
[18] Tanaka Y. *J. Opt. Soc. Amer.* 1955 **45** 710.
[19] Wilkinson P. G. *J. Opt. Soc. Amer.* 1955 **45** 1044.
[20] Bloch L. et E. *J. Phys. Radium.* 1925 **6** 105.
[21] Servant R. *Ann. Physique Paris* 1939 **12** 424.
[22] Bills K. M. *Communication au Congrès de Spectroscopie de Munster (Allemagne). Septembre* 1953.
[23] Shenstone A. G. *J. Opt. Soc. Amer.* 1954 **44** 749.
[24] Wahr J. C., McCormick W. W. et Sawyer R. A. *J. Opt. Soc. Amer.* 1953 **43** 151.
[25] Weissler G. L. et Po Lee *J. Opt. Soc. Amer.* 1952 **42** 80.
[26] Po Lee et Weissler G. L. *J. Opt. Soc. Amer.* 1952 **42** 200.
[27] Po Lee et Weissler G. L. *J. Opt. Soc. Amer.* 1953 **43** 512.
[28] Po Lee *J. Opt. Soc. Amer.* 1955 **45** 703.
[29] Ditchburn R. W. *Proc. Roy. Soc.* 1955 **229** 44.
[30] Vodar B. et Astoin Mlle N. *Nature* 1950 **166** 1029.
[31] Astoin Mlle N. *C.R. Acad. Sci. Paris* 1952 **234** 2050.
[32] Astoin Mlle N. et Vodar B. *J. Phys. Radium* 1953 **14** 494.
[33] Romand J. et Balloffet Mlle G. *J. Phys. Radium* 1955 **16** 489.
[34] Bockasten K. *Ark. för Fysik* 1955 **9** 457.

[35] Balloffet Mlle G. et Romand J. *J. Phys. Radium.* 1955 **16** 490.
[36] Romand J. et Balloffet Mlle G. *Communication au 18 ème Congrès du G.A.M.S. (Paris Juin* 1955) (en cours d'impression).
[37] Balloffet Mlle G. Diplôme d'Etudes Supérieures, Paris 1955.
[38] Balloffet Mlle G. et Romand J. *C.R. Acad. Sci. Paris* 1956 **242** 2333.
[39] Schwetzoff V., Robin Mme S., et Vodar B. *C.R. Acad. Sci. Paris* 1952 **234** 426.
[40] Schwetzoff V. et Robin Mme S. *C.R. Acad. Sci. Paris* 1952 **234** 316.
[41] Schwetzoff V. *Rev. Gen. Elec.* 1954 **63** 71.
[42] Piore E. R., Harvey G. G., György E. M., et Kingston R. H. *Rev. Sci. Instrum.* 1952 **23** 8.
[43] Schwetzoff V., Robin Mme S., et Vodar B. *J. Phys. Radium* 1952 **13** 369.
[44] Romand J. *Ann. Phys. Paris* 1949 **4** 529.
[45] Johannin-Gilles Mme A. *J. Rech. C.N.R.S. Bellevue* 1955, no. 31 205.
[46] Johannin-Gilles Mme A. *C.R. Acad. Sci. Paris* 1953 **236** 676.
[47] Johannin-Gilles Mme A. *C.R. Acad. Sci. Paris* 1953 **236** 1345.
[48] Gilles Mlle A., Bauple R., Romand J., et Vodar B. *C.R. Acad. Sci. Paris* 1949 **229** 876
[49] Gilles Mlle A. *C.R. Acad. Sci. Paris* 1952 **234** 822.
[50] Gilles Mlle A. *J. Phys. Rad.* 1952 **13** 247.
[51] Thomas H. *Ann. der Phys.* 1940 **38** 604.
[52] Romand J. et Vodar B. *J. Phys. Rad.* 1951 **12** 631.
[53] Romand J. et Vodar B. *C.R. Acad. Sci. Paris* 1951 **233** 930.
[54] Romand J. et Granier-Mayence Mme J. *C.R. Acad. Sci. Paris* 1952 **235** 1023.
[55] Granier-Mayence Mme J. et Romand J. *J. Phys. Rad.* 1953 **14** 428.
[56] Granier-Mayence Mme J. et Romand J. *C.R. Acad. Sci. Paris* 1953 **236** 1148.
[57] Romand J. et Granier-Mayence Mme J. *J. Phys. Rad.* 1954 **15** 62.
[58] Robin S. et Romand J. *C.R. Acad. Sci. Paris.* 1950 **231** 1455.
[59] Robin S., Romand J., et Oksengorn B. *C.R. Acad. Sci. Paris* 1950 **231** 689.
[60] Astoin Mlle N. et Vodar B. *J. Phys. Rad.* 1953 **14** 424.
[61] Ditchburn R. W. *Proc. Roy. Soc.* 1955 **229** 48.
[62] Weissler G. L., Po Lee et Mohr I. *J. Opt. Soc. Amer.* 1952 **42** 84.
[63] Ditchburn R. W. et Heddle D. W. O. *Proc. Roy. Soc.* 1953 **220** 61.
[64] Hammond V. J. et Price W. C. *J. Sci. Instrum.* 1954 **31** 104.
[65] Hinteregger H. E. et Watanabe K. *J. Opt. Soc. Amer.* 1953 **43** 604.
[66] Friedman H., Lichtman S. W., et Byram E. T. *Phys. Rev.* 1951 **83** 1025.
[67] Byram E. T., Chubb T., Friedman H., et Gailar N. *Phys. Rev.* 1953 **91** 1278.
[68] Chubb T. A. et Friedman H. *Rev. Sci. Instrum.* 1955 **26** 493.
[69] Astoin Mlle N., Vodar B., et Romand J. *J. Phys. Radium* 1955 **16** 491.
[70] Terrien J. *Rev. Optique* 1937 **16** 343.
[71] Johnson F. S., Watanabe K., et Tousey R. *J. Opt. Soc. Amer.* 1951 **41** 702.
[72] Robin Mme S. et Vodar B. *J. Phys. Radium* 1951 **12** 634.
[73] Packer D. M. et Lock C. *J. Opt. Sod. Amer.* 1951 **41** 699.
[74] Robin Mme S. *J. Phys. Radium* 1953 **14** 551.
[75] Namioka T. *Sci. of Light* 1954 **3** 15.
[76] Robin Mme S. et Vodar B. *J. Phys. Radium* 1952 **13** 492.
[77] Fabre D. Diplôme d'Etudes Supérieures Paris 1956.
[78] Fabre D. et Romand J. *C.R. Acad. Sci. Paris* 1956 **242** 893.
[79] Kandare S. et Fabre D. *C.R. Acad. Paris* 1956 **242** 1150.
[80] Robin Mme S. *Rev. Optique* 1954 **33** 377.
[81] Robin Mme S. *J. Phys. Radium* 1952 **13** 493.
[82] Gibson G. E., Rice O. K., et Bayliss N. S. *Phys. Rev.* 1933 **44** 193.
[83] Vodar B. *J. Phys. Radium* 1948 **9** 166.
[84] Goodeve C. F. et Taylor A. W. C. *Proc. Roy. Soc.* 1935 **152** 221.
[85] Goodeve C. F. et Taylor A. W. C. *Proc. Roy. Soc.* 1936 **154** 181.
[86] Fink P. et Goodeve C. F. *Proc. Roy Soc.* 1937 **163** 592.
[87] Porret D. et Goodeve C. F. *Proc. Roy. Soc.* 1938 **165** 31.

[88] ROMAND J. et VODAR B. *C.R. Acad. Sci. Paris* 1948 **226** 2062.
[89] ROMAND J. *C.R. Acad. Sci. Paris* 1948 **227** 117.
[90] ROMAND J. et MAYENCE Mlle J. *C.R. Acad. Sci. Paris* 1949 **228** 998.
[91] MAYENCE Mlle J. *Ann. Physique Paris* 1952 **7** 453.
[92] ROMAND J. et GRANIER-MAYENCE Mme J. *C.R. Acad. Sci. Paris* 1952 **234** 824.
[93] STEARN A. E. et EYRING H. *J. Chem. Phys.* 1935 **3** 778.
[94] SUN H. et WEISSLER G. L. *J. Chem. Phys.* 1955 **23** 1160.
[95] EHLER A. W. et WEISSLER G. L. *J. Opt. Soc. Amer.* 1955 **45** 1035.
[96] PO LEE et WEISSLER G. L. *Phys. Rev.* 1955 **99** 540.
[97] ASTOIN Mlle N. et GRANIER-MAYENCE Mme J. *C.R. Acad. Sci. Paris* 1955 **241** 1736.
[98] GRANIER-MAYENCE Mme J. et ASTOIN N. Melle *C.R. Acad. Sci. Paris* 1956 **242** 1431.
[99] ASTOIN Mlle N. *C.R. Acad. Sci. Paris* 1956 **242** 2327.
[100] WAINFAN N., WALKER W. C. et WEISSLER G. L. *Phys. Rev.* 1955 **99** 542.
[101] PRICE W. C. et TUTTE W. T. *Proc. Roy. Soc.* 1940 **174** 207.
[102] WALSH A. D. *Trans. Faraday Soc.* 1946 **42** 779.
[103] PRICE W. C. et WALSH A. D. *Proc. Roy. Soc.* 1946 **185** 182 et 1947 **191** 22.
[104] WALSH A. D. *Proc. Roy. Soc.* 1947 **191** 32.
[105] ROMAND J., SCHWETZOFF V., et VODAR B. *Le Vide* 1951 n° 34–35 1046.
[106] PO LEE et WEISSLER G. L. *Proc. Roy. Soc.* 1953 **220** 71.
[107] PRICE W. C. *J. Chem. Phys.* 1936 **4** 146–539–547.

VOL.
8
1956/5

Spectrochimica Acta, 1956, Vol. 8, pp. 249 to 261. Pergamon Press Ltd., London

The infra-red absorption bands associated with the COOH and COOD groups in dimeric carboxylic acid—II

The region from 3700 to 1500 cm^{-1}

S. Bratož,* D. Hadži,* and N. Sheppard†

(*Received June* 1956)

Abstract—The infra-red spectra of a number of dimeric carboxylic acids and their deutero (COOD) analogues have been investigated in the region of 3700 to 1500 cm^{-1}. The substances were studied in the vapour, liquid, and crystalline solid states, and in solution in carbon tetrachloride. In some cases observations were made over a range of temperature which extended down to that of liquid air. Particular attention was paid to the main broad νOH (νOD) absorption regions centred at 3000 cm^{-1} (2300 cm^{-1}) and also to the weaker satellite bands to lower frequencies centred near 2650 cm^{-1} (2100 cm^{-1}). The structure of the satellite bands, the presence of intensity submaxima on the main νOH (νOD) bands, and the general differences in appearance of the νOH and νOD absorption regions have been shown to be reasonably explicable in terms of combination, mostly summation, frequencies involving lower-frequency fundamentals of the COOH (COOD) groups. The summation bands are probably enhanced in intensity by Fermi resonance with the fundamentals responsible for the main νOH (νOD) absorption regions.

Introduction

An investigation of the infra-red spectra of a number of carboxylic acids in the dimeric state $(R{\cdot}COOH)_2$, was reported by Hadži and Sheppard [1] for the frequency range 1500 to 500 cm^{-1}. In this communication the experimental results obtained in the region 3700 to 1500 cm^{-1} are presented and discussed.

The most prominent feature attributable to the COOH group in this region is the strong and very broad band, of half-width about 500 cm^{-1}, centred near 3000 cm^{-1}. This is caused by the stretching vibration of the OH bond (νOH), as has previously been discussed by Davies and Sutherland [2] and Buswell, Rodebush, and Roy [3]. A less intense band centred near 2650 cm^{-1} with a narrower half-width appears consistently as a satellite on the low-frequency side of the main νOH band. This subsidiary band overlaps to some extent the νOH band, but its separate existence is clear when the overall contours of this absorption region is considered, such as is observed directly when the spectra are run under fairly low resolution, [4]. Under higher resolution both the main and satellite bands are found to have a number of sharper subsidiary absorption maxima associated with them as shown in the figures. Several attempts have previously been made to interpret the breadth and the submaxima of these bands (see later discussion) but no generally acceptable explanation has as yet been proposed. The principal aim of the present work was to investigate these absorption bands over as wide a range of experimental conditions as possible

* Kemični Inštitut "Borisa Kidriča," and the University Chemical Laboratory, Ljubljana, Yugoslavia.
† Department of Colloid Science, The University, Cambridge, England

and to reconsider their interpretation. A number of different acids have been studied, many of them in several of the physical states, viz. vapour, liquid, and crystalline solid, and in solution in carbon tetrachloride. In a few cases measurements were made over a wide range of temperatures. The analogous absorption bands of the CO∩D group* have also been studied in a number of cases.

Other prominent features of these spectra of the acids in the region investigated are the bands usually centred in the range 1720 ± 30 cm^{-1} caused by the stretching vibration of the C=O bonds (νC=O) of the dimeric units. These bands are much sharper than these due to the νOH vibrations and they have half-widths of 50 cm^{-1} or less. This paper adds little to the existing data on these bands.

Experimental

Thoroughly dried carboxylic acids of analytical grade were used without further purification. The solution spectra were taken in carbon tetrachloride which had been dried by refluxing over phosphorus pentoxide. The preparation of the D acids has been described in Part I. The majority of the spectra were obtained with a Perkin-Elmer 21 double-beam spectrometer equipped with prisms of LiF and NaCl. A few of the spectra of the D acids were studied with an Hilger D-209 spectrometer, using a CaF_2 prism. Low temperature spectra were obtained in a simple vacuum-jacketed cell using liquid air as the refrigerant. The spectra obtained are shown in Figs. 1 to 4, and the detailed frequencies of a selection of the acids are listed below. The experimental data are in good general agreement with those published previously [1, 2, 4-11] although in a few cases the presence of a number of the weaker submaxima previously reported in the 3500 to 2500 cm^{-1} region has not been confirmed (compare references [6] and [7]).

The observed frequencies in cm^{-1} of the absorption bands between 3700 and 1600 cm^{-1} of a number of the acids are listed below; the more prominent features of the spectra are *italicized*.

Formic acid: (*vapour*) *3581*, *3543*, 3385, 3290, 3196, 3137, *3106*, 3055, *3015*, *2942*, *2876*, 2808, 2765, 2721, *2611*, *2568*, 2423, *1793*, *1779*, *1749*.
(*Solution, 0·003 M in CCl_4*) *3509*, 3350, 3175, 3120, *3077*, *2994*, *2941*, *2857*, 2804, 2778, 2755, 2721, *2606*, *2564*, 2410, *1756*, *1724*.
(*liquid*) *3150* (broad), 2950, 2700, 2560, 2339, *1727*,
(*crystal at C −150°*) *2890*, *2703*, *2538*, 2326, 2123, 1890, 1764, *1613*.

Acetic acid: (*vapour*) *3571*, 3125, 3067, *3021*, 2940, 2777, 2702, *2632*, *2564*, *1783*, *1730*.
(*solution, 0·003 M in CCl_4*) *3527*, 3170, 3100, *3008*, *2924*, 2841, 2793, *2684*, *2632*, *2554*, *1768*, *1718*.
(*liquid*) ~ 3080, *2941*, 2793, *2688*, *2632*, *2561*, 1759, *1718*.
(*crystal at −150°C*) *2924*, 2820, *2674*, *2618*, 2538, 2169, 1802, 1764, *1658*, 1645.

Dichloroacetic acid: (*solution, 0·004 M in CCl_4*) *3509*, 3115, *3003*, 2915, *2681*, 2600, *1786*, *1742*.
(*liquid*) *3115*, 3021, 2688, 2604, 2342, *1799*, *1739*.

Trichloroacetic acid: (*solution, 0·004 M in CCl_4*) *3502*, 3150, *3096*, *3030*, 2882, *2627*, *2494*, *1789*, *1745*.
(*liquid*) *3120*, 3059, 2890, *2604*, 2481, *1742*.
(*crystal*) 3106, *3012*, 2882, *2631*, 2494, *1742*.

Benzoic acid: (*solution 0·003 M in CCl_4*) *3521*, 3077, *3007*, *2878*, *2667*, 2601, *2547*, 1741, *1698*.
(*liquid*) *3012*, *2890*, *2653*, *2564*, *1700*.
(*crystal*) 3077, *3003*, 2890, *2833*, *2681*, 2617, *2571*, 1792, *1689*.

Formic acid D: (*vapour*) *2940*, 2312, *2299*, 2262, 2229, *2075*.

Acetic acid D: (*vapour*) *2941*, 2632, 2370, *2283*, *2128*, *2083*, 1934, *1795*, *1733*.
(*liquid*) 2900, 2370, *2270*, 2130, 2060, *1710*.

* The acids containing COOD groups will be subsequently referred to collectively as D acids, or individually as acetic acid D, benzoic acid D etc.

VOL. 8 1956/5

Trichloroacetic acid D: (*crystal*) 2860, 2625, 2385(P) *2258*, 2180, 2150, *2090*, 1983, 1870, *1750*.
Benzoic acid D: (*solution, 0·003 M in CCl_4*) 3067, *2242*, 2170, *2083*, 1969, 1912, 1739, *1695*.
(*crystal*) 3067, *2240*, 2173, *2070*, 1910, 1853, *1680*.

The spectroscopic results

The collected spectra (Figs. 1–4) show a number of similarities which are independent of the particular acid studied. These are listed as follows.

(1) The νOH and νC=O absorption bands characteristic of dimeric units dominate the spectra in nearly all cases, irrespective of the physical state of the substance under investigation. Only the spectra of formic acid and acetic acid

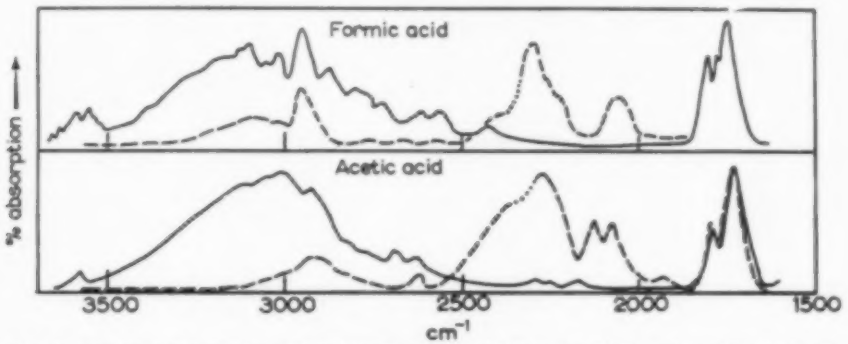

Fig. 1. The infra-red spectra of formic acid, acetic acid, formic acid D, and acetic acid D (D acids dashed curves) in the vapour state at room temperature. Dotted portions of the curves indicate regions of interference due to atmospheric absorption.

in the solid state are exceptional: these show νC=O bands at abnormally low frequencies. However, HOLTZBERG, POST, and FANKUCHEN [12] have shown that the hydrogen bonding is polymeric rather than dimeric in solid formic acid; this may be the cause of the unusual spectroscopic behaviour of both of the above acids.

It is important to note that all the characteristic features, e.g breadth and submaxima, of the νOH region of the spectra of the acids persist in the vapour phase, i.e. they must be explicable in terms of a quantum-mechanical treatment of the dimeric unit alone.

(2) Owing to the occurrence of a certain fraction of monomeric acid molecules in the vapour phase and in solution in carbon tetrachloride, the spectrum obtained under these conditions shows extra sharp and weak absorption bands corresponding to the νOH and νC=O vibrations of the single molecules [2,9]. In solution these have frequencies near 3500 cm^{-1} (νOH) and in the range 1770 ± 30 cm^{-1} (νC=O); in the vapour phase the frequencies are somewhat higher. These bands of formic acid vapour are resolved as doublets because of the presence of relatively widely spaced rotational fine structure [13].

(3) Most of the spectra show fairly sharp absorption bands due to νCH vibrations in the regions 3000 — 2800 cm^{-1} (aliphatic acids) or 3100 — 2900 cm^{-1} (aromatic acids). These are superimposed on the broad νOH bands. As is to be expected, they are strong in the spectra of acids containing considerable numbers

of CH groups. They are also relatively more prominent in the vapour and solution spectra where the strength of the dimeric νOH absorption is diminished (see Section 2 above).

(4) The subsidiary absorption maxima associated with both the main νOH band near 3000 cm^{-1} and the satellite band near 2700 cm^{-1} are less pronounced

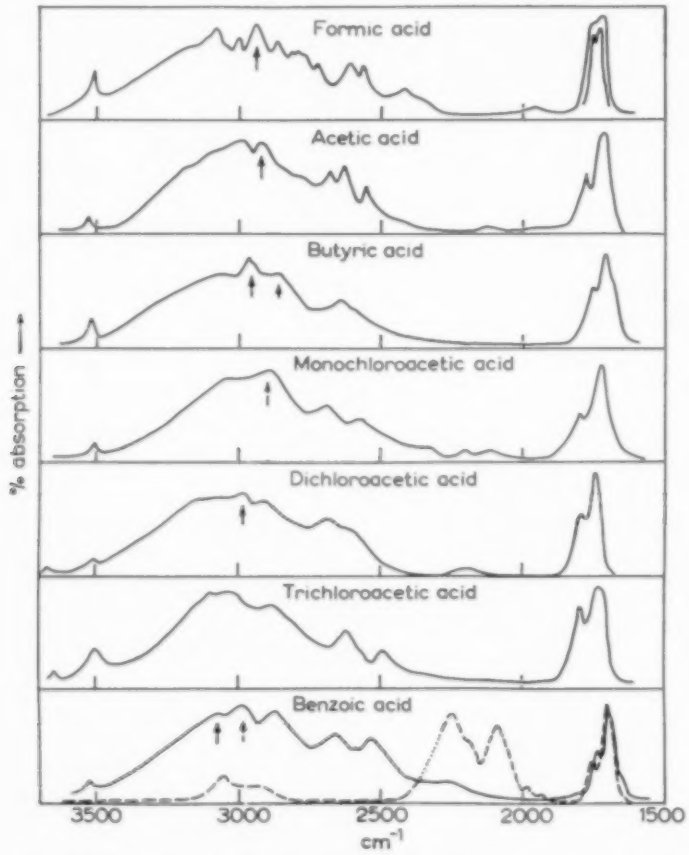

Fig. 2. The infra-red spectra of a number of carboxylic acids (D-acid spectra, dashed curves) in solution in carbon tetrachloride (concentration 0·003 to 0·004 molar, cell thickness 2 mm). Arrows indicate νCH bands.

(i.e. the main bands exhibit the smoothest overall contours) in the spectra of the liquids. The νOH band usually also extends to somewhat higher frequencies in in the liquid-state spectra as shown earlier by Shubin [4]. These additional broadening phenomena are probably the result of intermolecular forces between a given dimer and its differently oriented neighbours in the liquid.

(5) Many of the weaker absorption bands are relatively more prominent in the spectra of the solids. This is an optical phenomenon often encountered in the study of the spectra of polycrystalline materials.

VOL. 8 1956/5

(6) The spectra of *n*-butyric acid and dichloroacetic acid were obtained as liquids at room temperature and as solids near liquid-air temperature. In the case of *n*-butyric acid the low-temperature spectrum is similar to that of the liquid except that some contraction occurs at the high-frequency end of the

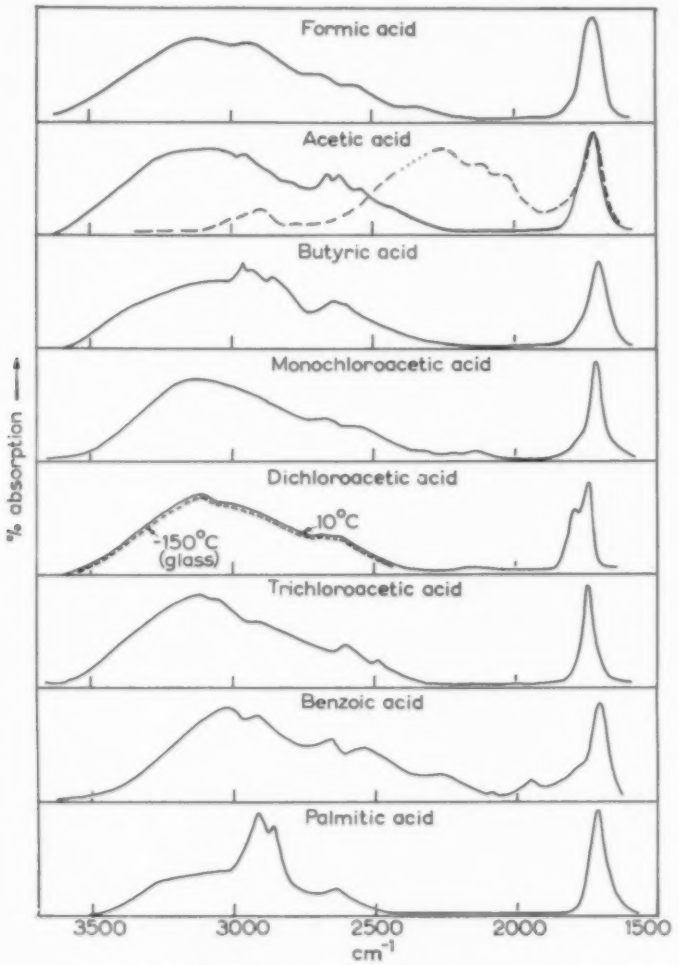

Fig. 3. The infra-red spectra of a number of carboxylic acids (D-acid spectra, dashed curves) in the liquid phase.

broad νOH band. No change is observed in the spectrum of dichloroacetic acid at low temperature, perhaps because the liquid has frozen into a disordered glass rather than a crystalline solid. However, in neither of these cases does any consistent or marked change occur in the relative intensities of absorption maxima of the νOH or satellite bands on lowering the temperature. This is also true for the dimer band of acetic acid which has been studied in the vapour phase between 20°C and 150°C (spectra not illustrated). Formic acid and acetic acid do show

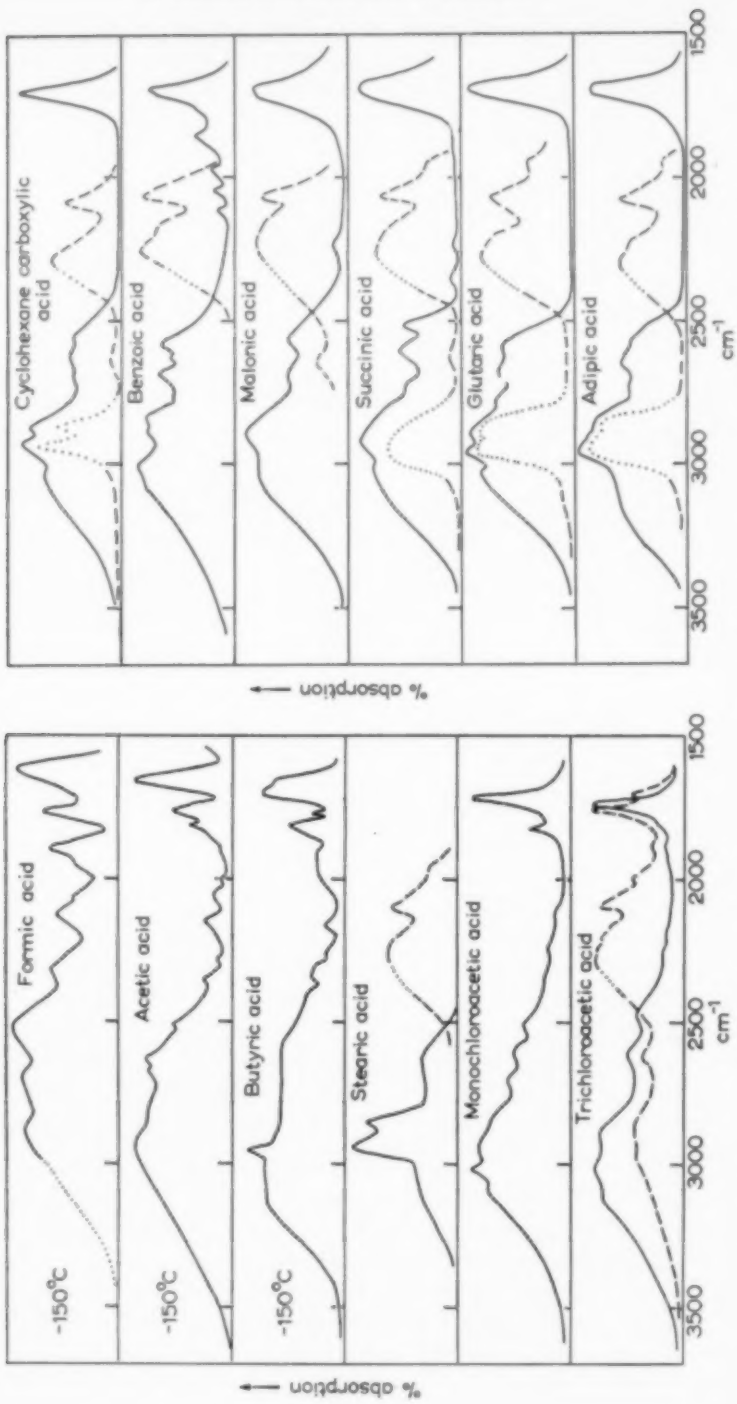

Fig. 4 (*a and b*) The infra-red spectra of a number of carboxylic acids in the crystalline phase (D-acid spectra, dashed curves). Dotted portions of the curves indicate regions of interference due to atmospheric absorption, or to the Nujol mulling agent.

VOL.
8
1956/5

some changes in the νOH region on solidification at low temperatures but, as mentioned in Section 1, the changes in the νC=O region indicate probable alterations in the type of hydrogen bonding.

(7) If polarized infra-red radiation is used on crystalline specimens, it is found that the whole of the broad νOH band has the same polarization properties [14, 15].

(8) In the spectrum of the dimeric D acids the νOD band near 2300 cm^{-1} is also accompanied by a satellite band at lower frequencies (*ca.* 2100 cm^{-1}). The main νOD band is considerably broader than its satellite, the approximate half-widths being 200—250 cm^{-1} and ~100 cm^{-1} respectively compared with 500 and *ca.* 250 cm^{-1} for the analogous OH bands. The overall width of the absorption band due to OD is markedly less than that for OH, as shown by WALL and CLAUSSEN [5] in the case of benzoic acid.

(9) The sharpness of the sub-maxima of the satellite band in the spectra of the H acids varies with the nature of the substituent group, R. They are particularly broad and poorly resolved when the COOH group is attached either to a long hydrocarbon chain or to a saturated alicyclic ring.

Interpretation of the spectra

The discussion will be confined principally to the νOH (and νOD) bands and their satellites at lower frequencies. Two phenomena require separate comment, viz. the origin of the satellite bands, and the cause of the subsidiary absorption maxima accompanying both the main νOH (and νOD) bands and their satellites. The intrinsic breadth of the main νOH (νOD) bands is also of interest, although it is a phenomenon of general occurrence in the spectra of hydrogen-bonded compounds.

1. The origin of the satellite band

This band occurs consistently in the region of 2700 cm^{-1} in the spectra of the COOH acids and near 2100 cm^{-1} in those of the D acids. Its occurrence is independent of the nature of the group R in the R·COOH (R·COOD) molecules. A number of possible explanations for this band can be put forward:

(α) It may be caused by the second νOH (νOD) fundamental of the dimeric unit;

(β) It may correspond to a difference frequency of the type $\nu\text{OH} - \nu'$, where ν' is a fundamental of approximate frequency 300 cm^{-1} (200 cm^{-1} for the COOD groups);

(γ) It may represent summation frequencies involving lower frequency fundamentals of the COOH (COOD) groups, perhaps brought up in intensity by Fermi resonance with the νOH (νOD) vibration.

Explanation (α) is ruled out by the fact that the second νOH fundamental, which is Raman active (and for a truly centrosymmetric dimer structure infra-red inactive), is observed in the region of 2900–3100 cm^{-1} [16, 17]. Explanation (β) leads to a number of predictions that are at variance with the experimental results. Thus a corresponding summation band $\nu\text{OH} + \nu'$ would be expected near 3300 cm^{-1} of greater strength than the 2700 cm^{-1} difference band; no such absorption is observed. Further, a difference band should be greatly reduced

in intensity at low temperatures because its intensity partly depends upon the Boltzmann factor exp $(-hc\nu'/kT)$. With $\nu' \sim 300$ cm^{-1} this factor should reduce the intensity of the satellite band by a factor of about 9 on passing from room temperature (300°K) to −150°C (∼120°K); no marked reduction in intensity of the band is actually observed on cooling (Figs. 3 and 4a).

Explanation (γ) implies that there should be two fundamentals of the COOH (COOD) dimeric grouping, whose summed frequencies approximate to 2700 cm^{-1} (2100 cm^{-1}). The lower-frequency COOH (COOD) fundamentals were discussed in Part I, where it was concluded that the COOH acids have characteristic frequencies near 1420 and 1300 cm^{-1} in the infra-red spectrum (coupled νC—O and δOH vibrations of symmetry B_u), and that the analogous Raman-active fundamentals of symmetry A_g have closely similar values. Combinations of B_u and A_g frequencies in pairs could give rise to summation frequencies in the region of 2700 cm^{-1} which might be enhanced in intensity in the observed spectrum by Fermi resonance with the B_u νOH fundamental. For the D acids, the corresponding infra-red frequencies are near 1350 and 1050 cm^{-1} (νC—O and δOD respectively) and their Raman counterparts may be presumed to have similar values. In this case the combination of *ca.* 1050 cm^{-1} (B_u) and 1050 cm^{-1} (A_g) again gives a summation frequency near 2100 cm^{-1} of the same symmetry class as νOD in the correct position for the satellite band. Other combination frequencies might be expected in this case near 2400 and 2700 cm^{-1}; in a number of cases there are well-defined absorption maxima between 2300 and 2400 cm^{-1}, but not at 2700 cm^{-1}. However, the latter frequency may be too far removed from the νOD band for Fermi resonance to occur.

It can be concluded that this type of explanation of the satellite bands is in general agreement with the experimental facts. It is noteworthy that for both D and H acids, the summation frequencies which are assumed to interact strongly with the νOH (νOD) fundamentals involve δOH (δOD) vibrations.

2. An interpretation of the subsidiary maxima associated with the νOH (νOD) and satellite bands

An interpretation of the subsidiary maxima associated with the satellite bands readily follows from an extension of the reasons presented in Section 1 for the occurrence of the satellite bands as a whole. In this region (2500 to 2700 cm^{-1}) there are two, sometimes three, fairly prominent absorption peaks in the spectra of the H acids. The combination in pairs of the B_u and A_g fundamentals near 1420 and 1300 cm^{-1} can give four summation frequencies of the correct symmetry class, viz., one near 2800, two near 2700, and one near 2600 cm^{-1}. When allowance is made for anharmonicity these usually account for the observed absorption peaks without difficulty. For comparison, the lower-frequency fundamentals near 1350 and 1050 cm^{-1} of the D-acid spectra can give only one combination frequency, ($\sim 1050\, A_g + \sim 1050\, B_u$) near 2100 cm^{-1}. Usually there is only a single strong peak in the satellite region for the D-acid spectra. Acetic acid D (Fig. 1) and trifluoroacetic acid-D [8] are exceptional in that they appear to have doublet peaks on the satellite bands. In the latter case, however, it is

VOL. 8 1956/5

probable that combinations of the strong νC—F fundamentals contribute to the spectrum in this region.

It is of interest to consider the extent to which the summation-band hypothesis also accounts for the observed subsidiary maxima in the region of the main νOH (νOD) band. Table 1 gives the relevant frequencies and their proposed interpretation for a selection of molecules, particularly those for which infra-red and Raman low-frequency data are available for the same physical state. No Raman data appear to be available for the vapour state or for solutions in carbon tetrachloride; this is unfortunate, as it is often under these conditions that the most detail is discernible in the νOH and νOD bands. Nevertheless, an attempt has been made to analyse the particularly detailed νOH band of the formic-acid dimer as observed in solution, with the help of solution infra-red data and semi-schematic values for the A_g (Raman-active) fundamental frequencies.

In making an overall assessment of the agreement between the observed and calculated frequencies shown in Table 1, allowance must be made for the fact that the observed frequencies are often likely to be a few per cent lower than those calculated, because of the effect of anharmonicity. As the magnitude of these differences cannot be predicted in specific cases, the general result is to give more flexibility to the correlation procedure. However, even when this factor is taken into account it seems reasonable to conclude that the summation-band hypothesis does provide a satisfactory interpretation of the observed spectra; it is particularly successful in accounting for the position and appearance of the satellite bands. Only in the case of formic acid has it been necessary to consider

Table 1. An interpretation of the 3500–2000-cm^{-1} region of the carboxylic acid spectra in terms of fundamental and combination (summation) frequencies of the COOH or COOD groups.

(a) *Trichloroacetic acid (crystalline)*[a]

lower-frequency COOH fundamentals: (B_u) 1742, 1407[b], 1206; (A_g) (1689)[c], 1434, 1260.

3106(s)	1742 + 1434 = 3176
3012(s)	νOH
2882(s)	1260 + 1689 = 2949
2631(m)	1407 + 1260 = 2667
2494(m)	1260 + 1260 = 2520

(b) *Acetic acid (liquid)*[a, d]

lower-frequency COOH fundamentals: (B_u) 1718, 1412, 1290; (A_g) 1666, (1432), 1279.

~ 3080(s : bd)	νOH
2941(m)	νCH
2793(w)	1412 + 1432 = 2844
2688(m)	1290 + 1432 = 2722
2632(m)	1412 + 1279 = 2691
2561(w)	1290 + 1279 = 2569

(c) *Acetic acid D (liquid)*[a, f, g]

lower-frequency COOD fundamentals: (B_u) 1710, 1320, 1058; (A_g) 1656, 1325, 1102.

2900(m)	νCH
2370(m)	1058 + 1325 = 2383
2270(s)	νOD
2130(m)	1058 + 1102 = 2160
2060(m)	?

Table 1. (*contd.*)

(d) *Benzoic acid (crystalline)*[a, e]

lower frequency COOH fundamentals: (B_u) 1689, 1420, 1287; (A_g) 1637, 1441, 1314.

3077(*m*)	νCH
3003(*s*)	νOH (+ νCH)
2890(*m*)	1287 + 1637 = 2924
2833(*m*)	1420 + 1441 = 2861
2681(*m*)	1420 + 1314 = 2734 1287 + 1441 = 2728
2617(*w*)	?
2571(*m*)	1287 + 1314 = 2601

(e) *Benzoic acid D (crystalline)*[a, b]

lower-frequency fundamentals: (B_u) 1680, 1367, 1042; (A_g) (1630) (1390) (1070).

3067(*m*)	νCH
2240(*s*)	νOD
2173(*m*)	?
2070(*s*)	1042 + 1070 = 2112

(f) *Formic acid (solution)*[b, i]

lower-frequency fundamentals: (B_u) 1720, 1183, 1360, 1390 (δCH); (A_g) (1670), (1200), (1360), (1390), (δCH).

3350(*w*)	1724 + 1670 = 2394
3175(*w*)	?
3120(*w*)	1724 + 1390 = 3114
3077(*m*)	νOH
2994(*m*)	1360 + 1670 = 3030
2941(*s*)	νCH
2857(*m*)	1724 + 1200 = 2924
2804(*w*)	1183 + 1670 = 2853
2778(*w*)	1390 + 1390 = 2780
2755(*w*)	1390 + 1360 = 2750
2721(*w*)	1360 + 1360 = 2720
2606(*m*)	1390 + 1200 = 2590
2564(*m*)	1183 + 1390 = 2573

(*s*)—strong: (*m*)—medium: (*w*)—weak: (*bd*)—broad.

[a] Hadži and Sheppard, ref. (1).

[b] mean value from 1415, 1398 cm^{-1} doublet.

[c] taken from liquid-state data, [16].

[d] Kohlrausch K. W. F. *Ramanspektren*, Becker and Erler, Leipzig, 1943, p. 264.

[e] A_g frequencies are mean values from Bai K. S. *Proc. Ind. Acad. Sci.*, 1940 **A11** 212, and Herz G., Kahovec L. and Kohlrausch K. W. F. *Monatsh. Chem.*, 1943 **74** 253.

[f] Angus W. R. Leckie A. H. and Wilson C. L. *Proc. Roy. Soc.* 1936 **A155** 183.

[g] Engler W. *Zeit. phys. Chem.* 1936 **B32** 471; 1937 **B35** 433.

[h] A_g frequencies are estimated from relative values of B_u and A_g fundamentals of other acids.

[i] B_u fundamentals from Bratož and Hadži (unpublished work).

fundamentals other than those directly associated with the COOH (COOD) group in order to account for all the observed features in the complex spectra. It should be noted that the common polarization properties observed for the whole νOH band would be expected if all the submaxima are of the same symmetry class for Fermi resonance to occur with the fundamental νOH frequency.

Analogous explanations of extra absorption bands in the νNH region have been made for the amides by Newman and Badger [18], and for methylamine hydrochloride by Waldron [19]. Further, the νCH region in the spectra of

hydrocarbons commonly shows extra peaks due to Fermi resonance between νCH fundamentals and summation bands of the δCH type [20]. In connection with their study of the spectra of percarboxylic acids, GIGUÈRE and OLMOS [21] have previously given assignments of this type for some of the extra absorption peaks in the νOH region of the carboxylic acids. In doing so, however, they appear to have used low frequency fundamentals from both monomers and dimers.

Discussion

A number of alternative explanations of the submaxima of the νOH (νOD) absorption bands have been proposed in the literature. These are now discussed in relation to the present results.

Several authors have suggested that the breadth of the νOH band and the presence of submaxima are both caused by interaction between the νOH vibration and modes of much lower frequency in which the two molecules which constitute the dimer vibrate to and fro with respect to each other by stretching the hydrogen bonds, ν(OH . . . O) (see, for example, BADGER and BAUER [22]). In other cases, low-frequency angle-deformation vibrations involving the hydrogen bonds have also been invoked, δ(OH . . . O). The Russian authors STEPANOV [22,24] and BATUEV [25, 26] have proposed quantum-mechanical and classical models respectively for these interactions and their relative merits have been discussed [27]. On either of these formulations it is to be expected that series of submaxima might be found in the νOH region with a separation equal in frequency to the ν(OH . . . O) vibration, although STEPANOV visualizes that these may individually be broadened due to "predissociation" and blur together to form a single wide band. CHULANOVSKII and SIMOVA [7] appear to have been the first to apply these ideas specifically to the spectra of the carboxylic acids and to pick out and assign a series of bands of the type νOH + n ν(OH . . . O). DAVIES and EVANS [28] have also identified a series of submaxima in the spectrum of trichloroacetic acid [6] as representing νOH − n ν(OH . . . O) frequencies; in this latter case νOH signifies the stretching frequency of the OH bond under conditions of no hydrogen bonding. This formulation of the series as difference frequencies seems less likely as it would imply a marked temperature dependence of the spectrum (see earlier). FUSON and JOSIEN [8] have also listed series occurring in the spectra of several acids, but have interpreted them as being caused by a type of quantized hydrogen bonding. CHAPMAN [11] has picked out a regular series of submaxima in the spectrum of liquid formic acid, but could not make a similar analysis of the solid-state data.

A general criticism of these attempted analyses of the COOH bands is that the maxima chosen to form series are often weak and irregularly spaced, and a number of those listed [6, 7] are not confirmed in the present work. Furthermore there are no really dominating series immediately discernible in the spectra. This difficulty is illustrated by the fact that different authors among those mentioned above have picked out different series from very similar experimental data. Thus series spacings of approximately 200 cm^{-1} and 160 cm^{-1} have been proposed at different times for acetic acid, and of 210 and 100 cm^{-1} for trichloroacetic acid. Moreover, absorption bands additional to those assigned to the main

series are always observed; they have to be ascribed to the combination of νOH with δ(OH . . . O) frequencies [7].

This type of interpretation of the submaxima runs into particular difficulties when the experimental data for the D acids are considered. From these Fuson and Josien have picked out analogous series with spacings of about 100–120 cm^{-1}, i.e. about half in value of those found by the same authors in the COOH spectra. However, both the ν(OH . . . O) and δ(OH . . . O) vibration frequencies of the hydrogen bonds will depend mainly on the masses and moments of inertia of the whole monomer molecules that are vibrating with respect to each other. These frequencies should therefore be little changed by the substitution of one hydrogen atom by deuterium, a conclusion that is at variance with the experimental results. Fuson and Josien [8] state that the change in spacings of the submaxima in the COOH and COOD spectra is understandable on their quantized hydrogen-bond picture, but they have not explained in detail how this is so.

Another type of explanation of some of the submaxima in the νOH bands has been put forward by Buswell, Rodebush, and Roy [3], and by Wall and Claussen [5]. These authors point out that the structure of the νOH band in the infra-red spectrum of benzoic acid is more complex than that of the νOD band; in particular doublets in the νOH band become single bands in the νOD spectrum. They interpret the doublets as being possibly caused by the tunnelling motions of hydrogen atoms in the OH groups of the acid dimers from one equivalent position to another as below.

Such a phenomenon would give rise to splitting of the νOH energy levels into pairs, and hence to the occurrence of doublets in the spectrum. The splitting of the energy levels in such cases is very sensitive to the mass of the moving atom, and it would be expected to be much less in the case of D atoms; hence single unresolved bands may be observed. However, although the present experimental data for benzoic acid are in good agreement with those of the earlier workers, similar well-marked doublet to singlet changes do not occur consistently in the νOH—νOD spectra of other acids; it seems probable that the agreement found in the spectra of benzoic acid with predictions based on the tunnelling phenomenon is fortuitous. Kovner and Chuenkov [29] have discussed theoretically the effect of such tunnelling motions on the Raman-active νOH vibrations. Although this type of interaction is probably more effective than in the infra-red, the correlation between theoretical expectations and experimental results [17] is again unconvincing.

Conclusion

In contrast to the ideas discussed above, the summation-band hypothesis developed in this paper accounts in a satisfactory fashion for the observed pattern of submaxima. It should be noted, however, that this approach does not attempt to explain the great intrinsic breadth of the νOH and νOD bands as does the Stepanov hypothesis. It cannot be ruled out that the breadth of these bands, and also some of the submaxima, may be caused by interaction of the OH vibration

with ν(OH . . . O) and δ(OH . . . O) motions, but the observed spectroscopic phenomena do not appear to be wholly explicable on this basis. In particular the detailed structure of the satellite bands and the considerable differences in structure of the νOH and νOD absorption regions of the analogous acids are much more readily explicable on the summation-band hypothesis as developed here. It seems certain, at least, that this type of summation band plays an important rôle in the observed spectra.

Throughout the discussion it has been assumed that only those summation bands which might be enhanced in intensity by Fermi resonance are to be taken into account in interpreting the submaxima. However, if the νOH vibration is sufficiently anharmonic, summation frequencies of other symmetry classes could also be involved.

Acknowledgements—The first two authors would like to thank Professor PETERLIN of the Physics Institute of the Academy of Science and Arts, Ljubljana, for the gift of a sample of D_2O.

The other author (N. S.) is grateful to the Hydrocarbon Research Group of the Institute of Petroleum (London) for financial assistance of this work.

We are grateful to Dr. D. M. SIMPSON (Mrs. J. N. AGAR) for helpful discussions, and to Mr. C. G. CANNON of British Nylon Spinners for translations of the Russian articles [4, 27, 29].

References

[1] HADŽI D. and SHEPPARD N. *Proc. Roy. Soc.* 1953 **A216** 274.
[2] DAVIES M. M. and SUTHERLAND G. B. B. M. *J. Chem. Phys.* 1938 **6** 755.
[3] BUSWELL A. M. RODEBUSH W. H. and ROY M. F. *J. Amer. Chem. Soc.* 1938 **60** 2239.
[4] SHUBIN A. A. *Izvest. Akad. Nauk SSSR.* (Ser. Fiz.) 1950 **14** 442.
[5] WALL F. T. and CLAUSSEN W. F. *J. Amer. Chem. Soc.* 1939 **61** 2812.
[6] DAVIES M. M. *Trans. Faraday Soc.* 1940 **36** 1114.
[7] CHULANOVSKII V. M. and SIMOVA P. D. *Doklady Akad. Nauk SSSR.* 1949 **68** 1033.
[8] FUSON N. and JOSIEN M. L. *J. Optical Soc. Amer.* 1953 **43** 1102.
[9] GOULDEN J. D. S. *Spectrochim. Acta* 1954 **6** 129.
[10] FLETT M. St. C. *J. Chem. Soc.* 1951 962.
[11] CHAPMAN D. *J. Chem. Soc.* 1956 225.
[12] HOLTZBERG F. POST B. and FANKUCHEN I. *Acta Cryst.* 1953 **6** 127.
[13] WILLIAMS V. Z. *J. Chem. Phys.* 1947 **15** 232.
[14] MANN J. and THOMPSON H. W. *Proc. Roy. Soc.* 1948 **A192** 489.
[15] AMBROSE E. J. ELLIOTT A. and TEMPLE R. B. *Proc. Roy. Soc.* 1951 **A206** 192.
[16] SAKSENA B. D. *Proc. Ind. Acad. Sci.* A. 1940 **12** 312.
[17] BATUEV M. I. *Doklady Akad. Nauk. SSSR.* 1948 **59** 1117.
[18] NEWMAN R. and BADGER R. M. *J. Chem. Phys.* 1951 **19** 1147.
[19] WALDRON R. D. *J. Chem. Phys.* 1953 **21** 734.
[20] SHEPPARD N. and SIMPSON D. M. *Quart. Rev.* 1953 **7** 19.
[21] GIGUÈRE P. A. and OLMOS A. W. *Canad. J. Chem.* 1952 **30** 821.
[22] BADGER R. M. and BAUER S. H. *J. Chem. Phys.* 1937 **5** 839.
[23] STEPANOV B. I. *Zhur. Fiz. Khim.* SSSR. 1945 **19** 507; 1946 **20** 907.
[24] STEPANOV B. I. *Nature* 1946 **157** 808.
[25] BATUEV M. I. *Zhur. Fiz. Khim.* 1949 **23** 1399.
[26] BATUEV M. I. *Izvest. Akad. Nauk. SSSR.* (*Ser. Fiz.*) 1950 **14** 429.
[27] WOLKENSTEIN M. V. and others General discussion on spectra of hydrogen bonds, *Izvest. Akad. Nauk SSSR.* (*Ser. Fiz*) 1950 **14** 447–451.
[28] DAVIES M. M. and EVANS J. C. *J. Chem. Phys.* 1952 **20** 342.
[29] KOVNER M. A. and CHUENKOV V. A. *Izvest. Akad. Nauk SSSR.* (*Ser. Fiz.*) 1950 **14** 435.

Spectrochimica Acta, 1956, Vol. 8, pp. 262 to 279. Pergamon Press Ltd., London

A linear-plate characteristic and an intensity scale

C. CANDLER
Department of Scientific and Industrial Research, Baghdad*

(*Received in revised form May* 1956).

Abstract—To ensure the uniform illumination of the slit image in a Littrow-system spectrograph, certain conditions must be fulfilled. These are critically examined, all sources of error specified, and a two-step sector preferred to either a multi-step sector or a step filter.

If T_1 and T_2 are the transmittances of the two halves of a spectral line recorded through a two-step sector, a graph of $(T_1 - T_2)$ against $\frac{1}{2}(T_1 + T_2)$ takes the form of a hump. That the Kaiser transform $K = D - G/\phi$, where D is the density $-\log T$ and $G = -\log(1 - T)$ is nearly linear in $\log E$, is now generally accepted, provided that the constant $\emptyset$ is assigned an appropriate value. The form of the hump dictated by the Kaiser transform is studied, and the near-linearity of the transform confirmed.

The constant ϕ varies with wavelength, but the product $\phi\, dK/d \log E$ remains constant over the range 260–360 mμ on all the nine makes of plate examined. So when a new transform, the lambda transform, defined as $\Lambda = \phi D - G$, is introduced, the slope $d\Lambda/d \log E$ is independent of wavelength, and thus a constant of a particular plate. This slope is written Π, and the maximum contrast factor γ is shown to be Π/ϕ.

A simple mathematical manipulation converts any linear transform into an intensity equation, and the equation appropriate to either the Kaiser or lambda transforms is shown to be

$$I = I_0[(1 - T)/T^{\phi}]^{1/\Pi}$$

The scales published by NOBBS, and obtained from first principles, confirm this.

The behaviour of the two parameters ϕ and Π shows that ϕ is a measure of the ultra-violet absorption of the emulsion, and that Π is the mean number of photons required to render a halide crystal capable of development.

PAGE

1. Experimental procedure 262
2. The Kaiser transform 266
3. The λ transform 271
4. Scales of intensity 276

1. Experimental procedure

1.1. *Random variations of density.* When the density of a spectrum line is anomalous, there are six, and it is believed only six, possible causes; (1) The densitometer, (2) The stepped sector, (3) The optical system, (4) Stray light, (5) Absorption, (6) The photographic plate.

The densitometer is placed first, because it is available in a form which is as accurate as the reproducibility of an arc source warrants, and the source is likely to place a limit on the accuracy of an analysis. If the densitometer is taken as accurate to 0·5%, the cumulative error of the next four items can be held below this, only when no single item is allowed to contribute more than 0·1%. This high standard necessitates stringent precautions, but it can be met in three of the four.

1.2. *The densitometer.* The Hilger microphotometer and galvoscale projector is generally recognized as giving some margin of accuracy over what the spectrochemist requires, and needs only one comment. A scale reading 0 to 50 had its origin in a 50-cm scale placed 1 m away, but with the introduction of a projected scale the unit became arbitrary, and 100 would be more

* Formerly at the Department of Preventive Medicine, University of Bristol.

convenient than 50, for 50 faces an author with a dilemma. On the one hand, the density or other transform should be tabulated in terms of the raw reading l and on the other the text should use an international quantity independent of the instrument, and approved by a British Standard Specification. This can only be the transmittance T defined as l/l_0. When l differs from T only in the position of the decimal point, the dilemma is sufficiently resolved.

The transmittance is more reliably measured on a large area than a small, so the spectrograph slit was opened to a width of 0·125 mm, and an area 1·5 by 0·3 mm of uniform density obtained on the plate. The densitometer slit, set to 0·7 by 0·1 mm, passed the central part of this.

When the potentiometer is adjusted to give a full-scale deflection on the clear plate, the accuracy in ΔT falls at high and low densities, but at both ends of the scale this can be countered by a change in procedure.

At high densities the large area gives a margin of sensitivity, and the potentiometer is set to give a full-scale deflection on a step of a rhodium filter, whose transmittance is about 0·2.

At low densities, advantage was taken of the pair of photocells fitted to the galvoscale projector and designed to locate the point of balance in an absorption spectrum. The two cells are wired in opposition, one receiving light from the upper, and the other from the lower half of a spectrum line. The two potentiometers are first adjusted so that the deflection is zero when both cells receive light through areas of the same transmittance. The deflection produced by areas of different transmittance is then proportional to ΔT, and is independent of the plate area and photocell sensitivity.

The theory is simple. Let the photocells receive light of mean intensity i and i' from areas A and A' of a clear plate; if the sensitivities of the photocells and their potentiometers are s and s' in volts per lumen, a balance will be obtained when

$$Asi = A's'i' \tag{1.1}$$

OL.
8
6/57

In practice, one makes A as nearly equal to A' as is possible by eye.

When the slit is transferred to cover two areas of plate of transmittance T and T', the deflection θ will be proportional to the out-of-balance e.m.f.

$$\begin{aligned}\theta &= (T - T')Asi/R \\ &= k(T - T')\end{aligned} \tag{1.2}$$

where R is the resistance, and k is a constant. This theory has been confirmed on a multi-step rhodium filter, which incidentally determines the constant k.

1.3. *The stepped sector.* Consider a six-step sector with an angle ratio of 2 : 1 and a first opening of 160°. The sixth step with an opening of 5° must be accurate to 20″ of arc, or 0·0003 in. on a radius of 3 in., if the error is to be down to 0·1%. As four other steps must be worked, this specification is very tight, and one may well wonder how many sectors have been cut to meet it. Certainly the author's sector, cut with what he had supposed was reasonable care, was found to have errors of 15′ of arc and to introduce errors in transmittance greater than the densitometer and plate combined.

Nor is this the whole trouble with the multi-step sector, for of the remaining requirements, the most difficult to satisfy is uniform illumination. This difficulty, which is chiefly one of eliminating absorption, increases rapidly with the length of slit, and so with the number of steps.

To one faced with a specification so nearly unattainable, the two-step sector offers a welcome escape. The specification is no more than three short lines radial. The angle ratio is measured after the sector is cut, and need not be near that intended. Two discs have been used with ratios intended to be antilog (0·3) and antilog (0·1), and measured as 2·007 and 1·260.

The two-step sector does not merely reduce the error arising in inequality of the angle ratio, but eliminates it. Until this has been done, other errors are difficult to control because they are so elusive.

The advantages to be gained by calibration with a constant intensity ratio have not gone unnoticed, although the method of producing the two exposures differs from that proposed here. Churchill [1], and later Schmidt [2] used two spectrum lines, and varying the exposure, measured the slope of the characteristic at various densities. In the varying field of an electric arc, however, the intensity ratio of the lines is unlikely to remain precisely constant; and with

only one reading from each spectrum, too few readings are obtained on a single plate to permit the checks essential in precision work. With a two-step sector, one may obtain fifty readings from a single square centimetre. For the sector divides every spectrum line into two halves, whose relative exposure is constant, and thus provides the numerous readings so essential, if random errors are to be smoothed and unsuspected errors identified. Indeed, in the early stages of this work, when every step was empirical, no progress would have been possible without a smoothed curve.

When the transmittances, T_1 and T_2, of the two halves of each line are measured with a densitometer, a graph of ΔT or $(T_1 - T_2)$ against T or $\frac{1}{2}(T_1 + T_2)$ takes the form of a hump (Fig. 1).

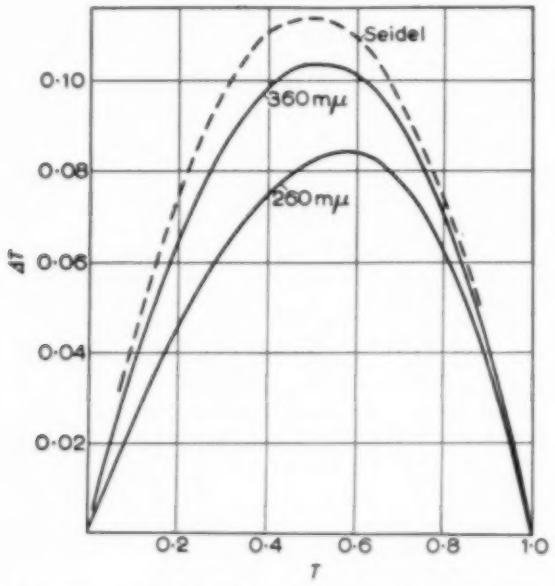

Fig. 1. Variation of ΔT with T on an Ilford chromatic plate at 260 and 360 mμ. The third curve is the Seidel parabola.

1.4. *The optical system.* The laws governing the illumination of an optical image have been known for over a century, and have been recently expounded by MARTIN [3]. MARTIN, however, does not apply them to the spectrograph, and almost every other textbook states that a line of uniform density is produced, whenever the source is imaged on the collimator lens. Experiment with a short arc and a Littrow system will soon convince the least-suspecting student that this is something less than the whole truth, and accordingly the argument is best re-examined.

A spectrograph is conveniently discussed without the prism, as in principle it may be when the source is monochromatic (Fig. 2). A slit S is imaged by the collimator and camera lenses, L_2 and L_3, on the plate P, while the source B is imaged by the condenser L_1 on a plane Q, where an aperture is placed so small that the lenses L_2 and L_3 do not further restrict the beam. An eye, which moves up and down the monochromatic image at P, sees always the same area of source; so the illumination is uniform, provided that no error arises from obliquity. The error of obliquity can be calculated and shown to be negligible, when the apertures are no more than $f/50$.

The essential conditions are thus clear. First, the slit must be uniformly illuminated; second, between the slit and plate not more than one aperture must restrict the beam, and on that aperture the source must be imaged. Moreover, when light is lost by reflection or absorption, all parts of the beam must be reduced in the same ratio.

VOL.
8
1956/5

The Littrow system of the large spectrograph makes the precise fulfilment of these conditions impossible, when an aperture inside the instrument restricts the beam; for the only plane where such an aperture might legitimately be placed is the back surface of the prism. As this is impracticable, the makers have chosen the plane of the collimator lens, but collimator and camera lenses are identical, so inevitably they have introduced a second aperture. Could the arc be imaged near the centre of the prism, this would matter little; but the ghosts formed by reflection at the collimator lens can be kept within bounds only if a bar is placed across it, and inevitably the image of a short arc wanders on and off the bar with disastrous changes of intensity along each spectrum line.

The remedy is to restrict the beam outside the spectrograph so that the apertures inside do not further vignette it. To secure this, the arc is imaged on an aperture B' (Fig. 2b), and the latter imaged by the condenser on the back surface of the prism, an adjustment, which is hardly

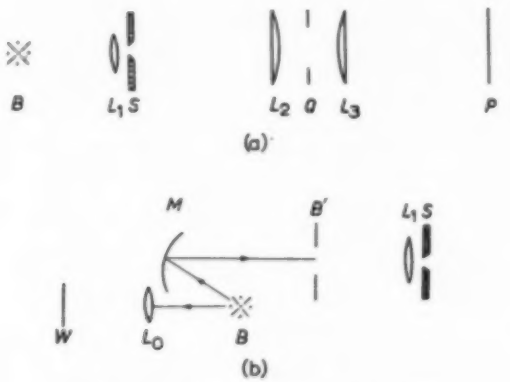

Fig. 2a. Optical system of a spectrograph.
Fig. 2b. Illumination of the spectrograph slit.

possible in the ultra-violet without much waste of valuable prism surface, unless the condenser is a quartz-fluorite achromat.

The arc is imaged on the aperture B' with a concave mirror, for this too should be achromatic. The position of the arc during an exposure is conveniently controlled by back projection onto a wall W with a glass lens L_0.

1.5. *Stray light.* That stray light is objectionable even at a level which is likely to escape detection, follows from the shape of the intensity curve (Fig. 10). Thus a background of transmittance 0·98 to a line of transmittance 0·4 necessitates a correction of 11% in the intensity, yet a transmittance of 0·98 can be overlooked on the plate all too easily.

Only two surfaces return light to the plate after a single reflection, the front and back surfaces of the collimator. Light from these two images, each 5% as bright as the incident beam, is kept from the centre line of the plate by a rod placed 2 mm in front of B' (Fig. 2b), that is, in a plane conjugate to the collimator lens.

A plate inserted in the holder with the glass surface in front shows that much of the light scattered on to the plate at 300 mμ is visible or near-visible. It is largely excluded by a Chance OX7 filter, which passes only the range 250–400 mμ. An upper limit of 370 mμ to exclude the carbon bands would be better, but no suitable filter is known.

When the intensity allows, a film of aluminium on a quartz plate near the OX7 filter is an additional help, for the reflectivity of aluminium decreases rapidly with wavelength, so that it enhances weak lines near 260 mμ at the expense of strong lines near 360 mμ. In the present work the aluminium film was also required to increase the exposure, which would otherwise have been under 1 sec, and in so short a period a stepped sector may produce errors of sampling.

To make sure that these precautions were adequate, the diaphragm was opened to 18 mm, and a plate exposed for ten times as long as any plate measured. The test plate showed no signs of stray light.

1.6. *Absorption.* Absorption which is uniform over the beam cannot produce a variation of density along a spectrum line, and even irregular absorption, which occurs on a surface conjugate or nearly conjugate to the arc, as on the collimator lens or refracting prism, is unobjectionable. But any dirt on the condenser lens or reflecting prism, which both lie near the slit, produces a non-uniform line.

In a chemical analysis, which depends on the density difference of two adjacent lines, absorption is unlikely to lead to error. But directly a stepped sector is introduced, absorption requires the most careful and continuous attention, for it cannot be measured or eliminated,

Table 1.

ILFORD	
Chromatic	1¾ min
Ordinary	3 min
Process	1¾ min
Special rapid	4½ min
Thin-film half-tone	4¼ min
KODAK	
B.10.	3 min
B.20.	3 min
L.15.	3 min
Uniform gamma	5 min

The nine plates examined with the times of development at 20°C. All Ilford plates were developed in ID2 diluted 1 : 2, and all Kodak plates in D19b at full strength.

and once brought under control, it may suddenly reappear. Moreover, when absorption has been eliminated at 360 mμ, it may still exist at 260 mμ, for a rapid increase in absorption with decreasing wavelength is common.

To ensure reliable measurements, the author makes an exposure with the sector stationary at the top and bottom of each plate. If three lines of different wavelengths are uniform along their length, the stepped spectrum is measured. When the lines are not uniform, the plate is best discarded.

A step filter has several advantages over a step sector, but there seems no method by which one can ensure that in introducing it, one does not also introduce some grease, whose absorption varies with wavelength in the ultra-violet. And until a security check is evolved, this must remain an absolute bar.

1.7. *The photographic plate.* The nine makes of plate examined are listed in Table 1. All were developed in a dish 20 × 30 cm containing solution to a depth of 1 cm. The developer was rocked by hand, but was not further agitated, nor were the plates brushed. After development, the plates were placed in a bath of ammonium thiosulphate solution and washed.

The lines measured were all more than 1½ cm from the edges of the plate, but the border apart, the emulsion appeared to be uniform over the body of the plate. Certainly the values of ΔT examined were as consistent, when taken from different spectra, as when taken from the same.

2. The Kaiser transform

2.1. *A linear characteristic.* Many authors [2, 4–8] have sought a characteristic linear at low densities in the logarithm of the exposure, but none seems to have noticed that in principle he need only measure the area under an empirical curve.

VOL. 8 1956/5

The hump (Fig. 1) is a graph of $(dT/d \log E)/\Delta \log E$, where $\Delta \log E$ or $\log (E_1/E_2)$ is a constant, whose value depends on the angle ratio of the sector. So that when we postulate a function J linear in $\log E$, so that $dJ/d \log E$ is constant, the reciprocal of the ordinate is

$$\frac{dJ}{d \log E}, \quad \frac{d \log E}{dT} = \frac{dJ}{dT} \tag{2.1}$$

on an arbitrary scale. And as experiment gives dJ/dT as a function of T over the whole range, J can be evaluated and a characteristic linear in $\log E$ is always available, although the numerical work would be laborious if no equation could be found.

2.2. *The density.* Many functions of the transmittance have been used to measure the blackening of a photographic plate. All are arbitrary, and in the absence of a reliable theory, the choice is one of convenience, and of convenience alone.

By long tradition, the density D claims precedence, though why it dominated the scene for many decades is far from clear. Some perhaps were swayed by a false analogy with the colour filter; for if the developed plate consisted of silver granules uniformly distributed in the emulsion and the number of granules increased with the exposure, or if all the halide crystals were sensitized in a surface layer and exposure increased the thickness, the plate would obey the same laws as a colour filter. But in fact the number of silver granules formed per unit volume decreases with depth in the emulsion, so the analogy is false.

More important probably is the linearity of D as a function of $\log E$ at densities greater than 0·4, for the densities used in photography are high, and in spectrochemical analysis, although lower densities offer higher sensitivity and greater accuracy, reproducible readings at densities lower than 0·4 have been difficult to obtain.

2.3. *The Seidel transform.* The transform S, defined as $\log \{(1 - T)/T\}$, was proposed at a discussion group in 1939 by Dr. Walter Seidel, who was then, and indeed still is, head of the spectrographic laboratories of the Bayerwerk. As Seidel did not publish the transform, its value might well have gone unrecognized, had not Kaiser [4] adopted it and spent much time in proving its value, for earlier it had been used by Baker [3] and had passed unregarded.

As S, like D, is a measure of blackening, it has been called the Seidel density, but this may confuse the reader unless D is renamed the true density. And difficulties mount when other functions are introduced. Accordingly, density is here used for D alone, and other functions of the transmittance are called transforms.

The word characteristic, however, may be conveniently extended to cover a plot of any transform against $\log E$, and in due course the Seidel and Kaiser characteristics will be compared with the density characteristic.

Although the scanty evidence available suggests that Seidel reached his transform by an inspired guess, a logical argument is easily supplied. The first approximation to the empirical hump (Fig. 3) is an inverted parabola, whose equation is $kT(1 - T)$, where k depends on the angle ratio of the stepped sector

and is here a constant. Thus

$$dT/d \log E = kT(1 - T) \tag{2.2}$$

Thus when we postulate a **function** J linear in $\log E$, so that

$$dJ/d \log E = j \tag{2.3}$$

where j is a constant,

$$J = (j/k)\int dT/T(1 - T) \tag{2.4}$$

and the Seidel transform follows.

2.4. *The Kaiser transform.* Measurement of a stepped spectrum shows that

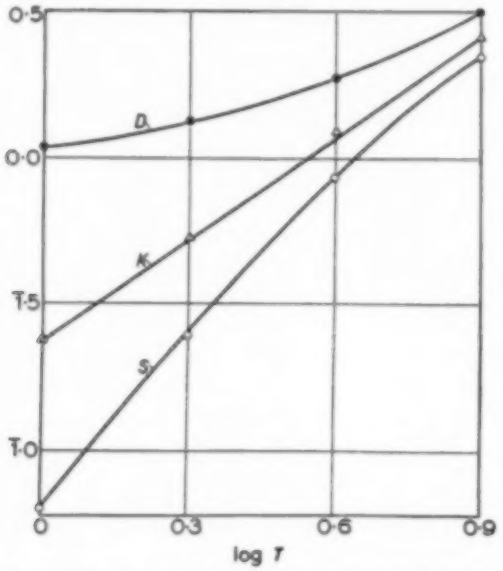

Fig. 3. The density, Seidel, and Kaiser characteristics of a line.

the density and Seidel curves have the form shown in Fig. 3. The D curve is concave on all plates and at all wavelengths, while the S curve is convex in the range 260 to 320 mμ, but becomes concave at some longer wavelength. Thus a function K, which divides the distance between the D and S curve in the ratio $f/(1 - f)$, will be more nearly linear than either D or S, when f is properly chosen.

$$K = (1 - f)D + fS \tag{2.5}$$

As D and S are functions of the transmittance T, K is also a function of T, and may be tabulated for a given value of f.

The Kaiser transform may also be written

$$K = D - fG \tag{2.6}$$

when G is defined as $(D - S)$, and inspection shows that

$$G(T) = D(1 - T) \tag{2.7}$$

A set of five tables giving K as a function of T for the five values of f, 0·6 by 0·1 to 1·0 has been prepared on microfilm, and this can be borrowed from the author.

KAISER [4–5] studied this transform at length, but for some years it was curiously little used. In retrospect, one can see that KAISER [5] himself contributed to this, when he devoted twenty-five out of thirty pages to second-order corrections, although careful measurement suggests that the equations given in the first five pages yield a remarkably close fit at all wavelengths and on all types of plate.

Today, however, its value in spectrochemical analysis is more and more widely recognized. BLACK [7] noted the linearity of S at a wavelength of 350 mμ, and PRICE that of $\frac{1}{2}(D + S)$ at 280 mμ, while NOBBS [10] used $(D + S)$ on Kodak plates at all wavelengths from 230 to 360 mμ. Although these papers are cited at random from a larger number, they appear to be typical in that the authors have thought it unnecessary to determine f more closely than to the nearest half-unit, although it can be measured to 0·1, and the linearity is then much improved.

One notes too that the transform has been used always to increase the accuracy of some analysis. No one seems to have considered how the two parameters f and $dK/d \log E$ depend on the wavelength and type of plate.

2.5. *Experimental choice of f.* The factor f may always be chosen to make three points on the Kaiser characteristic collinear. For when three pairs of points PP', QQ', and RR' are given (Fig. 4), a line may be drawn which divides each pair in the same ratio. When PQ and

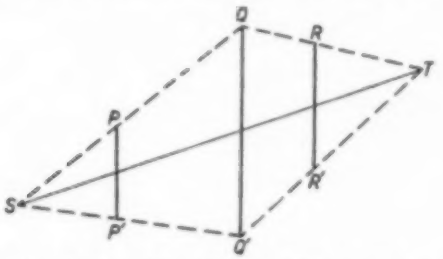

Fig. 4. Three pairs of points PP', QQ', and RR' are given, and the line ST is so constructed that each is divided in the same ratio.

$P'Q'$ meet in S, any line through S divides PP' and QQ' in the same ratio; and by the same argument a line through T similarly divides QQ' and RR'. Thus, if the line ST meets the lines PP', QQ', and RR' in L, M, and N respectively, the ratios PL/LP', QM/MQ', and RN/NR' are equal.

Let the points P, Q, and R lie on the density curve with ordinates D_1, and D_2, and D_3 and abscissa log E_1, log E_2 and log E_3, while P', Q', and R' lie on the Seidel curve with ordinates S_1, S_2, and S_3. The slope of the line LM is therefore

$$\{(1 - f)\Delta D_{21} + f\Delta S_{21}\}/\Delta \log E_{21} \tag{2.8}$$

where ΔD_{21} is an abbreviation for $(D_2 - D_1)$. So the slopes of LM and MN will be equal when f is determined by the equation

$$f/(1 - f) = -(D_1 - 2D_2 + D_3)/(S_1 - 2S_2 + S_3) \tag{2.9}$$

In practice the curvature may be masked by random errors, and f is better chosen so that two lengths of the characteristic some distance apart are made parallel, as they will be if ΔK is the same for two lines of different density.

$$f/(1 - f) = -(\Delta D' - \Delta D'')/(\Delta S' - \Delta S'') \tag{2.10}$$

An equation of this type was given by KAISER [5].

When a two-step sector is used and many lines are measured, ΔD and ΔS may be regarded as current co-ordinates, so that f is constant only when ΔS is a linear function of ΔD (Fig. 5). Differentiating equation (2.5) shows that

$$\Delta S = \{(1 - f)/f\}\,\Delta D + \Delta K/f \tag{2.11}$$

so the slope determines f and the intercept ΔK.

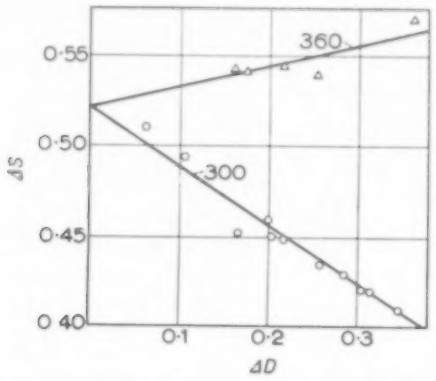

Fig. 5. ΔS as a function of ΔD for lines at 300 and 360 mμ on an Ilford process plate.

2.6. *The form of the hump.* Assuming that the Kaiser transform is linear in log E, consider how the shape of the hump differs from the parabola required by SEIDEL. Differentiation shows that

$$\frac{dK}{dT} = -\left\{\frac{1}{T} + \frac{f}{(1 - T)}\right\} \log_{10} e \tag{2.12}$$

A stepped sector produces a finite change $\Delta \log E$ in the logarithm of the exposure, and thus a change ΔT in the transmittance. In the equations, which follow, the sign of ΔT will be ignored, since it cannot cause confusion.

The Kaiser transform is linear in log E, when ΔK is independent of T, that is, when

$$\Delta T = \Delta K \log_e 10 \Big/ \left\{\frac{1}{T} + \frac{f}{(1 - T)}\right\} \tag{2.13}$$

This equation gives ΔT as a function of T, and is the equation of the hump. Five properties are easily derived.

(1) ΔT is zero, when T is zero or unity.

(2) The value of T at which ΔT is a maximum is

$$T_{\max} = 1/(1 + f^{\frac{1}{2}}) \tag{2.14}$$

so that $T_{\max}$ increases from 0·5 to 0·6 as f decreases from 1·0 to 0·6. The corresponding value of ΔT is

$$\Delta T_{\max} = \Delta K \log_e 10/(1 + f^{\frac{1}{2}})^2 \tag{2.15}$$

VOL. 8 1956/5

HUGHES and MURPHY (1948) apparently noticed that the maximum is shifted to a value of T higher than the $\frac{1}{2}$ required by SEIDEL, for their equation allows this.

(3) The slopes at the two ends of the curve should be in the ratio of $-f : 1$.

$$Lt_{T\to 0}(\Delta T/T)/Lt_{T\to 1}\{\Delta T/(1-T)\} = -f \tag{2.16}$$

The slope at the end of a curve is not easily measured, but there is no reason to doubt that this prediction is satisfied. The equation of HUGHES and MURPHY [6], which makes the two slopes equal, conflicts with experiment, as the authors doubtless realized, for they claimed only that it was valid at transmittances less than 0·97.

(4) When $T = \frac{1}{2}$,

$$\Delta T = \Delta K\,(\log_e 10)/2(1+f) \tag{2.17}$$

2.7. *Variation of f with wavelength.* On all the nine types of plate examined, f and $dK/d\log E$ vary with wavelength, but the ratio $(1/f)\,dK/d\log E$ remains constant. This suggests that some function more fundamental than the Kaiser transform should not be difficult to find. A later paper will also attempt to show that it unlocks the door to an adequate theory.

3. The λ transform

3.1. *A rational function linear in log E.* The Kaiser transform is nearly linear in log E, but its form is adventitious. As K is the area under a curve, the scale of whose ordinate is arbitrary, both the slope of K and its value at a selected point are arbitrary. In other words, the function $(a + bK)$ will be linear in log E, while a and b may be chosen to give it advantages not possessed by K.

Consider therefore the function

$$\Lambda - \Lambda_s = \phi\,(D - D_s) - (G - G_s) \tag{3.1}$$

where the suffix s refers to the value at a standard transmittance T_s. Three-point plate calibration has often been criticized, because the slope varies with the wavelength and from one batch of plates to the next, so that the concentration calibration is affected. However, as stated in the preceding section, $\phi\,dK/d\log E$ is constant for a particular plate, when ϕ is defined as $1/f$, and if we call the constant Π, the slope of the Λ transform is independent of wavelength.

$$= \Lambda_0 + \Pi \log E \tag{3.2}$$

At the densities chiefly used in analysis, Λ should vary little with ϕ. This condition is met by making $(\partial\Lambda/\partial\phi)_T$ zero at a standard transmittance T_s, which, following MITCHELL [11], we take as 0·4. D_s and G_s are then the values of D and G at this point. Finally, when the lambda function is tabulated, Λ_s is assigned the value 2, so that no negative values of Λ occur in the working range.

3.2. *Measurement of ϕ and Π.* When the transmittances T_1 and T_2 of the two halves of two or more spectrum lines have been measured, ΔD and ΔS may be read from tables, for they are merely abbreviations for $(D_1 - D_2)$ and $(S_1 - S_2)$. Now

$$\Delta S = \Delta\Lambda - (\phi - 1)\,\Delta D \tag{3.3}$$

so that a plot of ΔS against ΔD will be linear, since $\Delta\Lambda$ is constant, provided that the Kaiser transform is linear in log E. The slope of this line (Fig. 6) is $(1 - \phi)$ and the intercept ΔS_0, or $\Delta\Lambda$.

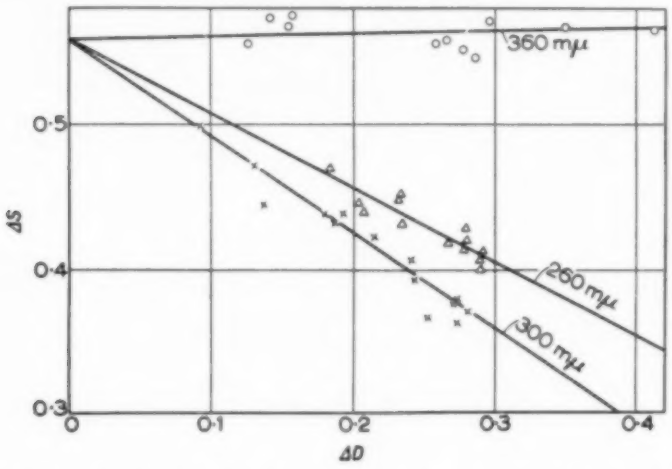

Fig. 6. ΔS as a function of ΔD for three wavelengths on an Ilford thin-film half-tone plate

When two lines of different density are measured, $\Delta\Lambda$ may be eliminated and ϕ obtained from the equation

$$\phi = 1 - (\Delta S' - \Delta S'')/(\Delta D' - \Delta D'') \tag{3.4}$$

or in a convenient shorthand

$$\phi = 1 - \Delta^2 S/\Delta^2 D \tag{3.5}$$

where the first difference is between the upper and lower halves of a line, and the second between the two lines. This, like equation (2.10), is only a variant of an equation given originally by KAISER.

The value of ΔS_0 follows from the equation

$$\Delta S_0 = \Delta S + (\phi - 1)\,\Delta D \tag{3.6}$$

applied to either line. And finally, Π is obtained from

$$\Pi = \Delta S_0/\log\,(E_1/E_2) \tag{3.7}$$

where E_1/E_2 is the angle ratio of the two-step sector.

3.3. *The plate contrast.* The plate contrast, Π, is independent of the wavelength in all the nine makes of plate examined, and over the range 260 to 360 mμ, as shown in Section 2. Moreover, when these plates are developed according to the makers' instructions, Π lies in the narrow range 1·7 to 2·3 (Table 2) if the Ilford special rapid plate is excluded.

The contrast of a plate is usually measured by the maximum contrast factor γ defined as the value of $dD/d\log E$ at the point of steepest slope. The definition of Λ shows that

$$d\Lambda/d\log E = \phi\, dD/d\log E - dG/d\log E \tag{3.8}$$

and at high densities the last term is negligible, so that

$$\gamma = \Pi/\phi \tag{3.9}$$

The Seidel transform is linear in log E, when $\phi = 1$, so that $\gamma = \Pi$ at the particular wavelength at which this occurs. At all shorter wavelengths, γ is less than Π, while at longer wavelengths it is greater.

The plate contrast may well vary with the age of the plate, and from batch to batch. But if these changes are small, they can perhaps be compensated by

Table 2.

Emulsion	Π
ILFORD	
Chromatic	1·93
Ordinary	1·77
Process	2·01
Special rapid	1·45
Thin-film half-tone	1·89
KODAK	
B.10.	2·29
B.20.	1·91
L.15.	1·77
Uniform gamma	2·24

Values of Π, when the nine makes of plate were developed under the conditions recorded in Fig. 1.4. Considerable variations in the values may perhaps occur from batch to batch, and even from plate to plate.

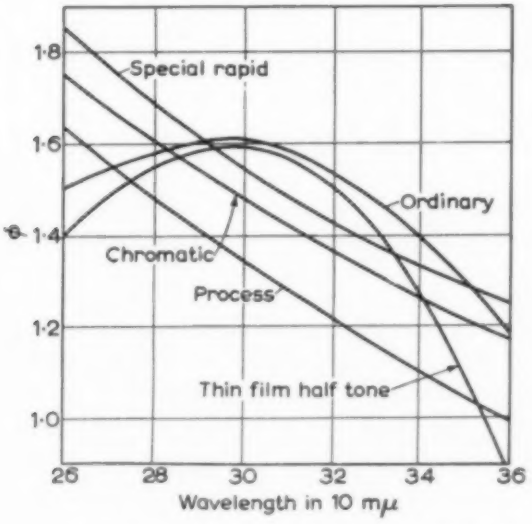

Fig. 7. Variation of ϕ with wavelength on Ilford plates.

altering the time of development, until $\Delta\Lambda$ returns to its old value. Thus the age-old complaint of the spectrochemical analyst that a new batch of plates means a new concentration calibration should be heard less frequently. This is a point which calls for examination in a later paper.

3.4. *The gelatine factor.* Theory apart, the variation of ϕ with wavelength (Figs. 7 and 8) strongly suggests that it is proportional to the coefficient of absorption of the gelatine, and so without being too specific it may for the present be called the "gelatine factor."

The absorption or $\phi - \lambda$ curves divide the nine makes of plate examined into two groups, *g* and *s*. The *g* group consists of three Ilford plates, chromatic, process, and special rapid. In these plates the absorption increases almost uniformly with the wave number of the radiation, as one might expect it to do in natural gelatine.

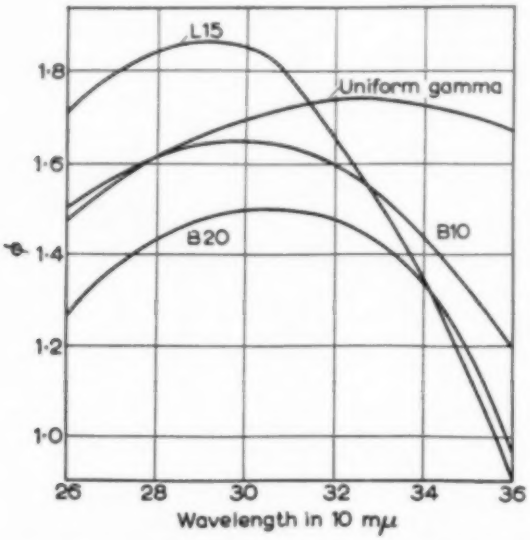

Fig. 8. Variation of ϕ with wavelength on Kodak plates.

The *s*-group plates are Ilford ordinary and thin-film half-tone, and the Kodak plates, B.10, B.20, L.15, and uniform gamma. In all these plates the makers have produced an emulsion such that ϕ varies slowly with λ in the working range, with ϕ given a maximum between 280 and 320 mμ.

3.5. *Validity of the* Λ *transform.* The validity of the Λ transform is best examined in three overlapping ranges of density. Accordingly, the words high, medium, and low will be taken to connote the ranges:—

High density	T from 0·02 to 0·4
Medium density	T from 0·3 to 0·8
Low density	T from 0·7 to 1·0

The points which need consideration vary from level to level.

VOL. 8 1956/5

At high densities, D has been widely accepted as adequate, although some routine laboratories reveal their doubts by refusing to accept any reading outside a range as narrow as $0{\cdot}3 \pm 0{\cdot}1$. Even at high densities a function which will give a better fit at all wavelengths and on all plates should be welcome. As ϕ seldom lies outside the range 1·0 to 1·8, the Λ transform for $\phi = 1{\cdot}4$ meets this requirement. This is well shown by Table 3 of ΔD and $\Delta\Lambda$ for a stepped sector producing an exposure ratio of 1·26. In the ΔD column the trend to lower values exceeds the random error, when T exceeds 0·3, but no significant change occurs in $\Delta\Lambda$ even when T rises to 0·4.

Table 3

T_1	T_2	ΔD	$\Delta\Lambda$
0·128	0·174	134	210
0·130	0·173	126	196
0·199	0·266	126	214
0·207	0·276	125	214
0·263	0·337	108	196
0·301	0·388	110	213
0·313	0·398	105	203

Validity of the Λ transform at high densities on a Chromatic plate at 320 mμ. ϕ was assigned the value 1·4. The decimal point is omitted in the first and fourth columns; in the following table it is omitted from the T columns as well.

Table 4

T_1	T_2	$\Delta\Lambda$
106	231	641
123	270	660
126	274	654
166	349	656
227	457	670
230	463	674
252	498	676
279	530	660
284	538	662
311	563	636
394	668	651
442	716	650
486	760	661
494	760	642
526	790	651
564	820	661
676	890	672

Thin-film half-tone plate at 300 mμ. Validity of the Λ transform assuming $\phi = 1{\cdot}7$.

Lines in the transmittance range 0·4 to 0·8 have been considered unsuited to spectrochemical analysis, because D is no longer even approximately linear in log E. Extension of the permitted range to lower densities should increase both the sensitivity and the accuracy, so some spectroscopists may wish to work in this region, even at the expense of extra trouble.

On the thin-film half-tone plate recorded in Table 4 the standard deviation of $\Delta\Lambda$ is no more than 0·011, a figure which indicates a random variation of 2·7% in the intensity ratio. Although the range of transmittance is 0·1 to 0·9, this standard deviation is not much greater than that often accepted as unavoidable in ΔD, when the transmittance is restricted to the range 0·1 to 0·4.

This high consistency is not, however, always achieved. On many plates $\Delta\Lambda$ shows a tendency to increase at high and low densities. The opposite effect, decrease of $\Delta\Lambda$ at high and low densities, has never been observed, and this is the more noteworthy in that stray light would make $\Delta\Lambda$ decrease as T approaches unity. So this deviation appears to show that the Kaiser transform is not quite linear in log E.

The low-density range is used only in background correction, so the validity of the intensity curve is at issue, and this will be considered in a later section.

4. Scales of intensity

4.1. *The search for an intensity scale.* A densitometer calibrated in intensity has been widely advocated [12–14] and as little used.

That it has been widely advocated is not surprising, for the concentration of a trace metal is proportional to the intensity, while background correction is greatly facilitated, since the intensity of line-plus-background is the sum of the intensity of line and background separately.

These cogent arguments have persuaded the Australian Defence Laboratory [10, 15, 16], to persist with intensity scales over ten years and half a million samples. But a reading of NOBBS's paper [10] shows that his method is still laborious, and its successful application calls for personal judgement as well as patience.

In this work an intensity scale is derived from the Kaiser and Lamda transforms, so that when these are linear the intensity scale can be expressed in terms of two empirical parameters. But this is still very far from a theory proper; indeed, it can scarcely claim to be the prolegomena to a theory.

4.2. *A scale derived from first principles.* The unit of intensity is arbitrary, and an intensity which produces a line of transmittance 0·4 is here assigned the value 100.

When the empirical hump is plotted in the form $(T_1 - T_2)$ against T_1, an intensity curve follows by iteration. For if the angle ratio of the sector is ρ, the value of $(T_1 - T_2)$ read at $T_1 = 0{\cdot}4$, gives the value of T, at which the intensity is $100/\rho$. And repetition gives successively the transmittance of points, whose intensities are $100/\rho^2, 100/\rho^3, \ldots, 100/\rho^n$. The intermediate points may either be interpolated, or measured with a step sector of different angle ratio.

4.3. *A scale derived from the Lamda transform.* The Lamda transform is linear

VOL. 8 1956/5

in the logarithm of the exposure and has a slope Π, as in equation (3.2)

$$\Lambda = \Lambda_0 + \Pi \log E$$

A simple mathematical manipulation converts this into the exposure equation

$$E = E_0 10^{\Lambda/\Pi} \tag{4.1}$$

And when a number of spectrum lines are all exposed for the same time, the relative intensities are given by a similar equation:

$$I = I_0 10^{\Lambda/\Pi} \tag{4.2}$$

where I_0 is arbitrary.

Moreover, as Λ is a function of T (equation 3.1), the intensity may be made explicit in the transmittance

$$I = I_0 \{(1 - T)/T^{\phi}\}^{1/\Pi} \tag{4.3}$$

The type of curve dictated by this equation is shown in Figs. 9 and 10.

This equation has been fitted to the empirical curves obtained by NOBBS [10], and the agreement is excellent, Π and ϕ remaining constant along any one curve, but changing their values from one curve to another.

OL.
8
6/57

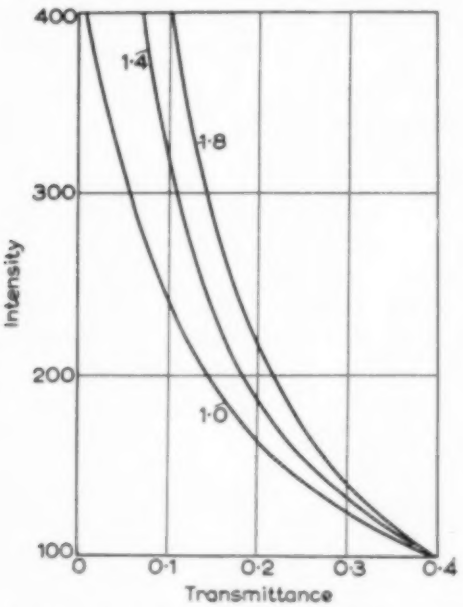

Fig. 9. A set of intensity scales at high densities for $\Pi = 2$ and $\phi = 1{\cdot}0$, 1·4, and 1·8.

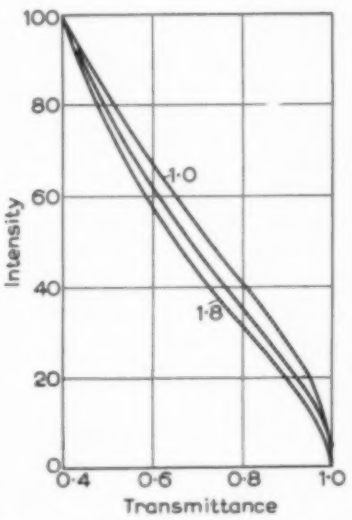

Fig. 10. A set of intensity scales at low densities for $\Pi = 2$ and $\phi = 1{\cdot}0$, 1·4, and 1·8.

4.4. *The conflict of time and intensity scales.* Either a step filter or a step sector will calibrate a plate; the filter yields an intensity curve and the sector a time curve.

Plate calibration should aim at the highest possible precision, for otherwise unsuspected errors creep into the succeeding concentration calibration and bedevil it. In the ultra-violet a step filter is liable to introduce unsuspected absorption, so one is forced to use a rotating sector and a time scale.

When a time scale is used in the concentration calibration of spectrochemical analysis, no conflict can occur. But when a time scale is used to correct for background, an error creeps in, even though in practice it is unlikely to be significant. For, according to SCHWARZCHILD, the effective exposure E is It^p, and the intensity of line-plus-background is the sum of line and background separately.

$$I = I_L + I_B \tag{4.4}$$

In correction for background, the time is the same for line and background, so this equation states that

$$E = E_L + E_B \tag{4.5}$$

And if the plate calibration employed a step sector, so that E was obtained on a time scale, while I was constant

$$t^p = t_L{}^p + t_B{}^p \tag{4.6}$$

Moreover, if a scale has been obtained with a step sector, and thereafter called colloquially an "intensity scale," whose values are I' in contradistinction to the true intensity I, then while I' may be used in the concentration calibration, the background should be corrected with the equation

$$I'^p = I_L{}'^p + I_B{}'^p \tag{4.7}$$

There is, however, little evidence that p ever differs from unity by an amount which would make this equation of more than theoretical interest in this wavelength region.

4.5. *Validity of the scale at low intensities.* Transmittances greater than 0·7 are used only in correction for background, so that the linearity of Λ is less important than the validity of the intensity equation. In one sense this is irrelevant, for the two are interrelated, but the intensity curve is easier to visualize, and therefore more easily discussed. When T differs little from unity, and Π is approximately 2,

$$I = I_0(1 - T)^{\frac{1}{2}} \tag{4.8}$$

so that the intensity curve takes the form of a parabola, in which $dI/dT \to \infty$ as $T \to 1$.

This infinite slope may surprise some spectroscopists, but it is fully confirmed by the intensity curves published by NOBBS [10, 16], curves which were obtained by a direct empirical approach. In theory it derives from the value of Π, and is inevitable whenever Π is greater than unity. Of this, theory offers a simple explanation, if Π is the mean number of photons required to render a halide crystal capable of development. Incidentally, this identification is in no way a new discovery, it was made by BAKER [9] thirty years ago.

VOL. 8 1956/5

Acknowledgements—This paper had its origin in an attempt to estimate lead and tin in food at the lowest possible concentrations, although the preliminaries have run to such length that they must be applied to spectrochemical analysis in a later paper. All the work was carried out in the Department of Preventive Medicine at Bristol University, and the author is glad to acknowledge the encouragement he has received from both Professor R. H. PARRY and the Public Analyst, Mr. E. G. WHITTLE.

He is much indebted to Dr. W. CHESTER and Dr. H. B. GRIFFITHS for help with the mathematics, to Dr. J. BURCH for advice on the optics of uniform illumination, and to Dr. H. D. KEITH for discussions of photographic theory. He also wishes to express his thanks to Mr. N. J. ATHERTON, who has taken and measured many of the spectrograms.

References

[1] CHURCHILL J. R. *Ind. Eng. Chem.* (*Analyt. Ed.*) 1944 **16** 653.
[2] SCHMIDT R. *Trav. chim. Pays-Bas.* 1948 **67** 737.
[3] MARTIN L. C. *Technical Optics* 1948.
[4] KAISER H. *Spectrochim. Acta* 1941 **2** 4.
[5] KAISER H. *Spectrochim. Acta* 1948 **3** 159.
[6] HUGHES H. K. and MURPHY R. W. *J. Opt. Soc. Amer.* 1949 **39** 501.
[7] BLACK I. A. *Spectrochim. Acta* 1952 **4** 519.
[8] PRICE W. J. *Spectrochim. Acta* 1952 **5** 278.
[9] BAKER E. A. *Proc. Roy. Soc. Edin.* 1925 **45** 166; 1926 **47** 34; 1928 **48** 106.
[10] NOBBS J. McK. *Spectrochim. Acta* 1955 **7** 552.
[11] MITCHELL R. L. *Commonwealth Bureau of Soil Science* 1948 Tech. Comm. 44.
[12] MINNAERT M. and HOUTGAST J. *Z. Astrophys.* 1938 **15** 354.
[13] LANGSTROTH G. O. and MCRAE D. R. *J. Opt. Soc. Amer.* 1938 **28** 440.
[14] BROWN W. N. and BIRTLEY W. B. *Rev. Sci. Instrum.* 1951 **22** 67.
[15] SINCLAIR D. A. *J. Opt. Soc. Amer.* 1944 **34** 689.
[16] NOBBS J. McK. *Spectrochim. Acta* 1953 **5** 286.

OL.
8
6/57

Spectrochimica Acta, 1956, Vol. 8, pp. 280 to 316. Pergamon Press Ltd., London

REPORTS OF MEETINGS

Symposium On Molecular Structure and Spectroscopy

THE tenth anniversary of the Symposium on Molecular Structure and Spectroscopy was held at the Ohio State University, Columbus, Ohio, 11 to 15 June 1956. This meeting was held jointly with the Joint Commission on Spectroscopy of the International Union of Pure and Applied Physics and the International Astronomical Union, and the National Research Council Committee on Line Spectra of the Elements. The following papers were presented at the symposium.

Electronic Band Spectra

Invited papers

Configuration interaction as applied to two-electron systems: JOHN SLATER, Department of Physics, Massachusetts Institute of Technology, Cambridge, Massachusetts.

Some recent developments in the molecular quantum theory: PER-OLOV LÖWDIN, University of Uppsala, Uppsala, Sweden.

The spectra of charge-transfer complexes: Some problems and new developments: ROBERT S. MULLIKEN, Department of Physics, University of Chicago, Chicago, Illinois.

Ultra-violet spectra of simple polyatomic molecules: G. HERZBERG, National Research Council, Ottawa, Canada.

Contributed papers

A quantum mechanical derivation of an internuclear potential function for polyelectronic bonds: ELLIS R. LIPPINCOTT, Department of Chemistry, University of Maryland, College Park, Maryland.

A simple quantum mechanical model of bond formation is presented which allows the derivation of an internuclear potential function of the form

$$V = D_e e^{-n\Delta R^2/2R} \qquad \text{where } n = k_e R_e/D_e.$$

The method makes use of a delta function model whereby bond formation is described by the shifting of atomic delta functions into molecular delta functions. The predicted results for H_2^+ are nearly exact for all bond properties while the results for H_2 are more accurate than those of all but the most elaborate methods used previously. In particular the method appears superior to both the valence bond and molecular orbital theories in both results and ease of calculation. Advantages of the method are that the same form for the internuclear potential is obtained for polyelectronic bonds as for one and two electron bonds, and that polyelectronic bond systems can be handled by one-dimensional methods. Theoretical values of the parameter, n, for polyelectronic molecules are calculated which agree well with values obtained from experimental data. Application to the excited states of H_2, He_2 and He_2^+ gives good results.

Lifetime measurements of metastable state of molecules: WILLIAM LICHTEN, Laboratory of Molecular Spectra and Structure, University of Chicago, Chicago, Illinois.*

The molecular beam method for the measurement of the lifetime of metastable states has been improved by the introduction of differential pumping, control of the energy of the bombarding electrons, and use of a movable detector.

* Present address: Columbia Radiation Laboratory, Columbia University, New York, N.Y.

VOL. 8 1956/5

A lower limit for the lifetime of the $A^3\Sigma_u^+$ state of N_2 is obtained; the measured value for the $a^1\Pi g$ state is $(1{\cdot}7 \pm 0{\cdot}3) \times 10^{-4}$ sec.

Some observations on metastable states of other molecules and atoms are mentioned briefly.

Hyperfine structure and electron densities in aromatic free radicals:* E. DE BOER and S. I. WEISSMAN, Department of Chemistry, Washington University, St. Louis 5, Missouri.

The paramagnetic resonance absorption spectra of anthracene and biphenyl univalent anion contain 21 and 9 peaks respectively.

With the aid of HUCKEL's m.o. approximation the electron densities of these radicals were calculated. Assuming the charge density as the determining factor for the hyperfine splitting, we were able to explain our experimental results. In accordance with the charge density at the connecting carbon atoms of the two phenyl rings in a biphenyl negative ion, the paramagnetic resonance absorption spectrum of this compound proved to be about 23% shorter than the spectrum of naphthalene anion, where HUCKEL puts the odd electron in an orbital with zero densities at the two central carbon atoms.

The optical spectra of uni- and bi-valent anions of anthracene were measured.

Spectroscopic determination of electron exchange between naphthalene negative ion and naphthalene:† R. L. WARD, Department of Chemistry, Washington University, St. Louis 5, Missouri.

The rate constants for the electron exchange between sodium naphthalenide and naphthalene and between potassium naphthalenide and naphthalene in tetrahydrofuran and 1,2-dimethoxyethane have been determined by paramagnetic resonance techniques.

Addition of small amounts of naphthalene leads to broadening of the individual hyperfine components. Larger amounts of naphthalene cause the hyperfine components to merge into a single peak with broad tails. In the case of $K^+C_{10}H_8^-$ in 1,2-Dimethoxyethane it has been possible to add quantities of naphthalene such that exchange narrowing begins to take place.

The rate constants, for the bimolecular exchange, vary between $6{\cdot}2 \times 10^6$ litres/mole sec and $1{\cdot}2 \times 10^8$ litres/mole sec.

The electronic structure and the hfs coupling constants of SH_2 molecule: K. OHNO and Y. MIZUNO, Department of Physics, Faculty of Science, University of Tokyo, Tokyo, Japan. and M. MIZUSHIMA, Department of Physics, University of Colorado, Boulder, Colorado.

BURRIS and GORDY [1] observed in the microwave spectra of SH_2 that the apex angle is 92°6′ and the quadrupole hfs coupling constants are $\chi_{aa} = -32$ Mc/sec, $\chi_{bb} = -8$ Mc/sec and $\chi_{cc} = 40$ Mc/sec, where the axis a lies between two hydrogen atoms, b is in the molecular plane and perpendicular to a, and c is perpendicular to that plane. The very large asymmetry of χ_{aa} and χ_{bb} does not agree with the fact that the angle is nearly 90° if the s-p hybridization only is considered. It can be explained, however, if we take d-orbitals into account. The bonding orbital of 73·6% p character, 15·8% d character and 10·6% s character was found appropriate.

Molecular calculations by a one-centre method:‡ R. K. NESBET, Lincoln Laboratory, Massachusetts Institute of Technology, Lexington, Massachusetts.

An electronic-wave function can be approximated near one nucleus in a molecule by expanding in terms of analytic orbitals centred on that nucleus. This expansion cannot be expected to be of practical value beyond the nearest neighbour nuclei to the centre of expansion. However, it is possible to obtain reliable mean values of certain "local" operators which heavily weigh

* This work has been supported by the United States Air Force through the Office of Scientific Research of the Air Research and Development Command.

† This research was supported by the United States Air Force, through the Office of Scientific Research of the Air Research and Development Command, and by the joint programme of the US Office of Naval Research and US Atomic Energy Commission.

‡ The research reported in this document was supported jointly by the Army, Navy, and Air Force under contract with Massachusetts Institute of Technology.

[1] BURRUS C. A. JR. and GORDY W. *Phys. Rev.* 1953 **92** 274.

the electronic density in the vicinity of the centre of expansion. The mean value of an operator localized at one of several inequivalent nuclei can be calculated from a one-centre wave function obtained independently for that particular nucleus. Calculations on the isoelectronic systems He_2, LiH, and Be will be described. Ground state energy curves for LiH and He_2 have been obtained by integrating mean values of "local" operators, parametric derivatives of the electronic Hamiltonian, calculated by the one-centre method.

Electron interaction in FE Mo Theory: H. LABHART, University of Basel, University of Chicago, Physics Department, Chicago, 37 Illinois.

Coulomb and exchange integrals are calculated assuming wave-functions of the form $\phi_i = \xi(x)\,\eta(y)\,\zeta i(z)$. z is the co-ordinate in the direction of the line connecting adjacent nuclei. x and y are the co-ordinates perpendicular to z and to one another. ξ and η are for all states taken to be the same normalized optimum trigonometric functions of adequate symmetry calculated by KUHN and HUBER. (*Helv. chim. acta*, 1952, **35**, 1155). When the potential may be set $V(x, y, z) = V_x(x) + V_y(y) + V_z(z)$ then ζ_i is an eigenfunction of

$$\left(\frac{\hbar^2}{2m}\frac{d^2}{dz^2} + V_z^{\circ}\right)\zeta = E\zeta$$

Application to ethylene gives with

$$V = -\int \xi^2\eta^2 \frac{e^2 Z_{\text{eff}}}{r_{1e}}\,dx\,dy - \int \xi^2\eta^2 \frac{e^2 Z_{\text{eff}}}{r_{1r}}\,dx\,dy$$

where r_{1e} and r_{1r} are the distances between the volume element and the left and right nucleus respectively, with $Z_{\text{eff}} = 3{\cdot}25$ for the lowest excited singlet state an energy $V = 11{\cdot}6\,\text{eV}$ over the ground state and for the lowest triplet state $T = 7{\cdot}6$ eV. Further approximation by the Hartree-Fock method does not appreciably alter these values. LCAO MO treatment by PARR and CRAWFORD (*J. Chem. Phys.* 1948 **16**, 526), gives $V = 11{\cdot}5\,\text{eV}$ and $T = 3{\cdot}1\,\text{eV}$. Experimental values are $V = 7{\cdot}6\,\text{eV}$ and $T = 3{\cdot}1$–$5{\cdot}6\,\text{eV}$. It is suggested that better agreement with experiment can be achieved taking after PAULING and SHERMAN (*Zs. Krist.* **81**, 7, 1932) $Z_{\text{eff}} = 2{\cdot}04$. This leads to $V = 9{\cdot}7\,\text{eV}$ and $T = 5{\cdot}7$ eV.

VOL. 8 1956/5

The effect of hydrogen bonding on the near ultra-violet absorption of naphthol: S. NAGAKURA and M. GOUTERMAN, Laboratory of Molecular Structure and Spectra, Department of Physics, University of Chicago, Chicago, Illinois.

The effect of hydrogen bonding on the near ultra-violet absorption band of α- or β-naphthol has been studied. Triethylamine, ether and nitromethane have been used as the proton acceptor. Experimental results show that proton accepting ability increases in the order of triethylamine > ether > nitromethane and that the red shift of absorption maximum caused by the hydrogen bonding increases in the order of α-naphthol > phenol > α-naphthol. On the basis of these results, the mechanism of hydrogen bonding and of the red shift will be discussed.

Additional evidence supporting the existence of intramolecular charge transfer absorption: S. NAGAKURA, Laboratory of Molecular Structure and Spectra, Department of Physics, University of Chicago, Chicago, Illinois.

It was shown that the strong absorption band observed with some molecules containing electron donating and accepting groups can be explained by the simple treatment and can be regarded as the intramolecular charge transfer absorption [1]. The same method was applied to explain the difference between the absorption spectrum of *p*-disubstituted benzene molecule and that of *o*-, *m*-disubstituted one. Furthermore, on the basis of the result obtained by the improved treatment, the accuracy of our method will be discussed.

---

[1] NAGAKURA S. and TANAKA J. *J. Chem. Phys.* 1954 **22** 23b; NAGAKURA S. *J. Chem. Phys.* 1955 **23** 1441.

On the U.V. absorption spectra of thionyl-aniline: A. MANGINI and G. LEANDRI, Industrial Chemistry Department, University of Bologna, Bologna, Italy.

The thionyl-aniline (ThA), $R—N=S=O$, prepared condensing the amines with thionyl-chloride are generally coloured in the yellow shades.

The authors have recorded the u.v. absorption spectra.

The phenyl-thionyl-aniline presents the band of aniline, and also the band in the 320 mμ region, $\lg\epsilon \sim 4$: the latter is shifted towards the red by some substituents (Me, Alg, OR . . . .) and the intensity remains about of the same order of magnitude: In the case of *p*-nitro-derivative the spectrum is practically similar to that one of *p*-nitro-acetanilide.

The authors considering also the results on dipole moments and on the chemical behaviour, formulate the hypothesis that the ThA are in a highly dipolar state.

The π-electron structure of butadiene: R. STEPHEN BERRY and WILLIAM E. MOFFITT, Mallinckrodt Chemical Laboratory, Harvard University, Cambridge, Massachusetts.

The energy levels of the π electron systems of butadiene have been computed for six spatial configurations of the molecule; of these, three are *cis* and three *trans*. The levels were determined by the following methods;

(a) Valence Bond Theory including covalent structures only;
(b) Antisymmetrized Molecular Orbital Theory including self-consistent field orbitals;
(c) "full" configuration interaction;
(d) perturbation theory applied to two neighbouring vinyl radicals represented by ASMO functions, and
(e) the method of Atoms in Molecules as applied to (a), (b), (c), and (d) above.

From these calculations, it is concluded that the method of Atoms in Molecules with full configuration interaction is the only one of the methods used which predicts quantitatively the ultra-violet spectrum of butadiene. On the basis of the calculation, the observed band at 6·0 eV is assigned as $^1Ag \rightarrow {}^1Bu$, corresponding essentially to the one-electron excitation $N \rightarrow V_1$. (The band is predicted at 6·0 eV). The observed 7·2 eV absorption is assigned as $^1Ag \rightarrow {}^1Ag$ (predicted 7·7 eV). This band system is attributed to V_{23}^+, the higher energy state of the pair V_{23} and V_{23}^+, the first two excited orbital configurations which are degenerate in a simple molecular orbital treatment. Excitation to the lower ^1Ag excited state, V_{23}, is predicted to lie at 6·1 eV, and being a forbidden transition, would be masked by the strongly allowed $^1Ag \rightarrow {}^1Bu$ transition.

Continuous emission spectra of O_2 in the ultra-violet and the vacuum regions: Y. TANAKA, A. JURSA and F. LEBLANC, Geophysics Research Directorate, Air Force Cambridge Research Centre, Air Research and Development Command, Cambridge Massachusetts.

Several emission continua were observed, in a transformer discharge of ($A + O_2$), in the ultra-violet and vacuum regions. Approximate wavelengths of their peaks are 1490, 1840, 2100, and 2315 Å. When krypton was used instead of argon, most of them showed a slight shift in wavelength at their peaks, except one at 2100 Å. But, with xenon, all others disappeared completely except the longest at 2350 Å, which also was observed by HERMAN [2]. In consideration of the experimental conditions, these are probably due to the O_2 produced by transitions from upper stable states to unstable lower states.

Absorption spectra of benzene and benzene-d_6 in the vacuum ultra-violet:* P. G. WILKINSON, Department of Physics, The University of Chicago, Chicago 37, Illinois.

The absorption spectra of benzene and benzene-d_6 have been photographed in the 1300° Å to 1800° Å region using the first order of a 21-foot vacuum spectrograph and the xenon and krypton continue as absorption backgrounds. Four Rydberg series were identified in each

* This research was assisted in part by the Office of Ordnance Research under project TB 2-0001 of Contract DA-11-022-ORD-1002 with the University of Chicago.

[1] HERMAN R. and HERMAN L. *J. Phys. Radium* 1950 **11** 69.
[2] A preliminary account of this work was given in *J. Chem. Phys.* 1956 **24.**

molecule, converging to ionization potentials of 9·247 eV (benzene) and 9·251 eV (benzene-d_6). Progressions of the ν_2, ν_{18}, and ν_{20} vibrations are associated with most of the 31 observed Rydberg transitions. The strong intensity and unusual length of the upper state $\nu_{18}(e_{2g})$ progression in comparison with the $\nu_2(a_{1g})$ progression are interpreted in terms of the Jahn-Teller theorem, and it is concluded that the stable equilibrium nuclear configuration in the Rydberg states is of D_{2h} symmetry [1].

Effect of substituents on the near U.V. spectrum of benzene: JOHN A. PETRUSKA*, Laboratory of Molecular Structure and Spectra, University of Chicago, Chicago 37, Illinois.

The changes in intensity and excitation energy of the lowest singly excited states of benzene accompanying the replacement of one or more hydrogen atoms on the ring by other groups are considered in the light of theoretical results based on approximate MO theory. Simple formulas are given for relating the frequency shift and intensity increment of the 2600-Å band (in benzene) to two parameters characteristic of each different substituent. The formulas are shown to hold for a wide variety of substituent groups. Suitable values for the parameters are obtained from the observed spectra of the corresponding monosubstituted derivatives.

Rotational structure of the 3800Å absorption system of SO_2:† J. B. COON, R. K. RUSSELL, and B. L. LANDRUM, Department of Physics, A. and M. College of Texas, College Station, Texas.

The geometry of the excited electronic state associated with the 3800-Å absorption system of SO_2 vapour has been recently determined by a quantitative application of the Frank-Condon principle [1]. The results reported are $r = r'' + 0{\cdot}060 = 1{\cdot}492$ Å, and $2\theta' = 2\theta'' + 5°4' = 124°36'$. These data yield the constants of the rotational structure, namely $2\Delta\,(A - \bar{B}) = 0{\cdot}396$ cm^{-1} and $2\Delta\bar{B} = -0{\cdot}071$ cm^{-1}. In order to check these results, and in order to remove the uncertainty as to the polarization of the bands of this system [2, 3], the resolvable features of the rotational structure of the bands are being examined. Preliminary measurements yield $2\Delta\,(A - \bar{B}) = 0{\cdot}438 \pm 0{\cdot}03$ cm^{-1} and $2\Delta\bar{B} = -0{\cdot}080 \pm 0{\cdot}008$ cm^{-1} confirming the results based on the Frank-Condon principle. Although the polarization of these bonds has not yet been determined with certainty, it is expected that this can be reported soon.

Vibrational analyses of the triplet-singlet emission spectra of several alkylbenzenes:‡ YOSHIYA KANDA and LAWRENCE BLACKWELL, Department of Physics, Duke University, Durham, North Carolina.

The triplet-singlet emission spectra of toluene, ethyl-benzene, *n*-propylbenzene, and *n*-butylbenzene were studied at several concentrations in a rigid solution (EPA) and in the crystalline state at liquid nitrogen and liquid helium temperatures. A comparison of the vibrational analyses of these spectra was made with the analysis of the toluene spectrum given by DIKUN and SVESHNIKOV. The crystalline spectra of these compounds were shifted to the red and found to have a different vibrational structure from that of the solution spectra. Special bearing of concentration effects on the interpretation of the spectra will be discussed.

Triplet-singlet emission spectra of some heterocyclic and related molecules: RICHARD C. HECKMAN,§ Department of Physics, Duke University, Durham, North Carolina.

Triple-singlet emission spectra taken in rigid glass solutions (EPA) will be presented for indene, indole, thianaphthene, fluorene, carbazole, dibenzofuran and dibenzothipohene. Except for indene, vibrational analyses of the spectra are possible on the basis of known Raman

---

* Holder of a Shell Oil Fellowship in the Department of Chemistry, University of Chicago, September 1955—June 1956.

† Supported by the Air Force Office of Scientific Research of the ARDC under contract No. AF18 (600)—439.

‡ Supported by the National Science Foundation.

§ CHARLES F. KETTERING Foundation Fellow at time of this work. Present address: CHARLES F. KETTERING Foundation, Yellow Springs, Ohio.

[1] COFFMAN M. L., CORGAN J. M., LOYD C. M., and COON J. B. *Bull. Amer. Phys. Soc.* 1956 **1** 90.

[2] METROPOLIS N. *Phys. Rev.* 1941 **60** 283.

[3] MULLIKEN R. S. *Rev. Mod. Phys.* 1942 **14** 204.

VOL. 8 1956/5

and infra-red vibrations. Four other compounds namely cyclopentadiene, purrole, furan and thiophene showed no corresponding emission within the limitations of the experiment. The phosphoroscope permitted observation of emission with lifetimes above 0·002 sec. The results will be discussed.

Triplet-singlet emission spectra of benzene and naphthalene crystals at low temperatures:* H. Sponer, Lawrence Blackwell and Yoshiya Kanda, Department of Physics, Duke University, Durham, North Carolina.

The triplet-singlet transition of benzene at 3400 Å sharpens at liquid-helium temperature to a spectrum with remarkably well-defined structure. With naphthalene crystals the known lowest triplet-singlet emission was observed at 5200 Å as a fairly sharp spectrum at liquid nitrogen and at liquid helium temperatures. In addition, evidence of another T–S transition at 3600 Å was obtained from plates taken at liquid-helium temperature. The results in the experiments with naphthalene are very sensitive to the purity of the sample. For example, with a commercial sample of naphthalene studied at liquid-helium temperature the TS emission of thianapthene is present and, in addition a spectrum at shorter wavelengths which proved to be identical with the fluorescence spectrum of naphthalene described by Obreimov and Shabaldas at liquid-hydrogen temperature, usually not observable with a phosphoroscope. We consider that a second triplet state of thianaphthene may be so located as to sensitize the fluorescence emission of naphthalene.

Electronic and vibrational states of the pleiadienes [1]: Jerome W. Sidman [2], Department of Chemistry, The University of Rochester, Rochester, New York.

The electronic spectra of acepleiadiene [3] and acepleiadylene [4] have been studied in rigid glassy solution at 77°K, in dilute single mixed crystals with pyrene at 77°K and at 4°K, and in single crystals at 77°K. The electronic transitions are assigned, using both the semi-empirical (Platt) and the symmetry classifications. Comparisons with theory where possible, indicate that the LCAO-MO, FEMO, and cyclicpolyene (Moffitt perturbation) theories are in good agreement with the observed results. Aromaticity in pericondensed systems is discussed, and possible extensions of the Huckel $(4n + 2)$ rule are suggested. Vibrational analyses and assignments are given for the lowest absorption and fluorescence transitions in acepleiadylene and for the lowest absorption transition in acepleiadiene.

A 1890 cm^{-1} (K) crystal splitting which is observed for the lowest transition in acepleiadylene is interpreted on the basis of the Frenkel-Davydov exciton theory. The lowest absorption transition of acepleiadiene shows evidence of crystal-induced mixing of molecular transitions. The crystal spectra give information regarding some of the gross features of the crystal structure.

Effect of solvent on the electronic spectra of the polyacenes: B. H. Johnson, Humble Oil and Refining Company, Baytown, Texas, and F. A. Matsen, The University of Texas, Austin, Texas.

The wavelengths of an electronic absorption band of a chromophore, C in a medium M is given to the second order of perturbation by

$$\lambda = \lambda_0 \left(1 + \frac{\phi}{R^6} \frac{^a M}{^1 M} |r_c|^2 \right) + \text{terms relating to other transitions} \qquad (1)$$

where α_M, I_M, r_C, ϕ, and R are respectively polarizability, ionization energy, transition moment, co-ordination number and internuclear distance. The solvents used were ROH $(\alpha/I \sim 0{\cdot}298)$$RNH_2$

* Supported by the National Science Foundation.

[1] *J. Amer. Chem. Soc.* **78** in press (1956): This research was supported by the U.S. Office of Ordnance Research under contract DA-30-115-Ord 620 with the University of Rochester.

[2] Post-doctoral fellow under a grant by the Shell Fellowship Committee to the Department of Chemistry of the University of Rochester.

[3] Boekelheide V., Langeland W. E., and Liu C. T. *J. Amer. Chem. Soc.* 1951 **73** 2432.

[4] Boekelheide V. and Vick G. K. *J. Amer. Chem. Soc.* 1956 **78** 653.

(0·525) and RSH (0·930), which have in common an unshared pair of electrons on a single atom and no multiple bonds. The effect of these solvents on the first and second transitions of naphthalene, anthracene, and naphthacene have been determined. The results obtained are in good qualitative agreement with respect to variation in α/I. The dependency on $|r_C|^2$ is similar to that obtained in the pressure experiments described in the following paper.

The addition of mercaptan to naphthacene completely changes the naphthacene spectrum. Because of the high electron affinity of the naphthacene and the low ionization energy of the mercaptan, this result may be attributable to a charge-transfer interaction.

If the change in solubility of the chromophore can be attributed to the change in dispersion forces one may write

$$RT \ln S/S = \frac{(\lambda - \lambda_0)\, I_B}{\lambda_0}$$

This relation was found to be qualitatively obeyed.

The ultra-violet absorption spectrum of CF_3I: S. R. Polo, Division of Pure Physics, National Research Council, Ottawa, Canada.

The absorption spectrum of CF_3I in the vacuum ultra-violet has been studied in a 3-m grating spectrograph. Three absorption systems at 1739 Å, 1599 Å, and 1416 Å have been observed. The system at 1739 Å has been photographed in the fourth order and the vibrational structure analysed. The values of the totally symmetric vibrations in the upper state are 969·1, 681·9, and 231·3 cm^{-1}.

The emission spectrum of P_2^+: N. A. Narasimham, Division of Pure Physics, National Research Council, Ottawa, Canada.

A discharge through helium containing a little phosphorus in a hollow cathode discharge tube has been found to emit a number of new bands between 3400 and 9000 Å. These bands have been photographed with a 35-ft. grating spectrograph and their rotational and vibrational structures studied. Analysis of the 3900–4400 Å bands show that they arise from a $^2\Sigma_u^+ - {}^2\Sigma_g^+$ transition of the P_2^+ molecule. Two lower state progressions have been analysed but the vibrational numbering is as yet unknown. A second band system has been found in the region 3400-3850 Å and, on the basis of an incomplete analysis, has been assigned to a $^2\Pi$–$^2\Pi$ transition of P_2^+. When a small amount of hydrogen was added to the gas in the discharge, three hydride bands were found at 3648 Å, 3850 Å, and 4227 Å. From a preliminary study of the bands, it appears probable that these bands arise from a $^2\Delta$–$^2\Pi$ transition of PH^+.

The near ultra-violet spectrum of carbon disulphide: B. Kleman, Division of Pure Physics, National Research Council, Ottawa, Canada.

The 3100 Å system of CS_2 has been photographed in absorption with a 35-ft. grating spectrograph. Multiple reflection mirrors have been used in the absorption cell to obtain path lengths of up to 100 metres. The spectrum extends from 2700 Å to 4000 Å. The long-wavelength end of the spectrum consists of regular progressions involving excitation of the bending frequency of the upper state. In addition to the bending frequency, one quantum of the symmetric stretching frequency of the upper state is also excited in some progressions. The lowest states range from the ground state up to $5\nu_2$ and the bands have the appearance of Σ–Σ, Π–Π, Δ–Δ, and Φ–Φ bands. A detailed study of the vibrational and rotational structure shows that the molecule is nonlinear in the upper state.

Electronic spectrum and structure of the free NH_2 radical: D. A. Ramsay, Division of Pure Physics, National Research Council, Ottawa, Canada.

The a bands of ammonia which lie in the region 4000–8300 Å have long been known in emission from oxyammonia flames and discharges through streaming ammonia. The bands were recently observed in absorption during the flash photolysis of ammonia and hydrazine. Isotopic

VOL. 8 1956/5

shifts were observed when N^{14} was replaced by N^{15} and when H was replaced by D. The bands were assigned to NH_2 for a variety of reasons and this assignment has now been conclusively confirmed by a rotational and vibrational analysis of the bands.

The bands are found to be due to a Type-C transition between a ground state in which NH_2 is bent to an excited state in which it is linear. A progression of sixteen bands of the bending frequency in the upper state has been identified, the quantum number v_2' taking the probable values 5, 6, 7, . . . 20. The vibrational intervals are found to increase from $\sim$650 cm^{-1} to $\sim$1000 cm^{-1} with increasing vibrational quantum number. A vibrational perturbation has been observed in the region $v' = 13$–16. No bands involving excitation of the N–H stretching vibrations in the upper state have yet been identified.

Ground state combination differences are found to repeat in alternate bands, but not in successive bands of the progression. This provides strong confirmation that the upper state is linear since, for a progression of the bending vibration of a linear molecule, the vibrational symmetries alternate between Σ, Δ, Γ . . . for the even members and Π, Φ, . . . for the odd members of the progression. The expected 3 : 1 alternation in the intensities of successive rotational lines of various branches has been observed and provides conclusive proof of the presence of a twofold axis of symmetry. The sign of the intensity alternation is consistent with the assignment of the ground state to an electronic $^2B_1$ state as predicted by MULLIKEN.

Rotational constants for the ground state have been determined by the application of MECKE'S Sum Rules are $A''_{000} = 23{\cdot}6_2\ cm^{-1}$ $B''_{000} = 12{\cdot}9_4\ cm^{-1}$ $C''_{000} = 8{\cdot}3_6\ cm^{-1}$. From these constants, the following bond lengths and angles may be deduced:

$$r''_{000}\,(NH) = 1{\cdot}025\ \text{Å}\quad H\text{–}\hat{N}\text{–}H = 103°.$$

Detailed rotational constants for the upper state have not yet been obtained due to large displacements of subbands with different values of l. Very roughly these displacements are of the form gl^2 where $g \sim 30$–$40\ cm^{-1}$. The upper state is probably an electronic $^2\pi$ state and the displacement of subbands with different l values is probably due to interaction between the electronic orbital angular momentum $\frac{\Lambda h}{2\pi}$ (where $\Lambda = 1$) and the vibrational angular momentum $\frac{lh}{2\pi}$ associated with the bending vibration. A small spin splitting has also been observed.

Thermochemical determination of the dissociation energies of YO, LaO, and CeO: MICHAEL HOCH, Department of Chemistry, The Ohio State University, Columbus, Ohio.

The vaporization into vacuum of the sesquioxides Y_2O_3, La_2O_3, and Ce_2O_3 was studied between 2000 and 2500°K. The major components of the gas phase are the respective metal monoxides YO, LaO, CeO, and oxygen. From the rates of evaporation the partial pressures of the gaseous monoxides in equilibrium with the solid sesquioxides can be calculated. These values combined with known thermochemical quantities, permits calculation of the dissociation energies $D_0°$ of the monoxides.

Programming the IBM 701 computer for double numerical integration of the overlap integral between two hydrogen-like wave functions: D. S. VILLARS, U.S. Naval Ordnance Test Station, China Lake, California.

The 701 Computer has been programmed to derive, to 10-decimal-digit accuracy, the coefficients of the polynomial terms representing hydrogen-like wave functions. The results from this computation are recorded on punched cards, and then used as data input for a second programme which computes the values of the individual polynomials, multiplies them together with the volume element for polar co-ordinates, and supplies the product as the integrand for a double numerical quadrature over radial distance and polar angle. Subtraction of the "Simpson" error, used to define the (adjustable) interval of integration, from the computed value of the integral, effects the removal of error terms up to (but excluding) the sixth derivative. This amounts to fitting groups of five points by quartic equations. A study has been made of dependence of speed of the double integration on maximum Simpson-error specification.

Nonplanar structure of formaldehyde in its low-lying excited electronic state:* G. WILSE ROBINSON and WILLIAM S. BENEDICT, The Johns Hopkins University, Baltimore, Maryland.

The rotational analysis of the high-resolution emission spectrum of formaldehyde in the near ultra-violet region gives evidence that the upper state of this transition has an equilibrium configuration that is slightly nonplanar. The inertial defect, $\Delta = I_C - I_B - I_A$, calculated for the upper level of the α-band is small but definitely negative. For a rigid planar structure it should be zero, while in the lowest level of the planar ground state [1] it is of the same order of magnitude as here but positive, due to zero-point vibrations. A re-examination of part of the absorption spectrum [2] similarly shows negative defects. If the equilibrium configuration of the upper state is nonplanar as suggested by the rotational analysis, but with the potential energy of the planar configuration only slightly higher, one would expect inversion doubling of the lowest upper state vibrational levels. The puzzling 125 cm^{-1} energy difference between the lowest observed vibrational states of the emission system (α band) and absorption system (A band) may thus be interpreted. As a consequence of this difference in geometry between the ground and excited electronic states, progressions of the out-of-plane bending vibration are observed as predicted by the Franck-Condon Principle.

Effects of high pressure upon the near ultra-violet absorption spectra of the polyacenes:† W. W. ROBERTSON, O. E. WEIGANG, and F. A. MATSEN, Departments of Physics and Chemistry, The University of Texas, Austin, Texas.

The absorption spectra of naphthalene, anthracene, and naphthacene in n-pentane have been recorded in the near ultra violet at pressures up to 5500 bars. The wavelength of absorption increases linearly with the dielectric constant of the pressurized solvent, $\lambda = \Delta\lambda/\Delta K\,(K-1) + \lambda^\circ$. $\Delta\lambda/\Delta K$ varies from 26 Å for the naphthalene ${}^1A_{1g}^- - {}^1B_{3u}$ transition to 235 Å for the naphthalene ${}^1A_{1g}^- - {}^1B_{2u}^-$ transition. Since $\Delta\lambda/\Delta K$ can be accurately measured, a practical method exists for distinguishing between transitions.

Values of λ_0 obtained by extrapolating to $K = 1$ are within a few ångströms of the measured values that are obtainable for the vapour state.

$\frac{1}{\lambda_0}\,\Delta\lambda/\Delta K$ increases generally with the oscillator strength of the transition as is predicted by theory. However, no simple relation exists between slope and oscillator strength.

VOL. 8 1956/5

Atomic Spectroscopy

Some attempts to obtain ground-state wave functions of considerable accuracy for two-electron systems: L. C. GREEN, Strawbridge Observatory, Haverford College, Haverford, Pennsylvania.

Simple wave functions for first-row atoms and ions: C. C. J. ROOTHAAN, Department of Physics, University of Chicago, Chicago, Illinois.

Atomic theory in non-euclidian space: R. E. TREES, Palmer Physical Laboratory, Princeton University, Princeton, New Jersey.

The configurations d^n, $d^{n-1}s$, and $d^{n-2}s^2$ in the spectra of the third group of transition elements: M. A. CATALÁN and R. VELASCO, Institute of Optics, Madrid, Spain.

* One of us (GWR) is grateful to the Office of Ordnance Research, U.S. Army, for support of part of this work under OOR Project No. TB2-0001 of Contract No. DA-36-034-ORD-2169.

† This work was supported in part by the Office of Scientific Research, Air Research and Development Command, under Contract No. AF 18(600)-430.

[1] LAWRANCE R. B. and STRANDBERG M. W. P. G. *Phys. Rev.* 1951 **83** 363.

[2] DIEKE H. and KISTIAKOWSKY G. B. unpublished data.

A revision of some simple atomic spectra: (Na I, K I, Mg II, Ca II) Bengt Edlén, Physical Institute, University of Lund, Sweden.

Developments in atomic emission spectra in the lead sulphide region since 1954: C. J. Humphreys, U.S. Naval Ordnance Laboratory, Corona, California.

Isotope effects in the hyperfine structure of the resonance lines of gallium I: D. A. Jackson, Laboratoires de Bellevue, Seine-et-Oise.

The hyperfine structure of the two resonance lines of gallium I, in the visible, $4^2P_{1/2} - 5S_{1/2}$, 4033 Å, and $4^2P_{3/2} - 5S_{1/2}$, 4172 Å, has been investigated by means of the absorption of a multiple atomic beam of high collimation, observed with a double Fabry-Perot etalon. The combined Doppler and instrumental width was approximately 5 mK.

In the line 4033 Å, the components of the two isotopes Ga^{69} and Ga^{71} were very well resolved, their separation being about 4 times their line width, and since 68 independent measurements were made, the probable error in the positions of the *hfs* components was reduced to approximately 0·1 mK. From these measurements are derived:—the *hfs* intervals of the terms $4^2P_{1/2}$ and $5S_{1/2}$ for Ga^{69} and for Ga^{71}, the ratio of the magnetic moments of the nuclei given by each of these terms and the isotope shift for the line.

The line 4172 was less well resolved, due to the smaller separations of the components of the two isotopes, and they were mostly observed as blends, but the structure of the level $^2P_{3/2}$ can be derived with an accuracy of the order of 2 mK and an approximate value can be found for quadrupole moments of the nuclei.

Calcium beam experiments: K. W. Meissner, Department of Physics, Purdue University, Lafayette, Indiana.

The first spectrum of iodine: C. C. Kiess and C. H. Corliss, Spectroscopy Section, National Bureau of Standards, Washington. D.C.

Spectral structure of the rhenium atom: P. F. A. Klinkenberg, Zeeman Laboratorium University of Amsterdam, Amsterdam, Holland.

By a joint effort of three research groups (National Bureau of Standards, Washington, D.C.; Instituto de Optica "Daza de Valdés", Madrid; Zeeman Laboratory, Amsterdam) the analysis of the Reare spectrum has been improved and extended to include 2769 classified lines in the spectral region 1700–12,000 Å. To the existing level system 12 low even, 3 high even and 46 odd levels could be added, so that there are now 51 low even, 20 high even and 212 odd levels known. Thanks to extensive Zeeman effect observations on plates obtained at the MIT Spectroscopy Laboratory g values could be evaluated for 75% of all levels. These confirmed most of the earlier identifications, but a few had to be changed and many levels could be interpreted for the first time. In the ground systems the evidence for $5d^7$ levels has not been confirmed. In the high even group the term $5d^46s^2\ (^5D)\ 7s^6D$ was detected except the level $^6D_{1/2}$. In the odd group the ^6D and ^6F terms from $5d^46s^2(^5D)6p$ could be located and also $5d^56s(^5G)\ 6p^6G$ in close agreement with the low position of the ^5G parent term in Re II and with correspondingly irregular spacings. A few ^6D levels derived from the parent term $5d^56s\ ^5P$ have been detected. The spectrum is characterized by wide hyperfine structure patterns which were used as additional evidence for the correctness of the classifications.

Extension of the analysis of the first spectrum of ruthenium with digital computers: K. G. Kessler, Spectroscopy Section, National Bureau of Standards, Washington, D.C.

The second spectrum of ruthenium: A. G. Shenstone, Palmer Physical Laboratory, Princeton University, Princeton, New Jersey.

Survey of isotope shift for elements near the middle of the atomic table: J. E. MACK, Department of Physics, University of Wisconsin, Madison, Wisconsin.

Isotope shift in the arc spectrum of osmium and application to the identification of the electron configurations: JEAN BLAISE and P. JACQUINOT, Laboratoires du C.N.R.S., Bellevue, (S & O) France.

The isotope shifts have been measured in a number of lines of Os I, allowing the classification of the following types of transitions:

transitions	shifts 190–192(mK)
$d^6s^2 - d^6sp$	−55
$d^7s - d^6sp$	+28
$d^7s - d^7p$	−96
$d^6sp - d^66s7p$	+15
$d^6s^2 - d^5s^2p$	0

The terms classified by ALBERTSON W. (*Phys. Rev.* 1934 **45,** p. 304), have been confirmed and electron configurations have been attributed to a number of them.

The term 53°(36818·1 K above the ground level) is the term $d^7p^5F_5{}^\circ$. The classification of the term 103 (47198·8 K), $d^66s7s\,{}^7D_5$ is confirmed.

Investigation of the nuclear moments of the separated isotopes of hafnium: F. A. JENKINS, Department of Physics, University of California, Berkeley, California.

The emission spectra of actinium: W. F. MEGGERS, National Bureau of Standards, Washington, 25, D.C. and M. FRED and F. S. TOMKINS, Argonne National Laboratory, Lemont, Illinois.

Spectra of triplyionized rare earths: G. H. DIEKE, Department of Physics, Johns Hopkins University, Silver Spring, Maryland.

Preliminary classification of the spectrum of singlyionized plutonium: J. RAND MCNALLY, JR., Oak Ridge National Laboratory, Oak Ridge, Tennessee.

Survey of the spectra of americium and neptunium: M. FRED, Argonne National Laboratory, Lemont, Illinois.

The astrophysical importance of rare-earth spectra: CHARLOTTE M. SITTERLY, Spectroscopy Section, National Bureau of Standards, Washington, D.C.

Spectra of Molecules

Invited papers

A case history of the NO molecule: J. H. VAN VLECK, Division of Engineering and Applied Physics, Harvard University, Cambridge, Massachusetts.

The spectrum of NO_2: CHUN C. LIN, Department of Physics, University of Oklahoma, Norman, Oklahoma.

The far infra-red spectrum of methyl alcohol: DAVID M. DENNISON, Randall Laboratory of Physics, University of Michigan, Ann Arbor, Michigan.

In 1939 BORDEN and BARKER mapped the infra-red spectrum of methanol and observed a considerable number of irregularly spaced lines in the region from 860 to 380 cm^{-1} which they correctly interpreted as arising from hindered rotation transitions. Twelve years later BURKHARD measured the rotation spectrum out to 50 cm^{-1}. Recently PALIK and OETJEN have re-examined the region and have refined many of the details.

The goal of the present work is the identification of the observed lines and hence the evaluation of the energy levels of the molecule. Since the lines are crowded together with an apparently

VOL. 8 1956/5

irregular distribution, both of spacings and of intensities, it is necessary to start with a calculated spectrum which is quite accurate if one hopes to make an unambiguous correlation. The following steps were employed. (1) The microwave spectrum of methanol furnishes reliable values for the barrier height and the molecular dimensions. From these the energy levels and transition probabilities were calculated for $n = 0$, 1 and 2 and for $K = 0$ up to 10. (2) The centrifugal stretching is quite large for methyl alchohol and gives a correction to the energy levels which, while it is negligible for the lower levels of $n = 0$, becomes as large as 10 cm^{-1} for the levels of $n = 2$. Knowing the molecular force constants from the near infra-red spectrum it is possible to calculate these corrections without introducing any additional empirical constants. (3) With the aid of the calculated spectrum, including the corrections, it was possible to identify the more intense lines and consequently to find the actual energy levels. The weaker lines now furnished self-consistency checks. (4) The observed levels were examined to see whether they would fit into the structure of levels demanded by the theory of hindered rotation. This last step furnished a strong check on the whole process and constitutes convincing evidence for the correctness of the identifications.

The determination of potential barriers hindering internal rotation: E. Bright Wilson, jr., Department of Chemistry, Harvard University, Cambridge, Massachusetts.

Contributed papers

Intramolecular strain constants: pyramidal XY_3 molecules: Emil J. Slowinski, jr., and Harold E. Bellis, Department of Chemistry, University of Connecticut, Storrs, Connecticut.

The potential function $V = \Sigma_{\text{all bonds}} k_i(d_i - D_i^0)^2 + \Sigma_{\text{all angles}} k_\alpha(\alpha_j - A_j^\circ)^2$, where D_i^0 and A_i^0 are the "Strain free" values of bond length and bond angle respectively, has been extended to NH_3-type molecules. Improved mathematics are described. Sufficient equations exist to determine all 6 parameters. Results in part support the conclusions made on H_2O-type molecules. There appears to a be "preferred" strain free bond angle.

New terms in the potential function of the Y_2X_2 molecule:† Fred L. Keller and Alvin H. Nielsen, Department of Physics, The University of Tennessee, Knoxville, Tennessee, and Wave H. Shaffer, Department of Physics and Astronomy, Ohio State University, Columbus Ohio.

A re-examination of the infra-red spectrum of acetylene at high dispersion, recently concluded, disclosed some serious difficulties with regard to band assignments and consistency among the vibrational constants. These difficulties led to a re-examination of the paper on the theory of the linear Y_2X_2 molecule by Shaffer and Nielsen. [1] From this study it became apparent that several permitted terms had been omitted from the cubic and quartic portions of their expression for the potential energy, namely:

$$hc\beta_{345}q_3(r_4s_5 - r_5s_4),\quad hc\sum_{i=1i}^{2}\gamma_{345i}q_iq_3(r_4s_5 - r_5s_4),\quad hc\gamma'_{4455}(r_4s_5 - r_5s_4)^2 \text{ and } hc\gamma''_{4455}(r_4r_5 - s_4s_5)^2,$$

where the notation is the same as in the original paper. With polar co-ordinate substitutions the above terms may all be seen to depend upon the phase angle between the degenerate vibrations $\tilde{\nu}_4$ and $\tilde{\nu}_5$. As they have A_{1g} symmetry it seems reasonable to include them in the potential energy expression.

The new terms affect the energy of the molecule by contributing to x_{34}, x_{35}, and x_{45}, and by introducing an entirely new constant X_{45} which is the coefficient of $(l_4l_5 - 1)$. While the contributions to x_{34}, x_{35} and x_{45} do not affect the interpretation of the spectrum or the experimental values previously obtained for them, the new constant X_{45} does affect the agreement between theory and experiment; the interpretation and assignment of the bands; and the values obtained for several of the other constants. The experimental value of X_{45} was found to be

† This paper constitutes a portion of a Ph.D. thesis submitted to the Graduate Council of The University of Tennessee. The work was supported by the Office of Ordnance Research, US Army.

[1] Shaffer W. H. and Nielsen A. H. *J. Chem. Phys.* **1941** **9** 847.

4·91 cm^{-1}. The new terms become important in the accidental degeneracy involving $\tilde{\nu}_3$ and $\tilde{\nu}_1 + \tilde{\nu}_4^1 + \tilde{\nu}_5^1$, which are separated by only 13 cm^{-1}. A resonance between these levels is postulated in order to make their observed positions consistent with data from other observed bands. The term $hcq_1q_3(r_4s_5 - r_5s_4)$ has nonzero, off-diagonal matrix elements, connecting the upper levels of these bands, which remove the difficulty about their position, while the Shaffer-Nielsen potential function contains no such terms.

The emission spectrum of the hydrogen-fluorine flame:* D. E. Mann and J. J. Ball, National Bureau of Standards, Washington 25, D.C. and Gordon E. Moore, Applied Physics Laboratory, The Johns Hopkins University, Silver Spring, Maryland.

The emission spectrum of the hydrogen-fluorine flame has been photographed over the range 5500–10,400 Å with a 2-metre grating spectrograph. The 3–0, 4–1, 5–2, 4–0, 5–1, 6–2, 7–3, 5–0, 6–1, 7–2, 8–3, and 9–4 bands of hydrogen fluoride have been measured. For several bands levels above $J = 20$ have been observed. These data have permitted improved molecular constants to be established.

ν_1, $2\nu_2^\circ$, $(\nu_3-\nu_1)$ and $(\nu_3-2\nu_2^\circ)$ of N_2O†: K. Narahari Rao and Harald H. Nielsen, Department of Physics and Astronomy, The Ohio State University, Columbus 10, Ohio.

The bands ν_1 and $2\nu_2$ of N_2O have been remeasured with a vacuum-grating infra-red spectrometer. Interference due to "hot" bands occurring in the region of absorption of these two bands was minimized by keeping the absorbing gas at low temperatures. The scatter in the previously published data could thus be reduced, and therefore, it was possible to investigate the effect of Fermi resonance on the rotational constants of the levels 10°O and 02°O of N_2O. The results have been examined using the theory developed by Nielsen, Amat, and Goldsmith [1].

Two bands were observed in the region of about 10 μ and they were identified as $(\nu_3-\nu_1)$ and $(\nu_3-2\nu_2)$. It is anticipated that the frequencies of the P and R structure of these "difference" bands along with the positions of the rotational lines of ν_1, $2\nu_2$ and ν_3 can conveniently be used to evaluate the merits or otherwise of the techniques employed in a laboratory for obtaining wavelength measurements of infra-red lines.

The infra-red spectra of T_2O and TCN: P. A. Staats, H. W. Morgan, and J. H. Goldstein, Oak Ridge National Laboratory, Oak Ridge, Tennessee.

The vapour phase spectra of T_2O and TCN have been studied in the region 400 to 5000 cm^{-1}. A single beam double-pass spectrometer was used with prisms of LiF, NaCl, and KBr. The fundamentals ν_2 and ν_3 were measured in T_2O. Small quantities of the H and D substituted species were produced by exchange, and ν_2 and ν_3 were observed for THO and ν_3 for the TDO molecule. The three fundamentals of TCN were measured. Anharmonicity corrections and zero order frequencies have been computed, and will be discussed. The techniques employed for the synthesis and handling of the tritiated samples will also be presented.

High-resolution, temperature-dependent spectra of calcite:‡ R. M. Hexter and D. A. Dows, Baker Laboratories, Cornell University, Ithaca, New York.

High-resolution absorption spectra of the 2·0–3·5-μ region of a basal section of calcite are reported and analysed. The resolution was accomplished with a 7500 l.p.i. "Merton-N.P.L." replica grating mounted in place of the Littrow mirror of a Perkin-Elmer Model 13 Spectrometer, with a KBr prism left in place. The spectrum is of the "double beam" type, although it envelopes

* This work was supported in part by the United States Air Force through the Office of Scientific Research of the Air Research and Development Command.

† Supported, in part, by the office of ordnance research through contracts with the Ohio State University Research Foundation.

‡ This research was in part supported by the Office of Ordnance Research, US Army.

[1] Nielsen H. H., Amat G., and Goldsmith M. (to be published).

VOL. 8 1956/5

the region of the 3700 cm^{-1} water vapour fundamentals. The methods of accomplishing the necessary compensation are discussed.

Further details of the well known splittings of degenerate vibrations of the $CO_3^=$ ion were observed and will be discussed in terms of the relative importance of the terms $V_{mm'}$ and $V_{jms}{}^r$ in the complete expression for the vibrational potential energy function of a crystal suggested by HORNIG [1]. In this analysis, the expected differences in the spectra of the so-called ordinary and extraordinary rays is discussed in terms of the theory of the motions of molecules in condensed systems developed since such spectra were obtained.

An alternative explanation of some of the observed "splittings" in the 2·0–3·5-μ region, will be presented. This analysis will be similar to that suggested previously as an explanation of observed fine structure in the spectra of crystalline iodoform and brucite. In this test of the explanation, spectra of calcite were obtained from 78°K to 873°K; the observed modifications in the spectra confirm the hypothesis of "librational interaction."

Vibrational spectrum of dislane:* GEORGE W. BETHKE and M. KENT WILSON, Mallinckrodt Chemical Laboratory, Harvard University, Cambridge, Massachusetts.

Raman spectra of the liquid and infra-red spectra of the gaseous phase have been obtained for both Si_2H_6 and Si_2D_6. With the exception of the torsional mode all fundamental frequencies have been observed and assigned to the proper normal modes. The coarse rotational structure of the perpendicular bands has been resolved and the corresponding Coriolis coupling coefficients determined. Comparisons with the spectra of ethane and methyl silane have been made.

***I*-type doubling in N_2O:†** J. N. SHEARER, T. A. WIGGINS, A. H. GUENTHER, and D. H. RANK, The Pennsylvania State University, University Park, Pennsylvania.

I-doublet separations in nine π–π bands of N_2O have been measured in the region 1·4–2·4 μ with a high-resolution spectrometer. The data indicate that the doubling constant, q_v, is in general a function of all three vibrational quantum numbers. By analogy with past theoretical work on *I*-doubling one is led to the semi-empirical equation

$$q_v = \sum_i Q_i(v_i + 1)$$

for the functional relationship, where v_i are the vibrational quantum numbers, $i = 1, 2, 3$, and the Q_1 are called Coriolis constants. It is shown that the data fits this equation within experimental error.

High-resolution infra-red spectra of methyl amine and its deuterium derivatives: ALLAN P. GRAY and R. C. LORD, Spectroscopy Laboratory, Massachusetts Institute of Technology, Cambridge 39, Massachusetts.

Methyl amine, methyl amine-d_2, methyl-d_3 amine and methyl-d_3 amine-d_2 of high chemical and isotopic purity have been synthesized and their infra-red spectra studied at both prism and grating resolution. The vibration-rotation band centres of methyl amine have been measured with improved accuracy over previous investigations and with the aid of the spectra of the deuterium analogues a vibrational assignment differing in some important respects from those hitherto suggested has been made.

The grating spectra in some cases show irregularities in the rotational fine structure but none which can be associated with effects due to hindered internal rotation. Recent studies in the microwave region have shown that these effects should not be observed within the resolution limits of the grating spectrometers used in this work. However the first overtone of the torsional frequency in methyl amine, methyl amine-d_2 and methyl-d_3 has amine been observed in a position consistent with calculations based on a barrier height of 690 cm^{-1}.

* This work was supported in part by the United States Air Force under Contract AF 18(600)—590 monitored by the Office of Scientific Research.

† This research was assisted by support from Contract Nonr-656 (12), NR 019–401 of the U.S. Office of Naval Research.

[1] HORNIG D. F. *J. Chem. Phys.* 1948 **16** 1063.

The rotational structure of a number of unperturbed vibrational bands has been analysed in terms of equations applicable to an approximate symmetric top and rotational constants have been obtained in good agreement with values calculated from parameters obtained from microwave investigations.

The infra-red spectra and structure of ethylene carbonate:* C. L. ANGELL, University of Michigan, The Harrison M. Randall Laboratory of Physics, Ann Arbor, Michigan.

The infra-red spectra of ethylene carbonate (CH_2—O—CO—O—CH_2) in the solid, liquid and vapour states and its solutions in water, chloroform, benzene, carbon tetrachloride and carbon disulphide have been studied between 3600 and 400 cm^{-1}, together with the Raman spectrum in aqueous solution. Previous X-ray crystal structure determination [1] has shown that the five-membered ring of the ethylene carbonate molecule is not planar and has symmetry C_2 in the crystal. Evidence will be presented from the spectroscopic work that the symmetry of the molecule changes from C_2 in the solid state to C_{2v} in the other states and that the five-membered ring becomes planar. An assignment of all the observed absorption bands will be given in terms of the fundamental vibrations of the molecule.

The vibrational frequencies, rotational barriers and thermodynamic properties of several polymethylbenzenes: S. H. HASTINGS and D. E. NICHOLSON, Humble Oil and Refining Company, Baytown, Texas.

Tentative vibrational frequency assignments have been made for a number of polymethylbenzenes so that the thermodynamic functions of systems containing these compounds could be computed by statistical mechanical methods. All of the methylbenzenes for which vibrational assignments had not previously been made were included: namely, 1, 2, 3-trimethylbenzene, 1, 2, 4-trimethylbenzene, the three tetra-methylbenzene isomers, pentamethylbenzene and hexamethylbenzene. A minor change in the assignment of the 1, 2-dimethylbenzene frequencies by PITZER was also made. PITZER's modification of the Teller-Redlich product rule (PITZER and SCOTT, *J. Amer. Chem. Soc.* 1943, **65** 803) was employed extensively to aid in all of the assignments.

The translational and free rotational contributions to the various thermodymanic functions were computed according to the method outlined by TAYLOR (TAYLOR, WAGMAN, WILLIAMS, PITZER, and ROSSINI, *J. Res. N.B.S.* 1946, **37**, 95. The vibrational contributions were calculated on the IBM 650 electronic computer using the harmonic oscillator expressions given by TAYLOR and GLASSTONE (*Treatise on Physical Chemistry* 1942, p. 654. These data were then combined to yield the thermodynamic functions uncorrected for the effect of restricted rotation. The value of the barrier assigned by TAYLOR *et al.*, for isolated methyl groups in methylbenzene, 1, 3-dimethylbenzene and 1, 4-dimethylbenzene (750 cal/mole) was accepted. The value of 2100 cal/mole assigned to adjacent methyl groups (as in 1, 2-dimethylbenzene) appears to be too high based upon our vibrational assignment for 1, 2, 4-trimethylbenzene and the recent experimental entropy for this compound by KILPATRICK (Southwest Regional Meeting ACS, Houston, Texas, Dec. 1955). A value of 1400 cal/mole appears to be more reasonable. Employing this barrier for the outside methyl groups in 1, 2, 3-trimethylbenzene and the experimental entropy for this compound by KILPATRICK one obtains a barrier of 3200 cal/mole for the central methyl group. This is to be contrasted with the value of 750 cal/mole for this methyl group assumed by TAYLOR *et al.* These barriers were employed to obtain the restricted rotation contributions for the three tetramethylbenzenes, pentamethylbenzene and hexamethylbenzene (e.g., six 3200 cal/mole barriers were used for hexamethylbenzene).

On the basis of these assignments thermodynamic equilibria were calculated for the tri- and tetramethylbenzenes at several temperatures. The calculated equilibria are compared with experimental data at two temperatures below:

* This work was carried out at the University of Cambridge, England during the tenure of an Oliver Gatty Studentship.

[1] BROWN C. J. *Acta Cryst.* 1954 **7** 92.

VOL. 8 1956/5

Temperature, °K.	298		700	
Mol Per Cent	Calculated	Experimental	Calculated	Experimental
1, 2, 3-Trimethylbenzene	—	—	9	9
1, 2, 4-Trimethylbenzene	—	—	67	65
1, 3, 5-Trimethylbenzene	—	—	24	29
			100	100
1, 2, 3, 4-Tetramethylbenzene	8	7	17	19
1, 2, 3, 5-Tetramethylbenzene	52	47	50	46
1, 2, 4, 5-Tetramethylbenzene	40	46	33	35
	100	100	100	100

Although no definitive estimates of error have yet been made, it is believed that the differences shown above will fall within these error limits and that further refinements in the vibrational assignments would not affect the results significantly.

Vibrational spectra and normal co-ordinate treatment of *cis-* and *trans*-BrHC=CHBr, and *cis-* and *trans*-BrDC=CDBr:* JEROME M. DOWLING, P. G. PURANIK,† ARNOLD G. MEISTER and SIDNEY I. MILLER, Spectroscopy Laboratory, Department of Physics, Illinois, Institute of Technology, Chicago 16, Illinois.

Raman spectral data for the liquid and infra-red spectral data for both liquid and gas have been obtained for *cis-* and *trans*-BrHC = CHBr and *cis-* and *trans*-Br = CDBr. The assignments are:

Type	*cis*-$C_2H_2Br_2$	*cis*-$C_2D_2Br_2$	Type	*trans*-$C_2H_2Br_2$	*trans*-$C_2D_2Br_2$
a_1	3070K(a)	2312	a_g	3089	2323
a_1	1586	1548	a_g	1581	1531
a_1	1147	819	a_g	1249	972
a_1	580	567	a_g	746	670
a_1	114	113	a_g	216	214
b_1	3059	2282	b_u	3085	2289
b_1	1254	993	b_u	1165	858
b_1	746	671	b_u	680	648
b_1	464	453	b_u	192 (b)	191 (b)
a_2	866	679	a_u	898	658
a_2	369	336	a_u	188 (c)	183 (c)
b_2	671	517	b_g	736	628

(a) K = kayser = cm^{-1}
(b) Deduced from combinations and overtones.
(c) Calculated value.

* This investigation was part of a research programme which has been aided by grants from the Research Corporation and the National Science Foundation.
† Present address: Department of Physics, Osmania University, Hyderabad 7, India.

The vibrational spectra and molecular structure of some halogenated methyl cyanides: Samuel C. Wait, jr., and George J. Janz, Department of Chemistry, Rensselaer Polytechnic Institute, Troy, New York.

The series of halogenated methyl cyanides: CCl_3CN, CCl_2FCN, $CClF_2CN$, and CF_3CN, presents the interesting case where the substituent X in the CX_3 group is progressively replaced by an atom of greater electronegativity. The present communication reports the infra-red and Raman spectra and vibrational assignments for the fundamental bands of the molecules in this series. Comparison of the results clearly shows regularities in certain fundamentals (C ≡ N stretch, C − C ≡ N symmetric and antisymmetric bends, C − F symmetric and antisymmetric stretches) which may be attributed to the changes in the force field caused by increasing electronegativity of the CX_3 group. Force constants are calculated for CX_3CN molecules belonging to the C_{3v} point group by the Wilson FG matrix method, the potential function containing all possible second degree terms. The limits of the invariancy of the force constants are examined in this series.

Vibrational spectra and molecular structure of 1,2-dicyanoethane: Warren E. Fitzgerald and George J. Janz, Department of Chemistry, Rensselaer Polytechnic Institute, Troy, New York.

The infra-red spectrum is presented from 2 to 25 μ and $-100°$ to $+180°$C for 1,2-dicyanoethane in the liquid and solid states. The results clearly show the presence of two rotational isomers of C_{2h} (trans and C_2 (gauche) symmetry at temperatures above $-43{\cdot}7°$C. The variation of the intensities of the infra-red bands with temperature gives a value of 360 ± 50 cal mole^{-1} for the energy difference, ΔH, between the two forms, with the C_2 isomer having the lower energy. At temperatures less than $-43{\cdot}7°$C, 1,2-dicyanoethane exists entirely in gauche isomeric form. In the vapour state, it is predicted, that the C_{2h} isomer will be the lower energy form, the energy difference between the isomeric forms, estimated from these results, now being 1·0 kcal mole^{-1}. The infra-red spectrum, when combined with the known Raman spectrum, permits a tentative vibrational assignment.

VOL. 8 1956/5

Vibrational spectrum and thermochromism of $VOCl_3$: Foil A. Miller, Lauren R. Cousins, and William B. White, Department of Research in Chemical Physics, Mellon Institute, Pittsburgh 13, Pennsylvania.

The infra-red spectrum of $VOCl_3$ has been measured for the first time, covering the range 300–3000 cm^{-1}. The Raman spectrum has been obtained with qualitative depolarizations. The interpretation of the spectrum (using C_{3v} symmetry) is straightforward. Species a_1 fundamentals are at 1035 (V = O stretch), 408, and 165 cm^{-1}; those of species e are 504, 249, and 129 cm^{-1}.

$VOCl_3$ provides a striking and unique example of thermochromism. At room temperature it is a pale yellow liquid, whereas it becomes cherry red on cooling. This is unique in two respects: (a) it occurs in the pure liquid, and (b) the colour deepens on cooling. To find an explanation, the visible and ultra-violet absorption have been measured at several temperatures. The results will be discussed.

The use of infra-red spectroscopy to determine the kinetics of polypeptide synthesis: M. Idelson and E. R. Blout, Children's Cancer Research Foundation, The Children's Medical Centre, Boston 15, Massachusetts and Chemical Research Laboratory, Polaroid Corporation, Cambridge 39, Massachusetts.

The polymerization of N-carboxyanhydrides of α-amino acids to yield high molecular weight polypeptides may be initiated by small amounts of basic compounds. Both monomer and polymer (N-carboxyanhydride and polypeptide respectively) each show two strong absorption bands. The monomer bands, associated with the C=O groups of the anhydride, are observed at 1860 and 1790 cm^{-1}; the polymer bands, characteristic of secondary amide groups, lie at 1655 and 1550 cm^{-1}. In the region 1500 to 1900 cm^{-1} the monomer shows no absorption where the polymer absorbs, and vice versa. Thus, one may follow the course of the reaction with time,

either by measuring the decrease in the intensity of the monomer bands, or by measuring the increase in the intensity of the polymer bands.

Data will be presented showing the use of infra-red spectroscopy to determine the kinetics of the polymerization of several amino acid anhydrides in solution. The advantages and limitations of the method will be discussed.

Potential constants and energy distributions of nitrous acid: Ann Palm, Illinois Institute of Technology, Chicago 16, Illinois.

Both *cis*- and *trans*-rotational isomers of nitrous acid have the C_s symmetry. A normal co-ordinate treatment based on a general quadratic force field has been completed following the Wilson FG matrix method. Although observed fundamentals of HNO_2 and DNO_2 are available in the literature, the number of unknown parameters exceeds the number of knowns, thereby precluding a unique solution. Hence, several sets of potential constants have been evaluated and the most likely ranges of values have been established by applying bond order criteria together with potential and kinetic-energy distributions among the internal co-ordinates.

Vibration spectra of ClF_3 and BrF_3: Howard H. Claassen, John G. Malm and Bernard Weinstock, Argonne National Laboratory, Lemont, Illinois.

The interhalogens, ClF_3 and BrF_3, were originally assigned a pyramidal structure of symmetry C_{3v} on the basis of electron-diffraction studies. Early vibrational spectra were also interpreted in terms of this model. More recently, however, investigation of ClF_3 by X-ray diffraction and microwave spectroscopy, indicates that this molecule is plane and of symmetry C_{2v}; the angles being nearly right angles.

We have studied the infra-red spectrum of ClF_3 vapour from 3 to 38 μ and its Raman spectrum. These data provide a strong confirmation for the plane structure. The fundamental frequencies obtained in the present work, together with the moments of inertia from the microwave results lead to a calculated entropy in good agreement with that obtained from thermal measurements.

The spectral data obtained for BrF_3 are less complete but the similarity of its infra-red spectrum to that of ClF_3 suggests that it also has the plane C_{2v} structure.

The vibrational spectrum of N-methyl formamide:† D. E. deGraaf and G. B. B. M. Sutherland Harrison M. Randall Laboratory, University of Michigan, Ann Arbor, Michigan.

A correct assignment of the fundamental frequencies in N-methyl formamide is of considerable importance since it is probably the simplest model compound for the peptide link in proteins. The infra-red spectrum of N-methyl formamide has been studied between 300 and 3600 cm^{-1} in the gaseous and liquid states and also in solution in nonpolar solvents. In addition, the Raman spectrum of the liquid has been obtained. From these results and similar studies on the corresponding N-deuterated compound it is possible to establish the majority of the fundamental frequencies.

Infra-red Spectroscopy

Solid-state Spectra

Solid state effects in infra-red spectroscopy: A. W. Baker, The Dow Chemical Company, Western Division, Pittsburg, California, Research Department.

The spectra of organic compounds under stress by mechanical deformation show that the deformation is roughly correlatable with crystal class and crystal energy. Some compounds give spectra which in KBr pellets are nearly identical to solution spectra, thus indicating existence of a molecularly dispersed state. Stress relaxation in KBr pellets can be followed by changes in the infra-red spectra. Polymorphism and second order transitions can be induced by mechanical vibration, precipitation from solvents, or by compression in KBr. The plastic flow in KBr is

* Based on the work performed under the auspices of the U.S. Atomic Energy Commission.
† Supported in part by U.S. Public Health Service.

sufficiently different from the flow in KCl that crystal deformation will frequently occur in one and not the other.

Infra-red spectra of lithium halides: WILLIAM KLEMPERER and STUART A. RICE, Department of Chemistry, Harvard University, Cambridge 38, Massachusetts.

The infra-red spectra of the molecules, LiI, LiBr, LiCl have been measured in the region of the fundamental vibration frequency. The vibrational frequencies are calculated from the observed spectra to be

$$\begin{aligned} &\text{LiI} \quad \omega_e = 501\ \text{cm}^{-1} \\ &\text{LiBr} \quad \omega_e = 576\ \text{cm}^{-1} \\ &\text{LiCl} \quad \omega_e = 662\ \text{cm}^{-1} \end{aligned}$$

The observed spectra are composed of many overlapping bands. The calculated spectra are in good agreement with those observed. There is no evidence in the spectra for the existence of appreciable quantities of dimeric molecules.

The apparatus used appears suitable for absorption measurements above 2000°C.

The librational frequency in water and ice: PAUL A. GIGUÈRE and KENNETH B. HARVEY, Laval University, Quebec, Canada.

The infra-red spectrum of H_2O in condensed states was measured between 2 and 30 μ. In the liquid a strong absorption band appears at 710 cm^{-1} due to the restricted rotation, or liberation, of the H_2O molecule. Upon crystallization this band is shifted to 800 cm^{-1} at −15°C and 850 cm^{-1} at −175°C. The corresponding frequencies in D_2O are at 530, 590, and 630 cm^{-1}.

From the frequency of this mode ν_R it is possible to differentiate between supercooled water and ice. Thus it was found that, under certain conditions, thin films of water do not crystallize even in liquid air. The contribution of lattice vibrations to the low-temperature heat capacity of ice will be discussed briefly.

Structure of the infra-red "atmospheric" bands in liquid oxygen: C. W. CHO, ELIZABETH J. ALLIN and H. L. WELSH, Department of Physics, University of Toronto, Toronto, Canada.

The 0–0, 1–0, and 2–0 bands of the $^1\Delta_g$–$^3\Sigma_g^-$ electronic transition have been studied in liquid O_2 and in liquid O_2–N_2 and O_2–A mixtures. Two cryostats were used; one enabled absorption to be observed for any path length up to 60 cm, the other for a fixed path length of 300 cm. In pure O_2 the bands are broad with their intensities degraded towards higher frequencies. On dilution of the oxygen they become sharper and the 1–0 and 2–0 bands show two well defined components, the stronger of which is at the band origin, ν_0, as calculated from the constants for the free molecule. The frequency difference between the two components indicates that the weaker is due to simultaneous transitions in two oxygen molecules; one molecule makes the electronic transition together with the 0–0 or 1–0 vibrational transition and the other molecule makes only the 1–0 vibrational transition of the ground electronic state. The integrated absorption coefficient of the bands varies in a complex way with increasing dilution. The behaviour of the bands in the gas phase at high pressures will also be discussed.

The spectroscopy of crystals of low symmetry: by MICHAEL BEER, The Harrison M. Randall Laboratory of Physics, University of Michigan, Ann Arbor, Michigan.

In anisotropic crystals of orthorhombic or higher symmetry the dichroic ratios can be correlated with the inclinations of the transition moment vectors if the radiation is incident normally on principal planes and it is plane polarized so that the electric vector is parallel to the principal axes [1]. In crystals of lower symmetry this condition cannot be met. The case of triclinic crystals is discussed. It is shown by electromagnetic theory and the theory of anomalous dispersion that in those cases

1. Strong absorption bands can give rise to very high dichroic ratios.

---

[1] NEWMAN R. and HALFORD *J. Chem. Phys.* 1950 **18** 1276.

VOL. 8 1956/5

2. Strong absorption bands will in general show a spurious splitting with different polarization characteristics for the components of the doublet. These can be used to obtain an expression for the orientation of the transition moment vector.
3. Weak bands as overtone and combination bands will in general show small dichroic ratios.

The theory is illustrated with reference to the spectra of NN^1 diacetylhexamethylenediamine [1].

The infra-red spectrum of solid dinitrogen tetroxide: EUGENE R. NIXON and ROBERT N. WIENER,* Department of Chemistry, University of Pennsylvania, Philadelphia 4, Pennsylvania.

According to the commonly accepted V_h symmetry of the N_2O_4 molecule and the X-ray crystal structure of BROADLEY and ROBERTSON [2], present theory [3] predicts one infra-red active component in the crystal for each infra-red active fundamental of the gaseous molecule. These components, with one exception, have been observed in polycrystalline films of N_2O_4 at liquid air temperature as sharp bands only slightly shifted from the gas frequencies. The 684 cm^{-1} fundamental is apparently too weak to be observed. Additional bands, associated with the fundamentals and some combinations, indicate at least two lattice modes in the frequency range 17 to 24 cm^{-1}.

The spectrum will be discussed along with that of solid N_2O_4 containing about 35 atom % of N^{15}.

Absorption spectra of solids condensed from an electrical discharge through oxygen:† ARNOLD M. BASS and HERBERT P. BROIDA, National Bureau of Standards, Washington, D.C.

The products of a high-frequency electrical discharge in flowing oxygen are frozen out on a fused silica plate maintained near the temperature of liquid helium. The absorption spectra of the collected material are studied as a function of layer thickness and of temperature. Spectra are obtained over the range 2200 to 8500 Å with prism spectrographs, and from 1 to 3·5 microns with a grating spectrometer, using a cooled lead-sulphide detector.

The absorption spectrum of the condensate from the discharge through oxygen shows some 25 diffuse bands in the range 3500 to 7000 Å. A few of these bands correspond to bands observed in solid molecular oxygen. In the ultraviolet there is a strong continuous absorption starting at about 3500 Å and increasing very rapidly toward shorter wavelengths. In the infra-red two bands, about 20 cm^{-1} wide, are observed peaking at 3030 and 3499 cm^{-1}. The band at 3030 cm^{-1} may be due to ozone, which in the gas phase has an absorption band at 3050 cm^{-1}. In addition there are observed six narrow lines (about 2 cm^{-1} wide) coming from the fused-silica collecting plate. The two strongest lines, at 3364 and 3470 cm^{-1}, show marked broadening and shift by about 10 cm^{-1} to shorter wavelengths upon warming the plate from liquid-helium temperature to room temperature.

Infra-red spectrum and crystal structure of cellulose:† MASAMICHI TSUBOI,‡ Harrison M. Randall Laboratory of Physics, University of Michigan, Ann Arbor, Michigan.

Infra-red absorption spectra of oriented cellulose fibres have been observed using polarized radiation. Natural fibres are in general too thick but swelling them in NaOH solution followed by pressing and drying is an effective way of obtaining a suitable thickness in the 900–1100 cm^{-1} and 3100–3600 cm^{-1} regions. The dichroism observed for the bands which can be assigned agrees well with that predicted from the crystal structure [4], e.g. the CH stretching bands are polarized perpendicular to the fibre axis. In the region of CH and OH deformation frequencies

* Present address: Department of Chemistry, Rutgers University, New Brunswick, New Jersey.

† This research was supported in part by the United States Air Force through the Air Force Office of Scientific Research of the Air Research and Development Command under Contract CSO-680-56-30.
† Supported by the U.S. Public Health Service.

‡ Fulbright Fellow.

[1] SANDEMAN I. *Proc. Roy. Soc.* 1955 **A232** 105.
[2] BROADLEY J. S. and ROBERTSON J. M. *Nature* 1949 **164** 915.
[3] HORNIG D. F. *J. Chem. Phys.* 1948, **16** 1063; WINSTON H. and HALFORD R. S. *J. Chem. Phys.*
[4] MEYER K. H. and MISCH L. *Helv.* 1937, **20** 232; PEIRCE E. T. *Trans, Faraday Soc.* 1946 **42** 545; 1949 **17** 607.

(1200–1500 cm^{-1}) nine bands are observed, of which four are polarized parallel and five, perpendicular to the fibre axis. Probable assignments will be given for these bands. In the region of CO and CC stretching frequencies (800–1200 cm^{-1}) all the bands are polarized parallel to the fibre axis. Observations were also made on deuterated cellulose, i.e. cellulose which had been swelled in NaOD. Of the six OD stretching bands observed, five show parallel dichroism, indicating that the OH bands in cellulose are arranged predominantly parallel to the fibre axis. The deuteration of amorphous cellulose will also be discussed.

High Dispersion

Invited papers

Vibration-rotation bands of some small molecules under high resolution: H. W. Thompson, The Physical Chemistry Laboratory, Oxford, England.

A survey will be made of measurements carried out during the past few years at Oxford on some vibration-rotation bands of a number of simple diatomic and polyatomic molecules, using high resolving power. A grating spectrometer has been used mainly in the region 2–6 μ with photoconductive cells as detectors. At 5 μ it is possible to resolve sharp lines about 0·1 cm^{-1} apart. Various rotational and vibrational constants have been derived, such as the rotational constants B_i, B_s, the centrifugal stretching constants D_J, DJ_K, the ϵ-doubling factors q and Coriolis factors ζ_i. The bond lengths of some carbon–carbon linkages have been determined, and the effects of Fermi resonance have been examined. The molecules which have been studied include hydrogen and deuterium halides, acetylene and deuteroacetylenes, hydrogen cyanide and deuterium cyanide, methyl acetylene and its deutero derivatives, cyanogen diacetylene, allene and allene-d_4, deuteromethanes, dimethyl acetylene, methyl halides, diazomethane and keten. The results derived from this work have been correlated with other infra-red and Raman measurements.

The structure of pyridine, furan, pyrrole, and thiophene: Børge Bak, Chemical Laboratory, University of Copenhagen, Copenhagen, Denmark.

Inversion splitting of NH_3 in the far infra-red: Ludwig Genzel, Physikalisches Institut der Universität Frankfurt a.M, Frankfurt, Germany.

According to Randall and Wright who discovered the inversion doubling of the NH_3 rotational lines in the far infra-red, the splitting is 1·33 to 1·36 cm^{-1}. More recent measurements of Oetjen *et al.* and of McCubbin and Sinton confirmed this result. The line splitting should be just twice the splitting of the inversion terms which was found to be 0·794 cm^{-1} from microwave measurements. Two times 0·794, however, disagrees with 1·34 beyond the limit of error. On the other hand, Bleaney and Loubser found an anomalous pressure dependence of width and position of microwave inversion lines which the theories of Margenau and of Anderson explained semiquantitatively by the dipole interaction of the molecules at higher pressures. Up to pressures of 1 atmosphere Margenau's theory agrees well with the experiments which were recently extended to ND_3 by Birnbaum and Maryott.

It seemed of interest to examine whether this anomalous pressure shift of the inversion spectrum shows up in the splitting of the rotational line doublets in the far infra-red, and whether the discrepancy mentioned above can be explained by the pressure effect.

Measurements were made on the NH_3 lines of $J = 1$, $J = 2$, and $J = 0$. The latter line is not doubled, but its position should be shifted to lower frequencies by one half of the inversion splitting. Our experiment shows in fact a decrease of the inversion splitting with increasing pressure, but the effect differs for the different J values. We should like to interpret the microwave results tentatively as an averaged effect with respect to the different J (and K) values.

A new look at the fundamentals of lattice vibrations: Wave H. Shaffer, Department of Physics and Astronomy, The Ohio State University, Columbus, Ohio.

Lattice vibrations are considered on basis of characteristic modes of a large molecule rather than as standing wave patterns in a quasi-continuous medium with arbitrary boundary

VOL. 8 1956/5

conditions. Symmetry properties are used in solution of problem for uniform linear chain without recourse to the controversial Born-Von Karman cyclic end conditions. An iterative process, based on LAGRANGE's equation with "extra" forces, is developed for treating such modifications of the uniform linear chain as: alternating masses, both nearest and next-nearest neighbour coupling, change in masses and/or force constants near ends of the chain, "impure" mass in midst of the chain, coupling of linear chains to form planar and three-dimensional arrays, etc. The method permits proper approximations as the number of particles becomes very large. Interesting results are obtained for two- and three-dimensional arrays on the basis of valence-type vibrational forces similar to those employed in small molecules.

Application to Chemical Problems

Invited papers

Infra-red investigation with polarized light: R. MECKE, Institute for Physical Chemistry, The University of Freiburg, i. Br., Freiburg, i. Br., Germany.

Spectres d'absorption infrarouges dans la région au dela de 20μ, obtenus avec des spectrographes à prisme ou réseau: J. LECOMTE, Laboratoire des Recherches Physique, Sorbonne, Paris, France.

We intend to give a brief summary of the results obtained in the region beyond 20 μ, in our department of the Laboratoire des Recherches Physiques in Sorbonne.

Prism spectrographs. We have tried to gather systematically data on the absorption of inorganic or organic substances in the region beyond 20 μ, as we did in the field of sodium chloride some 25 or 30 years ago.

We have examined saturated hydrocarbons, saturated alcohols, ketones, esters, all belonging to the aliphatic series; many benzene derivatives (from the mono- to the hexasubstituted derivatives, more than 150 compounds), sulphur derivatives.

Grating spectrographs. This work has been carried out by Dr. A. HADNI. He has built a recording spectrograph with an echelette grating (14 and 28 lines per mm); as a receiver, it has a thermopile, which may be changed to work with a window suitable to the region studied. Another recording spectrograph—this one of small dimensions—with gratings with only a few lines per mm is in the process of being adjusted and has already reached about 200 μ (with a Golay pneumatic detector).

For the building of these spectrographs, the theory of echelette gratings has been discussed particularly in view of determining the regions where the superposition of various orders is not disturbing. The best dimensions of the receiver, mirrors grating, etc., have also been specially investigated.

With these instruments, absorption spectra of gases and vapours (CS_2, NH_3, Freons 11 and 13, ethyl aldehyde, acetone, methyl alcohol, etc.), of solids (fluorspar, etc,) have been recorded between about 20 and 48 μ.

Further spectroscopic studies on the internal rotation about a single bond: S. MIZUSHIMA, Laboratory of Physical Chemistry, University of Tokyo, Tokyo, Japan.

Contributed papers

The infra-red spectra of substituted 1, 3, 5, triazines: W. M. PADGETT and W. F. HAMNER, Monsanto Chemical Company, Texas City, Texas.

The infra-red spectra of a series of substituted 1, 3, 5 triazines have been obtained in order to identify bands characteristic of the triazine ring. Empirical correlation of the spectra of substituted 2, 4-diamino- and 2, 4, 6 triamino- triazines confirms the assignment of strong bands near 1560 cm^{-1} and 1450 cm^{-1} to in-plane vibrations involving the ring. These bands are shifted to lower frequency in the spectra of cyanuric chloride, cyanuric acid and N, N′, N″-trichloroisocyanuric acid. In the spectra of amino-substituted triazines the 1560 cm^{-1} band

appears to be extremely consistent and stable, while the 1450 cm^{-1} absorption is more erratic, perhaps disappearing altogether in the spectra of two dialkyl-amino chloro triazines.

The medium-strength band occurring consistently near 813 cm^{-1} was assigned a ring vibrational origin also, and may be related to the 735 cm^{-1} A_2'' vibration of unsubstituted 1, 3, 5 triazine. The 813 cm^{-1} band, which has found analytical application previously in melamine determinations, has proved to be an excellent identifying characteristic of amino-substituted triazines in general.

The observed spectra of some monosubstituted melamines, trisubstituted melamines, diamino alkoxy triazines, and diamino chloro triazines will be presented.

High-precision differential infra-red analysis of gases: J. Paul Pemsler and Walter G. Planet, Technical Division, Goodyear Atomic Corporation, Portsmouth, Ohio.

The principles of differential spectrophotometry have been applied to the analysis of gaseous mixtures with a resulting precision of 0·1 to 0·2 per cent. A standard gas at a pressure calculated to give an absorbance of 1·2 at an absorption peak is placed in both cells of a double-beam spectrophotometer. The optical null position is read on the chart, the reference cell closed, and the sample cell evacuated. The sample is then metered into the sample cell until the pen is nearly rebalanced. The ratio of the reference pressure to the resulting sample pressure gives the analysis directly in mole per cent. The difference between observed pen position and true balance necessitates an additional correction factor which can be readily calculated. The application of this technique to mixtures containing overlapping bands is discussed. A possible adaption of these procedures to precision automatic multicomponent analysis in a gas stream also is considered.

Quantitative infra-red determinations in mixtures of unknown qualitative composition: Homer L. Cupples, Pesticide Chemicals Research Section, U.S. Department of Agriculture, Beltsville, Maryland.

The basic rule that quantitative infra-red determinations may only be made in systems of known qualitative composition is subject to well-known qualifications. The known qualitative composition may be replaced by a comparison which is known to interfere at selected wavelengths, or which produces a reproducible interference which may be handled by techniques employing "blanks" or base-line-density methods.

Mixtures of truly unknown composition may introduce substantial inaccuracies into base-line-density methods. One possible solution is to select analytical wavelengths where the interference is least, with the objective of obtaining checks at several such wavelengths. A second approach, of a statistical nature, involves measurement of the component with a maximum number of base-line-density correlations, discarding results on a statistical basis, and averaging the remaining data.

A valuable limiting value for a given component in a given mixture is obtained by referring the true absorbance of the mixture at selected wavelengths to the absorbance-concentration curve for that component. The lowest value so obtained is a limiting maximum value for the component.

The infra-red spectra of olefines chemisorbed on nickel: W. A. Pliskin and R. P. Eischens, Beacon Laboratories, The Texas Company, Beacon, New York.

The infra-red spectra of ethylene and propylene chemisorbed on silica-supported nickel (9·2 wt.%) have been obtained. Interpretation of the spectra is based on analogy with the spectra of hydrocarbons of known structure neglecting any possible effects of strain on the spectra of the adsorbed hydrocarbons. In the case of chemisorbed ethylene the position of the absorption due to C-H stretching was essentially in the region characteristic of saturated hydrocarbons. In addition a band attributed to CH_2 deformation was observed at 6·91 microns. On the basis of these data it was concluded that the chemisorbed species consists mainly of $H_2\overset{*}{C}—\overset{*}{C}H_2$ (asterisk indicates bonding to the nickel surface). Evidence was obtained for the existence of a half-hydrogenated state, $\overset{*}{C}H_2CH_2$, by exposing the chemisorbed ethylene to hydrogen.

VOL. 8 1956/5

Infra-red spectra of chemisorbed propylene and hydrogen exposed chemisorbed propylene were also obtained.

The infra-red spectrum of acetylene chemisorbed on nickel: W. A. PLISKIN and R. P. EISCHENS, Beacon Laboratories, The Texas Company, Beacon, New York.

The infra-red spectrum of acetylene chemisorbed on silica-supported nickel (9·2 wt. %) has been obtained. As in chemisorbed ethylene the absorption due to C-H stretching was essentially in the region characteristic of saturated hydrocarbons. But unlike chemisorbed ethylene, the chemisorbed acetylene spectrum shows evidence of the existence of $-CH_3$ groups by a sharp absorption band at 7·25 microns. Attempts were made to rule out effects due to residual surface hydrogen by chemisorbing acetylene on a dehydrogenated surface and also on a deuterated surface. However, in both cases the presence of CH_2 and CH_3 groups was indicated in the spectra of the chemisorbed acetylene. It was therefore concluded that self-hydrogenation takes place with some acetylene molecules giving up hydrogen atoms to others to form chemisorbed ethyl groups, CH_2CH_3, and a surface carbide.

Structure of the hexafluorobenzene molecule: LUC DELBOUILLE (paper presented by M. MIGEOTTE, Institut d'Astrophysique, University of Liége, Liége, Belgium).

Infra-red and Raman spectra of hexafluorobenzene have been observed. It has been possible to select eleven fundamental bands and lines whose frequencies as well as polarization character indicate that the molecule is planar and belongs to the D_{6h} symmetry, as in the case of benzene.

A potential function containing four valency deformation force constants and seven other parameters characterizing certain bond–bond and angle–angle interactions was calculated. The C-C force constant, amounting to $5{\cdot}741 \times 10^5$ dynes/cm, is weaker than in benzene where it is equal to $6{\cdot}3 \times 10^5$. The C–F force constant, which is equal to $7{\cdot}5 \times 10^5$, is greater than in *p*. $C_6H_4F_2$ where it was found to be equal to $6{\cdot}5 \times 10^5$. This should mean a small decrease in the CF bond-length when the number of these bonds in the benzene ring increases. The signs obtained for the bond–bond and bond–angle interactions nicely check the theory.

Vibrational spectra and calculated thermodynamic properties of 1, 1-difluorobromoethylene: ROSE THEIMER and J. RUD NIELSEN, Department of Physics, University of Oklahoma, Norman, Oklahoma.

The infra-red spectrum of gaseous CF_2 : CHBr has been obtained with a Perkin-Elmer double-pass spectrometer equipped with LiF, NaCl and CsBr prisms and a 1-m absorption cell. The Raman spectra of the compound in the gaseous and liquid states have been photographed with a 3-prism glass spectrograph of linear dispersion 15 Å/mm at 4358 Å. The 12 fundamental vibration frequencies have been assigned, and the spectra have been interpreted in detail. Thermodynamic functions have been calculated for the compound in the ideal gas state at a number of temperatures above the boiling point.

Vibrational spectra of crystalline polyethylene and long-chain paraffins: J. RUD NIELSEN and A. H. WOOLLETT, Department of Physics, University of Oklahoma, Norman, Oklahoma.

The Raman spectra of highly crystalline polyethylene (Marlex 50 and hydrogenated Marlex 50), and of solid n-$C_{28}H_{58}$ and n-$C_{36}H_{74}$, have been obtained. On the basis of the space group V_h^{16} and unit cell determined by BUNN [1], the eight Raman-active unit cell fundamentals have been assigned as follows:

1061 (skel. def., $a_g + b_{1g}$), 1131 (skel. def., $b_{2g} + b_{3g}$), 1168 (CH_2 rock., $b_{1g} + a_g$), 1295 (CH_2 twist., $b_{3g} + b_{2g}$), 1415 (CH_2 wag., $b_{2g} + b_{3g}$), 1440 (CH_2 def., $a_g + b_{1g}$), 2848 (sym. CH str., $a_g + b_{1g}$), and 2883 cm^{-1} (asym. CH str., $b_{1g} + a_g$).

[1] BUNN C. W. *Trans. Faraday Soc.* 1939 **35** 482.

No splitting was observed for any of these fundamentals.

The infra-red spectrum of Marlex 50, at room temperature and at —180°C, has been investigated with a Perkin-Elmer Model 112 spectrometer equipped with LiF, NaCl, and CsBr prisms. In terms of the Raman-active fundamentals listed and the four infra-red active fundamentals assigned by previous workers, it has been possible to assign all of the 60 observed infra-red bands, except for nine very weak ones. Several of the combination bands violate the u,g selection rule, indicating that they involve non-unit-cell fundamentals. A few combination bands are interpreted in terms of fundamentals of the atmosphere phase. The infra-red active CH_2 wagging fundamental (species b_{1u}), which must be extremely weak, appears to be masked by a band of the amorphous phase. For this reason it has not been possible to determine its wave number from combination bands. The same is true of the twisting fundamentals of species $a_u + b_{1u}$.

Discussion of the intensities of some vibrational bands of crystalline polyethylene: O. Theimer
Department of Physics, University of Oklahoma, Norman, Oklahoma.

The integrated absorption coefficients (in 10^{13} sec^{-1}) of the five infra-red active factor group fundamentals of long straight polymethylene chains are approximately: O(CH_2 wagging), 2(CH_2 rocking), 5(CH_2 deformation), 20(sym. CH stretching), and 41 (asym. CH stretching) These results are incompatible with the usual bond moment theory according to which the rocking and wagging fundamentals should have almost equal intensities proportional to the square of the permanent dipole moment μ_{CH} of the CH bond. A modification of the theory consistent with the observed intensities has been developed on the assumption that the dipole moment of the CH bond is directed along the bond axis even when the latter is displaced from its equilibrium position. Taking into account also the symmetry of the polymethylene chain, one obtains from the observed infra-red intensities the following numerical values:

$$|\mu_{CH}| \cong 0, \ (\partial|\mu_{CH}|/\partial\gamma)/(\partial|\mu_{CH}|/\partial|_l) \cong -2{\cdot}1 \quad \text{and} \quad \partial|\mu_{CH}|/\partial x = 0.$$

Here x, y, z are the components of the displacement of the hydrogen atom, the x axis being parallel to the chain and the z axis being perpendicular to the plane of the carbon skeleton. The bond moment obtained in this manner is smaller than previous estimates.

The Raman spectrum of long polymethylene chains contains three lines assigned to CH_2 rocking (1168 cm^{-1}), twisting (1295 cm^{-1}) and wagging (1415 cm^{-1}). These assignments have been supported by intensity calculations based on the bond polarizability theory and the symmetry of the chain. The following calculated intensity ratios were obtained $I_{\text{twisting}} : I_{\text{wagging}} : I_{\text{rocking}} = 6 : 3 : 1$ in qualitative agreement with the observed intensities.

Infra-red studies of rotational isomerism in CF_2CL—CF_2CL and CF_2BR—CF_2CL: R. E. Kagarise,
Naval Research Laboratory, Chemistry Division, Washington 25, D.C.

The phenomenon of rotational isomerism has been studied in CF_2CL—CF_2CL and CF_2BR—CF_2CL by observing the temperature and state dependence of their infra-red absorption spectra in the 2–18 μ region. In CF_2CL—CF_2CL, the trans isomer persists in the crystalline solid, and is also the more stable form in the liquid and vapour states. The energy difference between the trans (C_2H) and gauche (C_2) forms in the vapour was observed to be 500 $\pm$ 200 calories/mole.

In CF_2BR—CF_2CL, the selection rules for the two probable isomeric species (C_s and C_1) are not sufficiently different to facilitate a direct determination of the symmetry of the form which persists in the solid state. However, a comparison of the infra-red spectrum of CF_2BR—CF_2CL with those of CF_2CL—CF_2CL and CF_2BR—CF_2BR indicates that the persistent isomer is the pseudo-trans form (C_s symmetry). This trans form is also the more stable isomer in both the liquid and vapour phases, the energy difference being 520 $\pm$200 and 600 $\pm$200 calories/mole respectively.

Infra-red spectra of quinol clathrate compounds: R. M. Hexter and T. D. Goldfarb, Baker
Laboratories, Cornell University, Ithaca, New York.

The ease of synthesis of "inclusion compounds" of hydroquinone with small molecules, such as HCl, H_2S, SO_2 and CO_2, affords an unique opportunity to study restricted rotational

VOL. 8 1956/5

and translational motion of such molecules, as well as to elucidate the nature of the binding of the lattices of such compounds. Spectra, both absorption and differential, of such compounds, when suspended in KBr pellets, covering the range 0·8–15 μ, are reported, which demonstrate the proposed [1] difference in crystal structure between α-hydroquinone and its β allomorph. In addition, some results are presented which indicate the extent of freedom of rotational motion of the small molecules included in the clathrate, and the extent of the binding of the small molecules to the clathrate lattice.

Shifts in the characteristic carbonyl wavelength: RICHARD A. JEWELL, Commercial Solvents Corporation, Terre Haute, Indiana, and ROBERT A. SPURR, Hughes Research and Development Laboratories, Culver City, California.

The infra-red spectra of complexes formed between twelve benzoylic compounds (benzoyl bromide, benzoyl chloride, phenyl benzoate, methyl benzoate, ethyl benzoate, benzaldehyde, benzoic anahydride, benzoic acid, acetophenone, propiophenone, benzamide, and benzophenone) and six metal halides ($SbBr_3$ $SbCl_3$, $FeCl_3$, AlI_3, $AlCl_3$, and $SbCl_5$) together with the $SnCl_4$, $TiCl_4$, and $AlBr_3$ complexes of benzaldehyde have been studied in the 5·0 to 7·5 μ carbonyl region.

A shift in the characteristic carbonyl wavelength of each benzoylic compound has been taken as *prima-facie* evidence of complex formation. The decreasing order of these metal halides to effect a shift in the characteristic carbonyl wavelength is: $SbCl_5$, $AlCl_3$, $AlBr_3$, AlI_3, $FeCl_3$, $TlCl_4$, $SnCl_4$, $SbCl_3$, $SbCr_3$. No wavelength shifts were observed with either SnI_4 or SbI_3. This order bears a striking resemblance to the catalytic effectiveness of these metal halides in a Friedel-Crafts reaction.

The investigation has further shown the existence of a straight-line relationship between the amount of shift in the characteristic carbonyl wavelength and the bond energy of the complex [1, 2] provided the comparison be made for complexes of a single benzoylic compound and halides of metals in the same valence state.

OL.
8
6/57

The infra-red spectra of HDO in ionic solutions: ROBERT D. WALDRON, Laboratory for Insulation Research, Massachusetts Institute of Technology, Cambridge, Massachusetts.

The infra-red spectra of HDO in H_2O and D_2O solutions saturated with metal halides were investigated in the region from 1200-8000 cm^{-1}. The effect of hydrogen bonding with various ions present on the fundamental and overtone vibrations of the OH and OD bonds was measured. The dependence of frequency shift and anharmonicity on ionic species and H bond energy was investigated. It is shown the vibrational frequency of the OH or OD vibration decreases with decreasing anion size, and the vibrational anharmonicity is nearly independent of the presence of ions.

Synthesis of organic deuterated compounds of spectroscopic interest: L. C. LEITCH, Division of Pure Chemistry, National Research Council, Ottawa, Canada.

Several methods of introducing deuterium into organic molecules of interest to spectroscopists will be discussed with special reference to the scope of the reactions involved. From this viewpoint the synthesis of compounds ranging in complexity from deuterated methanes to deuterated heterocycles will be described.

The infra-red spectrum of N_2O_4 in the gas, liquid and solid phases: R. G. SYNDER, I. C. HISATSUNE and BRYCE CRAWFORD, JR., School of Chemistry, University of Minnesota.

In connection with our kinetic studies of some oxides of nitrogen, we have reinvestigated the infra-red spectrum of N_2O_4. In the gas phase the spectrum is that of an equilibrium mixture

---

[1] PALIN D. E. and POWELL H. M. *J. Chem. Soc.* 1947 208.
[1] DILKE M. H. and ELEY D. D. *J. Chem. Soc.* 1949 2601–2620.
[2] DILKE M. H., and ELEY D. D., and SHEPPARD M. G. *Trans. Faraday Soc.* 1950 **46** 261–270.

of NO_2 and N_2O_4. In order to obtain the spectrum of N_2O_4 alone, we have measured its infra-red absorption spectrum in both the liquid phase and the solid phase. A special low-temperature liquid cell was constructed for this purpose. Our spectral data can be interpreted adequately in terms of a V_h symmetry for the molecule, as is found to be the case in X-ray single-crystal studies. The liquid and the solid spectra as well as the height of the internal rotational potential barrier estimated from these spectra will be discussed. The general applicability of the low-temperature liquid cell for other gases will also be discussed.

Hydroxyl absorption in the 3μ region: URNER LIDDEL and EDWIN D. BECKER, National Institutes of Health, Bethesda, Maryland.

The variation of the absorption of methanol and ethanol as a function of temperature and of concentration has been investigated quantitatively. Solutions of methanol and ethanol in CCl_4 and CS_2 in the range 1 molar to 0·005 molar have been studied from $-10°C$ to $+50°C$. The peak height of the "polymer" band near 3325 cm^{-1} decreases logarithmically with increasing temperature. In 0·005 molar solutions, where no absorption in the polymer region is apparent, the molar absorption coefficient of the 3640 cm^{-1} band, assigned to the OH stretching mode of unassociated molecules, also decreases with increasing temperature in apparently a linear fashion. This change in monomer absorption is interpreted as resulting from an interaction (hydrogen bonding) between the solvent and solute molecules. The same phenomenon is observed in chloroform solutions in CCl_4, indicating that a similar interaction occurs with the CH bond. *n*-Heptane solutions show practically no temperature dependence.

Acetone, ether, dioxane and pyridine have been added to dilute solutions of alcohol in CCl_4. The monomer band decreases in intensity with the appearance of bands at lower frequencies ascribed to intermolecular aggregates. Benzene apparently has no effect on the solutions.

The infra-red spectrum and structure of polyvinyl alcohol: S. KRIMM, C. Y. LIANG and G. B. B. M. SUTHERLAND, Harrison M. Randall Laboratory of Physics, University of Michigan, Ann Arbor, Michigan.

The infra-red spectrum of polyvinyl alcohol has been obtained from 3600 cm^{-1} to 70 cm^{-1}. Polarization measurements on stretched specimens were made down to about 330 cm^{-1}. The spectrum of a deuterated specimen (about 90% of the OH having been converted to OD) has also been obtained. From X-ray diffraction studies, MOONEY [1] and BUNN [2] have proposed slightly different structures for polyvinyl alcohol. On the basis of the parallel dichroism of the band near 650 cm^{-1}, the structure proposed by MOONEY can be ruled out. The observed spectrum does, however, appear to be consistent with BUNN's structure. As a result of recent detailed studies on the infra-red spectra of alcohols [3], it is possible to make definite assignments of all of the OH bands in polyvinyl alcohol with the exception of one near 1445 cm^{-1}. This band presumably corresponds to the 1410 cm^{-1} band in the alcohols, whose interpretation has been uncertain. A possible assignment of this band will be discussed, as well as an interpretation of the remainder of the spectrum.

Shapes, breadths and shifts of HF lines broadened by foreign gases:* D. F. SMITH, Technical Division, Oak Ridge Gaseous Diffusion Plant, Union Carbide Nuclear Company, Oak Ridge, Tennessee.

The ratio of the foreign gas broadening efficiency to the self broadening efficiency can be determined for the lines of the HF fundamental vibration band with a prism spectrometer. These ratios, together with self broadened line widths determined by Kuipers, can be used to evaluate line width parameters for foreign gas broadeners. These line breadths show different

* Portion of this work was supported by the United States Navy, Bureau of Ordnance, through contract with the University of Minnesota.

[1] MOONEY C. L. R. *J. Amer. Chem. Soc.* 1941 **63** 2828.
[2] BUNN C. W. *Nature* 1948 **161** 929.
[3] STUART A. V. and SUTHERLAND G. B. B. M. *J. Chem. Phys.* 1956 **24** 559.

VOL. 8 1956/5

J variations for different foreign gases. A rather detailed agreement between collision diameters derived from the R(O) line breadth and the collision diameter for the NH_3 3–3 microwave line [1] is found.

The University of Tennessee grating spectrometer has been used to examine some of the R branch lines of the HF vibration spectrum in samples containing 0·1 to 0·2 mole per cent HF at 5 atmospheres pressure. In eighteen experiments involving some combination of the five lines and six foreign gases, line centre shifts were observed in twelve instances. Shifts as large as 0·65 cm^{-1} were observed for the R(O) line broadened with SO_2. When shifts were observable, the R(O) line was always shifted to higher wave numbers, and the other lines to lower wave numbers. With the more efficient broadeners the line was broad compared with the spectrometer-transmission function, and the shape of the line was directly determined with fair accuracy. When broadened with HCl the line is nicely fit by a Lorentz line shape. When broadened with SO_2 there is not only a shift, but also a pronounced asymmetry about the line peak with the high-frequency side of the line being the stronger.

The shapes and intensities of hydrogen fluoride lines:* G. A. Kuipers, Technical Division, Oak Ridge Gaseous Diffusion Plant, Union Carbide Nuclear Company, Oak Ridge, Tennessee.

The intensities and shapes of the lines in the fundamental band of hydrogen fluoride have been studied at 117°C and pressures ranging from 200 to 3860 mm Hg. Slit corrections, performed with the aid of an IBM calculating machine, amounted to less than 3% in the absorption coefficient at 3860 mm Hg for the lines $R(5)$ to $P(7)$ and went as high as 25% on even the strong lines at 700 mm Hg. The lines were found to be symmetrical about the line centre. A shift in the line centre of the order of tenths of a wave number at 3860 mm Hg was observed. The line breadths vary with J from 0·5 to less than 0·2 cm^{-1}/atmosphere. A study of the line intensities gives

$$|d\mu/dr| = 1{\cdot}6 \times 10^{-10} \text{ e.s.u.}$$

with the dipole moment increasing with increase in r. In the wings of the lines where no slit corrections are required the absorption coefficient was found to be quadratic in the pressure and always appreciably higher than calculated for a Lorentz line of the same height and breadth. At the centre of the $R(2)$ line the absorption coefficient was observed to decrease 11% with increase in pressure from 700 to 3860 mm Hg. A decrease of 3% was observed between 2310 and 3860 mm Hg, in which pressure range the maximum slit correction was 3%. Polymer absorption peak was found adjacent to the band centre, on the high-wave number side.

Instrumentation

Invited papers

Some new techniques in optical spectroscopy: P. Jacquinot, Bellevue Laboratories, Bellevue, France.

Interferometry in the infra-red: John Strong, Johns Hopkins University, Baltimore, Maryland.

Some interferometric secondary standards in the near infra-red: D. Rank, Pennsylvania State University, State College, Pennsylvania.

Contributed papers

Measurements on efficiency of echelette gratings: Pierre Connes and Pierre Jacquinot, Laboratoires de C.N.R.S., Bellevue, France.

The efficiency (ratio of the flux diffracted in the best order to the incident flux) has been measured for a number of echelette gratings as a function of the wave number in the visible

* This work was done at the Oak Ridge Gaseous Diffusion Plant operated for the Government by Union Carbide and Carbon Corporation.

[1] Smith W. V. and Howard R. *Phys. Rev.* 1950 **79** 132.

region. The results are in good agreement with a very simple theory according to which the curve (efficiency versus wave number) is periodical and composed of selections similar to the upper half of the central maximum of the conventional diffraction curve. When properly used all the gratings investigated have efficiency varying as a function of the wave number, between a maximum value and approximately the half of this maximum value. The case of gratings used far from the Littrow position has been examined, both theoretically and experimentally and it will be proved that this is not unfavourable.

Recent developments on the Beckman IR-4 spectrophotometer. WILLIAM M. WARD, Beckman Instruments, Inc., Fullerton, California.

A new optical null double beam, double monochromator infra-red spectrophotometer has been designed. New features include a method for easy repetitive scan, higher resolution, and automatic control of wavelength scanning speed. New accessories, including a simple variable path cell and calcium fluoride interchange unit, have been developed and results obtained. Conventional beam-size potassium-bromide pellets have been examined.

Rapid scan infra-red spectroscopy with a Fabry-Perot interferometer:* R. W. TERHUNE and C. W. PETERS, Randall Laboratory, University of Michigan, Ann Arbor, Michigan.

An experimental instrument using a Fabry-Perot interferometer as the basic dispersing element will be described. The intensity of the central fringe is recorded. Generally the order of this fringe is less than 10, and overlapping orders are removed by fixed interference filters. Multilayer dielectric films on the interferometer plates provide the necessary high reflectivity. The plates are mounted independently of each other, and are supported by parallelogram type frames that inhibit any motion other than a shear. As the frames are distorted, the separation of the plates is altered, and the spectrum is scanned. The instrument was designed primarily to scan one order of interference 10 times per second. The spectrum appears as an oscilloscope trace which may be photographed. Results have been obtained with scan rates up to 500 scans per second with small scan amplitudes. Fused quartz optical flats and a PbS detector are presently being used in the instrument. The primary advantages of this instrument is that at a given resolution the power output is approximately 1000 times that of a comparable prism instrument.

A high-resolution spectrometer for the 20μ region: ROBERT P. MADDEN, Laboratory of Astrophysics and Physical Meteorology, The Johns Hopkins University, Baltimore 18, Maryland.

In an effort to push back the energy barrier to high resolution in the infra-red, the Laboratory of Astrophysics and Physical Meteorology of the Johns Hopkins University began construction some years ago on a high-flux Ebert spectrometer using a 30″ Ebert mirror. A discussion of the aberrations of this particular system has been given [1].

This spectrometer is now in operation accommodating a grating with a 12″ × 14″ ruled area which is placed in the 20 micron spectral region. The spectrometer is driven by a precision screw capable of yielding very accurate wavelength measurements. A resolution of 0·1 cm^{-1} has already been obtained throughout the 15 to 24 micron region, and considerably better resolution is to be expected.

The principal components of the spectrometer will be discussed, and spectra demonstrating its performance will be shown. This work was supported by Navy contract Nonr 248 (01).

New grating monochromator:† T. NAMIOKA, Laboratory of Molecular Structure and Spectra, Department of Physics, The University of Chicago, Chicago 37, Illinois.

A 15,000 line per inch, 54-cm-grating monochromator based on the new mounting was constructed. The entrance and exit slits are fixed; the grating rotates about a vertical axis

---

* This research was partially supported by a triservice contract administered by the Signal Corps.
† A part of this work was given in *Science of Light* 1952 **2** 8 and 1954 **3** 15.
This work has been supported by the United States Air Force, Office of Scientific Research, Baltimore Maryland.
[1] FASTIE WM. G. *J. Opt. Soc. Amer.* 1952 **42** 647.

VOL. 8 1956/5

through the centre of the grating and different wavelengths are obtained in good focus over a wide range simply by this rotation of the grating. This mounting is also applicable to infra-red region if grating and detector are changed.

The absorption coefficients of methane which was measured using this monochromator will be presented.

An infra-red rapid scanning spectrometer and its use in the measurement of the spectra of short-lived molecules: K. NOLEN TANNER and RAYMOND L. KING, U.S. Naval Ordnance Laboratory, Corona, California.

A rapid scanning infra-red spectrometer has been designed and constructed to search for certain fundamental bands of the free radicals NH_2, CH_3, and CH_2. The monochromator uses the same off-axis parabola design as the Perkin-Elmer Mod. 12, but the Littrow mirror has been replaced by a Littrow-Wadsworth combination in which the Littrow mirror rotates continuously. The detector is a cooled lead-telluride photoconductive cell. The spectrum is presented on a double-beam oscilloscope. An "optical vernier" system synchronizes the oscilloscope sweep and also generates a set of linear fiduciary marks, each corresponding to about 4 minutes of Littrow mirror rotation, which are presented on the second trace of the oscilloscope. The radicals are generated by flash photolysis in one meter quartz absorption cell. This spectrometer is capable of scanning the 3 mμ band of ammonia in about 4 milliseconds with essentially no loss in resolution from conventional slow speed, narrow band scanning, in about 2 msecs with slight loss, and in less than one msec with somewhat greater resolution loss. The results of using this instrument to search for the 3 micron bands of NH_2, CH_3, and CH_2 will be presented.

Design and performance of a double beam, double pass infra-red spectrophotometer: E. H. SIEGLER, JR., and T. F. FLYNN, The Perkin-Elmer Corporation, Norwalk, Connecticut.

Last year at Columbus, M. GOLAY described studies made by Perkin-Elmer comparing various spectrometric systems. Eight systems for double-beam, double-pass infra-red spectrometers were discussed.

Of these, one system was chosen as the most desirable for conversion of the Perkin-Elmer Model 21 to a double-pass, double-beam spectrophotometer. This system, which operates on an optical null principle, is characterized by beam switching at a frequency $2f$, by chopping of an intermediate slit image at $3f$ and by decoding at f.

A double-pass spectrophotometer has been constructed according to this principle. The conversion parts consist of a single mechanical subassembly and quite minor electronic modifications. As expected, the reduction of scattered light is the main performance advantage.

The performance of a small grating, infra-red spectrometer in the region from 2 to 25μ: WALTER F. EDGELL, J. AMY, and NORMAN TIDESWELL, Department of Chemistry, Purdue University, Lafayette, Indiana.

A small, versatile, infra-red spectrometer has been constructed (Perkin-Elmer Corporation) which eliminates the unwanted radiation by means of a fore-prism monochromator already described (E. SIEGLER, JR. and J. HULEY). Separation of the various orders is facilitated by good optical imagery in the fore-prism monochromator and the ready exchangeability of prisms. A cooled, lead-telluride cell and a thermocouple have been employed with a Perkin-Elmer monochromator suitably modified for the use of gratings and these detectors. Bausch and Lomb gratings blazed for the first order at 6 μ, 12 μ, and 112 μ have been used to date. The separation of the wavelengths obtained with the fore-prism monochromator makes it possible to use these gratings in the higher orders with ease.

The performance of the instrument has been tested with water vapour, ammonia, hydrogen bromide, etc. Good wavelength accuracy and resolution of 0·3 cm^{-1} or better have been obtained except at the longer wavelength end of the accessible region where suitable gratings are not yet available to us. Typical results observed for CD_3F, CD_2HF, NF_3, CF_4 $Co(CO)_4H$, etc. will be presented.

Frequency linear-drive for spectrographic recorder: W. E. DEEDS, The University of Tennessee, Knoxville, Tennessee.

A drive system for a spectrographic recorder can easily be made which is accurately linear with frequency. If radiation passing through the spectrometer is also passed through a Fabry-Perot interferometer, the transmitted radiation will exhibit intensity maxima, or fringes, at equal frequency intervals. If the transmitted radiation is detected and the a.c. signal is amplified, it can drive the synchronous motor which moves the chart paper.

If the spectrometer scanning rate is very slow, several methods can be used to increase the motor-driving frequency: the Fabry-Perot plates can have greater separation; ultra-violet light in high order can be superimposed on the regular beam; a frequency-multiplier can be employed; a separate oscillator can be used, with servocontrol system to maintain constant rate of appearance of Fabry-Perot fringes; or the synchronous motor drive can be replaced by an electromagnetic stepping ratchet.

A scaling circuit can be used to provide a marker signal of the recorder every time N more fringes have passed, M being presumably a large integer.

Microwave and Raman Spectroscopy

The microwave spectrum of methyl difluorosilane:* JEROME D. SWALEN,† Department of Chemistry, Harvard University, Cambridge 38, Massachusetts.

The microwave spectrum of two isotopic species of methyl difluorosilane has been observed and assigned. From these spectra the structure, dipole moment and barrier to internal rotation have been determined. Several series of Q branch lines, assigned from $J = 6$ to $J = 12$, have been observed to be split into doublets. From these splittings the barrier has been calculated to be 122 ± 50 cal.

VOL. 8 1956/5

Microwave spectrum of methyl monofluorosilane:* LOUIS PIERCE, Department of Chemistry, Harvard University, Cambridge 38, Massachusetts.

The rotational constants of two isotopic species of methyl monofluorosilane, as determined from microwave data, have been used to calculate its structure. Quantitative Stark-effect data have been obtained and used to calculate the dipole moment. Certain absorption lines in the microwave spectrum were found to be split into doublets. These splittings are due to internal rotation and have been used to determine the barrier to internal rotation. This barrier was found to be 1450 cal ± 50 cal.

Internal barrier and structure of methyl silane:* R. W. KILB‡ and LOUIS PIERCE, Department of Chemistry, Harvard University, Cambridge 38, Massachusetts.

The microwave spectrum of CH_3SiHD_2 has been studied and from the splitting of the $J = 1$–2 lines the barrier to internal rotation has been determined, using an extension of the Wilson, Lin and Lide theory [1]. If the barrier is assumed to be $V_3/2(1 - \cos 3\alpha)$, then V_3 is 1630 ± 50 cal. If a V_3 term of about 100 cal is assumed, of the form $V_6/2(1 - \cos 6\alpha)$, then V_3 is 1595 ± 50 cal. This barrier is in agreement with KIVELSON's [2] work, where the barrier, 1959 ± 50 cal was obtained from a study of the $J = 0 - 1$ satellites of CH_3SiH_3. A dipole moment study and structural analysis have also been carried out for this molecule.

---

* This research was made possible in part by support extended Harvard University by the Office of Naval Research under ONR Contract N5ori 76, Task Order V.

† Proctor and Gamble Fellowship, 1955–56.

‡ Standard Oil of Indiana Fellowship, 1955-56.

[1] WILSON, LIN and LIDE *J. Chem. Phys.* 1955 **23** 136.

[2] KIVELSON *J. Chem. Phys.* 1954 **22** 1733.

The microwave spectrum of methylamine—d_5: David R. Lide, jr., National Bureau of Standards, Washington 25, D.C.

The microwave spectrum of CD_3ND_2 has been investigated in an effort to elucidate the structure of the methylamine molecule. A series of lines in which the rotational transition is of the type $J_{0J} \rightarrow J_{1J}$ has been studied in the 24,000–35,000 Mc regions. Each rotational transition is split into four lines, with spacings of the order of 100 Mc, as a result of the internal motion. These splittings have been analysed on the basis of a hindered internal rotor with additional terms to include the possibility of inversion of the ND_2 group. Preliminary values for molecular constants are: reciprocal principal moments: 52,420 Mc, 16,550 Mc, 15,570 Mc; quadrupole coupling constants: $\chi_{aa} = 2{\cdot}4$ Mc, $\chi_{bb} = 2{\cdot}1$ Mc, $\chi_{cc} = -4{\cdot}5$ Mc; barrier to internal rotation: $V_0 = 590$ cm^{-1}.

Paramagnetic resonance spectra of some isotopically substituted naphthalene negative ions:* T. R. Tuttle, jr., Department of Chemistry, Washington University, St. Louis 5, Missouri.

The paramagnetic resonance spectra of three isotopically substituted naphthalene negative ions have been studied under moderate resolution to determine the α and β proton, and α-C^{13} hyperfine splitting factors. The spectrum of the α-deutero compound has 15 peaks and that of the β-deutero 14 peaks. These facts, along with the relative intensities of lines, lead to values of the proton splitting on the α position of 5·1 gauss and on the position of 1·7 gauss. Naphthalene negative ion with 53 atom per cent C^{13} in the α position gives a spectrum of 21 lines. An assignment of 5·4 gauss for the α-C^{13} splitting gives good agreement with the observed spectrum.

The observed splittings will be compared with those calculated using S. I. Weissman's method involving configurational interaction [1].

The microwave spectrum identification and structure of disulphur monoxide: D. J. Meschi and R. J. Myers, Department of Chemistry, University of California, Berkeley, California.

The previous work [2] on the ultra-violet and infra-red spectra of so-called sulphur monoxide has been interpreted on the basis of a molecule with the formula of S_2O_2. An examination of the microwave spectrum shows conclusively that the major component of so-called sulphur monoxide is in reality disulphur monoxide, S_2O.

The low-J-valued microwave transitions of S_2O consist of R branch lines (a-dipole) and Q branch lines (b-dipole). The values of B-C obtained from the a-dipole and b-dipole lines agree within experimental error. The rotational constants for the $S_2{}^{32}O^{16}$ species are $A = 41{,}914{\cdot}3$; $B = 5{,}059{\cdot}1$; $C = 4{,}507{\cdot}0$ mc/s. These data are consistent with an S—S—O structure and angle of about 120°. A new interpretation will be given of the ultra-violet and infra-red spectra of S_2O.

The raman spectra of gaseous and liquid cyclopropane: P. M. Mathai, G. G. Shepherd, and H. L. Welsh, Department of Physics, University of Toronto, Toronto, Canada.

The Raman spectra of gaseous and liquid cyclopropane were photographed with a reciprocal linear dispersion of 10·5 cm^{-1} per mm. The resolved rotational spectrum of the gas gave $B_0 = 0{\cdot}6697 \pm 0{\cdot}0005$ cm^{-1}. Although no rotational structure in the vibrational bands was resolved, the spectrum of the gas clarifies the vibrational assignments. The spectrum of the liquid, because of hindered rotation and consequent overlapping of bands, has led to incomplete frequency assignments. Nine of the ten Raman active fundamentals were recorded; of particular interest are $\nu_1 = 3038{\cdot}0$, $\nu_8 = 3019{\cdot}9$, and $\nu_{13} = 1188{\cdot}0$ cm^{-1}. An infra-red band centred at 3024 cm^{-1}

---

* This research was supported by the United States Air Force through the Office of Scientific Research of the Air Research and Development Command.

[1] Weissman S. I. to be published.
[2] Jones A. V. *J. Chem. Phys.* 1950 **18** 1263.

has been previously assigned to ν_8; it is suggested that this band should be classified as $2\nu_{10} + \nu_5$. The inactive frequency ν_4 was assigned to a faint line at 1132·5 cm^{-1}. The ζ constants of some of the degenerate vibrations were determined from the intensity contours of the bands.

Raman spectra of *s*-triazine and butatriene: B. P. Stoicheff, Division of Pure Physics, National Research Council, Ottawa, Canada.

The pure rotational spectra of gaseous *s*-triazine ($C_3N_3H_3$ and $C_3N_3D_3$) and butatriene ($H_2C_4H_2$) have been photographed in the second order of a 21 ft. grating spectrograph. The C-N bond length in *s*-triazine was found to be 1·338 Å, a value which is 0·02 Å larger than that found in the solid phase by X-ray diffraction. The central C=C bond length in butatriene was found to be 1·284 Å. This double bond is considerably shorter than in ethylene (1·344 Å) and allene (1·309 Å). An apparatus for exciting Raman spectra with $\lambda 2537$ from Hg^{198} lamps will be described and some preliminary results will be discussed briefly.

Nuclear magnetic resonance effects in systems with sterically interfering protons: C. Reid. Department of Chemistry, The University of British Columbia, Vancouver 8, Canada.

The nuclear magnetic resonance spectra of about 40 polynuclear aromatic hydrocarbons have been examined. It has been found that the largest chemical shifts are due to direct proton–proton interference between suitably placed neighbours. These may be in identical or non-identical environments and are consequently not electron coupled spin–spin effects, but "repulsive" chemical shifts. Using ring systems of different shapes and sizes, a correlation between proton–proton distance and shifts has been found. Some new ideas about steric hindrance are suggested.

Intensities, Line Breadths, etc.

Coupled anharmonic vibrations as a cause of broadening of spectral bands: Hydrogen-bonded systems: H. L. Frisch and G. L. Vidale, Department of Chemistry, University of Southern California, Los Angeles 7, California.

The broadening of molecular-spectral bands in hydrogen-bonded systems is calculated for a simple model of the hydrogen-bonded molecule on the assumption that it is due to the precession of coupled anharmonic vibrations. The approximate classical mechanics of such a generalized system is developed in terms of known results in the theory of nonlinear mechanics. It is shown that when reasonable molecular parameters are substituted into the calculated broadening one obtains values consistent in all respects with the experimental data.

The intensity distribution in ν_2 of hydrogen sulphide:* D. F. Eggers, jr., and M. T. Emerson, Department of Chemistry, University of Washington, Seattle, Washington.

The complete understanding of the vibration-rotation spectrum of hydrogen sulphide has long been hindered by the observation of an unusually weak *P* branch and strong *R* branch in most of the type-*B* bands. By measuring the intensity of the ν_2 band and using the first-order part of the theory which Herman and Wallis [1] applied to the diatomic molecule, we have calculated the envelope of this band. The molecule was treated as an asymmetric rotor, and the resulting spectrum shows quantitative agreement with that observed. The actual computation was performed on an IBM 604 electronic calculator, and after summing over a slit function, the calculated spectrum was plotted with the aid of the IBM 407 accounting machine. Details of the treatment will be present.

Dispersion and electric dipole moment of gaseous hydrogen chloride: P. Barchewitz, Laboratoire D'Infrarouge, 12, Rue Cuvier, Paris V^e, France.

Study of the dispersion in the 3·4 μ and $\lambda f \mu$ vibration-rotation bands, using a Twyman interferometer in connection with a grating spectrometer. Determination of the coefficients M_0,

* Supported by the National Science Foundation.

[1] Herman R. and Wallis R. F. *J. Chem. Phys.* 1955 **23** 637.

M_1, and M_2 in the expansion of the dipole moment with respect to the variation $(r - r_e)$ of the internuclear distance.

$$M(2) = M_0 + M_1(r - r_e) + M_2(r - r_e)^2$$

The data is from the research of F. LEGAY of our laboratory.

Vibrational relaxation times from infra-red emission intensities: DAVID A. DOWS, Baker Laboratory, Cornell University, Ithaca, New York.

Two general processes can contribute to the rate of change of population of a molecular energy level in a gaseous sample. These are (a) emission or absorption of radiation, and (b) collisional excitation or de-excitation. A simple steady state treatment gives the intensity of emission, which is proportional to an excited state population, in terms of the rate constants for processes (a) and (b).

The two processes have different dependences on pressure, (a) being first ordér and (b) second order; thus measurement of intensity of emission as a function of pressure allows a comparison of the rate constants of (a) and (b). Since the emission and absorption constants may be found from absolute absorption intensity measurements, it should be possible to determine vibrational relaxation times by this method.

Some experimental results obtained on gases heated to 2–300°K at pressures down to a few tenths of a millimetre will be presented and experimental difficulties discussed.

The band shape of ν_3 of liquid CS_2: G. A. GALLUP. Department of Chemistry and Chemical Engineering, University of Nebraska, Lincoln, Nebraska.

Measurements of the infra-red active fundamental of liquid CS_2(1510 cm^{-1}) indicate as is to be expected that there is a breakdown of the gaseous rotational selection rules. The general aspect of the band is Gaussian. However, deviations from the Gaussian shape strongly suggest that there are a number of subbands or branches on either side of the central maximum. As many as 8 of these branches are visible.

Theoretical considerations using simple potential functions indicate that the selection rules for a parallel band of a linear molecule in a liquid could be $\Delta M = O$; $\Delta J = O, \pm 2, \pm 4, \ldots$ and $\Delta M = \pm 1$; $\Delta J = 1$ with perhaps the addition of $\pm 3, \pm 5, \ldots$ An interpretation of the band shape in terms of these selection rules and potential functions allows an estimate of the force tending to hold the molecule in a given direction in the liquid.

Band intensities of methyl and olefin groups in polyethylenes: R. S. SILAS, Phillips Petroleum Company, Bartlesville, Oklahoma.

Model hydrocarbons containing up to 50 carbon atoms were used to determine peak-height and integrated band intensities near 7·25 μ for terminal methyl groups, methyl branches, and methyl groups on ethyl branches. Surprisingly, the intensities at 300°F differ by a factor of three for these structures.

Methyl Structure	Peak-Height Intensity per Group
End Groups	7,900 (cm_2/mole)
Ethyl Branches	13,700 (cm_2/mole)
Methyl Branches	22,200 (cm_2/mole)

The intensities of bands associated with ethyl branches and various olefin structures were also determined.

Structure	Wavelength	Peak-Height Intensity per Group
Ethyl Branch	13·0 μ	3,400 (Cm^2-/mole)
trans Olefin	10·3 μ	64,000 (Cm-/mole)
Vinyl	11·0 μ	70,000 (Cm-/mole)
Branched Vinyl	11·3 μ	~ 80,000 (Cm-/mole)

Application of these data to the determination of branching and unsaturation in typical polyethylenes is summarized.

Changes in intensity of some infra-red bands of benzene in solution: ELDON FERGUSON, Naval Research Laboratory, Washington 25, D.C.

Fundamental vibrational frequencies which are infra-red inactive in the vapour state are commonly observed in the liquid state. This breakdown of the selection rules is generally attributed to the influence of intermolecular forces. In an attempt to utilize this phenomenon as a means of studying intermolecular forces, data have been obtained on the intensities of some of the inactive fundamentals of benzene in several solvents.

The Raman-active fundamental at 1179 cm^{-1} is less intense in carbon tetrachloride, chloroform, cyclohexane, and N-Decane solutions than it is in pure benzene while in carbon disulphide solutions it is stronger. The magnitude of the change is considerable. In a 10% by volume solution of benzene in carbon tetrachloride the extinction coefficient is 0·6 of its value in pure benzene, while in a 10% solution of benzene in carbon disulphide, the extinction coefficient is twice that of pure benzene. A similar effect is observed for other inactive fundamentals corresponding to both planar and nonplanar vibrations. The infra-red-active fundamental at 1037 cm^{-1}, on the other hand, shows no such marked intensity change in solution.

The observed intensity changes appear to correlate with the dispersion forces between molecules. In the case of the carbon disulphide solutions, where the inactive fundamentals are enhanced, the London dispersion force (induced-dipole–induced-dipole interaction) between solute and solvent molecules is greater than the dispersion force between two benzene molecules. In the case of the carbon tetrachloride, chloroform, and cyclohexane solutions where the bands are weakened, the solute–solvent interactions are less than in pure benzene.

Some data on the effect of temperature on these bands in pure benzene has also been obtained. In going from 10°C to 70°C, a decrease in intensity of approximately 30% is observed for the inactive fundamentals at 850, 1179, and 1310 cm^{-1}. However, the two active fundamentals at 1030 and 1485 cm^{-1} show the same change so that a relationship between the effects of temperature and dilution in various solvents is not apparent.

Line-widths and shapes in CO at pressures above one atmosphere:* HENRY J. KOSTKOWSKI and ARNOLD M. BASS, National Bureau of Standards, Washington, D.C.

The widths of self-broadened lines in the first overtone band of CO at pressures from $2\frac{1}{2}$ to 20 atmospheres were measured directly with a small grating monochromator whose spectral slit-width was approximately 0·25 cm^{-1}. Line intensities were also determined but at pressures below one atmosphere. Both the line widths and intensities are believed to be in error by less than 5%. These independently determined parameters were then used with assumed line shapes to calculate the absorption, as a function of pressure, at various troughs throughout the band. Comparisons were made with actual measurements to try to obtain some information about the line shape and widths for pressures up to 60 atmospheres. The method for determining the width and intensity of the lines as well as the results obtained on widths and shapes will be presented.

Vibrational intensities in CH_3 and CD_3 chloride, bromide, and iodide: A. D. DICKSON, BRYCE CRAWFORD, JR., W. T. KING, IAN M. MILLS and W. B. PERSON, School of Chemistry, University of Minnesota, Minneapolis 14, Minnesota.

Absolute intensities have been measured for all the fundamental vibrations of the six molecules CH_3Cl, CD_3Cl, CH_3Br, CD_3Br, CH_3I and CD_3I. The intensities were measured by integrating the optical density over each band, high pressures of nonabsorbing gas being used to broaden the fine-structure and so overcome the spectrometer slit effect. Nitrogen, helium and argon were used at 1200 psi to pressure broaden the samples, and some special high-pressure absorption cells designed for this work will be described. The band areas Γ_i were determined by integrating against the logarithm of the frequency, according to the relation

$$\Gamma_i = \frac{1}{nl} \int_{\text{band}} ln(I_0/I) \cdot d\ln\nu$$

* This research was supported in part by the United States Air Force through the Air Force Office of Scientific Research of the Air Research and Development Command under contract CSO-680-56-30.

VOL. 8 1956/5

Here n is the concentration of sample gas and l is the path length. Γ_i is then related to $(\partial p/\partial Q_i)_\eta$ for the ith fundamental vibration as follows:

$$\Gamma_i = \left(\frac{d_i}{\omega_i} \cdot \frac{N\pi}{3c^2} \cdot \frac{\partial p}{\partial Q_i}\right)^2$$

where d_i is the degeneracy and ω_i the harmonic vibration frequency. These relations have certain advantages over the definitions used previously by WILSON and WELLS [1]. The individual areas of overlapping bands were determined by assuming symmetrical shapes for the perpendicular bands, and a complete error treatment was carried out in order to ascertain the effects of possible errors in the separations.

Normal co-ordinates were calculated from the potential function recently derived by CHANG [2], which was adjusted to fit both the vibration frequencies, corrected for anharmonicity, and in certain cases the Coriolis ζ values. These normal co-ordinates were used to derive values of $(\partial p/\partial S_j)$ where S_j is a symmetry co-ordinate in the molecule, in the degenerate symmetry class, which contains a pair of infra-red-active rotations, the known dipole moments of the molecules were used to correct the observed $(\partial p/\partial S_j)$ values to a standard state in which there is no rotation of the carbon-halogen bond during the deformation. Ambiguities arising from the unknown relative signs of the $(\partial p/\partial Q_i)$ were eliminated by comparing data on the isotopic species. Finally bond-effective moments were calculated for each symmetry co-ordinate.

Line widths and intensities in resolved vibration-rotation bands of NH_3:* W. S. BENEDICT, Laboratory of Astrophysics and Physical Meteorology, The Johns Hopkins University, Silver Spring, Maryland, and EARLE K. PLYLER, National Bureau of Standards, Washington 25, D.C.

The absorption spectrum of NH_3 has been observed with high resolution in the region 2745–4720 cm^{-1}. The conditions were varied from long paths and low pressures (1000 cm × 0·003 atm), which permits resolution and analysis of weak lines, including the K-fine-structure, to short paths (5 cm) at atmospheric pressure, under which condition the width and intensity of single isolated lines can be measured.

From the high resolution studies molecular constants have been derived for the bands listed in Table 1. Total band intensities are also given; the intensities of individual lines agree quite well in general with rigid-rotator calculations. The line widths show marked variations with J and K, paralleling those observed in the microwave region, but averaging 20% narrower. At one atmosphere pressure the lines appear quite closely of Lorentz shape out to $|\nu-\nu_0| = 3\ cm^{-1}$, and show no shift ($<0{\cdot}03\ cm^{-1}$) of central frequency from their low-pressure position.

Table 1. Constants for some Rotation-Vibration Bands of NH_3

Transition $(V_1V_2{}^PV_3)-(V_1V_2{}^PV_3)$	Type	ν_0 cm^{-1}	$B-B$ cm^{-1}	$[(A'-B')]$ $(A''-B'')$ cm^{-1}	ζ	$S_v{}^0$ cm^{-2} atm^{-1}
0 1^s 1 — 0 0^a 0	⊥	4434·566	−0·2431	+0·1784	0·0204	10
0 1^a 1 — 0 0^s 0	⊥	4416·854	−0·1498	+0·0441	0·0239	10
1 1^a 0 — 0 0^s 0	∥	4230·012	−0·1904	+0·0895		1·7
1 1^s 0 — 0 0^a 0	∥	4293·668	−0·0589	−0·0911		1·7
0 0^a 1 — 0 0^s 0	⊥	3443·59	−0·178	+0·188	0·0325	4
0 0^s 1 — 0 0^a 0	⊥	3443·15	−0·174	+0·182	0·0325	4
1 0^a 0 — 0 0^s 0	∥	3337·18	−0·091	+0·004		11
1 0^s 0 — 0 0^a 0	∥	3335·39	−0·079	+0·001		11
0 3^a 0 — 0 0^s 0	∥	2895·60	−0·76	+0·85		0·17

[1] WILSON E. B. and WELLS A. J. *J. Chem. Phys.* 1946 **14** 578.
[2] TSU-SHEN CHANG, Ph.D. Thesis, University of Michigan, Ann Arbor, Michigan; 1953.
* Work supported in part by the Office of Scientific Research, ARDC.

Infra-red intensities of the fundamental frequencies of CF_3Br: WILLIS B. PERSON, Department of Chemistry, State University of Iowa, Iowa City, Iowa, and S. R. POLO, Department of Pure Physics, National Research Council, Ottawa 2, Canada.

Absolute intensities have been measured for the fundamental bands of CF_3Br, using the extrapolation technique of WILSON and WELLS, at a total pressure of one atmosphere. These have been interpreted in terms of bond moments and derivatives, using normal co-ordinates calculated from the potential function of MCGEE *et al.* (*J. Chem. Phys.* 1953 **21** 242). While the sign ambiguity is not completely removed, there is one choice which seems most favourable. The relationship between these results and those for other CF_3–x molecules will be discussed.

Letter to the Editors

BEMERKUNG zu einer Notiz von Herrn BARDÓCZ. In einer Notiz am Schlusse seiner Publikation (Spectrochim. Acta 1955 **7** 320) meint Herr BARDÓCZ, daß ich eine Arbeit von ihm in der "Nature" (Nature 1953, **171** 1156) nicht zitiert hätte, obwohl darin das Prinzip einer Kombination von Elektronenröhren mit Funkenstrecken zuerst für die Steuerung spektrographischer Funkenerzeuger verwendet worden sei. Ich vermag bei genauer Nachprüfung nicht zu erkennen, daß ich in meiner Arbeit ein Prinzip benutzt hätte, das erstmalig von Herrn BARDÓCZ verwendet worden ist. Abgesehen davon, daß die naheliegende Kombination elektronischer Elemente mit Funkenstrecken zur Steuerung eines Funkenerzeugers m. E. noch kein Prizip konstituiert, stammt die erste in der spektroskopischen Literatur angegebene Kombination dieser Art von MALPICA und BERRY. Wenn also schon die Literaturangaben im Hinblick auf den in meiner Arbeit beschriebenen Hochspannungsteil ergänzt werden sollen, so ist in erster Linie auf die Arbeit der eben erwähnten Autoren (Gen. Elect. Rev. 1941, **44**, 563) zu verweisen. Was die "tandem-gap"-Anordnung anbetrifft, so ist die Arbeit von ENNS und WOLFE (J. Opt. Soc. Am. 1949, **39**, 298) zu zitieren.

K. BUNGE

Leverkusen 5.
Mettlacherstr. 17, *Germany*

VOL. 8 1956/5

Spectrochimica Acta, 1957, Vol. 8, pp. 317 to 328. Pergamon Press Ltd., London

An atomic-absorption spectrophotometer and its application to the analysis of solutions

BARBARA J. RUSSELL, J. P. SHELTON, and A. WALSH
Chemical Physics Section, Division of Industrial Chemistry, Commonwealth Scientific and Industrial Research Organization, Melbourne, Australia

(*Received* 18 *September* 1956)

Abstract—The construction of an atomic-absorption spectrophotometer is described and its performance is illustrated by results obtained in applying the instrument to the analysis of solutions. The sample is sprayed into a flame and the absorption by the latter of an atomic resonance line of the element to be estimated is measured, the apparatus being so arranged that the absorption measurement is independent of any radiation emitted by the flame. The results confirm that, in contrast with the emission method, the sensitivity of the absorption method is independent of the excitation potential of the spectral line used.

1. Design and construction of an atomic absorption spectrophotometer

(a) *General design*

IN a previous paper [1] it was shown, from a consideration of the theoretical factors governing the relationship between atomic absorption and atomic concentration, that atomic absorption spectra provide a promising method of chemical analysis with vital advantages over emission methods, particularly from the viewpoint of absolute analysis. This paper describes an atomic absorption spectrophotometer [2, 3] which has been constructed to test the practical possibilities of this method of analysis and to investigate some of the factors involved in recording atomic absorption measurements. The design adopted has been determined to a large extent by the items of equipment, such as monochromators, atomizers, etc., which were readily available for these experiments. Whilst this apparatus has proved admirably suited for testing the principle of the atomic absorption method, it will be apparent that it is possible to use simpler and more inexpensive forms of apparatus for various analytical problems.

There are two main features in the design of the atomic absorption spectrophotometer. In the first place, since it is practically impossible to design an instrument which will accurately record the profiles of atomic absorption lines having half-widths of the order of 0·01 Å, the approach adopted has been to construct a series of light sources which emit atomic spectra of the various elements under conditions favouring the production of sharp lines having half-widths of the same order, or less than, those of the corresponding absorption lines. The absorption by the sample of these lines, which will usually be resonance lines, is a function of the profiles of the emission line of the source and the absorption line of the sample. If the former can be considered as being infinitely narrow compared to the absorption line, a measure of the peak absorption is obtained. The second feature of the design is the provision of compensation for the spectrum

emitted by the sample. This is necessary, since the atomized sample will generally emit at precisely the same wavelength as that at which the absorption measurement is made.

The general arrangement of the apparatus is shown in Fig. 1. The operation of the apparatus shown in Fig. 1 is as follows. The source emits a sharp atomic-line spectrum of the element to be estimated and this emitted radiation is modulated before it passes through the atomized sample. The monochromator isolates a given spectrum line, which then falls on a photo-electric detector. The output from the latter is passed to an amplifier tuned to the same frequency as the modulator so that only the signal due to radiation from the source is amplified: any radiation emitted by the atomized sample is not modulated and thus produces

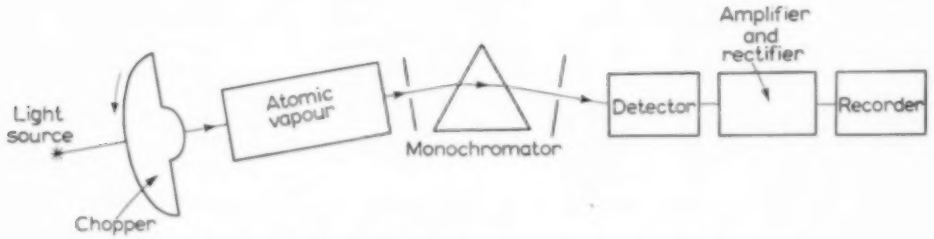

Fig. 1. Schematic diagram illustrating the principle of the atomic absorption spectrophotometer.

VOL. 8 1956/5

no signal at the output of the amplifier. After rectification, the amplified signal is passed to a recorder which indicates the signal with and without the absorbing sample in the radiation path. Alternatively, a ratio recorder can be used in conjunction with a double-beam method, so that per cent absorption is recorded directly. The various components are shown in Figs. 2 and 3, and are discussed below.

In Fig. 2 the console on the right contains (reading from bottom to top): regulated power-supply for the hollow-cathode tubes which were used as atomic line sources; Speedomax recorder converted to ratio recording; and a twin-channel homodyne amplifier. The close-up of the optical system (Fig. 3) shows, reading from right to left: hollow-cathode tube; beam splitter; twin-frequency modulator and sector controlling the synchronous rectifiers; condensing lenses; atomizer and burner; beam combiner; photo-multiplier; and monochromator.

(b) *Atomic line source*

Since the atomic line source used must not exhibit erratic fluctuations in intensity, which would preclude accurate absorption measurements, it is not possible to use any electrical discharge operating in an open atomsphere. Apart from instability, such sources would also be unsatisfactory, since the lines would be too broad and the resonance lines would certainly show some self-reversal. Some form of enclosed discharge is essential, and there are three main possibilities: laboratory discharge lamps similar to the Wotan spectral lamps supplied by

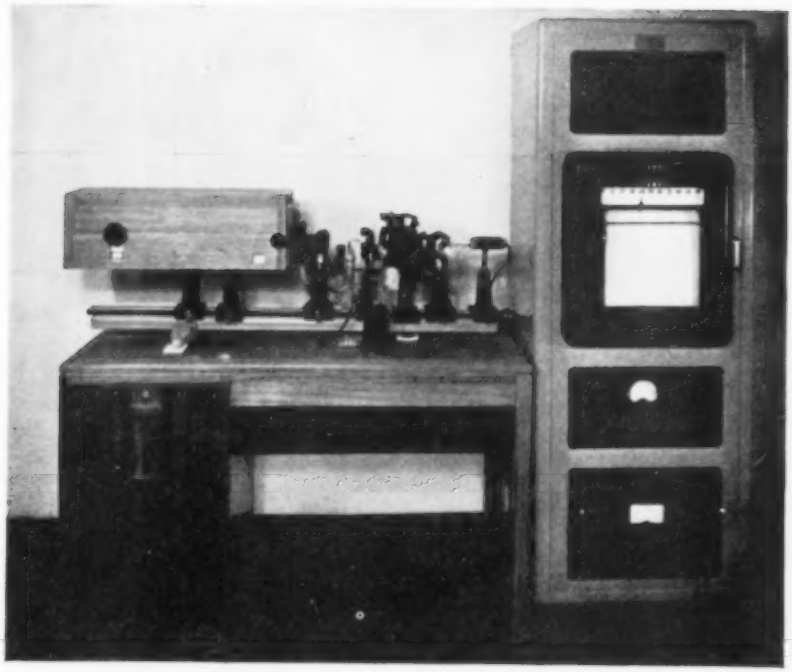

Fig. 2. Photograph of the atomic absorption spectrophotometer.

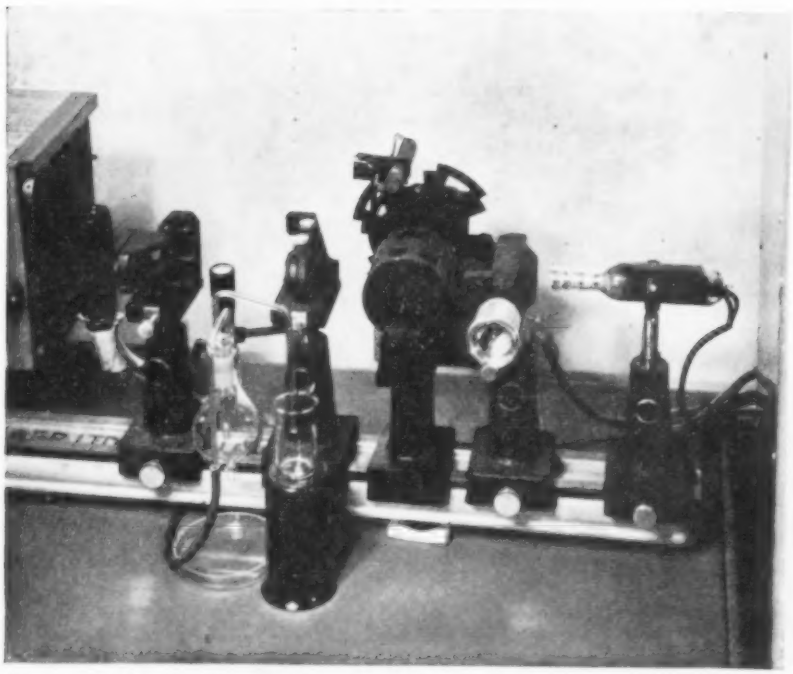

Fig. 3. Photograph of the optical system of the atomic absorption spectrophotometer

facing p. 318

VOL.
8
1956/5

Osram; high-frequency electrodeless discharge lamps; and hollow-cathode tubes.

Of the Wotan lamps, those containing sodium, potassium, thallium, rubidium, and caesium are probably more convenient sources for these elements than any other type of discharge. It is essential, however, to under-run the lamps, since at the recommended operating currents the resonance lines exhibit self-reversal

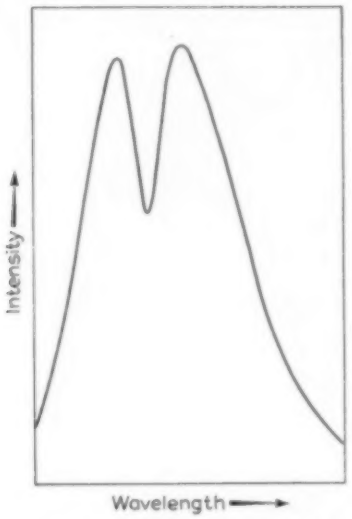

Fig. 4. Contour of Cd-2888-line Å emitted by Wotan lamp at recommended current.

and thus reduce the sensitivity of the absorption method. This is illustrated in Fig. 4 which shows a microphotometer tracing of an echelle spectrum of the 2288-Å line emitted by a Cd Wotan lamp operating at the recommended current. Similarly, instead of operating the sodium lamp at a recommended current of 1·3 amp, it is necessary to decrease the current to 0·8 amp to remove self-reversal, and although the manufacturers warn that such under-running may harm the tube, we have not yet damaged any bulb. Whilst the zinc and cadmium lamps, provided with silica envelopes to transmit the resonance lines at 2138 Å and 2288 Å respectively, may also be used as sources, they are not so satisfactory, since even when they are under-run the lines are not nearly so narrow as those provided by hollow-cathode tubes, and consequently the sensitivity of detection is not so high. This type of lamp is, of course, limited to a restricted range of elements having a low boiling-point.

High-frequency electrodeless discharge lamps of the type developed by Meggers and Westfall [4] and others [5] would suffice for elements having low boiling-points or which form volatile halides, but they require an expensive power-pack, and our experience is that their light-output is not so constant as that from hollow-cathode lamps.

The most suitable source for a wide range of elements is the hollow-cathode

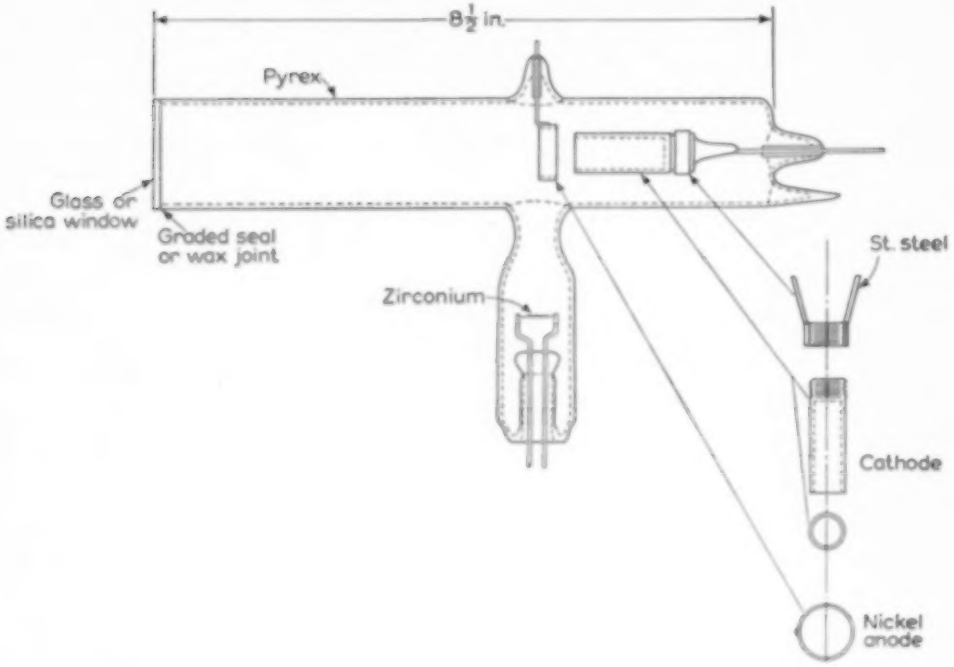

Fig. 5. Diagram of hollow-cathode tube with separate getter assembly.

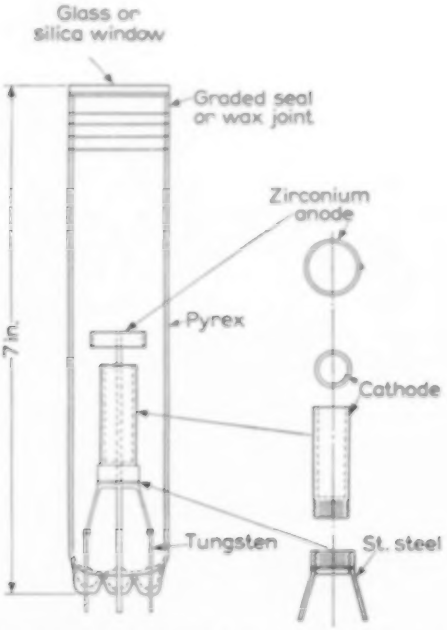

Fig. 6. Diagram of hollow-cathode tube in which the getter and the anode are combined.

discharge tube. Our early experiments involved the use of a closed gas-circulating system, of the type described by TOLANSKY [6], for purification of the rare gas filler. However, following the success of DIEKE [7, 8] and his co-workers in making sealed-off iron hollow-cathode tubes, we have abandoned the gas-circulating system and all our hollow-cathode tubes are of the sealed-off variety. Whereas these workers used activated uranium as a getter and state that this is much more effective than other methods of purification of rare gases, we have adopted the suggestion of Dr. A. L. G. REES and made sealed-off tubes using zirconium as a getter. Our general experience has been that the preparation of sealed-off tubes presents little difficulty, and that any standard gettering technique is satisfactory, provided the tube and electrode assembly is thoroughly outgassed before sealing off the tube. Early forms of tube employed an electrode assembly and a separate getter arrangement similar to that shown in Fig. 5. The anode is made of nickel and the electrode assembly outgassed by induction heating or by running the discharge in argon at currents up to 150 mA, according to the material of the cathode. After several fillings and evacuations of the tube, the latter is filled with spectroscopically pure argon and sealed. The getter, consisting of zirconium wire, is then fired by passage of an electrical current or by induction heating. Many of these tubes are now two years old and are quite satisfactory, including some in which the quartz window is sealed on with black wax.

Whilst the above design of hollow-cathode tube has proved quite satisfactory, we believe the design given in Fig. 6 is preferable, although this design has only been in use for a short time and in this respect cannot be regarded as having been so fully tested as the original models. To date, however, all tubes of this new design have been entirely satisfactory.

The basis of the design is to make the anode of zirconium (or tantalum) strip, and this getter is fired simply by reversing the polarity of the discharge or by induction heating. In this fashion it is possible to dispense with the separate getter and the construction of the tube then becomes extremely simple.

The cathode may be open at both ends or have one end sealed with a plug of the metal whose spectrum is required. For low melting-point metals such as cadmium and lead, it is sufficient to place a pellet of the metal in the cathode, which can be made of any suitable metal, but preferably one such as aluminium, which has a simple spectrum. The tube is then used in a vertical position. Operating currents for the tubes vary from 5 to 100 mA, and should be as small as possible consistent with a satisfactory signal/noise ratio. This is particularly essential for tubes of the low-melting-point metals, which, even at current as low as 10 mA, produce sufficient vapour to cause appreciable resonance broadening. The tubes are operated from a regulated d.c. supply giving 600 V and currents up to 150 mA.

(c) *Sprayer*

Our work to date has been restricted to the analysis of solutions, and these have been atomized by spraying into the air supply of a Meker burner operating on air and coal-gas. The sprayer is similar to that used in early types of

Perkin-Elmer flame photometers and the flame has a diameter of 2 cm at the base. A rate of flow of 1850 c.c./min of gas and 8200 c.c./min of air was found to provide a convenient flame. The consumption of solution is then 0·2–0·3 c.c./min. This type of flame is suitable for many elements, but it is not hot enough to atomize elements such as aluminium, silicon, and hafnium, which form refractory compounds, and these are not decomposed in the flame.

It may be noted that if the flame is strongly emitting, then it is important that it be placed before the monochromator so that the emitted light is dispersed before falling on the detector. Otherwise, although the emitted light will give no resultant d.c. signal, it will give rise to noise which will lower the accuracy of the absorption measurement.

(d) *Monochromator*

The required resonance line has been isolated from all other lines by means of a Beckman monochromator which is mounted so that the entrance slit is horizontal. The resolution is adequate for many elements, but for those such as iron and nickel, which have complex spectra, a slightly higher dispersion is desirable to facilitate isolation of the desired line. If lines other than the resonance line are transmitted by the monochromator, there will obviously be a loss in sensitivity, since only a portion of the signal will be attenuated by passage of the beam through the flame. For many analyses the monochromator can be replaced by an appropriate filter, or by an arrangement similar to that used by Alkemade and Milatz [9] for the analysis of sodium.

VOL. 8 1956/5

(e) *Detector*

The detector in the ultra-violet and visible is a R.C.A. IP28 photomultiplier tube operated from a regulated supply. A sodium salicylate film deposited on the window of the photomultiplier permits satisfactory recording of lines below 2500 Å down to the zinc line at 2138 Å. For caesium and rubidium with resonance lines in the near infra-red a red-sensitive IP22 photomultiplier tube has been used.

(f) *Amplifier*

It was originally assumed that some form of double-beam method would be necessary in order to compensate for variations in the light output from the hollow-cathode tubes. It has been found, however, that when the tubes are operated from stabilized supplies, the light output is highly stable and single-beam operation is perfectly satisfactory, provided the photomultiplier also is operated from a regulated supply. Consequently, double-beam working is not essential but is valuable if rapid analysis is required, and obviates the necessity for regulated supplies.

We have followed Oberley's [10] method of phase discrimination in which the sample signal is chopped at frequency f (in our case 93 c/s) and the reference signal at frequency $2f$ (186 c/s), the a.c. signals being amplified and then rectified by synchronous rectifiers operating at the corresponding frequencies. Rectification is controlled by interrupting the light falling on a photo-cell using the

rotating sector shown in Fig. 3. The ratio of the two d.c. signals is then measured on a Speedomax Type-G recorder which has been converted to ratio recording. This measurement is quite satisfactory provided that the amplifier or dynode voltage is adjusted so that the d.c. signal from the reference beam is approximately 10 mV.

Whilst this method of double-beam operation has proved very satisfactory, it is not claimed that it is better than other well-known methods for this purpose. The selection of this particular method was determined by the fact that it is wished to use the same system in a double-pass ozone spectrophotometer, for which this two-frequency method has decided advantages over other methods. It may be noted that in one respect the design of double-beam systems for use in atomic-absorption spectrophotometers is much simpler than when recording spectra using a source which emits a continuous spectrum, since with atomic spectra the spectral slit-width of the monochromator is greater than the line-width and thus matching of the two beams in the monochromator is not nearly so important.

2. Application of the atomic absorption spectrophotometer to the analysis of solutions

(a) *Comparison of peak absorption with oscillator strength*

The work to date has been restricted to solutions, and no attempt has been made to develop the method for application to any specific analytical problem. The main aim of the work has been to investigate some of the factors involved in the recording of atomic absorption measurements in terms of peak absorption and to assess the possibilities of absolute analysis. We have therefore confined most of our investigations to those elements for which the oscillator strengths of the resonance lines are known. In this connection it may be noted that measurement or calculation of oscillator strengths is by no means simple and the values obtained are therefore not highly accurate, as witnessed by the discrepancies between the results of various workers.

To test the absorption method we have taken measurements on aqueous solutions containing salts of different elements and compared the peak absorption measurements with the known oscillator strengths (see equation 8, ref. 1). By using the oscillator strength of the strongest resonance line of copper as the reference, the oscillator strengths of the resonance lines of other elements have been determined from the measurements of peak absorption. The results of this comparison are shown in Table 1, in which the oscillator strengths, expressed as f-values, indicate the extent to which the atom, for the line concerned, behaves as a classical oscillator for which $f = 1$.

It will be seen that the agreement between these values and those obtained by other methods, whilst by no means perfect, is extremely encouraging. It means that if the instrument is calibrated for one element, then it is also approximately calibrated for the other elements listed. In this respect we believe that the absorption method, even in its present form, represents a significant advance on any emission method.

Table 1. Relative *f*-values measured on atomic absorption spectrophotometer

Resonance line	*f* (previous work)	*f* (atomic absorption)
Cu-3247	0·62	0·62
Mg-2852	1·74	1·8
Na-5890	0·70	1·0
K-7665	0·64	0·5
Cd-2288	1·20	2·8
Tl-2769	0·20	0·15
Zn-2138	—	1·9
Ag-3280	—	1·3
Au-2428	—	0·8
Fe-3720	·013	0·01
Ni-3415	0·02	0·04
Cr-4254	0·08	0·01

At this stage in the development of the absorption method there are various reasons why perfect correlation between our measurements of peak absorption and oscillator strength is not to be expected. In the first place, the unjustifiable assumption has been made that the shape of the absorption line is the Doppler contour, whereas it is known that there will be a pressure-broadening width, of the order of the Doppler width, and this broadening will be different for the lines of the various elements. Similarly, the widths of the lines emitted by the hollow-cathode lamps are not known, and it is necessary to establish that this width is negligible compared to the width of the absorption line. Fortunately, it is possible to obtain some indication whether this is so by making absorption measurements with the hollow-cathode tube operating at different currents. For high-melting-point metals such as iron, chromium, and nickel, the peak absorption is sensibly independent of the tube current, and this suggests that the emitted line must be much narrower than the absorption line. For low-melting-point metals such as cadmium and zinc, on the other hand, the absorption varies rapidly with current. This is shown in Fig. 7, which gives calibration curves for cadmium with the hollow cathode operated at various currents. It will be seen that at lower currents there is a marked increase in absorption, which must be due to a decrease in the width of the line emitted. It would, of course, be quite possible to extrapolate the results to zero current, and this may prove desirable in absolute analysis. It may also be noted that in those cases where the absorption varies rapidly with current in the light source, it is important to operate the source from a well-regulated supply.

(b) *Sensitivity*

The limit of sensitivity of the method depends on various factors such as the oscillator strength of the line involved, the intensity of the line emitted by the source, and the spectral slit-width required to isolate the required line.

VOL. 8 1956/5

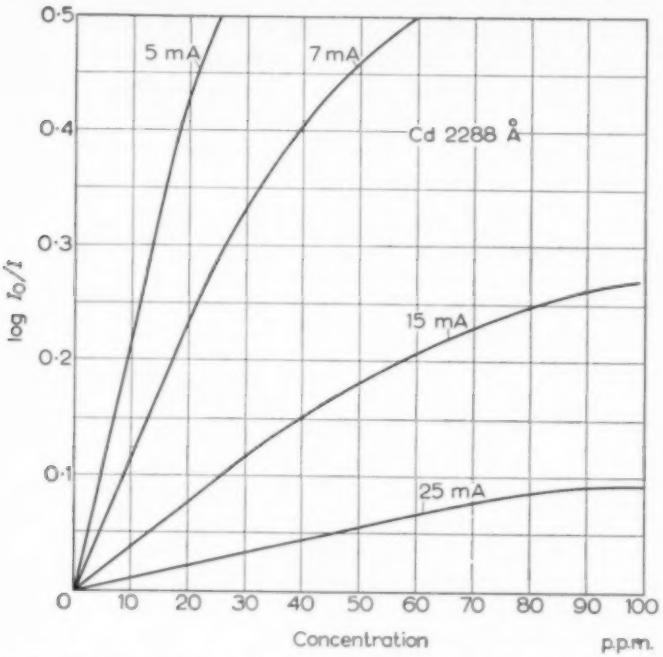

Fig. 7. Calibration curves for cadmium for different currents in the hollow-cathode tube.

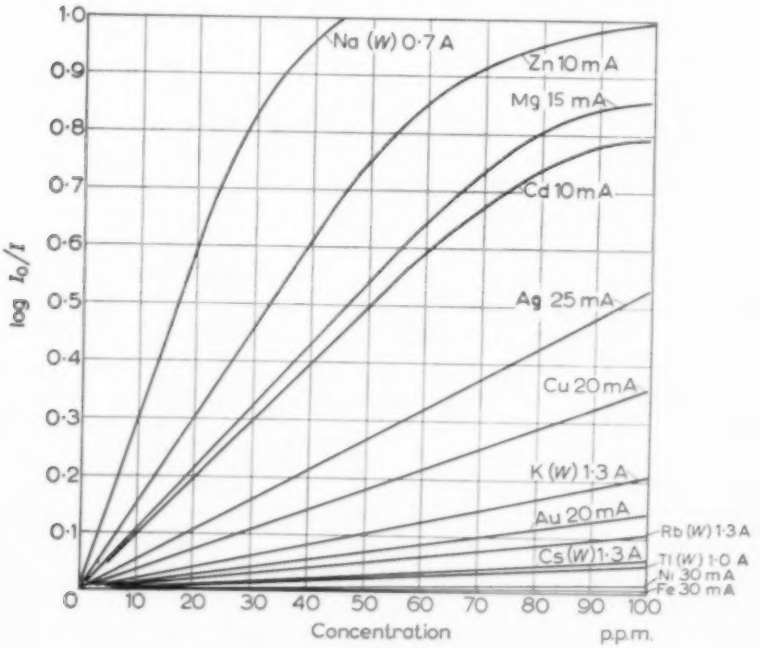

Fig. 8. Calibration curves for various elements.

Consequently, it is difficult to give any precise figures for sensitivity. However, in Table 2 are given our estimates, which it is believed are conservative, for the elements studied. Those marked with an asterisk indicate that Osram lamps were used as source. For all other elements the sources were hollow-cathode tubes. The calibration curves are shown in Fig. 8. These curves are linear over a limited concentration range. The tail-off is presumably due to pressure-broadening.

Table 2. Limits of detection

Element	p.p.m.
Na*	0·1
K*	0·5
Cu	1
Zn	0·1
Cd	0·1
Au	2
Ag	2
K	0·5
Rb*	2
Cs*	10
Tl*	10
Mg	0·1
Fe	40
Cr	40
Ni	20

VOL. 8 1956/5

Possibly the most interesting result is the confirmation of the expected result that elements such as zinc and cadmium, with resonance lines in the extreme ultra-violet, have the same order of sensitivity as sodium with its resonance line at the long-wave end of the visible spectrum. This is in marked contrast to emission spectra, where the limit of detection depends critically on the excitation energy of the first resonance level. Thus in emission, zinc, for example, has a much lower sensitivity than sodium. This is because a flame is not hot enough to excite an appreciable proportion of zinc atoms. In absorption, on the other hand, where we are concerned only with the atoms in the ground state, this is of no consequence, and in this respect the absorption measurement is independent of the wavelength of the resonance line. There is, of course, a much smaller effect due to the variation in the Doppler width of the absorption line.

It may be noted that the sensitivity for rubidium and caesium is not nearly so high as for sodium. This is due to the fact that the resonance lines emitted by the rubidium and caesium lamps are self-reversed at the lowest current (1 A) which can be used in order to obtain a satisfactory signal-noise ratio.

The sensitivities quoted in Table 2 are for a single passage of the radiation through the flame. It is possible to achieve higher sensitivities by multiple traversals. For example, using a J. U. White system to give twelve traversals,

we have obtained an increase in sensitivity of approximately tenfold. The effect of increasing pathlength on sensitivity is shown by the iron calibration curves in Fig. 9.

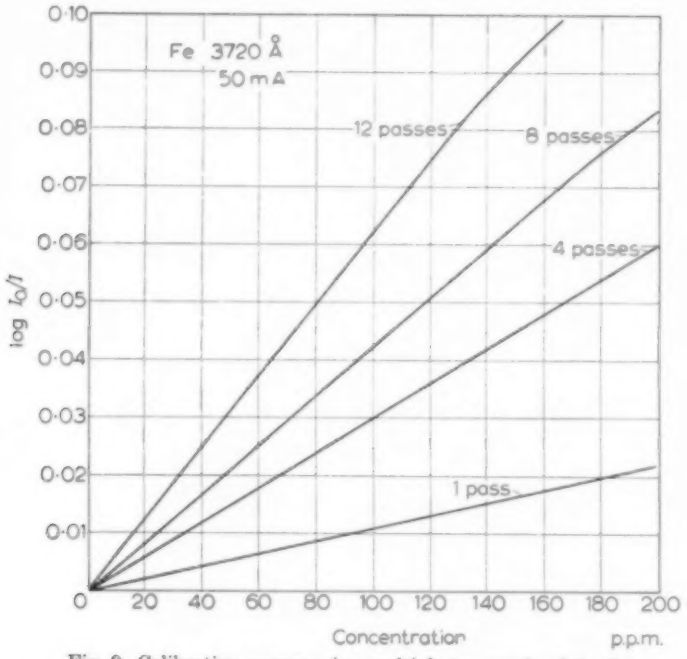

Fig. 9. Calibration curves using multiple traversals of the flame.

(c) *Limitations*

At the present state of its development, by far the most serious difficulty in the absorption method is due to the difficulty in atomizing various elements. For example, highly oxidizable elements such as aluminium, silicon, hafnium, etc. are not atomized in the air–coal-gas flame used in this work and thus are not detectable in absorption. Similarly, many other elements will not be completely atomized, thus decreasing the sensitivity and providing a serious obstacle to accurate absolute analysis. In this respect the cyanogen-oxygen flame, having a temperature of about 4600°C, which has recently been applied by BAKER and VALLEE [11] to emission methods, may prove to be extremely valuable. This problem of complete atomization of the sample seems to us to be the outstanding problem at the present time.

Acknowledgement—We are grateful to Mr. W. G. JONES for the construction of all hollow-cathode tubes used in this work.

References

[1] WALSH A. *Spectrochim. Acta* 1955 **7** 108.
[2] *Handbook of Third Exhibition of Institute of Physics* Melbourne, March 1954.
[3] Patent Specifications: Australia, Provisional Spec. 12041/1953; Complete 23041/53; Great Britain 33,068/54; USA 469,221; France 679,886; Germany C10276 IXb/421; Holland 192,460; Italy 82/322; Sweden 10436/54.

[4] Meggers W. F. and Westfall F. O. *J. Res. Nat. Bur. Standards* 1950 **44** 447.
[5] Zelikoff M., Wyckoff P. H., Aschenbrand L. M., and Loomis R. S. *J. Opt. Soc. Amer.* 1952 **42** 818.
[6] Tolansky S. *High Resolution Spectroscopy* 1947 Methuen, London.
[7] Dieke G. and Crosswhite H. M. *J. Opt. Soc. Amer.* 1952 **42** 433.
[8] Crosswhite H. M., Dieke G. H., and Legagneur *J. Opt. Soc. Amer.* 1955 **45** 270.
[9] Alkemade C. T. J. and Milatz J. M. W. *App. Sci. Res.* 1955 **B4** 289.
[10] Oberley J. J. *Rev. Sci. Inst.* 1953 **24** 125.
[11] Baker M. R. and Vallee B. L. *J. Opt. Soc. Amer.* 1955 **45** 773.

VOL.
8
1956/5

Spectrochimica Acta, 1957, Vol. 8, pp. 329 to 347. Pergamon Press Ltd., London

Photoelectric Fabry-Perot interferometer for assay of lead and uranium isotopes*

J. K. Brody, F. S. Tomkins, and M. Fred
Argonne National Laboratory, Lemont, Illinois

(*Received* 25 *April* 1956)

Abstract—The Fabry-Perot interferometer was used with photoelectric detection for precise intensity measurements of the complex pattern of Pb-4057·82 Å. The central fringe was scanned by a change of pressure in the interferometer housing. Optical and electronic arrangements for employing the internal-standard principle with the interferometer are described. The concentration of Pb^{208}, Pb^{206}, Pb^{204}, and Pb^{207} determined by the method are essentially in agreement with mass spectroscopic results.

Small isotope shifts in the uranium spectrum were examined because of similarities with other heavy-element spectra, particularly plutonium for which it was hoped a method might be developed. Partially resolved U^{235} hyperfine structure necessitated a search for U^{235} lines with negligible structure. Low intensity of the hollow cathode source limited the usefulness of the interferometer method for uranium.

OL.
8
6/57

Introduction

The optical spectroscopic method of isotope assay employing photoelectric detection has been used successfully for isotopes of hydrogen [1, 2], helium [3], lithium [4, 5], and uranium [6]. All of these elements exhibit comparatively large isotope shifts. Smaller isotope shifts of the order of 0·01 Å were studied with a view toward extending the usefulness of the optical spectroscopic method. Shifts of this magnitude may be resolved in the high orders of a grating spectrograph which could be used for isotope assay, provided the grating was blazed to give sufficient intensity in high orders.

Alternatively, the Fabry-Perot interferometer might be used with a spectrograph of moderate dispersion to resolve small isotope shifts. The present investigation is devoted to the development of the interferometric method.

The complex pattern of Pb-4057·82 Å was used to demonstrate the problems involved in making isotope assays with the Fabry-Perot interferometer. This line consists of six isotope and hyperfine components with a total width of about 0·07 Å. The shift from Pb^{206} to Pb^{208} is 0·014 Å. The arrangement of the pattern is shown in Fig. 1 with the separations given by Steudel [7]. The position of Pb_{80}^{207} component is dotted to show its position in the pattern when a 10-mm spacer is used in the interferometer. The theoretical intensities of the Pb^{207} hyperfine components were employed to determine the total Pb^{207} intensity.

Rose and Stranathan [8] made an isotope assay of "ordinary" lead with the Fabry-Perot interferometer by photographing the patterns for Pb-II lines 5372 Å and 5367 Å. The Pb^{204} component was superimposed on one of the Pb^{207} hyperfine components. They calculated the relative intensity of the Pb^{207} components by the

*Based on work performed under the auspices of the US Atomic Energy Commission.

sum rule for intensities, and the Pb^{204} intensity was obtained by difference in their measurements.

Small shifts of about 0·03 Å in the uranium spectrum were also studied in the present work. Although the large shift in the U line 4244·37 Å would prove more useful for uranium-isotope determinations [6], it appeared that the techniques developed for the small uranium shifts might be used for similar determination in plutonium and other heavy elements.

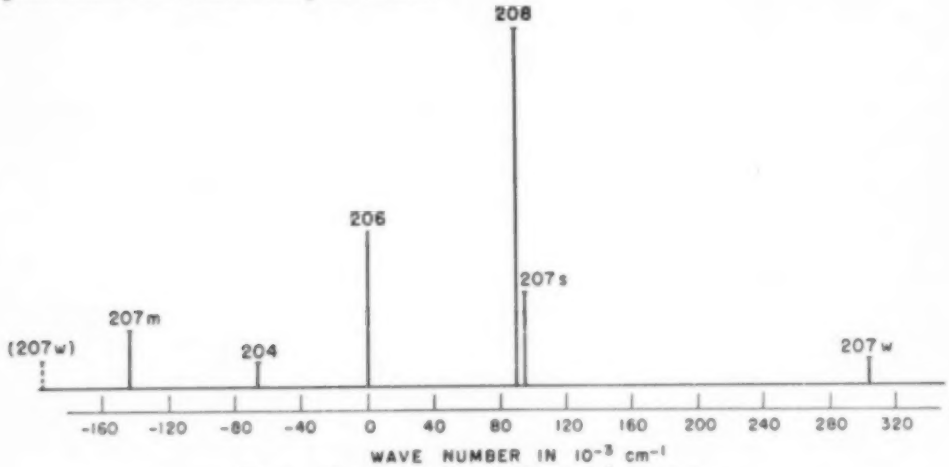

Fig. 1. Schematic diagram of Pb-4058-Å structure.
The shifts taken from Steudel [7] are in $cm^{-1} \times 10^{-3}$. The dashed 207_w line shows its relative position in the Fabry-Perot pattern, using a 10-mm spacer. The strong, medium, and weak 207 components are designated by subscripts *s*, *m*, *w*, respectively.

Experimental

A water-cooled Schüler-type hollow cathode [9] was used for the lead and uranium studies. Samples of 3 mg of PbO in an aluminium cathode were excited in an argon atmosphere at 2·5-mm mercury pressure, using currents of 15 to 50 mA. Samples of 5 mg of U_3O_8 containing equal amounts of U^{235} and U^{238} were excited in an iron cathode in an atmosphere of argon at 4-mm mercury pressure with currents of 100 mA. For purposes of intensity comparisons, uranium metal was also used in the hollow cathode and an electrodeless discharge tube containing neon and UCl_4 with an equal mixture of U^{235} and U^{238} was excited by a high-frequency field.

The first order of the 30-ft grating spectrograph equipped with an 8-in. Bausch and Lomb grating with 15,000 lines per inch was used, giving a reciprocal dispersion of 1·6 Å/mm. The large instrument was used as a matter of convenience, although a smaller commercial instrument could have been used as well. Photoelectric detection was employed with a.c. amplifiers built by W. K. Brookshier of the Electronics Division. Leeds and Northrup* experimental amplifiers and ratio recorder were also used for the time-proportioned internal-standard procedure described below.

* We wish to express our appreciation to the Leeds and Northrup Company for the use of their experimental amplifiers and ratio recorder

VOL. 8 1956/5

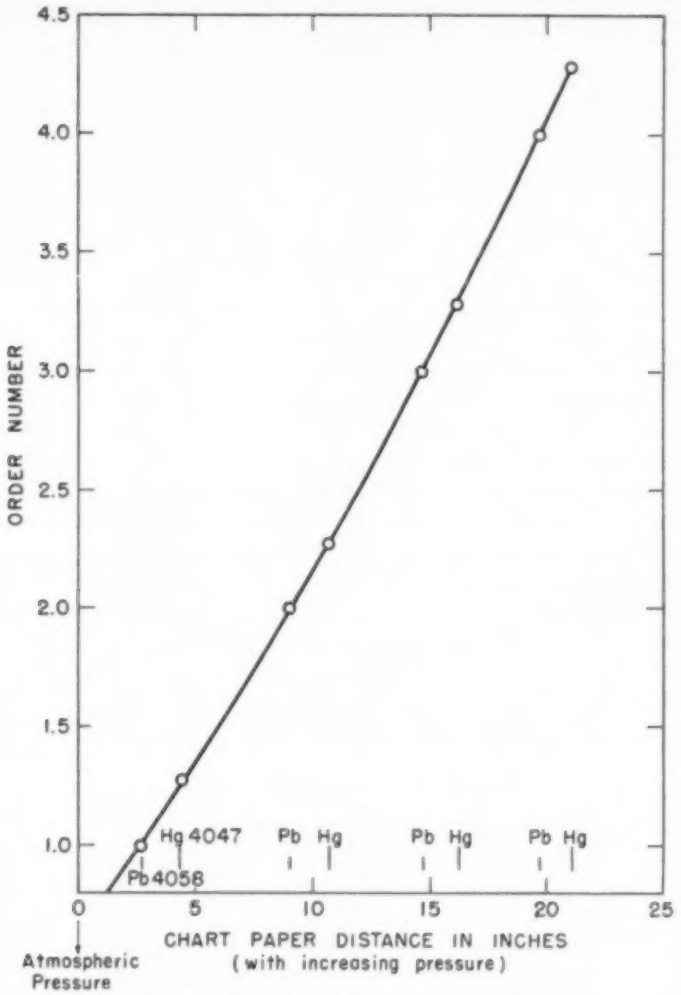

Fig. 2. Correction for nonlinear scanning rate.

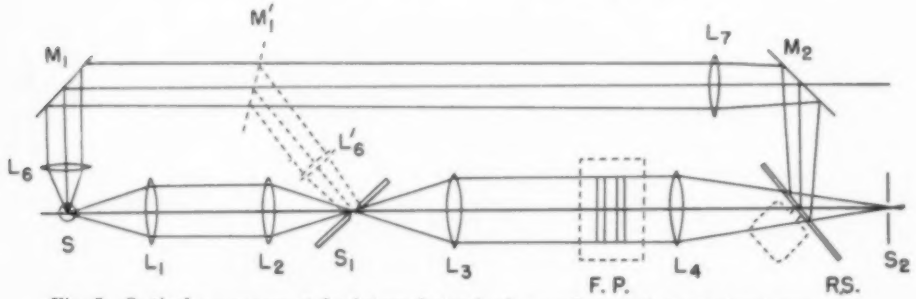

Fig. 3. Optical arrangement for internal standard procedure with the Fabry-Perot interferometer. The dotted beam shows the equivalent internal-standard optical path used for the hollow cathode tube. The angle of the auxiliary slit is exaggerated. RS is the rotating sector with polished stainless-steel blades.

The Fabry-Perot interferometer enclosed in a pressure-tight box was designed and built in the Argonne shops. The 25-mm-diameter interferometer plates with zinc sulphide-cryolite multilayer coating* were used with a 10-mm quartz spacer.

K. W. Meissner [10] first pointed out to the authors the advantage in resolving power and dispersion at the central fringe of the interferometer ring system. Jacquinot [11] has utilized a pressure scanning technique for the analysis of hyperfine structures. In order to realize the advantage mentioned above for isotope analysis, a similar scanning procedure was developed in which the change in the central spot was observed as the pressure (and therefore the optical path between the interferometer plates) was slowly changed. As the pressure increases, the central fringe expands gradually until it forms the first ring. The pressure was changed by moving a piston in a steel cylinder 24 in. long by 6 in. inside diameter. The piston was connected to a motor-driven screw which displaced the piston 0·3 in. per minute. The inside of the cylinder was honed to a smooth finish and lubricated with light grease. An O-ring on the circumference of the piston made a tight seal. One end of the cylinder was connected to the interferometer housing by Neoprene pressure tubing and the other end vented by a small hole. A linear rate of piston displacement does not effect a linear rate of pressure change and therefore results in a nonlinear scanning rate. However, the nonlinearity of scanning was held to a minimum by making the total volume of the cylinder large. The plot of Fig. 2 was used to convert the chart paper distance between successive orders to fractional order. This was obtained by scanning four successive orders of both Pb-4058 Å and Hg^{198}-4047 Å, starting from atmospheric pressure, which served as the reference point for the chart-paper measurements.

VOL.
8
1956/5

Internal standard procedure

The internal-standard procedure commonly used to compensate for fluctuations in the light source proved to be a worthwhile technique for intensity measurements with the Fabry-Perot interferometer. Although the hollow-cathode discharge is a very stable source under ideal conditions, more precise intensity measurements were realized with an internal standard. When the electrodeless discharge tube was used, an internal standard was quite essential, due to the fact that the UCl_4 gradually distilled to the cooler parts of the tube, causing rather large changes in the intensity.

For intensity measurements with the Fabry-Perot interferometer a photomultiplier tube placed on a line of interest would see the constantly changing intensity of the fringe system as it was scanned. A second photomultiplier on another line to serve as internal standard would see the intensity distribution of its own fringe system. The ratio of the two photocurrents would represent the ratio of the two fringe systems, each varying independently of the other. Obviously this would not correct for fluctuation in the light source.

To solve this problem, a second beam from the light source was utilized for the internal standard, as shown in Fig. 3. In the case of the discharge tube operated in a vertical position, lens L_6 rendered the light parallel from the same part of the discharge tube seen by the interferometer. After reflection from mirror M_1, lens

* We are indebted to Dr. J. G. Hirschberg, University of Wisconsin, Physics Department, for the excellent dielectric coatings.

L_7 focused an image of the tube on the spectrograph slit by reflection from mirror M_2 and the polished blades of the rotating sector, RS. As the sector rotated, the photomultiplier on the line of interest observed the interferometer fringe intensity on one half cycle and the source directly on the next half cycle. For the 60-cycle signal system used, the sector rotated 1800 r.p.m. For the interferometer beam, the source S was imaged by lenses L_1 and L_2 on the auxiliary slit S_1, which was used to eliminate secondary fringes according to the method of TOLANSKY [12]. The interferometer was used in parallel light and the fringes focused on the slit by lens

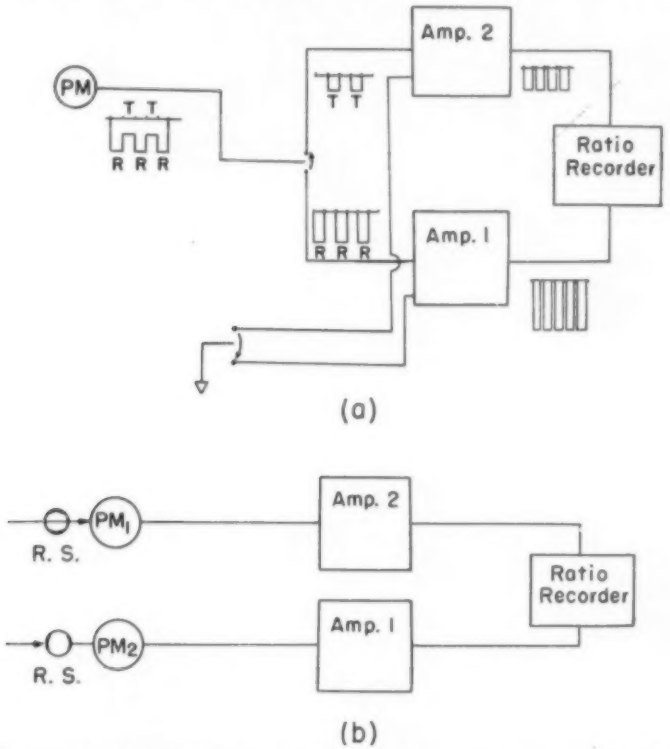

Fig. 4. Schematic diagram of the signal system, *a*, for the time-proportioned internal standard, using a single photomultiplier, and *b*, using two photomultipliers. *R* is the signal for the reflected beam and *T* the signal for the transmitted beam. RS is a rotating shutter.

L_4. The output of the photomultiplier was fed to a vibrator-type switch, which switches the fringe photocurrent to one amplifier and the internal standard signal to a second amplifier. The vibrator is operated in synchronism with the sector. The amplifier outputs are fed to the ratio recorder, so that the trace shows the ratio of the fringe intensity distribution of the line to the unresolved line directly.

Fig. 4a shows a schematic diagram of the switching system. Each amplifier was grounded during the half cycle in which it received no signal. The square wave signal is shown with the internal standard signal designated by R, since it was reflected by the sector, and the interferometer fringe intensity by T, since it was

transmitted by the sector. A trace of U-4362 Å in the electrodeless discharge tube is compared with Hg^{198}-4358 Å in Fig. 5, using the internal-standard system above. The system had one serious disadvantage when it became necessary to operate the photomultiplier at high gain. The vibrator switch chopped the d.c. component of the dark current so that it was amplified by the a.c. amplifiers along with the signal resulting in rather high backgrounds. The advantage of the a.c.

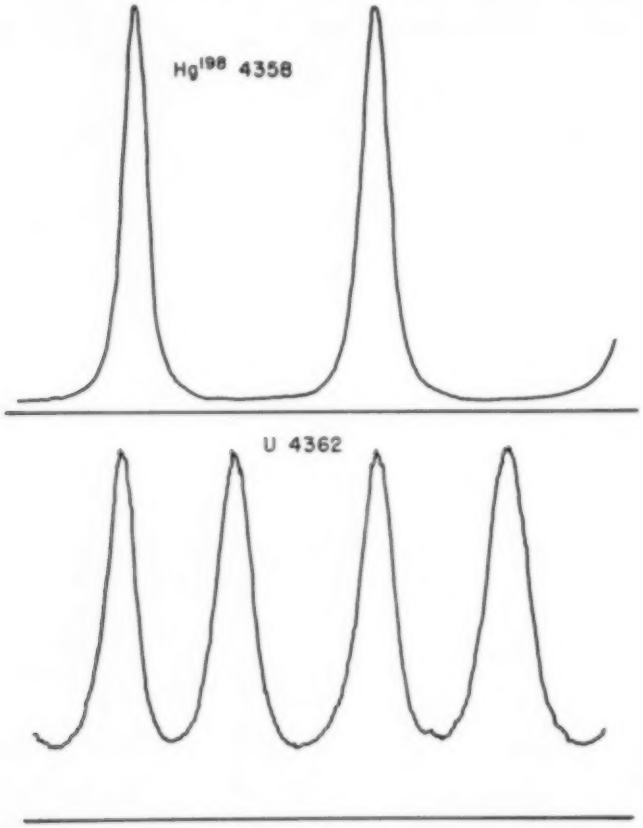

Fig. 5. Recorder trace of U-4362·05 Å compared with Hg^{198}-4358·35 Å, using a single photomultiplier and the time-proportioned internal-standard system. Since the tube contained equal amounts of U^{235} and U^{238}, equal peak heights indicate negligible hyperfine structure.

signal system in automatically subtracting the d.c. component of the dark current was consequently lost. The d.c. dark current could be eliminated by a small d.c. current of opposite polarity. However, it was felt that a second internal-standard system described below might serve as well without revision of the electronics.

The advantages of the a.c. signal system were restored with a second internal-standard technique used in the lead isotope assay. A 1P21 photomultiplier tube with a 1-mm-wide slit placed on the Pb-4058-Å line observed the interferometer pattern, while a second 1P21 photomultiplier with a 2-mm slit on the same line in

VOL.
8
1956/5

the second order observed the unresolved line in the source reflected from the sector. The second phototube eliminated the need for the vibrator switch. The output from each photomultiplier was fed to its own amplifier, whose output was fed to the ratio recorder, as shown in Fig. 4b. In order to prevent the one photomultiplier receiving the transmitted beam from observing the reflected beam, and vice versa, synchronous shutters, operated 180 degrees out of phase, were placed directly in front of the exit slits.

Since the hollow cathode tube used for the lead determination was unidirectional, a change in the optical set-up was required, as shown by the dotted optical path in Fig. 3. An image of the source reflected from the polished jaws of the auxiliary slit S_1 is made parallel by lens L_6', reflected by M_1', and focused on the spectrograph slit by lens L_7 in the same manner as described above. Although the internal standard beam did not observe precisely the same area of the source as the interferometer, it was found that the closely adjacent area provided excellent internal standard compensation.

Selection of slit-width and hole diameters

Since the central fringe of the interferometer ring system is a circular spot, the light may be utilized more efficiently by using a hole rather than a slit at the entrance to the spectrograph. The hole would be imaged in the focal curve of the spectrograph except for the astigmatism which expands the image in the vertical direction.

To determine the diameter of the hole for Pb-4058 Å, the fundamental equation for the Fabry-Perot interferometer was used.

$$n = 2\mu t\nu \cos \theta/2 \tag{1}$$

In this formula, n is the order of interference, μ the index of refraction of air between the plates, t the plate separation, ν the wave number of the line, and θ the angular diameter of the ring. At the centre of the system, equation (1) becomes

$$n_0 = 2\mu t\nu \tag{2}$$

and

$$dn_0 = 2\mu t d\nu. \tag{2a}$$

Substituting equation (2) in equation (1), the latter becomes

$$n = n_0 \cos \theta/2.$$

Expanding $\cos \theta/2$ and rearranging

$$n = n_0 = -n_0\theta^2/8.$$

Considering a full order at the centre bright spot, the angular diameter of the Kth ring is

$$\theta = (8K/n_0)^{\frac{1}{2}}$$

The linear diameter was obtained by multiplying the angular diameter by the focal length of the projection lens.

$$D = f\theta = f(8K/n_0)^{\frac{1}{2}} \tag{3}$$

For the Hg^{198}-4047-Å line an 80-cm-focal-length lens and a 1-cm quartz spacer was used, so that the diameter of the first ring out from the centre bright spot was calculated to be

$$D = 80\left(\frac{8}{5 \times 10^4}\right)^{\frac{1}{2}} = 10{\cdot}1 \text{ mm}.$$

In the Pb-4058-Å line, the separation between Pb^{208} and Pb^{206} has been shown to be 0·089 cm^{-1} [13]. Substituting this value in equation $2a$, $dn_0 = 0{\cdot}178$ order. Substituting 0·178 for K in equation (3), the diameter was found to be 4·27 mm. The central bright fringe had a finite size due to the combined Doppler and instrumental broadening effects, the total of which was estimated to be 0·04 cm^{-1} at half the intensity. The diameter of the central fringe was calculated as above and

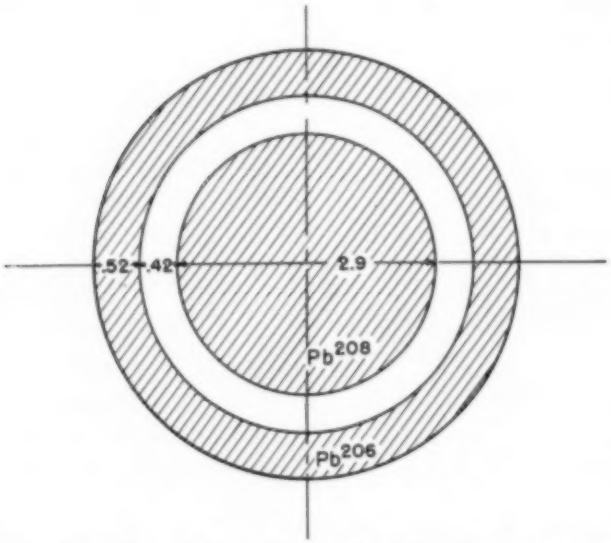

Fig. 6. Central fringe and first-ring diameter in millimetres for Pb-4058 Å, drawn to scale. Although it is recognized that the intensity distribution follows the Airy formula, half intensity widths are represented as discreet quantities.

found to be 2·9 mm. The 4·27-mm diameter calculated above for the adjacent isotope line represents the diameter at the centre of gravity. However, this line also has a finite width, for the reasons mentioned above. Although the dispersion changes rapidly at the centre of the ring system, the width of the first ring was calculated as a first approximation, using the formulas above, and found to be 0·52 mm. The ring system is represented in Fig. 6, and shows that a 2·9 mm-diameter hole clearly resolves the two isotopic components.

This was verified experimentally by scanning the line with 1-, 1·5-, 2-, 2·5-, 2·75-, 3·0-mm-diameter holes successively. The 3-mm hole resolves the pattern well. However, the peak-to-background ratio became progressively smaller with larger holes, starting with the 2·5-mm hole. In order to minimize the background

corrections explained below, the largest hole possible without appreciable reduction of peak to background ratio was used. This was determined experimentally as 2·5-mm diameter.

A hole may be used at the entrance of the spectrograph in place of the slit when relatively simple spectra such as lead are being studied. Also a large exit slit may be used. An exit slit 1 mm wide was used for the Pb-4058-Å line.

However, for complex spectra such as uranium, very few lines were sufficiently isolated from neighbouring lines to use the larger entrance area. For uranium, entrance- and exit-slit widths of 100 and 250 microns were used. The entrance-slit height was determined by the size of the central fringe. A 2·5-mm slit height was used, since the optical conditions were the same as for the Pb determinations.

Background corrections

Background corrections were made in a manner similar to that described for Li isotope determinations [4]. Since the Fabry-Perot interferometer has an intensity distribution given by the Airy formula, the minimum intensity between orders never goes to zero. In the complex pattern of Pb-4058 Å each isotope and hyperfine component superimposed its own contour upon the others to give the observed pattern. The background intensity for a particular line consisted of contributions from all the other components in the pattern and could not be observed directly. The amount of background intensity, and hence the correction, was determined by observing the contour of a single line pattern. The Hg^{198}-4047 Å line was used. From the known or observed separations of the lead components, the contribution of each component to the others may be determined. The Hg^{198}-Å-line contour

Table 1. Background corrections as a function of the peak intensity of the interfering line

Interfering lines	Measured lines						Check Point
	208	206	204	207 *m*	207 *w*	207 *s*	
208	—	0·022	0·007	0·005	0·005	0·78†	0·007
Fractional order	—	0·16	0·30	0·43	−0·46	0·025	−0·30
206	0·02	—	0·022	0·008	0·005	0·015	0·005
Fractional order	0·16	—	0·16	0·27	0·38	0·19	−0·46
204	0·007	0·022	—	0·032	0·010	0·006	0·007
Fractional order	0·30	0·16	—	0·13	0·21	0·35	−0·30
207 *m*	0·005	0·008	0·032	—	0·065	0·005	0·007
Fractional order	0·43	0·27	0·13	—	0·10	−0·45	0·26
207 *w*	0·005	0·005	0·010	0·065	—	0·005	0·022
Fractional order	−0·46	0·38	0·21	0·10	—	0·45	0·16
207 *s*	0·78†	0·015	0·006	0·005	0·005	—	0·007
Fractional order	0·025	0·19	0·35	−0·45	0·45	—	−0·30

† Pb_s^{207} and Pb^{208} were not resolved. This correction was determined from the plot of Fig 11 and is explained below.

(Fig. 7) was assumed to be nearly identical to Pb-4058 Å, since there are only slight differences in mass and wavelength. Since the mercury discharge tube was water-cooled, the Doppler broadening should be the same as for lead in the water-cooled hollow cathode. This was found to be the case judging from a comparison of the observed Hg-λ4047 and Pb^{206}-λ4058 half-widths. The Hg contour is shown in Fig. 7 with the relative positions of the components of the lead pattern. The background corrections determined in this manner are given in Table 1 as a fraction of the peak intensity contributing to the background intensity.

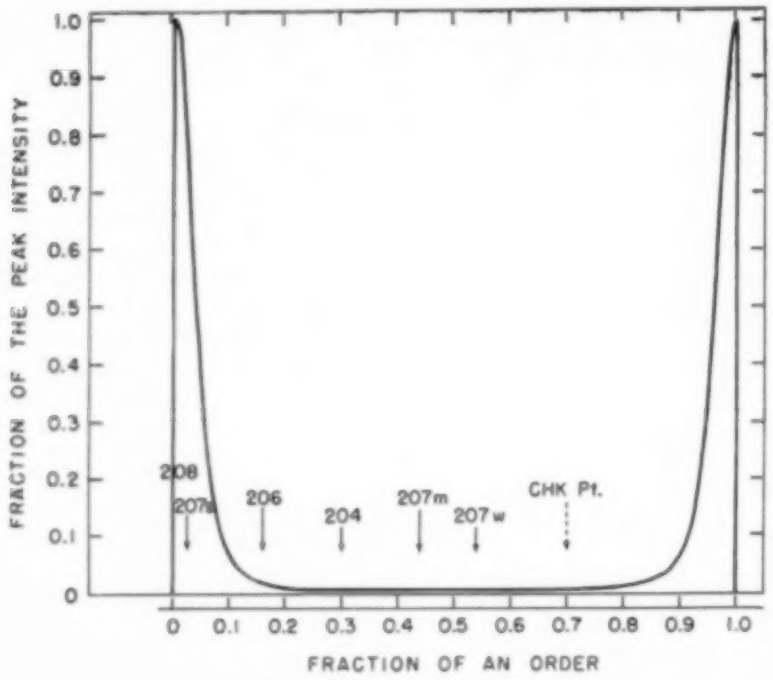

Fig. 7. Hg^{198}-4047-Å line contour.
This line excited in a water-cooled electrodeless discharge tube was assumed to have the same contour as a single component of the lead pattern for λ4058 in the water-cooled hollow cathode tube. The position of the components in the lead pattern is shown.

The validity of the background correction was verified by observing the minimum intensity of the pattern which was used as a "check point." The intensity at this point consists of contributions from all of the line contours by the fraction of the peaks shown in Table 1. In cases when the lead spectrum was strong compared to the overall spectrum, good agreement was obtained between the observed and calculated intensity at the check point. When the lead spectrum was relatively weaker, the gain of the system was increased, thus bringing up the intensity of the light-source continuum relative to the lead-line intensities. In this case the small difference between the calculated and observed intensity at the check point was subtracted from all lines as light-source background.

VOL.
8
1956/5

Self-absorption correction

The ratio I^{208}/I^{207} for normal lead decreased with increasing intensity. Similarly, other ratios for the enriched samples increased or decreased with increasing intensity, depending upon which line was the stronger. This effect was attributed to self-absorption, for which a correction was empirically derived from the measurements on the sample enriched in Pb^{207}. This sample provided the best measurements of the hyperfine structure components I_m^{207}, and I_w^{207}. The observed weak line, I_w^{207}, was plotted against the observed intermediate intensity line, I_m^{207} to give the curve of Fig. 8. The straight line of Fig. 8 shows the theoretical I_m^{207}/I_w^{207}

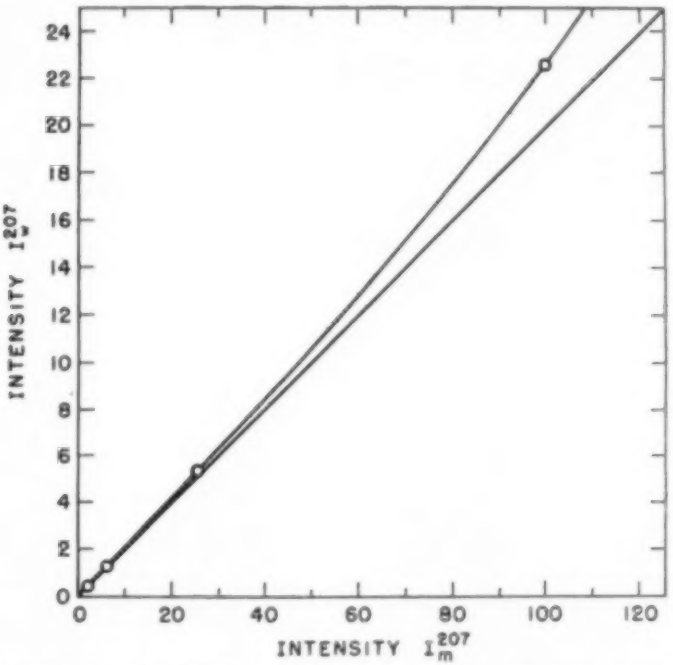

Fig. 8. Plot of I_w^{207} against I_m^{207}, showing self-absorption. The straight line shows the plot for the absence of self-absorption, assuming an I_m^{207}/I_w^{207} ratio of 5 : 1.

ratio = 5·0. It was possible to make observations at sufficiently low intensity to observe an I_m^{207}/I_w^{207} ratio of 5·0 : 1. In starting from the lowest intensity and gradually increasing, the first differences between the two curves of Fig. 8 were assumed to be due to the self-absorption of the stronger component only. This was a reasonable assumption for a ratio of 5 : 1 which was observed at low intensity. The initial differences between the curves became the corrections to be added to the stronger component. At somewhat higher intensity where both lines were self-absorbed, the initial corrections were used to correct the weak line. Knowing the unabsorbed intensity of the weak line $I_{0,w}^{207}$, the unabsorbed intensity of the stronger line, $I_{0,m}^{207}$, was obtained by multiplying $I_{0,w}^{207}$ by 5, the unabsorbed ratio.

This procedure was repeated for the intensity range of the experimental observations and provided a correction curve for self-absorption.

Since the Pb^{207} intermediate intensity component was 5/15 the total Pb^{207} intensity and since the Pb^{207} concentration was 61%, the empirically derived correction curve did not extend to sufficiently high intensities to correct the Pb^{206} line in the sample containing 65% Pb^{206} or the Pb^{208} line in the sample containing 88% Pb^{208}. It became necessary to extend the correction curve to higher intensities, and this was done in the following manner.

The correction curve for the experimental range of intensities was observed to fit very closely the general formula for a parabola, $x^2 = 4fy$, or in terms of the

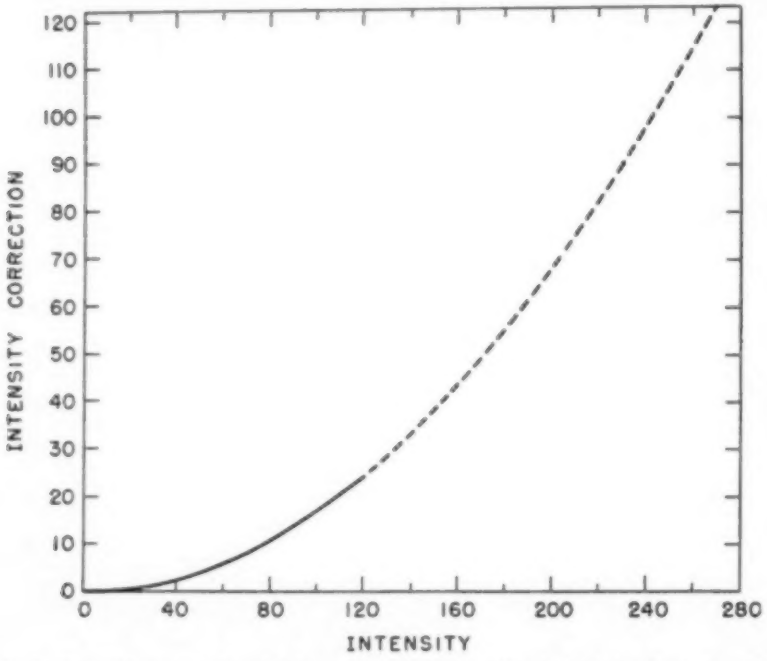

Fig. 9. Correction curve for self-absorption. The correction is the intensity to be added to the observed intensity. The solid curve is the experimental intensity range for Pb_m^{207} and the dashed curve is the extrapolation described in the text.

co-ordinates of Fig. 9, $(I_m^{207})^2 = 4fC$, where C is the correction. The focal length of the parabola, f, was determined for the experimental intensity range and, by substituting hypothetical values of I_m^{207}, the correction, C, for an extended range of intensities was obtained. The correction curve is shown in Fig. 9 with the extrapolation based on the above considerations dotted.

With the self-absorption correction, the same Pb^{208}/Pb^{207} and Pb^{206}/Pb^{207} ratios were observed for a wide range of intensities. Evidently the correction derived above was valid.

In the case of lithium [4] two equations were derived using a 2 : 1 doublet intensity ratio and were used to derive a self-absorption correction. To make the

VOL. 8 1956/5

same correction in a similar manner for Pb where the $I_m^{207}/I_w^{207} = 5$, the equations would take the form,

$$I_m = \frac{1}{K}(1 - e_{0,w}^{-5KI})$$

$$I_w = \frac{1}{K}(1 - e_{0,w}^{-KI}).$$

The observed ratio I_m/I_w was calculated from the two equations as a function of KI_0 for which values of 0·005 to 0·060 were found to cover the experimental intensity range. The value of K over this range was 0·003 and could subsequently be used to derive values of $I_{0,w}$ over an extended range.

Either method could be used to provide the self-absorption corrections. However, the method first described was used for the lead determinations.

Measurements at the high intensity were made with better precision due to the reduction in the statistical fluctuations of the light source relative to the intensity.

Results

Although the 4057·8-Å line of lead has been extensively investigated by a number of workers [13–17], the pattern according to STEUDEL [7] is shown in Fig. 1 for purposes of comparison with the recorder tracing of the interferometer pattern shown in Fig. 10 for normal lead. Referring to Fig. 1, it will be noted that three hyperfine components of Pb^{207} are present. The theoretical intensities were calculated, using the sum rule for intensities, and found to be 1 : 5 : 9 for Pb_w^{207}, Pb_m^{207}, and Pb_s^{207} respectively, giving a total intensity of 15. The total Pb^{207} intensity was calculated from the measured intensity of Pb_m^{207} by multiplying by 15/5. The intensity of the Pb_s^{207} peak unresolved from Pb^{208} as shown in Fig. 10 was calculated by multiplying the total Pb^{207} intensity by 9/15.

The Pb_s^{207} and Pb^{208} peaks were not precisely superimposed. According to STEUDEL [7], these two components had a separation of 0·011 cm^{-1}. In order to determine the fraction of the theoretical Pb_s^{207} peak to subtract from the observed peak, the two lines were plotted as in Fig. 11. The Hg^{198}-4047-Å contour was used to make the plot, and the sums of the intensities at various points along the contours were used to plot the combined peak, which corresponded to the observed peak. From the plot of Fig. 11 it was determined that 78% of the theoretical Pb^{207} peak calculated as explained above should be subtracted from the observed peak to give the Pb^{208} intensity. The Pb^{208}/Pb^{207} ratio was calculated as follows:

$$Pb^{208}/Pb^{207} = \frac{I^{208,207s} - 0{\cdot}78\,(9/15)\,(15/5)\,I_m^{207}}{(15/5)\;I_m^{207}}$$

The Pb^{206} and Pb_m^{207} intensities were measured directly and the ratio calculated as follows:

$$Pb^{206}/Pb^{207} = \frac{I^{206}}{(15/5)I_m^{207}}.$$

The isotope ratios Pb^{208}/Pb^{207}, Pb^{206}/Pb^{207}, Pb^{204}/Pb^{207} were determined for normal lead and several enriched samples. The results in terms of per cent of the isotopes present are compared with the mass spectrometric values in Table 2.

With the exception of the Pb^{207} enriched sample, the results of Table 2 were based on measurements at relatively high intensity to which self-absorption corrections were applied. The Pb^{208}/Pb^{207} ratio for the Pb^{207} sample decreased about 10% for a tenfold increase in intensity. Evidently, when the Pb^{207} concentration becomes high enough so that the Pb_s^{207} line is stronger than Pb^{208} and becomes

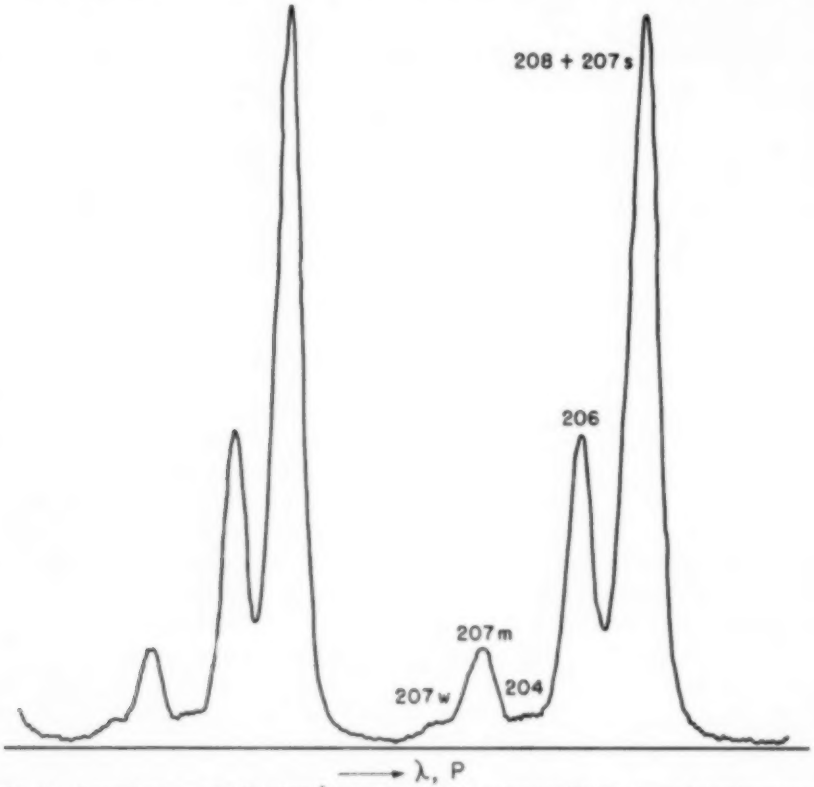

Fig. 10. Recorder trace of Pb-4058 Å for normal lead, using the Fabry-Perot interferometer with dielectric coated plates and 10-mm spacer. λ, P refer to the wavelength and pressure, respectively.

appreciably self-absorbed with increasing intensity, the change in the Pb_s^{207} line contour makes the correction to the combined Pb^{208}, Pb_s^{207} peak derived from Fig. 11 less accurate. Rather than attempting to evaluate the self-absorption of the Pb_s^{207} line at a point on the contour slightly removed from the peak, it appeared simpler to make measurements at somewhat lower intensity where the effect was minimized. This problem was not apparent in any of the other samples, because the Pb_s^{207} line was always appreciably weaker than Pb^{208} line and the self-absorption of Pb_s^{207} line was very small.

The precision of the results depended to a large degree upon the reproducibility of the Pb_m^{207} line. Any errors in the intensity measurements of this line were multiplied by 3 when the total Pb^{207} intensity was calculated. Furthermore, the

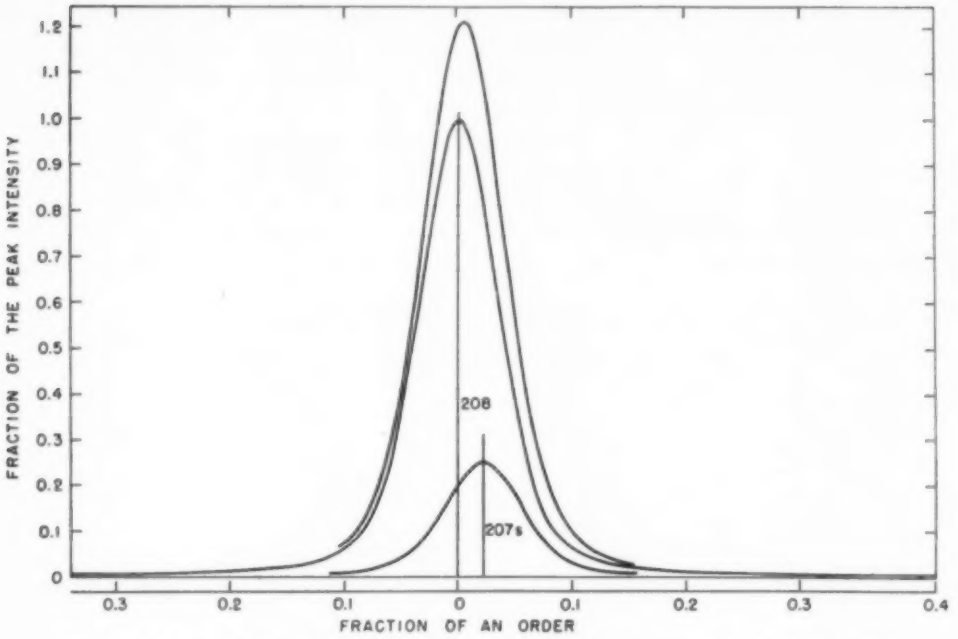

Fig. 11. Plot of Pb^{208} and Pb_s^{207}, using the Hg^{198}-4047-Å contour to give the "observed" contour. The plot shows that 78% of the Pb_s^{207} peak must be subtracted from the observed peak to give the Pb^{208} peak.

Table 2. Comparison of mass spectrometric and optical spectrographic results

Lead isotope assay

Sample	Method	Pb^{208} (%)	Pb^{206} (%)	Pb^{204} (%)	Pb^{207} (%)
Normal	Opt. spec.[a]	52·5	23·7	1·7	22·1
Normal	Mass. spec.[b]	53·2	22·6	1·54	22·6
Normal	Mass spec.[c]	52·3	24·8	1·4	21·5
Normal	Mass. spec.[d]	52·3	23·6	1·48	22·6
Enriched Pb^{206}	Opt. spec.	16·6	64·9	—	18·4
	Mass spec.[e]	16·55	64·93	0·172	18·35
Enriched Pb^{208}	Opt. spec.	87·0	2·94	—	10·1
	Mass. spec.[e]	87·97	1·99	0·069	9·97
Enriched Pb^{204}	Opt. spec.	24·5	34·2	26·0	15·1
	Mass. spec.[e]	26·2	33·8	25·7	14·3
Enriched Pb^{207}	Opt. spec.	30·6	7·76	—	61·6
	Mass. spec.[e]	31·09	7·73	—	61·06

[a] Optical spectroscopic values on Merck reagent PbO.

[b] Nominal values for normal lead from LANDOLT-BÖRNSTEIN, *Zahlenwerte und Funktionen*, 1 Band, 5 Teil, Atom Kerne, Springer-Verlag Pg. 60, 1952.

[c] Nominal values for normal lead by EHRENBURG as quoted by STEUDEL [7].

[d] Natural abundance accepted by K. T. BAINBRIDGE and A. O. NIER, *Relative Isotopic Abundances of the Elements, Prelim. Report No.* 9. Nuclear Science Series, National Research Council, Washington, D.C., 1950.

[e] Mass spectrometric values on the same sample supplied by Stable Isotope Research and Production Division, Oak Ridge National Laboratory, Oak Ridge, Tennessee.

errors in the measurement of Pb_m^{207} were reflected in the Pb^{208} intensity, due to the correction for the interference of Pb_s^{207}. Even so, the Pb^{208}/Pb^{207} ratio could be determined with the precision shown in Table 3 where the mean deviation of from four to eight successive measurements is given for the samples.

Systematic errors due to the evaluation of the background corrections become increasingly important with lower concentration, which probably explains the greater deviation from the mass spectrometric values at 1 or 2%. However, on the whole, the comparisons between mass spectrometric and optical results appear to be within experimental error.

Table 3. Precision of optical spectroscopic results

Sample	208/207[a]	206/207[a]	204/207[a]
Normal	2·37 ± 0·04	1·07 ± 0·02	0·077 ± 0·003
Enriched Pb^{206}	0·899 ± 0·03	3·52 ± 0·08	—
Enriched Pb^{208}	8·62 ± 0·08	0·292 ± 0·006	—
Enriched Pb^{204}	1·62 ± 0·04	2·26 ± 0·04	1·72 ± 0·03
Enriched Pb^{207}	0·497 ± 0·03	0·126 ± 0·001	—

[a] Uncertainty expressed as mean deviation of from four to eight consecutive traces.

The uranium isotope determinations with the Fabry-Perot interferometer involved a search for lines with small U^{235} hyperfine structure and sufficient intensity. The electrodeless discharge tube containing Ne and UCl_4 with an equal mixture of U^{235} and U^{238} was studied and gave very intense, sharp lines. Equal U^{235} and U^{238} peak heights were observed for U-4202·67 Å and U-4362·05 Å. The latter is shown in Fig. 5. However, the preparation of the tube was rather time-consuming and was eliminated from consideration as an analytical source except for occasional samples. The water-cooled iron hollow cathode tube containing a few milligrams of U_3O_8 with an equal mixture of U^{235} and U^{238} was then investigated. The two lines mentioned above were found unsuitable because of poor intensity and interferences. Equal U^{235} and U^{238} peak heights were observed for the U-4516·73-Å line, as shown in Fig. 12. However, insufficient intensity was obtained to determine ratios of 25 : 1 or greater. Uranium metal was used in the hollow cathode and gave a fivefold increase in intensity which would have considerably extended the usefulness of the method. Unfortunately, it was not expected that samples would be submitted in metallic form.

To demonstrate the analytical difficulties associated with the U^{235} hyperfine structure, tracings of U-4090·13 Å and U-4246·26 Å are shown in Figs. 13 and 14, respectively. Peak heights of these lines could not be used for analytical purposes without standardization with known mixtures or mass spectroscopically analysed standards. Determination of the area under line contours appeared to be excessively laborious.

The intensities of the discharge tube, metallic uranium in the hollow cathode, and uranium oxide in the hollow cathode were in the ratio of 50 : 5 : 1 respectively. The more intense sources were not investigated further, for reasons already cited.

VOL. 8 1956/5

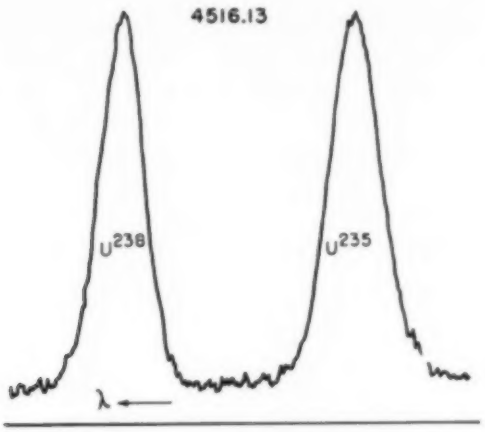

Fig. 12. Recorder trace of U-4516·73 Å in the hollow cathode tube, showing equal peak heights for equal U^{235}/U^{238} isotope ratio.

OL.
8
6/57

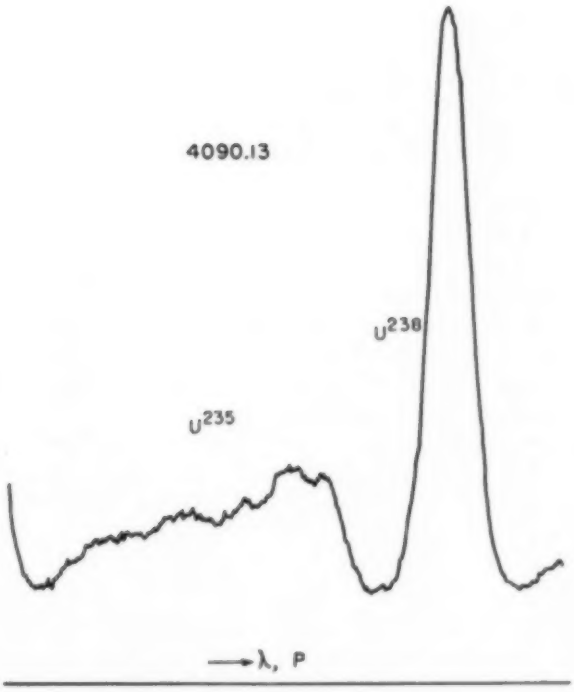

Fig. 13. Recorder trace of U-4090·13 Å in the hollow cathode, showing partially resolved U^{235} hyperfine structure in the Fabry-Perot pattern

Discussion

The procedure described for the lead isotope determination was completely independent of the mass spectroscopic method. In the plot of Fig. 11 used to determine the amount of interference of Pb_s^{207} with Pb^{208}, the mass spectroscopically determined concentrations for normal lead were used. However, similar plots for widely different Pb^{208}/Pb_s^{207} ratios also revealed the same 78%

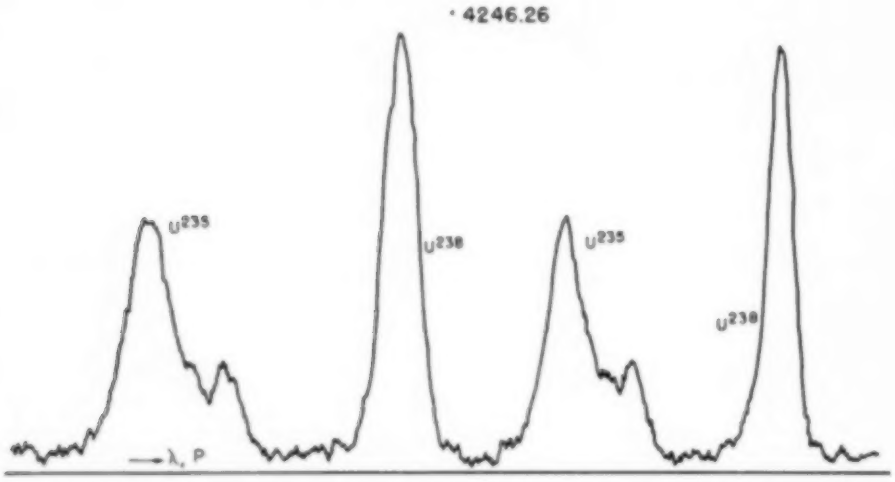

Fig. 14. Recorder trace of U-4246·26 Å in the hollow cathode showing partially resolved U^{235} hyperfine structure in the Fabry-Perot pattern.

correction, so that the mass spectroscopic values for normal lead were not essential. The correction was found to be independent of the Pb^{208}/Pb^{207} ratio in the absence of self-absorption.

The intensities of the components in the Pb-4058-Å pattern were quite different for normal lead and the enriched samples. The agreement between the optical and mass spectroscopic method shown in Table 2 indicates that the corrections of Table 1 for the Airy formula distribution were essentially correct and the corrections can be properly made in a complex pattern.

In isotope determinations where the shift may be resolved by either the interferometer or the grating in higher orders, the former method may be more favourable from the standpoint of intensity when the greater area of a hole may be utilized in place of an entrance slit. The interferometer uses the grating as a monochromator in a wavelength region of maximum intensity. If the grating intensity is appreciably reduced in higher orders and if narrow slits are required to resolve the isotope shift, less intensity may be realized, using the grating to resolve the lines directly. For example, the grating used in these experiments exhibited in higher orders 0·02 the maximum intensity which occurred in the first order. The loss of intensity in the interferometer may be more than compensated for by the larger spectrograph aperture and use of the grating in a region of maximum intensity.

The usefulness of the interferometer method appeared to be somewhat limited

for spectra similar to uranium because of intensity considerations and partially resolved hyperfine structure. The advantage of a hole in place of the entrance slit could not be realized in the region 4000 to 4600 Å because of the complexity of the uranium spectrum.

Conclusions

Some of the problems involved in extending the optical method of isotope assay by utilizing smaller isotope shifts were encountered in the preceding investigation. The increased resolving power required for the smaller isotope shift may also resolve to some degree any existing hyperfine structure. This problem may be overcome providing at least one hyperfine component is completely resolved and its relationship to the rest of the hyperfine pattern is known. These conditions were fulfilled in the case of the 4057·8-Å-lead line, and apparently the intensity ratios of the Pb^{207} hyperfine components did not deviate appreciably from the theoretical values.

The problem presented by the partially resolved U^{235} hyperfine structure was solved in the case of small uranium shifts by locating lines with negligibly small hyperfine structure. Lines with partially resolved hyperfine structure might be used with standardization with known isotopic mixtures.

Because of similarities between uranium and plutonium spectra, it was concluded that plutonium isotopes might be determined in a similar manner. However, because of intensity considerations using the hollow cathode source, ratios of 25 : 1 or greater would be difficult to determine.

Acknowledgement—The authors wish to express their appreciation to Dr. T. E. MANNING* for valuable discussions during the course of the investigation.

References

[1] BRODY J. K. *Argonne National Laboratory Report* 1949 *ANL*-4359, 94.
[2] BROIDA H. P. and MOYER J. W. *J. Opt. Soc. Amer.* 1952 **42** 37.
[3] BRODY J. K. 1949 unpublished data.
[4] BRODY J. K., FRED M., and TOMKINS F. S. *Spectrochim. Acta.* 1954 **6** 383.
[5] WERNER G. K., SMITH D. D., OVENSHINE S. J., RUDOLPH O. B., and MCNALLY J. R. JR. *J. Opt. Soc. Amer.* 1955 **45** 203.
[6] BRODY J. K. *J. Opt. Soc. Amer.* 1952 **42** 408.
[7] STEUDEL A. *Z. Phys.* 1952 **133** 438.
[8] ROSE J. L. and STRANATHAN R. K. *Phys. Rev.* 1936 **49** 916.
[9] SCHÜLER H. and GOLLNOW H. *Z. Phys.* 1935 **93** 611.
[10] MEISSNER K. W. private communication.
[11] JACQUINOT P. and DUFOUR C. *C.R.M.S. Journal des recherches* 1948 **61** 91.
[12] TOLANSKY S. *High Resolution Spectroscopy*, Methuen and Co., Ltd., London 1947 p. 155.
[13] KOPFERMANN H. *Z. Phys.* 1932 **75** 363.
[14] SCHÜLER H. and JONES E. G. *Z. Phys.* 1932 **75** 563.
[15] ROSE J. L. and GRANATH L. P. *Phys. Rev.* 1932 **40** 760.
[16] MANNING T. E., ANDERSON C. E., and WATSON W. W. *Phys. Rev.* 1950 **78** 417.
[17] MURAKAWA K. and SUWA S. *J. Phys. Soc. Japan* 1950 **5** 382.

* On leave from Department of Physics, Oberlin College, Oberlin, Ohio.

Spectrochimica Acta, 1957, Vol. 8, pp. 348 to 355. Pergamon Press Ltd., London

Steric effects in the electronic spectra of substituted benzophenones*

R. F. REKKER† and W. TH. NAUTA‡

(*Received* 10 *October* 1955)

Abstract—A previous study on the ultra-violet absorption of a series of symmetrically substituted benzophenones [1] has been extended to include methyl-substituted benzophenones in which the methyl groups are arranged in a non-symmetrical way. In addition, a small number of ethyl-, *i*-propyl-, and *t*-butyl-benzophenones were involved in this research. The steric effects due to *ortho* substitution could be derived from the U.V. absorption spectra and were mutually compared.

In a previous study we have investigated the ultra-violet absorption of a number of methyl-substituted benzophenones. The main features of this investigation have been summarized in Table 1.

Table 1§

	COMPOUND	C BAND	f	f_0	f/f_0	θ
1	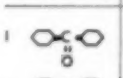	2530 (16000)	0·38	0·40	0·96	15°
2	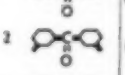	2580 (17000)	0·37	0·39	0·96	15°
3	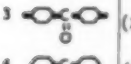	2650 (21000)	0·50	0·52	0·96	15°
4		2530 (13750)	0·30	0·52	0·58	53°
5	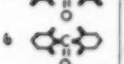	2550 (11950)	0·29	0·52	0·56	55°
6	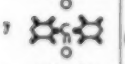	2615 (9400)	0·24	0·64	0·38	68°
7	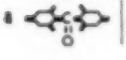	2700 (10400)	0·25	0·64	0·39	67°
8		2710 (12100)	0·30	0·76	0·39	67°

Explanation

The third column of Table 1 shows the oscillator strengths calculated from molecular extinctions and half-bandwidths. The fourth column shows the oscillator strengths which might be expected for these molecules when special *ortho* effects were absent, and *ortho*-methyl groups would give increases in oscillator strength similar to those of *para*-methyl groups.

* Paper presented at the Oxford meeting of the European Molecular Spectroscopy Group, 7–11 July 1955.

† Chemical Laboratory of the Free University, Amsterdam.

‡ Research Laboratories of the N.V. Koninklijke Pharmaceutische Fabrieken v/h Brocades-Stheeman & Pharmacia, Amsterdam

§ All data in this and other tables refer to alcoholic solutions.

VOL. 8 1956/5

The values of f_0 for benzophenone, 3,3′-dimethyl-benzophenone, and 4,4′-dimethyl-benzophenone were derived as follows:

In a benzophenone the two phenyl groups cannot be accommodated in the same

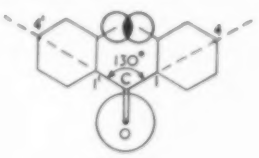

Fig. 1.

plane because of interference between the hydrogen atoms at the 2 and 2′ positions. JONES [2] assumed an angle of 130° between the 1-4 axes of the phenyl groups, and calculated a minimum angle between the planes of the benzene nuclei of about 30° (see Fig. 1). We have distributed this angle equally between the two halves of the

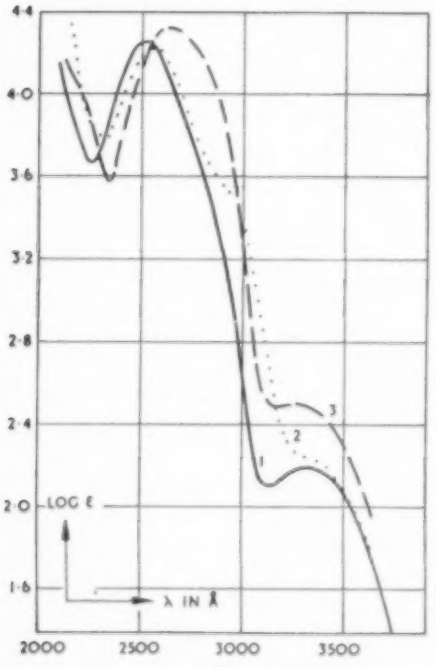

Fig. 2.
(1) Benzophenone.
(2) 3,3′-Dimethyl-benzophenone.
(3) 4,4′-Dimethyl-benzophenone. Solvent: ethanol.

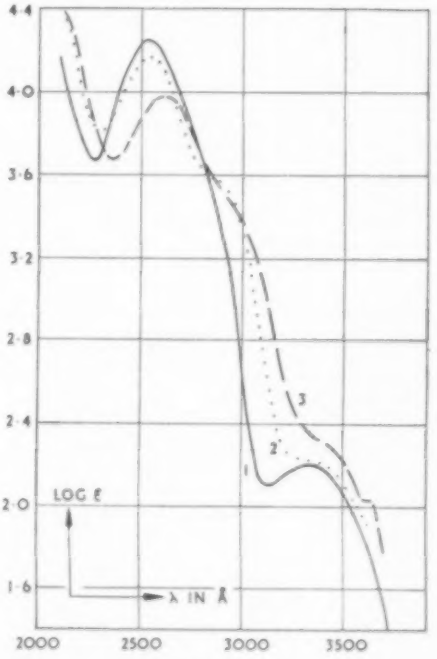

Fig. 3.
(1) Benzophenone.
(2) 2,2′-Dimethyl-benzophenone.
(3) 2,6,2′,6′-Tetramethyl-benzophenone. Solvent: ethanol.

molecule, assuming that both phenyl rings are completely symmetrical and are striving for a maximum of conjugation with the carbonyl group.

Using the cosine relationship between f/f_0 and the angle of twist θ, f_0 amounts to 0·40, 0·39, and 0·52 respectively. These values make the calculation of the

OL.
B
6/57

remaining f_0's possible; 2,2′-dimethyl-benzophenone equals 4,4′-dimethyl-benzophenone, just like 2,3,2′,3′-tetramethyl-benzophenone, as meta substitution is ineffective (compare benzophenone and 3,3′-dimethyl-benzophenone); f_0 for 2,6,2′,6′-tetramethyl-benzophenone amounts to 0·40 + 2 × difference 1 and 3 = 0·64 a.s.o.

Division of f by f_0 gives the remaining f/f_0 values from which the θ's were calculated.

Table 2

COMPOUND	f	f CALCULATED FROM SYMM. B.P'S.	f_0	f/f_0
	0·38		0·40	0·96
	0·37	0·37	0·39	0·95
	0·45	0·44	0·46	0·98
	0·35	0·34	0·46	0·76
	0·32	0·33	0·46	0·70
	0·30	0·31	0·52	0·58
	0·35	0·34	0·46	0·76
	0·27	0·27	0·58	0·47
	0·36	0·37	0·58	0·62
	0·44	0·44	0·46	0·96
	0·33	0·34	0·58	0·58
	0·31	0·30	0·64	0·48

In 2,2′-dimethyl-benzophenone the effective angle of twist amounts to 53° for each phenyl-carbonyl combination. This value agrees quite well with that found by other investigators [3] for 2-methyl-acetophenone: 55°. Substitution of two more methyl groups in *ortho* position gives a further increase of θ to 68°. This value is in good agreement with the θ value for 2,6-dimethyl-acetophenone: Braude found 71°. Additional *meta* or *para* substitution does not affect the steric relations in 2,6,2′,6′-tetra-methyl-benzophenone.

Table 2 shows the results of our spectral measurements with asymmetrically substituted methyl-benzophenones.

The values for the oscillator strengths obtained for asymmetrical methyl-benzophenones agree excellently with values calculated from symmetrically substituted benzophenones, as may be seen by comparing columns 2 and 3.

The values in column 3 were obtained by adding together half the amounts of f, found for the two symmetrical benzophenones, that can be derived from the two

component parts of each asymmetrical benzophenone. It is clearly shown that f is a purely additive factor for the compounds under investigation.

The f_0 values were calculated as before. The ratios f/f_0 give an idea of the total amount of steric inhibition of resonance, and they may be compared as such with the ratios f/f_0 given in Table 1. On the other hand, it is impossible to use them for the derivation of the angles of twist between phenyl and carbonyl groups.

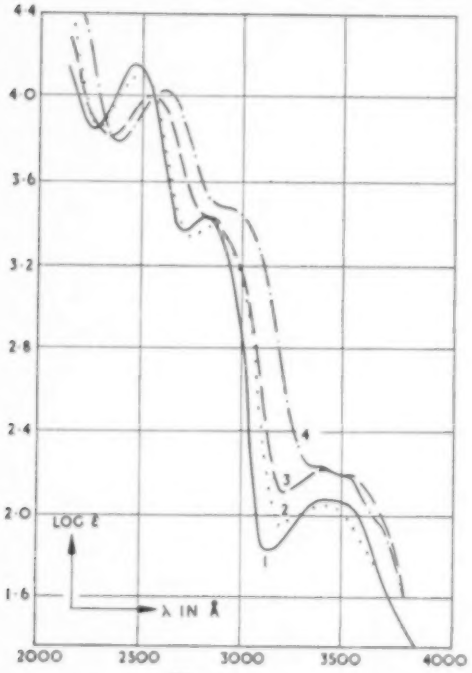

Fig. 4.
(1) 2,2′-Dimethyl-benzophenone.
(2) 2,3,2′,3′-Tetramethyl-benzophenone.
(3) 2,6,2′,6′-Tetramethyl-benzophenone.
(4) 2,3,5,6,2′,3′,5′,6′-Octamethyl-benzophenone.
Solvent: *iso*-octane.

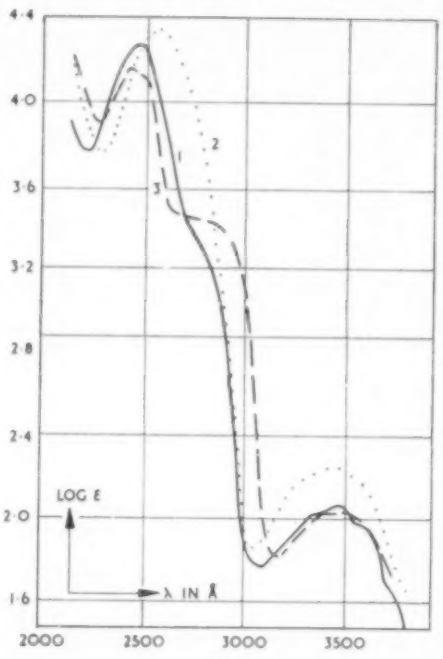

Fig. 5.
(1) Benzophenone.
(2) 4,4′-Dimethyl-benzophenone.
(3) 2,4,6,2′-Tetramethyl-benzophenone.
Solvent: *iso*-octane.

More detailed information about the steric relations in some typical asymmetrical benzophenones is given in Table 3.

Some of the main features are:

(a) The introduction of two *ortho*-methyl groups in one phenyl group of benzophenone (11, Table 3) causes a *decrease* in wavelength of 20 Å. This decrease can only be interpreted when we accept a strong increase of resonance between unsubstituted phenyl group and carbonyl at the cost of the *diortho*-substituted group (see Fig. 9): The molecule assumes, slightly, the character of acetophenone ($\lambda_c = 2420$, $\varepsilon = 13{,}000$). The introduction of two more methyl groups on *ortho* positions makes the molecule symmetrical again, and the phenyl positions become identical with respect to carbonyl; increase in λ: 105 Å.

Substitution of *para*-methyl in the unsubstituted phenyl group gives a λ-increase of 110 Å, being 40 Å larger than the effect of *para*-substitution in benzophenone, whereas substitution of *para*-methyl in the other phenyl group is ineffective (14, Table 3).

(b) The same reasoning can also be applied to 2,6,2′-trimethyl-benzophenone (compare 15, 16, 17). Comparison of (13 — 14) with (16 — 17) demonstrates the special character of the third methyl group in its ability to neutralize, to some extent, the strong tendency for coplanarity of an unsubstituted phenyl-CO system when it is partnered by a heavily *ortho*-substituted phenyl group (110 → 100; 0 → 10).

Table 3

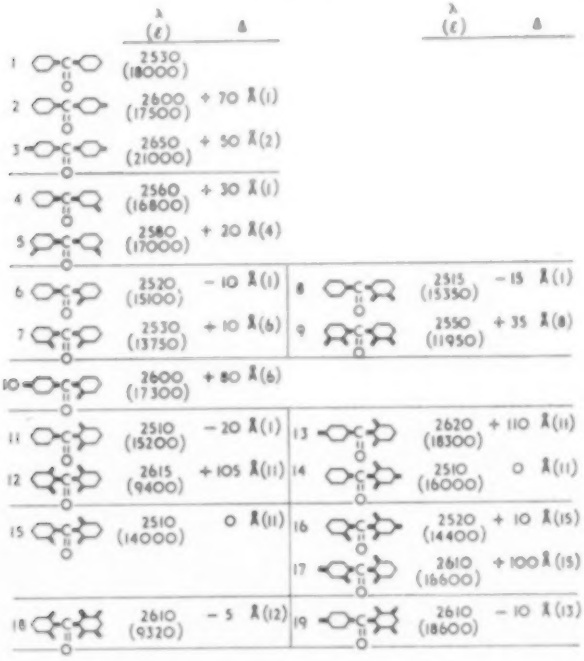

(c) While the introduction of *meta*-methyl groups in benzophenones results in an increase in wavelength (4 and 5), the introduction of *meta* groups in 2,6,2′,6′-tetramethyl-benzophenone is ineffective. As a matter of fact, a small decrease is observed. This strongly suggests a buttressing effect of the two *meta*-methyl groups, causing an increase in coplanarity of the system 2,6-dimethylphenyl-CO at the cost of a loss in coplanarity in the rest of the system.

A similar effect is observed in 2,3,5,6,4′-pentamethyl-benzophenone, where the introduction of two *meta*-methyl groups causes a decrease of 10 Å (compared with 13).

VOL. 8 1956/5

(d) One *ortho*-methyl group in benzophenone causes a hypsochromic shift of 10 Å, whereas a second *ortho*-methyl group, when symmetrically placed, causes an increase of 10 Å. The different behaviour of the two phenyl groups in 2-methyl-benzophenone finds proof in the observation that the introduction of a *para*-methyl group in the unsubstituted phenyl group gives a bathochromic shift of 80 Å. Compare benzophenone and 4-methyl-benzophenone: $\Delta = 70$ Å.

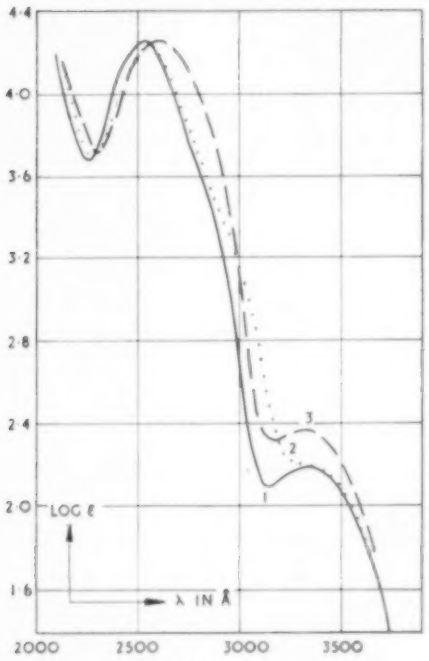

Fig. 6.
(1) Benzophenone.
(2) 3-Methyl-benzophenone.
(3) 4-Methyl-benzophenone. Solvent: ethanol.

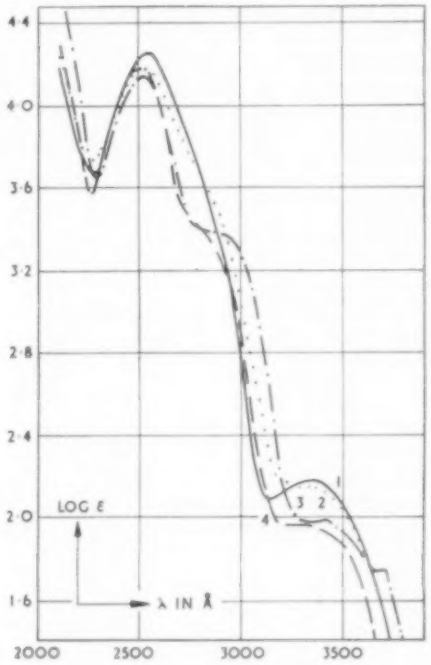

Fig. 7.
(1) Benzophenone.
(2) 2-Methyl-benzophenone.
(3) 2,6-Dimethyl-benzophenone.
(4) 2,6,2′-Trimethyl-benzophenone.
Solvent: ethanol.

(e) A buttressing effect seems also to be present in 2,3-dimethyl-benzophenone; compare 1 and 8: $\Delta = -15$ Å, 8 and 9: $\Delta = +35$ Å.

(f) We are inclined to accept for 4-methyl-benzophenone a decrease of coplanarity of the system ph-CO together with an increase of coplanarity for the combination 4-Me-ph-CO, the introduction of the first *para*-methyl in benzophenone being without effect on the molecular extinction, whereas the introduction of the second *para*-methyl gives a rather strong increase. Strong support for this idea is found in the fact that the introduction of an *ortho*-methyl group in 4-methyl-benzophenone (to give 10) only gives a slight decrease in extinction (compare 1 and 6: 18,000 → 15,000).

(g) The reasoning under (f) holds perhaps to a much lesser extent also for *meta* substitution (compare 4 and 5).

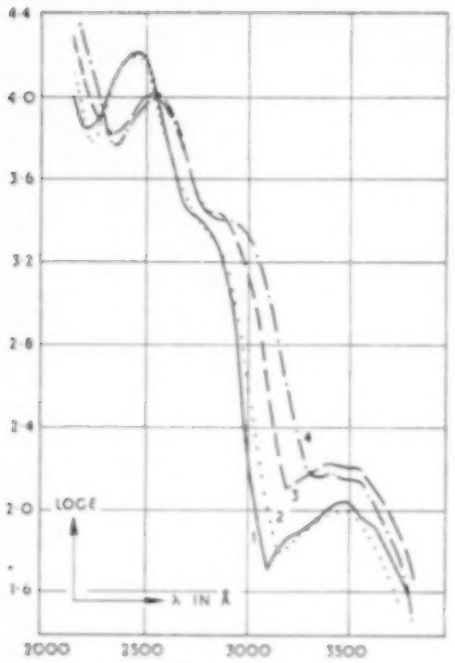

Fig. 8.
(1) 2-Methyl-benzophenone.
(2) 2,3-Dimethyl-benzophenone.
(3) 2,6,2′,6′-Tetramethyl-benzophenone.
(4) 2,3,5,6,2′,6′-Hexamethyl-benzophenone.
Solvent: iso-octane.

Table 4

	COMPOUND	C BAND	f	f_0	f/f_0
1		2530 (18000)	0·38	0·40	0·96
2	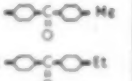	2650 (21000)	0·50	0·52	0·96
3	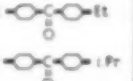	2660 (22000)	0·53	0·55	0·96
4	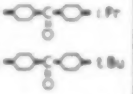	2640 (20700)	0·53	0·55	0·96
5	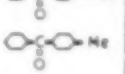	2660 (22600)	0·53	0·55	0·96
6	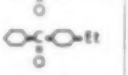	2600 (17500)	0·45	0·46	0·96
7	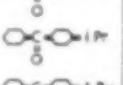	2590 (17000)	0·46	0·475	0·97
8	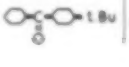	2600 (17200)	0·46	0·475	0·97
9		2590 (16900)	0·47	0·48	0·98

Table 5

	COMPOUND	C BAND	f	f_0	f/f_0	Θ
1		2520 (15100)	0·35	0·46	0·76	
2		2520 (15400)	0·34	0·475	0·72	
3		2510 (15200)	0·34	0·475	0·72	
4		2490 (14600)	0·30	0·475	0·64	
5		2510 (15200)	0·30	0·52	0·58	
6	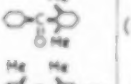	2710 (12100)	0·30	0·76	0·39	67°
7	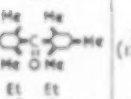	2660 (12000)	0·29	0·85	0·34	70°
8	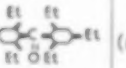	2640 (11700)	0·29	0·85	0·34	70°

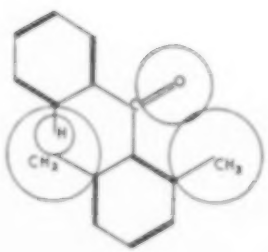

Fig. 9.

Table 4 gives an idea of the effects of *para* substitution by means of ethyl, *i*-propyl, *t*-butyl groups. The data are in good agreement with our findings for *para*-methyl substitution. Observe the ineffectiveness of all *mono-para* substitutions on the molecular extinction in connection with our remarks on 4-methyl-benzophenone. The introduction of a second *para*-alkyl group always gives a strong hyperchromic effect.

Some *ortho*-alkyl-substituted benzophenones are summarized in Table 5. *Ortho*-ethyl and *i*-propyl groups are found to have the ability to occupy such a position in the molecule that no additive steric effects are encountered when compared with *ortho*-methyl. The complexity of the *tert*-butyl group, however, shows an extra effect which is hypsochromic as well as hypochromic. This results in an oscillator strength equal to that found for 2,6-dimethyl-benzophenone, and an f/f_0 ratio which has markedly decreased with respect to the other *ortho*-substituted compounds. The symmetrically *hexa*-substituted derivatives with ethyl and *i*-propyl groups co-ordinate excellently with 2,4,6,2′,4′,6′-hexamethyl-benzophenone.

Conclusions

1. In benzophenone and in symmetrically substituted derivatives, both phenyl groups have the same degree of coplanarity with respect to C=O. Though in cases of *ortho* substitution there is an attempt to maintain this situation, a definite increase of coplanarity is observed between the least-hindered ring and carbonyl groups, whereas at the same time the coplanarity between the most-hindered ring and carbonyl decreases.

In a way *para* substitution can also change the coplanarity-relations between the parts of the molecule.

2. There is not much difference between the methyl, ethyl, and *i*-propyl groups in their respective abilities to give decreases in oscillator strength.

t-Butyl has an exceptional position. The complexity of this group is of such a character that it causes effects which are comparable with the effects of two *ortho*-methyl groups in one phenyl group of benzophenone.

Some of the absorption spectra are shown in Figs. 2, 3, 4, 5, 6, 7, and 8.

Acknowledgement—The authors wish to thank Miss J. Spierdijk for her great help in the spectral measurements.

References

[1] Rekker R. F. and Nauta W. Th. *Recueil Trav. chim. Pays-Bas.* 1954 **73** 969.
[2] Jones R. N. *J. Amer. Chem. Soc.* 1945 **67** 2127.
[3] Hedden G. D. and Brown W. G. *J. Amer. Chem. Soc.* 1953 **75** 3744; Braude E. A., Sondheimer F., and Forbes W. F. *Nature* 1954 **173** 117.

Spectrochimica Acta, 1957, Vol. 8, pp. 356 to 373. Pergamon Press Ltd., London

Contribution à la spectrométrie Raman—I
Construction d'un spectromètre enregistreur à grande dispersion

GILBERT MICHEL et GEORGES DUYCKAERTS
Service de Chimie Analytique, Université de Liège, Belgique

(*Received* 26 *May* 1956)

Abstract—The authors describe the photoelectric recording Raman spectrometer which they have built; it consists of the following parts:

(a) a light source of the Toronto-type helical mercury arc furnished by ARL.

(b) a monochromator, which is the result of the transformation of a three-prism Huet spectrograph (9 Å/mm), the scanning of the spectrum on a fixed exit slit, in front of the 1P21 photomultiplier tube is obtained by a plane mirror located between the camera lens and the focal plane.

(c) a tuned amplifier giving the maximum positive reaction for the chopping frequency of light (about 31 cycles/sec) and a Brown recorder.

The authors discuss the choice of optical and electronic parameters to obtain the following performances:

1. reproducibility of intensity measurements of about 2%.

2. a signal/noise ratio of about 500 : 1 is obtained for the 992-cm^{-1} Raman line, with a time constant of 4 seconds.

3. the resolution is excellent; the two lines 992 cm^{-1} of benzene and 1001 cm^{-1} of cyclohexane, are fairly well separated.

VOL.
8
1956/5

EN 1954, nous avons présenté, au Congrès de Chimie Industrielle tenu à Bruxelles, une note succinte sur quelques performances d'un spectromètre enregistreur pour l'effet Raman à grande dispersion [1].

Nous nous proposons de faire une description détaillée de cette installation.

Introduction

Dans une publication antérieure [2], nous avons montré combien la mesure des intensités des raies Raman était délicate. L'utilisation de la plaque photographique, malgré certains avantages, est incompatible avec le travail analytique de contrôle, surtout à cause de sa lenteur et de sa complexité.

La technique d'enregistrement de l'effet Raman a franchi un pas considérable lorsque RANK et ses collaborateurs [3] utilisèrent le multiplicateur d'électrons comme récepteur.

Depuis lors, un certain nombre de publications ont paru sur le sujet. Les pionniers, comme CHIEN et BENDER [4], SUSCHINSKII [5] décrivent des montages utilisant l'enregistrement galvanométrique sur papier photographique. Dans la suite, les chercheurs [6, 7, 8, 9] préfèrent la solution plus commode de l'enregistreur à plume précédé d'un amplificateur plus élaboré. En général, ils ont adopté des spectrographes très lumineux et peu dispersifs comme le montre le tableau 1.

Nous avions le choix entre deux spectrographes Huet, l'un du type BII, l'autre du type BIII.

Le premier a une dispersion réciproque de l'ordre de 110 cm^{-1}/mm vers 1000 cm^{-1} de nombre d'onde (4358 Å du Hg comme excitatrice); nous avons préféré le second, qui, bien que moins lumineux (f/11), a une dispersion nettement plus élevée de 45 cm^{-1}/mm.

DUPEYRAT [11] utilise dans son installation le même spectrographe.

Tableau 1

Auteurs	Ouverture	Dispersion réciproque (vers 1000 cm^{-1}	Eléments dispersants
BRANDMÜLLER *et alii* [7]	f: 3,7	155 cm^{-1}/mm	3 prismes
KINELL et TRAYNARD [8]	f: 11	150 cm^{-1}/mm	1 prisme
LUTHER *et alii* [9]	f: 3,7	155 cm^{-1}/mm	3 prismes
ROBERT [10]	f: 3,7	155 cm^{-1}/mm	3 prismes
STAMM [6]	f: 3,0	185 cm^{-1}/mm	réseau
SUSCHINSKII [5]		100 cm^{-1}/mm vers 4358 Å	prismes

Description de l'installation

La figure 1 représente le schéma de principe fort simplifié de l'installation complète.

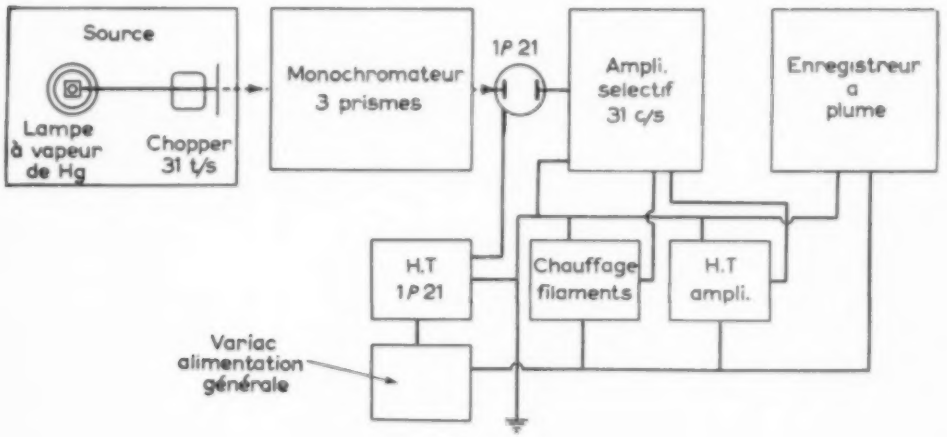

Fig. 1.

Le tube contenant la substance à étudier est disposé verticalement dans l'arc d'une lampe à vapeur de mercure de forme hélicoïdale, travaillant sous basse pression. La lumière diffusée est hachée à 31 cycles/seconde et focalisée sur la fente d'entrée du spectrographe Huet transformé en monochromateur.

Le faisceau dispersé par un train de 3 prismes fixes est focalisé sur la fente de sortie derrière laquelle est logé un multiplicateur d'électrons; le courant photoélectrique est amplifié sélectivement et alimente un potentiomètre à plume.

1. *Système optique*

A. *Source.* Elle est constituée par une lampe hélicoïdale à vapeur de mercure du type Toronto construite par la firme A.R.L. Elle est refroidie complètement par un courant d'air tandis qu'une circulation d'eau maintient une température d'électrode de l'ordre de 50°C. Dans ces conditions, elle est autostabilisée pour un courant de 15 A, pour autant que la tension d'alimentation soit constante.

La puissance est de 1500 watts et les caractéristiques spectrales sont excellentes: le fond continu est faible et le rapport d'intensités entre la raie 4358 Å et ses satellites est suffisamment élevé pour que l'on n'observe que les raies Raman correspondant à la 4358 Å.

La mesure précise des intensités de raies Raman exige évidemment une source de grande stabilité.

Nous avions constaté au début d'importantes fluctuations de l'intensité à caractère périodique et allant jusqu'à 9% pic à pic. Le refroidissement trop intense de certaines parties de la lampe était la cause des condensations de mercure dont la chute périodique provoquait des variations brusques de courant. Une modification apportée au refroidissement a permis de remédier à cet inconvénient.

B. *Tubes Raman et système de focalisation sur la fente d'entrée.* Les tubes Raman utilisés sont du type droit et de section circulaire; ils sont placés dans l'axe d'une jaquette verticale dont les 2 compartiments concentriques contiennent l'un une solution filtrante de nitrite ou de nitrite + éosine et l'autre l'eau qui assure la thermostatisation.

La lumière diffusée par le tube Raman est réfléchie à l'horizontale par un prisme à réflexion totale bleuté et envoyée dans le monochromateur au moyen d'une lentille condensatrice. Le choix de la position de cette dernière est fonction du tube Raman et de l'objectif collimateur du monochromateur. Pour ce faire, nous nous sommes inspirés des travaux de NIELSEN [11a], WELSH [12], repris par STAMM [13].

Nous avons considéré les variables suivantes:

D = diamètre de la colonne de liquide
l = longueur de la colonne de liquide
n = indice de réfraction du liquide
F = focale de la lentille condensatrice
f_1 = focale du collimateur
H_1 = hauteur utile du collimateur (= diamètre si le collimateur est complètement utilisé)

Les tubes que nous utilisons ont une contenance approximative de 14 ml, une longueur $l = 170$ mm et un diamètre intérieur $D = 10$ mm; la fente d'entrée du spectromètre a une hauteur de 10 mm, le collimateur a une focale de 1594 mm et un diamètre de 112 mm.

En supposant que le liquide le moins réfrigérant que nous étudierons aura un indice de réfraction égal à 1,3, nous calculons que:

$F = 156$ mm
$l = 185$ mm (longueur maximum couverte par l'optique).

Ce calcul montre que le tube de 170 mm sera complètement utilisé.

VOL. 8 1956/5

C. *Le monochromateur.* Comme nous l'avons déjà signalé, nous utilisons un spectrographe Huet BIII à 3 prismes en flint dense de 59,3 degrés d'angle réfringent; les longueurs des faces sont respectivement 146, 154, et 170 mm.

L'objectif collimateur est du type achromatique à deux éléments; il possède une distance focale de 1594 mm et une ouverture libre de 112 mm.

L'objectif de chambre, non achromatique, est d'un type spécial à 3 lentilles séparées dont les ouvertures sont respectivement 130, 116 et 120 mm de diamètre données dans l'ordre de la lumière incidente; sa distance focale moyenne est de 986 mm pour la longueur d'onde de 4341 Å.

La dispersion du spectrographe vaut:

λ	Dispersion réciproque.
4500 Å	9,4 Å/mm, soit 45 cm^{-1}/mm
4700 Å	11,2 Å/mm, soit 50 cm^{-1}/mm
5000 Å	14,6 Å/mm, soit 58 cm^{-1}/mm

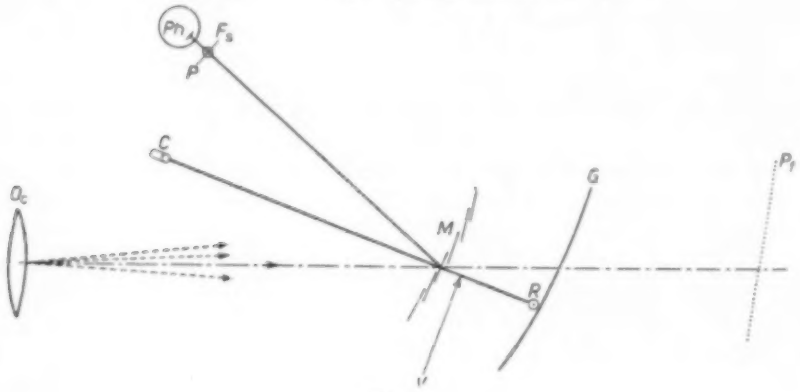

Fig. 2.

La transformation du spectrographe en spectromètre pouvait se faire de deux façons, soit en balayant le plan focal au moyen d'une fente mobile, soit en faisant défiler le spectre sur une fente fixe au moyen d'un miroir plan disposé entre l'objectif de chambre et le plan focal.

Nous avons adopté cette dernière solution afin d'éviter de longs déplacements du multiplicateur d'électrons qui risquent par torsions des cables de connexions, d'engendrer un bruit de fond non négligeable aux fortes amplifications; nous voulions aussi nous mettre à l'abri du bruit de fond microphonique provoqué par le mouvement de l'ensemble sur la vis micrométrique.

La figure 2 donne le schéma de principe du mécanisme de balayage du spectre.

Le changement de distance focale d'une optique en verre avec la longueur d'onde requiert, pour la focalisation de la lumière sur une fente fixe, un miroir animé d'un mouvement de rotation combiné à une translation. Ce mouvement composé est obtenu par la rotation du miroir (M) autour du pseudo-centre C; la longueur du bras de levier de rotation du miroir est variable et commandée par le roulement du galet (R) assujetti au miroir (M), le long d'une came (G) de profil calculé à partir des données optiques du spectrographe. Le miroir (M) est monté

sur un équipage à roulements à billes à semelles cylindriques de façon à réduire au minimum les frottements et les vibrations.

La fente de sortie (F_s) et le multiplicateur d'électrons (Ph) sont disposés sur une plateforme pouvant pivoter autour du point (P); un bras de levier relié au miroir maintient constamment la fente perpendiculaire à l'axe optique.*

Le multiplicateur d'électrons est logé dans le boitier situé derrière la fente de sortie.

Le défilé du spectre devant la fente de sortie est obtenu par une vis micrométrique (V) agissant sur l'équipage mobile du miroir; elle est actionnée par un moteur avec changement de vitesse à pignons hélicoïdaux.

L'élément réflecteur (M) est un miroir plan en Pyrex de 140 mm de diamètre et d'une épaisseur de 20 mm; il est taillé au quart d'onde et aluminisé; il peut être enlevé de manière à permettre l'enregistrement des spectres sur plaque photographique.

Le monochromateur ainsi conçu garde les caractéristiques du spectrographe; seul le facteur de transmission T est légèrement diminué par l'introduction d'un miroir d'aluminium (réflectivité = 0,90).

Nous pouvons en calculer la "figure de mérite" (voir relation (11) de la note) en adoptant pour les différents termes qui interviennent, les hypothèses proposées par STAMM [13]

La transmission d'un interface air/verre est, sous incidence normale, égale à 0,96, si le verre n'est pas bleuté et 0,99 si le verre est bleuté; la transmission de n interfaces air/verre (prisme dont l'incidence est proche de 56°) peut être calculée au moyen de la relation $(1 + 0{,}82^n)/2$ pour des surfaces non bleutées et $(1 + 0{,}92^n)/2$ pour des surfaces bleutées; quant à l'absorption des prismes, elle est supposée être de 3,6% par cm de matériau traversé pour la radiation de 4500 Å de longueur d'onde; l'absorption des lentilles est jugée négligeable.

Dans ces conditions,

$$\mathscr{L} = T \cdot S \cdot \frac{h_1}{f_1} \cdot \frac{d\theta}{d\lambda} = 2{,}1 \times 10^{-5} \qquad (5)$$

formule dans laquelle le facteur de transmission T du spectromètre est égal à: $0{,}90 \times (0{,}96)^2 \times (1 + 0{,}83)/2 \times 0{,}42 = 0{,}27$; la surface S de l'ouverture utile de l'optique est égale dans notre cas à la surface du collimateur diminuée de 10% environ, soit $(11{,}2)^2/4 \,.\, - 10\% = 98{,}5 \text{ cm}^2 - 9{,}85 \text{ cm}^2 \simeq 89 \text{ cm}^2$; le rapport $\frac{h_1}{f_1} = \frac{1{,}0}{159{,}4} = 0{,}063$ et la dispersion angulaire $\frac{d\theta}{d\lambda} = 1{,}38 \cdot 10^{-4}$ radian/Å.

La valeur de $\mathscr{L}$ ainsi obtenue est comparée dans le tableau 2 à celle que nous avons calculée pour le spectromètre monté par BUSING† ainsi que à celle des installations réalisées par plusieurs auteurs dont la plupart sont cités par STAMM.

* La réalisation de ce dispositif mécanique a pu être menée à bien grâce aux conseils éclairés de Monsieur MOSSOUX, Ingénieur en chef de la Fabrique Nationale d'armes de Herstal; nous nous plaisons à le remercier chaleureusement, ainsi que ses adjointe Mrs. VAN DE VOORT et COLLAS.

† Communication privée.

Note sur la "figure de mérite" d'un spectromètre à prismes

Le flux lumineux utile Φ_1 passant au travers de la lentille collimatrice est donné par la relation

$$\Phi_1 = B_\lambda \cdot w_1 \cdot h_1 \cdot \frac{W_1 \cdot H_1}{f_1^2} \tag{6}$$

où B_λ est la brillance de la fente d'entrée; la signification des autres symboles est indiquée sur la figure 3.

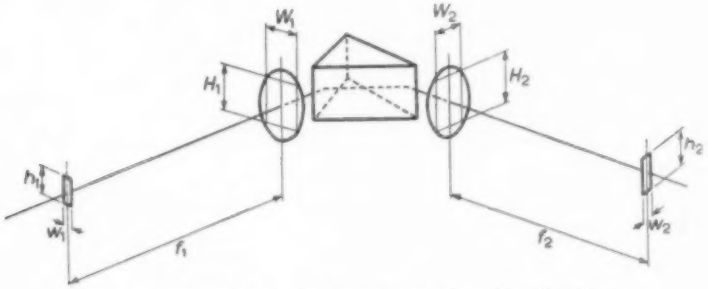

Fig. 3. Schéma de principe d'un monochromateur à prisme:
h_1, h_2 hauteur des fentes d'entrée et de sortie
w_1, w_2 largeur des fentes d'entrée et de sortie
f_1, f_2 distances focales des objectifs collimateur et de chambre.
H_1, W_1 hauteur et largeur efficace de l'objectif collimateur.
H_2, W_2 hauteur et largeur efficace de l'objectif de chambre.

Le produit $W_1 \cdot H_1 = S$ représente la surface de l'ouverture utile du système optique.

L'énergie lumineuse arrivant sur la photocathode du multiplicateur d'électrons est proportionnelle à T, le facteur de transmission du système optique, et à la largeur de fente spectrale $\Delta\lambda$:

$$\Phi_2 = B_\lambda \cdot T \cdot w_1 \cdot h_1 \cdot \frac{S}{f_1^2} \cdot \Delta\lambda \tag{7}$$

Si la largeur de la fente d'entrée, w_1, est choisie, celle de la fente sortie, w_2, est fixée par la relation

$$\frac{w_1}{w_2} = \frac{f_1}{f_2} \tag{8}$$

et sa largeur exprimée en fente spectrale s'écrira:

$$w_2 = f_2 \cdot \frac{d\theta}{d\lambda} \cdot \Delta\lambda. \tag{9}$$

où $(d\theta/d\lambda)$ est la dispersion exprimée en radians/Å.

L'introduction des relations (8) et (9) dans l'expression (7) nous donne:

$$\Phi_2 = B_\lambda \cdot T \cdot S \cdot \frac{h_1}{f_1} \cdot \frac{d\theta}{d\lambda} \cdot (\Delta\lambda)^2 \text{ watt} \tag{10};$$

or la brillance B_λ de la fente d'entrée dépend du coefficient de diffusion k_λ de la substance, de la longueur l du tube qui contient la substance et l'efficience I_s du système d'illumination de l'échantillon, nous pouvons prendre la relation (10) sous sa forme la plus explicite:

$$\Phi_2 = k_\lambda \cdot l \cdot I_s \cdot T \cdot S \cdot \frac{h_1}{f_1} \cdot \frac{d\theta}{d\lambda} \cdot (\Delta\lambda)^2 \tag{11}$$

où apparaît nettement l'origine des différents termes.

Ainsi le terme $k_\lambda \cdot l$ caractérise l'échantillon diffusant, I_s la source lumineuse excitatrice,

$$\mathscr{L} = T \cdot S \cdot \frac{h_1}{f_1} \frac{d\theta}{d\lambda}$$

les constantes du spectromètre, et est appelée "figure de mérite" et finalement $(\Delta\lambda)^2$ est le terme qui dépend de la fente spectrale choisie.

$\mathscr{L}$ mesure l'efficacité lumineuse d'un spectromètre, tout comme la luminosité caractérise un spectrographe à plaque photographique; dans le dernier cas, L est égal à

$$L = \frac{\text{éclairement}}{w_2 \cdot h_2} = \frac{\Phi_2}{B_\lambda \cdot w_2 \cdot h_2} = \frac{T \cdot S \cdot}{f_2^2} \cdot \Delta\lambda \cdot \qquad (12)$$

Tableau 2

Auteurs	S (cm²)	h_1 (cm)	f_1 (cm)	h_1/f_1	(rad/Å) $\frac{d\theta}{d\lambda} \times 10^4$	T	$\mathscr{L} \times 10^5$
1. BUSING*	69,0	0,7	60,0	0,0117	1,0	0,27	2,18
2. STAMM [13]	44,2	1,0	27,0	0,037	1,26	0,40	8,2
3. HILGER	58,1	0,6	58,4	0,0103	2,4	0,3	4,3
4. HEIGL [14]	28,3	2,2	66,0	0,033	0,65	0,65	4,0
5. SUSCHINSKII [5]	17,6	0,44	12,0	0,037	1,6	0,30	3,2
6. RANK [3]	146,7	1,0	240	0,0042	1,26	0,36	2,8
7. STAMM [6]	137,1	0,6	100	0,006	0,629	0,44	2,3
8. A. R. L.†	49,0	0,53	92,0	0,0058	1,6	0,24	1,2
9. MICHEL-DUYCKAERTS	89,0	1,0	159,4	0,0063	1,38	0,27	2,1

* Communication privée.

† L'un de nous (G. MICHEL) a eu l'occasion d'utiliser cette installation à l'Université de Bologne chez le professeur G. B. BONINO; nous profitons de cette occasion, pour l'en remercier bien chaleureusement, ainsi que son chef de laboratoire le Dr. P. CHIORBOLI.

La valeur de h_1 du tableau 2 se rapporte à l'utilisation d'un tube de 4,5 ml; pour des volumes de 10 ml, h_1 était égal à 0,8 cm, ce qui portait $\mathscr{L}$ à $1{,}8 \times 10^{-5}$; pour des tubes de 21 ml, nous avions $h_1 = 1{,}6$ et $\mathscr{L} = 3{,}6 \times 10^{-5}$.

Nous voyons que bien peu d'appareils peuvent réellement être considérés comme de bons "spectromètre Raman"; seuls les n° 2, 3, 4, 5 pourraient répondre aux conditions, encore que le n° 4 ait une dispersion angulaire bien faible. Dans la plupart des cas, le rapport (h_1/f_1) devrait être amélioré ce qui ne pourrait se faire pour un système d'illumination classique de la fente qu'en adoptant des volumes d'échantillons prohibitifs.

Ainsi, dans notre cas, le bleutage de l'optique du spectrographe-prismes et lentilles—ferait gagner environ 18% au facteur de transmission T:

$$T \text{ (non bleuté)} = 0{,}27\,\mathscr{L} = 2{,}1 \times 10^{-5}$$
$$T \text{ (bleuté)} \quad = 0{,}33\,\mathscr{L} = 2{,}56 \times 10^{-5}$$

seul l'emploi d'un "slicer" permettrait un gain d'énergie plus important; ce système a été préconisé par STRONG et BENESCH [15] et par J. U. WHITE [16].

2. *Système électronique*

L'emploi de multiplicateurs d'électrons nous impose le respect de certaines conditions de travail et par là même le choix de l'amplificateur. Celui-ci doit

VOL. 8 1956/5

nécessairement être construit de telle sorte qu'il élimine le plus possible les bruits de fond dont les plus gênants sont engendrés par le multiplicateur d'électrons lui-même.

A. *Le multiplicateur d'électrons et son stabilisateur*

Les caractéristiques moyennes du multiplicateur d'électrons 1P21 RCA sont bien connues, elles ont été définies par ENGSTRÖM [17]. Cependant, elles peuvent varier fortement d'un multiplicateur à l'autre.

Le meilleur phototube dont nous disposions donnait un courant noir ($I_{\text{D.C.}}$) de $2{,}7 \times 10^{-9}$ A pour un voltage entre dynodes (E) égal à 100 volts.

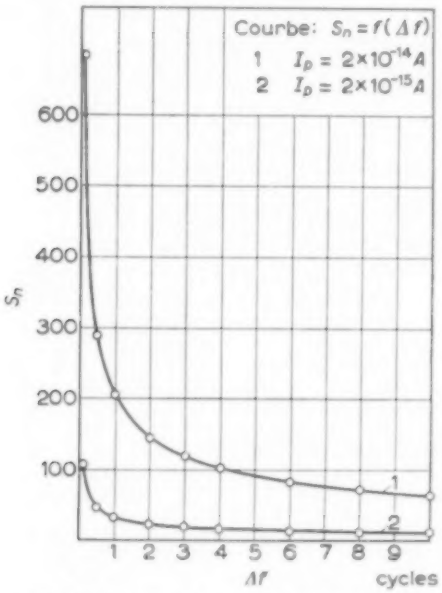

Fig. 4. Rapport signal-bruit de fond en fonction de la largeur de la bande passante.

Nous avons recherché les conditions optima d'utilisation en déterminant I_p, le courant de sortie du phototube, $I_{\text{D.C.}}$, son courant noir, et $I_p/I_{\text{D.C.}}$ leur rapport en fonction de E. Le meilleur phototube dont nous disposions donnait un courant noir de $2{,}7 \cdot 10^{-9}$ A pour un voltage entre dynodes égal a 100 volts. A l'encontre des résultats obtenus par DIEKE [18] pour de nombreux phototubes, nous avons constaté que le multiplicateur selectionné par nous présentait ses meilleures performances pour une tension de 100 volts entre dynodes. Ainsi alimenté le 1P21 RCA fournit avec des flux lumineux de 10^{-14} lumen qu'on observe en Raman, un courant au niveau de la cathode $i_p = 2 \cdot 10^{-14}$ A à peine plus élevé que le courant d'émission thermionique i_t ($\sim 10^{-14}$ A). La valeur quadratique moyenne de fluctuations du courant anodique I engendrée par cette émission thermionique et par l'effet "shot" des photoélectrons est représentée assez exactement par la relation suivante:

$$[(\bar{I})_f^2]^{\frac{1}{2}} = \mu \cdot [2e \cdot \Delta f \cdot (i_t + i_p)]^{\frac{1}{2}} \tag{13}$$

où e est la charge de l'électron, Δf la bande passante de l'amplificateur et μ le gain du phototube ($\sim 2 \cdot 10^6$).

Dans ces conditions, le rapport signal/bruit de fond S_n en fonction de Δf est donné par la formule suivante:

$$S_n = \frac{1}{[2e \cdot \Delta f]^{\frac{1}{2}}} \cdot \frac{i_p}{[i_t + i_p]^{\frac{1}{2}}} \tag{14}$$

La courbe $S_n = f(\Delta f)$ de la figure 4 nous a incité à construire un amplificateur très sélectif (Δf de 1 à 4 cycles au maximum) qui permet d'éliminer la réfrigération du phototube.

L'alimentation du phototube accuse une variation de 0,02% lorsque le secteur passe de 95 à 115 volts; sa composante alternative est à peine de 1 mV (mesurée à l'oscillographe) pour une tension de 100 volts entre dynodes.

B. *L'amplificateur et ses stabilisateurs*

Nous avons construit un amplificateur à couplage résistance-capacité à bande passante étroite réglable tant en fréquence (24 à 35 cycles/seconde), qu'en largeur de la bande passante (1 à 8 cycles/seconde).

Il comprend les 3 parties suivantes: les 4 étages d'amplifications proprement dits, un étage de couplage en "cathode follower" et la détection.

(a) *les étages d'amplifications.* Les tubes 5693 RCA des premier, second et quatrième étages ont été choisis pour leur faible bruit de fond et leur faible microphonisme.

Le troisième étage, le plus important, est l'étage sélectif basé sur un système dont la contre-réaction variable positive est maximum pour la fréquence d'accord ($\sim$31 cycles/seconde).

La largeur de la bande passante est réglée commodément par le potentiomètre P_2 (Fig. 5) qui impose le taux de contre-réaction. La position de la bande passante est ajustée par la valeur de P_1 et P_1' qui sont accouplés sur le même axe, elle peut être ainsi accordée à la fréquence de hachage du faisceau lumineux entrant dans le spectromètre.

La proportionnalité de ces 4 étages est excellente pour toute la zone d'utilisation.

(b) *l'étage de couplage.* Il est monté en "cathode follower," il élimine les écarts importants à la linéarité qui prennent naissance par couplage des étages d'amplification et de détection.

(c) *la détection et l'amplification de puissance.* La détection de l'alternance négative du courant modulé est réalisé par un tube 6H6 de telle sorte que le potentiel de grille de la 6C5 de l'amplificateur de puissance soit constamment négatif.

Le réglage du zéro de l'appareil se fait au moyen du potentiometre P_0, le gain est réglé au moyen des sélecteurs à résistances S_1 et S_2, tandis que le sélecteur à capacités S_3 impose au système une constante de temps de 1,5, 4, 6,5 ou 10,5 secondes.

La proportionnalité signal-réponse est très satisfaisante. Pour une bande passante de 1,5 cycles/seconde de large réglée à la fréquence 31 cycles/seconde, le

VOL. 8 1956/5

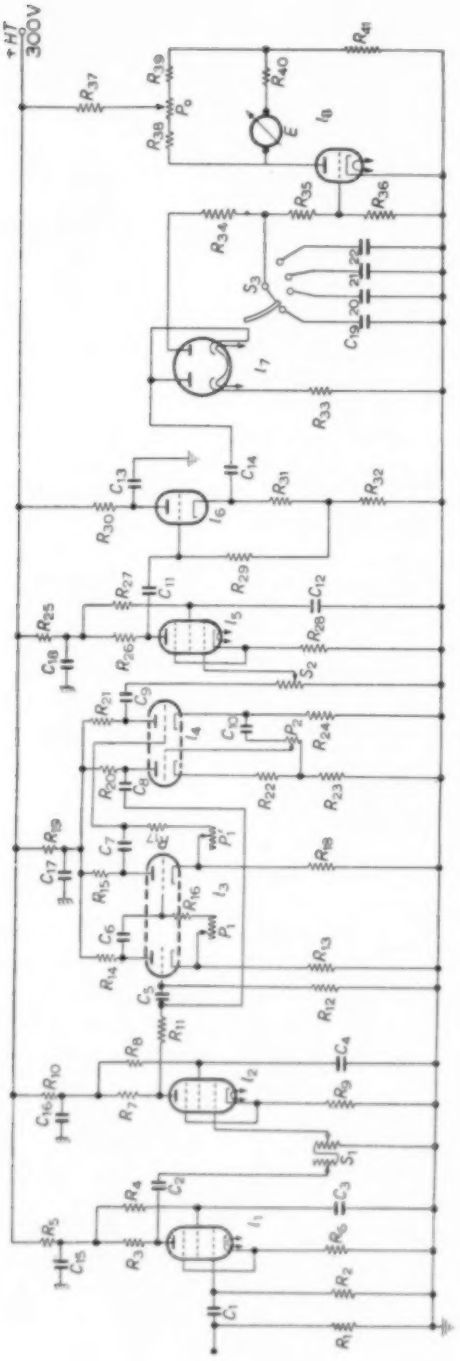

Fig 5. Amplificateur.

l_1, l_2, l_5 = 5693; l_3, l_4 = 12 A × 7; l_6, l_8 = 6C5; l_7 = 6H6; R_1 = 1 MΩ; R_2 = 2,9 MΩ; R_3 = 0,2 MΩ; R_4 = 1,R MΩ; R_5 = 91 kΩ; R_6 = 2 kΩ; R_7 = 0,21 MΩ; R_8 = 1 MΩ; R_9 = 2 kΩ; R_{10} = 22 kΩ; R_{11} = 0,3 MΩ; R_{12} = 1 MΩ; R_{13}, R_{14}, R_{21} = 1,8 kΩ; R_{15}, R_{23} = 3,9 kΩ; R_{16}, R_{17} = 50 kΩ; R_{19} = 35 kΩ; R_{20}, R_{31} = 22 kΩ; R_{24} = 5,6 kΩ; R_{25} = 27 kΩ; R_{26} = 0,22 MΩ; R_{27} = 1 MΩ; R_{28} = 1,3 kΩ; R_{29} = 1,2 MΩ; R_{30} = 22 kΩ; R_{31} = 250 Ω; R_{32} = 3 kΩ; R_{33} = 50 kΩ; R_{34} = 0,22 MΩ; R_{35} = 0,27 MΩ; R_{36} = 50 kΩ; R_{37} = 5 kΩ; R_{38}, R_{39} = 7,5 kΩ; R_{40} = 2,5 kΩ; R_{41} = 10 kΩ; P_1, P_1' = 50 kΩ (montés en tandem); P_2 = 0,5 MΩ; P_3 = 5 kΩ (hélipot); S_1 et S_2 sélecteurs à résistances; C_1 = 0,25 μF; C_2 = 1 μF; C_3 = 0,1 μF; C_4 = 0,5 μF; C_5 = 0,05 μF; C_6, C_7, C_8 = 0,1 μF; C_9 = 1 μF; C_{10} = 0,1 μF; C_{11}, C_{12} = 0,5 μF; C_{13} = 12 μF; C_{14} = 0,5 μF; C_{15}, C_{16}, C_{17}, C_{18} = 12 μF; C_{19} = 25 μF; C_{20} = 4,0 μF; C_{21} = 8 μF; C_{22} = 6 μF;
S_3 = sélecteur; E = enregistreur potentiométrique Brown (10 mV d'échelle).

bruit de fond (effet Johnson) au niveau de la grille d'entrée est inférieur au microvolt, la stabilité du zéro est remarquable et la dérive est de l'ordre de 1% par heure.

La tension anodique de l'amplificateur est de 300 volts et sa variation est de moins de 0,09 volt pour des fluctuations de secteur de 10 pourcent.

3. *Performances de l'installation*

A. *Détermination des fréquences Raman*

La détermination des nombres d'ondes des raies Raman se fait au moyen de la courbe de dispersion du monochromateur; celle-ci a été tracée au moyen des spectres d'une série de substances dont les nombres d'ondes des raies ont été déterminés par voie photographique sur le même appareil. A cet effet, nous avions photographié et agrandi 14 fois les spectres des substances suivantes dont nous avons pu déterminer par comparaison avec un arc au fer les nombres d'ondes de raies Raman avec une précision de l'ordre du cm^{-1}: benzoate d'éthyle, salicylate d'éthyle, fumarate d'éthyle et phthalate d'éthyle (voir Fig. 6).

Nous avons éprouvé la courbe de dispersion ainsi obtenue en calculant les fréquences Raman de substances bien connues, comme le tétrachlorure de carbone, le benzène, le toluène et le bromo-benzène dont nous avons fait des enregistrements photoélectriques (Fig. 6) et en les comparant aux fréquences trouvées dans le livre de KOHLRAUSCH: *Ramanspektren* (1943); l'accord est excellent.

Il est bon de noter que certaines substances avaient été distillées 6 mois plus tôt et que nous nous sommes contentés de les transvaser telles quelles dans les tubes Raman, ce sont le bromo-benzène, le benzoate d'éthyle, le salicylate d'éthyle, l'o-phthalate d'éthyle; le fond continu de ces spectres a augmenté mais est encore très acceptable.

VOL.
8
1956/5

B. *Pouvoir de résolution de l'installation*

Le pouvoir de résolution d'une telle installation dépend de plusieurs facteurs; en effet, si les caractéristiques et la qualité de l'optique fixent la limite de résolution, celle-ci ne sera jamais atteinte pour des raisons que nous allons développer.

En principe, un choix de fentes d'entrée et de sortie aussi fines que possible nous fera approcher cette résolution-limite, seulement à l'encontre de l'enregistrement photographique, nous nous trouvons rapidement à court de flux lumineux.

Lorsque le signal du multiplicateur devient trop faible, c'est à dire de l'ordre de grandeur du courant noir ($\sim 10^{-8}$ A), les oscillations de l'enregistrement deviennent tellement fortes qu'il est nécessaire d'avoir recours à une constante de temps importante pour rendre le spectrogramme utilisable, or, comme nous le verrons plus loin, l'emploi de constante élevée diminue la résolution.

(a) *Fente spectrale.* Nous avons fait une série d'enregistrements (voir Fig. 7) d'un groupe de deux raies rapprochées, la 992 cm^{-1} du benzène et la 1001 cm^{-1} du toluène, en opérant sur un mélange 40% benzène-60% toluène (% molaire).

La diminution du pouvoir de résolution avec une augmentation de la largeur spectrale de la fente est nette et nous remarquons que pour les conditions expérimentales choisies, la résolution de ce "doublet" est cependant encore satisfaisante pour une fente de largeur spectrale de 6 cm^{-1}; nous ferons aussi remarquer que pour cette valeur de la largeur spectrale, le rapport d'intensité des deux raies I_B^{992}/I_T^{1001}

ne s'écarte que de 2% à peine de la valeur moyenne de 1,46 obtenue pour la fente de 3 cm^{-1}.

Largeur spectrale de la fente	3 cm^{-1}	4,5 cm^{-1}	6 cm^{-1}	8 cm^{-1}	10 cm^{-1}
. I_B^{992}/I_T^{1001}	1,46	1,46	1,43	1,41	1,40

(*b*) *Vitesse de balayage et constante de temps.* Ces deux facteurs ont une importance énorme et leur choix est à déterminer en fonction de la largeur de la fente spectrale. Le temps de réponse de l'enregistreur Brown étant de l'ordre de 2 secondes pour l'échelle totale, c'est la constante de temps de l'amplificateur qui joue le rôle principal.

La valeur instantanée de la tension E prise aux bornes d'un élément de circuit résistance-capacité varie suivant une fonction exponentielle représentée par l'équation (15).

$$E = E_{\max} \cdot [1 - e]^{-(t/RC)} \tag{15}$$

où t est le temps compté en secondes.

le produit $R\ (\Omega) \times C\ (F)$ est appelé constante de temps.

Après un intervalle de temps t égal à $R.C.$ et compté à partir de l'application de la tension maximum E_{max}, le potentiel instantané E est égal à 0,632 E_{max}. Dans ces conditions, pour que la mesure d'intensité d'une raie soit égale à 99,5% de sa valeur réelle, il faut que la constante de temps ne dépasse pas le cinquième du temps de balayage de la portion maximum de la raie considérée à intensité constante.

Une série d'essais à constantes de temps croissantes et à vitesses de balayage croissantes (Fig. 7) montre nettement l'effet de ces facteurs; ainsi pour une fente assez fine (5 cm^{-1}), la diminution d'intensité est remarquable et le rapport d'intensité varie non moins fortement:

R.C. sec	1,5	4,5	6,5	10
I_B^{992}/I_T^{1001}	1,46	1,48	1,41	1,33

Scan cm^{-1}/min	6	10	15
I_B^{992}/I_T^{1001}	1,48	1,48	1,42

Plus la largeur de la fente sera faible, plus le balayage du spectre devra être lent pour une constante de temps donnée. Dans ces conditions, nous préférons enregistrer les spectres avec une fente un peu large quitte à perdre un peu de résolution, quand elle n'est pas indispensable, comme c'est d'ailleurs souvent le cas des mesures quantitatives.

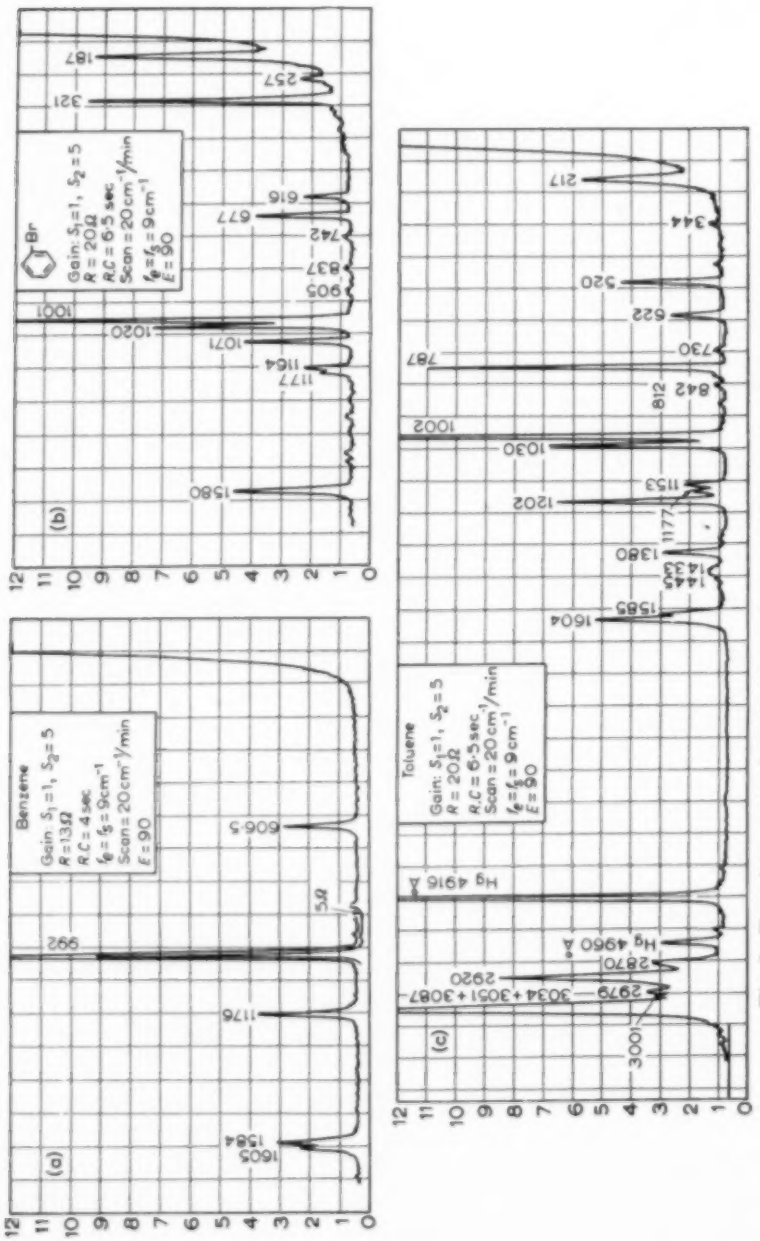

Fig. 6. Enregistrements photoélectriques du spectre Raman de substances diverses.

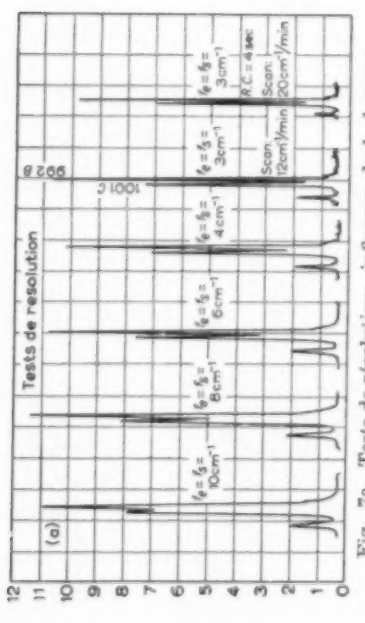

Fig. 7a. Tests de résolution: influence de la largeur spectrale des fentes.

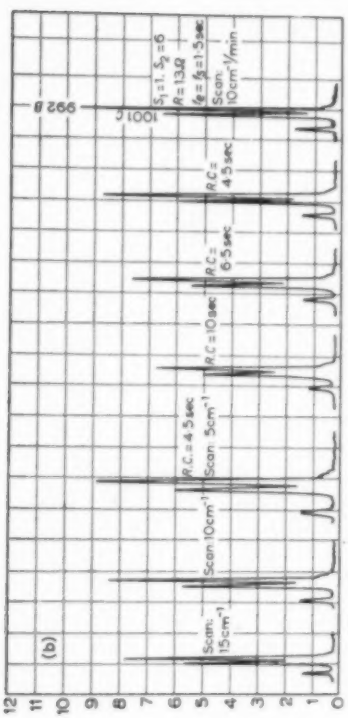

Fig. 7b. Tests de résolution: influence de la constante de temps et de la vitesse de balayage du spectre.

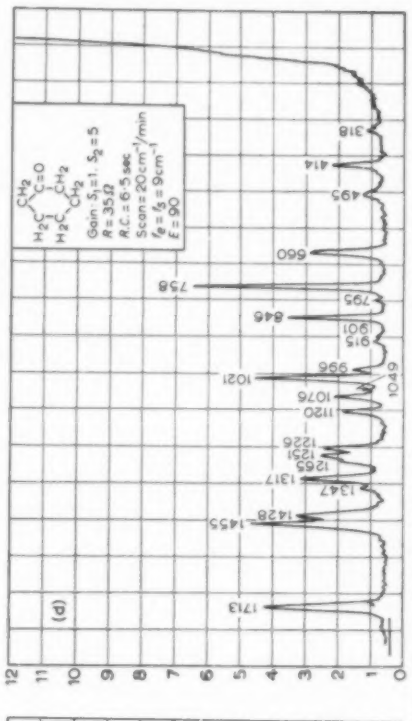

Fig. 7c et 7d. Enregistrements photoélectriques des spectres Raman du tétrachlorure de carbone et de la cyclohexanone.

Le rapport d'intensités peut dépendre des conditions d'enregistrement si les profils des deux raies utilisées sont différents comme c'est souvent le cas.

Lorsque nous n'avons besoin que de mesures qualitatives ou semi-quantitatives, la vitesse de balayage peut être augmentée; ainsi les spectres rassemblés dans la fig. 6 sont enregistrés à la vitesse de 20 cm^{-1}/min avec une fente spectrale de 9 cm^{-1} et une constante de temps de 4 ou 6,5 sec; nous avons relevé dans ces spectres une série de raies proches qui sont pourtant bien séparées:

Benzène:	1584 — 1605 cm^{-1} = 21 cm^{-1}
Bromobenzène:	1001 — 1020 cm^{-1} = 19 cm^{-1}
	1164 — 1177 cm^{-1} = 13 cm^{-1}
Toluène	1002 — 1030 cm^{-1} = 28 cm^{-1}
	1585 — 1609 cm^{-1} = 24 cm^{-1}
Benzoate d'éthyle:	1160 — 1177 cm^{-1} = 17 cm^{-1}
Fumarate d'éthyle:	1643 — 1658 cm^{-1} = 15 cm^{-1}

Nous avons aussi enregistré à titre d'exemple le spectre de la cyclohexanone et le spectre du tétrachlorure de carbone dans lequel le fameux doublet 762–791 cm^{-1} est bien résolu (Fig. 7).

Lorsque des mesures d'intensités plus précises sont nécessaires, la région du spectre à enregistrer est balayée avec une vitesse de 10 cm^{-1}/min au maximum.

(c) *Le rapport signal/bruit de fond.* En plus des considérations d'ordre électronique que nous avons développées plus haut sur la largeur de bande passante de l'amplificateur et sur le courant noir du phototube, il en est d'autres très importantes qui se rapportent au flux lumineux Φ_2 qui tombe sur la photocathode du multiplicateur d'électrons.

Nous avons déjà vu précédemment dans la note sur la "figure de mérite" que ce flux était égal à $\Phi_2 = k_\lambda \cdot l \cdot I_s \cdot \mathscr{L} \cdot (\Delta\lambda)^2$.

Pour des conditions expérimentales fixées—*R.C.*, fentes spectrales—les seules variables sur lesquelles nous pouvons jouer sont I_s, qui est fonction de l'intensité de la raie excitatrice, des filtres employés et du pouvoir réfléchissant de la boite à lumière, l, longueur du tube Raman adopte et k_λ qui est fixé par la substance étudiée.

(1°) Rôle de la source lumineuse. Le choix judicieux des filtres peut améliorer le rapport signal/bruit de fond en diminuant l'intensité du fond continu de la lampe. En effet, si le filtre a une transmission T_X à la longueur d'onde de la raie excitatrice et T pour la fréquence Raman choisie, l'intensité de la raie Raman est égale à $T_X \cdot I_s$, tandis que les fluctuations du bruit de fond Δi sont proportionnelles à $[i \cdot T]^{\frac{1}{2}}$.

où $i = i_t = i_p$ de l'equation (13).

Le rapport signal/bruit de fond est proportionnel à $[T_X/T]^{\frac{1}{2}}$. Nous avons fait l'essai du filtre au nitrite potassique à 100% seul (I) ou additionné d'éosine (II).

Avec le filtre (II) à 0,01% en éosine, le rapport signal/bruit de fond serait amélioré d'un facteur $\dfrac{0{,}56}{(0{,}16)^{\frac{1}{2}}} = 1{,}4$ pour autant que le courant noir i_t du phototube soit négligeable par rapport au courant photoélectrique i_p (1P21 réfrigéré) dû au fond continu lumineux.

VOL. 8 1956/5

Mais à $t°$ ordinaire, $i_t \simeq i_p$, dès lors l'augmentation du gain (environ 2×) nécessaire pour compenser l'absorption du filtre (II) donne rapport signal/bruit de fond un peu inférieur à l'unité:

$$\left\{\frac{0{,}56}{[0{,}16 + 0{,}16]^{\frac{1}{2}}}\right\} \times 2 \simeq 0{,}99$$

Nous travaillons dans la plupart des cas avec le filtre (I) sans réfrigérer le phototube.

(2°) Rôle du tube Raman. Le flux lumineux Φ_2 est directement proportionnel à la longueur l du tube Raman; celle-ci étant fixée, seul l'emploi d'un "slicer" (16) peut accroître l'intensité du flux entrant dans le monochromateur.

(3°) Le coefficient de diffusion k varie d'une raie à l'autre; le rapport signal/bruit de fond subit les mêmes variations; cette notion n'a une signification que si on précise la raie choisie.

Tableau 3

Enregistrement	R.C	k_{219}	k_{315}	k_{459}	k_{762}	k_{791}
I	4″	0,775	0,923	1,000	0,238	0,240
II	4″	0,792	0,915	1,000	0,231	0,231
III	4″	0,770	0,910	1,000		
IV	6,5″	0,772	0,908	1,000	0,225	0,238
V	10″	0,748	0,882	1,000	0,236	0,241
k_{moyen}		0,774 ± 0,010	0,908 ± 0,010		0,232 ± 0,004	0,238 ± 0,003
Δk		1,3%	1,1%		1,7%	1,3%
$\Delta k_{\max}$		3,5%	3,0%		3,0%	3,0%

Stamm [13] donne le rapport signal/bruit de fond pour la raie 992 cm^{-1} du benzène et A.R.L. pour la raie 459 cm^{-1} du CCl_4; nous même pour une constante de temps de 4 secondes nous trouvons les valeurs suivantes:

pour la raie 992 cm^{-1} ~ 500/1 et pour la 459 cm^{-1} ~ 350/1

Pour ces deux raies intenses, il semble bien que le rapport signal/bruit de fond soit bien proportionnel à la racine carrée de leur intensité — $k_{992} = 2{,}12$ et $k_{459} = 1{,}000$-; en supposant exact le rapport signal/bruit de fond de la 459 cm^{-1}, nous obtenons pour la raie 992 cm^{-1}

$$350 \times \left[\frac{2{,}12}{1}\right]^{\frac{1}{2}} = 510.$$

Pour les raies moins intenses ($k_\nu < 0{,}1$) cette loi n'est plus vérifiée et le rapport signal/bruit de fond diminue de plus en plus, en cela nous rejoignons les conclusions de Marrinan [19].

Le rôle de la composante du courant noir augmente au fur et à mesure de la diminution du signal.

(d) *Mesures de l'intensité des raies Raman.* La précision des mesures d'intensités des raies Raman dépendra essentiellement de la stabilité dans le temps de l'installation: source, récepteur, amplificateur et enregistreur—et de la reproductibilité

des conditions opératoires—sélection des tubes Raman et leur position dans la source.

Bien que le courant d'alimentation de la source excitatrice ne soit pas stabilisé, nous avons observé une bonne constance de l'intensité au cours de la prise du spectre; en effet l'enregistrement du spectre du tétrachlorure de carbone (Fig. 7) effectué à différentes reprises nous donne des valeurs assez constantes des coefficients de diffusion relatifs des différentes raies comparées à la 459 cm^{-1}.

Notons cependant que pour la constante de temps de 10 secondes, les coefficients de diffusion des raies intenses et fines (219 cm^{-1} et 315 cm^{-1}) ont quelque peu

Tableau 4.

N° tube	Elongation de la raie 459	Ecart à la moyenne
1	234,5 mm	−3,5
2	237,5 mm	−0,5
3	241,5 mm	+3,5
4	233,5 mm	−4,5
5	238,5 mm	+0,5
6	241,5 mm	+3,5

Valeur moyenne: 238,0 mm ± 2,7 mm
Erreur relative moyenne: 1,13%
Erreur relative maximum: 1,89%

Tableau 5.

cm^{-1}	Auteurs						
	A.R.L.†	BERNSTEIN [20]	BUSING*	CHIEN-BENDER [4]	KINELL [8]	MICHEL-DUYCKAERTS	Y. MORINO [21]
219	0,690	0,755	0,760	0,820	0,726	0,774	0,962
315	0,850	0,877	0,900	0,930	0,864	0,908	1,05
459	1,000	1,000	1,000	1,000	1,000	1,000	1,000

* Communication privée.
† Mesures faites sur l'installation A.R.L. de l'Université de Bologne.

diminué, alors que ceux des raies plus larges et faibles (762 et 791 cm^{-1}) n'ont guère changé.

On peut donc conclure que malgré des conditions d'enregistrement assez différentes l'erreur relative moyenne oscille entre 1 et 1,7% et l'erreur relative maximum se situe aux environs de 3%. Nous avons également voulu nous faire une opinion sur la reproductibilité des conditions opératoires: à cet effet nous avons enregistré la raie 459 cm^{-1} du CCl_4:

(1°) en déplaçant le tube contenant le CCl_4 après chaque prise de spectre nous n'avons pas constaté de variations plus fortes de l'intensité que celles qui sont tolérées pour les variations de l'installation électronique.

(2°) En prenant le tétrachlorure de carbone dans des tubes différents numérotés de 1 à 6, nous avons obtenu les élongations au maximum suivantes:

Ces écarts sont très acceptables lorsque l'on sait que les fluctuations dues à la source sont de l'ordre de 2%. Nous avons rassemblé dans le tableau 5, les coefficients de diffusion des raies du tétrachlorure de carbone obtenues par divers auteurs; les différences observées par les différents auteurs sont tout à fait normales si l'on considère que ces enregistrements ont été obtenus avec des appareils très différents les uns des autres et dans des conditions opératoires différentes (fente, constante de temps, récepteur, etc).

Remerciements—Il nous est agréable de pouvoir adresser ici nos remerciements au Patrimoine de l'Université de Liège ainsi qu'au F.N.R.S. dont les subsides nous ont permis de mener à bonne fin la construction de ce spectromètre Raman.

Nous remercions également Mr. le Prof. L. D'Or qui par ses encouragements et sa collaboration nous a grandement facilité le travail.

Nous tenons aussi à marquer notre gratitude à Messieurs H. Mertens et M. Debot pour les discussions fructueuses que nous avons eues ensemble.

Bibliographie

[1] Michel G. et Duyckaerts G. *Ind. Chim. Belge, Compte Rendu XXVII Congrès Chim. Ind. Bruxelles Sept.* 1954 **T.XX Vol. 1** 193–198 N° spécial.
[2] Michel G. *Spectrochim. Acta* 1952 **5** 218–37.
[3] Rank D. H. et coll. *J. Opt. Soc. Amer.* 1942 **32** 390; 1943 **33** 31; 1946 **36** 325.
[4] Chien J.-Y. et Bender P. *J. Chem. Phys.* 1947 **15** 376.
[5] Suschinskii M. *Doklady Akad. Nauk. S.S.S.R.* 1950 **70** 221.
[6] Stamm R., Salzmann C., et Mariner Th. *J. Opt. Soc. Amer.* 1953 **43** 119–125.
[7] Brandmuller J. et Moser H. *Ann. Phys.* 1953 **13** 253–56.
[8] Kinell P. O. et Traynard Ph. *Acta Chem. Scand.* 1948 **2** 193–203.
[9] Luther H., Bergmann G., et Muhlfeld A. *Naturwiss.* 1952 **39** 255–6.
[10] Robert L. *Spectrochim. Acta* 1953 **6** 115–23.
[11] Dupeyrat R. *J. Physique et le Radium* 1953 **14** 131.
[11'] Nielsen J. R. *J. Opt. Soc. Amer.* 1930 **20** 701; 1947 **37** 494.
[12] Welsh, Crawford et Scott *J. Chem. Phys.* 1948 **16** 97.
[13] Stamm R. et Salzmann C. *J. Opt. Soc. Amer.* 1953 **43** 126–137.
[14] Heigl J. J., Dudenbostel Jr. B. F., Black J. F., et Wilson J. A. *Analyt. Chem.* 1950 **22** 154.
[15] Benesch W. et Strong J. *J. Opt. Soc. Amer.* 1951 **41** 252.
[16] White J. U. *J. Opt. Soc. Amer.* 1951 **41** 732.
[17] Engström R. W. *J. Opt Soc. Amer.* 1947 **37** 420.
[18] Dieke C. H. *Instruments and measurements Conference, Stockholm Transactions* 1947 17.
[19] Marrinan H. J. *J. Opt. Soc. Amer.* 1953 **43** 1211.
[20] Bernstein H. J. et Allen G. *J. Opt. Soc. Amer.* 1955 **45** 237.
[21] Morino Y. et coll. *J. Chem. Soc. Japan* 1954 **75** 861.

Spectrochimica Acta, 1957, Vol. 8, pp. 374 to 389. Pergamon Press Ltd., London

Effects of grinding during the preparation of alkali-halide disks on the infra-red spectra of hydroxylic compounds

V. C. FARMER
Department of Spectrochemistry, The Macaulay Institute for Soil Research, Craigiebuckler, Aberdeen

(*Received 5 October* 1956)

Abstract—Changes in the spectra of phenols and organic acids induced by grinding with alkali halides are ascribed to the adsorption of molecules on the surface of the alkali halides through their hydroxyl groups. Carboxylic acids are shown to be adsorbed principally as monomers, linked to halide ions by hydrogen bonding, so that the spectral changes which occur serve to identify vibrations to which the carboxyl group contributes. In addition, a rearrangement of the crystalline structures of cinnamic acid and hydroquinone on grinding with alkali halides is reported. Glucose gives a new crystalline spectrum when ground with potassium iodide, but other sugars are either unchanged or converted to an amorphous state; similar effects occur with some samples of potassium bromide. The pressed-disk technique is discussed in the light of these results.

Introduction

THE infra-red spectra of solid materials can be conveniently obtained by the pressed-disk technique, whereby a powdered alkali halide, in which a little of the sample has been finely dispersed, is converted into a transparent disk under pressure [1, 2]. To obtain the best results, it is important that the particle size of the sample should be small, since then little radiation is lost by scattering, and the Christiansen effect [3], which shifts absorption maxima and obscures the finer details of the spectrum, is eliminated. For quantitative purposes it is essential that the particle size should be below the level at which this variable affects the intensity of absorption bands [4, 5, 6]. A number of methods have been used to obtain the necessary degree of fineness, among which the vibratory grinder of ARDENNE [7] seems to be both rapid and effective [6, 8]. It has been found, however, that the spectra of acids, alcohols, and phenols often undergo marked changes on grinding with alkali halides [9], and further work has shown that amides may also be affected. Even in the mineral-oil mull technique, however, spectral changes may be expected where the sample is soluble in the oil, and as the pressed-disk technique has many advantages in convenience, reproducibility and economy of material, the present work was undertaken to determine conditions under which the pressed-disk technique might be confidently used. The results also lead to an understanding of the nature of some of the spectral changes which occur.

Materials and methods

Pure samples of sodium and potassium chloride were prepared by the method of HALES and KYNASTON [10]. The fine crystals obtained by pouring concentrated solutions of these salts into concentrated hydrochloric acid were dried and heated to 500° for 8 hr to remove adsorbed hydrochloric acid. The potassium bromide and iodide used were selected samples of

reagent quality. They were ground in a mechanical mortar and then heated to 500°. Windows prepared from these materials showed the usual weak absorption near 3 μ and 6 μ, due to adsorbed water, but the bromide and iodide showed in addition a weak band near 9 μ (10% absorption in 1-mm disks).

The sample and the alkali halide together with three ball-bearings (diameters $\frac{3}{16}$, $\frac{1}{8}$, and $\frac{5}{16}$ in.) were placed in a stainless-steel capsule, and ground in the electromagnetic vibrator shown in Fig. 1. The steel strip vibrated at 100 c/sec, the peak-to-peak amplitude being 1 cm.

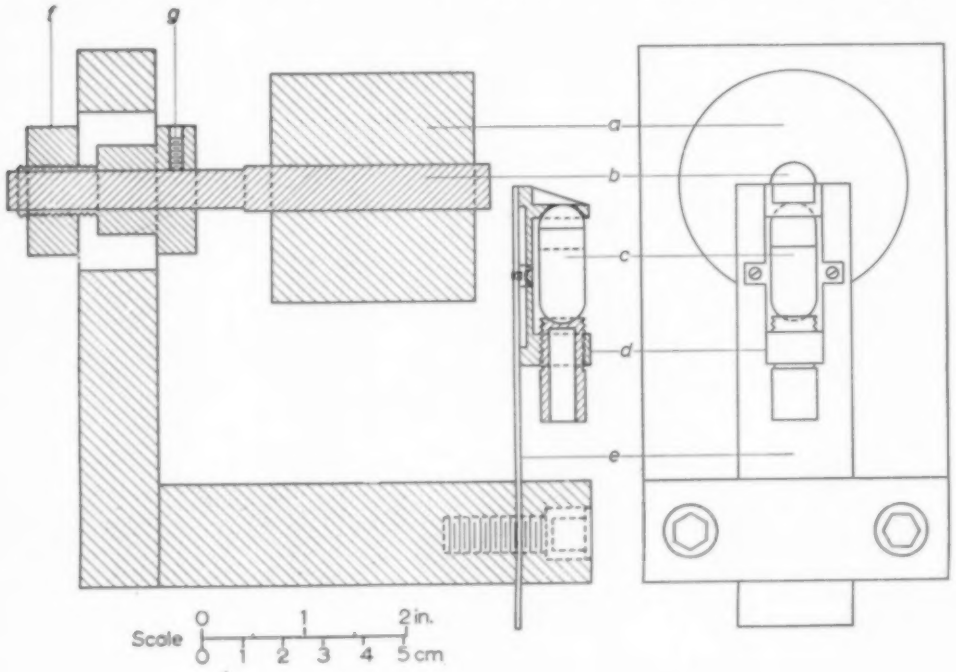

Fig. 1. Solenoid vibratory grinder. (a) Solenoid, supplied with 50-cycle a.c. through control resistor. (b) Soft iron core. (c) Stainless-steel capsule, wall thickness 0·4 mm with push fit lid. (d) Duralumin capsule holder. (e) Tempered steel strip, 1·08 mm thick, length adjusted to resonance. (f) Lock nut for vertical adjustment of solenoid. (g) Set screw for horizontal adjustment.

The ground powder was pressed in the mould shown in Fig. 2, using a thrust of 8 tons. The construction of the mould, which is based on the design of FORD and WILKINSON [11], differs from it in that the barrel of the mould is fitted with two hardened sleeves S_1 and S_2, which are a sliding fit in the barrel B. The alkali halide disk is formed within the short sleeve, in which it is then handled and used. The longer sleeve acts as a guide to the plunger D, which presses the disk on the anvil F. The sleeves are standard, hardened, jig liner bushes (type P.L.2 of Boneham and Turner Ltd., Mansfield, Notts, England), so that a stock of interchangeable sleeves can be cheaply obtained. For $\frac{1}{2}$-in. disks they have an external diameter of $\frac{3}{4}$ in., their lengths are $\frac{5}{16}$ in. and $1\frac{1}{4}$ in. The plunger and anvil are made of silver steel, hardened and tempered to a light straw, while the rest of the mould is of mild steel.

The infra-red spectra were recorded on a Grubb-Parsons Doublebeam Spectrometer, type $S4$, equipped with sodium chloride prism. The positions of sharp absorption bands were determined to within $\pm 0{\cdot}02$ μ.

Results and interpretation

The infra-red spectra of all the solid organic acids studied, which included substituted benzoic and acetic acids, and $\alpha\beta$-unsaturated acids, were found to change markedly on prolonged grinding with sodium chloride, potassium chloride, and potassium bromide, but potassium iodide proved to have little effect on their infra-red spectra. The interpretation of the changes observed follows most readily from a study of the benzoic acids, and these will be discussed first, although it seems likely that all the effects are fundamentally similar.

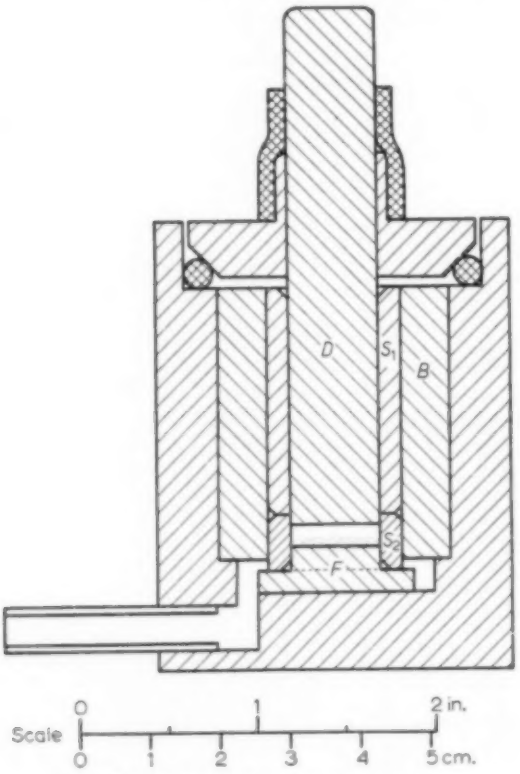

Fig. 2. Vertical section of mould.

Adsorption effects in benzoic acids

The spectra given by benzoic acid after grinding with the alkali halides are shown in Fig. 3. In potassium iodide the spectrum (a) is essentially that of the normal dimeric crystalline form, and absorption bands of the dimer at 7·02 and 7·73 μ are also present in the spectra of the potassium bromide (b) and chloride (c) disks, although weakened relative to the rest of the spectrum. These bands are absent from the spectrum of the sodium chloride disk, (d), where they are replaced by bands at longer wavelengths. Displaced bands corresponding to these are also present in the spectra of the other alkali halide disks, although in potassium iodide

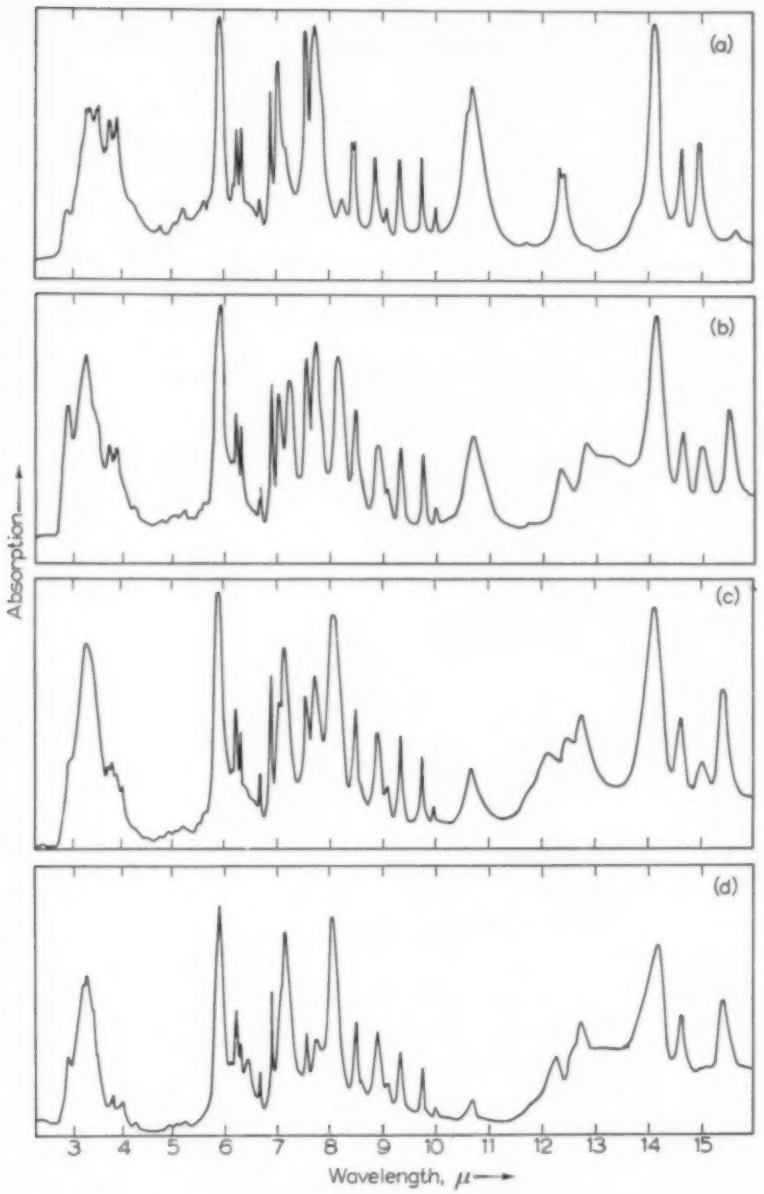

Fig. 3. Spectra of benzoic acid dispersed in pressed disks of (a) KI. (b) KBr, (c) KCl, and (d) NaCl. 0·7 mg benzoic acid ground 16 min with 300 mg alkali halide. The ground mixtures with NaCl and KCl were heated 2 hr at 80° before pressing.

they are only just detectable. *p*-Chloro- and *p*-methoxybenzoic acids were found to behave like benzoic acid itself.

The new bands in the spectra, as will be shown, can be ascribed to monomeric benzoic-acid molecules adsorbed on the surface of the alkali halide particles. The crystalline dimer is readily volatile, and on heating the ground mixture of benzoic acid and alkali halide in a thin layer at 80° before pressing, excess benzoic acid is lost, leaving the adsorbed form alone in sodium chloride disks. Some of the dimer, however, is retained by the other alkali halides, even after long heating (16 hr) and the spectra of the monomers alone has not been obtained. Some of the monomer is also volatilized from potassium bromide under these conditions.

The spectrum given by the sodium chloride disk shows a close analogy to that of benzoic acid in dioxan solution (Table 1), even though solvent absorption

Table 1. Wavelength (μ) of absorption bands of benzoic acid in dimeric and in monomeric states

Assignments	Dimer crystalline	Monomer				
		Dioxan	NaCl	KCl	KBr	KI
OH (str.) and summation bands	3·45	*o*	3·26	3·26	*o*	*o*
	3·76	3·82	3·83	3·84	*o*	*o*
	3·92	3·98	4·03	4·04	*o*	*o*
C=O (str.)	5·91	5·81	5·83 5·89 6·45	5·89	5·91	*o*
OH (def.) + C—O (str.)	7·02	7·17	7·15	7·16	7·22	7·16
benzene ring	7·54	*o*	7·57	7·57	*o*	*o*
OH (def.) + C—O (str.)	7·73	8·13	8·04	8·05	8·12	8·21
OH (def.)	10·71	—	—	—	—	—
unassigned	12·32	(12·03)*	12·24	12·11	12·33	*o*
	12·42	12·44		12·48		
		12·82	12·74	12·76	12·82	—
C_6H_5·X and/or O=C—O (def.)	14·97	15·38	15·34	15·34	15·43	15·60

o obscured by solvent or dimer absorption
— not detected
str. stretching; def. : deformation
* probably a displaced dioxan vibration

obscures part of the spectrum. In dioxan, carboxylic acids are present as monomers, as they associate more readily with solvent molecules rather than their own species. This strongly suggests that the spectrum of the sodium chloride disk is to be ascribed to monomeric molecules of benzoic acid, which are adsorbed on the sodium chloride particles by hydrogen bonds between the acid hydroxyl groups and the chloride ions on the crystal surfaces.

VOL. 8 1956/5

A detailed study of the individual spectra confirms this interpretation. Thus, those bands which have been ascribed to the hydroxyl groups are found to be displaced in the spectrum of the adsorbed form. These shifts and other changes in the spectrum are listed in Table 1, together with the corresponding data for the other alkali halides, and for a dioxan solution. The strong bands of the dimer at 7·02 and 7·73 μ, which have been ascribed to the coupled C-O stretching and OH in-plane deformation vibrations by HADZI and SHEPPARD [12], are displaced to longer wavelengths in the adsorbed monomers. The displacement of the band near 8 μ increases in the order: chloride, bromide, iodide, corresponding to the weakening of the hydrogen bond expected with increasing ionic radius, until in potassium iodide it lies close to the corresponding bands of the free monomers of CD_3·COOH [13] and CCl_3·COOH [14] at 8·22 and 8·20 μ respectively. The band near 7μ does not show this regular displacement, nor does it reach the wavelengths of the corresponding bands in the free monomers, which lie between 7·4 and 7·5 μ. In contrast to the in-plane vibration, the out-of-plane OH deformation vibration of the dimer at 10·72 μ has no clear counterpart in the spectrum of the adsorbed monomer. It may, however, give rise to the broad flat absorption below 12·5 μ in the spectrum of the sodium chloride and potassium bromide disks, but the absence of a corresponding band in the potassium chloride disk is then difficult to understand.

In the hydrogen stretching region, the complex hydroxyl absorption of the dimer, centred on 3·45 μ, is replaced by a simpler band displaced to shorter wavelengths consistent with a weaker hydrogen bond in the adsorbed state. It is noteworthy, however, that the outlying peaks of the dimer at 3·75 and 3·91μ are displaced to longer wavelengths in the monomers. The 3·91-μ band can be readily accounted for as an overtone of the strong hydroxyl deformation vibration at 7·73 μ, greatly enhanced by coupling with the overlying hydroxyl stretching absorption, but an assignment of the 3·75-μ band to an overtone of the dimer absorption at 7·54 μ is less likely, as the fundamental is little displaced although much weaker in the monomer. It seems more probable that this is a summation band, as suggested by BRATOZ, HADZI, and SHEPPARD [15].

Apart from the hydroxyl vibrations discussed above, there are few other differences between the spectra of the benzoic-acid monomers and the crystalline dimer. The band of the dimer at 14·97 μ, which is displaced to longer wavelengths in the monomers, lies in a region where HADZI and SHEPPARD [12] have suggested that the O=C—O deformation vibration of the carboxyl group may occur, but as there is no corresponding band in the spectra of *p*-methoxy and *p*-chlorobenzoic acid, it seems likely that an X-sensitive vibration of the C_6H_5·X molecule which is to be expected in this region [16] contributes to it. The absorption of the crystalline dimer at 8·42 μ is absent in the monomer, but is also absent from the spectrum of the dimer in nonpolar solvents. Of more general interest is the strong band of the dimer at 7·54 μ which appears only weakly in the spectrum of the monomer adsorbed on sodium chloride. A strong band near this wavelength can be seen in the spectrum of all three toluic acids [17], and was also found to be present in the spectra of crystalline *p*-methoxy and *p*-chlorobenzoic acid, but weak or absent in the spectra of the monomers. There is no corresponding

band in the spectra of substituted acetic acids. MECKE and ROSSMY [18] have suggested that a band in this region given by phenols may be ascribed to coupling between a planar vibration of the benzene ring and the hydroxyl deformation vibration, and a similar assignment seems reasonable in the benzoic acids. As the hydroxyl group may well lie out of the plane of the benzene ring in the adsorbed state, and as the wavelengths of the coupled vibrations lie further apart, a marked reduction in the intensity of the 7·54 μ band in the monomer is easily understandable. No explanation can be offered of the spectral changes which occur near 12·5μ, where the spectra of the sodium and potassium chloride disks differ markedly. The resemblance between the absorption pattern of the dioxan solution and that of the potassium chloride disk in this region (Table 1) is at least partly adventitious, since the band at 12·03 μ in dioxan is almost certainly a vibration of those dioxan molecules which are linked by hydrogen bonds to benzoic-acid molecules. It was found to be present in the spectra of dioxan solutions of other acids, but absent from the spectrum of an acetone solution of benzoic acid which is in other respects similar to that of the dioxan solution.

Although the position of the hydroxyl bands of the monomers adsorbed on sodium and potassium chloride agrees closely, the spectrum of the sodium chloride disk has some distinctive features. In addition to differences already noted near 12·5 μ, these include two additional bands at 5·83 and 6·45 μ (probably displaced carbonyl frequencies) and a marked dissymmetry of the band at 14·11 μ, which is a C-H out-of-plane vibration [19]. It seems likely that these are effects of the greater electrostatic field associated with the smaller sodium ion, but no detailed interpretation can be given.

VOL. 8 1956/5

Monomeric adsorption in other carboxylic acids

Examination of substituted acetic acids and $\alpha\beta$-unsaturated acids under conditions similar to those used with benzoic acid revealed spectral changes which could again be ascribed to the formation of adsorbed monomers, as changes in their hydroxyl bands near 3, 7, and 10·8 μ similar to those found with benzoic acid occurred. The spectra of the substituted acetic acids, which included ω-phenyl substituted acetic, propionic and butyric acids, and the dicarboxylic adipic and succinic acids, showed marked changes on fusion, since in the liquid state free rotation can occur about at least two C-C bonds [20]. The spectra of the adsorbed monomers, of course, approximated that of the fused state; this is illustrated by the spectra of γ-phenylbutyric acid in Fig. 4. Here the spectral changes in the 8 μ region are of particular interest: the doublet at 7·80 and 8·05 μ in Fig. 4b is typical of substituted acetic acids in the fused state and in solution [21, 22] and the assignment of either or both of these bands to the carboxyl group has been discussed [23]. The 7·80-μ band of the dimer is displaced to 8·09 μ in the monomer adsorbed on sodium chloride (Fig. 4c), and so can confidently be ascribed to one of the coupled OH and CO vibrations. The 8·05-μ band of the dimer is not displaced, suggesting that it should be assigned to a vibration of the methylene group adjacent to the carboxyl group.

Complete conversion to the monomers was achieved for the monocarboxylic acids in sodium chloride disks, but, in potassium bromide, overlying dimer absorption

obscured points of interest in the monomer spectrum. Monomer absorption could not be detected in potassium iodide disks. With the dicarboxylic acids, which associate in chains, only partial conversion to the monomer was achieved even after prolonged grinding in sodium chloride.

The spectral changes in the 8-μ region shown by the $\alpha\beta$-unsaturated acids are also of considerable interest. In the spectrum of the crotonic acid dimer there are

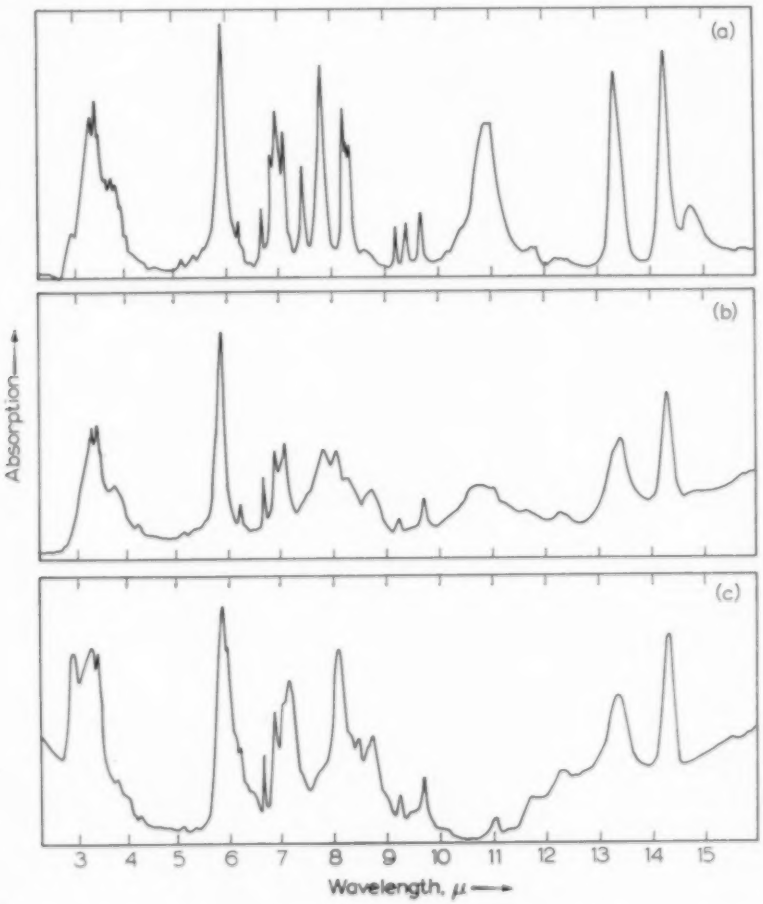

Fig. 4. Phenylbutyric acid. (a) Crystalline dimer; 0·8 mg in 170 mg KBr, ground 0·5 min. (b) Fused dimer; capillary film. (c) Adsorbed monomer; 1 mg in 400 mg NaCl, ground 16 min.

three strong bands between 7·5 and 8·2 μ (Table 2), all of which undergo displacement in the adsorbed monomers. In addition to the vibration of the carboxyl group already observed in other acids, the two in-plane hydrogen deformation frequencies of the R·CH=CH·R′ group are to be expected in this region [24], so that the three bands are readily accounted for. As these vibrations are co-planar, strong coupling is to be expected between them, and clearly does occur, so no

Table 2. Wavelength (μ) of absorption bands of crotonic acid in dimeric and monomeric states

Assignments	Dimer crystalline	Monomer		
		Dioxan	NaCl	KBr
C=O (str.)	5·87	5·82	5·87	5·88
C=C (str.)	6·05	6·02	6·02	6·05
OH (def.) + C—O (str.)	7·03	7·17	7·12	7·17
OH (def.) + C—O (str.) + H—C=C—H (def.)	7·58	o	7·79	7·85
	7·68	8·13	8·05	o
	8·14	8·44	8·31	8·39
OH (def.)	10·82	—	—	—
O=C—O (def.)?	14·27; 14·52*	15·02	14·97	15·21

* single absorption band in CCl_4 solution at 14·41μ
o obscured by solvent or dimer absorption
— not detected

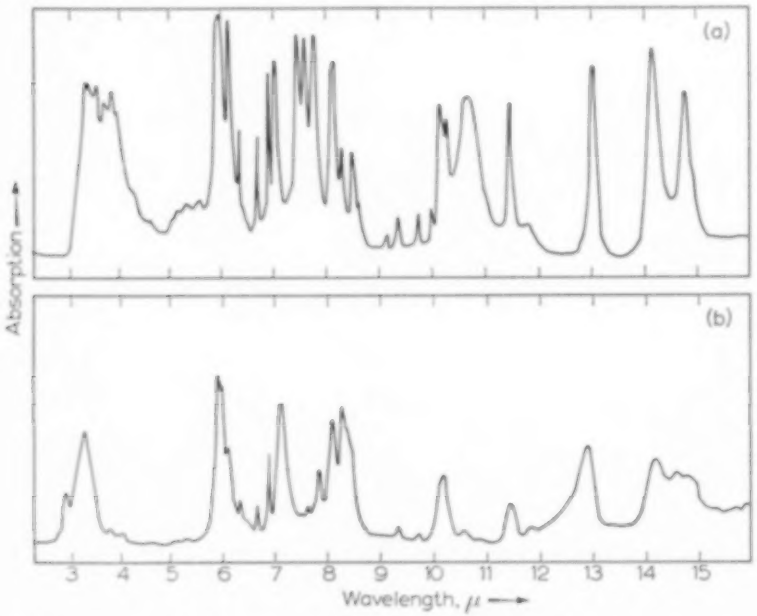

Fig. 5. Cinnamic acid. (a) Crystalline dimer; 0·9 mg in 150 mg KI, ground 1 min. (b) Adsorbed monomer; 0·7 mg in 300 mg NaCl, ground 16 min and heated 2 hr at 80° before pressing.

attempt is made to distinguish between them. The crotonic-acid dimer, like benzoic acid, has a vibration at longer wavelengths which is displaced in the adsorbed monomers and which is ascribed to O—C=O deformation (Table 2). None of the other acids examined showed bands of this type, but in their spectra the corresponding band may lie beyond 16 μ, as low-frequency vibrations are not in general stable in position.

The dimer of cinnamic acid (Fig. 5a) has even more complex absorption in the 8-μ region than crotonic acid, there being four strong bands at 7·45, 7·60, 7·77, and 8·14 μ. Here the 7·6-μ vibration of the benzene ring may well contribute to the absorption, as already suggested for benzoic acid. Adsorbed on sodium chloride, the cinnamic-acid monomer has only three bands in this region (Fig. 5b), the pattern closely resembling that of the crotonic-acid monomer in this alkali halide. This suggests that, as with benzoic acid, the benzene-ring vibration is effectively decoupled from the side chain in the adsorbed state. The formation of the cinnamic-acid monomer in potassium chloride and bromide was well defined, but, in addition, other changes in the spectra occurred which were best seen in potassium iodide disks, where little monomer was formed. Here grinding led to a modified dimer spectrum identical with that of the α-crystalline form, the original sample being the β-modification [25]. The presence of alkali halide is not necessary for this transformation, which could be effected by grinding cinnamic acid alone, when an X-ray study confirmed a change in the crystalline structure. This crystalline rearrangement is rapid; it is already detectable after 1 min grinding (the weak 10·19-μ band in Fig. 5a is from the α-form), and is almost complete after 4 min.

Retention of carboxylic-acid dimers by alkali halides

When the ground mixture of acid and potassium iodide is heated to 80° in a thin layer before pressing, some of the benzoic and cinnamic-acid dimers are retained if the grinding time is long (16 min), but phenylacetic acid and crotonic acid are not. In potassium bromide, after long grinding, some dimer is always retained, so that the spectrum of the monomer alone was never obtained with any of the acids studied. From the results with potassium iodide it seems unlikely that the retention is purely mechanical in nature, due, for example, to trapping of traces of the dimer within particles of the alkali halide. On the other hand, there is no evidence for adsorption forces acting on these acid dimers, since the spectra of both cinnamic and benzoic acid retained in potassium iodide on heating differed little from those of the crystalline forms.

Adsorption and other effects in phenols

An examination of several phenols, including α- and β-napthol, *p*-hydroxybenzaldehyde, vanillin, resorcinol, catechol, and hydroquinone, showed that grinding with the alkali halides converted them in part to an adsorbed form, the amount adsorbed being again dependent on the alkali halide. Here again the spectra of the adsorbed form were best obtained by volatilizing the unchanged crystalline material in an oven at 80°. Unlike the acids, however, the spectrum of the adsorbed forms of the phenols differed little from that of the fused form. Thus, although the spectrum of the adsorbed form of resorcinol in potassium chloride (Fig. 6b) differs markedly from that of the crystalline state (Fig. 6a), it differs from that of the fused state only in the two bands at 7·90 and 8·23 μ, which are more sharply defined when adsorbed. These bands were shifted 0·06 μ to longer wavelengths in a potassium bromide disk, but in sodium chloride there was an additional band in this region at 8·03 μ. These bands are clearly hydroxyl deformation frequencies [18], and the results suggest that the phenols form hydrogen bonds with

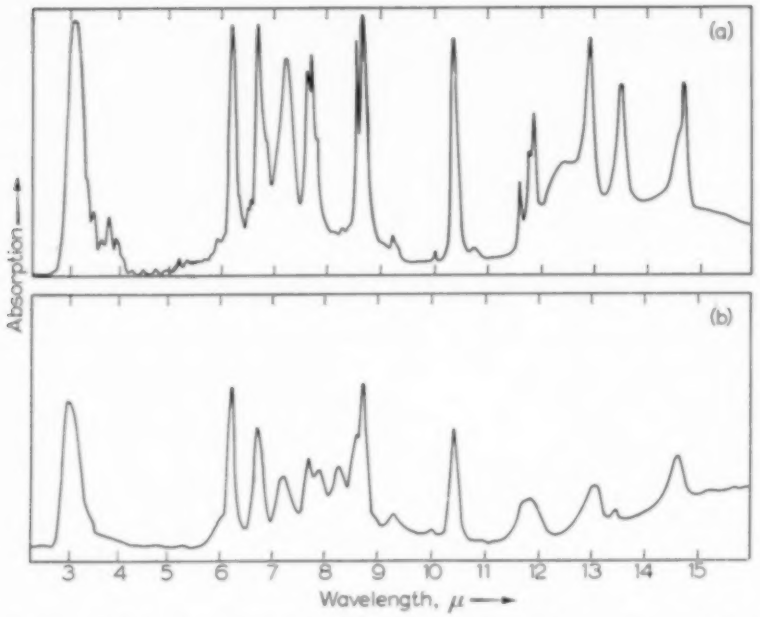

Fig. 6. Resorcinol. (a) Crystalline; 0·6 mg in 300 mg KI, ground 8 min. (b) Adsorbed form; 0·7 mg in 300 mg KCl, ground 16 min and heated 2 hr at 80° before pressing.

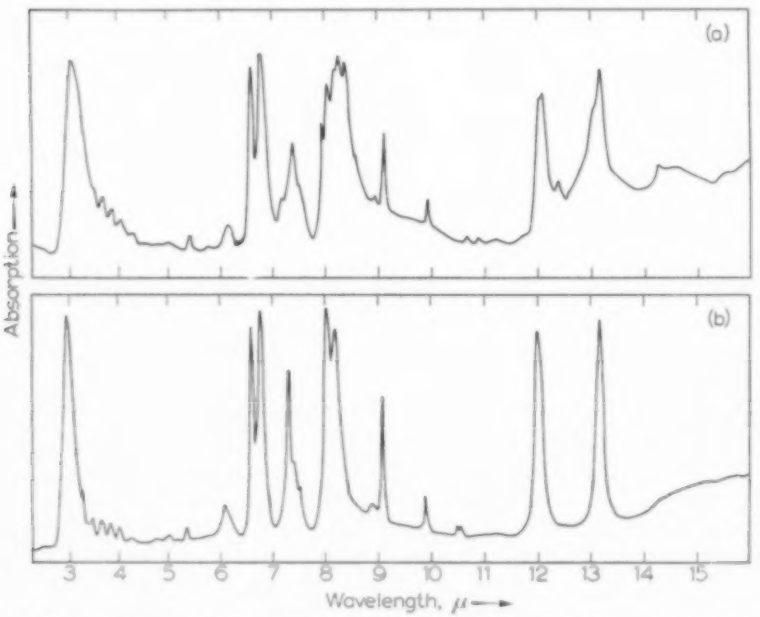

Fig. 7. Hydroquinone. (a) Original crystalline form; 0·65 mg in 300 mg KBr, ground 1 min. (b) Modified crystalline form; 0·6 mg in 300 mg KBr, ground 8 min.

VOL. 8 1956/5

the halide ions, although differences between sodium and potassium chlorides indicate that the cation also contributes to the adsorption forces In the spectrum of the sodium chloride disks there was further evidence of strong adsorption through the hydroxyl groups, since the out-of-plane deformation frequency of the aromatic hydrogen atom between the two hydroxyl groups of resorcinol was also affected. Its absorption band, lying at 11·90 μ in the spectrum of the fused state [26], was markedly broadened in that of the adsorbed state, while the deformation frequency of the other aromatic hydrogens at 13·05 μ was unaffected.

The other phenols, apart from hydroquinone, gave results broadly similar to those found with resorcinol, and a brief examination of benzamide indicated that it behaved like the phenols.

Hydroquinone, however, showed a new effect. Grinding with the alkali halides was found to give rise to a spectrum (Fig. 7b) differing markedly from both that of the original crystalline form (Fig. 7a) and that of the fused state. The sharpness of the absorption bands and the fine structure of the O-H stretching frequency between 3 and 4 μ show that this spectrum arises from a new crystalline state. The conversion proceeded almost equally rapidly in potassium chloride, bromide, and iodide, but could not be effected by grinding hydroquinone alone. It may be that the new crystalline state is formed on the layer of adsorbed hydroquinone molecules, whose presence was detected at low concentrations of hydroquinone (i.e. 0·1%) in potassium bromide, chloride, and iodide. Such a layer of adsorbed molecules, if attached to the alkali halides through their hydroxyl groups, will still have hydroxyl groups in the *para* position available for hydrogen bonding to a second layer of hydroquinone molecules. This effect may be related to the phenomenon of epitaxy, i.e. the oriented growth of crystals on the surface of other crystalline materials, which is believed to proceed from an initial adsorbed layer [27].

Spectral changes in polyhydroxyalcohols

The sugars fall into this catagory, as only their hydroxylic groups can be active in the solid state, where they exist as pyranose or furanose ring compounds. Examples of these ground for 8 min at a concentration of 0·2% in the alkali halides showed markedly different effects. The spectra of xylose, lactose, and cellobiose remained unchanged on grinding with potassium chloride, bromide, and iodide, but those of sucrose, sorbose, and mannose, although essentially unchanged in chloride and bromide, were markedly altered in potassium iodide, the sharp bands of the original crystalline state being replaced by broad diffuse bands of what must be an amorphous form. Glucose (α-glucopyranose), however, was found to be completely converted to a new crystalline modification by grinding with potassium iodide (Fig. 8), whereas with sodium and potassium chloride, and with potassium bromide, no such effect could be detected, although partial conversion to the amorphous state was perceptible. The interpretation of the spectral changes observed in potassium iodide disks is made more difficult by the observation that very similar, if not identical, changes were produced by some samples of potassium bromide, although the activity of the bromides (all "reagent" quality) varied with their source. With the material generally used in the course of this work ("Analar" reagent of British Drug Houses Ltd., London) no trace of the new crystalline form

of glucose could be detected under varying conditions of humidity and grinding. Changes in the spectrum of glucose in potassium bromide disks have been previously reported [28], and the new spectrum has been identified with that of glucose monohydrate [29]. It was also reported that the potassium bromide lost its activity on thorough drying at 650°. The spectrum we have obtained, however, is not that of glucose monohydrate, nor was the activity lost on heating. A study of active and inactive samples of potassium bromide failed to identify the causative factor.

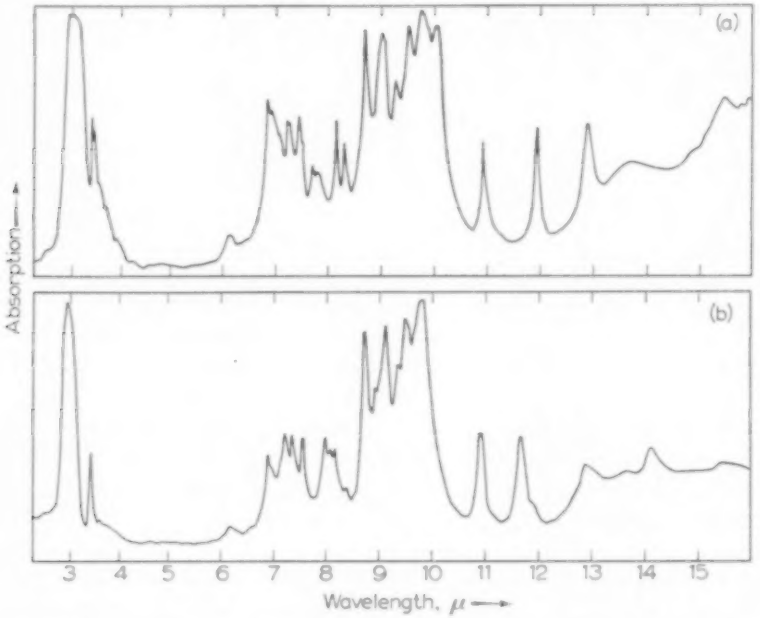

Fig. 8. α-Glucopyranose. (a) Original crystalline form; 0·7 mg in 150 mg KBr, ground 4 min. (b) Modified crystalline form; 0·7 mg in 300 mg KI, ground 8 min.

Evidence was obtained that the spectral changes observed with the sugars may also occur with simple polyhydroxy-alcohols. Mannitol and inositol were examined as described for the sugars, and under these conditions the spectrum of mannitol was unchanged, but that of inositol indicated partial conversion to the amorphous state in all four alkali halides. Heating the ground mixture of sample and alkali halide to 80° for 2 hr before pressing was found to give the spectra of the amorphous state of both compounds in potassium iodide disks, but little additional change occurred in other alkali halides.

Although a full interpretation of these effects is not yet available, it seems possible, in view of the variability of potassium bromide samples, that not all samples of potassium iodide will give the effects reported here.

Discussion

The adsorption of compounds containing hydroxyl groups on alkali halides, and the spectral changes associated therewith, are clearly of importance in the

VOL. 8 1956/5

application of the pressed-disk technique to such compounds. The results reported above, however, make it possible to select conditions under which good quality spectra of the crystalline state can be obtained, at least for qualitative purposes.

With acids, the amount of the adsorbed form in disks of sodium chloride, potassium chloride, and potassium bromide decreases in that order, while little or none appears in potassium iodide disks. Two factors certainly contribute to this variation in the amount of the adsorbed monomer. On the one hand, the strength of hydrogen bonding between the hydroxyl group and the halide ion decreases with increasing size of the halide ion, i.e. in the order chloride, bromide, iodide; while on the other, the number of available sites where adsorption can occur may be expected to vary with the number of halide ions per unit weight of alkali halide, i.e. in the ratios 2·85: 2·23: 1·40: 1·00 in NaCl, KCl, KBr, and KI respectively.

With phenols, too, adsorption effects are least in potassium iodide disks,

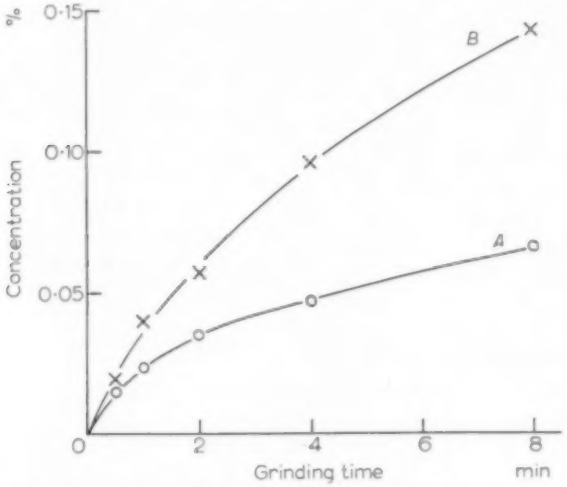

Fig. 9. Effect of grinding time on the concentration of benzoic-acid monomer formed in KBr (curve A) and KCl (curve B) disks.

and this suggests that potassium iodide is the most suitable alkali halide to use with these materials. There is no doubt that for special purposes it has many advantages, giving spectra of excellent quality, almost entirely free of Christiansen effect. (Potassium chloride gives pronounced Christiansen effects, while potassium bromide is intermediate between chloride and iodide.) Unfortunately, however, potassium iodide disks are easily fogged, and soon deteriorate under normal conditions, and for general use they cannot be recommended, particularly as the iodide is far from inert to polyhydroxy-alcohols and sugars. With such compounds, spectral changes are least in potassium chloride or bromide, although it is to be noted that the activity of different samples of potassium bromide may differ markedly. Here, however, the spectrum of glucose may provide a simple test for the suitability of a given sample.

These considerations point to the widely used potassium bromide as the most suitable material for general qualitative purposes, although some compromise

must be made in grinding time. Fig. 9 shows how the concentration of the benzoic-acid monomer varies with grinding time in potassium bromide and chloride, and these results are at least approximately true for other acids and phenols. Nevertheless, there is considerable variation among compounds in the permissible grinding time before any marked change in their spectra occurs. Thus, the benzoic-acid monomer, which gives strong sharp bands in regions where the dimer does not absorb, can be detected in 300-mg potassium bromide disks after only 0·5 min grinding, but spectral changes with phenylbutyric acid only become noticeable after 4 min grinding at a concentration of 0·33% in 300-mg potassium bromide disks. Such differences can scarcely be predicted, but in practice it is found that by using the minimum amount of potassium bromide consistent with the mechanical stability of the disk (about 150 mg for a 0·5-in. disk) and concentrations of sample such that the strongest bands have over 95% absorption (0·5 to 1·0%), then with a grinding time of 0·5 min, the effects of adsorption and crystalline transformation are generally negligible. The quality of the spectra is good, provided that the sample is initially finely divided, but this is not always possible where material is limited or of a waxy nature. Under such conditions, regrinding the pressed disk followed by another pressing is an effective technique [30].

The use of the pressed-disk technique for quantitative purposes must, however, present difficulties with compounds of the type examined, especially at low concentrations. Nevertheless, it would appear that, even where adsorption effects do occur, satisfactory results can be obtained, as with benzoic acid in potassium bromide [6], by selecting an absorption band which is unaffected by adsorption.

Acknowledgement—The author is indebted to Mr. A. M. FRASER for the design and construction of the mould and vibratory grinder.

VOL.
8
1956/5

References

[1] SCHIEDT U. and REINWEIN H. *Z. Naturf.* 1952 **7b** 270.
[2] STIMSON M. M. and O'DONNELL M. *J. Amer. chem. Soc.* 1952 **74** 1805.
[3] PRICE W. C. and TETLOW K. S. *J. Chem. Phys.* 1948 **16** 1157.
[4] DUYCKAERTS G. *Spectrochim. Acta* 1955 **7** 25.
[5] BONHOMME J. *Spectrochim. Acta* 1955 **7** 32.
[6] HAUSDORFF H. *Appl. Spectroscopy* 1954 **8** 131.
[7] ARDENNE M. v. *Angew. Chem.* 1941 **54** 144.
[8] SCHIEDT U. *Z. Naturf.* 1953 **8b** 66.
[9] FARMER V. C. *Chem. and Ind.* 1955 586.
[10] HALES J. L. and KYNASTON W. *Analyst* 1954 **79** 702.
[11] FORD M. A. and WILKINSON G. R. *J. sci. Instrum.* 1954 **31** 338.
[12] HADZI D. and SHEPPARD N. *Proc. Roy. Soc.* 1953 **A216** 247.
[13] WELTNER W. *J. Amer. chem. Soc.* 1955 **77** 3941.
[14] KURATANI K. *J. chem. Soc. Japan*, Pure Chem. Sect. 1952 **73** 758.
[15] BRATOZ S., HADZI D., and SHEPPARD N. *Bull. sci. Conseil acad. RPF Yougoslav.* 1953 **1** 71.
[16] RANDLE R. R. and WHIFFEN D. H. *Molecular Spectroscopy* Institute of Petroleum, London, 1954.
[17] BARNES R. B., GORE R. C., LIDDEL U., and WILLIAMS V. Z. *Infra-red Spectroscopy* Reinhold Publishing Co., New York, 1944, p. 83.

[18] Mecke R. and Rossmy G. *Z. Electrochem.* 1955 **59** 866.
[19] Bellamy L. J. *J. chem. Soc.* 1955 4221.
[20] Sinclair R. G., McKay A. F., and Jones R. N. *J. Amer. chem. Soc.* 1952 **74** 2570.
[21] Freeman N. K. *J. Amer. chem. Soc.* 1952 **74** 2523.
[22] Rigaux C. *C.R. Acad. Sci., Paris* 1954 **238** 63.
[23] Bellamy L. J. *The Infra-red Spectra of Complex Molecules* Methuen, London, 1954, p. 147.
[24] Sheppard N. and Sutherland G. B. B. M. *Proc. Roy. Soc.* 1949 **A196** 195.
[25] Guy J. *Bull Soc. chim. Fr.* 1949 731.
[26] Bellamy L. J. *J. chem. Soc.* 1955 2818.
[27] Seifert H. in *Structure and Properties of Solid Surfaces*, ed. Gomer R. and Smith C. S. University of Chicago Press, 1953, p. 318.
[28] Barker S. A., Bourne E. J., Neely W. B., and Whiffen D. H. *Chem. and Ind.* 1954 1418.
[29] Barker S. A., Bourne E. J., Weigle H., and Whiffen D. H. *Chem. and Ind.* 1956 318.
[30] Clauson-Kaas N., Nedenskov P., Bak B., and Rastrup-Andersen J. *Acta chem. Scand.* 1954 **8** 1088.

OL.
3
6/57

Spectrochimica Acta, 1957, Vol. 8, pp. 390 to 394. Pergamon Press Ltd., London

REPORTS OF MEETINGS

Society for Applied Spectroscopy

Eleventh Annual Meeting

1-2 November 1956

New York, N.Y.

The spectrochemical analysis of copper and copper-base alloys

Quantitative analysis of various wrought brass and bronze alloys with a production control quantometer, P. A. LEICHTLE, R. BURNHAM, and F. SULLIVAN, Chase Brass and Copper Co., Inc., Waterbury, Conn.

A production control quantometer is being successfully used for the quantitative analysis of the eight major alloying elements and impurities in ten types of wrought brasses and bronzes. The method is a conventional point-to-plane method using a selected multisource case which permits simultaneous quantitative analysis of nearly all important major constituents and impurities in the alloys studied; namely, zinc, lead, iron, tin, nickel, manganese, silicon, and aluminium in:

1. Binary brasses; with copper from 58% to 96%.
2. Leaded brasses; with copper from 58% to 66%, lead up to 4%.
3. Tin brasses, admiralty, naval, and leaded naval brasses.
4. Manganese bronze.
5. Aluminium brass.
6. Silicon aluminium bronze.
7. Olympic bronze.
8. Cupro-nickel with 10% nickel.
9. Cupro-nickel with 30% nickel.
10. Talnic and phosnic bronze.

The prescribed method, without modification, is satisfactory except for the analysis of impurities in 95–5 brass and for nickel in the 9 to 32% range.

Working curves for each type of alloy will be compared. It is apparent that separate standards and working curves are needed for each type of alloy if accurate results are to be obtained. Extraneous element effects will be discussed. Cast standards will be compared with wrought standards.

Some notes on the quantitative spectrochemical analysis of copper-base alloys, R. CARLS, Federated Metals Division, American Smelting and Refining Co., Barbar, N.J.

The effects of working and heat-treatment on the spectrochemical analysis of ingot brasses will be given. Major and minor element determinations using American Smelting and Refining Company continuous cast standards and chill-cast samples will be described. Also the effect of lead on the determination of tin in ingot brasses will be discussed.

Spectrographic analysis of impurities in refined copper, F. V. SCHATZ, Revere Copper and Brass Company, Rome, N.Y.

Three methods that have been the most useful in the analyses of impurities in refined copper and high-purity brasses will be outlined. The first, a solution method of analysis utilizing the d.c. arc, is useful for general surveys and trouble shooting when the samples are submitted

VOL. 8 1956/5

in a variety of forms. The second, the so-called globule analysis utilizing the d.c. copper arc with the sample as the negative electrode, is useful when extreme sensitivity is desired. The third, a spark method utilizing the cathode layer in a unidirectional spark discharge, is useful for the determination of impurities in the routine control specimens submitted by the mill casting department.

The role of the X-ray spectrograph in the copper-base control laboratory, G. CRUMRINE, North American Smelting Co., Wilmington, Del.

A review of the use of the X-ray spectrograph in the analysis of copper-base alloys will be presented. Comparisons with chemical analysis, problems involved, and the future aspects of the instrument's applications, will be given.

Infra-red and related techniques

Recent innovations in instrumentation for infra-red spectroscopy, E. H. SIEGLER JR., The Perkin-Elmer Corporation, Norwalk, Conn.

Infra-red instrumentation has recently been extended in a number of somewhat diverse directions. Some of these developments will be discussed, with emphasis on the new types of instruments which are of interest to industrial and governmental laboratories. The following topics will be included: rapid-scan spectrometers, infra-red fore prism-grating spectrometers, and absorbance integrators.

Some applications of infra-red spectroscopy to chemical analysis, W. J. POTTS JR., The Dow Chemical Company, Midland, Mich.

1. Correlation of infra-red absorptions with organic structures continues to be a growing field. Some of the limitations of the out-of-plane hydrogen bending absorption correlations in aromatic structures will be discussed, and some new correlations of aliphatic hydrogen stretching absorptions will be given.

2. New instrumental techniques are continually being developed. Two examples to be discussed are the quantitative use of water solutions and adaption of vapour-phase chromatographic cuts to infra-red investigation.

3. Often, quantitative analysis of amines can best be done with infra-red by converting to the hydrochloride. This technique will be discussed.

Nondispersive gas analysis, MAX D. LISTON, Liston-Becker Plant, Beckman Instruments, Inc., Stamford, Conn.

The coming of age of nondispersion infra-red continuous analysers has been marked by a greatly accelerated sale and use over the past year. Some of the more important new industrial applications in safety and hygiene techniques will be discussed.

The development of mobile nondispersion infra-red analysers over the past year has facilitated taking measurements under conditions that were heretofore difficult. These mobile analysers have been successfully employed for combustion studies on vehicles under road conditions, for location of leaks in gas-mains, measurement of gas seepage for geological surveys and photosynthesis measurements.

Still another new nondispersion infra-red analyser which promises to overcome many of the shortcomings of the present instruments has been developed. This instrument is unique in that it measures the ratio of the signals from two detectors which are viewing the sample cell and source from the same aspect. It promises to minimize greatly the effects of sample cleanliness, deterioration of the optical elements, and overlapping spectra.

Gas chromatography—complementary to spectroscopy, E. F. WILLIAMS, American Cyanamid Co., Stamford, Conn.

Gas chromatography functions both as a tool for separation and as an analytical instrument. Its maximum utility in analysis may frequently be attained when it is used in conjunction with other instrumental methods. Several such applications will be considered along with a few of the problems encountered.

Infra-red radiometry and thermal photography, Eric Wormser, Barnes Engineering Co., Stamford, Conn.

Basic properties of thermistor infra-red detectors will be briefly reviewed and recent developments in these detectors reported.

The application of thermistor infra-red detectors to a family of radiometers for remote temperature measurements will be described. The radiometers when combined with optical mechanical scanning systems can be used for two-dimensional scanning. The results of the two-dimensional scan of objects or scenes are presented as thermal photographs with the visual brightness of the points on the photograph proportional to the infra-red radiance of the corresponding point in space.

The infra-red radiance is a function of the "apparent" or "equivalent black body" temperature of the object. If the emissivity of the object is known, its temperature distribution can then be read off the thermal photograph.

Thermal photography using the evaporograph, David Robinson, Baird Associates-Atomic Instruments Co., Cambridge, Mass.

An approximate ten-minute paper will be presented describing the use of the evaporograph in thermal photography.

Fundamental aspects of emission and X-ray spectroscopy

Atomic collision processes occurring in gas discharges, Manfred A. Biondi, Westinghouse Research Laboratories, Pittsburgh 35, Pa.

A brief discussion will be given of some of the fundamental atomic collision processes which lead to light emission in gas-discharge tubes. The processes will be divided into the following categories (1) Direct excitation—the excitation by electron impact of an atom from its ground state; (2) Indirect excitation—(a) the excitation by electron impact from an excited state to a higher state, and (b) the excitation to a higher state of an excited atom upon collision with another excited atom; (3) Excitation transfer—the excitation of an atom in its ground state by transfer of excitation from an excited atom; (4) Electron-ion recombination—the formation of an excited atom as a result of recombination between an electron and a positive ion; (5) Impurity effects—for example, excitation of one atomic species as a result of collisions with excited atoms of a different species. Possible consequences of the action of these processes in light sources used in spectrochemical analysis will be touched upon.

The fundamental facts of atomic spectra, W. F. Meggers, National Bureau of Standards, Washington, D.C.

The present status of wavelengths, intensities, and excitation potentials associated with spectral lines of atoms and ions will be summarized.

Early chemical analysis by X-ray emission, L. Thomassen, University of Michigan, Ann Arbor, Mich.

The possibility of using the characteristic X-ray spectra for chemical analysis is as old as X-ray spectroscopy itself. In Siegbahn's laboratory a number of demountable X-ray tubes and spectrographs were developed and some of these were used for chemical analysis by direct emission, notably by Hadding [1], Goldschmidt [2], and von Hevesy [3]. By means of X-ray spectroscopy von Hevesy also discovered the unknown element No. 72 (hafnium). In the present paper the methods used and the results of these early investigations will be reviewed and an evaluation of the results attempted.

[1] Hadding A. *Z. f. Phys.* 1921 **3**, 369.
[2] Goldschmidt V. M. and Thomassen L. *Geochemische Verteilungsgesetze* III. *Videnskapsselskapets Skrifter I. Mat. Naturv. Klasse*, 1924 No. 5.
[3] von Hevesy G. *Chemical Analysis by X rays and Its Applications*, 1932. McGraw-Hill Book Co., New York.

VOL. 8 1956/5

Applied and theoretical papers in ultra-violet absorption, mass, and pertinent nuclear spectroscopic techniques

X-ray emission spectroscopy, H. FRIEDMAN, Naval Research Laboratory, Washington, D.C.

The application of X-ray spectroscopy to elemental analysis has had spectacular success in recent years. Since the basic principles of X-ray analysis have been well known for many decades, the new popularity can be attributed directly to the development of electronic means of intensity measurement. Geiger counters, proportional counters, and scintillation counters detect characteristic X rays over the entire spectrum with high efficiencies. These detectors have been incorporated in various forms of spectrographs using crystal analysers, and in simple X-ray photometers. Routine analyses may now be made of all elements of higher atomic numbers than magnesium. The applications cover the entire range of concentrations from major constituents to traces of the order of a part per million. X-ray analysis is nondestructive and requires no direct contact with the sample. It handles many routine laboratory analyses with great speed compared to wet-chemical methods and is readily applicable to production problems such as the control of continuous flow processes.

Nuclear magnetic resonance spectroscopy, W. D. PHILLIPS, E. I. duPont de Nemours and Co., Wilmington, Del.

The utility of nuclear magnetic resonance spectroscopy as a tool in structural analysis has been expanded by the addition of surveys of P^{31}, N^{14}, O^{17}, and Si^{29} resonances in different bonding situations to the existing surveys of H^1 and F^{19} resonances. Theoretical analyses of these chemical shifts, as well as of the spin-spin splitting fine structure, in terms of electron densities, ionic characters of bonds, bonding hybrids, and molecular symmetries, are proceeding. In addition, nuclear magnetic resonance spectroscopy is proving of value in elucidating some of the more subtle aspects of molecular structure such as the hindered rotation that occurs in substituted ethanes and nitrosamines. A recent application of the technique utilizing the sensitivity of *n-m-r* spectral characteristics to molecular rate process has been the study of fluorine exchange in CF_3, BrF_3, BrF_5, and IF_5.

Mass spectrometer techniques for the analysis of solids*, LEWIS FRIEDMAN, Brookhaven National Laboratory, Upton, L.I., N.Y.

The problems of solids analysis in the mass spectrometer is closely related to problems of development of ion sources suitable for handling of low vapour-pressure materials. A brief review of the capabilities and limitations of electron impact, surface ionization, and vacuum-spark techniques will be presented. Some detailed consideration will be given to isotope dilution studies, with particular emphasis on analyses at the millimicrogram level and lower.

Spectroscopic instrumentation in the Soviet Union, ROBERT J. MELTZER, Bausch and Lomb Optical Company, Rochester, New York.

This paper will describe and illustrate those spectroscopic instruments developed in the Soviet Union which are in production as standard instruments, rather than special-purpose instruments. They include instruments for emission spectroscopy, absorption spectroscopy in the ultra-violet visible and infra-red, and Raman spectroscopy.

Use of machine-sorted punched cards in ultra-violet spectrophotometry, R. C. HIRT, American Cyanamid Co., Stamford, Conn.

Ultra-violet spectrophotometry may be used effectively in organic group analysis for the identification of chromophoric groups rather than for identification of particular compounds. A knowledge of the correlation of molecular structure of chromophoric groups with absorption-band wavelength, intensity, contour, and solvent or pH changes is essential. In addition, a large library of spectra is needed for ready reference. Practical economic factors severely limit

* Research performed under the auspices of the U.S. Atomic Energy Commission.

the extent of the library of spectra that may be built up by the individual library, so recourse must be made to the published literature.

Prior to the advent of Kuentzel-Wyandotte or A.S.T.M.-I.B.M. system of machine-sorted punched cards, the Stamford Laboratories of the American Cyanamid Company had built up a sizable library of spectra of pure compounds and of published spectra contained in reprints from journals. These were elaborately indexed. The A.S.T.M.-I.B.M. system was adopted and co-ordinated with the existing files, and the growth and operation of this system will be described.

Two major types of information are generally desired: (1) the chromophoric groups responsible for the observed spectrum of an unknown sample, and (2) the spectrum of a particular compound for comparison with an observed spectrum. The machine-sorted cards are most suitable for the first case, while empirical formula and alphabetical compound-name files are better for the second. The co-ordination of these two major uses, and other uses (such as literature searching and bibliography preparation) will be illustrated. For example, the machine-sorted cards have been used for the rapid construction of an empirical formula index and for a bibliography on vacuum ultra-violet spectra.

Performance specifications for a recording spectrophotometer, R. H. Noble and C. W. Warren, Perkin-Elmer Corporation, Norwalk, Conn.

The best description of a measuring instrument is its list of specifications. This list delineates the instrument's field of usefulness, its probable effectiveness in that field, and usually its price range. It forms the basis for the design during development and the testing after manufacture.

As an example the operation of the Spectracord-400 is described. Reasons for the choice of particular specifications are discussed. Performance tests are described and the test results on a typical instrument listed.

VOL.
8
1956/5

NOTICES OF MEETINGS

Pittsburg Conference on Analytical Chemistry and Applied Spectroscopy—4–8 March 1957, Pittsburgh, Pa.

American Association of Spectrographers—Eighth Annual Symposium, 29 April–1 May 1957, Chicago, Ill.

Organizers of gatherings of spectroscopists, of national or international scope, are invited to send to this journal not only the dates of the meetings, but also the names and addresses of the organizing secretaries.

OL.
8
6/57